



U.S. Department
of Transportation

**Federal Highway
Administration**

PB2001-105207



Publication No. FHWA-TS-89-045
September 1989

ROCK SLOPES: Design, Excavation, Stabilization

Research, Development, and Technology
Turner-Fairbank Highway Research Center
6300 Georgetown Pike
McLean, Virginia 22101-2296



NOTICE

This document is disseminated under the sponsorship of the Department of Transportation in the interest of information exchange. The United States Government assumes no liability for its contents or use thereof.

The contents of this report reflect the views of Golder Associates, which is responsible for the facts and the accuracy of the data presented herein. The contents do not necessarily reflect the official views or policy of the Department of Transportation.

This report does not constitute a standard, specification or regulation.

ACKNOWLEDGEMENTS

Golder Associates wishes to express their appreciation to the Federal Highway Administration for their funding of the preparation of this manual. We also appreciate the assistance and advice provided by many members of the Federal and State Government geotechnical engineering community with whom we have worked in the past. In particular, we acknowledge Gerry DiMaggio, Dick Cheney, Bob Leary, and Ron Chassie with the Federal Highway Administration, and Verne McGuffey (NYDOT), Hal Apper (NJDOT), Dave Bingham (NCDOT), Bob Smith, Bill Capaul and Jim Winger (IDT), Al Killian and Steve Lowell (WSDOT), and Harry Moore (TNDOT).

We also appreciate the generosity of Dr. Evert Hoek and John Bray for allowing the adaptation of their book "Rock Slope Engineering" (published by Institute of Mining and Metallurgy, London 1981) as the basis for this manual. Examples and experience quoted in this manual have been drawn from many organizations including railway, highway, logging and mining companies located in many parts of the world. In addition, we are grateful to the manufacturers of drilling equipment, explosives and movement monitoring instruments for the use of their technical data.

PROTECTED UNDER INTERNATIONAL COPYRIGHT
ALL RIGHTS RESERVED.
NATIONAL TECHNICAL INFORMATION SERVICE
U.S. DEPARTMENT OF COMMERCE

Reproduced from
best available copy.



PREFACE

This manual has been prepared by Golder Associates, Seattle, Washington, in conjunction with a series of Rock Slope Engineering courses sponsored by the Federal Highway Administration.

The manual is based on a book entitled "Rock Slope Engineering" authored by Dr. Evert Hoek and Dr. John Bray. A third edition of this book has been published in 1981. The book has been modified for these courses by expanding the chapter on Blasting and preparing new chapters on Sloe Stabilization, Movement Monitoring and Construction Contracts and Specifications. A glossary of excavation terms, Listings and documentation of two slope stability programs and a data collection manual have been added as appendices. The entire text has been edited to make it applicable to transportation engineering.

TABLE OF CONTENTS

	<u>PAGE</u>
Chapter 1: Principles of rock slope engineering for highways	1.1
Economic consequences of instability	1.1
Planning stability investigations	1.6
Chapter 1 references	1.11
Chapter 2: Basic mechanics of slope failure	2.1
Continuum mechanics approach to slope stability	2.1
Maximum slope height - slope angle relationship for excavated slopes	2.1
Role of discontinuities in slope failure	2.2
Friction, cohesion and unit weight	2.2
Sliding due to gravitational loading	2.7
Influence of water pressure on shear strength	2.7
The effective stress law	2.8
The effect of water pressure in a tension crack	2.9
Reinforcement to prevent sliding	2.9
Factor of safety of a slope	2.10
Slope failures for which factors of safety can be calculated	2.11
Critical slope height versus slope angle relationships	2.12
Slopes for which a factor of safety cannot be calculated	2.14
Probabilistic approach to slope design	2.16
Chapter 2 references	2.18
Chapter 3: Graphical presentation of geological data	3.1
Definition of geological terms	3.1
Definition of geometrical terms	3.3
Graphical techniques for data presentation	3.4
Equal-area projection	3.4
Construction of a great circle and a pole representing a plane	3.9
Determination of the line of intersection of two planes	3.9
To determine the angle between two specific lines	3.10
Alternative method for finding the line of intersection of two planes	3.11
Plotting and analysis of field measurements	3.11
Evaluation of potential slope problems	3.19
Suggested method of data presentation and analysis for highway design	3.23
Chapter 3 references	3.26
Chapter 4: Geological data collection	4.1
Regional geological investigations	4.1
Mapping of exposed structures	4.2
Photographic mapping of exposed structures	4.6
Measurement of surface roughness	4.8
Diamond drilling for structural purposes	4.8
Presentation of geological information	4.16
Chapter 4 references	4.18

TABLE OF CONTENTS (Cont'd)

	PAGE
Chapter 5: Shear strength of rock	5.1
Shear strength of planar discontinuities	5.1
Influence of water on shear strength of planar discontinuities	5.2
Shearing on an inclined plane	5.3
Surface roughness	5.4
Shear testing of discontinuities in rock	5.7
Estimating joint compressive strength and friction angle	5.14
Shear strength of filled discontinuities	5.19
Shear strength of closely jointed rock masses	5.22
Testing closely jointed rock	5.25
Shear strength determination by back analysis of slope failures	5.30
Sample collection and preparation	5.33
Chapter 5 references	5.39
Chapter 6: Groundwater flow; permeability and pressure	6.1
Groundwater flow in rock masses	6.2
Flow nets	6.8
Field measurement of permeability	6.10
Measurement of water pressure	6.17
General comments	6.20
Chapter 6 references	6.22
Chapter 7: Plane failure	7.1
General conditions for plane failure	7.1
Plane failure analysis	7.1
Graphical analysis of stability	7.8
Influence of aroundwater on stability	7.10
Critical tension crack depth	7.12
The tension crack as an indicator of instability	7.15
Critical failure plane inclination	7.16
Influence of undercutting the toe of a slope	7.17
Reinforcement of a slope	7.17
Analysis of failure on a rough plane	7.18
Practical example No. 1	7.19
Practical example No. 2	7.25
Practical example No. 3	7.30
Practical example No. 4	7.41
Practical example No. 5	7.47
Chapter 7 references	7.49
Chapter 8: Wedge failure	a.1
Definition of wedge geometry	a.4
Analysis of wedge failure	a.4
Wedge analysis including cohesion and water pressure	a.5
Wedge stability charts for friction only	8.11
Practical example of wedge analysis	a.12
Chapter B references	a.25

TABLE OF CONTENTS (Cont'd)

	PAGE
Chapter 9: Circular failure	9.1
Conditions for circular failure	9.1
Derivation of circular failure chart	9.3
Groundwater flow assumptions	9.4
Production of circular flow charts	9.5
Use of the circular failure charts	9.5
Location of critical failure circle and tension crack	9.14
Practical example No. 1	9.17
Practical example No. 2	9.18
Practical example No. 3	9.19
Bishop's and Janbu's methods of slices	9.22
Chapter 9 references	9.29
Chapter 10: Toppling failure	10.1
Types of toppling failure	10.1
Analysis of toppling failure	10.3
Factor of safety for limiting equilibrium analysis of toppling failures	10.13
General comments on toppling-failure	10.13
Chapter 10 references	10.14
Chapter 11: Blasting	11.1
I Principles of blasting	11.1
Mechanism of rock failure by explosive	11.1
Production blasting	11.2
Blast design	11.11
Evaluation of a blast	11.13
Modification of blasting methods	11.13
II Controlled blasting to improve stability	11.15
Line drilling	11.16
Cushion blasting	11.20
Preshear blasting	11.24
Buffer blasting	11.30
Controlled blasting: construction practices and economics	11.30
III Blast damage and its control	11.32
Structural damage	11.34
Control of flyrock	11.37
Airblast and noise problems associated with production blasts	11.39
Chapter 11 references	11.43
Chapter 12: Stabilization and protection measures	12.1
Stabilization methods	12.2
I Stabilization methods that reduce driving forces	12.3
II Reinforcement and support stabilization methods	12.8
III Protection measures	12.18
Example of slope stabilization project	12.24
Chapter 12 references	12.32

TABLE OF CONTENTS (Cont'd)

	<u>PAGE</u>
Chapter 13: Slope movement monitoring	13.1
Methods of measuring slope movements	13.2
Surface methods	13.3
Subsurface surveying methods	13.10
Interpreting movement results	13.11
Chapter 13 references	13.15
Chapter 14: Construction contracts and specifications	14.1
Selecting the type of construction contract	14.1
Writing specifications	14.6
Typical specifications	14.7
Chapter 14 references	14.20
Appendix 1: Analysis of laboratory strength test data	A1-1
Appendix 2: Wedge solution for rapid computation	A2-1
Appendix 3: Factors of safety for reinforced rock slopes	A3-1
Appendix 4: Conversion factors	A4-1
Appendix 5: Glossary of blasting and excavation terms	A5-1
Appendix 6: Geotechnical data collection manual	A6-1
Appendix 7: HP67 slope design programs	A7-1
Appendix 8: Practicums	A8-1
Appendix 9: Rock mass classification systems	A9-1

Chapter 1 Principles of rock slope engineering for highways.

Introduction

This manual is concerned with the stability of rock slopes, with methods for assessing this stability and with techniques for improving the stability of slopes which are potentially hazardous. It is intended that it serve as both an instruction manual for engineers carrying out slope stability investigations and designing rock slopes, and a guide for construction engineers involved with excavation and stabilization. With this purpose in mind, the manual contains sections on methods of rock slope design, practical exercises demonstrating the application of these methods, sections on blasting, slope stabilization, contracts and contract management.

Economic consequences of instability

Rock slope failures, or the remedial measures necessary to prevent them, cost money and it is appropriate that, before becoming involved in a detailed examination of slope behavior, some of the economic implications of this behavior should be examined. On transportation routes rock slope stability involves both overall slope failure, and rock falls from slope faces. Obviously, slopes are cut at the steepest possible angle in order to minimize the excavation volume and the disturbance to adjacent property. However, in designing rock slopes it is essential that the long-term stability of the slope be considered because it is likely that the excavation must be stable for many years. During this time the rock will weather, it will be subject to ice and water action, plant root growth and possible change in loading conditions due to such activities as ditch widening at the toe and construction on the crest. Adequate safeguards to account for these changes should be incorporated in the design because the consequences of instability, as discussed below, can be costly.

In examining the economic consequences of slope failures one should consider both direct and indirect costs*(1). For the case of a slope failure during construction, direct costs would include such items as equipment damage, claims for delays, excavation of the failed material and stabilization of the remaining slope. Indirect costs would include such items as extra engineering time, legal fees and, the most significant item, delay to opening of the new highway, or the need to reroute traffic.

In the event of rock fall on an operational highway the direct costs are usually limited to cleaning rock from the road surface, repairing the pavement and doing some stabilization work. Indirect costs include such items as injury to highway users, damage to vehicles, lost wages, hospital charges, legal fees and highway closure.

One approach to examining the cost benefits of slope stabilization programs to reduce the incidence of slope failures that disrupt highway operations, is to use decision analysis(2,3,4). This technique relates the cost of uncertain events, that can be expressed in terms of probabilities of failure, to the costs of alternative stabilization programs. The results give expected total costs of failure and stabilization for different op-

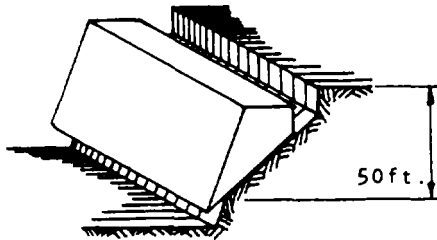
*Numbers refer to list of references at the end of each Chapter.

tions which helps the engineer to decide which action produces the greatest economic benefit. Decision analysis is beginning to be used in engineering(5,6) following its more widespread use in the business community.

A further consideration is that motorists are sometimes successfully suing highway departments for damages and injury caused by rock falls(7). One possible protection against such action is to show that reasonable steps were taken to prevent failure. Usually, reasonable steps are the application of proven engineering methods and techniques. The methods described in this manual have been used successfully in practice(8,9) and can be applied, in appropriate conditions, with confidence in the design of rock slopes. This means that designs for individual rock slopes can be prepared rather than using a standard specification such as 1/4 (horizontal) : 1 (vertical).

Example of slope stabilization costs

Possibly the best illustration of slope design can be given by an example which includes a consideration of the most important factors which control rock slope behavior as well as the economic consequences of failure.



Geometry of planar failure in example of bench stability analysis.

Details of slope geometry and material properties used in analysis. Discontinuity surface upon which sliding occurs dips at 45° . The friction angle of the surface is 35° and the cohesion is 1200 lb/sq.ft.

In the slope illustrated in the margin sketch which has been designed to be excavated at our angle of 76° (1/4:1), a discontinuity has been exposed during the early stages of excavation. Measurement of the orientation and inclination of this discontinuity and projection of these measurements into the rock mass shows that the line of intersection of the discontinuity will daylight in the slope face when the height of the slope reaches 50 ft. It is required to investigate the stability of this slope and to estimate the costs of the alternative methods of dealing with the problem which arises if the slope is found to be unstable.

The factor of safety* of the slope, for a range of slope angles, is plotted in Figure 1.2 for the two extreme conditions of a dry slope and a slope excavated in a rock mass in which the groundwater level is very high. It will become clear, in the detailed discussions given later in this manual, that the presence of groundwater in a slope can have a very important influence upon its stability and that drainage of this groundwater is one of the most effective means of improving the stability of the slope.

A slope will fail if the factor of safety falls below unity and from Figure 1.2, it will be seen that the saturated slope will fail if it is excavated at an angle steeper than 72 degrees. The dry slope is theoretically stable at any angle but the minimum factor of safety of approximately 1.1 is not considered sufficiently high to ensure that the slope will remain stable. Slopes adjacent to highways are considered to be permanent and a factor of safety of 1.5 should usually be used for design purposes.

*The definition of this and of other terms used in the stability analysis is given later in the manual. A detailed knowledge of the method of analysis is not necessary in order to follow this example.



Figure 1.1 : Example of a planar failure.

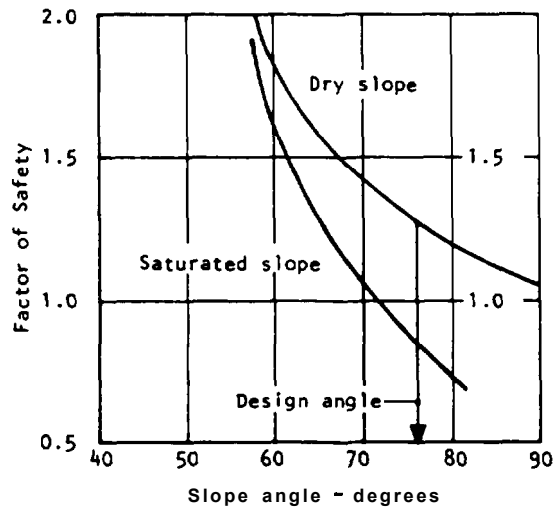
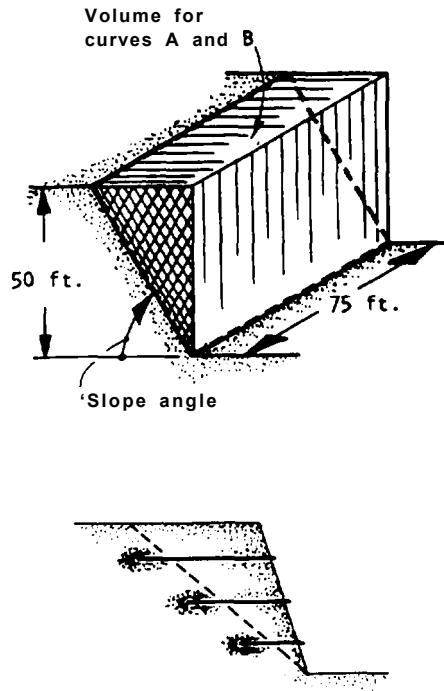


Figure 1.2: Variation in Factor of Safety with slope angle.



In this example it would be necessary to cut the slope at an angle of 68 degrees for the dry slope and 61 degrees for the saturated slope in order to achieve a factor of safety of 1.5.

A comparison of costs if failure was to occur, with costs of alternative stabilization measures, can be made by first calculating the estimated volume of failure with increasing slope angle (curve A on Figure 1.3). A slope length of 75 ft. has been taken in this example. One means of stabilizing the slope would be to flatten the slope angle, and curve B shows the extra volume that must be excavated to flatten the slope from 76 degrees.

Also included in this figure are two curves giving the external load, applied by means of cables installed in horizontal holes drilled at right angles to the strike of the slope and anchored in the rock behind the discontinuity planes, required to give a factor of safety of 1.5 for both saturated and dry slopes (curves C and D).

The cost of the various options which are now available to the engineer will depend upon such factors as the physical constraints at the site, e.g. property ownership, and the availability of men and equipment to install drain holes and rock anchors. In deriving the costs presented in Figure 1.4, the following assumptions were made:

- a) The basic cost unit is taken as the contract price per cubic yard of rock measured in place. Hence line B in Figure 1.4, the cost of flattening the slope, is obtained directly from line B in Figure 1.3.
- b) The cost of clearing up a slope failure is assumed to be twice the basic excavating cost. This gives line A which starts at a slope angle of 72 degrees, theoretically the steepest possible saturated slope (see Figure 1.2).
- c) The cost of tensioned cables is assumed to be 2 1/2 cost units per ton of cable load. This gives lines C and D on Figure 1.4 for saturated and dry slopes respectively (factor of safety = 1.5, Figure 1.3).

On the basis of a set of data such as that presented in Figure 1.4, the engineer is now in a position to consider the relative costs of the options available to him. Some of these options are listed below:

- a) Flatten slope to 61 degrees to give a factor of safety of 1.5 under saturated conditions (line B).

Total Cost = 900 Units

- b) Flatten slope to 67 degrees and install a drainage system to give a factor of safety of 1.5 for a dry slope (line B and E).

Total Cost = 1250 Units

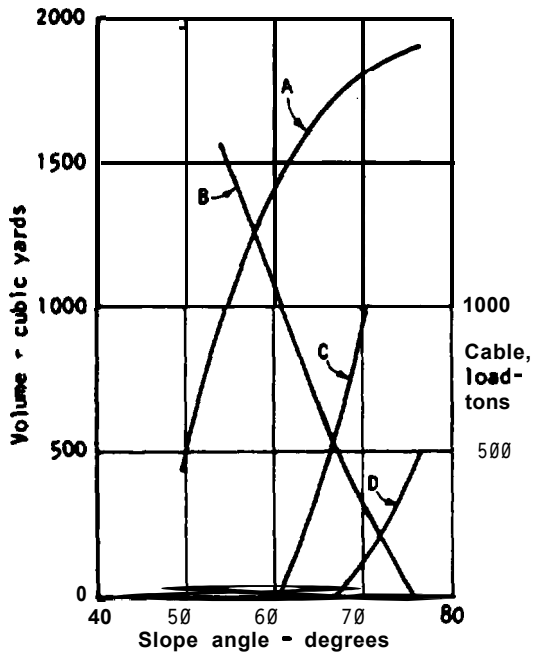
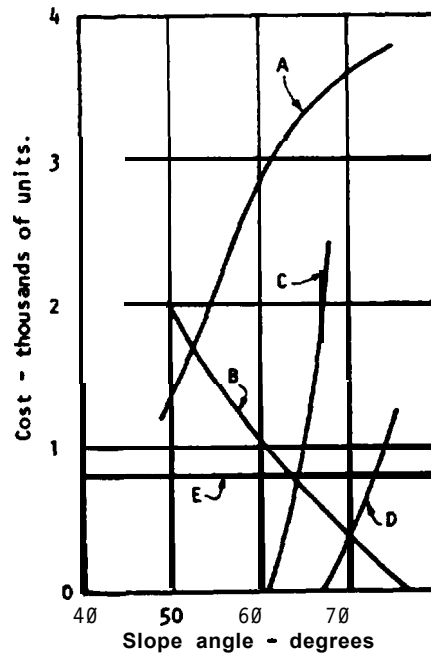


Figure 1.3: Excavation volumes and bolt loads.

- Line A - Volume to be cleared up if failure occurs.
- Line B - Volume excavated in flattening slope from angle of 76° for 75 ft. long slope.
- Line C - Cable load required for Factor of Safety of 1.5 for saturated slope.
- Line D - Cable load required for Factor of Safety of 1.5 for dry slope.

Figure 1.4: Comparative cost of options.

- Line A - Cost of clearing up slope failure.
- Line B - Cost of flattening slope.
- Line c - Cost of installing cables in saturated slope.
- Line D - Cost of installing cables in dry slope.
- Line E - Cost of draining slope.



- c) Cut slope to 72 degrees to induce failure and clean up failed material (lines A and B).

Total Cost = 3800 Units

- d) The option of cutting this slope at 76 degrees and installing anchors to give a factor of safety of 1.5 for a standard slope is not feasible because it would be impractical to install the number of cables required (curve C).

- e) Cut slope at 76 degrees, install drains and anchors to give a factor of safety for a dry slope of 1.5 (lines D and E).

Total Cost = 2000 Units

- f) Cut slope to 67 degrees on the assumption that it may not fail and make provision to clean up any failure that may occur (lines A and B).

Minimum Total Cost = 450 Units

Maximum Total Cost = 3850

It must be emphasized that these estimates are hypothetical and apply to this particular slope only. The costs of these and other options will vary from slope to slope and no attempt should be made to derive general rules from the figures given.

The lowest cost option (option (f)) if the slope does not fail, is to cut the slope to 67 degrees and accept the risk of failure. This risk may be acceptable for a temporary or infrequently used road if it is expected that the slope will not become saturated. However, if the slope were to fail then the total cost would be greater than any of the other options. The option with the next lowest cost is option (a) which involves flattening the slope to 61 degrees so that a factor of safety of 1.5 is obtained under saturated conditions. This has the advantage that no artificial support, which may not work as designed in the long term, is required, but would not be feasible if property restrictions preclude cutting back the slope. If it was necessary that the slope be cut at 76 degrees then it would be necessary to drain the slope as well as put in anchors (option (e)). The effectiveness of the drainage system would be most important because of the sensitivity of the slope to water pressures.

Planning stability investigations

Typically, rock cuts above highways may only suffer very occasional slope failures during their life. How can these isolated slopes which are potentially dangerous be detected in the many miles of slopes along the highway?

The answer lies in the fact that certain combinations of geological discontinuities, slope geometry and groundwater conditions result in slopes in which the risk of failure is high. If these combinations can be recognized during the preliminary geological and highway layout studies, steps can be taken to deal with the slope problems which are likely to arise in these areas. Slopes in which these combinations do not occur require

no further investigation. It must, however, be anticipated that undetected discontinuities will be exposed as the slope is excavated and provision must be made to deal with the resulting slope problems as they arise.

This approach to the planning of slope stability studies is outlined in the chart presented in Figure 1.5, and it will be seen that there are two distinct categories:

- a) Design of slopes for new construction
- b) Evaluation of stability of existing slopes, and design of stabilization programs where required.

Details of the different approaches are as follows:

- a) **New construction:** the first task involves a preliminary evaluation of the geological data available from the route exploration program, which normally includes air photo interpretation, surface mapping and study of natural slopes. The study should include the stability of large, regional movements as well as the stability of individual rock cuts.

The preliminary assessment of stability can be done using a number of simple techniques which will be described in the first part of this manual. This preliminary study should identify those slopes in which no failure is likely, and which can, therefore, be designed on the basis of operational considerations, and those slopes in which the risk of failure appears to be high and which require more detailed analysis.

This analysis involves a much more detailed study of the geology, possibly requiring drilling, the groundwater conditions, and the mechanical properties of the rock mass. A detailed analysis of stability is then carried out on the basis of this information to determine maximum safe slope angle, or support requirements.

Chapters 7 - 10 of this manual will deal with the techniques which can be used for these detailed stability studies.

- b) **Existing slopes:** the major difference between these stability studies and those for new construction, is the greater amount of information available in the case of existing slopes. The exposed face will usually give excellent information on geological conditions and study of past failures will demonstrate the type of failure most likely to occur. Back-analysis of these failures would be the most reliable means of determining the rock strength although in some cases it may also be necessary to carry out laboratory testing on fractures not involved in previous failures. If it is suspected that groundwater pressures played a part in the failure it may be necessary to install piezometers to measure the pressure because it is rarely possible to obtain this information from observations on the face. In many cases drilling programs will not be required because more information on geology will be

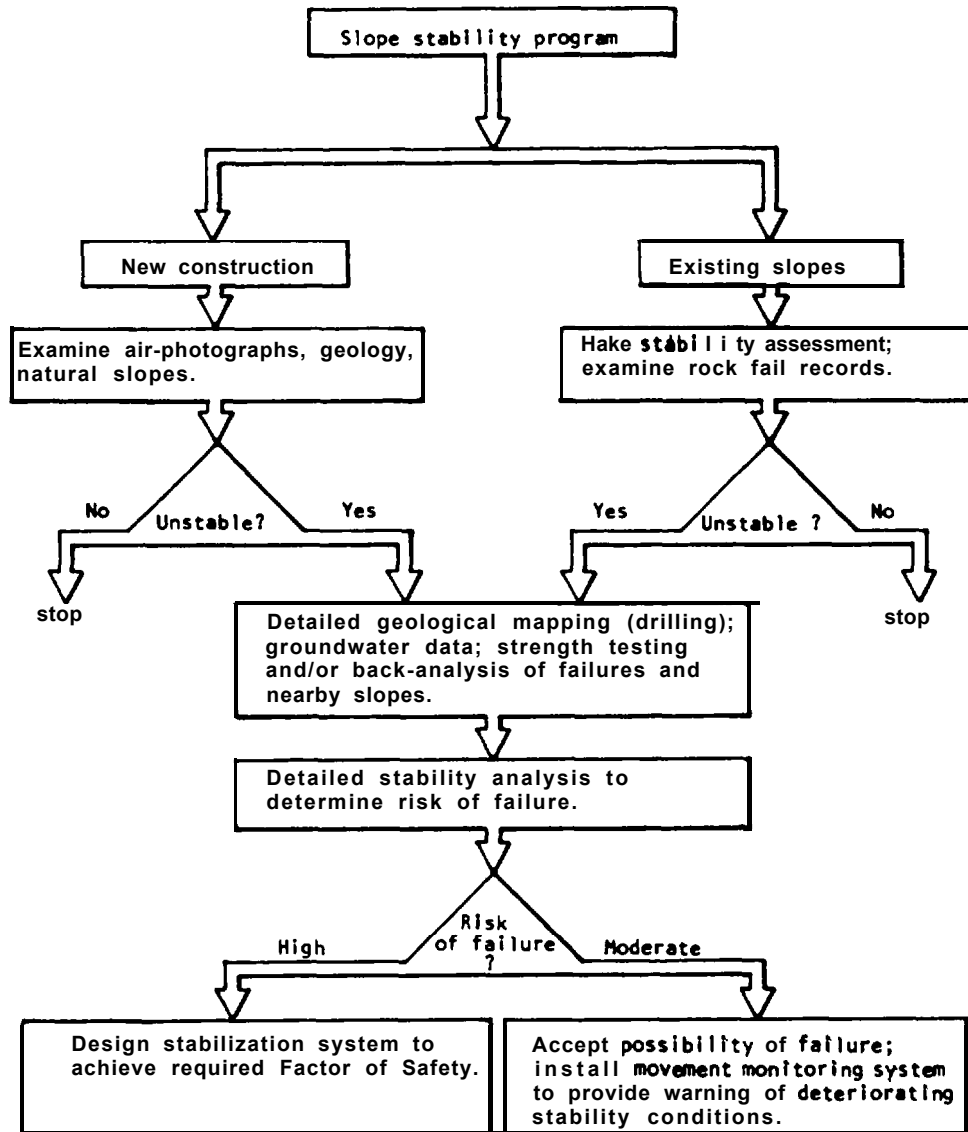


Figure 1.5: Planning a slope stability program.

available from surface mapping than will be obtained from drill core. This information can be used to design appropriate stabilization measures.

In some cases there may be a number of unstable slopes along many miles of highway and there will be insufficient time and funds available to carry out all the stabilization work. One method of drawing up a long term stabilization program in which the most hazardous slopes are stabilized first, is to make an inventory of stability conditions. This inventory would describe the physical and geotechnical conditions of each site, from which a priority rating, related to the probable risk of failure, to be assigned to each slope (10, 10A). This information would identify the most hazardous locations, and the stabilization work required, and would be used to plan a program which would start with the slopes having the highest priority rating.

An example of the information that would be collected in making an inventory of stability conditions is shown in Figure 1.6. The information for all the slopes is stored in a computerized data base which can be used to retrieve selected data, such as the mileage and priority rating of all slopes where previous rock falls have occurred. Also, the data base facilitates updating of records such as rock fall events. Once an inventory of slopes has been completed, priority ratings can be assigned to each slope.

In assigning priority ratings, it is important that a method be used that is consistent, both between sites, and when data is collected by different personnel. The system shown in Figure 1.7 assigns points to each category of data that has an influence on stability conditions. The total number of points is then added to determine the priority rating number. The sites can then be ranked according to their rating number, or they can be grouped as shown on the lower part of Figure 1.7. It is considered that grouping of sites with similar ratings is appropriate because assignment of rating numbers is imprecise and requires a certain amount of judgement. One means of describing priority ratings based on groupings of priority numbers is as follows:

<u>Point Total</u>	<u>Priority</u>	<u>Description of Risk</u>
>500	A)	Moderate probability of failure of sufficient volume to cause hazard if failure undetected.
400 to 500	B)	Some probability of failure of sufficient volume to cause hazard if failure undetected.
250 to 400	C)	Moderate probability of failure of small volumes which might reach the highway.
250 to 150	D)	Moderate probability of localized rocks or rock falls occurring during extreme climatic conditions - wry heavy rainfall or run-off, extreme freeze-thaw cycles, etc.
<150	E)	Slight possibility of localized failures under extreme climatic conditions. Generally shallow cuts.

Finally, how long will a slope design program take? The time will range from one half to two hours for a stability assessment (Figure 1.61, to several days for a preliminary investigation for a new construction site, to possibly two months for a detailed study of a critical slope.

STABILITY ASSESSMENT	


Date: March 22, 1988	Priority: A
Region: Western	Route: SR 1002A
Mileage: 81.2	Traffic: Heavy
Alignment: Tangent.	
Sight Visibility: 500 yards, east and west.	
Average Climatic Conditions:	
Coastal - wet with freeze/thaw cycles in spring and fall.	
Past Stability Records:	
A rockfall in late 1983 was struck by a truck. There are other falls lying in the ditch with volumes up to 1/2 cu.yd; the Foreman report equipment has been used in the past to remove substantial quantities of rock from the ditch.	
DESCRIPTION OF SITE	
cut: x	Fill: Other: Height: 40 ft. Length: 300 ft.
Rock: x	Soil: Other:
Notes : Through-cut.	
Geologic Description:	
Strong massive granite with blast damage that has opened substantial cracks. Note heavy tree cover along crest of cut.	
Evidence of Water:	
Nil.	
Work Space Available:	
Limited.	
DESCRIPTION OF POTENTIAL INSTABILITY	
Further rockfalls with volumes up to at least 5 cu.yds.	
RECOMMENDED STABILIZATION	
Clean end widen existing ditches, to minimum of 15 ft. width. Where ditch cannot be excavated, scale loose rock on slope face.	
PHOTOGRAPH OF SITE	
Gold® Associates	

Figure 1.6: Example of Slope Stability Assessment Sheet.

	POINTS 1	POINTS 3	POINTS 9	POINTS 27	POINTS 81
SLOPE HEIGHT	<15 FT	15 TO 25 FT	25 TO 35 FT	35 TO 45 FT	> 45 FT
SLOPE LENGTH	< 50 FT	50 TO 100 FT	100 TO 150 FT	150 TO 200 FT	> 200 FT
VISIBILITY/ SHOULDER	Adequate stopping distance, full shoulder	Good visibility and shoulder width	Moderate visibility and shoulder width	Limited visibility and shoulder width	Very limited visibility, no shoulder
TRAFFIC	Very light	Recreational only	Moderate	Heavy	Very heavy/ continuous
DITCH DIMENSIONS	Meets Ritchie criteria	Adequate width, inadequate depth	Moderate catchment	Limited catchment	Nil
GEOLOGY	Massive, no fractures dipping out of slope	Discontinuous fractures, random orientation	Fractures form wedges	Discontinuous fractures dipping out of slope	Continuous fractures dipping out of slope
BLOCK SIZE	< 6 IN	6 TO 12 IN	1 TO 2 FT	2 TO 5 FT	> 5 FT
ROCK FRICTION	Rough, irregular	Undulating	Planar	Smooth, slickensided	Clay, gouge faulted
WATER/ICE	Dry, warm winters	Moderate rainfall, warm winters	Moderate rainfall, some freezing	Moderate rainfall, cold winters	High rainfall, cold winters
ROCK FALL	No falls	Occasional minor falls	Occasional falls	Regular falls	Major falls/ slides

Priority

Point Total

A	Greater than 500
B	400 to 500
C	250 to 400
D	150 to 250
E	Less than 150

Figure 1.7: Slope Stability Rating System

Chapter 1 references

1. CHIN, SHIH-MIAO. Cost as a criterion for evaluating highway level of service, ITE Journal, August 1978, Page 16.
2. WYLLIE, D.C., McCAMMON, N.R., BRUMUND, W. Planning slope stabilization programs using decision analysis. TRB, Annual Meeting, January 1978.
3. RUSSELL, S.O. Civil engineering risks and hazards. The B.C. Professional Engineer, January 1976.
4. RAIFFA, H. Decision analysis. Addison-Wesley, Massachusetts, 1970.
5. ACTON, J. E. Assessment of hazards associated with highway engineering. Proc. Inst. Civ. Engrs., Part 1, 1978, 64, Aug. 381-391.
6. BENJAMIN, J.R. Applied statistical decision theory for dam construction. Conference on Dam Safety, Stanford University, 1978.
7. ROYSTER, D.L. Landslide Remedial Measures. Bull. Assoc. Eng. Geol., Vol XVI, No. 2, 1979, Page 301.
8. HOEK, E. and BRAY, J. Rock Slope Engineering I.M.M., Second Edition, 1977.
9. FOKES, P.G. and SWEENEY, M. Stabilization and control of local rock falls and degrading rock slopes. Quart. Jour. Eng. Geol, Vol 9, No. 1, 1976, pp. 37-55.
10. BRAWNER, C.O. and WYLLIE, D.C. Rock slope stability on railway projects. American Railway Engineering Association, Vancouver, B.C. October 1975.
- 10A. WYLLIE, D.C. Rock slope inventory/maintenance programs. FHWA, 13th Northwest Geotechnical Workshop, Portland, OR, 1987.

Chapter 2 Basic mechanics of slope failure.

Continuum mechanics approach to slope stability

A question which frequently arises in discussions on slope stability is how high and how steep can a rock slope be cut. One approach to this problem, which has been adopted by a number of investigators(11-15), is to assume that the rock mass behaves as an elastic continuum. The success which has been achieved by the application of techniques such as photoelastic stress analysis or finite element methods in the design of underground excavations has tempted many research workers to apply the same techniques to slopes. Indeed, from the research point of view, the results have been very interesting but in terms of practical rock slope engineering, these methods have limited usefulness. These limitations arise because our knowledge of the mechanical properties of rock masses is so inadequate that the choice of material properties for use in the analysis becomes a matter of pure guesswork. For example, if one attempts to calculate the limiting vertical height of a slope in a very soft limestone on the basis of its intact strength, a value in excess of 3,500 ft. is obtained(16). Clearly, this height bears very little relation to reality and one would have to reduce the strength properties by a factor of at least 10 in order to arrive at a reasonable slope height.

It is appropriate to quote from a paper by Terzaghi(17) where, in discussing the problem of foundation and slope stability, he said "... natural conditions may preclude the possibility of securing all the data required for predicting the performance of a real foundation material by analytical or any other methods. If a stability computation is required under these conditions, it is necessarily based on assumptions which have little in common with reality. Such computations do more harm than good because they divert the designer's attention from the inevitable but important gaps in his knowledge ...".

Muller and his co-workers in Europe have emphasized for many years the fact that a rock mass is not a continuum and that its behavior is dominated by discontinuities such as faults, joints and bedding planes. Most practical rock slope designs are currently based upon this discontinuum approach and this will be the approach adopted in all the techniques presented in this book. However, before leaving the question of the continuum mechanics approach, the authors wish to emphasize that they are not opposed in principle to its application and indeed, when one is concerned with overall displacement or groundwater flow patterns, the results obtained from a numerical method such as the finite element technique can be very useful. Developments in numerical methods such as those reported by Goodman(19) et al and Cundall(20) show that the gap between the idealized elastic continuum and the real discontinuum is gradually being bridged and the authors are optimistic that the techniques which are currently interesting research methods will eventually become useful engineering design tools.

Maximum slope height - slope angle relationship for excavated slopes

Even if one accepts that the stability of a rock mass is dominated by geological discontinuities, there must be situations where the orientation and inclination of these discontinuities is such that simple sliding of slabs, blocks or wedges is not possible. Failure in these slopes will involve a combination

of movement on discontinuities and failure of intact rock material and one would anticipate that, in such cases, higher and steeper slopes than average could be excavated. What practical evidence is there that this is a reasonable assumption?

A very important collection of data on excavated slopes was compiled by Kley and Lutton(21) and additional data has been obtained by Ross-Brown(22). The information refers to slopes in open cut mines, quarries, dam foundation excavations and highway cuts. The slope heights and corresponding slope angles for the slopes in materials classified as hard rock have been plotted in Figure 2.1 which includes both stable and unstable slopes. Ignoring, for the moment, the unstable slopes, this plot shows that the highest and steepest slopes which have been successfully excavated, as far as is known from this collection of data, fall along a fairly clear line shown dashed in Figure 2.1. This line gives a useful practical guide to the highest and steepest slopes which can be contemplated for normal transportation planning. In some exceptional circumstances, higher or steeper slopes may be feasible but these could only be justified if a very comprehensive stability study had shown that there was no risk of inducing a massive slope failure.

Role of discontinuities in slope failure

Figure 2.1 shows that, while many slopes are stable at steep angles and at heights of several hundreds of feet, many flat slopes fail at heights of only tens of feet. This difference is due to the fact that the stability of rock slopes varies with inclination of discontinuity surfaces, such as faults, joints and bedding planes, within the rock mass. When these discontinuities are vertical or horizontal, simple sliding cannot take place and the slope failure will involve fracture of intact blocks of rock as well as movement along some of the discontinuities. On the other hand, when the rock mass contains discontinuity surfaces dipping towards the slope face at angles of between 30° and 70° , simple sliding can occur and the stability of these slopes is significantly lower than those in which only horizontal and vertical discontinuities are present.

The influence of the inclination of a failure plane on the stability of a slope is strikingly illustrated in Figure 2.2 in which the critical height of a dry rock slope is plotted against discontinuity angle. In deriving this curve, it has been assumed that only one set of discontinuities is present in a very hard rock mass and that one of these discontinuities "daylights" at the toe of the vertical slope as shown in the sketch in Figure 2.2. It will be seen that the critical vertical height H decreases from a value in excess of 200 ft., for vertical and horizontal discontinuities, to about 70 ft. for a discontinuity inclination of 55° .

Clearly, the presence, or absence, of discontinuities has a very important influence upon the stability of rock slopes and the detection of these geological features is one of the most critical parts of a stability investigation. Techniques for dealing with this problem are discussed in later chapters of this book.

Friction, cohesion and unit weight

The material properties which are most relevant to the discussion on slope stability presented in this book are the angle of



A planar discontinuity

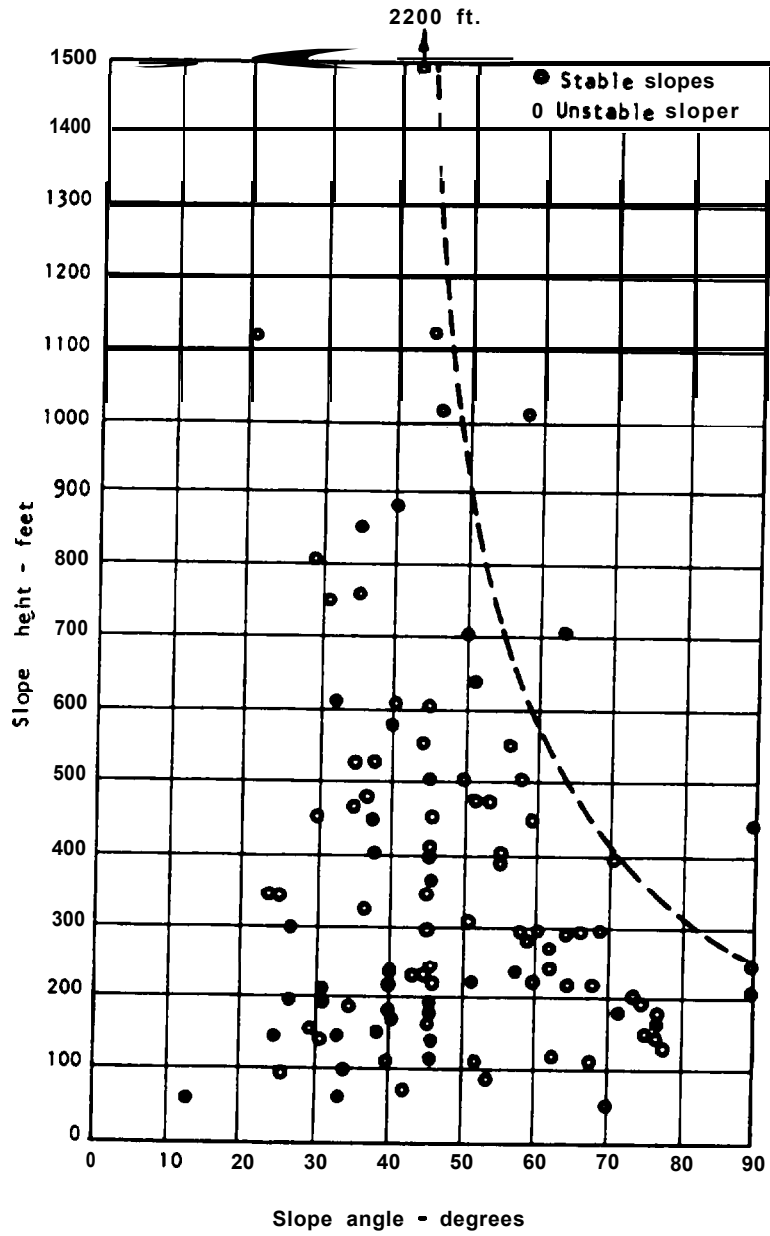
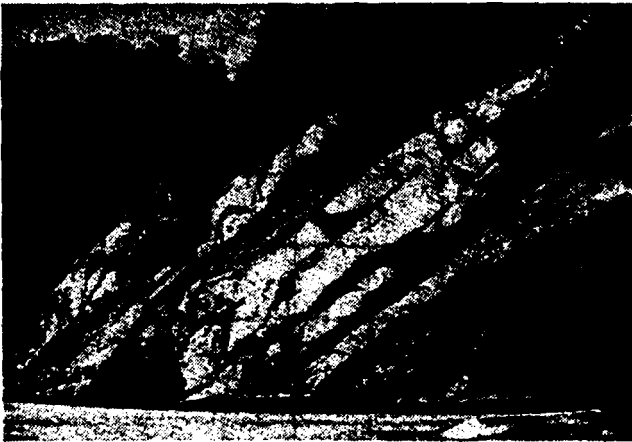


Figure 2. 1: Slope height versus slope angle relationships for hard rock slopes, including data collected by Kley and Lutton ²¹ and Ross-Brown ²².



Inclined planar discontinuities which daylight at the toe of a rock slope can cause instability when they are inclined at a steeper angle than the angle of friction of the rock surfaces

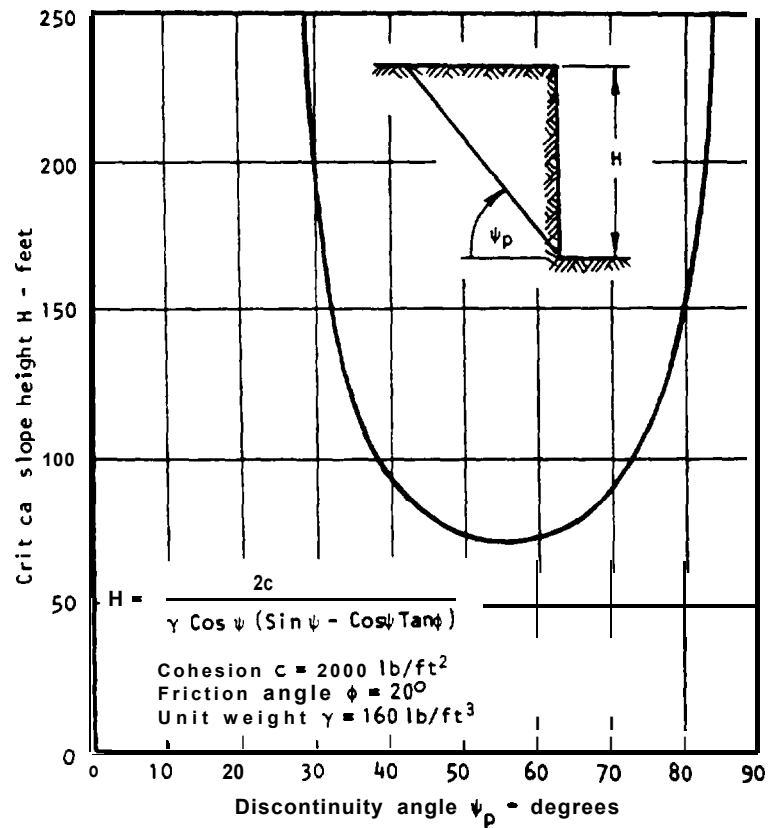


Figure 2.2: Critical height of a drained vertical slope containing a planar discontinuity dipping at an angle ψ_p .

friction, the cohesive strength and the unit weight of the rock and soil masses.

Friction and cohesion are best defined in terms of the plot of shear stress versus normal stress given in Figure 2.3. This plot is a simplified version of the results which would be obtained if a rock specimen containing a geological discontinuity such as a joint is subjected to a loading system which causes sliding along the discontinuity. The shear stress τ required to cause sliding increases with increasing normal stress σ . The slope of the line relating shear to normal stress defines the angle of friction ϕ . If the discontinuity surface is initially cemented or if it is rough, a finite value of shear stress τ will be required to cause sliding when the normal stress level is zero. This initial value of shear strength defines the cohesive strength c of the surface.

The relationship between shear and normal stresses for a typical rock surface or for a soil sample can be expressed as:

$$\tau = c + \sigma \tan \phi \quad (1)$$

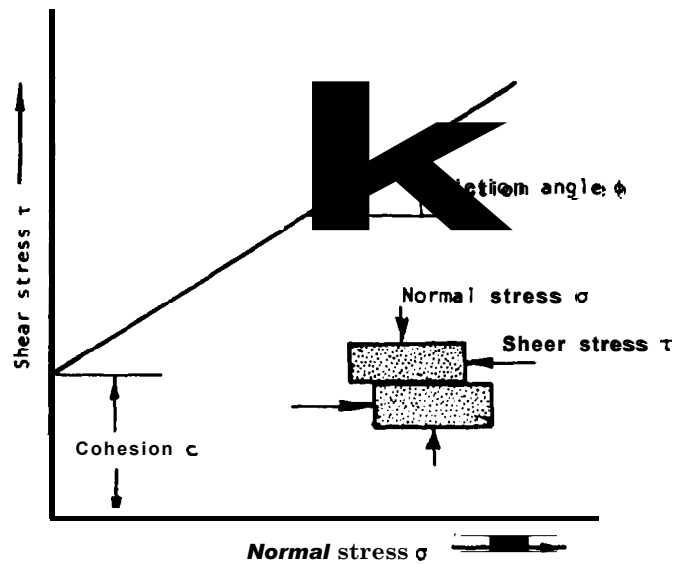


Figure 2.3: Relationship between the shear stress τ required to cause sliding along a discontinuity and the normal stress σ acting across it.

TABLE 1 - TYPICAL SOIL AND ROCK PROPERTIES							
Description		Unit weight (Saturated/dry)		Friction angle degrees	Cohesion		
Type	Material	lb/ft ³	kN/m ³		lb/ft ²	kPa	
Cohesionless	Sand	Loose sand, uniform grain size	118/90	19/14	28-34°		
		Dense sand, uniform grain size	130/109	21/17	32-40°		
		Loose sand, mixed grain size	124/99	20/16	34-40*		
		Dense sand, mixed grain size	135/116	21/18	38-46*		
	Gravel	Gravel, uniform grain size	140/130	22/20	34-37*		
		Sand and gravel, mixed grain size	120/110	19/17	48-45°		
	Blasted/broken rock	Basalt	140/110	22/17	40-50*		
		Chalk	80/62	13/10	30-40°		
		Granite	125/110	20/17	45-50°		
		Limestone	120/100	19/16	35-40*		
Sandstone		110/80	17/13	35-45*			
Shale		125/100	20/16	30-35°			
Cohesive	Clay	Soft bentonite	80/30	13/6	7-13	200-400	10-20
		Very soft organic clay	90/40	14/6	12-16	200-600	10-30
		Soft, slightly organic clay	100/60	16/10	22-27	400-1000	20-50
		Soft glacial clay	110/76	17/12	27-32	600-1500	30-70
		Stiff glacial clay	130/105	20/17	30-32	1500-3000	70-150
		Glacial till, mixed grain size	145/130	23/20	32-35	3000-5000	150-250
	Rock	Hard igneous rocks - granite, basalt, porphyry	160** to 190	25 to 30	35-45	720000- 1150000	35000- 55000
		Metamorphic rocks - quartzite, gneiss, slate	160 to 180	25 to 28	30-40	400000- 800000	20000- 40000
		Hard sedimentary rocks - limestone, dolomite, sandstone	150 to 180	23 to 28	35-45	200000- 600000	10000- 30000
		Soft sedimentary rock - sandstone, coal, chalk, shale	110 to 150	17 to 23	25-35	20000 - 400000	1000- 20000

* Higher friction angles in cohesionless materials occur at low confining or normal stresses as discussed in Chapter 5.

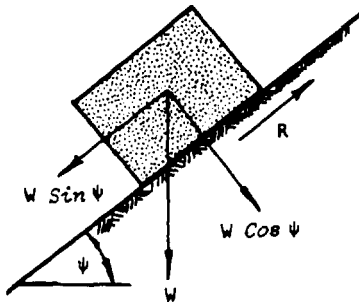
** For intact rock, the unit weight of the material does not vary significantly between saturated and dry states with the exception of materials such as porous sandstones.

Typical values for the angle of friction and cohesion which are found in shear tests on a range of rocks and soils are listed in Table 1 together with unit weights for these materials. The values quoted in this table are intended to give the reader some idea of the magnitudes which can be expected and they should only be used for obtaining preliminary estimates of the stability of a slope.

There are many factors which cause the shear strength of a rock or soil to deviate from the simple linear dependence upon normal stress illustrated in Figure 2.3. These variations, together with methods of shear testing, are discussed in Chapter 5.

Sliding due to gravitational loading

Consider a block of weight W resting on a plane surface which is inclined at an angle ψ to the horizontal. The block is acted upon by gravity only and hence the weight W acts vertically downwards as shown in the margin sketch. The resolved part of W which acts down the plane and which tends to cause the block to slide is $W \sin \psi$. The component of W which acts across the plane and which tends to stabilize the slope is $W \cos \psi$.



The normal stress σ which acts across the potential sliding surface is given by

$$\sigma = (W \cos \psi) / A \quad (2)$$

where A is the base area of the block.

Assuming that the shear strength of this surface is defined by equation (1) and substituting for the normal stress from equation (2)

$$\tau = c + \frac{W \cos \psi}{A} \cdot \tan \phi$$

$$\text{or } R = cA + W \cos \psi \cdot \tan \phi \quad (3)$$

where $R = \tau A$ is the shear force which resists sliding down the plane.

The block will be just on the point of sliding or in a condition of limiting equilibrium when the disturbing force acting down the plane is exactly equal to the resisting force:

$$W \sin \psi = cA + W \cos \psi \cdot \tan \phi \quad (4)$$

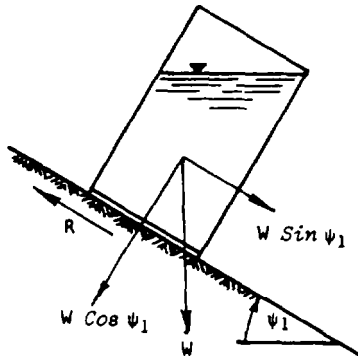
If the cohesion $c = 0$, the condition of limiting equilibrium defined by equation (4) simplifies to

$$\psi = \phi \quad (5)$$

Influence of water pressure on shear strength

The influence of water pressure upon the shear strength of two surfaces in contact can most effectively be demonstrated by the beer can experiment.

An opened beer can filled with water rests on an inclined piece of wood as shown in the margin sketch.



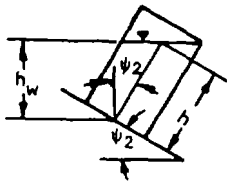
The forces which act in this case are precisely the same as those acting on the block of rock as shown in the diagram on the previous page. For simplicity the cohesion between the beer can base and the wood is assumed to be zero. According to equation (5) the can with its contents of water will slide down the plank when $\psi_1 = \phi$.

The base of the can is now punctured so that water can enter the gap between the base and the plank, giving rise to a water pressure u or to an uplift force $U = uA$, where A is the base area of the can.

The normal force $W \cos \psi_2$ is now reduced by this uplift force U and the resistance to sliding is now

$$R = (W \cos \psi_2 - U) \tan \phi \quad (6)$$

If the weight per unit volume of the can plus water is defined as γ_c while the weight per unit volume of the water is γ_w , then $W = \gamma_c \cdot h \cdot A$ and $U = \gamma_w \cdot h_w \cdot A$, where h and h_w are the heights defined in the small sketch. From this sketch it will be seen that $h_w = h \cdot \cos \psi_2$ and hence



$$U = \gamma_w / \gamma_c \cdot W \cos \psi_2 \quad (7)$$

Substituting in (6)

$$R = W \cos \psi_2 (1 - \gamma_w / \gamma_c) \tan \phi \quad (8)$$

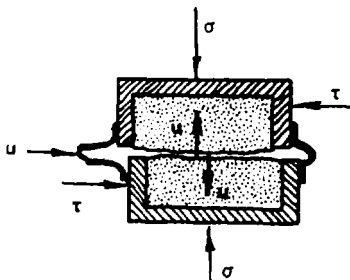
and the condition for limiting equilibrium defined in equation (4) becomes

$$\tan \psi_2 = (1 - \gamma_w / \gamma_c) \tan \phi \quad (9)$$

Assuming the friction angle of the can/wood interface is 30° , the unpunctured can will slide when the plane is inclined at $\psi_1 = 30^\circ$ (from equation (5)). On the other hand, the punctured can will slide at a much smaller inclination because the uplift force U has reduced the normal force and hence reduced the frictional resistance to sliding. The total weight of the can plus water is only slightly greater than the weight of the water. Assuming $\gamma_w / \gamma_c = 0.9$ and $\phi = 30^\circ$, equation (9) shows that the punctured can will slide when the plane is inclined at $\psi_2 = 3^\circ 18'$.

The effective stress law

The effect of water pressure on the base of the punctured beer can is the same as the influence of water pressure acting on the surfaces of a shear specimen as illustrated in the margin sketch. The normal stress σ acting across the failure surface is reduced to the effective stress $(\sigma - u)$ by the water pressure u . The relationship between shear strength and normal strength defined by equation (1) now becomes



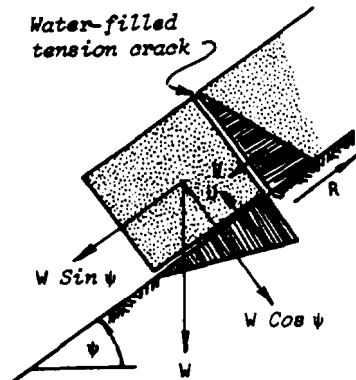
$$\tau = c + (\sigma - u) \tan \phi \quad (10)$$

In most hard rocks and in many sandy soils and gravels, the cohesive and frictional properties (c and ϕ) of the materials are not significantly altered by the presence of water and hence,

reduction in shear strength of these materials is due, almost entirely to the reduction of normal stress across failure surface. Consequently, it is water pressure rather than moisture content which is important in defining the strength characteristics of hard rocks, sands and gravels. In terms of the stability of slopes in these materials, the presence of a small volume of water at high pressure, trapped within the rock mass, is more important than a large volume of water discharging from a free draining aquifer.

In the case of soft rocks such as mudstones and shales and also in the case of clays, both cohesion and friction can change markedly with changes in moisture content and it is necessary, when testing these materials, to ensure that the moisture content of the material during test is as close as possible to that which exists in the field. Note that the effective stress law defined in equation (10) still applies to these materials but that, in addition, c and ϕ change.

The effect of water pressure in a tension crack



Consider the case of the block resting on the inclined plane but, in this instance, assume that the block is split by a tension crack which is filled with water. The water pressure in the tension crack increases linearly with depth and a total force V , due to this water pressure acting on the rear face of the block, acts down the inclined plane. Assuming that the water pressure is transmitted across the intersection of the tension crack and the base of the block, the water pressure distribution illustrated in the margin sketch occurs along the base of the block. This water pressure distribution results in an uplift force U which reduces the normal force acting across this surface.

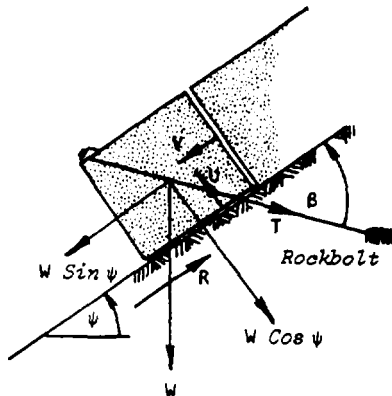
The condition of limiting equilibrium for this case of a block acted upon by water forces V and U in addition to its own weight W is defined by

$$W \sin \psi + V = cA + (W \cos \psi - U) \tan \phi \quad (11)$$

From this equation it will be seen that the disturbing force tending to induce sliding down the plane is increased and the frictional force resisting sliding is decreased and hence, both V and U result in decreases in stability. Although the water pressures involved are relatively small, these pressures act over large areas and hence the water forces can be very large. In many of the practical examples considered in later chapters, the presence of water in the slope giving rise to uplift forces and water forces in tension cracks is found to be critical in controlling the stability of slopes.

Reinforcement to prevent sliding

One of the most effective means of stabilizing blocks or slabs of rock which are likely to slide down inclined discontinuity surfaces is to install tensioned rock bolts or cables. Consider the block resting on the inclined plane and acted upon by the uplift force U and the force V due to water pressure in the tension crack. A rock bolt, tensioned to a load T is installed at an angle β to the plane as shown. The resolved component of the bolt tension T acting parallel to the plane is $T \cos \beta$



rock bolt installation to secure loose block.

Note: Other methods of slope stabilization are discussed in Chapter 12.

while the component acting across the surface upon which the block rests is $T \sin \beta$. The condition of limiting equilibrium for this case is defined by

$$W \sin \psi + V - T \cos \beta = cA + (W \cos \psi - U + T \sin \beta) \tan \phi \quad (12)$$

This equation shows that the bolt tension reduces the disturbing force acting down the plane and increases the normal force and hence the frictional resistance between the base of the block and the plane.

The minimum bolt tension required to stabilize the block is obtained by rearranging equation (12) to give an expression for the bolt tension T and then minimizing this expression with respect to the angle β , i.e. set $dT/d\beta = 0$, which gives

$$\beta = \phi \quad (13)$$

Factor of safety of a slope

All the equations defining the stability of a block on an inclined plane have been presented for the condition of limiting equilibrium, 1.0, the condition at which the forces tending to induce sliding are exactly balanced by those resisting sliding. In order to compare the stability of slopes under conditions other than those of limiting equilibrium, some form of Index is required and the most commonly used Index is the Factor of Safety. This can be defined as the ratio of the total force available to resist sliding to the total force tending to induce sliding. Considering the case of the block acted upon by water forces and stabilized by a tensioned rock bolt (see equation 12), the factor of safety is given by

$$F = \frac{cA + (W \cos \psi - U + T \sin \beta) \tan \phi}{W \sin \psi + V - T \cos \beta} \quad (14)$$

When the slope is on the point of failure, a condition of limiting equilibrium exists in which the resisting and disturbing forces are equal, as defined by equation (12), and the factor of safety $F = 1$. When the slope is stable, the resisting forces are greater than the disturbing forces and the value of the factor of safety will be greater than unity.

Suppose that, in a highway construction situation, the observed behavior of a slope suggests that it is on the point of failure and it is decided to attempt to stabilize the slope. Equation 14 shows that the value of the factor of safety can be increased by reducing both U and V , by drainage, or by increasing the value of T by installing rock bolts or tensioned cables. It is also possible to change the weight W of the falling mass but the influence of this change on the factor of safety must be carefully evaluated since both the disturbing and resisting forces are decreased by a decrease in W .

Practical experience suggests that, in a situation such as that described above, an increase in the factor of safety from 1.0 to 1.3 will generally be adequate for low slopes which are not required to remain stable for long periods of time. For critical slopes adjacent to major highways or important installations, a factor of safety of 1.5 is usually preferred.

This example has been quoted because it emphasizes the fact that the factor of safety is an index which is most valuable as a design tool when used on a comparative basis. In this case, the engineers and management have decided, on the basis of the observed behavior of the slope, that a condition of instability exists and that the value of the factor of safety is 1.0. If remedial measures are taken, their effect can be measured against the condition of slope failure by calculating the increase in the factor of safety. Hoek and Londe, in a general review of rock slope and foundation design methods (23), conclude that the information which is most useful to the design engineer is that which indicates the response of the structure to changes in significant parameters. Hence, decisions on remedial measures such as drainage can be based upon the rate of change of the factor of safety, even if the absolute value of the calculated factor of safety cannot be relied upon with a high degree of certainty. To quote from this general review: "The function of the design engineer is not to compute accurately but to judge soundly".

In carrying out a feasibility study for a proposed transportation or civil engineering project, the geotechnical engineer frequently is faced with the task of designing slopes where none have previously existed. In this case there is no background experience of slope behavior which can be used as a basis for comparison. The engineer may compute a factor of safety of 1.35 for a particular slope design, based upon the data available to him, but he has no idea whether this value represents an adequately stable slope since he has not had the opportunity of observing the behavior of actual slopes in this particular rock mass. Under these circumstances, the engineer is well advised to exercise caution in the choice of the parameters used in the factor of safety calculation. Conservatively low values of both cohesion and friction should be used and, if the groundwater conditions in the slope are unknown, the highest anticipated groundwater levels should be used in the calculation. Sensitivity analyses of the effects of drainage and rock bolting can still be carried out as in the previous case, but having chosen conservative rock strength parameters, the slope designer is unlikely to be faced with unpleasant surprises when the slope is excavated.

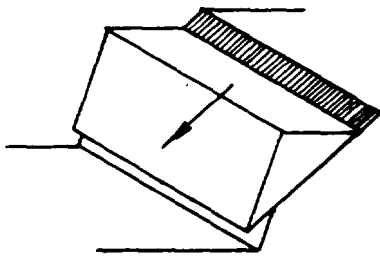
In later chapters of this book, a number of practical examples are given to illustrate the various types of rock slope design which are likely to be encountered by the reader. The problems of obtaining rock strength values, rock structure data and groundwater conditions for use in factor of safety calculations are discussed in these examples and guidance is given on the values of the factor of safety which is appropriate for each type of design.

Slope failures for which factors of safety can be calculated

In discussing the basic mechanism of slope failure, the model of a single block of rock sliding down an inclined plane has been used. This is the simplest possible model of rock slope failure and, in most practical cases, a more complex failure process has to be considered. In some cases, the methods of calculating the factor of safety, presented in this book, cannot be used because the failure process does not involve simple gravitational sliding. These cases will be discussed later in

this chapter. The method of limiting equilibrium can be used in analyzing the slope failures listed below.

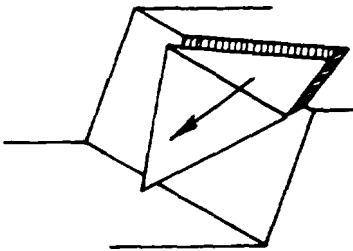
Plane failure



As shown in the margin sketch, plane failure occurs when a geological discontinuity, such as a bedding plane, strikes parallel to the slope face and dips into the excavation at an angle greater than the angle of friction. The calculation of the factor of safety follows precisely the same pattern as that used for the single block (equation 14). The base area A and the weight W of the sliding mass are calculated from the geometry of the slope and failure plane. A tension crack running parallel to the crest of the slope can also be included in the calculation.

A detailed discussion on the analysis of plane failure is given in Chapter 7.

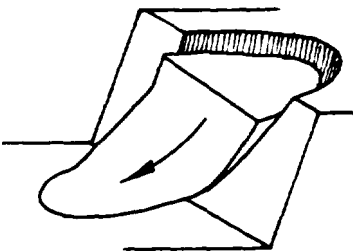
Wedge failure



When two discontinuities strike obliquely across the slope face and their line of intersection daylight in the slope face, the wedge of rock resting on these discontinuities will slide down the line of intersection, provided that the inclination of this line is significantly greater than the angle of friction. The calculation of the factor of safety is more complicated than that for plane failure since the base areas of both failure planes as well as the normal forces on these planes must be calculated.

The analysis of wedge failures is discussed in Chapter 8.

Circular failure

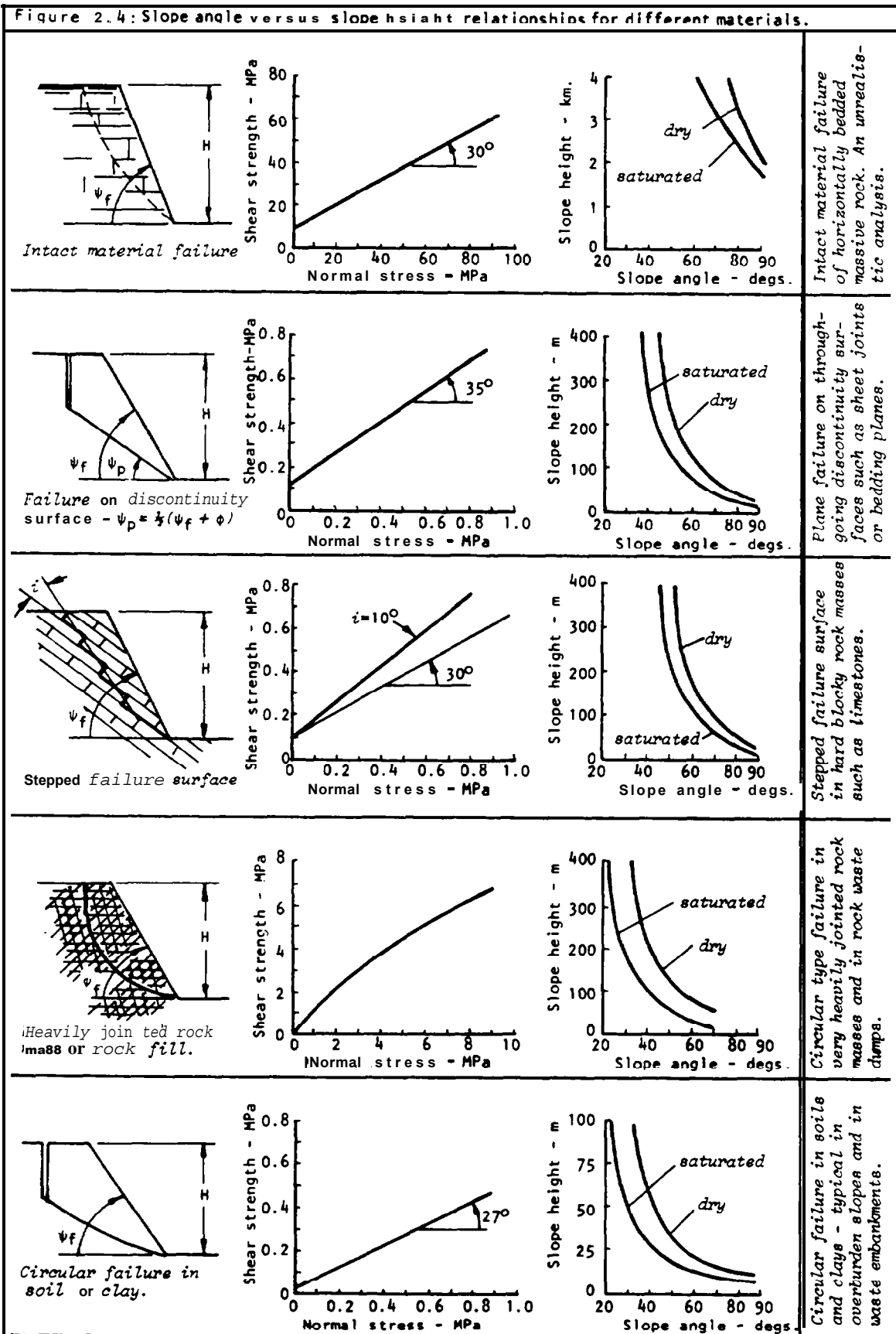


When the material is very weak, as in a soil slope, or when the rock mass is very heavily jointed or broken, as in a rock fill, the failure will not be defined by a single discontinuity surface but will tend to follow a circular failure path. This type of failure, illustrated in the margin sketch, has been treated in exhaustive detail in many standard soil mechanics textbooks and no useful purpose would be served by repetition of these detailed discussions in this book. A set of circular failure charts is presented in Chapter 9 and a number of worked examples are included in this chapter to show how the factor of safety can be calculated for simple cases of circular failure.

Critical slope height versus slope angle relationships

One of the most useful forms in which slope design data can be presented is a graph showing the relationship between slope heights and slope angles for failure, e.g. the dashed line in Figure 2.1. A number of typical slope failure cases have been analyzed and the relationships between critical slope heights and slope angles have been plotted in Figure 2.4. This figure is intended to give the reader an overall appreciation for the type of relationship which exists for various materials and for the role which groundwater plays in slope stability. The reader should not attempt to use this figure as a basis for the design of a particular slope since the conditions may differ from those assumed in deriving the results presented in Figure

Figure 2.4: Slope angle versus slope height relationships for different materials.



2.4. Individual slopes should be analyzed using the methods described in Chapters 7, 8 and 9.

Slopes for which a factor of safety cannot be calculated

The failure modes which have been discussed so far have all involved the movement of a mass of material upon a failure surface. An analysis of failure or a calculation of the factor of safety for these slopes requires that the shear strength of the failure surface (defined by c and ϕ) be known. There are also a few types of slope failure which cannot be analyzed by the methods already described, even if the strength parameters of the material are known, since failure does not involve simple sliding. These cases are discussed on the following pages.

Toppling failure

Consider, once again, a block of rock resting on an inclined plane as shown in Figure 2.5a. In this case, the dimensions of the block are defined by a height h and a base length b and it is assumed that the force resisting downward movement of the block is due to friction only, i.e. $c = 0$.

When the vector representing the weight W of the block falls within the base b , sliding of the block will occur if the inclination of the plane ψ is greater than the angle of friction ϕ . However, when the block is tall and slender ($h > b$), the weight vector W can fall outside the base b and, when this happens, the block will topple i.e. it will rotate about its lowest contact edge.

The conditions for sliding and/or toppling of this single block are defined in Figure 2.5b. The four regions in this diagram are defined as follows:

- Region 1: $\psi < \phi$ and $b/h > \tan \psi$, the block is stable and will neither slide nor topple.
- Region 2: $\psi > \phi$ and $b/h > \tan \psi$, the block will slide but it will not topple.
- Region 3: $\psi < \phi$ and $b/h < \tan \psi$, the block will topple but it will not slide.
- Region 4: $\psi > \phi$ and $b/h < \tan \psi$ the block can slide and topple simultaneously.

In analyzing the stability of this block, the methods of limiting equilibrium can be used for regions 1 and 2 only. Failure involving toppling, i.e. regions 3 and 4 to the right of the curve in Figure 2.5b, cannot be analyzed in this same way. Methods for dealing with toppling failure in slopes are discussed in Chapter 10.

Raveling slopes

Travelers in mountain regions will be familiar with the accumulations of scree which occur at the base of steep slopes. These scree are generally small pieces of rock which have become detached from the rock mass and which have fallen as individual pieces into the accumulated pile. The cyclic expansion and contraction associated with the freezing and thawing of water in cracks and fissures in the rock mass is one of the principal causes of slope raveling but a gradual deterioration



Toppling failure in a slate quarry.

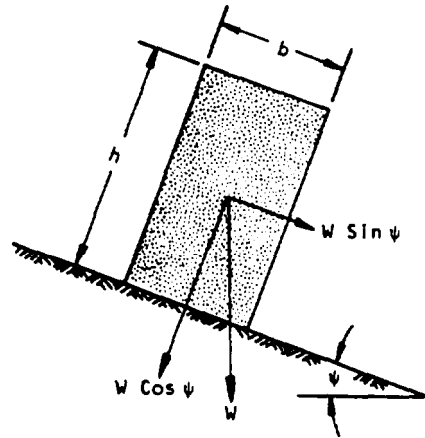


Figure 2.5a: Geometry of block on inclined plane.

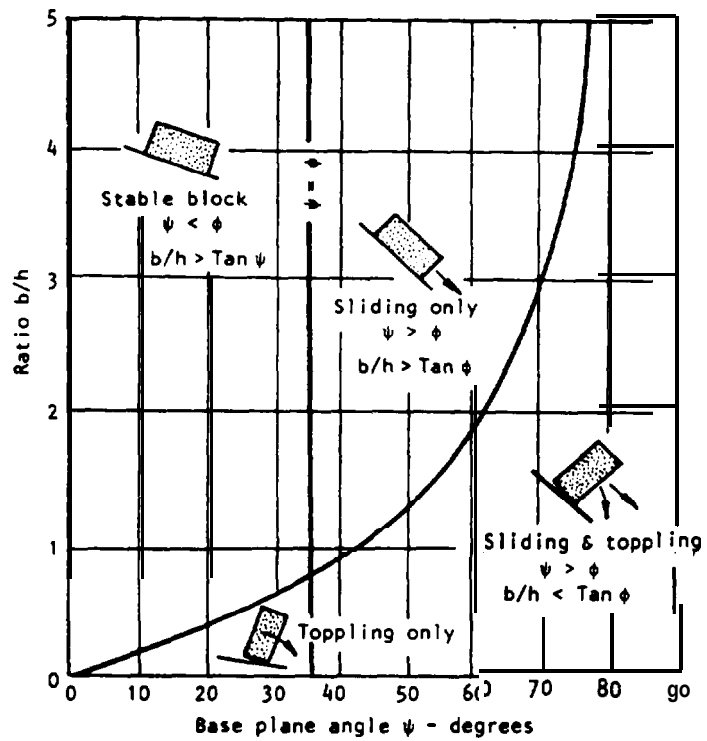
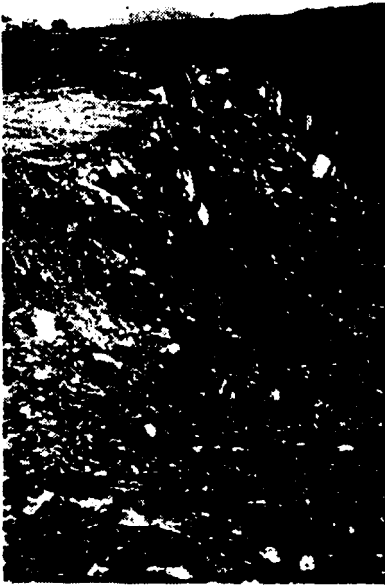


Figure 2.5b: Conditions for sliding and toppling of a block on an inclined plane.



Ravelling of the weathered surface material in a slope.



Slumping of columns in vertically jointed dolerite as a result of weathering in an underlying shale layer.

of the materials which cement the individual blocks together may also play a part in this type of slope failure.

Weathering, or the deterioration of certain types of rock on exposure, will give rise also to a loosening of a rock mass and the gradual accumulation of materials on the surface and at the base of the slope. Some of the engineering implications of weathering have been reviewed by Goodman(24) who gives a selection of useful references on the subject(25-30).

Few serious attempts have been made to analyze the process of slope failure by raveling since the fall of small individual pieces of rock does not constitute a serious hazard. When the stability of an accumulation of scree or of weathered material is likely to be altered by the excavation of a slope in this material, the stability of the excavation can be assessed by one of the methods described in Chapters 7, 8 and 9. Generally, the method of circular failure analysis, described in Chapter 9, would be used unless the size of the excavation is such that it is likely to cut back into the undisturbed rock mass.

It is important that the slope designer should recognize the influence of weathering on the nature of the materials with which he is concerned and this subject will be discussed in greater detail in Chapter 7.

Probabilistic approach to slope design

Probability theory has two distinct roles in the design of rock slopes:

- a. In the analysis of populations or families of structural discontinuities to determine whether there are dominant or preferred orientations within the rock mass.
- b. As a replacement for the factor of safety as an index of slope stability (or instability).

The first role is discussed in Chapter 3 which deals with the graphical presentation of geological data. The second role, that in which probability of failure replaces factor of safety as an index of slope stability, has been strongly advocated by McMahon(31) and has been utilized by a number of other authors(32-35).

It should clearly be understood that the use of probability theory in this latter role does not influence the other steps in a stability investigation. The collection of geological data follows the same basic pattern as that described in this book. The mechanics of failure are treated in the same way and the same limitations apply to the types of failure which can be analyzed. Probability theory does not, at present, offer any particular advantages in the analysis of toppling, raveling or buckling type failures.

The authors of this book have chosen to present all the detailed discussions on stability analysis in terms of the factor of safety. This decision has been made because it is believed that the discussion is less confusing for the non-specialist reader for whom this book is intended. The reader who feels that he has understood the basic principles of slope analysis is strongly recommended to examine the literature on the use of

probability theory to determine for himself whether he wishes to replace the factor of safety index by the probability of failure.

Chapter 2 references

11. BLAKE, W. Stresses and displacements surrounding an open pit in a gravity, loaded rock. *U.S. Bureau of Mines Report of Investigations* 7002, Aug. 1967, 20 pages.
12. BLAKE, W. Finite element model is excellent pit tool. *Mining Engineering, A.I.M.E.*, Vol. 21, No. 8. 1969, pages 79-80.
13. YU, Y.S., GYENGE, M. and COATES, O.F. Comparison of stress and displacement in a gravity loaded slope by photoelasticity and finite element analysis. *Canadian Dept. Energy, Mines and Resources Report MR 68-24 IO*. 1968.
14. WANG, F.O. and SUN, M.C. Slope stability analysis by finite element stress analysis and limiting equilibrium method. *U.S. Bureau of Mines Report of Investigations* 7341, January 1970. 16 pages.
15. STACEY, T.R. The stresses surrounding open-pit mine slopes. *Planning open pit mines*. Johannesburg Symposium, 1970. Published by A.A. Balkema, Amsterdam, 1971, pages 199-207.
16. HOEK, E. The influence of structure upon the stability of rock slopes. *Proc. 1st Symposium on Stability in Open Pit Mining*, Vancouver, 1970. Published by A.I.M.E. New York, 1971, pages 49-63.
17. TERZAGHI, K. Stability of steep slopes in hard unweathered rock. *Geotechnique*. Vol. 12, 1962, pages 251-270.
18. HULLER, L. The European approach to slope stability problems in open pit mines. *Proc. 3rd Symposium on Rock Mechanics. Colorado School of Mines Quarterly*, Vol. 54, No. 3, 1959, pages 116-133.
19. GOODMAN, R.E., TAYLOR, R.L. and BREKKE, T.L. A model for the mechanics of jointed rock. *A.S.C.E. Proceedings, J. Soil Mech. Foundation Div.* vol. 94, No. SM3, 1968, pages 637-659.
20. CUNOALL, P.A. A computer model for simulating progressive large-scale movements in blocky rock systems. *Symposium on Rock Fracture, Nancy, France*. October 1971, Section 2-8.
21. KLEY, R.J. and LUTTON, R.J. Engineering properties of nuclear craters : a study of selected rock excavations as related to large nuclear craters. *Report U.S. Army Engineers*, No. PNE 5010. 1967, 159 pages.
22. ROSS-BROWN, O.R. Slope design in opencast mines. *Ph. D Thesis*, Imperial College, London University, 1973, 250 pages.
23. HOEK, E. and LONDE, P. Surface workings in rock. *Advances in Rock Mechanics. Proc. 3rd Congress of the International Society for Rock Mechanics*, Denver, 1974. Published by National Academy of Sciences, Washington, D.C., 1974, Vol. 1A, pages 612-654.

24. GOOCHAN, R.E. Methods of *geological* engineering in *discontinuous rocks*. West Publishing Co., St Paul, Minnesota, 1976, 472 pages.
25. RUXTON, B.P. and BERRY, L. Weathering of granite and associated erosional features in Hong Kong, Bulletin *Geological Society of America*, Vol. 68. 1957, page 1263.
26. DEERE, D.U. and PATTON, F.D. Slope stability in residual soils, *Proc. 4th Pan American Conference on Soil Mechanics and Foundation Engineering*, San Juan, Puerto Rico, Vol. 1, 1971. pages 87-170
27. FOOKES, P.C. and HORSWILL, P. Discussion of engineering grade zones. *Proc. Conference on In-situ testing of Soils and Rock*, Institution of Civil Engineers, London, 1970, page 53.
28. SAUNDERS, H.K. and FOOKES. P.G. A review of the relationship of rock weathering and climate and its significance to foundation engineering. *Engineering Geology*, Vol. 4, 1970, pages 289-325.
29. DEERE, D.U., MERRITT, A.H and COON, R.F. Engineering classification of in situ rock. *Technical Report No. AFWL-67-144*, Air Force Systems Command, Kirtland Air Force Base, New Mexico. 1969.
30. SPEARS, D.A. and TAYLOR, R.K. The influence of weathering on the composition and engineering properties on in-situ coal measure rocks. *international Journal of Rock Mechanics and Mining Sciences*, Vol. 9, 1972. page 729-756.
31. McMAHON, B.K. A statistical method for the design of rock slopes. *Proc. First Australia-New Zealand Conference on Geomechanics*. Melbourne, 1971. Vol.1, pages 314-321.
32. McMAHON, B.K. Design of rock slopes against sliding on pre-existing fractures. *Advances in Rock Mechanics*, Proc. 3rd Congress of the International Society for Rock Mechanics, Denver 1974. Published by National Academy of Sciences, Washington D.C., 1974, Vol 118, page 803-808.
33. SHUK. T. Optimisation of slopes designed in rock. *Proc. 2nd Congress of the International Society for Rock Mechanics*, Belgrade, 1970. Vol. 3. Sect. 7-2.
34. LANCEJAN, A. Some aspects of safety factors in soil mechanics considered as a problem of probability. *Proc. 6th International Conference on Soil Mechanics and Foundation Engineering*, Montreal, 1965, Vol. 2. page 500- 502.
35. SERRANO, A.A. and CASTILLO, E. A new concept about the stability of rock masses. *Advances in Rock Mechanics*, Proc. 3rd Congress of the International Society for Rock Mechanics. Denver, 1974. Published by National Academy of Sciences, Washington D.C., 1974, Vol. 118, page 820-826.

Chapter 3 Graphical presentation of geological data.

Introduction

The dominant role of geological discontinuities in rock slope behavior has been emphasized already and few engineers or geologists would question the need to base stability calculations upon an adequate set of geological data. But what is an adequate set of data? What type of data and how much detailed information should be collected for a stability analysis?

This question is rather like the question of which came first - the chicken or the egg? There is little point in collecting data for slopes which are not critical but critical slopes can only be defined if sufficient information is available for their stability to be evaluated. The data gathering must, therefore, be carried out in two stages as suggested in Figure 1.5.

The first stage involves an examination of existing regional geology maps, air photographs, easily accessible outcrops and any core available from site investigations. A preliminary analysis of this data will indicate slopes which are likely to prove critical and which require more detailed analysis.

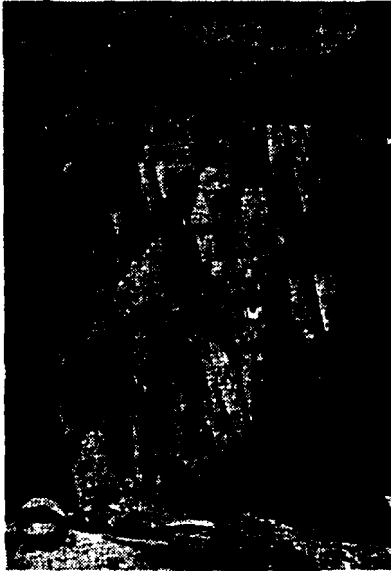
The second stage involves a much more detailed examination of the geological features of these critical regions and may require the drilling of special holes along the right-of-way, excavation of test pits and the detailed mapping and testing of discontinuities.

An important aspect of the geological investigations, in either the first or second stages, is the presentation of the data in a form which can be understood and interpreted by others who may be involved in the stability analysis or who may be brought in to check the results of such an analysis. This means that everyone concerned must be aware of precisely what is meant by the geological terms used and must understand the system of data presentation.

The following definitions and graphical techniques are offered for the guidance of the reader who may not already be familiar with them. There is no implication that these are the best definitions or techniques available and the reader who has become familiar with different methods should certainly continue to use those. What is important is that the techniques which are used in any study should be clearly defined in documents relating to that study so that errors arising out of confusion are avoided.

Definition of geological terms

Rock material or intact rock, in the context of this discussion, refers to the consolidated and cemented assemblage of mineral particles which form the intact blocks between discontinuities in the rock mass. In most hard igneous and metamorphic rocks, the strength of the intact rock is one or two orders of magnitude greater than that of the rock mass and failure of this intact material is not involved generally in the processes of slope failure. In softer sedimentary rocks, the intact material may be relatively weak and failure of this material may play an important part in slope failure.



An ordered structural pattern in slate.



An apparently disordered discontinuity pattern in a hard rock slope.

Rock mass is the in situ rock which has been rendered discontinuous by systems of structural features such as joints, faults and bedding planes. Slope failure in a rock mass is generally associated with movement of these discontinuity surfaces.

Waste rock or broken rock refers to a rock mass which has been disturbed by some mechanical agency such as blasting, ripping or crushing so that the interlocking nature of the in situ rock has been destroyed. The behavior of this waste or broken rock is similar to that of a clean sand or gravel, the major differences being due to the angularity of the rock fragments.

Discontinuities or weakness planes are those structural features which separate intact rock blocks within a rock mass. Many engineers describe these features collectively as joints but this is an over-simplification since the mechanical properties of these features will vary according to the process of their formation. Hence, faults, dykes, bedding planes, cleavage, tension joints and shear joints all will exhibit distinct characteristics and will respond in different ways to applied loads. A large body of literature dealing with this subject is available and the interested reader is referred to this for further information (36,37,38). For the purposes of this discussion, the term discontinuity will generally be used to define the structural weakness plane upon which movement can take place. The type of discontinuity will be referred to when the description provides information which assists the slope designer in deciding upon the mechanical properties which will be associated with a particular discontinuity.

Major discontinuities are continuous planar structural features such as faults which may be so weak, as compared with any other discontinuity in the rock mass, that they dominate the behavior of a particular slope. Many of the large failures which have occurred on transportation routes have been associated with faults and particular attention should be paid to tracing these features.

Discontinuity sets refers to systems of discontinuities which have approximately the same inclination and orientation. As a result of the processes involved in their formation (36), most discontinuities occur in families which have preferred directions. In some cases, these sets are clearly defined and easy to distinguish while, in other cases, the structural pattern appears disordered.

Continuity. While major structural features such as faults may run for many tens of feet or even miles, smaller discontinuities such as joints may be very limited in their extent. Failure in a system where discontinuities terminate within the rock mass under consideration will involve failure of the intact rock bridges between these discontinuities. Continuity also has a major influence upon the permeability of a rock mass since this depends upon the extent to which discontinuities are hydraulically connected.

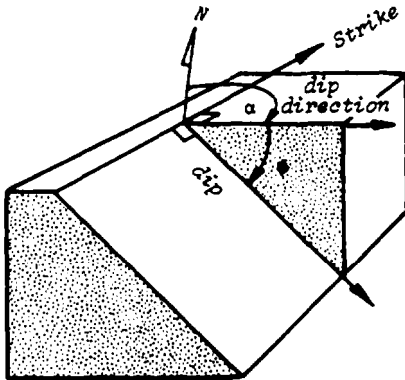
Gouge or infilling is the material between two faces of a structural discontinuity such as a fault. This material may be the debris resulting from the sliding of one surface upon another or it may be material which has been precipitated from solution or caused by weathering. Whatever the origin of the

infilling material in a discontinuity, its presence will have an important influence upon the shear strength of that discontinuity. If the thickness of the gouge is such that the faces of the discontinuity do not come into contact, the shear strength will be equal to the shear strength of the gouge. If the gouge layer is thin so that contact between asperities on the rock surfaces can occur, it will modify the shear strength of the discontinuity but will not control it (39).

Roughness. Patton (40,41) emphasized the importance of surface roughness on the shear strength of structural discontinuities in rock. This roughness occurs on both a small scale, involving grain boundaries and failure surfaces, and on a large scale, involving folds and flexures in the discontinuity. The mechanics of movement on rough surfaces will be discussed in the chapter dealing with shear strength.

Definition of geometrical terms

Dip is the maximum inclination of a structural discontinuity plane to the horizontal, defined by the angle α in the margin sketch. It is sometimes very difficult, when examining an exposed portion of an obliquely inclined plane, to visualize the true dip as opposed to the apparent dip which is the inclination of an arbitrary line on the plane. The apparent dip is always smaller than the true dip. One of the simplest models which can be used in visualizing the dip of a plane is to consider a ball rolling down an obliquely inclined plane. The path of the ball will always lie along the line of maximum inclination which corresponds to the true dip of the plane.



Definition of geometrical terms

Dip direction or dip azimuth is the direction of the horizontal trace of the line of dip, measured clockwise from north as indicated by the angle α in the margin sketch.

Strike is the trace of the intersection of an obliquely inclined plane with a horizontal reference plane and it is at right angles to the dip and dip direction of the oblique plane. The practical importance of the strike of a plane is that it is the visible trace of a discontinuity which is seen on the horizontal surface of a rock mass. In using strike and dip to define a plane for rock slope analysis, it is essential that the direction in which the plane dips is specified. Hence, one may define a plane as having a strike of N 45 E (or 045°) and a dip of 60° SE. Note that a plane dipping 60° NW could also have a strike of N 45 E.

Throughout this book, planes will be defined by their dip and dip direction. This convention has been chosen to avoid any possible confusion and to facilitate computation of slope geometries in later chapters. The same convention has been adopted by some geotechnical consulting organizations for stability computer programs. However, geologists are free to use strike and dip measurements for recording their field observations, if this is the convention preferred by them, and a supplementary program is used to transform these measurements into dips and dip directions before they are used as input in the slope stability programs.

Plunge is the dip of a line, such as the line of intersection of two planes or the axis of a borehole or a tunnel.

Trend is the direction of the horizontal projection of a line, measured clockwise from north. Hence, it corresponds to the dip direction of a plane.

In recording dip and dip direction data, many geologists use the system in which these quantities are written 35/085. Since the dip of a plane must lie between 0° and 90° , the angle defined by 35 refers to the dip. Similarly, the angle 085 refers to the dip direction which lies between 0° and 360° . The same convention can be used to define the plunge and trend of a line in space. The reader is encouraged to adopt this convention as it will help to eliminate recording errors in the field since, even if a figure is entered into an incorrect column, it will be clear that a two digit number refers to dip and a three digit number refers to dip direction.

Graphical techniques for data presentation

One of the most important aspects of rock slope analysis is the systematic collection and presentation of geological data in such a way that it can easily be evaluated and incorporated into stability analyses. Experience has shown that spherical projections provide a convenient means for the presentation of geological data. The engineer or geologist, who is not familiar with this technique, is strongly advised to study the following pages carefully. A few hours invested in such study can save many hours of frustration and confusion later when the reader becomes involved in studying designs and reading reports in which these methods have been used.

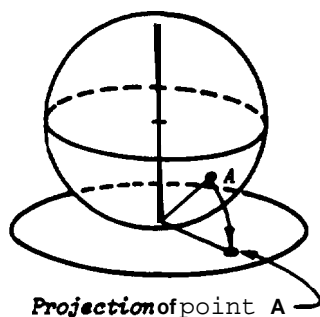
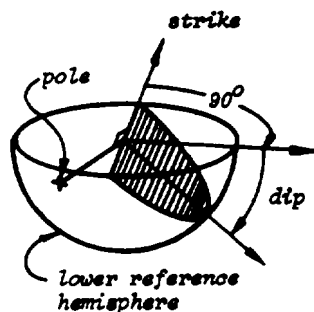
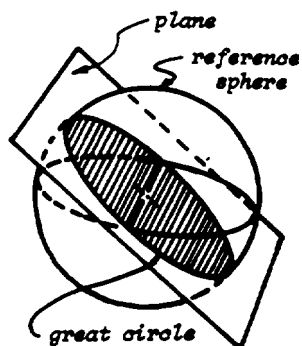
Many engineers shy away from spherical projection methods because they are unfamiliar and because they appear complex, bearing no recognizable relationship to more conventional engineering drawing methods. For many years the authors regarded these graphical methods in the same light but, faced with the need to analyze three-dimensional rock slope problems, an effort was made with the aid of a patient geologist colleague, and the mystery associated with these techniques was rapidly dispelled. This effort has since been repaid many times by the power and flexibility which these graphical methods provide for the rock engineer.

Several types of spherical projection can be used and a comprehensive discussion on these methods has been given by Phillips(42), Turner and Weiss(38), Badgley(43), Friedman(44) and Ragan(45). The projection which is used exclusively in this book is the equal area projection, sometimes called the Lambert projection or the Schmidt net.

The equal angle or stereographic projection offers certain advantages, particularly when used for geometrical construction, and is preferred by many authors. Apart from the techniques used in contouring pole populations, to be described later in this chapter, the constructions carried out on the two types of net are identical and the reader will have no difficulty in adapting the techniques, which he has learned using equal area projections, to analyses using stereographic projections.

Equal-area projection

The Lambert equal area projection will be familiar to most readers as the system used by geographers to represent the spheri-



cal shape of the sphere on a flat surface. In adapting this projection to structural geology, the traces of planes on the surface of a reference sphere are used to define the dips and dip directions of the planes. Imagine a reference sphere which is free to move in space but which is not free to rotate in any direction; hence any radial line joining a point on the surface to the center of the sphere will have a fixed direction in space. If this sphere is now moved so that its center lies on the plane under consideration, the great circle which is traced out by the intersection of the plane and the sphere will define uniquely the inclination and orientation of the plane in space. Since the same information is given on both upper and lower parts of the sphere, only one of these need be used and, in engineering applications, the lower reference hemisphere is used for the presentation of data.

In addition to the great circle, the inclination and orientation of the plane can also be defined by the pole of the plane. The pole is the point at which the surface of the sphere is pierced by the radial line which is normal to the plane.

In order to communicate the information given by the great circle and the position of the pole on the surface of the lower reference hemisphere, a two dimensional representation is obtained by projecting this information onto the horizontal or equatorial reference plane. The method of projection is illustrated in Figure 3.1. Polar and equatorial projections of a sphere are shown in Figure 3.2.

Polar and equatorial equal-area nets are presented on pages 3.7 and 3.8 for use by the reader. Good undistorted copies or photographs of these nets will be useful in following the examples given in this chapter and later in the book.

The most practical method of using the stereonet for plotting structural information is to mount it on a baseboard of 1/4 inch thick plywood as shown in Figure 3.3. A sheet of clear plastic film of the type used for drawing on for overhead projection, mounted over the net and fixed with transparent adhesive tape around its edges, will keep the stereonet in place and will also protect the net markings from damage in use. The structural data is plotted on a piece of tracing paper or film which is fixed in position over the stereonet by means of a carefully centered pin as shown. The tracing paper must be free to rotate about this pin end it is essential that it is located accurately at the center of the net otherwise significant errors will be introduced into the subsequent analysis.

Before starting any analysis, the North point must be marked on the tracing so that a reference position is available.

Figure 3.1: Method of construction of an equal-area projection.

Figure 3.2: Polar and equatorial projections of a sphere.

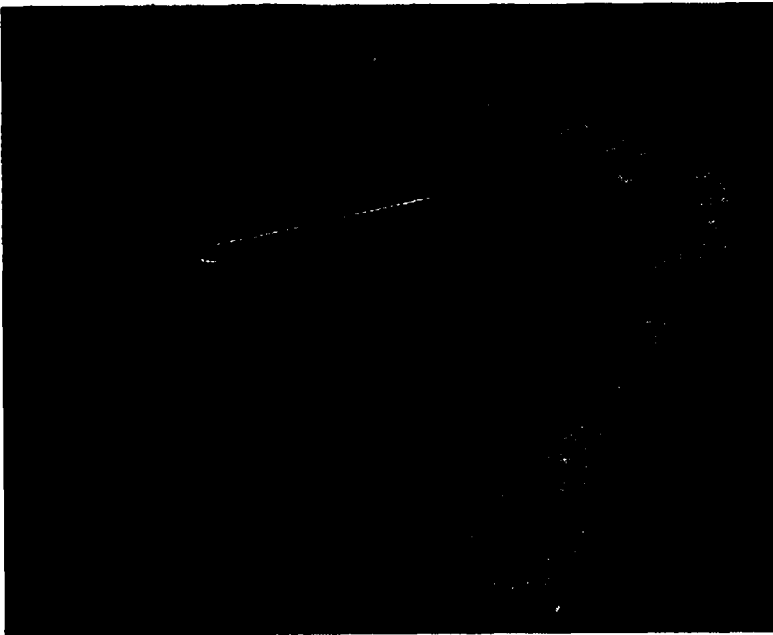
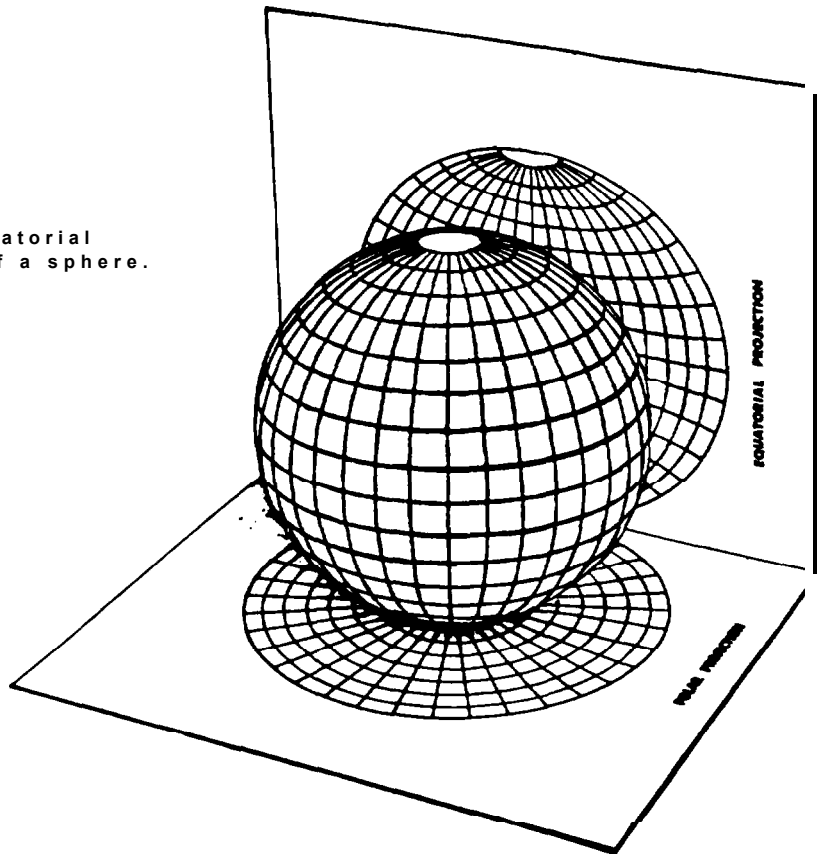
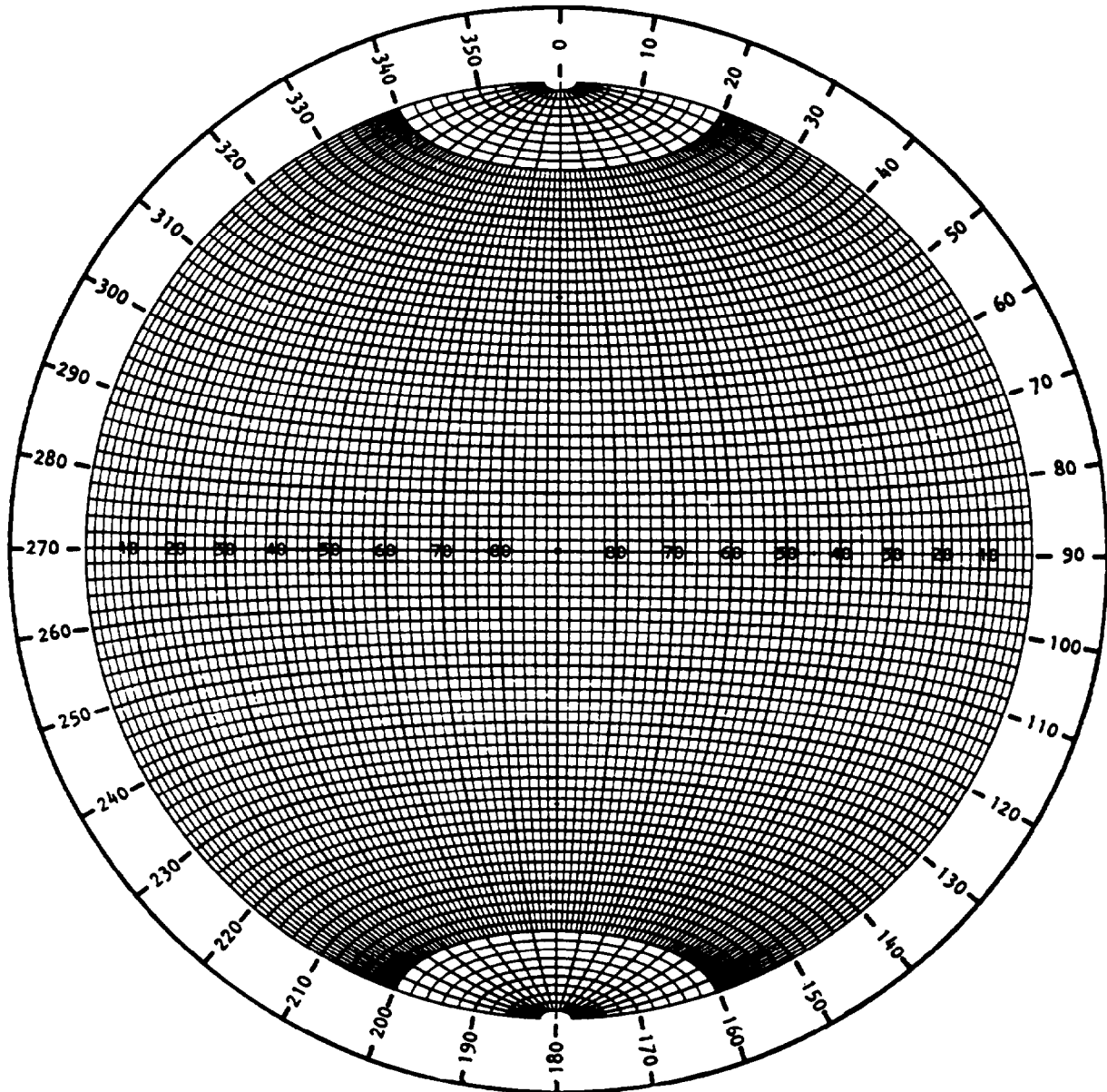


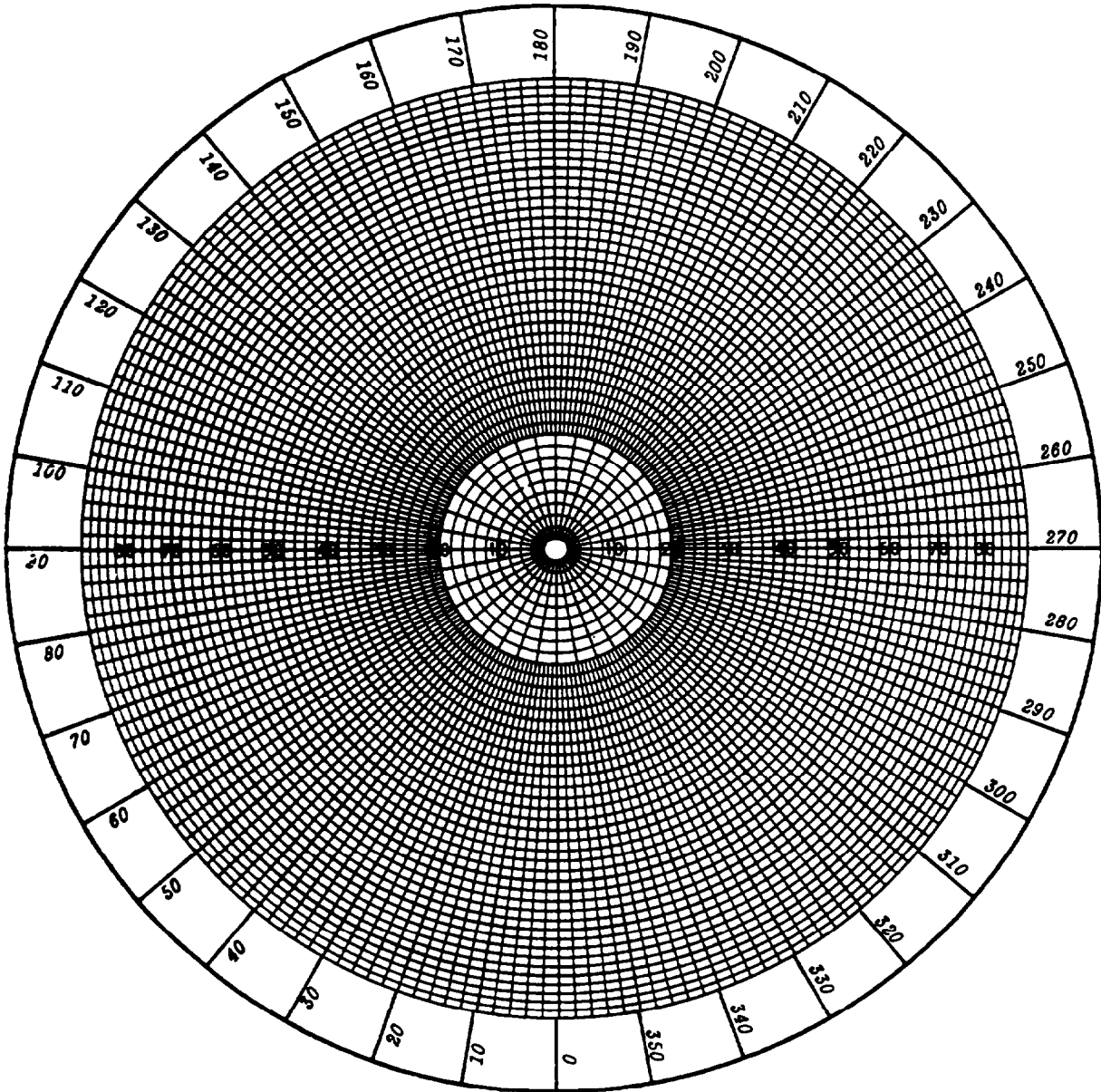
Figure 3.3: Geological data is plotted and analysed on a piece of tracing paper which is located over the centre of the stereonet by means of a centre pin as shown. The net is mounted on a base-board of plywood or similar material.



Equatorial equal-area stereonet marked in 2° intervals

Note: This stereonet is configured for the plotting of great circles of planes.

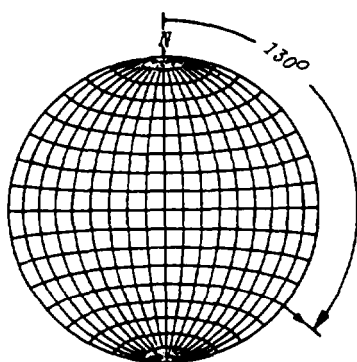
Computer drawn by Dr. C. M. St John of the Royal School of Mines, Imperial College, London.



Polar • equal-area stereonet marked in 2° interval

Note: This stereonet is configured for the direct plotting of poles of planes • xpressed in the dip/dip direction format.

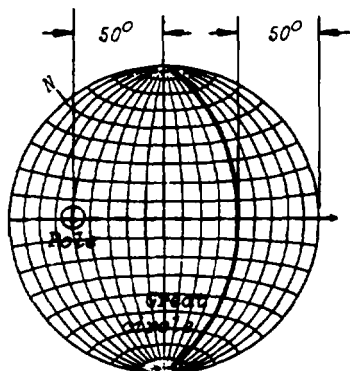
Computer drawn by Dr. C. M. St John of the Royal School of Mines, Imperial College, London.



Construction of a great circle and a pole representing a plane.

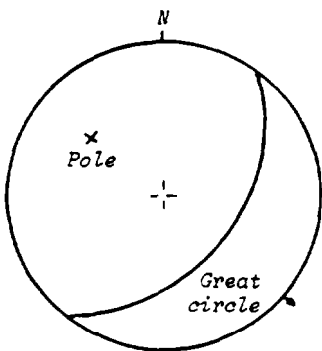
Consider a plane dipping at 50° in a dip direction of 130° . The great circle and the pole representing this plane are constructed as follows:

step 1: With the tracing paper located over the stereonet by means of the center pin, trace the circumference of the net and mark the north point. Measure off the dip direction of 130° clockwise from north and mark this position on the circumference of the net.

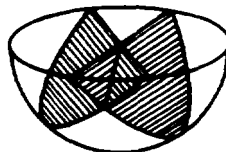


step 2: Rotate the tracing about the center pin until the dip direction mark lies on the W-E axis of the net, i.e. the tracing is rotated through 40° . Measure 50° from the outer circle of the net and trace the great circle which corresponds to a plane dipping at this angle.

The position of the pole, which has a dip of $(90^\circ - 50^\circ)$, is found by measuring 50° from the center of the net as shown or, alternatively, 40° from the outside of the net. The pole lies on the projection of the dip direction line which, at this stage in the construction, is coincident with the W-E axis of the net.



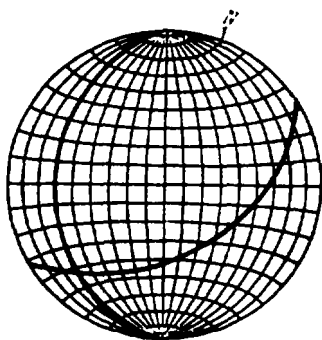
step 3: The tracing is now rotated back to its original position so that the north mark on the tracing coincides with the north mark on the net. The final appearance of the great circle and the pole representing a plane dipping at 50° in a dip direction of 130° is as illustrated.



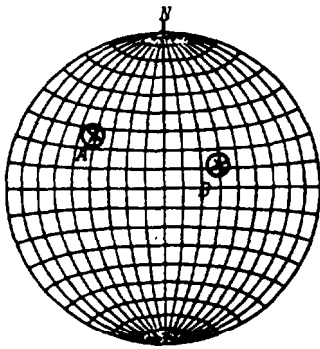
Determination of the line of intersection of two planes.

Two planes, having dips of 50° and 30° and dip directions of 130° and 250° respectively, intersect. It is required to find the plunge and the trend of the line of intersection.

Step 1: One of these planes has already been described above and the great circle defining the second plane is obtained by marking the 250° dip direction on the circumference of the net, rotating the tracing until this mark lies on the U-E axis and tracing the great circle corresponding to a dip of 30° .

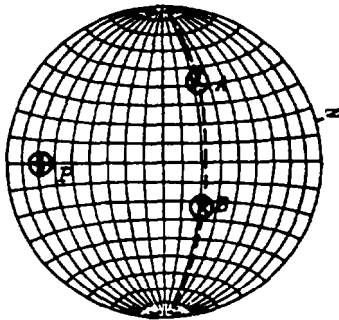






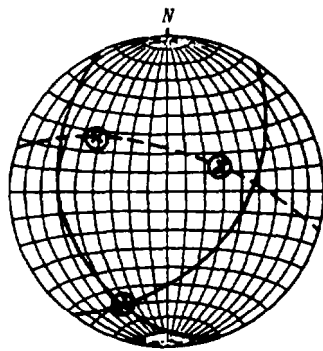
Alternative method for finding the line of intersection of two planes.

Two planes, dipping at 50° and 30° in dip directions of 130° and 250° respectively are defined by their poles A and B as shown. The line of intersection of those two planes is defined as follows:



step 1: Rotate the tracing until both poles lie on the same great circle. This great circle defines the plane which contains the two normals to the planes.

step 2: Find the pole of this plane by measuring the dip on the U-E of the stereonet. This pole P defines the normal to the plane containing A and B and, since this normal is common to both planes, it is, in fact, the line of intersection of the two planes.



Hence, the pole of a plane which passes through the poles of two other planes defines the line of intersection of those planes.

Plotting and analysis of field measurements

In plotting field measurements of dip and dip direction, it is convenient to work with poles rather than great circles since the poles can be plotted directly on a polar stereonet such as that given on Page 3.8. Suppose that a plane has dip direction and dip values of $050/60$, the pole is located on the stereonet by using the dip direction value of 50 given in italics and then measuring the dip value of 60 from the center of the net along the radial line. Note that no rotation of the tracing paper, centered over the stereonet, is required for this operation and, with a little practice, the plotting can be carried out very quickly.

There is a temptation to plot the compass readings directly onto the polar stereonet, without the intermediate step of entering the measurements into a field notebook, but the authors advise against this short-cut. The reason is that the measure-

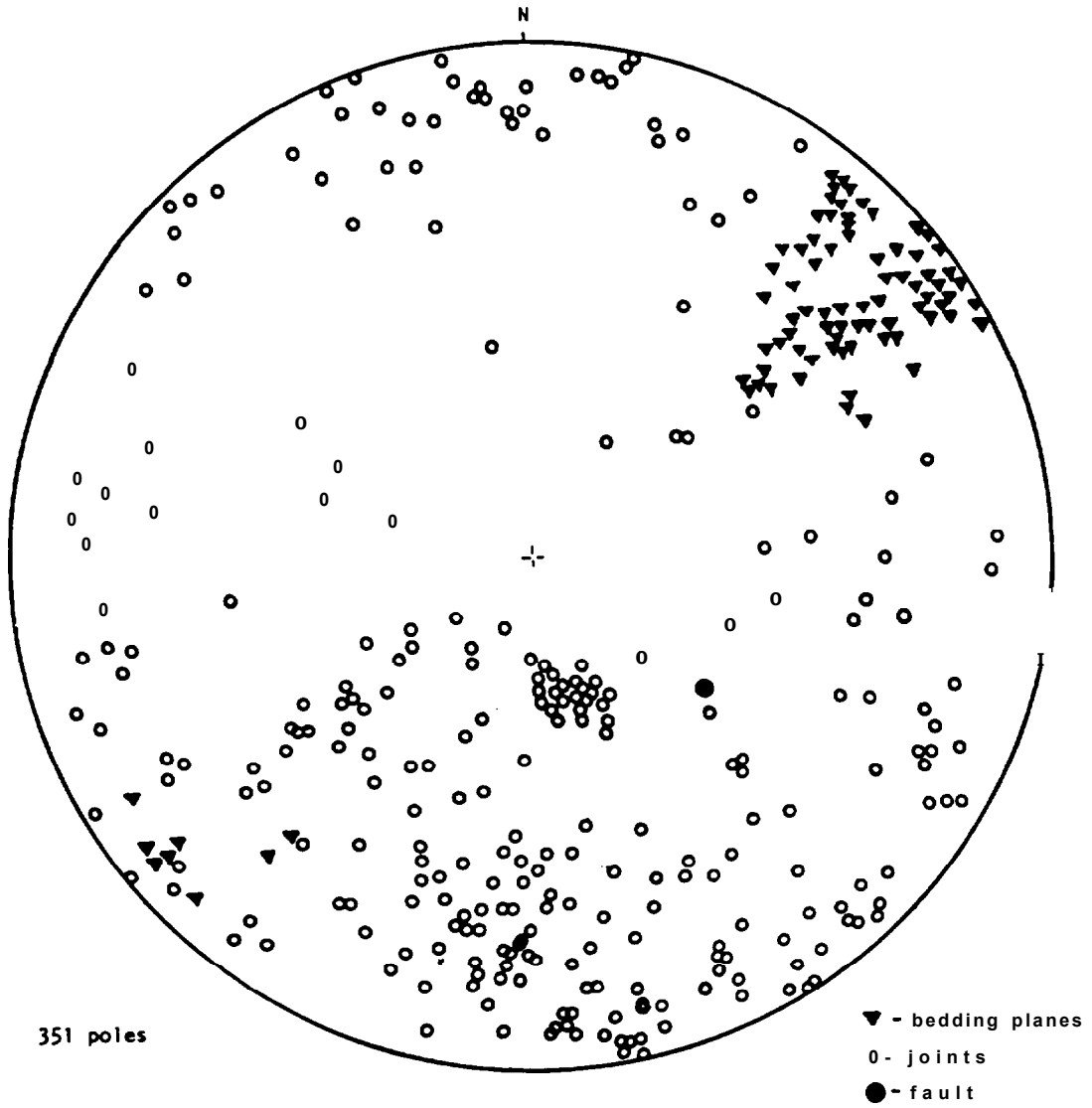


Figure 3.4: Plot of poles of discontinuities in a hard rock mass.

ments may well be required for other purposes, such as a computer analysis, and it is a great deal easier to work from recorded numbers than from the pole plot. Correcting errors on a pole plot on which several hundred measurements have been recorded is also difficult and information can be lost if it has not been recorded elsewhere. Some geologists prefer to use a portable tape recorder, instead of a notebook, for the recording of field data, and the reader should not hesitate to experiment to find the method which is best suited to his own requirements. When plotting field data it is recommended that different symbols be used to represent the poles of different types of structural features. Hence, faults may be represented by heavy black dots, joints by open circles, bedding planes by triangles and so on. Since these structural features are likely to have significantly different shear strength characteristics, the interpretation of a pole plot for the purposes of a stability analysis is simplified if different types of structure can easily be identified.

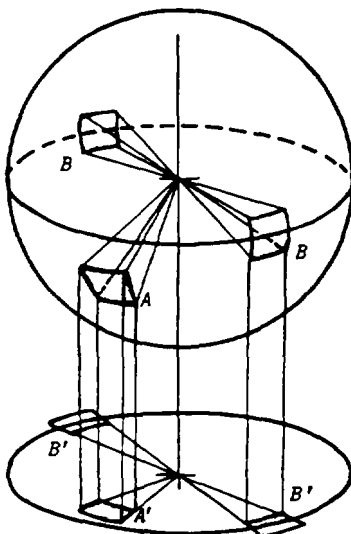
A plot of 351 poles of bedding planes and joints and of one fault in a hard rock mass is given in Figure 3.4. Since the fault occurs at one particular location in the rock mass, its influence need only be considered when analyzing the stability of the slope in that location. On the other hand, the bedding plane and joint measurements were taken over a considerable area of rock exposure and these measurements form the basis of the stability analysis of all other slopes in the proposed excavation.

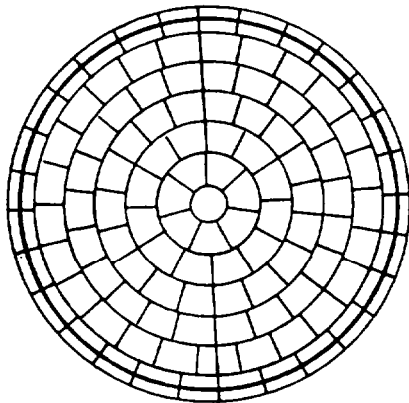
Two distinct pole concentrations are obvious in Figure 3.4; one comprising bedding plane poles in the north-eastern portion of the stereonet and the other, representing joints, south of the center of the net. The remainder of the poles appear to be fairly well scattered and no significant concentrations are obvious at first glance. In order to determine whether other significant pole concentrations are present, contours of pole densities are prepared.

Several methods of contouring pole plots have been suggested (41-47) but only two techniques will be described in this book. These techniques are preferred by the authors on the basis of numerous trials in which speed, convenience and accuracy of different contouring methods were evaluated.

Denness curvilinear cell counting method

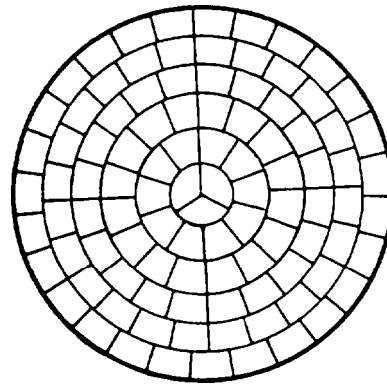
In order to overcome certain disadvantages of other contouring techniques, particularly when dealing with pole concentrations very close to the circumference of the net, Denness (46) devised a counting method in which the reference sphere is divided into 100 squares. A 1% counting square on the surface of the reference sphere, marked A in the margin sketch, projects onto the equal area stereonet as a curvilinear near Figure A'. When the counting cell falls across the equator of the reference sphere, only the poles falling in the lower half of the 1% cell will be shown on the stereonet since only the lower part of the reference sphere is used in the plotting process. The counting cell marked B and its projection B' illustrate this situation. Poles which fall above the equator are plotted on the opposite side of the stereonet and hence a count of the total number of poles falling in a 1% square falling across the equator is obtained





DENNESS TYPE A COUNTING NET

Cells per ring	Cell radius / Net radius	Angle
1	0.100	360.00
7	0.283	51.43
12	0.447	30.00
18	0.616	20.00
22	0.775	16.37
25	0.823	14.40
28	1.064	12.85



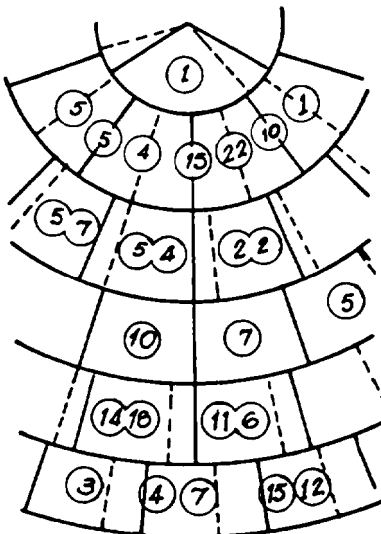
DENNESS TYPE B COUNTING NET

Cells per ring	Cell radius / Net radius	Angle
3	0.172	120.00
10	0.360	36.00
16	0.539	22.50
20	0.700	18.00
24	0.855	15.00
27	1.000	13.33

Figure 3.5: Dimensions of Denness curvilinear cell counting nets.

by summing the poles in the shaded portions of both projections marked B'.

Details of the two types of counting net devised by Denness are given in Figure 3.5. The type A net is intended for the analysis of pole plots with concentrations near the circumference of the net, representing vertically jointed strata. The type B net is more suited to the analysis of poles of inclined discontinuities and, since inclined discontinuities are of prime concern in the analysis of rock slope stability, this type of net is recommended for use by readers of this book. A type B counting net, drawn to the same scale as the stereonets on pages 3.7 and 3.8 and the pole plot in Figure 3.4 is reproduced in Figure 3.6.



In order to use this net for contouring a pole plot, a transparent copy or a tracing of the net must be prepared. Note that many photocopy machines introduce significant distortion and scale changes and care must be taken that good undistorted copies of nets with identical diameters are available before starting an analysis.

The transparent counting net is centered over the pole plot and a clean piece of tracing paper is placed over the counting net. The center of the net and the north mark are marked on the tracing paper. The number of poles falling in each 1% counting cell is noted, in pencil, at the center of each cell. Contours of equal pole density are obtained by joining the same numbers

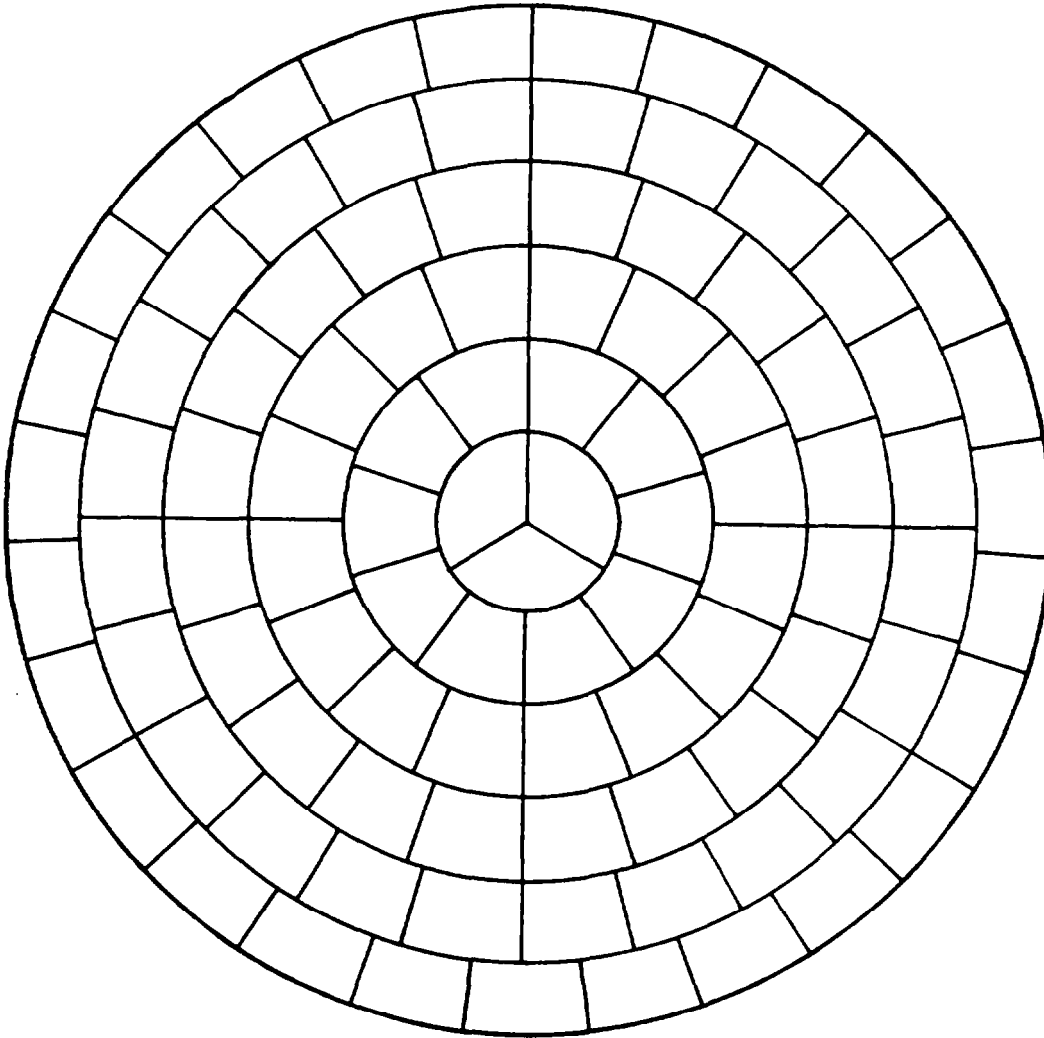


Figure 3.6: Denness Type B curvilinear cell mounting net.

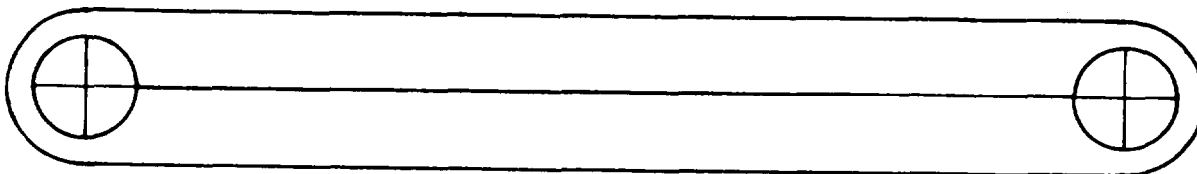


Figure 3.7: Counting circles for use in contouring pole plots.

on the diagram. If it is felt that insufficient information is available in certain parts of the diagram, the counting net can be rotated as indicated by the dashed lines in the margin sketch. The new counting cell positions are used to generate additional pole counts which are noted at the centers of these cells. If necessary, the counting net can be moved off center by a small amount in order to generate additional information in a radial direction.

Contours of equal pole densities are generally expressed as percentages. Hence, in the case of the 351 poles plotted in Figure 3.4, a 2% contour is obtained by joining pole counts of 7 and a pole count of between 17 and 18 corresponds to a contour value of 5%.

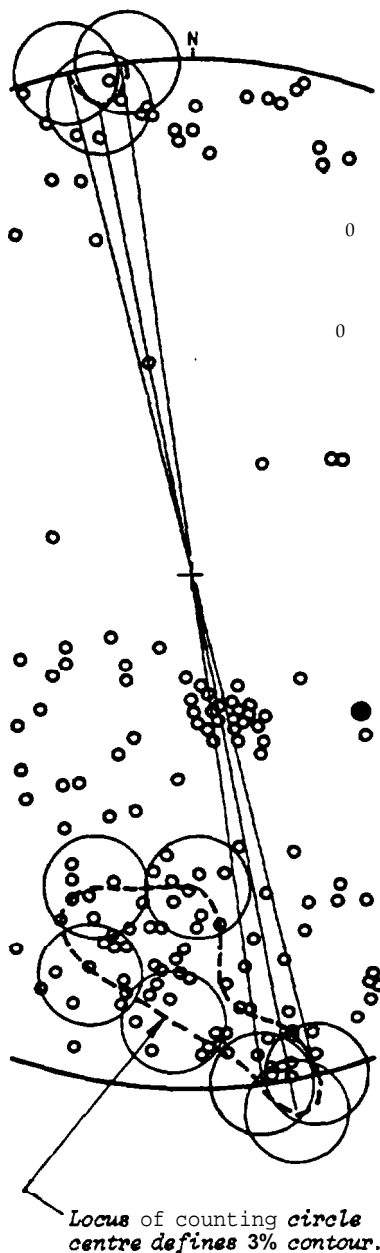
Floating circle counting method

One of the disadvantages of using a counting net to contour a pole plot is that the geometry of the counting net bears no direct relationship to the distribution of poles. When a cluster of poles falls across the boundary between two counting cells, a correct assessment of the pole concentration can only be obtained by allowing the cell to "float" from its original position and to center it on the highest concentration of poles. In some cases, several moves of the counting cell are needed to generate the quantity of information required for the construction of meaningful contours. Consideration of this counting procedure suggests that an alternative, and perhaps more logical, procedure is to use a single counting cell in a "floating" mode, its movements being dictated by the distribution of the poles themselves rather than by some arbitrarily fixed geometrical pattern. This reasoning lies behind the floating of free circle counting method (38) described below.

Figure 3.7 gives a pattern which can be used by the reader for the construction of a circle counter for use with stereonet of the diameter given on pages 3.7 and 3.8 and in Figure 3.4. The diameter of the circles is one-tenth of the diameter of the net and, therefore, the area enclosed by these circles is 1% of the area of the stereonet. The circles are exactly one net diameter apart and are used together when counting poles near the circumference of the net.

In order to construct a circle counter, trace the pattern given in Figure 3.7 onto a clear plastic sheet, using drawing instruments and ink to ensure an accurate and permanent reproduction. The plastic sheets used for drawing on for overhead projection, unexposed and developed photographic film or thin sheets of clear rigid plastic are all ideal materials for a counter. Punch or drill two small holes, approximately 1 mm in diameter at the center of each of the small circles.

The margin sketch illustrates the use of the circle counter to construct a 3% contour on the pole plot given in Figure 3.4. One of the small circles is moved around until it encircles 10 or 11 poles (3% of 351 poles = 10.5) and a pencil mark is made through the small hole at the center of the circle. The circle is then moved to another position at which 10 or 11 poles fall within its circumference and another pencil mark is made. When one of the small circles is positioned in such a way that a part of it falls outside the stereonet, the total number of poles falling in this circle is given by adding the poles in



this and in the other small circle, which must be located diametrically opposite on the stereonet as shown in the margin sketch. The locus of the small circle center positions defines the 3% contour.

Recommended contouring procedure

The following procedure is considered to provide an optimum compromise between speed and accuracy for contouring pole plots.

- Use a Denness type B counting net (Figure 3.6) to obtain a count of the number of poles falling in each counting cell.
- Sum these individual counts to obtain the total number of poles plotted on the net and establish the number of poles per 1% area which correspond to the different contour percentage values.
- Draw very rough contours on the basis of the pole counts noted on the tracing paper.
- Use the circle counter (Figure 3.7) to refine the contours, starting with low value contours (say 2 or 3%), and working inwards towards the maximum pole concentrations.

The contour diagram illustrated in the margin sketch was prepared from the pole plot in Figure 3.4 in approximately one hour by means of this technique.

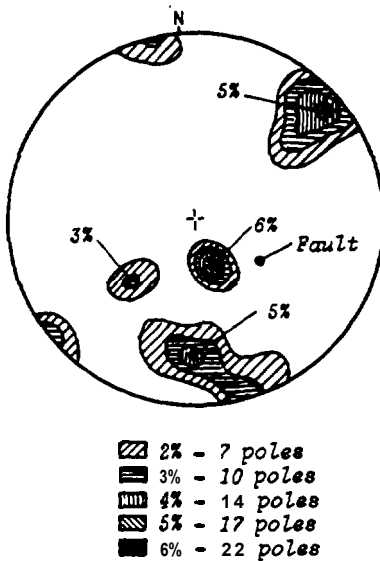
Computer analysis of structural data

Plotting and contouring a few sets of structural geology data can be both interesting and instructive and is strongly recommended to any reader who wishes completely to understand the techniques described on the previous pages. However, faced with the need to process large volumes of such data, the task becomes very tedious and may place an unacceptably high demand on the time of staff who could be employed more effectively on other projects.

The computer is an ideal tool for processing structural geology data on a routine basis and many engineering companies and geotechnical consulting organizations use computers for this task. A full discussion on this subject would exceed the scope of this chapter and the interested reader is referred to papers by Spencer and Clabaugh(48), Lam(49), Attewell and Woodman(50), and Mahtab et al(51) for details of the different approaches to the computer processing of structural geology data.

Optimum sample size

The collection of structural geology data is time consuming and expensive and it is important that the amount of data collected should be the minimum required to adequately define the geometrical characteristics of the rock mass. In considering what constitutes an adequate definition of the geometry of the rock mass, the object of the exercise must be kept clearly in mind. In the context of this book, the purpose of attempting to define the rock mass geometry is to provide a basis for choosing the most appropriate failure mode. This is one of the most important decisions in the entire process of a slope stability



Investigation since an incorrect choice of the failure mechanism will almost certainly invalidate the analysis. A hard rock mass, in which two or three strongly developed discontinuity sets show up as dense pole concentrations on a stereonet, will usually fail by sliding on one or two planes or by toppling. A single through-going feature such as a fault can play a dominant role in a slope failure and it is important that such features are identified separately in order that they are not lost in the averaging which occurs during the contouring of a pole plot. A soft rock mass such as a coal deposit which may be horizontally bedded and vertically jointed, or a hard rock mass in which joint orientations appear to be random, may fail in a circular mode similar to that which occurs in soil.

From this brief discussion, it will be clear that the collection and interpretation of structural geology data for the purposes of slope stability analysis cannot be treated as a routine statistical exercise. The rock mass knows nothing about statistics and there are many factors, in addition to the density of pole concentrations, which have to be taken into account in assessing the most likely failure mechanism in any given slope. An appreciation of the role of these other factors, which include the strength of the rock mass and the groundwater conditions in the slope, will assist the geologist in deciding on how much structural geology data is required in order that he may make a realistic decision on the slope failure mechanism.

For the reader who has not had a great deal of experience in slope stability analyses and may find it difficult to decide when he has enough structural geology data, the following guidelines on pole plots has been adapted from a paper by Stauffer(47):

1. First plot and contour 100 poles.
2. If no preferred orientation is apparent, plot an additional 300 poles and contour all 400. If the diagram still shows no preferred orientation, it is probably a random distribution.
3. If step 1 yields a single pole concentration with a value of 20% or higher, the structure is probably truly representative and little could be gained by plotting more data.
4. If step 1 results in a single pole concentration with a contour value of less than 20%, the following total numbers of poles should be contoured.
 - 12 - 20% add 100 poles and contour all 200.
 - 8 - 12% add 200 poles and contour all 300.
 - 4 - 8% add 500 to 900 poles and contour all 600 to 1,000.
 - less than 4% at least 1,000 poles should be contoured.
5. If step 1 yields a contour diagram with several pole concentrations, it is usually best to plot at least another 100 poles and contour all 200 before attempting to determine the optimum sample size.
6. If step 5 yields 1% contours less than 15° apart and with no pole concentrations higher than say 5%, the diagram is possibly representative of a folded structure for which the poles fall within a girdle distribution(45).

7. If step 5 yields a diagram with smooth 1% contours about 20° apart with several 3-6% pole concentrations, then an additional 200 poles should be added and all 400 poles contoured.
8. If step 7 results in a decrease in the value of the maximum pole concentrations and a change in the position of these concentrations, the apparent pole concentrations on the original plot were probably due to the manner in which the data were sampled and it is advisable to collect new data and carry out a new analysis.
9. If step 7 gives pole concentrations in the same positions as those given by step 5, add a further 200 poles and contour all 600 to ensure that the pole concentrations are real and not a function of the sampling process.
10. If step 5 yields several pole concentrations of between 3 and 6% but with very irregular 1% contours, at least another 400 poles should be added.
11. If step 5 yields several pole concentrations of less than 3% which are very scattered and if the 1% contour is very irregular, at least 1,000 and possibly 2,000 poles will be required and any pole concentration of less than 2% should be ignored.

Stauffer's work involved a very detailed study of the statistical significance of pole concentrations and his paper was not written with any particular application in mind. Consequently, the guidelines given above should be used for general guidance and should not be developed into a set of rules.

The following caution is quoted from Stauffer's paper:

"A practiced eye can identify point clusters, cell groupings and gross symmetry even for small samples of weak preferred orientations. It is probably true, however, that geologists are more prone to call a diagram preferred than to dismiss it as being random. This is understandable; most geologists examine a diagram with the intent of finding something significant, and are loath to admit their measurements are not meaningful. The result is a general tendency to make interpretations more detailed than the nature of the data actually warrants".

The authors feel that it is necessary to add their own words of caution in emphasizing that a contoured pole diagram is a necessary but not a sufficient aid in slope stability studies. It must always be used in conjunction with intelligent field observations and a final decision on the method of analysis to be used on a particular slope must be based upon a balanced assessment of all the available facts.

Evaluation of potential slope problems

Different types of slope failure are associated with different geological structures and it is important that the slope designer should be able to recognize the potential stability problems during the early stages of a project. Some of the structural patterns which should be watched for when examining pole plots are outlined on the following pages.

Figure 3.8 shows the four main types of failure considered in this book and gives the appearance of typical pole plots of

geological conditions likely to lead to such failures. Note that in assessing stability, the cut face of the slope must be included in the stereoplot since sliding can only occur as a result of movement towards the free face created by the cut.

The diagrams given in Figure 3.8 have been simplified for the sake of clarity. In an actual rock slope, combinations of several types of geological structures may be present and this may give rise to additional types of failure. For example, presence of discontinuities which can lead to toppling as well as planes upon which wedge sliding can occur could lead to the sliding of a budge which is separated from the rock mass by a "tension crack".

In a typical field study in which structural data has been plotted on stereonets, a number of significant pole concentrations may be present. It is useful to be able to identify those which represent potential failure planes and to eliminate those which represent structures which are unlikely to be involved in slope failures. John(52), Panet(53) and McMahon(32) have discussed methods for identifying important pole concentrations but the authors prefer a method developed by Markland(54).

Markland's test is designed to establish the possibility of a wedge failure in which sliding takes place along the line of intersection of two planar discontinuities as illustrated in Figure 3.8. Plane failure, Figure 3.8b is also covered by this test since it is a special case of wedge failure. If contact is maintained on both planes, sliding can only occur along the line of intersection and hence this line of intersection must "daylight" in the slope face. In other words, the plunge of the line of intersection must be less than the dip of the slope face, measured in the direction of the line of intersection as shown in Figure 3.9.

As will be shown in the chapter dealing with wedge failure, the factor of safety of the slope depends upon the plunge of the line of intersection, the shear strength of the discontinuity surfaces and the geometry of the wedge. The limiting case occurs when the wedge degenerates to a plane, i.e. the dips and dip directions of the two planes are the same, and when the shear strength of this plane is due to friction only. As already discussed, sliding under these conditions occurs when the dip of the plane exceeds the angle of friction ϕ and hence, a first approximation of wedge stability is obtained by considering whether the plunge of the line of intersection exceeds the friction angle for the rock surfaces. Figure 3.9b shows that the slope is potentially unstable when the point defining the line of intersection of the two planes falls within the area included between the great circle defining the slope face and the circle defined by the angle of friction ϕ .

The reader who is familiar with wedge analysis will argue that this area can be reduced further by allowing for the influence of "wedging" between the two discontinuity planes. On the other hand, the stability may be decreased if water is present in the slope. Experience suggests that these two factors will tend to cancel one another in typical wedge problems and that the crude assumption used in deriving Figure 3.9b is adequate for most practical problems. It should be remembered that this test is designed to identify critical discontinuities and, having iden-

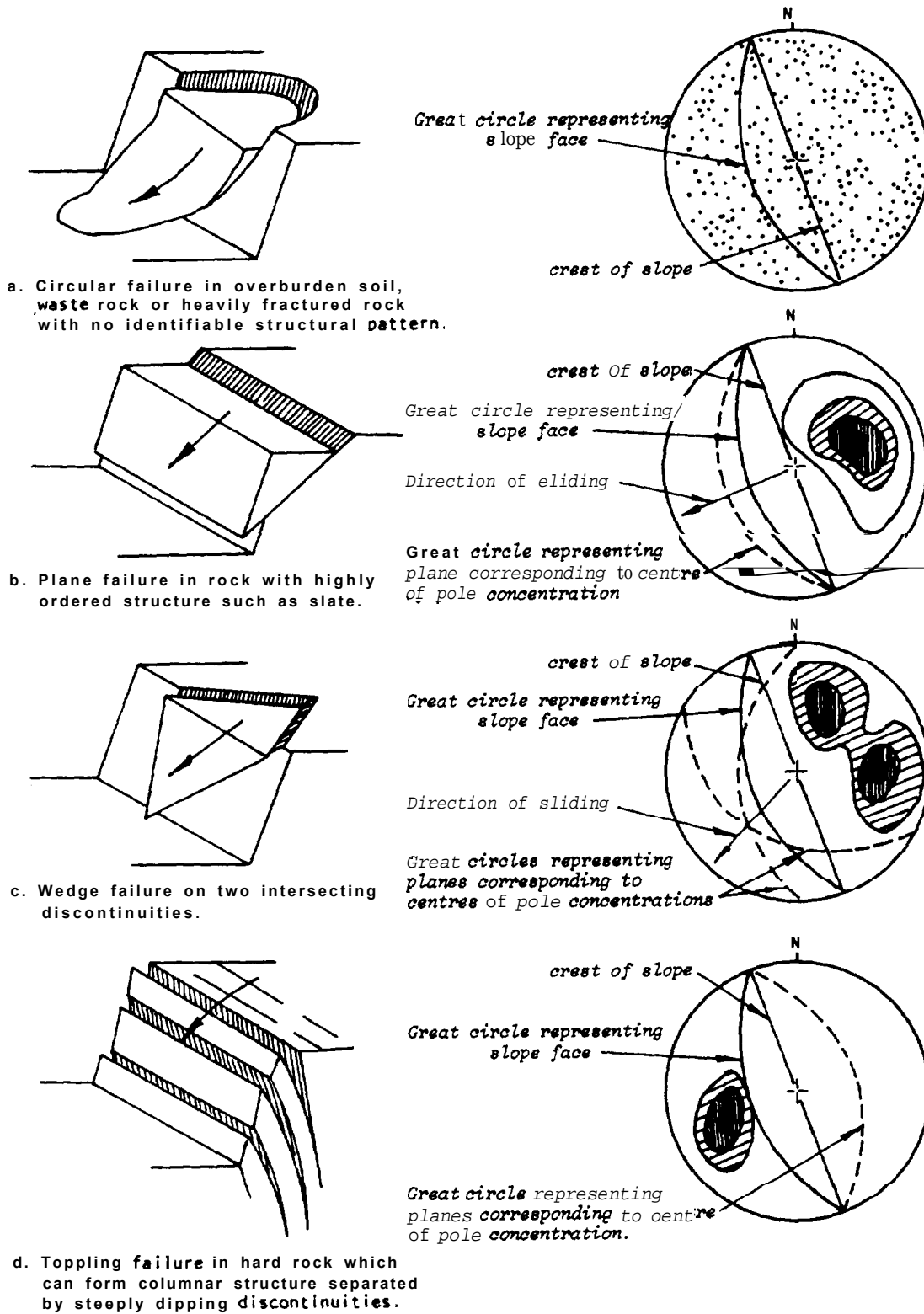


Figure 3.8: Main types of slope failure and stereoplots of structural conditions likely to give rise to these failures.

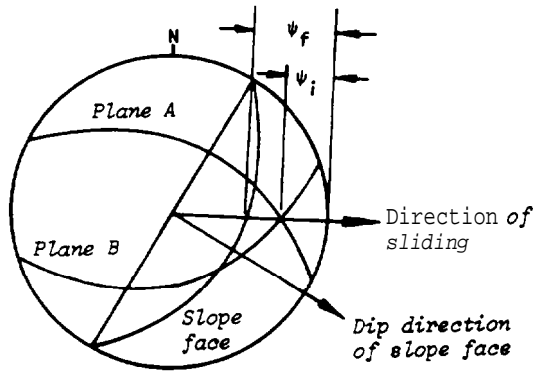


Figure 3.9a: Sliding along the line of intersection of planes A and B is possible when the plunge of this line is less than the dip of the slope face, measured in the direction of sliding, i.e.

$$\psi_f > \psi_i$$

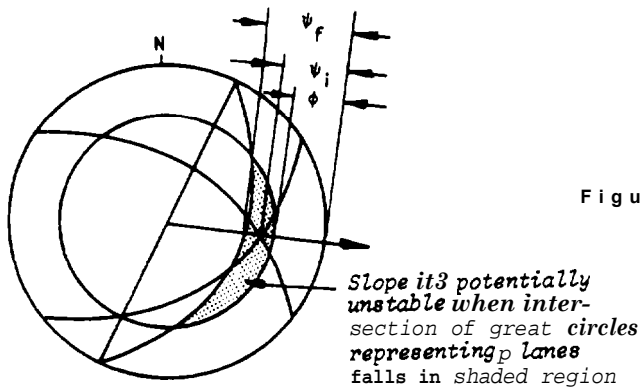


Figure 3.9b: Sliding is assumed to occur when the plunge of the line of intersection exceeds the angle of friction, i.e.

$$\psi_f > \psi_i > \phi$$

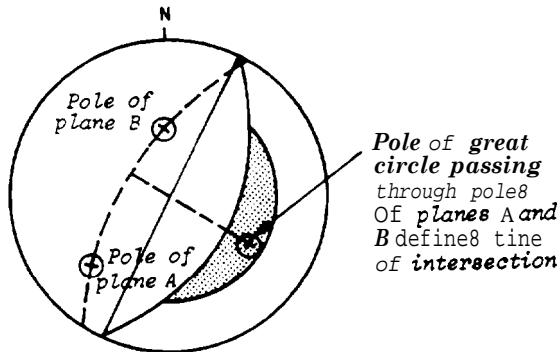


Figure 3.9c: Representation of planes by their poles and determination of the line of intersection of the planes by the pole of the great circle which passes through their poles.

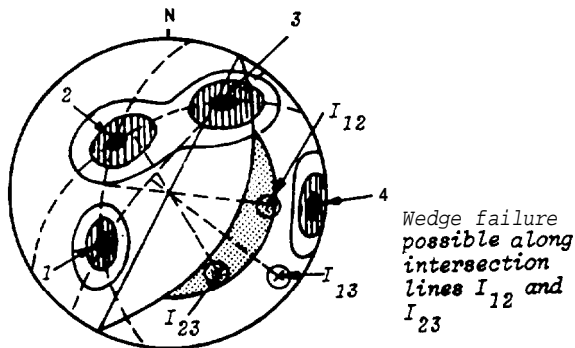
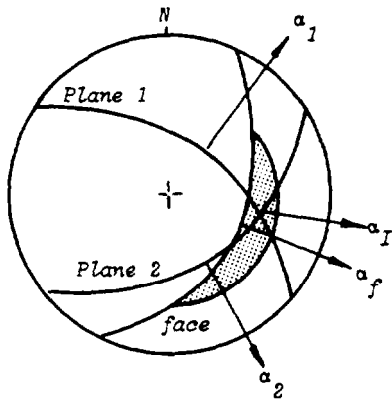
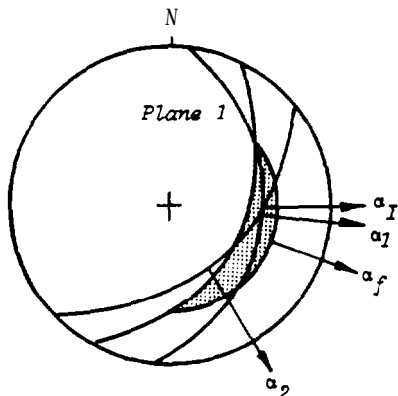


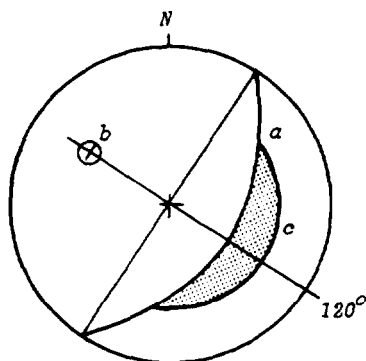
Figure 3.9d: Preliminary evaluation of the stability of a 50° slope in a rock mass with 4 sets of structural discontinuities.



Wedge failure along α_I



Sliding on plane 1 only



Overlay for checking wedge failure potential Z

tified them, a more detailed analysis would normally be necessary in order to define the factor of safety of the slope.

A refinement to Markland's test has been discussed by Hocking(55) and this refinement has been introduced to permit the user to differentiate between the sliding of a wedge along the line of intersection or along one of the planes forming the base of the wedge. If the conditions for Markland's test are satisfied, i.e. the line of intersection of two planes falls within the shaded crescent shown in the margin sketch, and if the dip direction of either of the planes falls between the dip direction of the slope face and the trend of the line of intersection, sliding will occur on the steeper of the two planes rather than along the line of intersection. This additional test is illustrated in the margin sketches on this page.

Figures 3.9a and 3.9b show the discontinuity planes as great circles but, as has been discussed on the previous pages, field data on these structures is normally plotted in terms of poles. In Figure 3.9c the two discontinuity planes are represented by their poles and, in order to find the line of intersection of these planes, the method described on page 3.111 is used. The tracing on which the poles are plotted is rotated until both poles lie on the same great circle. The pole of this great circle defines the line of intersection of the two planes.

As an example of the use of Markland's test consider the contoured stereoplot of poles given in Figure 3.9d. It is required to examine the stability of a slope face with a dip of 50° and dip direction of 120° . A friction angle of 30° is assumed for this analysis. An overlay is prepared on which the following information is included:

- a. The great circle representing the slope face.
- b. The pole representing the slope face.
- c. The friction circle.

This overlay is placed over the contoured stereoplot and the two are rotated together over the stereonet to find great circles passing through pole concentrations. The lines of intersection are defined by the poles of these great circles as shown in Figure 3.9d. From this figure it will be seen that the most dangerous combinations of discontinuities are those represented by the pole concentrations numbered 1, 2 and 3. The intersection I_{13} falls outside the critical area and is unlikely to give rise to instability. The pole concentration numbered 4 will not be involved in sliding but, as shown in Figure 3.8d, it could give rise to toppling or the opening of tension cracks. The poles of planes 1 and 2 lie outside the angle included between the dip direction of the slope face and the line of intersection I_{12} and hence failure of this wedge will be by sliding along the line of intersection I_{12} . However, in the case of planes 2 and 3, the pole representing plane 2 falls within the angle between the dip direction of the slope face and the line of intersection I_{23} and hence failure will be by sliding on plane 2. This will be the most critical instability condition and will control behavior of the slope.

Suggested method of data presentation and analysis for highway design

The following is an illustration of how the principles of structural geology and stability analysis can be used in high-

way design. Suppose that the proposed alignment passes through a spur of rock and it will be necessary to make a through-cut in order to keep the highway on grade (see Figure 3.10). The stability of the two slopes formed by this excavation is assessed in the following manner.

The structural geology of the rock forming the spur should be determined by surface mapping of outcrops. If there are no outcrops visible, then trenching or drilling may be required. If drilling is carried out then the core should be oriented (see Chapter 4) so that the dip and strike of the major structures can be determined. Suppose that the mapping (or drilling) showed three major joint sets which have the following orientations:

- A1: fractures dip to the south at angles between 20° and 30° .
- A2: fractures dip to the east at angles between 70° and 80° .
- A3: fractures dip to the west at angles between 30° and 40° .

Stereonet projections giving the orientations of these three sets are shown on Figure 3.10. Overlaid on each stereonet are great circles representing the dip and strike of the two slopes and the estimated friction angle of the fracture surface. These stereonet projections show that on the west slope, joint set A2 dips towards the excavation but at a steeper angle than the face so that sliding cannot occur. Set A3 dips away from the excavation and set A1 strikes at right angles to the excavation so that sliding cannot occur on either of these sets and the slope is likely to be stable.

On the east slope joint set A2 dips steeply away from the excavation and there is a possibility that the thin slabs formed by these joints will fall by toppling. There is also the possibility that sliding will occur on A2 joints that dip towards the excavation. This would not be a serious stability problem if the joints are discontinuous in which case only small failures would occur. There is also the possibility that wedge failures will occur where joint sets A1 and A2 intersect.

This preliminary analysis shows that the east cut slope has potential stability problems and that more detailed investigation of structural geology conditions would be required before finalizing the design. Since it is rarely possible to change alignment sufficiently to overcome a stability problem, it may be necessary to change the slope angle or implement stabilization measures in order to ensure that the slope is stable.

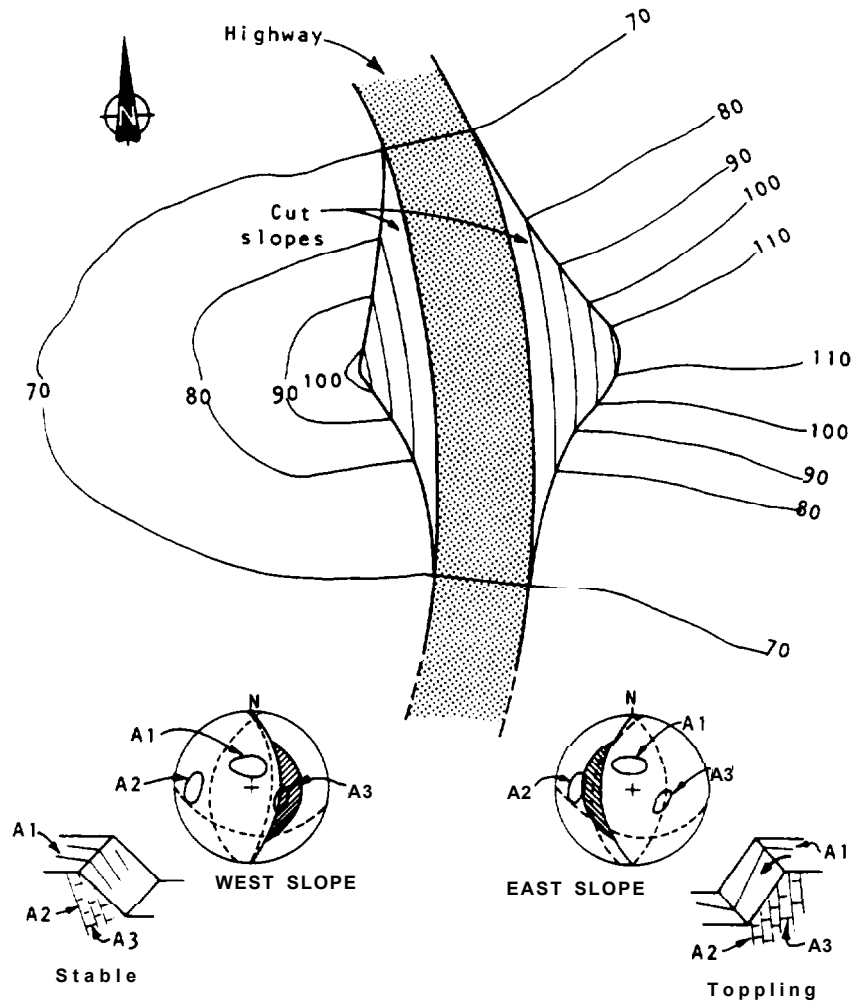


Figure 3. 10: Presentation of structural geology information and preliminary evaluation of slope stability of a proposed highway.

Chapter 3 references

36. PRICE, N.J. *Fault and joint development in brittle and semi-brittle rock*. Pergamon Press, London, 1966. 176 pages.
37. LOUDERBACK, G.D. Faults and engineering geology. In *Application of Geology to Engineering practice (Berkey volume)*. Geological Society of America, 1950, 327 pages.
38. TURNER, F.J. and WEISS, L.E. *Structural analysis of metamorphic tectonites*. McGraw-Hill Book Co., New York, 1963, 545 pages.
39. GOODMAN, R.E. The deformability of joints. In *Determination of the in-situ modulus of deformation of rock*. American Society for Testing and Materials Special Technical Publication, Number 477, 1970. Pages 174-196.
40. PATTON, F. D. Multiple modes of shear failure in rock. *Proc. 1st International Congress of Rock Mechanics*. Lisbon 1966, Vol. 1, pages 509-513.
41. PATTON, F.D. and DEERE, D.U. Significant geological factors in rock slope stability. *Planning open pit mines*, Johannesburg Symposium 1970. Published by A.A. Balkema, Amsterdam 1971. pages 143-151.
42. PHILLIPS, F.C. *The use of stereographic projections in structural geology*. Edward Arnold, London. Third edition (paperback), 1971, 90 pages.
43. BADGLEY, P.C. *Structural methods for the exploration geologist*. Harper Brothers, New York, 1959, 280 pages.
44. FRIEDMAN, M. Petrofabric techniques for the determination of principal stress directions in rock. *Proc. Conference State of Stress in the Earth's crust*. Santa Monica, 1963. Elsevier, New York, 1964, pages 451-550.
45. RAGAN, D.M. *Structural geology - an introduction to geometrical techniques*. John Wiley & Sons, New York, 2nd Edition 1973, 220 pages.
46. DENNESS, B. A revised method of contouring stereograms using variable curvilinear cells. *Geol. Mag.* Vol 109. Number 2, 1972. pages 157-163.
47. STAUFFER, M. R. An empirical-statistical study of three-dimensional fabric diagrams as used in structural analysis. *Canadian Journ. Earth Sciences*. Vol. 3. 1966, pages 473-498.
48. SPENCER, A.B. and CLABAUGH, P.S. Computer program for fabric diagrams. *American Journal of Science*. Vol.265, 1967, pages 166-172.
49. LAM, P.U.H. Computer methods for plotting beta diagrams. *American Journal of Science*. Volume 267, 1969, pages 1114-1117.
50. ATTEWELL P.B. and WOODMAN J.P. Stability of discontinuous rock masses under polyaxial stress systems. *Proc. 13th Symposium on Rock Mechanics*. University of Illinois, Urbana. 1971. pages 665 - 683.

51. MAHTAB, H.A., BOLSTAD, D.D., ALLDREDGE, J.R. and SHANLEY, R.J. Analysis of fracture orientations for input to structural models of discontinuous rock. *U.S. Bureau Of Mines Report of Investigations*. No.669, 1972.
52. JOHN, K.W. Graphical stability analysis of slopes in jointed rock. *Journal Soil Mechanics and Foundation Div. ASCE*. Vol. 94, No. SM2, 1968. pages 497-526 with discussion and closure in Vol. 95, No. SM6, 1969, pages 1541-1545.
53. PANET, H. Discussion on graphical stability analysis of slopes in jointed rock by K.W.John. *Journal Soil Mechanics and Foundation Div. ASCE* Vol.95, No. SM2, 1969, pages 685 - 686.
54. HARKLAND. J.T. A useful technique for estimating the stability of rock slopes when the rigid wedge sliding type of failure is expected. *Imperial College Rock Mechanics Research Report* No. 19, 1972, 10 Pages.
55. HOCKING, G. A method for distinguishing between single and double plane sliding of tetrahedral wedges. *Intl. J. Rock Mechanics and Mining Sciences*. Vol. 13, 1976, pages 225-226.

Chapter 4 Geological data collection.

Introduction

If one examines the amount of time spent on each phase of a rock slope stability investigation, by far the greatest proportion of time is devoted to the collection and interpretation of geological data. However, a search through slope stability literature reveals that the number of publications dealing with this topic is insignificant as compared with theoretical papers on the mechanics of slope failure (idealized slopes, of course). On first appearances it may be concluded that the engineer has displayed a remarkable tendency to put the proverbial cart before the horse. Deeper examination of the problem reveals that this emphasis on theoretical studies has probably been necessary in order that the engineer (and geologist) should be in a better position to identify relevant geological information and, as a consequence, be in a position to deal with this phase of the investigation more efficiently.

As engineers, the authors would not attempt to instruct the geologists on how to go about collecting and interpreting geological data. In fact, experience suggests that attempts by engineers to set up elaborate rock classification systems and standard core logging forms have been remarkably unsuccessful because geologists tend to be highly individualistic and prefer to work from their own point of view rather than that decreed by someone else. What has been attempted in this text, is to present an engineer's view of rock slope stability in such a way that the geologist can decide for himself what geological data is relevant and how he should go about collecting it.

When carrying out investigation programs for highway construction, cost savings can often be achieved by combining both soil and rock exploration work. For example, if drilling is carried out to determine the thickness and characteristics of the overburden, then a drill rig should be used that can also obtain core samples of the bedrock. Similarly, test trenches should be taken to bedrock so that mapping can be carried out in locations where there are few outcrops. Coordination of the rock and soil aspects of an exploration program requires close cooperation between the geologist and the soils engineer and some compromises may have to be made to make the best use of available funds.

On the following pages, a review is given of techniques which have been found useful in the geological data collection phase of slope stability investigations.

Regional geological investigations

A frequent mistake in rock engineering is to start an investigation with a detailed examination of drill cores. While these cores provide essential information, it is necessary to see this information in the context of the overall geological environment in which the proposed road is to exist. Structural discontinuities, upon which local failure of a bench can occur, are related to the regional structural pattern of the area and it is therefore useful to start an investigation by building up a picture of the regional geology.

Air photographs and topographic maps, in varying degrees of detail, are readily available and these provide an important source of information. Where detailed regional geology maps are

available, these should certainly be obtained as early as possible in the investigation.

Stereoscopic examination of adjacent pairs of air photographs is particularly useful and even an inexperienced observer can detect all near surface features which usually signify the presence of underlying geological structures. The experienced observer can provide a surprising amount of relevant information from an examination of air photographs and many consultants provide routine air-photo interpretation services. The interested reader is referred to the excellent text by Miller(56) on this subject.

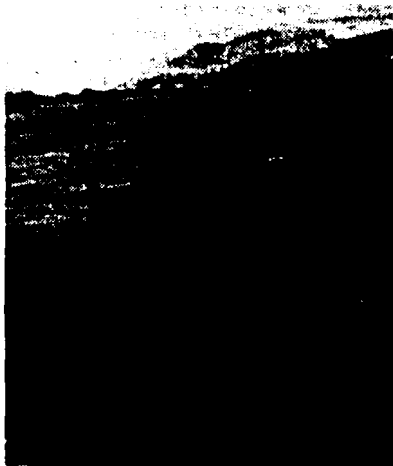
In addition to air photographs, full use should be made of any exposures available on site. Adjacent mines or quarries, road cuttings and exposures in river or stream beds are all excellent sources of structural information and access to such exposures can normally be arranged through local landowners.

Mapping of exposed structures

Mapping of visible structural features on outcrops or excavated faces is a slow and tedious process but there are unfortunately few alternatives to the traditional techniques used by the geologist. The most important tool for use in mapping is obviously the geological compass and many different types are available. An instrument which has been developed specifically for the type of mapping required for stability analyses is illustrated in Figure 4.1 and the use of this type of compass, reading directly in terms of dip and dip direction, can save a great deal of time. It must be emphasized that there are several other types of compass available and that all of them will do a perfectly adequate job of structural mapping. Which instrument is chosen, from those illustrated in Figure 4.1, is a matter of personal preference.

Several authors, including Broadbent and Ripperø(57), have discussed the question of the sampling of areas to be mapped and a line sampling method. This involves stretching a 100 ft. tape at approximately waist height along a face or a tunnel wall and recording every structural feature which intersects the tape line. Weaver and Call(58) and Halstead, et al(59) also used a technique, which they call fracture set mapping, which involves mapping all structures occurring in 20 ft. x 6 ft. bands spaced at 100 ft. intervals along a face. Da Silva, et al(60) mapped all structures exposed on the face of a rectangular tunnel.

All these methods can be used when an excavated slope or a tunnel is available but, during early exploration studies the geologist may simply have to make do with whatever exposures are available and use his ingenuity to compile as much relevant data as possible. The geologist concerned with mapping surface outcrops, as opposed to excavated faces, must contend with the problem of weathering and of surface coverings of soil and vegetation. A novel solution to this problem was used on the site investigation for the abutments of the Gordon arch dam in Tasmania where the vegetation and soil covering on the rock slopes were washed off by means of high pressure water jets. This process exposed the underlying rock and also accentuated structural features by washing out shallow fillings of weathering products. Obviously, this technique is only applicable



The Lake Edgar fault which stretches for many miles across Tasmania



Mapping exposed structures in a rock mass. An aluminium plate is being used for projecting planes.



A stereoviewer being used for the examination of a i r photographs.



A more elaborate stereoviewer which can be used for the measurement of differences in elevation from air photographs. The instrument illustrated is a model SB180 folding mirror stereoscope manufactured by Rank Precision Industries Ltd., P.O.Box 36, Leicester LE1 9JB, England.

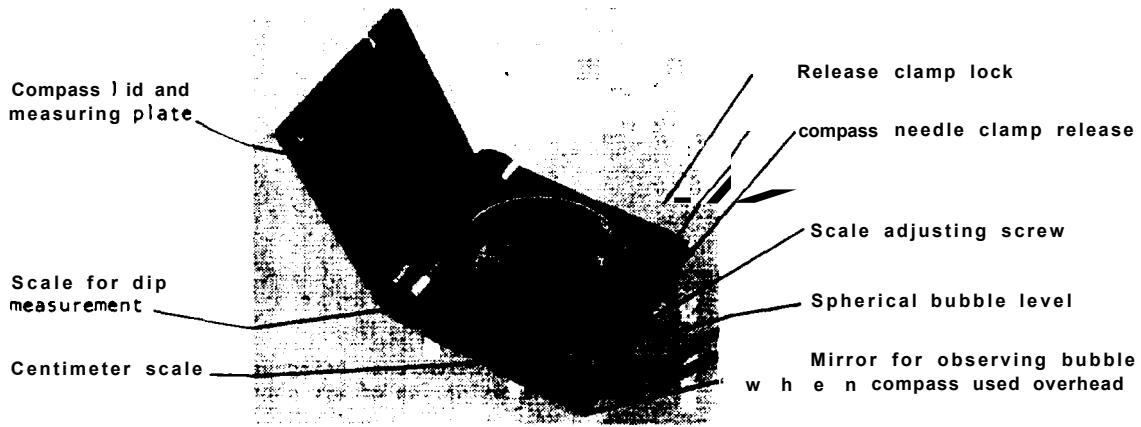
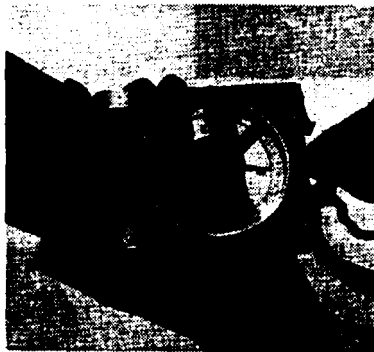


Figure 4.1: Geological compass designed by Professor Clar and manufactured by F.W.Breithaupt & Sohn, Adolfstrasse 13, Kassel 3500, West Germany.



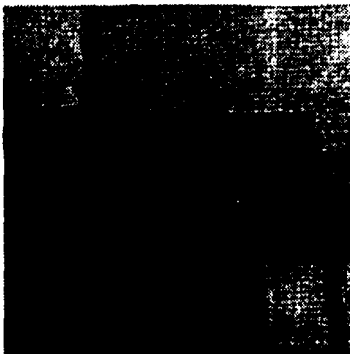
Level compass, release clamp and turn compass until needle points north. Clamp needle.



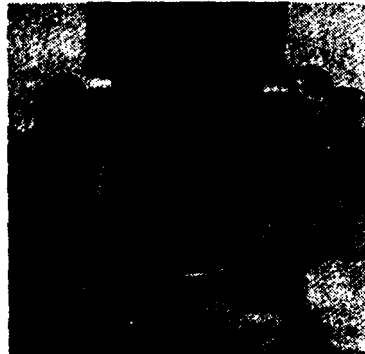
Use coin to turn adjusting screw to correct magnetic deviation. Zero on scale now reads true north.



Place measuring plate against rock face and level compass, release needle clamp and re-clamp after needle has settled.



Read dip of plane. In this example, dip is 35 degrees.



Read dip direction of plane. In this case, dip direction is 61°

The difference in magnetic declination in different hemispheres results in the needle jamming if a northern hemisphere compass is used in the southern hemisphere. Manufacturers will supply appropriate instrument if hemisphere is specified.

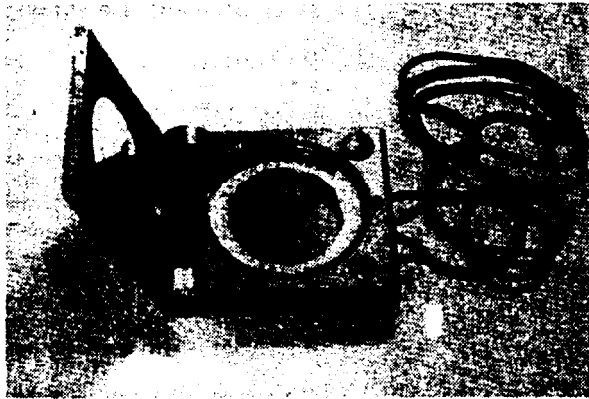


Figure 4.1a: A Clar type compass manufactured in East Germany and distributed by Carl Zeiss Jena Ltd., 2 Elmtree Way, Boreham Wood, Hertfordshire WD6 1NH, England. This instrument has sighting marks and a mirror fitted in the lid so that it can be used to take bearings in the same way as a Brunton compass. It also has a suspended pointer for measuring the inclination of the line of sight. The needle is undamped but it can be clamped in the same way as a Clar compass.

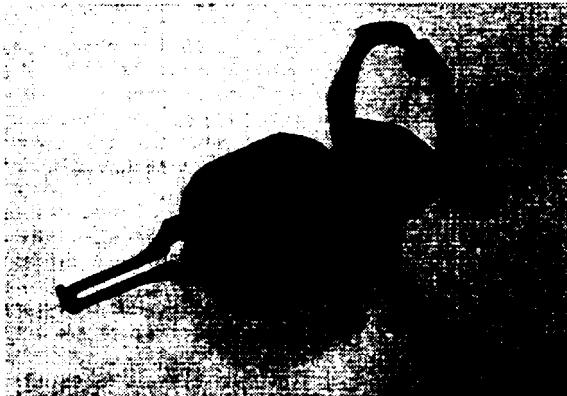


Figure 4.1b: A Brunton compass or pocket transit which is one of the most versatile field instruments for geologists although it is not as convenient as the Clar compass for the direct measurement of dip and dip direction of planes. This instrument is particularly convenient for taking bearings and for measuring the inclination of the line of sight.



Using a high pressure water jet to clean a rock face



A Wild P 30 phototheodolite set up for photography in an open-pit mine

In special cases but it is worth considering when critical slope problems are anticipated.

Good geological information can often be obtained by mapping in underground excavations which are in the same rock type as the proposed excavation. Although it is rare that a nearby tunnel will exist, there are circumstances where underground mapping may be possible. For example, tunnels are often excavated on hydro-electric and mining projects. Also, in mountainous terrain, tunnels are often required on railroads where the grade restrictions are more severe than on highways, so investigation of any nearby railroads is often worthwhile.

The rock exposed in a tunnel will often be less weathered than the rock outcropping at the surface. The tunnel may also provide useful information on ground water conditions.

All structural mapping techniques suffer from some form of bias since structures parallel or nearly parallel to an exposed face will not daylight as frequently as those perpendicular to the face. This problem has been discussed by Terzaghi(61) and most geologists apply Terzaghi's corrections to structural data obtained from surface mapping and borehole cores. However, Broadbent and Rippere(57) argue that these corrections are excessive when mapping on a typical excavated slope face which has been created by normal blasting. In this case the face will be highly irregular as a result of fracturing control led by discontinuities and the assumptions made by Terzaghi in deriving these corrections are no longer valid. Under such circumstances, Broadbent and Rippere suggest that the data should be presented without correction.

Photographic mapping of exposed structures

Before leaving the question of the mapping surface exposures, mention must be made of photogrammetric techniques which have been considered for use in structural mapping. Although not yet in wide use, photogrammetric methods offer considerable advantages and the authors believe that they will increasingly be used in rock engineering.

The equipment required consists of a phototheodolite such as that illustrated in the margin photograph which is simply a theodolite with a suitable camera located between the upper and lower circles. The field set-up is illustrated in Figure 4.2 and a rock face with targets painted on it for photogrammetric measurement is shown in Figure 4.3.

The two plates, taken at the left and right hand camera stations (Figure 4.2) are then viewed in a stereocomparator or similar instrument which produces a stereoscopic model of the overlapping region on the two plates. Measurements of the x, y and z coordinates of points in this three-dimensional model can be made to an accuracy of about 1 part in 5,000 of the mean object distance. Hence, a point on a face photographed from 5,000 ft. can be located to an accuracy of 1.2 inches.

Photogrammetric techniques can be used for both structural mapping and for quantity surveys of excavation volumes and a number of companies offer these services on a commercial basis. It would exceed the scope of this book to discuss details of photogrammetry and the interested reader is referred to the

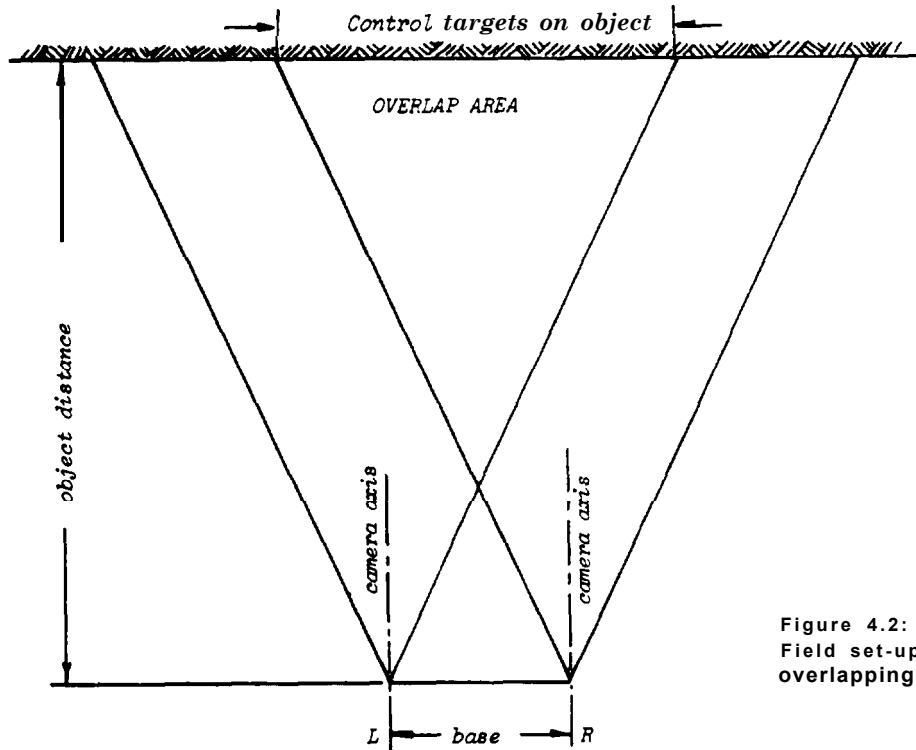


Figure 4.2:
Field set-up to obtain an
overlapping stereopair.

Figure 4.3:
Rock face with targets painted
on it as controls for photo-
grammetry. On high, steep faces
targets painted on metal plates
can be lowered on ropes.



publications listed at the end of this chapter for further information(62,63,64).

Most people think of photogrammetry in terms of expensive equipment and specialist operators and, while this is true for precise measurements, many of the principles can be used to quantify photographs taken with a normal hand-held camera. These principles are described in a useful text-book by Williams(65).

Measurement of surface roughness

Patton(40) emphasized the importance of surface roughness on the shear strength of rock surfaces and his concepts are now widely accepted. The influence of roughness on strength is discussed in the next chapter and the following remarks are restricted to the measurement of roughness in the field.

A variety of techniques have been used to measure roughness and, in the authors' opinion, the most practical method is that suggested by Fekker and Rengers(66) and illustrated in Figure 4.4, which is self-explanatory.

Diamond drilling for structural purposes

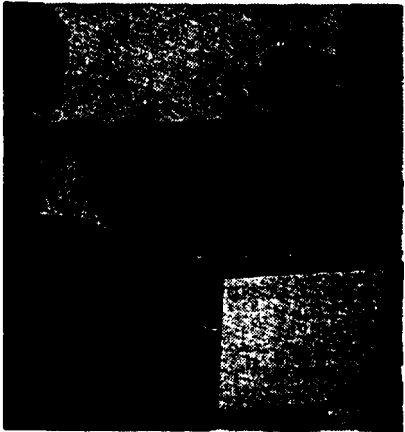
Many engineers are familiar with diamond drilling for mineral exploration and some would assume that the techniques used in exploration drilling are adequate for structural investigations. This is unfortunately not the case and special techniques are required to ensure that continuous cores which are as nearly undisturbed as possible are obtained. It should be remembered that it is the discontinuities and not the intact rock which control the stability of a rock slope and the nature, infilling, inclination and orientation of these discontinuities are of vital importance to the slope designer.

Contracts for mineral exploration drilling are normally negotiated on a fixed rate of payment per foot or meter drilled. In order to keep these rates low drilling contractors encourage their drillers to aim for the maximum length of hole per shift. In addition, machines are run frequently beyond their effective life in order to reduce capital costs. These practices result in relatively poor core recovery in fractured ground and it can seldom be claimed that the core is undisturbed.

To negotiate a geotechnical drilling contract on the same basis as a mineral exploration program is to invite trouble.

Good quality undisturbed core can only be achieved if the driller has time to "feel" his way through the rock and if he is using first class equipment. Consequently, many geotechnical engineers attempt to negotiate contracts in terms of payment for core recovery rather than the length of hole drilled. Alternatively, payment on an hourly rate rather than a drilling rate removes the pressure from the driller and permits him to aim at quality rather than quantity in his drilling.

In addition to providing financial incentives for the driller, it is essential to ensure that his equipment is designed for the job, in good working order and that it is correctly used.



A simple conducting paper electrical analogue model for the study of groundwater flow. Photograph courtesy Bougainville Copper Limited.

methods for constructing flow nets(174) have now largely been superseded by analogue(175,176) and numerical methods(177).

An example of an electrical resistance analogue for the study of anisotropic seepage and drainage problems is illustrated in Figure 6.8. Some typical examples of equipotential distributions, determined with the aid of this analogue, are reproduced in Figure 6.9.

Field measurement of permeability

Determination of the permeability of a rock mass is necessary if estimates are required of groundwater discharge from a slope or if an attempt is to be made to design a drainage system.

For evaluation of the stability of the slopes it is the water pressure rather than the volume of groundwater flow in the rock mass which is important. The water pressure at any point is independent of the permeability of the rock mass at that point but it does depend upon the path followed by the groundwater in arriving at the point (Figures 6.2 and 6.9). Hence, the anisotropy and the distribution of permeability in a rock mass is of interest in estimating the water pressure distribution in a slope.

In order to measure the permeability at a "point" in a rock mass, it is necessary to change the groundwater conditions at that point and to measure the time taken for the original conditions to be re-established or the quantity of water necessary to maintain the new conditions. These tests are most conventionally carried out in a borehole in which a section is isolated between the end of the casing and the bottom of the hole or between packers within the hole. The tests can be classified as follows:

- a. Falling head tests in which water is poured into a vertical or near vertical borehole and the time taken for the water level to fall to its original level is determined.
- b. Constant head tests in which the quantity of water which has to be poured into the borehole in order to maintain a specific water level is measured.
- c. Pumping tests or Lugeon tests in which water is pumped into or out of a borehole section between two packers and the changes induced by this pumping are measured.

The first two types of test are suitable for measurement of the permeability of reasonably uniform soils or rock. Anisotropic permeability coefficients cannot be measured directly in these tests but, as shown in the example given below, allowance can be made for this anisotropy in the calculation of permeability. Pumping tests, although more expensive, are more suitable for permeability testing in jointed rock.

Falling head and constant head tests

A very comprehensive discussion on falling head and constant head permeability testing is given by Horsley(179) and a few of the points which are directly relevant to the present discussion are summarized on page 6.12.

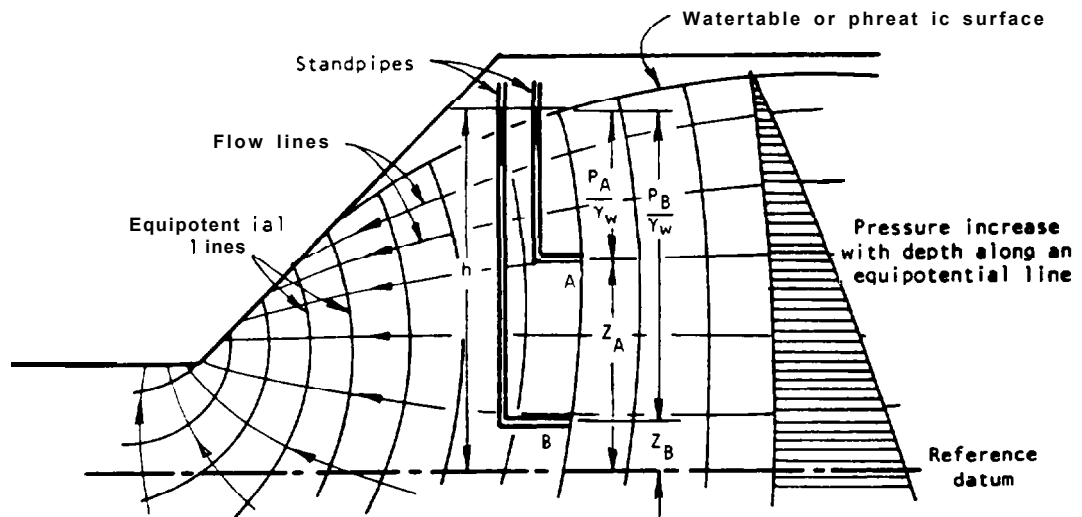


Figure 6.7 : Two-dimensional flow net in a slope.

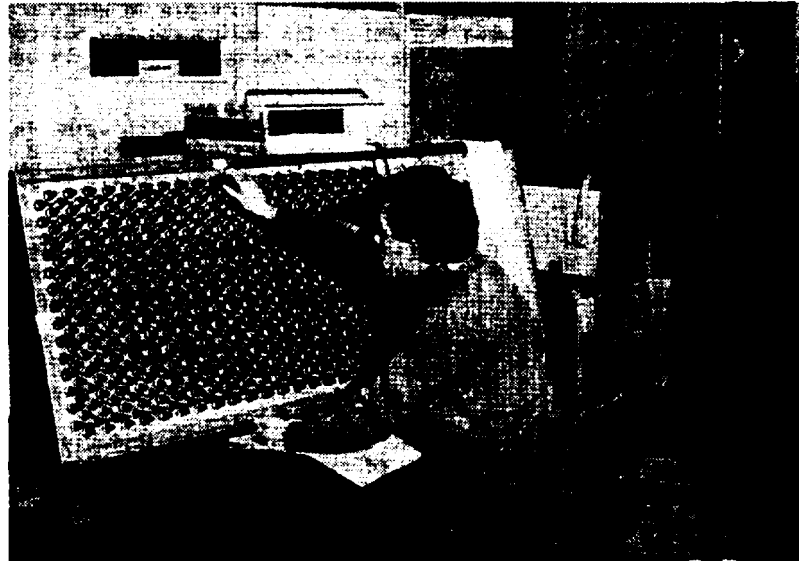


Figure 6.8 : Electrical analogue for the study of anisotropic groundwater flow and drainage problems ¹⁷¹.

Louis(170) points out that equation (33) only applies to laminar flow through planar parallel fissures and that it gives rise to significant errors if the flow velocity is high enough for turbulent flow to occur, if the fissure surfaces are rough or if the fissures are infilled. Louis lists no fewer than 8 equations to describe flow under various conditions. Equation (33) gives the highest equivalent permeability coefficient. The lowest equivalent permeability coefficient, for an infilled fissure system, is given by

$$k = \frac{e}{b} \cdot k_f + k_r \quad (34)$$

where k_f is the permeability coefficient of the infilling material, and

k_r is the permeability coefficient of the intact rock.

(Note that k_r has been ignored in equation (33) since it will be very small as compared with permeability of open joints).

An example of the application of equation (33) to a rock mass with two orthogonal joint systems is given in Figure 6.6. This shows a major joint set in which the joint opening e_1 is 0.10 m and the spacing between joints is $b_1 = 1$ m. The equivalent permeability k_1 parallel to these joints is $k_1 = 8.1 \times 10^{-2}$ cm/sec. The minor joint set has a spacing $b_2 = 1$ joint per meter and an opening $e_2 = 0.02$ cm. The equivalent permeability of this set is $k_2 = 6.5 \times 10^{-4}$ cm/sec., i.e. more than two orders of magnitude smaller than the equivalent permeability of the major joint set.

Clearly the groundwater flow pattern and the drainage characteristics of a rock mass in which these two joint sets occur would be significantly influenced by the orientation of the joint sets.

Flow nets

The graphical representation of groundwater flow in a rock or soil mass is known as a flow net and a typical example is illustrated in Figure 6.7. Several features of this flow net are worthy of consideration.

Flow lines are paths followed by the water in flowing through the saturated rock or soil.

Equipotential lines are lines joining points at which the total head h is the same. As shown in Figure 6.7, the water level is the same in boreholes or standpipes which terminate at points A and B on the same equipotential line.

Water pressures at points A and B are not the same since, according to equation (32), the total head h is given by the sum of the pressure head P/γ_w and the elevation z of the measuring point above the reference datum. The water pressure increases with depth along an equipotential line as shown in Figure 6.7.

A complete discussion on the construction or computation of flow nets exceeds the scope of this book and the interested reader is referred to the comprehensive texts by Cedergrön(166) and Haar(173) for further details. Traditional graphical

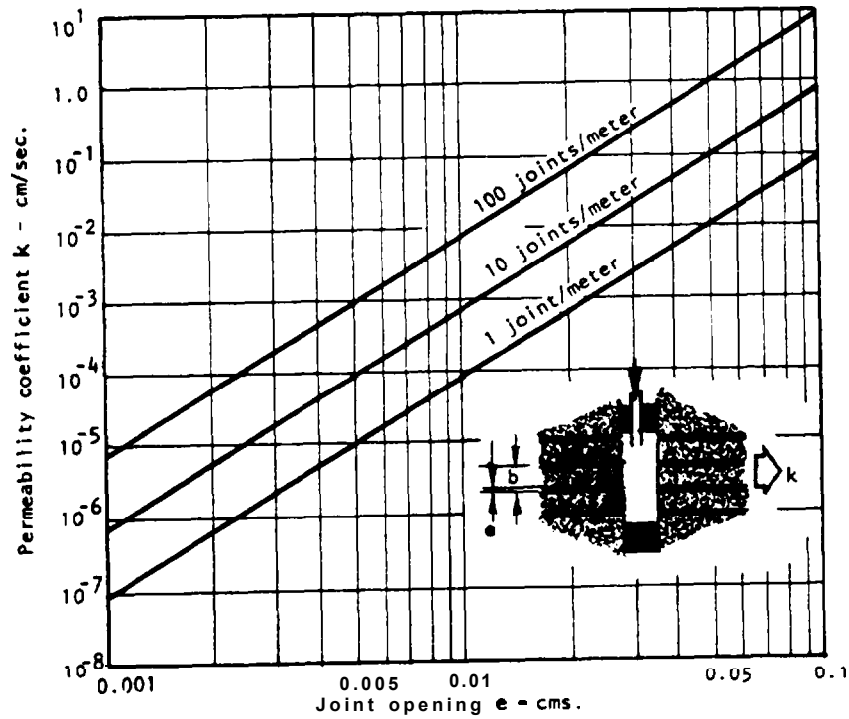


Figure 6.5: Influence of joint opening e and joint spacing b on the permeability coefficient k in the direction of a set of smooth parallel joints in a rock mass.

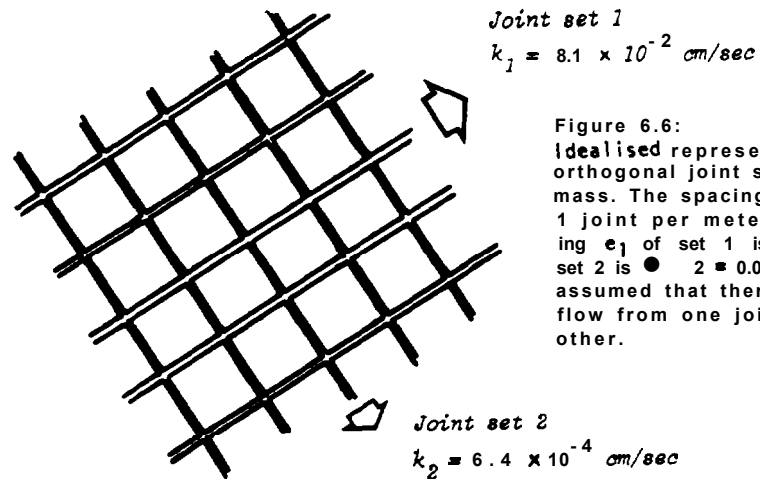


Figure 6.6: Idealised representation of two orthogonal joint systems in a rock mass. The spacing of both sets is 1 joint per meter. The joint opening e_1 of set 1 is 0.10 cm and for set 2 is $e_2 = 0.02$ cm. It is assumed that there is no cross-flow from one joint set to the other.

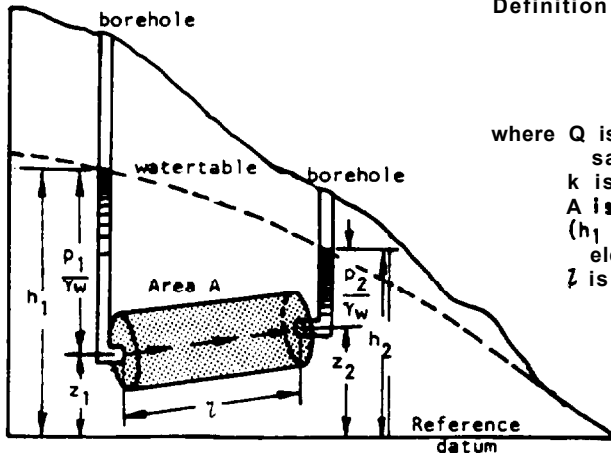


Figure 6.4:
Definition of permeability in terms of Darcy's law

$$Q = \frac{kA (h_1 - h_2)}{l}$$

where Q is the amount of water flowing through the sample in unit time,
 k is the coefficient of permeability
 A is the cross-sectional area of the sample
 $(h_1 - h_2)$ is the difference in watertable elevation between the ends of the sample
 l is the length of the sample.

TABLE V - PERMEABILITY COEFFICIENTS FOR TYPICAL ROCKS AND SOILS				
	$k - \text{cm/sec}$	<i>Intact rock</i>	<i>Fractured rock</i>	<i>Soil</i>
<i>Practically impermeable</i>	10^{-10}	Slate		Homogeneous clay below zone of weathering
	10^{-9}	Dolomite		
	10^{-8}	Granite		
<i>Low discharge poor drainage</i>	10^{-7}	Limestone ——— Sandstone ———		Very fine sands, organic and inorganic silts, mixtures of sand and clay, glacial till, stratified clay deposits
	10^{-6}			
	10^{-5}		Clay-filled joints	
	10^{-4}			
	10^{-3}			
<i>High discharge free drainage</i>	10^{-2}		Jointed rock	Clean sand, clean sand and gravel mixtures Clean gravel
	10^{-1}		Open-jointed rock	
	1.0			
	10^1			
	10^2		Heavily fractured rock	

above a reference datum and the quantity of water flowing through the sample in a unit of time is Q . According to Darcy's law, the coefficient of permeability of this sample is defined as (165,166,167):

$$k = \frac{Q \cdot L}{A(h_1 - h_2)} = \frac{V \cdot L}{(h_1 - h_2)} \quad (31)$$

To convert cm/sec to:	Multiply by
Meters/min	0.600
u/sec	10^4
ft/sec	0.0328
ft/min	1.968
ft/year	1.034×10^6

where V is the discharge velocity. Substitution of dimensions for the terms in equation (31) shows that the permeability coefficient k has the same dimensions as the discharge velocity V , i.e. length per unit time. The dimension most commonly used in groundwater studies is centimeters per second and typical ranges of permeability coefficients for rock and soil are given in Table V. Figure 6.5 shows that the total head h can be expressed in terms of the pressure p at the end of the sample and the height z above a reference datum. Hence

$$h = \frac{p}{\gamma_w} + z \quad (32)$$

where γ_w is the density of water. As shown in Figure 6.5, h is the height to which the water level rises in a borehole standpipe.

Permeability of jointed rock

Table V shows that the permeability of intact rock is very low and hence poor drainage and low discharge would normally be expected in such material. On the other hand, if the rock is discontinuous as a result of the presence of joints, fissures or other discontinuities, the permeability can be considerably higher because these discontinuities act as channels for the water flow.

The flow of water through fissures in rock has been studied in great detail by Huitt(168), Snow(169), Louis(170), Sharp(171), Maini(172) and others and the reader who wishes to pursue this complex subject is assured of many happy hours of reading. For the purposes of this discussion, the problem is simplified to that of the determination of the equivalent permeability of a planar array of parallel smooth cracks(170). The permeability parallel to this array is given by:

$$k = \frac{ge^3}{12\nu \cdot b} \quad (33)$$

where g = gravitational acceleration (981 cm/sec.²).

e = opening of cracks or fissures

b = spacing between cracks and

ν is the coefficient of kinematic viscosity (0.0101 cm²/sec. for pure water at 20°C).

The equivalent permeability k of a parallel array of cracks with different openings is plotted in Figure 6.5 which shows that the permeability of a rock mass is very sensitive to the opening of discontinuities. Since this opening changes with stress, the permeability of a rock mass will, therefore, be sensitive to stress.

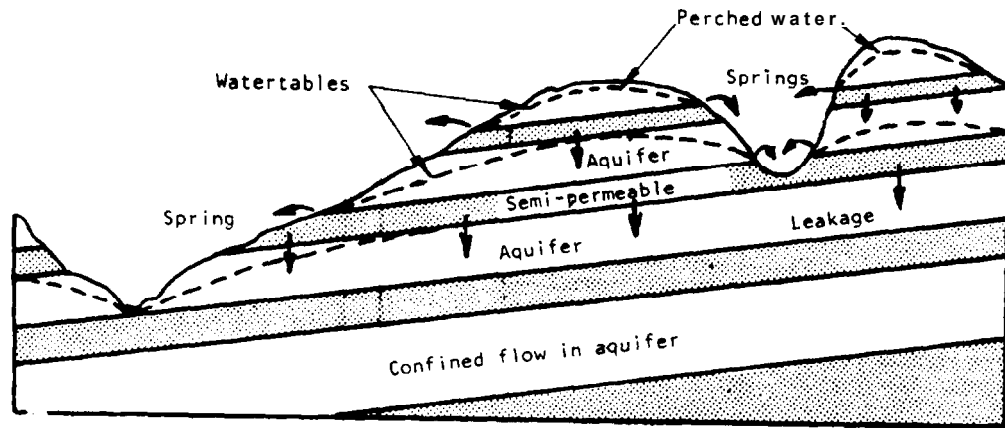


Figure 6.2: Confined, unconfined and perched water in a simple stratigraphic sequence of sandstone and shale. After Davis and de Wiest¹⁶³.

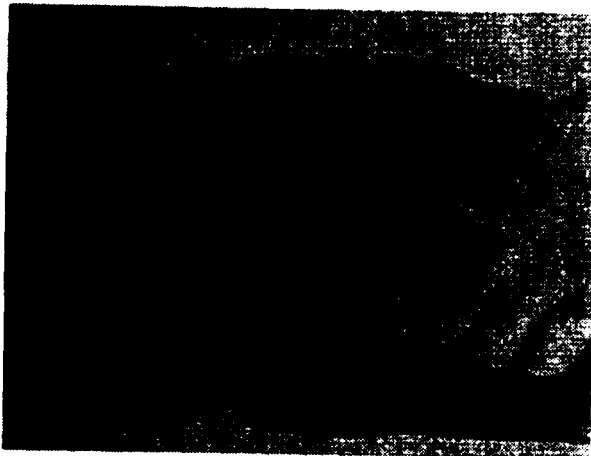


Figure 6.3:
Solution channel in limestone. The hydraulic conductivity of such a channel would be very high as compared with the permeability of the intact rock or of other discontinuities and it would have a major influence on the groundwater flow pattern in a rock mass.

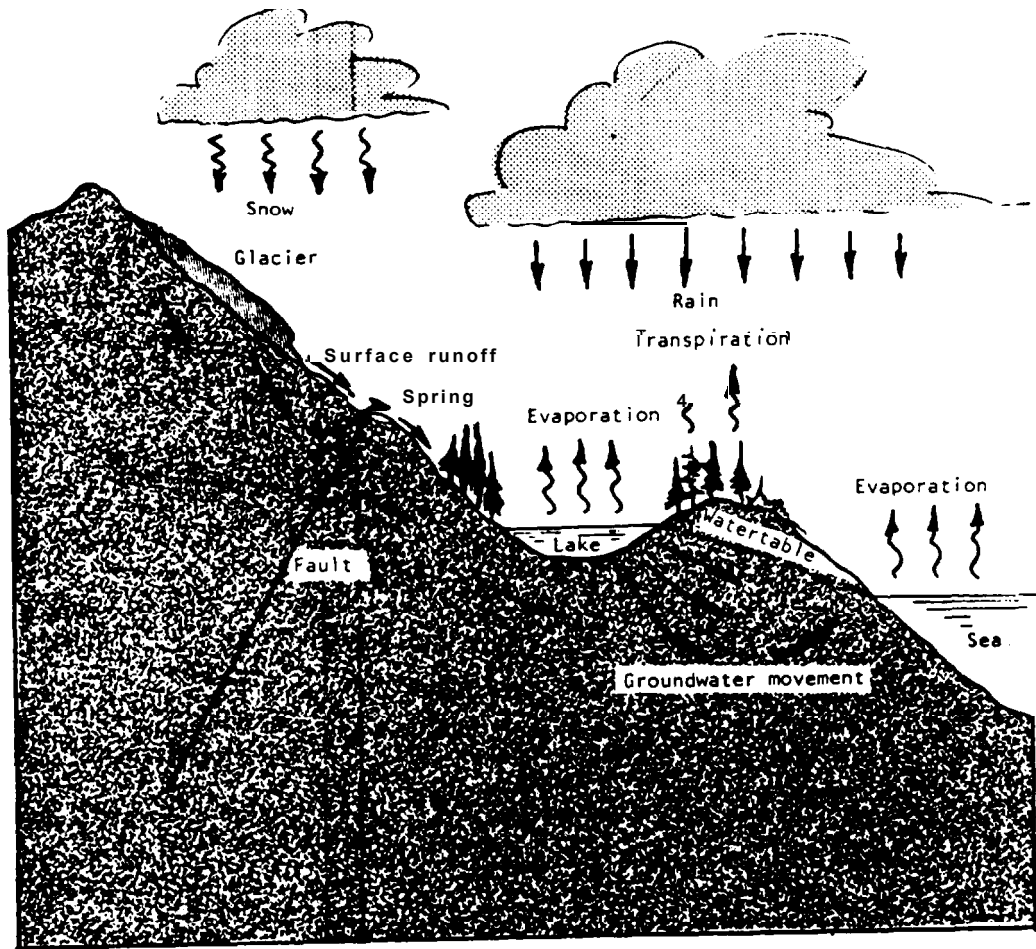
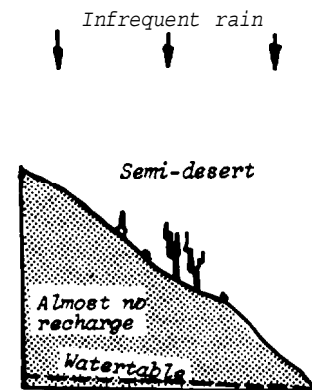
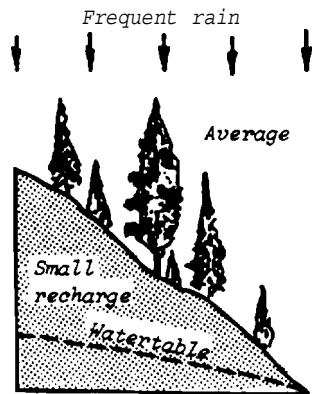
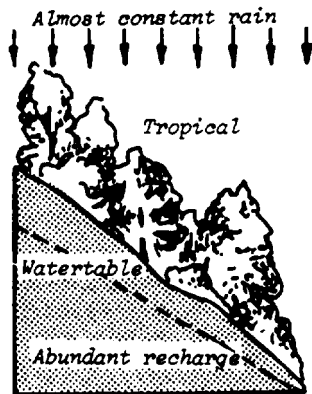


Figure 6.1 : Simplified representation of a hydrologic cycle showing some typical sources of groundwater.



After Davis and De Wiest¹⁶³.

Groundwater flow in rock masses

There are two possible approaches to obtaining data on water pressure distributions within a rock mass:

- Deduction of the overall groundwater flow pattern from consideration of the permeability of the rock mass and sources of groundwater.
- Direct measurement of water levels in boreholes or wells or of water pressure by means of piezometers installed in boreholes.

As will be shown in this chapter, both methods abound with practical difficulties but, because of the very important influence of water pressure on slope stability, it is essential that the best possible estimates of these pressures should be available before a detailed stability analysis is attempted. Because of the large number of factors which control the groundwater flow pattern in a particular rock mass, it is only possible to highlight the general principles which may apply and to leave the reader to decide what combinations of these principles is relevant to his specific problem.

The hydrologic cycle

A simplified hydrologic cycle is illustrated in Figure 6.1 to show some typical sources of groundwater in a rock mass. This figure is included to emphasize the fact that groundwater can and does travel considerable distances through a rock mass. Hence, just as it is important to consider the regional geology of an area when starting the design on a highway, so it is important to consider the regional groundwater pattern when estimating probable groundwater distributions at a particular site.

Clearly, precipitation in the catchment area is an important source of groundwater, as suggested in the sketch opposite, but other sources cannot be ignored. Groundwater movement from adjacent river systems, reservoirs or lakes can be significant, particularly if the permeability of the rock mass is highly anisotropic as suggested in Figure 6.2. In extreme cases, the movement of groundwater may be concentrated in open fissures or channels in the rock mass and there may be no clearly identifiable water table. The photograph reproduced in Figure 6.3 shows a solution channel of about 1 inch in diameter in limestone. Obviously, the hydraulic conductivity of such a channel would be so high as compared with other parts of the rock mass that the conventional picture of a groundwater flow pattern would probably be incorrect in the case of a slope in which such features occur.

These examples emphasize the extreme importance of considering the geology of the site when estimating water table levels or when interpreting water pressure measurements.

Definition of permeability

Consider a cylindrical sample of soil or rock beneath the water table in a slope as illustrated in Figure 6.4. The sample has a cross-sectional area of A and a length l . Water levels in boreholes at either end of this sample are at heights h_1 and h_2

Chapter 6 Groundwater flow; permeability and pressure.

Introduction

The presence of groundwater in the rock mass in a slope above a highway has a detrimental effect upon stability for the following reasons:

- a. Water pressure reduces the stability of the slopes by reducing the shear strength of potential failure surfaces as described on pages 2.6 and 2.7. Water pressure in tension cracks or similar near vertical fissures reduces stability by increasing the forces tending to induce sliding (page 2.8).
- b. High moisture content results in an increased unit weight of the rock and hence gives rise to increased haulage costs during construction. Changes in moisture content of some rock, particularly shales, can cause accelerated weathering with a resulting decrease in stability.
- c. Freezing of groundwater during winter can cause wedging in water-filled fissures due to temperature dependent volume changes in the ice. Freezing of surface water on slopes can block drainage paths resulting in a build-up of water pressure in the slope with a consequent decrease in stability.
- d. Erosion of both surface soils and fissure infilling occurs as a result of the velocity of flow of groundwater. This erosion can give rise to a reduction in stability and also to silting up of drainage systems.
- e. Discharge of groundwater from slopes above a highway can give rise to increased maintenance costs as a result of pavement deterioration and the need for higher capacity drainage systems. During construction there will be the difficulties of operating heavy equipment on wet ground and blasting costs are increased by wet blast holes.
- f. Liquefaction of overburden soils or fills can occur when water pressure within the material rises to the point where the uplift forces exceed the weight of the soil. This can occur if drainage channels are blocked or if the soil structure undergoes a sudden volume change as can happen under earthquake conditions.

Liquefaction is critically important in the design of foundations and soil fills and it is dealt with in the references numbered (159-162) listed at the end of this chapter. It will not be considered further in this book since it does not play a significant part in controlling the stability of rock slopes.

By far the most important effect of the presence of groundwater in a rock mass is the reduction in stability resulting from water pressures within the discontinuities in the rock. Methods for including these water pressures into stability calculations are dealt with in later chapters of this book. This chapter is concerned with methods for estimating or measuring these water pressures.

152. HAMEL, J. V. The slide at Brilliant cut. *Proc. 13th Symposium on Rock Mechanics*. Urbana, Illinois. 1971, pages 487-510.
153. LEY, G.M.M. The properties of hydrothermally altered granite and their application to slope stability in opencast mining. *M.Sc Thesis, London University, Imperial College*. 1972.
154. MIDDLEBROOK, T.A. Fort Peck slide. *Proc. American Society of Civil Engineers*. Vol. 107. paper 2144, 1942, page 723.
155. FLEMING, R.W., SPENCER, G.S and BANKS, D.C. Empirical study of the behaviour of clay shale slopes. *US Army Nuclear Cratering Group Technical Report No. 15, 1970*
156. HUTCHINSON. J.N. Field and laboratory studies of a fall in upper chalk cliffs at Joss Bay, Isle of Thanet. *Proc. Roeoe Memorial Symposium*. Cambridge, 1970.
157. HOEK. E. and RICHARDS, L.R. Rock slope design review. *Golder Associates Report to the Principal Government Highway Engineer, Hong Kong*. 1974, 150 pages.
158. STIMPSON, B., METCALFE, R.G and WALTON, G. A new technique for sealing and packing rock and soil samples. *Quarterly Journal of Engineering Geology*. Vol. 3, No. 2. 1970, pages 127-133.
- 15BA. Wyllie, D.C., Munn, F.J. The use of movement monitoring to minimize production losses due to pit slope failures. *Proc. of Frost International Conference on Stability in Coal Mining, Vancouver, Canada, 1978, Miller Freeman Publications*.

137. MARSAL, R.J. Mechanical properties of rockfill. *In hbankment Dwn Engineering - Caeagrande Volume.* Edited by R.C.Hirschfeld and S.J.Poulos, Published by J.Wiley b Sons, New York. 1973, pages 109-200
138. MARACHI, N.D., CHAN, C.K and SEED, H.B. Evaluation of properties of rockfill materials. *J. Soil Meckanics and Foundation Division, ASCE.* Vol. 98, No. SM1, 1972, pages 95-114.
139. WILKINS, J.K. A theory for the shear strength of rockfill. *Rock Mechanics.* Vol. 2, 1970, pages 205-222.
140. BARTON. N., LIEN, R. and LUNDE, J. Engineering clas-sification of rock masses for the design of tunnel support. *Rock Meckanics,* Vol. 6, 1974, pages 189-236.
141. BIENIAWSKI, Z.T. Geomechanics classification of rock masses and its application in tunnelling. *Proc. 3rd Intl. Cong. Rock Mech.,* Denver, Vol 11A, 1974.
142. JAEGER, J.C. The behaviour of closely jointed rock. *Proc. 11th Symposium on Rock Mechanics.* Berkeley, 1970, pages 57-68.
143. BISHOP, A.W and HENKEL, D.J. *The measurement of soil properties in the triaxial test.* Published by Edward Arnold, London. 2nd. Edition, 1962.
144. COATES, D. F. , CYENCE, M and STUBBINS, J.B. Slope stability studies at Knob Lake. *Proc. Rock Mechanics Symposium.* Toronto. 1965, pages 35-46.
145. WHITMAN, R.V. and BAILEY. W.A. Use of computers for slope stability analysis. *J. Soil Mechanics and Foundation Division, ASCE.* Vol. 93, 1967, pages 475-498.
146. HOEK, E. Estimating the stability of excavated slopes in opencast mines. *Trans. Institution of Mining and Metallurgy.* London. Vol. 79, 1970, pages A109-A132.
147. HOEK, E. Progressive caving induced by mining an inclined ore body. *Trans. Institution of Mining and Metallurgy.* London. Vol. 83, 1974, pages A133-A139.
148. ROBERTS, D. and HOEK, E. A study of the stability of a disused limestone quarry face in the Mendip Hills, England. *Proc. 1st. Intl. Conference on Stability in Open Pit Mining.* Vancouver. Published by AIME, New York, 1972, pages 239-256.
149. SKEMPTON, A.W. and HUTCHINSON. J.N. Stability of natural slopes and embankment foundations. State of the art report. *Proc. 7th Intl. Conference on Soil Mechanics.* Mexico. Vol. 1, 1969, pages 291-340.
150. HAHTEL, J.V. The Pima mine slide, Pima County, Arizona. *Geological Society of America Abstracts with Programs.* Vol. 2, No. 5, 1970, page 335.
151. HAHTEL. J.V. Kimberley plt slope failure. *Proc. 4th Panamerican Conference on Soil Meckanice and Foundation Engineering.* Puerto Rico. Vol. 2, 1971, pages 117-127.

123. BERNAIX, J. New laboratory methods of studying the mechanical properties of rocks. *Intl. J. Rock Mechanics and Mining Sciences*. Vol.6, 1969, pages 43-90.
124. SCHULTZE, E. Large scale shear tests. *Proc. 4th Intl. Conference on Soil Mechanics and Foundation Engineering*. London, Vol.1, 1957, pages 193-199.
125. EURENIUS, J. and FAGERSTROM, H. Sampling and testing of soft rocks with weak layers. *Geotechnique*. Vol.19, No.1, 1969, pages 133-139.
126. UNDERWOOD, B.L. Chalk foundations at four major dams in the Missouri River Basin. *Trans. 8th Intl. Congress on Large Dams*. Edinburgh, Vol.1, 1964, pages 23-47.
127. SERAFIM, J.L. and GUERREIRO, M. Shear strength of rock masses at three Spanish dam sites. *Proc. Intl. Rock Mechanics Symposium*. Madrid. 1968, pages 147-157.
128. COATES, D.L., McRORIE, K.L. and STUBBINS, J.B. Analysis of pit slides in some incompetent rocks. *Trans. Society of Mining Engineers. AIME*. 1963, pages 94-101.
129. MULLER, L. and PACHER, P. Modelversuche zur Klärung der Bruchgefahr geklufteter Medien. *Rock Mechanics and Engineering Geology*. Supplement 2, 1965, pages 7-24.
130. JOHN, K.W. Civil engineering approach to evaluate strength and deformability of regularly jointed rock. *Proc. 11th Symposium on Rock Mechanics*. Berkeley, 1969, pages 69-80.
131. BRAY, J.W. A study of jointed and fractured rock. *Rock Mechanics and Engineering Geology*. Vol.5, 1967, pages 119-136 and 197-216.
132. BROWN, E.T. Strength of models of rock with intermittent joints. *J. Soil Mechanics and Foundation Division. ASCE*. Vol.96, No. SM6, 1970, pages 1917-1934.
133. ROSENGREN, K.J. and JAEGER, J.C. The mechanical properties of an interlocked low-porosity aggregate. *Geotechnique*. Vol.18, No.3, 1968, pages 317-328.
134. HOEK, E. and BROWN, E.T. *Underground Excavations in Rock*. Published by the Inst. Min. Metall., London, 1980, 527 pages.
135. HOEK, E. and BROWN, E.T. Empirical strength criterion for rock masses, *J. Geotechnical Engineering Div., A.S.C.E.*, Vol. 106, No. GT9, 1980, pages 1013-1035.
136. HOEK, E. An empirical strength criterion and its use in designing slopes and tunnels in heavily jointed weathered rock. *Proc. Sixth Southeast Asian Conf. on Soil Engineering*, Taipei, Taiwan, Vol 2, 1980.

110. LINK, H. The sliding stability of dams. *Water Power*. 1969. Vol.21, No.3, pages 99-103, No.4, pages 135-139, No.5, pages 172-179.
111. SINCLAIR, S.R. and BROOKER, E.W. The shear strength of Edmonton shale. *Proc. Geotechnical Conference on shear properties of natural soils and rocks*. Oslo, Vol.1, 1967, pages 295-299.
112. SKEWPTON, A.W. and PETLEY, D.J. The strength along discontinuities in stiff clays. *Proc. Geotechnical Conference on shear strength properties of natural soils and rocks*. Oslo, Vol.2. 1968, pages 29-46.
113. LEUSSINK, H. and HULLER-KIRCHENBAUER, H. Determination of the shear strength behaviour of sliding planes caused by geological features. *Proc. Geotechnical Conference on shear strength properties of natural soils and rocks*. Oslo, Vol.1, 1967, pages 131-137.
114. STIMPSON, B. and WALTON, G. Clay mylonites in English coal measures. *Proc. 1st congress Intl. Assoc. Engineering Geology*. Paris, Vol.2, 1970. pages 1388-1393.
115. PIGOT, C.H. and MACKENZIE, I.D. A method used for an in situ bedrock shear test. *Trans. Intl. Congress on Large Dams*. Edinburgh. Vol.1, 1964. pages 495-512.
116. BRAWNER, C.O. Case studies of stability on mining projects. *Proc. 1st Intl. Conference on Stability in Open Pit Mining*. Vancouver, 1970. Published by AIME, New York, 1971, pages 205-226.
117. NOSE, M. Rock test in situ, conventional tests on rock properties and design of Kurobegwa No.4 Dam thereon. *Trans. Intl. Congress on Large Dams*. Edinburgh, Vol.1, 1964. pages 219-252.
118. EVDOKIMOV, P.D. and SAPEGIN, D.D. A large-scale field shear test on rock. *Proc. 2nd Congress Intl. Society for Rock Mechanics*. Belgrade, Vol.2, 1970, Paper 3.17.
119. DROZD, K. Variations in the shear strength of a rock mass depending upon the displacements of the test blocks. *Proc. Geotechnical Conference on shear strength properties of natural soils and rocks*. Oslo, Vol.1. 1967, pages 265-269.
120. KRSMANOVIC, D., TUFO, M. and LANGDF, Z. Shear strength of rock masses and possibilities of its reproduction on models. *Proc. 1st Congress Intl. Society for Rock Mechanics*. Lisbon, Vol.1, 1966, pages 537-542.
121. KRSMANOVIC, D. and POPOVIC, M. Large scale field tests of the shear strength of limestone. *Proc. 1st Congress Intl. Society for Rock Mechanics*. Lisbon, Vol.1, 1966, pages 773-779.
122. SALAS, J.A.J. and URIEL, S. Some recent rock mechanics testing in Spain. *Trans. Intl. Congress on Large Dams*. Edinburgh, Vol.1, 1964, pages 995-1021.

96. ROSS-BROWN, O.H. and WALTON, G. A portable shear box for testing rock joints. *Rock Mechanics*, Vol.7, No.3, 1975. pages 129-153.
97. BROCH, E. and FRANKLIN, J.A. The point-load strength test. *Intn2. J. Rock Mechanics and Mining Sciences*. Vol.9, 1972, pages 669-697.
98. BIENIAWSKI, Z.T. Estimating the strength of rock materials. *J. South African Institute of Mining and Metallurgy*, Vol. 74, 1974, pages 312-320.
99. BARTON, N.R and CHOUBEY, V. The shear strength of rock joints in theory and practice. *Rock Mechanics*, 1977, In press.
100. DEERE, D.U.. and MILLER. R.P. Engineering classification and index properties for intact rock. *Technical Report No. AFNL-TR-65-116 Air Force Weapons Laboratory. New Mexico, 1966.*
101. PITEAU, D.R. Geological factors significant to the stability of slopes cut in rock. *Proc. Symposium on Planning Open Pit Mines. Johannesburg. Published by A.A. Balkema, Amsterdam, 1971, pages 33-53.*
102. ROBERTSON, A.M. The interpretation of geological factors for use in slope theory. *Proc. Symposium on Planning Open Pit Mines. Johannesburg. Published by A.A. Balkema. Amsterdam, 1971, pages 55-70.*
103. SERAFIM, J.L. Rock Mechanics considerations in the design of concrete dams. *Proc. Intl. Conference on State of Stress in the Earth's Crust. Santa Monica, California. Published by Elsevier, New York, 1964, pages 611-645.*
104. HAMROL, A. A quantitative classification of the weathering and weatherability of rocks. *Proc. 5th Intl. Conference on Soil Mechanics and Foundation Engineering, Paris, Vol.2, 1961, pages 771-774.*
105. ROCHA, M. Mechanical behaviour of rock foundations in concrete dams. *Trans. 8th International Congress on Large Dams. Edinburgh. Vol.1, 1964, pages 785-831.*
106. FOOKES. P.G., DEARMAN, W.R. and FRANKLIN. J.A. Some engineering aspects of rock weathering with field examples from Dartmoor and elsewhere. *Quarterly J. Engineering Geology. Vol.4, 1971, pages 139-185.*
107. FRANKLIN, J.A and CHANDRA, A. The Slake-durability test. *Intl. J. Rock Mechanics and Mining Sciences. Vol 9, 1972, pages 325-341.*
108. BARTON, N.R. A review of the shear strength of filled discontinuities in rock. *Norwegian Geotechnical Institute Publication No. 105, 1974. 38 pages.*
109. RUIZ, M.D.. CAMARGO, F.P., MIDEA, N.F. and NIEBLE, C.H. Some considerations regarding the shear strength of rock masses. *Proc. Intl. Rock Mechanics Symposium, Madrid, 1968, pages 159-169.*

Chapter 5 references

82. BARTON, N.R. Review of a new shear strength criterion for rock joints. *Engineering Geology*, Elsevier. Vol.?, 1973. pages 287-332.
83. PAULDING, B.W.Jr. Coefficient of friction of natural rock surfaces. *Proc. ASCE J. Soil Mech. Foundation Div.* Vol. 96 (SM2), 1970, pages 385-394.
84. RENCERS, N. Roughness and friction properties of separation planes in rock. *Thesis*. Tech. Hochschule Fredericiana, Karlsruhe, Inst. Bodenmech. Felsmch. Veröff, 47, 1971, 129 pages.
85. LANDANYI, B. and ARCHAHBAULT, G. Simulation of shear behaviour of a jointed rock mass. *Proc. 11th Symposium on Rock Mechanics*, published by AIME, New York, 1970, pages 105-125.
86. LANDANYI, B. and ARCHAHBAULT, G. Evaluation de la résistance au cisaillement d'un massif rocheux fragmenté. *Proc. 24th International Geological Congress*, Montreal, 1972, Section 13D, pages 249-260.
87. FAIRHURST, C. On the validity of the Brazilian test for brittle materials. *Intl. J. Rock Mechanics and Mining Sciences*. Vol. 1, 1964, pages 535-546.
88. HDEK, E. Brittle failure of rock. *Rock Mechanics in Engineering Practice*. Edited by K.G. Stagg and O.C. Zienkiewicz, Published by J. Wiley, London, 1968, pages 99-124.
89. MARTIN, G.R. and MILLER, P.J. Joint strength characteristics of a weathered rock. *Proc. Third Congress International Society for Rock Mechanics*, Denver, Vol. 2A, 1974, pages 263-270.
90. BARTON, N.R. A relationship between joint roughness and joint shear strength. *Proc. International Symposium on Rock Fracture*. Nancy, France, 1971. Paper 1-8.
91. BARTON, N.R. A model study of the behaviour of excavated slopes. *Ph.D. Thesis*, University of London, Imperial College of Science and Technology. 1971, 520 pages.
92. SERAFIM, J.L. and LOPES, J.B. In-situ shear tests and triaxial tests on foundation rocks of concrete dams. *Proc. 5th International Conference on Soil Mechanics and Foundation Engineering*. Paris, Vol. VI, 1961, page 533.
93. HAVERLAND, H.L. and SLEBIR, E.J. Methods of performing and interpreting in-situ shear tests. *Proc. 13th Symposium on Rock Mechanics*. ASCE, 1972, pages 107-137.
94. RUIZ, M. and CAMARGO, F. A large scale field test on rock. *Proc. First Congress of the International Society for Rock Mechanics*. Lisbon, Vol. VI., 1966, page 257.
95. BRAUNER, C.D., PENTZ, D.L. and SHARP, J.C. Stability studies of a footwall slope in layered coal deposit. *Proc. 13th Symposium on Rock Mechanics*. ASCE, 1972, pages 329-365.

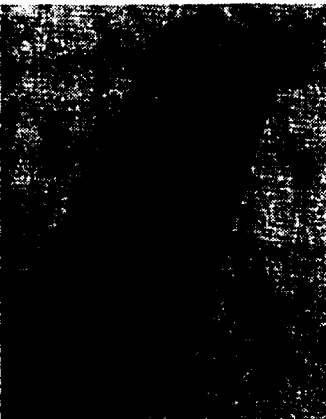
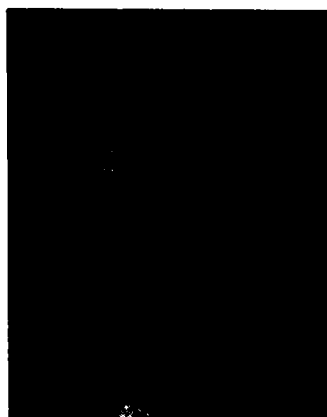
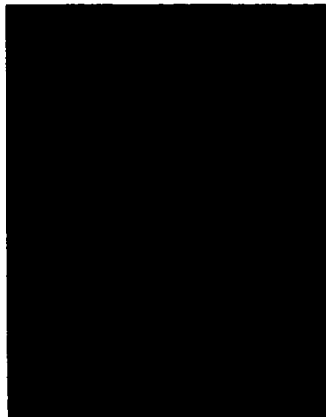
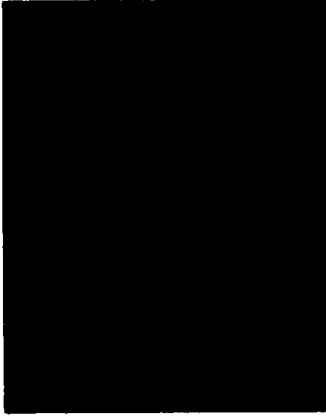


Figure 5.20 : Preservation of fragile rock core in foamed plastic as described by Stimpson, Metcalfe and Walton¹⁵⁸. Steps are described in the text on page 5.35

Note that rubber gloves should be worn when working with component liquids and with unset plastic foam.

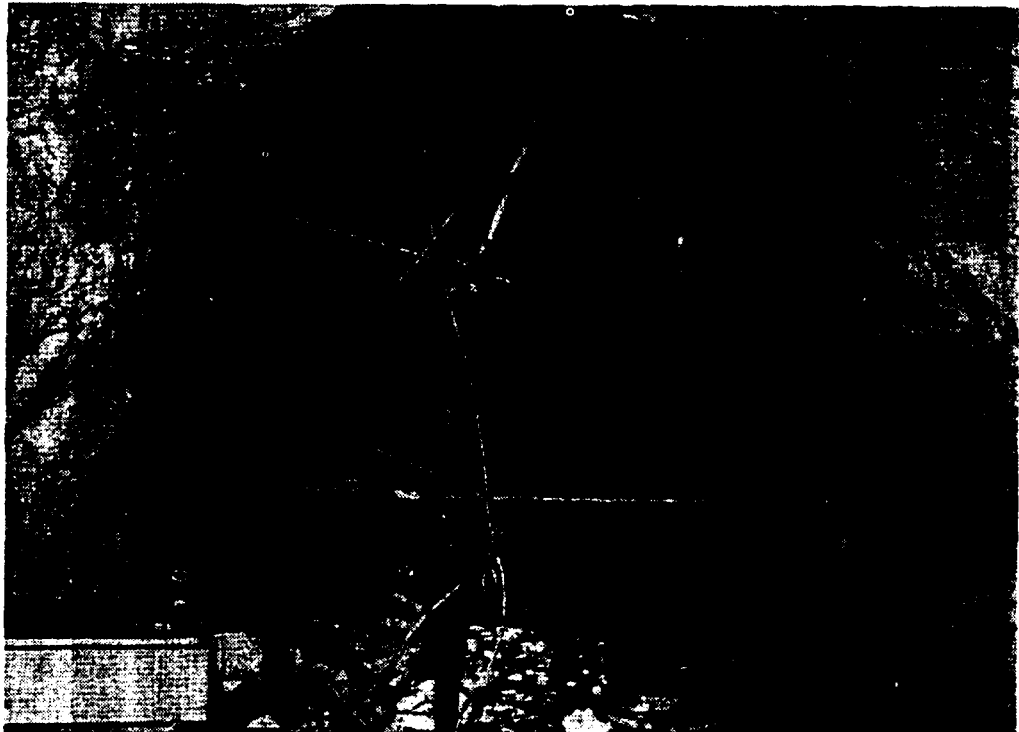


Figure 5.19 : Wire-sawing a shear specimen from the sidewall of a tunnel as described by Londe⁸¹. Photograph reproduced with permission of Pierre Londe, Coyne and Bellier, France.

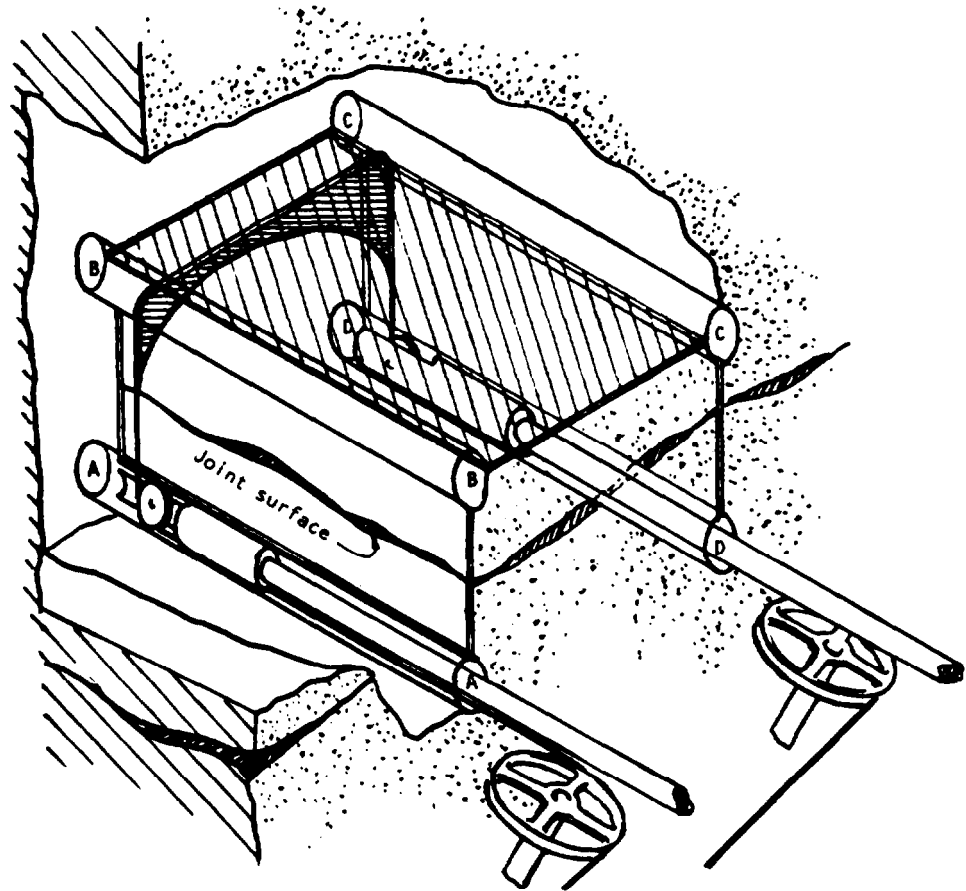


Figure 5.18 : Wire-sawing technique for sampling rock specimens for shear testing, described by Londe⁸¹. See text for details.

main drawback to such samples is their size and this means that the influence of surface roughness must be considered separately. Ideally, small samples should only be used to test infilled or planar joints which do not suffer from roughness effects. This may not always be possible and, when a rough joint is tested, the effect of surface roughness must be assessed and allowed for in the interpretation of the test results.

In order to overcome the size limitation of normal diamond drill core, some slope stability engineers have used large diamond core bits (8 to 10 inches, 200 to 250 mm) mounted on concrete coring rigs which are bolted to the rock face. Obviously, the length of core which can be obtained using such a system is limited to the length of the core barrel which can be supported by the rig and, in general, this is of the order of 1-1/2 to 3 ft. (0.5 to 1 m). In spite of this limitation, some excellent samples have been obtained with equipment of this type.

Londe(81) has described the use of a wire saw for specimen recovery and this technique is illustrated in Figures 5.18 and 5.19. Four holes, marked A, B, C and D in Figure 5.16 are drilled along the top and bottom edges of the specimen. These holes are large enough to accommodate small wheels which change the direction of the wire. Wire cuts are made between holes A-b, B-C and C-D and then the rear face of the specimen is cut free by passing the wire through the side end top cuts and cutting between holes A and D as illustrated in Figure 4.18. Finally, when the rear face has been cut free, the rods carrying the deflection wheels are withdrawn so that the base of the specimen, between holes A and D, is cut free. While this process may appear complex, it has a great deal of merit since wire-sawing is one of the gentlest rock cutting processes and, with care, the specimen can be recovered with very little disturbance.

When sampling rock cores which deteriorate very rapidly on exposure, a technique described by Stimpson, Metcalfe and Walton(158) can be used to protect the core during shipment and to prevent loss of in situ moisture. This technique is illustrated in Figure 5.20 and the steps are described below:

- Step 1 - The mould, consisting of a plastic pipe split along its axis, is prepared to receive the core. The core is supported on thin metal rods held in drilled spacers.
- Step 2 - The core, wrapped in aluminium foil, is placed on the supporting rods and the end spacers are adjusted to the length of the core.
- Step 3 - The upper half of the mould is fixed in place with adjustable steel bands and polyurethane foam is poured through the access slot.
- Step 4 - The foam sets in approximately 30 minutes after which the mould is stripped and the rods withdrawn.
- Step 5 - The core is removed just before testing by cutting the foam with a coarse-toothed wood saw.

does little for the quality of the results obtained from tests on such samples. The fault seldom lies with the geologists in such cases since they are simply doing the best possible job with the resources available. The fault generally lies with those responsible for planning the investigation and with the low priority allocated to shear strength testing.

The authors feel very strongly that poor quality shear tests are worse than no shear tests at all since the results of such tests can be extremely misleading and can give rise to serious errors in slope design. When the funding or the time available on a project is limited or when correct sample collection is impossible for some practical reason, it is recommended that one of the following alternative courses should be followed:

- a. Having established the geological conditions on site as accurately as possible, the slope designer should return to his office and devote the time which he would have spent in sample collection and testing to a thorough study of published papers and reports on slope stability in similar geological environments. It is frequently possible to find cases which have been studied which are very similar to that under consideration and the results presented in such studies may well provide an adequate basis for slope design. When using the results of a published study, extreme care should be taken in checking that the shear strength values were not derived from poor quality tests. It is also important that a sensitivity study should be carried out to determine the influence of shear strength variations on the proposed slope design. If this influence is significant, it may be necessary to insist that a few high quality shear tests be carried out in order to narrow the range of possible variation.
- b. When hand samples are available, shear test samples can be prepared by diamond saw cutting and then lapping the surfaces with a coarse grit. This removes surface roughness effects and reduces the test to one in which the basic angle of friction ϕ is determined. This value is then used, together with surface roughness and joint compressive strength measurements, observations or estimates, to calculate the shear strength of the rock joint by means of Barton's equation (26 on page 5.7) or Ladanyi and Archambault's equation (25 on page 5.6).

When both time and money are available for high quality shear strength testing, the slope designer has to decide upon the type of test which will give the results required. In the case of a critical slope, e.g. the abutment of a bridge, it may be justifiable to carry out in situ tests similar to that illustrated in Figure 5.4 on page 5.10. In many cases it is more economical and more convenient to collect samples in the field for subsequent testing in the laboratory.

The obvious source of samples for shear strength testing is the collection of diamond drill cores which usually are available on project sites. Provided that these cores have been obtained by careful drilling, using double or triple-tube equipment, and provided that the core size is in excess of about 2 inches (50 mm), reasonable samples can be obtained from these cores. The

SOURCE OF SHEAR STRENGTH DATA PLOTTED IN FIGURE 5.17					
<i>oint wnber</i>	<i>Material</i>	<i>Location</i>	<i>Slope height feet</i>	<i>Analysed by</i>	<i>Ref.</i>
1	Disturbed slates and quartzites	Knob Lake, Canada		Coates, Gyenge and Stubbins	144
2	Soil			Whitman and Bailey	145
3	Jointed porphyry	Rio Tinto, Spain	150-360	Hoek	146
4	Ore body hanging wall in granitic rocks	Grangesberg, Sweden	200-800	Hoek	147
5	Maximum height and angle of excavated slopes - see Figure 2.1 on page 2.3.				
6	Bedding planes in limestone	Somerset, England	200	Roberts and Hoek	148
7	London clay	England		Skempton and Hutchinson	149
8	Gravelly alluvium	Pima, Arizona		Hamel	150
9	Faulted rhyolite	Ruth, Nevada		Hamel	151
10	Sedimentary series	Pittsburgh, Pennsylvania		Hamel	152
11	Koal inised granite	Cornwall, England	250	Ley	153
12	Clay shale	Fort Peck Dam, Montana		Middlebrooks	154
13	Clay shale	Gardiner Dam, Canada		Fleming, et al	155
14	Chalk	Chalk cliffs, England	50	Hutchinson	156
15	Bentonite/clay	Oahe Dam, South Dakota		Fleming, et al	155
16	Clay	Garrison Dam, North Dakota		Fleming, et al	155
17	Weathered granites	Hong Kong	40-100	Hoek and Richards	157
18	Weathered volcanics	Hong Kong	100-300	Hoek and Richards	157
19	Folded sandstone, siltstone	Alberta, Canada	800	Wyllie and Munn	158A

Sample collection and preparation

Before leaving the subject of shear strength, the authors feel that some comments must be made on the question of sample collection and preparation for laboratory testing. From the discussion in this chapter it will be clear that samples for laboratory shear testing should be disturbed as little as possible during collection. The importance of the strength of the joint surface material has been emphasized and it is important that this material be retained on the joints to be tested. When the joints are infilled with clay or gouge materials, it is essential that this material should not be disturbed and that the two halves of the specimen should not be displaced relative to one another. When the materials to be tested are sensitive to changes in moisture content, the specimens must be sealed after collection in order to retain the in situ moisture content.

Because of difficulties of access, most samples for shear testing are collected by geologists whose only equipment consists of a geological pick and a backpack. While this may do a great deal to enhance the rugged pioneering spirit of geologists, it

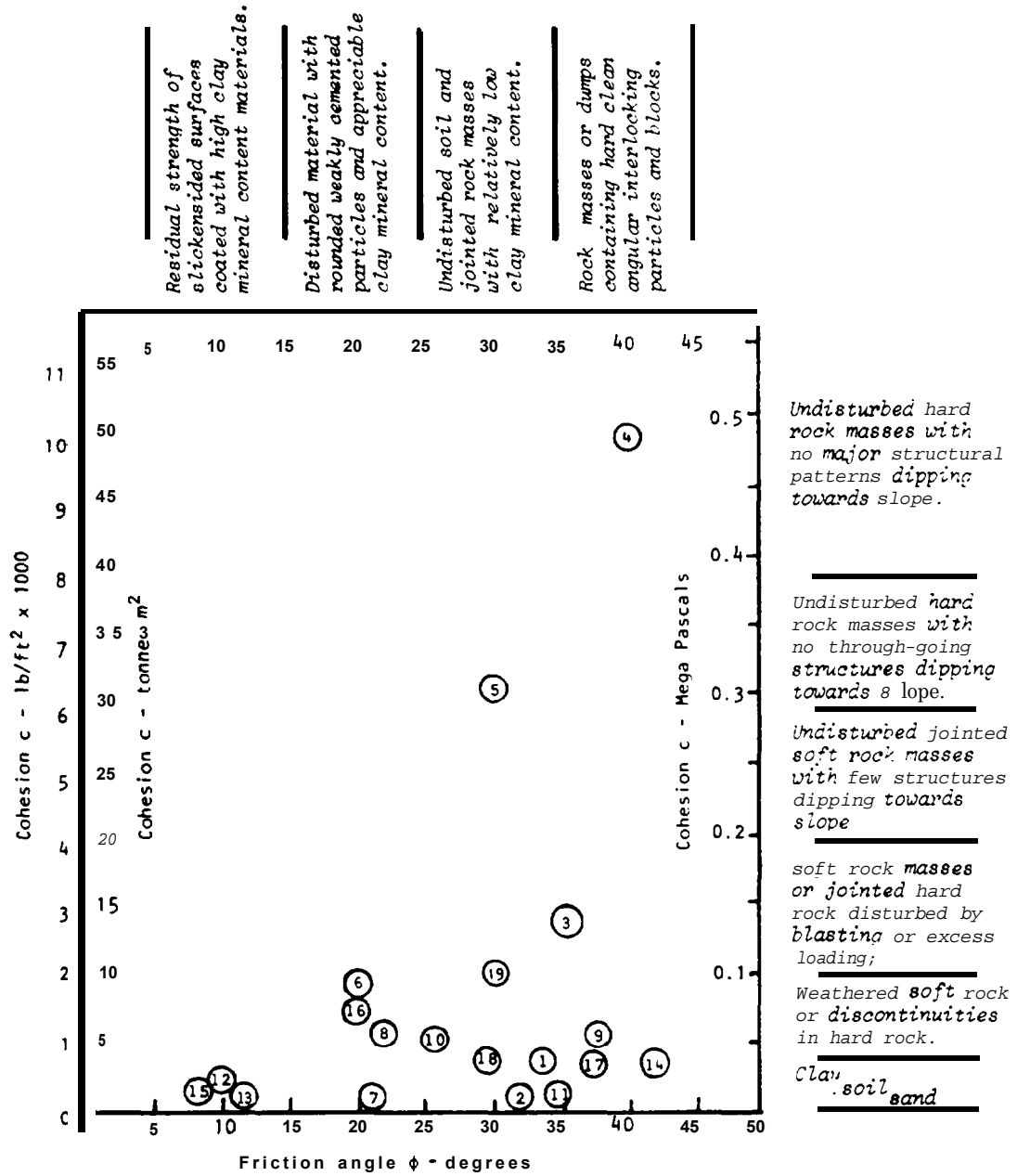


Figure 5.17 : Relationship between the friction angles and cohesive strengths mobilised at failure for the slope failure analyses listed in Table IV.

The simplest type of rock slope failure on which a back-analysis can be carried out is one in which strong structural control is evident. Examples of such failures are given in Figure 1.1 on page 1.3 and Figure 2.8 on page 2.4.

When the plane or planes upon which sliding has occurred are clearly defined and exposed, the dip and dip directions of these planes can be measured with a high degree of accuracy and an analysis can be carried out by means of one of the techniques outlined later in this book. The most significant unknown in these cases is usually the water pressure distribution in the slope at the time of failure. If this cannot be estimated from available data, upper and lower bound estimates of groundwater conditions can be made and a possible range of shear strength values determined by back-analysis. A good example of this type of analysis is given in the study of a limestone quarry slope failure presented on pages 7.25 to 7.30 of this book.

Another simple form of slope failure which can be back-analyzed is that in which the failure surface is approximately circular and it can be assumed that there are no dominant structural features involved in the failure process. In this case, measurement of the failure surface geometry by simple survey techniques together with a knowledge of the slope profile before failure will provide the basic information required for a back-analysis using one of the standard forms of analysis described in Chapter 9.

In carrying out a back-analysis of sliding on a plane or planes or on an approximately circular failure surface, the equations defining the condition of limiting equilibrium can only be solved if it is assumed that the shear strength of the failure surface or surfaces is represented by a simple Mohr-Coulomb failure criterion (equation 10 on page 5.2). Even when this assumption is made, it is not possible to determine the values for both material constants, the cohesive strength c and the angle of friction ϕ , from the back-analysis of a single slope failure. In order to define both material constants it is necessary to back-analyze several failures in the same material or to determine one of the constants, usually the friction angle, by some other means such as direct shear testing in the laboratory.

As pointed out earlier in this chapter, many rough discontinuity surfaces or shear zones in closely jointed rock masses exhibit strongly non-linear Mohr envelopes. The determination of the material constants c and ϕ by means of back-analysis of slope failures is equivalent to determining a tangent to a curved Mohr envelope. This tangent will only give an accurate assessment of the shear strength of the failure surface or zone at the normal stress level which existed during failure of the slopes back-analyzed. Consequently, care must be taken when applying the results obtained from the back-analysis of a particular slope to the design of a slope of different dimensions in which the normal stress levels may be different.

Figure 5.17 is a plot of cohesive strengths and friction angles obtained by back-analysis of the slopes listed in the accompanying table. This figure has been found to provide a useful starting point for stability analysis or a check on the reasonableness of assumed shear strength data. The reader is encouraged to add his or her own points on this plot.

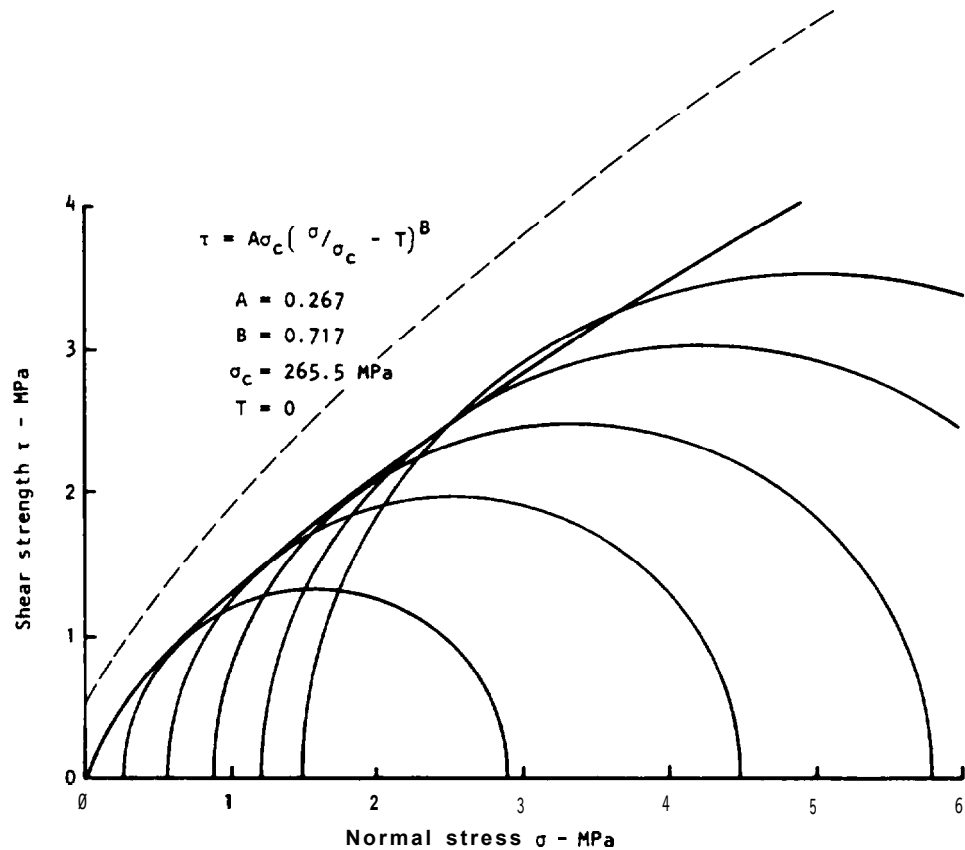


Figure 5.16: Mohr failure circles and fitted Mohr envelope for triaxial tests on recompacted graded samples of closely jointed andesite from Bougainville. Dashed Mohr envelope is for tests by Jaeger on undisturbed cores of the same material (from Figure 5.15).

which gives the lowest factor of safety. This means that it may be necessary to determine the strength characteristics of the individual discontinuity surfaces as well as that of the overall rock mass.

Shear strength determination by back analysis of slope failures

By this time the reader should have been convinced that the determination of the shear strength of rock surfaces or of closely jointed rock masses is not a simple matter. Even when successful tests have been carried out, the slope designer is still faced with the task of relating these test results to the full scale design.

In view of these difficulties, it is tempting to consider the possibility of back analyzing existing slope failures in order to determine the shear strength which must have been mobilized in the full scale rock mass at the time of failure. This technique has been used successfully in soil mechanics for many decades and has contributed significantly to the confidence with which soil slopes can be designed. With care, the same technique can be used to obtain useful data for rock slope design.

that all the individual pieces within the chosen sample volume are collected. A grading curve for the sample is obtained by running the material through a set of sieves and weighing the amount retained on each sieve. The maximum particle size which should be included in the test specimen is about one sixteenth of the diameter of the specimen and, if the grading curve of the field sample gives larger sizes than this, the grading curve should be scaled down. This is done by removing all particles larger than the permitted size and by adjusting the amount retained on each of the smaller sieve sizes until the grading curve is parallel to that of the original sample. Very fine material (less than 200 mesh U.S. standard sieve size) is removed from the sample since this could enter voids between the larger particles and give rise to strength characteristics similar to those of filled joints. The sample is then compacted by placing it in layers into a confining sleeve and subjecting it to vibration and/or direct axial load. If a significant axial load has to be used in order to achieve a unit weight equivalent to the in situ unit weight, some particle breakage will probably occur and the grading curve for the compacted material should be checked. The specimens are now ready for triaxial testing which would normally be carried out in a drained condition, in other words, any water pressure which could build up in the specimen is allowed to dissipate by loading at a sufficiently slow rate and by providing drainage in the loading platens.

Figure 5.16 gives a set of results obtained for such a series of tests which were carried out on 6 inch (153 mm) diameter specimens of recompacted graded andesite from Bougainville. The dashed curve included in this figure has been transferred from Figure 5.15 and represents the Mohr failure envelope for the undisturbed cores of the same material tested by Jaeger. The authors consider the two Mohr envelopes given in this figure to represent the upper and lower bounds for the shear strength of the closely jointed andesite in situ.

Note that test results such as those presented in Figures 5.15 and 5.16 should only be used for slope design purposes when the user is convinced that the failure mechanism in the sample is representative of that which is likely to occur in the rock mass in which the slope is to be excavated. In the case of closely jointed rock masses, this generally means that the failure would involve some form of kink band formation, such as that illustrated in the lower margin photograph on page 5.22, and that slope failure would occur along an approximately circular failure path similar to that which occurs in waste rock fills or soil slopes. If it is suspected that faults or dominant bedding planes or joints could control the slope failure, then this type of testing is inappropriate and the results could be misleading if used for slope design. In such cases, the shear strength characteristics of the individual planes of weakness should be determined, as discussed earlier in this chapter, and the slope design should be based upon a mechanism which recognizes the potential for failure along these planes rather than along a path of least resistance through the rock mass.

In cases in which the failure mechanism which could occur in a slope is not obvious, the only safe approach to follow is to analyze all those failure modes which are kinematically possible and to base the design of the slope upon that analysis

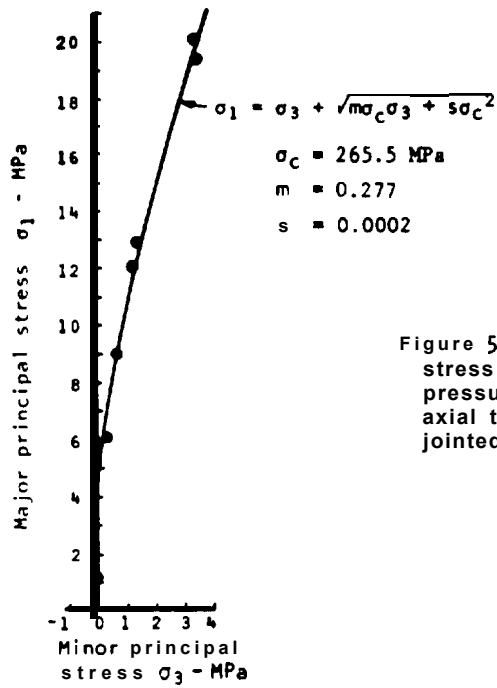


Figure 5.14 : Relationship between axial failure stress (major principal stress σ_1) and confining pressure (minor principal stress σ_3) from tri-axial tests on undisturbed cores of heavily jointed andesite tested by Jaeger¹⁴².

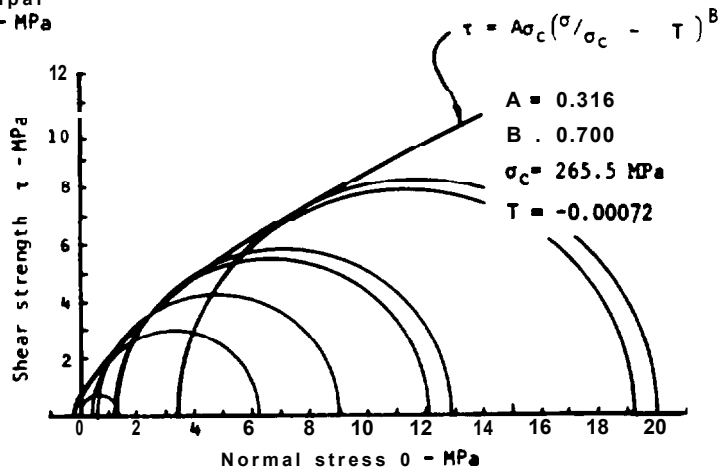


Figure 5.15: Mohr envelope for triaxial tests on heavily jointed andesite tested by Jaeger¹⁴².

Triaxial test results obtained by Jaeger^{1,2} on closely jointed andesite from Bougainville.

Axial failure stress σ_1 MPa	Confining pressure σ_3 MPa
1.24	0
6.07	0.35
8.96	0.69
12.07	1.24
12.82	1.38
19.31	3.45
20.00	3.45

In the inner core tubes to Jaeger's laboratory in Canberra. In the laboratory, the core tubes were cut carefully along two diametrically opposite axial lines so that one half of the tube could be lifted off, leaving the undisturbed core resting in the remaining half of the core tube. The core was then wrapped in thin copper sheeting and carefully rolled over to transfer the core from the core tube into the copper sheet which was then soldered to form a sealed sleeve. The specimen ends were prepared by careful diamond sawing through the copper sheathed core.

Cores, prepared in the manner described, were tested in a triaxial cell such as that illustrated diagrammatically in the margin sketch on page 5.24. The results obtained by Jaeger, for confining pressures of up to 3.5 MPa, are listed in the margin and are plotted in Figures 5.14 and 5.15.

Regression analysis of these data, using the analysis presented in Appendix 1, gives the following values for the constants required to solve equations 29 and 30:

$$\begin{aligned} \sigma_c &= 265.5 \text{ MPa}^* \\ m &= 0.277 \\ s &= 0.0002 \\ A &= 0.316 \\ B &= 0.700 \\ T &= -0.00072 \end{aligned}$$

Substitution of these values into equations 29 and 30 define the curves plotted in Figure 5.14 and 5.15. The correlation coefficient of 0.99 given by the regression analysis is reflected in the close fit of the empirical curves to the test data.

Many civil engineering laboratories have large triaxial cells designed for testing rock fill for dams and some of these cells are suitable for tests similar to those carried out by Jaeger. One such cell was used by the Snowy Mountains Authority and is illustrated in the margin photograph. Marsal(137) has described the design of a very large cell to accommodate 1130 mm diameter by 2500 mm high specimens. These large cells are very expensive to manufacture and to operate and most laboratories use smaller cells designed to accommodate 153 mm (6 inch) diameter cylindrical samples. Testing procedures should follow the guidelines set out by Bishop and Henkel(143) for the triaxial testing of soils.

The recovery of undisturbed samples of closely jointed rock is a very difficult process and, in many cases, may not be possible because of the lack of adequate facilities. Under such circumstances, the authors feel that a reasonable alternative is to approach the problem as one would that of testing compacted rock fill. The procedure for testing rock fill has been described by Marsal(137) and by Marachi, Chan and Seed(138) and is outlined briefly in the following notes.

A representative sample of the materials collected from an exposure of the rock mass. No attempt is made to prevent the particles from falling apart but care should be taken to ensure

*Determined by regression analysis of triaxial test data on intact andesite core(136).



Large triaxial cell for rock-fill testing in the laboratory of the Snowy Mountains Authority in Australia.

TABLE IV - APPROXIMATE RELATIONSHIP BETWEEN ROCK MASS QUALITY AND EMPIRICAL CONSTANTS •					
Empirical failure criterion $\sigma_1 = \sigma_3 + \sqrt{m\sigma_c\sigma_3 + s\sigma_c^2}$ $\tau = A\sigma_c(\sigma/\sigma_c - T)B$ where $T = \frac{1}{2}(m - \sqrt{m^2 + 4s})$	CARBONATE ROCKS WITH WELL-DEVELOPED CRYSTAL CLEAVAGE <i>dolomite, limestone and marble</i>	LITHIFIED ARGILLACEOUS ROCKS <i>mudstone, siltstone, shale and slate (normal to cleavage)</i>	ARENACEOUS ROCKS WITH STRONG CRYSTALS AND POORLY DEVELOPED CRYSTAL CLEAVAGE <i>sandstone and quartzite</i>	FINE-GRAINED POLYMINERAL-LIC IGNEOUS CRYSTALLINE ROCKS <i>andesite, dolerite, diabase and rhyolite</i>	COARSE-GRAINED POLYMINERAL-LIC IGNEOUS AND METAMORPHIC CRYSTALLINE ROCKS <i>amphibolite, gabbro, gneiss, granite, norite and quartz-diorite.</i>
INTACT ROCK SAMPLES <i>Laboratory size specimens free from joints</i> CSIR rating 100 NGI rating 500	m = 7.0 s = 1.0 A = 0.816 B = 0.658 T = -0.140	m = 10.0 s = 1.0 A = 0.918 B = 0.677 T = -0.099	m = 15.0 s = 1.0 A = 1.044 B = 0.692 T = -0.067	m = 17.0 s = 1.0 A = 1.086 B = 0.696 T = -0.059	m = 25.0 s = 1.0 A = 1.220 B = 0.705 T = -0.040
VERY GOOD QUALITY ROCK MASS <i>Tightly interlocking undisturbed rock mass to 3m. weathered rock to 10m.</i> CSIR rating 85 NGI rating 100	m = 3.5 s = 0.1 A = 0.651 B = 0.679 T = -0.028	m = 5.0 s = 0.1 A = 0.739 B = 0.692 T = -0.020	m = 7.5 s = 0.1 A = 0.848 B = 0.702 T = -0.013	m = 8.5 s = 0.1 A = 0.883 B = 0.705 T = -0.012	m = 12.5 s = 0.1 A = 0.998 B = 0.712 T = -0.008
GOOD QUALITY ROCK MASS <i>Fresh to slightly weathered rock with joints to 10m.</i> CSIR rating 65 NGI rating 10	m = 0.7 s = 0.004 A = 0.369 B = 0.669 T = -0.006	m = 1.0 s = 0.004 A = 0.427 B = 0.683 T = -0.004	m = 1.5 s = 0.004 A = 0.501 B = 0.695 T = -0.003	m = 1.7 s = 0.004 A = 0.525 B = 0.698 T = -0.002	m = 2.5 s = 0.004 A = 0.603 B = 0.707 T = -0.002
FAIR QUALITY ROCK MASS <i>Several sets of moderately weathered joints spaced at 1m.</i> CSIR rating 44 NGI rating 1.0	m = 0.14 s = 0.0001 A = 0.198 B = 0.662 T = -0.0007	m = 0.20 s = 0.0001 A = 0.234 B = 0.675 T = -0.0005	m = 0.30 s = 0.0001 A = 0.280 B = 0.688 T = -0.0003	m = 0.34 s = 0.0001 A = 0.295 B = 0.691 T = -0.0003	m = 0.50 s = 0.0001 A = 0.346 B = 0.700 T = -0.0002
POOR QUALITY ROCK MASS <i>Numerous weathered joints at 30 to 50mm with some clean waste rock.</i> CSIR rating 23 NGI rating 0.1	m = 0.04 s = 0.00001 A = 0.115 B = 0.646 T = -0.0002	m = 0.05 s = 0.00001 A = 0.129 B = 0.655 T = -0.0002	m = 0.08 s = 0.00001 A = 0.162 B = 0.672 T = -0.0001	m = 0.09 s = 0.00001 A = 0.172 B = 0.676 T = -0.0001	m = 0.13 s = 0.00001 A = 0.203 B = 0.686 T = -0.0001
VERY POOR QUALITY ROCK MASS <i>Numerous heavily weathered joints spaced <50mm with gouge - waste with fines.</i> CSIR rating 3 NGI rating 0.01	m = 0.007 s = 0 A = 0.042 B = 0.534 T = 0	m = 0.010 s = 0 A = 0.050 B = 0.539 T = 0	m = 0.015 s = 0 A = 0.061 B = 0.546 T = 0	m = 0.017 s = 0 A = 0.065 B = 0.548 T = 0	m = 0.025 s = 0 A = 0.078 B = 0.556 T = 0

* Note: The CSIR and NGI methods of classifying rock masses are described in Appendix 9.

The corresponding relationship between shear strength τ and the normal stress σ at failure is:

$$\tau = A\sigma_c (\frac{\sigma}{\sigma_c} - T)^B \quad (30)$$

where A and B are constants defining the shape of the Mohr failure envelope and

$$T = \frac{1}{2}(m - \sqrt{m^2 + 4s})$$

Hoek and Brown have assumed that the effective stress law (see page 2.8) applies to this failure criterion and that effective stresses may be calculated as follows:

$$\begin{aligned} \sigma_1' &= (\sigma_1 - u) \\ \sigma_3' &= (\sigma_3 - u) \\ \sigma' &= (\sigma - u) \end{aligned}$$

These effective stress values may be substituted directly into equations 29 and 30 when the pore water pressure u is known.

A regression analysis for the determination of the constants m , s , A and B from the results of laboratory triaxial tests on closely jointed rock is presented in Appendix 1 at the end of this book.

When laboratory test data are not available or when it is required to estimate the strength of a large rock mass, Hoek and Brown have proposed that the rock mass classifications of Barton, et al (140) and Bieniawski (141) be used to scale the values of the constants m , s , A and B. A full discussion on this scaling is given in the textbook by Hoek and Brown (134) and the proposed relationship between rock type and rock mass quality and the values of the constants has been summarized in Table IV on page 5.26.

An example of the application of Hoek and Brown's empirical failure criterion is discussed in the next section of this chapter and the application of this failure criterion in the analysis of circular failure in closely jointed rock slopes is discussed in Chapter 9.

Testing closely jointed rock

The determination of the strength of a closely jointed rock mass presents formidable experimental problems and relatively few attempts have been made to carry out direct shear or triaxial tests on these materials.

Jaeger (142) has described one of the most elaborate tests ever attempted on closely jointed rock and his paper is recommended reading for anyone faced with this problem. The rock mass tested by Jaeger was an andesite from the site of the open pit mine on Bougainville in Papua New Guinea. This hard rock is divided up by several sets of joints spaced at about one inch apart. The joints are free from infilling but are slightly weathered as a result of high water flows.

Six inch (153 mm) diameter cores were recovered by very careful triple-tube diamond drilling and these cores were transported

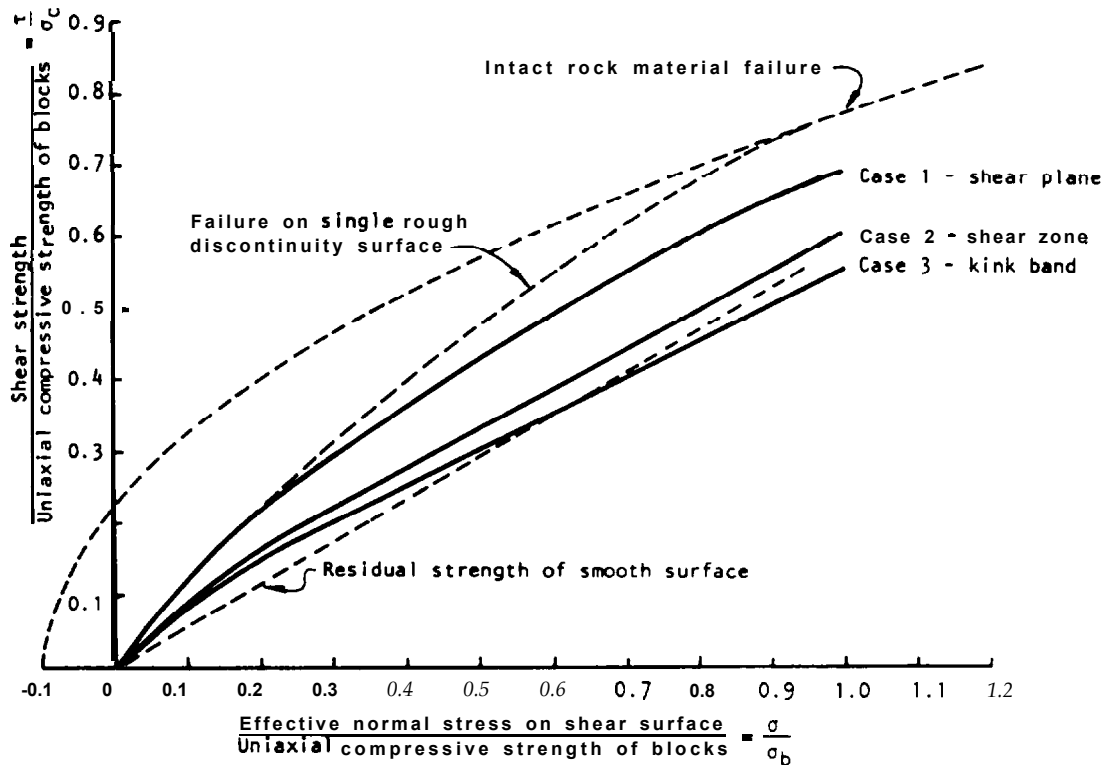


Figure 5.13 : Shear strength curves for three types of failure in closely jointed interlocking rock masses. Plotted for $i = 20^\circ$ and $\phi = 30^\circ$.

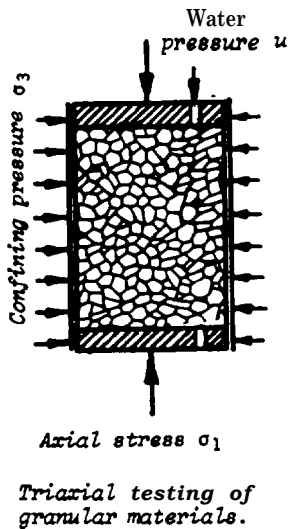
While Ladanyi and Archambault's approach is attractive because it involves a consideration of the mechanics of block movement and failure within a rock mass, it is difficult to apply in practice because of the choice of the various parameters ($\eta, n, \sigma_c, K, L, \phi$ and i) which are required to solve the equations. In fact, one generally has to guess most of these parameters in order to arrive at a solution.

In recognition of the problem of adequately defining the geometrical and material property parameters required in a mechanistic approach such as that adopted by Ladanyi and Archambault, Hoek and Brown (134, 135, 136) have proposed a very simple empirical failure criterion for closely jointed rock masses.

The basic empirical equation relating the axial failure stress σ_1 to the confining pressure σ_3 , in a triaxial test such as that illustrated in the margin sketch, is:

$$\sigma_1 = \sigma_3 + \sqrt{m\sigma_c\sigma_3 + s\sigma_c^2} \tag{29}$$

where σ_c is the uniaxial compressive strength of the intact rock pieces, and m and s are dimensionless constants which depend upon the shape and degree of interlocking of the individual pieces of rock within the mass.



where

$$\dot{v} = (1 - \frac{\sigma}{\sigma_c})^K \tan i \quad (28a)$$

$$a_s = 1 - (1 - \frac{\sigma}{\sigma_c})^L \quad (28b)$$

and σ_c is the uniaxial compressive strength of the individual blocks within the rock mass,

η is the degree of interlocking which defines the freedom of the blocks to translate and to rotate before being sheared or fractured*.

The suggested values for K, L and η for the three types of failure are as follows:

Case 1 - shear plane formation, K = 4 and L = 1.5 as for single rough discontinuity surfaces (page 5.7) with $\eta = 0.7$ to allow for loosening of the rock mass as a result of close jointing.

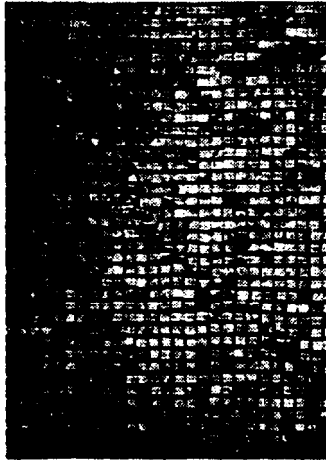
Case 2 - shear zone formation, K = 5 to allow for increased freedom of block to rotate, L = $\tan i$ and $\eta = 0.6$ which allows for a looser rock mass than in case 1.

Case 3 - kink band formation, K = 5 as for case 2 and L = $(2/n_r)^3 \tan i$ where n_r is the number of rows of blocks in the kink band which is normally 3 to 5. In this case $\eta = 0.5$ to allow for the very loose condition of the rock mass.

Figure 5.13 gives a set of shear strength curves, calculated by means of equations 28, 28a and b using $\phi = 30^\circ$, $i = 20^\circ$ and, for case 3, $n_r = 4$ in addition to the values suggested above. For comparison, the shear strengths for intact rock and for failure on a single rough discontinuity and the residual strength of a smooth plane are shown as dashed curves. These curves are reproduced from Figure 5.1 assuming $\sigma_j = \sigma_c$.

The curve for case 1, the formation of a single shear plane, coincides with that for a rough joint at very low normal stresses when the behavior is strongly dilatant. As the normal stress increases, the curve for the rock mass falls below that for the intact rock as a result of the weakening effect of the close jointing. Rosengren and Jaeger (133) noted this type of behaviour on tests on marble which had been heated to break the grain boundary material, resulting in a very tightly interlocking model rock mass. In spite of the fact that the grains were still in their original positions, the fact that the tensile strength of the grain boundaries has been reduced to zero gave rise to a strength reduction of about 20% at high normal stresses.

*In Ladanyi and Archambault's original equations, the term $\eta\sigma_c$ appears in equations 28, 28a and b. The authors have omitted η from equations 28a and b because they consider that it applies to the interlocking of the rock mass and not to the dilatation rate \dot{v} and the sheared area a_s which are functions of the shape and orientations of the individual blocks within the rock mass.



Shear plane



Shear zone



Kink band

Shear strength of closely jointed rock masses

When a hard rock mass contains a number of joint sets and when the joint spacing is very close, in relation to the size of slope being considered, the behavior of the rock mass may differ significantly from that of the single discontinuity surface considered in the first part of this chapter. The loosened state of the rock mass, resulting from the close jointing, permits individual blocks within the mass to translate and to rotate to a far greater degree than can occur in more intact rock and this gives rise to an overall strength reduction.

The determination of the shear strength of closely jointed rock masses has long been recognized as an important engineering problem and a number of excellent papers have been published on this subject (85,86,129-136). Closely related research has also been carried out on the shear strength characteristics of rock fill (137-139) and many similarities can be found between the results of this work and that on closely jointed rock. It would not be practical to attempt a detailed review of all of this work in this book and the discussion which follows will be limited to the relationship proposed by Ladanyi and Archambault (85,86) and the empirical equation published recently by Hoek and Brown (134,135) and Hoek (136).

Ladanyi and Archambault carried out a large number of model studies using small blocks of commercially compressed concrete. Each model contained 1800 blocks measuring 1/2" x 1/2" x 2.5" packed tightly together to form a 2.5" thick model slab. Biaxial loads were applied in the plane of the model slab, the loading direction being varied in relationship to the "joint" orientation.

Three distinct types of failure occurred and these are illustrated in the photographs reproduced in the margin.

- Case 1 - Shear along a well defined plane inclined to both discontinuity sets.
- Case 2 - Formation of a narrow failure zone in which block rotation has occurred in addition to the sliding and material failure of Case 1.
- Case 3 - Formation of a kink band of rotated and separated columns of 3, 4 or 5 blocks.

On the basis of these model studies, Ladanyi and Archambault proposed modified forms of equations 22, 23 and 24 (pages 5.6 and 5.7) which could be used in equation 21 to predict the shear strength of closely jointed rock masses. After very careful consideration of these modifications and after discussion with Ladanyi, the authors have introduced a further slight modification which removes an anomaly which can occur when using Ladanyi and Archambault's equations. The final equations resulting from these discussions and modifications are as follows:

$$\tau = \frac{\sigma(1 - a_s)(\dot{\nu} + \tan \phi) + a_s \gamma \sigma_c \frac{\sqrt{1+n} - 1}{n} (1 + n \frac{\sigma}{\gamma \sigma_c})^{\frac{1}{2}}}{1 - (1 - a_s) \dot{\nu} \tan \phi} \quad (28)$$

TABLE III - SHEAR STRENGTH OF FILLED DISCONTINUITIES

Rock	Description	Peak strength		Residual strength		Tested by
		'kg/cm'	ϕ°	'kg/cm'	ϕ°	
Basalt	Clayey basaltic breccia, wide variation from clay to basalt content.	2.4	42			Ruiz, Camargo Midea and Nieble ¹⁰⁹ .
Bentonite	Bentonite seam in chalk Thin layers Triaxial tests	0.15 9-1.2 6-1.0	7.5 2-17 9-13			Link ¹¹⁰ Sinclair and Brooker ¹¹¹
Bentonitic shale	Triaxial tests Direct shear tests	1-2.7	1.5-29	0.3	8.5	Sinclair and Brooker ¹¹¹
Clays	Over-consolidated, slips, joints and minor shears	1-1.8	2-18.5	0-0.03	0.5-16	Skempton and Petley ¹¹²
Clay shale	Triaxial tests	0.6	32			Sinclair and Brooker ¹¹¹
Clay shale	Stratification surfaces			0	9-25	Leusink and Muller-Kirchbauer ¹¹³
Coal measure rocks	Clay mylonite seams, 1.3 to 2.5cm thick	1.11-0.13	16	0	1-11.5	Stimpson and Walton ¹¹⁴
Dolomite	Altered shale bed, approximately 15 cm thick.	0.41	14.5	0.22	17	Pigot and Mackenzie ¹¹⁵
Diorite, granodiorite and porphyry	Clay gouge (2% clay, PI = 17%)	0	26.5			Brawner ¹¹⁶
Granite	Clay filled faults Weakened with sandy-loam fault filling Tectonic shear zone, schistose and broken granites, disintegrated rock and gouge.	1-1.1 0.5 2.42	14-45 40 42			Rocha ¹⁰⁵ Nose ¹¹⁷ Evdokimov and Sapagin ¹¹⁸
Greywacke	1-2mm clay in bedding planes			0	21	Drozd ¹¹⁹
Limestone	6mm clay layer			0	13	Krsmenovic et al ¹²⁰
	1-2cm clay fillings <1mm clay fillings	1.0 5-2.0	13-14 17-21			Krsmenovic & Popovic ¹²¹
Limestone, marl and lignites	Interbedded lignite layers Lignite/marl contact	0.8 1.0	38 10			Salas and Uriel ¹²²
Limestone	Marlaceous joints, 2cm thick	0	25	0	15-24	Bernaix ¹²³
Lignite	Layer between lignite and underlying clay	14-0.	5-17.5			Schultze ¹²⁴
Montmorillonite clay	8 cm seams of bentonite (montmorillonite) clay in chalk	3.6 16-0.	14 .5-11.	0.8	11	Eurenus ¹²⁵ Underwood ¹²⁶
Schists, quartzites and siliceous schists.	10-15cm thick clay filling Stratification with thin clay Stratification with thick clay	3-0.8 1-7.4 3.8	32 41 31			Serafim and Guerreiro ¹²⁷
Slates	Finely laminated and altered	0.5	33			Coates, McRorie and Stubbs ¹²⁸
Quartz/kaolin/pyrolusite	Remoulded triaxial tests	42-0.	16-38			

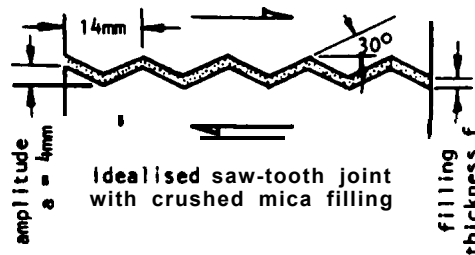
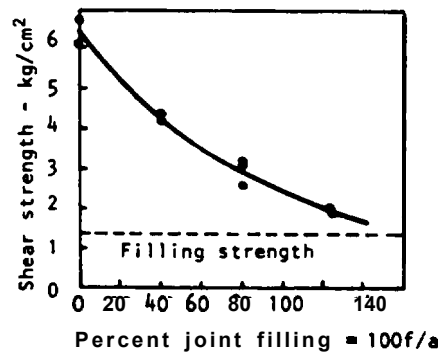


Figure 5.12: Influence of joint filling thickness on the shear strength of an idealised saw-tooth joint. After Goodman³⁹.



carried out in accordance with well established soil mechanics principles.

Another major factor which must be considered in relation to filled joints is the influence which they have on the permeability of the rock mass. The permeability of clay gouge and similar joint filling material may be three or four orders of magnitude lower than that of the surrounding rock mass and this can give rise to damming of ground water into compartments within the rock mass. When water pressure is allowed to build up behind a clay-filled discontinuity such as a fault, the overall stability of the slope can be jeopardized and the situation is made worse by the fact that this filling material has a very low shear strength and that failure of the slope may be initiated along this discontinuity.

From this discussion it will be clear that an extremely important aspect of a site investigation program for a rock slope design is the detection of major discontinuities which are filled with clay or other filling materials. If the presence of such discontinuities is suspected, a special effort should be made during the site investigation program to check whether they do exist. This may involve the drilling of holes in critical locations as well as the careful tracing of outcrops and intersections with any existing excavations. Determination of the orientation and inclination of such discontinuities for subsequent inclusion in stability analyses is important as is the sampling of the filling material for shear strength testing.

The roughness angle ζ which is required for an evaluation of Ladanyi and Archambault's equation can be obtained from measurements such as those described in Figure 4.4 on pages 4.9 and 4.10. Care should be taken to ensure that the scale of measurement is appropriate to the scale of the problem. In very large slopes features such as folds in the bedding planes may contribute to the effective roughness of the potential sliding surface. The average ζ value for such surfaces can be measured off photographs, as was done by Patton(40), or by measuring the dips, with a geological compass, along a line marked on the plane. This line should be in the direction of potential sliding and should be long enough to ensure that several roughness "wavelengths" are included in the measurement.

Barton's Joint Roughness Coefficient (JRC) is only approximately related to the roughness angle ζ and he suggests(82) that the value of JRC should be estimated by simple visual comparison with Figure 5.2. Note that two scales are given in this figure and that the user would use the scale most appropriate to the problem which he is considering.

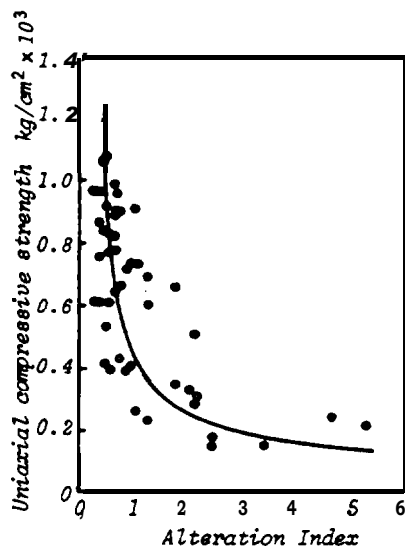
Shear strength of filled discontinuities

Up to this point the discussion has been restricted to the shear strength of surfaces in which rock-to-rock contact occurs along the entire length of the surface. A common problem which is encountered in rock slope design is a discontinuity which is filled with some form of soft material. This filling may be detrital material or gouge from previous shear movements, typical in faults, or it may be material which has been deposited in open joints as a result of the movement of water through the rock mass. In either case, the presence of a significant thickness of soft, weak filling material can have a major influence on the stability of the rock mass.

Goodman(39) demonstrated the importance of joint fillings in a series of tests in which artificially created sawtooth joint surfaces were coated with crushed mica. The decrease in shear strength with increasing filling thickness is illustrated in Figure 5.12 which shows that, once the filling thickness exceeds the amplitude of the surface projections, the strength of the joint is controlled by the strength of the filling material.

A very comprehensive review of the shear strength of filled discontinuities has been prepared by Barton(108) and this paper is highly recommended to any reader who wishes to study this subject in greater detail. A list of shear strength values for filled joints, based upon one compiled by Barton, is given in Table III.

When a major discontinuity with a significant thickness of filling is encountered in a rock mass in which a slope is to be excavated, it is prudent to assume that shear failure will occur through the filling material. Consequently, at least for the preliminary analysis, the influence of surface roughness should be ignored and the shear strength of the discontinuity should be taken as that for the filling material. Determination of the shear strength of this filling material should be



Variation of compressive strength with degree of alteration for a granite. After Serafim¹⁰³.

Approximate values for the basic friction angle ϕ for different rocks.

Rock	ϕ -degrees
Amphibolite	32
Basalt	31 - 36
Conglomerate	35
Chalk	30
Dolomite	27 - 31
Gneiss (schistose)	23 - 29
Granite (fine grain)	29 - 35
Granite (coarse grain)	31 - 35
Limestone	33 - 40
Porphyry	31
Sandstone	25 - 35
Shale	27
Siltstone	27 - 31
Slate	25 - 30

Lower value is generally given by tests on wet rock surfaces. After Barton⁸².

A final question which must be considered when estimating the compressive strength of the material adjacent to the discontinuity surface relates to the weathering or alteration of the material. This question has been discussed by Barton⁽⁸²⁾ who suggests that weathering can reduce the strength of the near surface material to as low as one quarter of the uniaxial compressive strength of the intact unweathered material. This process will vary according to the rock type since very dense and impervious rocks such as basalt would gradually acquire a thin skin of weathered material, granites would weather more deeply and, porous rock such as sandstone could weather more or less uniformly to considerable depth.

The graph reproduced in the margin is from Serafim⁽¹⁰³⁾ and shows the significant strength reduction with increasing alteration. The alteration index, described by Hemrol⁽¹⁰⁴⁾, is the weight of water absorbed by the rock in a quick absorption test, divided by the dry weight of rock, expressed as a percentage. Rocha⁽¹⁰⁵⁾ has also shown the rapid fall in shear strength of rock which is associated with the first few per cent increase in alteration index. Useful discussions on weathering have also been given by Fookes, Dearman and Franklin⁽¹⁰⁶⁾ and Franklin and Chandra⁽¹⁰⁷⁾.

Because of the wide range of conditions which can be encountered in the field, the authors have not attempted to give specific guidelines on the allowance which should be made for weathering when considering the uniaxial compressive strength of rock in order to determine the joint wall compressive strength σ_j . The reader should be aware of this problem and should give consideration to the allowance which he should make under each particular set of circumstances.

Turning to the question of the basic friction angle ϕ for use in Ladanyi and Archambault's and in Barton's equations, ideally, this quantity should be determined by direct shear testing on smooth rock surfaces which have been prepared by means of a clean, smooth diamond saw cut. Alternatively, residual shear strength values, obtained from shear tests in which the specimen has been subjected to considerable displacement, can be used to obtain the value of ϕ . Note that either of these tests should be carried out over a range of normal stress levels to ensure that a linear relationship between shear strength and normal stress with zero cohesion is obtained. This precaution is necessary because the shear strength at very low normal stresses can be influenced by extremely small surface roughness on the specimen. Tilting tests, in which the angle of inclination of the specimen required to cause sliding is measured, are not reliable for the determination of the basic friction angle because of the influence of very small scale surface roughness.

If a shear test is carried out on a field sample with rough surfaces, the surface profile can be measured, before testing, and the average roughness angle Z subtracted from the angle of inclination of the line relating shear strength to normal stress. This correction should only be used when the shear test results fall reasonably close to a straight line which passes through the origin.

When no test results are available, the tabulation given in the margin can be used to obtain an estimate of the basic angle of friction.

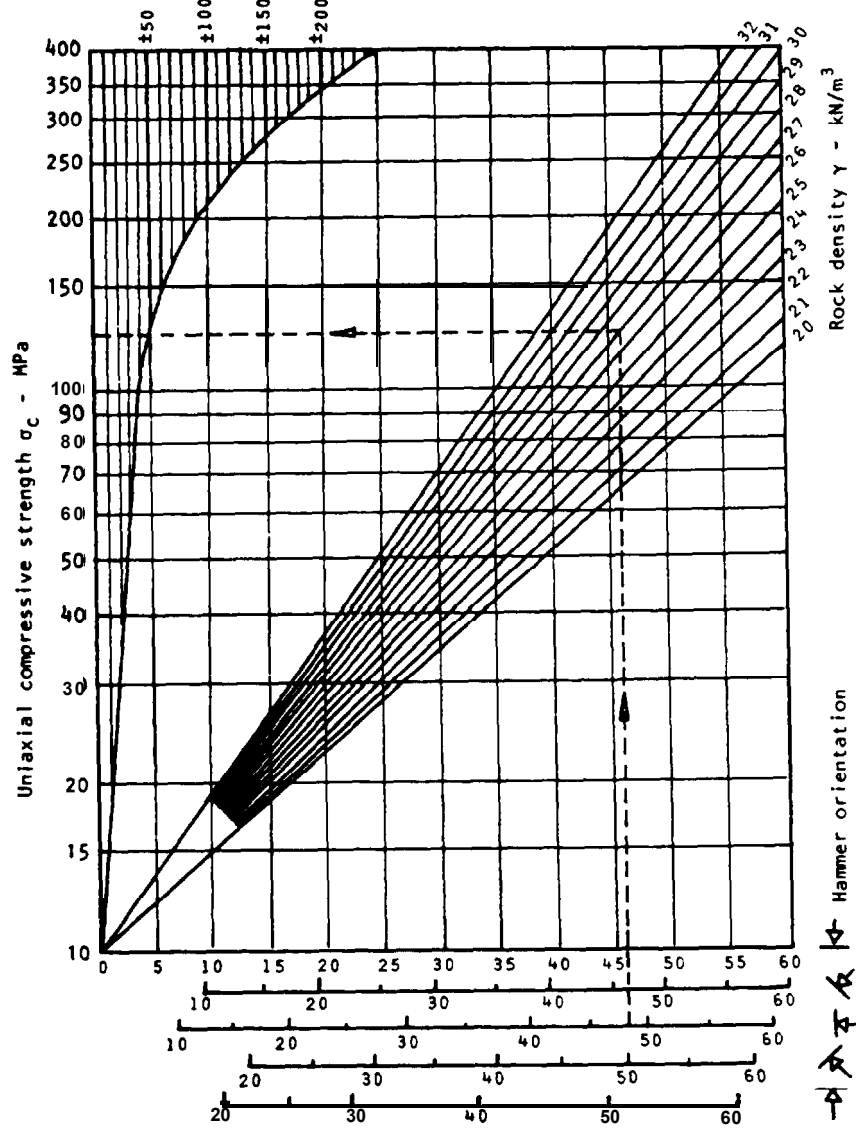
When the slope designer finds himself in a situation where no facilities at all are available, for example on a proposed highway during the earliest route location studies, he has to resort to a method of determining the compressive strength of the rock by a method which is best termed "kicking the rock". In order to assist such an adventurer, a very approximate set of guidelines have been tabulated below, based upon papers by Deere and Miller(100), Piteau(101), Robertson(102) and upon consulting experience. Cohesive soils have been included in this table since these are important as joint filling materials, to be discussed in the next section.

TABLE II - APPROXIMATE CLASSIFICATION OF COHESIVE SOIL AND ROCK

No.	Description	axial compressive strength			Examples
		lb/in ²	kg/cm ²	MPa	
S1	VERY SOFT SOIL - easily moulded with fingers, shows distinct heel marks.	<5	<0.4	0.04	
S2	SOFT SOIL - moulds with strong pressure from fingers, shows faint heel marks.	5-10	0.4-0.8	0.04-0.08	
S3	FIRM SOIL - very difficult to mould with fingers, indented with finger nail, difficult to cut with hand spade.	10-20	0.8-1.5	0.08-0.15	
S4	STIFF SOIL - cannot be moulded with fingers, cannot be cut with hand spade, requires hand picking for excavation.	20-80	1.5-6.0	0.15-0.60	
S5	VERY STIFF SOIL - very tough, difficult to move with hand pick. pneumatic spade required for excavation.	80-150	6-10	0.6-1.0	
R1	VERY WEAK ROCK - crumbles under sharp blows with geological pick point, can be cut with pocket knife.	150-3500	10-250	1-25	Chalk, rock salt
R2	MODERATELY WEAK ROCK - shallow cuts or scraping with pocket knife with difficulty, pick point indents deeply with firm blow.	3500-7500	250-500	25-50	Coal, schist, siltstone
R3	MODERATELY STRONG ROCK - knife cannot be used to scrape or peel surface, shallow indentations under firm blow from pick point.	7500-15000	500-1000	50-100	Sandstone, slate, shale
R4	STRONG ROCK - hand-held sample breaks with one firm blow from hammer end of geological pick.	15000-30000	1000-2000	100-200	Marble, granite, gneiss
R5	VERY STRONG ROCK - requires many blows from geological pick to break intact sample.	> 30000	> 2000	> 200	Quartzite, dolerite, gabbro, basalt

the graph as 125 ± 50 MPa. Note that the hammer should always be perpendicular to the rock surface.

Average dispersion of strength for most rocks - MPa



Schmidt hardness - Type L hammer.

Figure 5.11 : Relationship between Schmidt hardness and the uniaxial compressive strength of rock, after Deere and Miller (100).

$$1 \text{ MPa} = 1 \text{ MN/m}^2 = 10.2 \text{ kg/cm}^2 = 145 \text{ lb/in}^2$$

$$1 \text{ kN/m}^3 = 102 \text{ kg/m}^3 = 6.37 \text{ lb/ft}^3$$



Figure 5.9: Point load test equipment manufactured by Engineering Laboratory Equipment Limited, Hemel Hempstead, Hertfordshire, England.

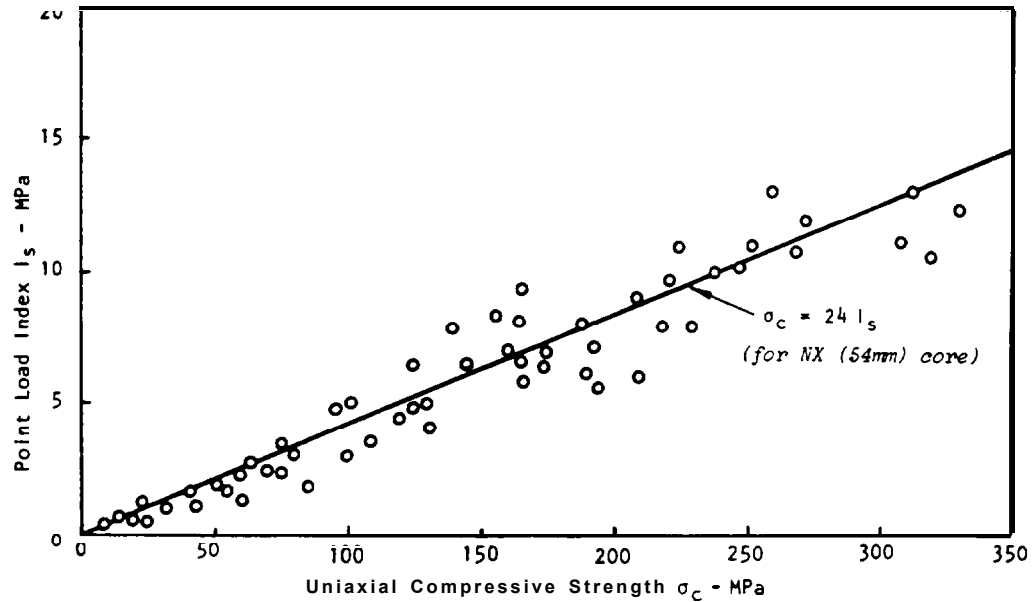


Figure 5.10: Relationship between point load strength index and uniaxial compressive strength. $1 \text{ MPa} = 10.2 \text{ kg/cm}^2 = 145 \text{ lb/in}^2$.

A less reliable but simpler alternative to the point load test for determining the uniaxial compressive strength of rock is the use of the Schmidt hammer (89,99). An advantage of this method is that it can be applied directly to an unprepared joint surface and can be used to obtain a direct estimate of the joint compressive strength σ_j .

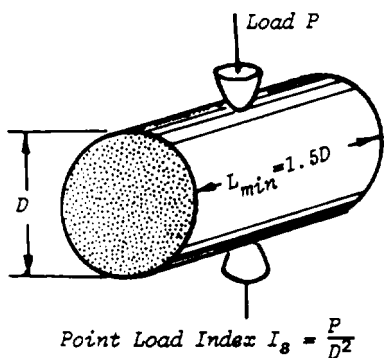
The relationship between compressive strength and Schmidt hardness is given in Figure 5.11. Suppose that a horizontally held type L hammer gives a reading of 48 on a rock with a density of 27 kN/m^3 , the uniaxial compressive strength σ_c is given by

specimen surface before testing, from the measured angle ($\phi + \lambda$) as determined in the test.

Estimating joint compressive strength and friction angle

When it is impossible to carry out any form of shear test, the shear strength characteristics of a rock surface can be approximated from Ladanyi and Archambault's equation or from Barton's equation. In order to solve either of these equations it is necessary to determine or to estimate values for σ_j , the joint material compressive strength, ϕ , the basic angle of friction of smooth surfaces of this rock type and λ , the average roughness angle of the surface or JRC, Barton's Joint Roughness Coefficient.

The uniaxial compressive strength of the joint wall material can be obtained by coring through the joint surface and then testing specimens prepared from this core. This is a complex process and, if facilities and time are available to carry out such tests, they would almost certainly be available for a direct shear test. Consequently, uniaxial compressive strength tests on material samples would seldom be a logical way in which to obtain the value of σ_j .



A simpler alternative which can be used in either the field or the laboratory is the Point Load Index test (97). This simple and inexpensive test can be carried out on unprepared core and the loading arrangement is illustrated in the margin sketch. Two types of commercially available point load testing machine are illustrated in Figures 5.8 and 5.9. A reasonable correlation exists between the Point Load Index and the uniaxial compressive strength of the material (98), as shown in Figure 5.10 and is given by:

$$\sigma_c = 24 I_s^* \quad (27)$$

where σ_c is the uniaxial compressive strength and I_s is the point load strength index.

Note that σ_j , the compressive strength of the rock material adjacent to the joint surface, may be lower than σ_c as a result of weathering or loosening of the surface.

In order to judge whether a point load test is valid, the fractured pieces of core should be examined. If a clean fracture runs from one loading point indentation to the other, the test results can be accepted. However, if the fracture runs across some other plane, as may happen when testing schistose rocks, or if the points sink into the rock surface causing excessive crushing or deformation, the test should be rejected.



Figure 5.8: Point Load Index test ● quipment manufactured by Robertson Research Ltd., Llandudno, North Wales.

*The constant of 24 in this equation is for a 54 mm core. Values for other core sizes are:
20 mm-17.5, 30 mm-19, 40 mm-21, 50 mm-23, 60 mm-24.5



Figure 5.7a: Sample , wired together to prevent premature movement along the discontinuity, is aligned in a mould and the lower half is cast in concrete, plaster or similar material. When the lower half is set, the upper half of the mould is fitted and the entire mould plus sample is turned upside-down in order that the second half of the casting can be poured.

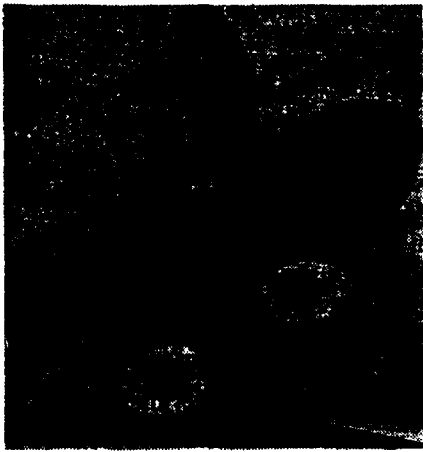
Figure 5.7b: Specimen, still wired together, is fitted into the lower shear box and the upper shear box is then fitted in place. Note that the load cables can be bent out of the way for easy access.



Figure 5.7c: The wires binding the specimen halves together are cut; and the normal and shear loads are applied.

specimen together are then cut and the shear load cable is placed in position.

- C. The specimen is now ready for testing and the normal load is increased to the value chosen for the test. This normal load is maintained constant while the shear load is increased. A note is kept of displacements during the application of the shear load.
- d. Once the peak strength has been exceeded, usually after a shear displacement of a few millimeters, the displacement is allowed to continue and it will be found that a lower shear load is required in order to sustain movement.
- e. The machine illustrated is limited to a displacement of approximately 1 inch (2.5 cm) and, in order to determine the residual shear strength, a displacement in excess of this value is normally required. This can only be achieved if the normal load is released and the upper half of the specimen is moved back to its starting position. In another version of the machine, manufactured by Robertson Research Ltd., a second jack acting in opposition to the shear load jack has been added to allow for shear reversal under constant normal load.



Portable shear machine with two shear load jacks which allow shear reversal under constant normal load.

Which of these systems is more representative of the shearing process in the rock mass is uncertain since, in one case, the detrital material is disturbed when the normal load is released while, in the other, the direction of rolling of the particles is reversed. It is possible that different rock structures behave differently under these conditions. The authors tend to prefer the single jack system since they feel that it is important that the direction of shearing under load should be kept constant.

- f. In this, as in most shear machines, the loads applied to the specimen are measured and these have to be divided by the surface area of the discontinuity surface in order to obtain normal and shear stresses. The initial area should be determined by direct measurement and the reduction in surface area with displacement should be calculated.
- g. The shear strength of rock is not generally sensitive to the loading rate and no difficulty should arise if the loads are applied at a rate which will permit measurements of loads and displacements to be carried out at regular intervals. A typical test would take between 15 and 30 minutes.

The specimen size which can be accommodated in the portable shear machine illustrated in Figure 5.6 is limited to about 4 inches x 4 inches (10 cm x 10 cm) and this means that it is very difficult to test joints with surface roughness which is representative of the in situ conditions. Consequently, it is recommended that the use of this machine should be restricted to the measurement of the basic friction angle ϕ . This can be done by testing sawn surfaces or by testing field samples and by subtracting the average roughness angle δ , measured on the

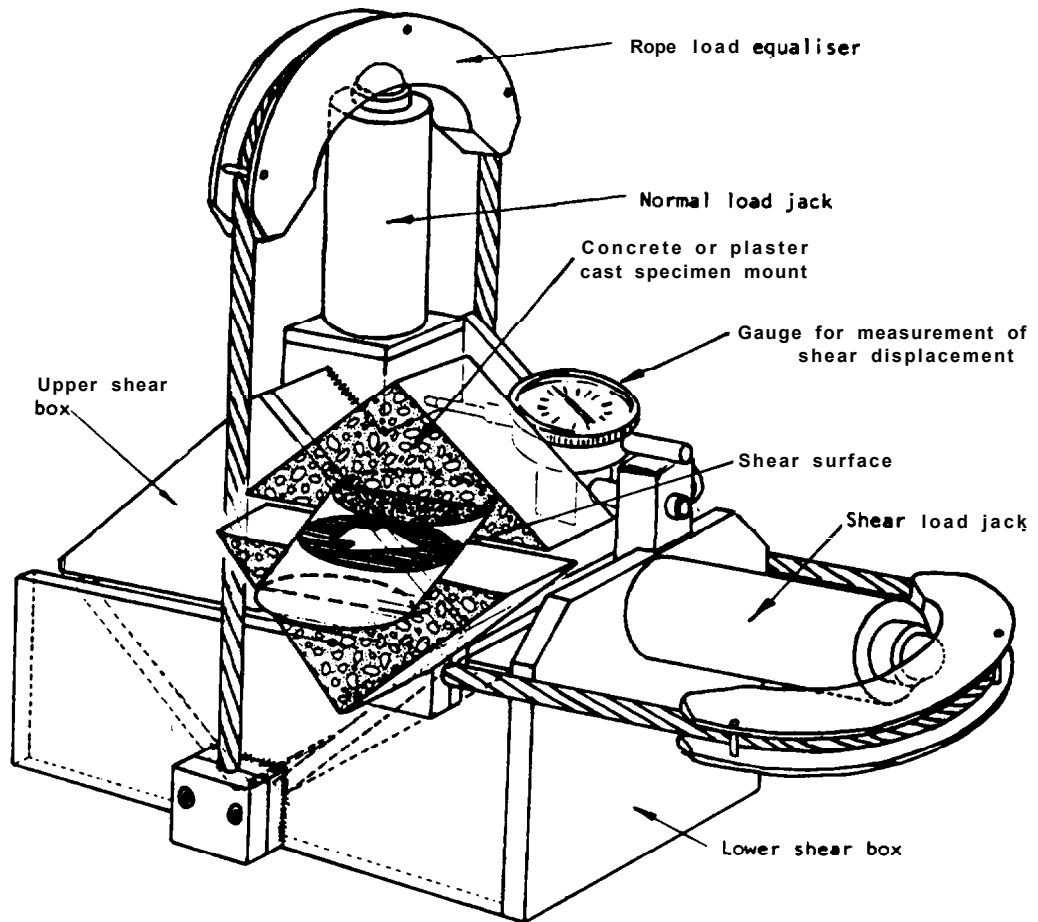


Figure 5.6: Drawing of a portable shear machine showing the position of the specimen and the shear surface. Drawing adapted from one by Robertson Research Ltd. A typical machine is 20 inches (51 cm) long and 18 inches (48 cm) high and weighs 85 lb. (39 kg.)

Figure 5.4: In situ direct shear test at Auburn dam site, after Haverland and Slebir⁹³.

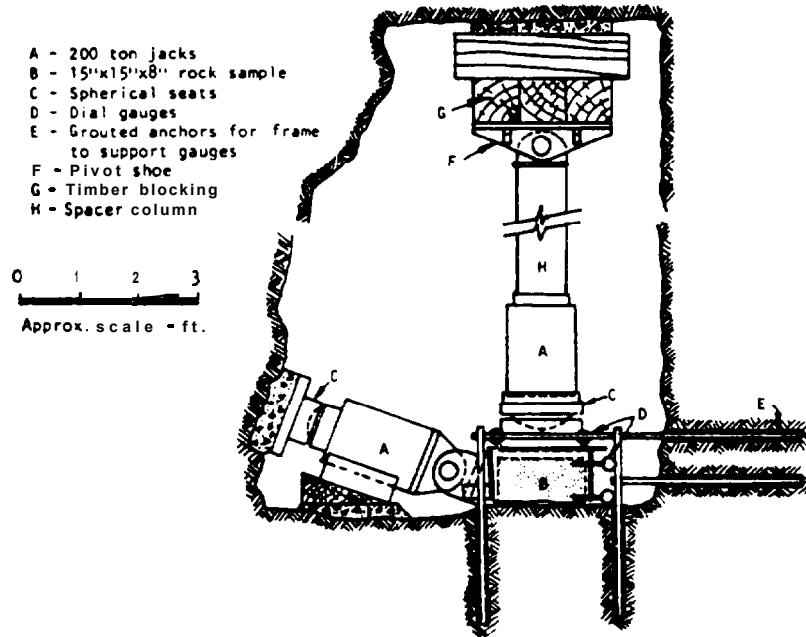


Figure 5.5: Large scale laboratory shear machine at the Imperial College of Science and Technology, London.

rock mass. On the other hand, preliminary stability calculations carried out during the route location studies for a new highway are generally restricted in terms of access to the rock mass and also time and money available for the study, hence elaborate and expensive testing is not justified. Under these circumstances, realistic estimates of the shear strength on the basis of the approaches proposed by Barton and by Ladanyi and Archunbault normally have to be used.

Figure 5.4 illustrates the arrangements for a large scale in-situ shear test to be carried out in an underground adit. This type of test costs several thousands of dollars and would only be justified under the most critical conditions. Alternative in situ shear test arrangements have been discussed by Serafim and Lopes(92), Haverland and Sieblir(93), Rulz and Camargo(94) and Brawner, Pentz and Sharp(95).

A laboratory shear machine designed and built at the Imperial College of Science and Technology in London is illustrated in Figure 5.5. This machine accepts samples of approximately 12 inches x 16 inches and has a capacity of 100 tons in both normal and shear directions. The loading rate is variable over a very wide range and normal and shear displacements can be monitored continuously during the test. Individual tests on this machine are relatively expensive and its use is normally only justified on major projects.

A portable shear machine for testing rock discontinuities in small field samples has been described by Ross-Brown and Walton(96) and a drawing of this machine is presented in Figure 5.6. This machine was designed for field use and many of the refinements which are present on larger machines were sacrificed for the sake of simplicity. Any competent machine shop technician should be capable of fabricating such a machine and the reader is encouraged to utilize the ideas presented in Figure 5.6 to develop his own shear testing equipment. Alternatively, machines manufactured to this design are available commercially from Robertson Research Ltd., Llandudno, North Wales.

The steps involved in testing a sample in the portable shear machine are illustrated in Figure 5.7 and these steps are described below:

- a. A sample containing the discontinuity to be tested is trimmed to a size which will fit into the mould. The two halves are wired together in order to prevent movement along the discontinuity and the sample is then cast in plaster or concrete. Care must be taken that the discontinuity is positioned accurately so that it lies in the shear plane of the machine. A bed of clean gravel, placed in the bottom of the first mould, is sometimes helpful in supporting the specimen during setting up and, provided that a wet mix is used, the gravel can be left in place so that it becomes part of the casting.
- b. Once the castings have set, the mould is stripped and the specimen is transferred into the shear machine. The upper shear box is set in position and a small normal load is applied in order to prevent movement of the specimen. The wires binding the two halves of the

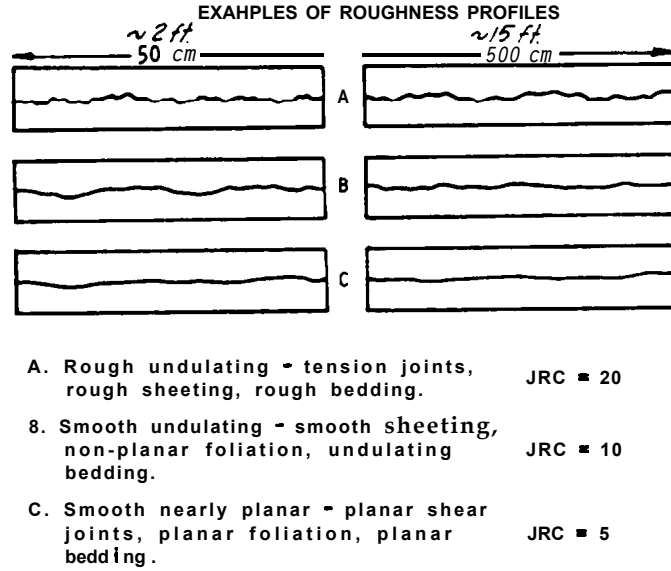


Figure 5.2: Barton's definition of Joint Roughness Coefficient JRC.

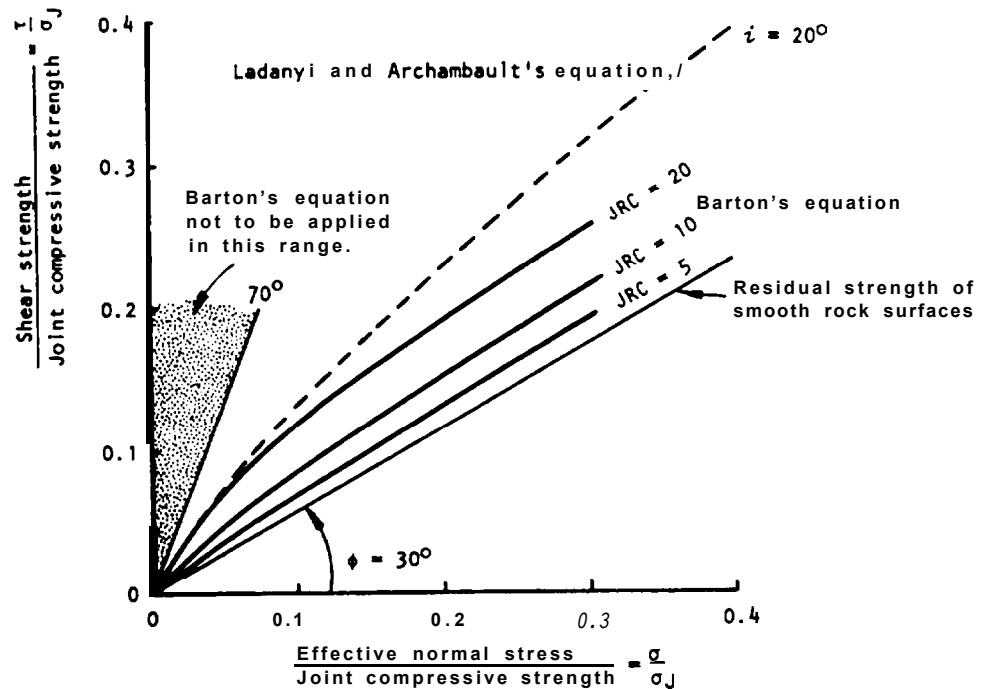


Figure 5.3 Barton's prediction for the shear strength of rough discontinuities.

An alternative approach to the problem of predicting the shear strength of rough joints was proposed by Barton (82). Based upon careful tests and observations carried out on artificially produced rough "joints" in material used for model studies of slope behavior (90,91), Barton derived the following empirical equation:

$$\tau = \sigma \tan(\phi + JRC \cdot \log_{10} \frac{\sigma_j}{\sigma}) \quad (26)$$

where JRC is a Joint Roughness Coefficient which is defined in Figure 5.2. The roughness angle ζ in equation 20 has been replaced by the normal stress dependent term containing JRC.

Barton's equation has been plotted in Figure 5.5, for JRC values of 20, 10 and 5. For comparison the residual strength of a smooth joint with $\phi = 30^\circ$ and Ladanyi and Archambault's equation for $\zeta = 20^\circ$ and $\phi = 30^\circ$ are included in the same figure.

Note that, while Barton's equation is in close agreement with Ladanyi and Archambault's (for $\zeta = JRC = 20$) at very low normal stress levels, the equations diverge as the normal stress level increases. This is because Barton's equation reduces to $\tau = \sigma \tan \phi$ as $\sigma_j/\sigma \rightarrow 1$ whereas Ladanyi and Archambault's equation reduces to $\tau = \tau_r$, the shear strength of the rock material adjacent to the joint surface. Barton's equation tends, therefore, to be more conservative than Ladanyi and Archambault's at higher normal stress levels.

Barton's original studies were carried out at extremely low normal stress levels and his equation is probably most applicable in the range $0.01 < \sigma/\sigma_j < 0.3$. Since the normal stress levels which occur in most rock slope stability problems fall within this range, the equation is a very useful tool in rock slope engineering and the authors have no hesitation in recommending its use within the specified stress range. Note that, as $\sigma/\sigma_j \rightarrow 0$, the logarithmic term in equation 26 tends to infinity and the equation ceases to be valid. Barton (82) suggests that the maximum value of the term in the brackets in equation 26 should be 70° as shown in Figure 5.3.

Shear testing of discontinuities in rock

From the discussion presented in the preceding pages it will be evident that, in order to obtain shear strength values for use in rock slope design, some form of testing is required. This may take the form of a very sophisticated laboratory or in situ test in which all the characteristics of the in situ behavior of the rock discontinuity are reproduced as accurately as possible. Alternatively, the test may involve a very simple determination or even estimate of the joint compressive strength σ_j , the roughness angle ζ and the basic friction angle for use in Barton's or Ladanyi and Archambault's equation. The choice of the most appropriate method depends upon the nature of the problem being investigated, the facilities which are available and the amount of time and money which has been allocated to the solution of the problem. In carrying out a detailed design for a critical slope such as that adjacent to a major item of plant or in the abutment of an arch dam, no expense and effort would be spared in attempting to obtain reliable shear strength values for critical discontinuities encountered in the

where, for rough rock surfaces, $K = 4$ and $L = 1.5$.

Substituting equations 22, 23 and 24 with $n = 10$, $K = 4$ and $L = 1.5$ into equation 21, and dividing through by σ_j , one obtains the following equation:

$$\frac{\tau}{\sigma_j} = \frac{\frac{\sigma}{\sigma_j} (1 - \frac{\sigma}{\sigma_j})^{1.5} \left[(1 - \frac{\sigma}{\sigma_j})^4 \tan i + \tan \phi \right] + 0.232 (1 - (1 - \frac{\sigma}{\sigma_j})^{1.5}) (1 + 10 \frac{\sigma}{\sigma_j})^{0.5}}{1 - (1 - \frac{\sigma}{\sigma_j})^{5.5} \tan i \tan \phi} \quad (25)$$

While this equation may appear complex, it will be noted that it relates the two dimensionless groups τ/σ_j and σ/σ_j , and that the only unknowns are the roughness angle i and the basic friction angle ϕ .

Figure 5.1, below, shows that Ladanyi and Archambault's equation 25 gives a smooth transition between Patton's equation 20 for dilation of a rough surface and Fairhurst's equation 22 for the shear strength of the rock material adjacent to the joints.

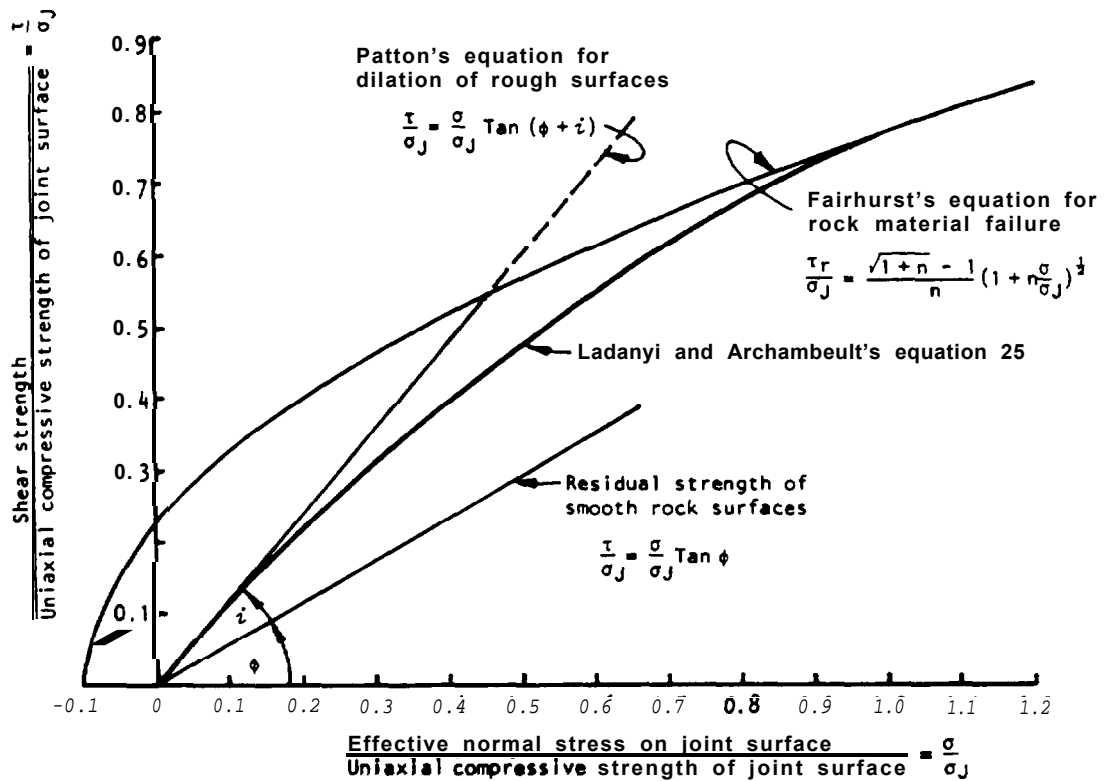


Figure 5.1: Transition from dilation to shearing predicted by Ladanyi and Archambault's equation. Plotted for $i = 20^\circ$ and $\phi = 30^\circ$.

The transition from dilation to shearing was studied theoretically and experimentally by Ladanyi and Archambault (85,86) who proposed the following equation for peak shear strength:

$$\tau = \frac{\sigma(1-a_s)(\dot{v} + \tan \phi) + a_s \cdot \tau_r}{1 - (1-a_s)\dot{v} \tan \phi} \quad (21)$$

where a_s is the proportion of the discontinuity surface which is sheared through projections of intact rock material,

\dot{v} is the dilation rate dv/du at peak shear strength, and

τ_r is the shear strength of the intact rock material.

At very low normal stress levels when almost no shearing through projections takes place, $a_s \rightarrow 0$ and $\dot{v} \rightarrow \tan i$, equation 21 reduces to equation 20. At very high normal stresses when $a_s \rightarrow 1$, $\tau \rightarrow \tau_r$.

Ladanyi and Archambault suggested that τ_r , the shear strength of the material adjacent to the discontinuity surfaces, can be represented by the equation of a parabola in accordance with a proposal by Fairhurst (87):

$$\tau_r = \sigma_c \frac{\sqrt{1+n} - 1}{n} \left(1 + n \frac{\sigma}{\sigma_c}\right)^{\frac{1}{2}} \quad (22)$$

where σ_c is the uniaxial compressive strength of the rock material adjacent to the discontinuity which, due to weathering or loosening of the surface, may be lower than the uniaxial compressive strength of the rock material within the body of an intact block,

n is the ratio of uniaxial compressive to uniaxial tensile strength of the rock material.

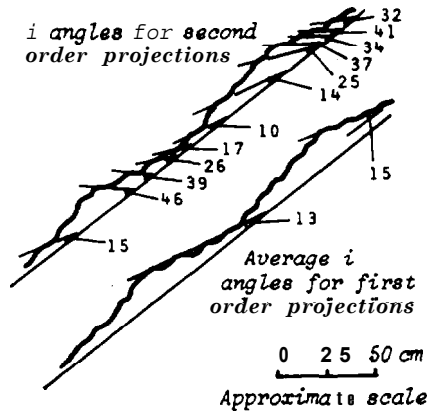
Hoek (88) has suggested that, for most hard rocks, n is approximately equal to 10.

Note that, in using Ladanyi and Archambault's equation, it is not necessary to use the definition of τ_r given by equation 22. Any other appropriate intact rock material shear strength criterion, such as $\tau_r = \sigma_c + \sigma \tan \phi_c$, can be used in place of equation 22 if the user feels that such a criterion gives a more accurate representation of the behavior of the rock with which he is dealing (89).

The quantity a_s in equation 21 is not easy to measure, even under laboratory conditions. The dilation rate \dot{v} can be measured during a shear test but such measurements have not usually been carried out in the past and hence it is only possible to obtain values for \dot{v} from a small proportion of the shear strength data which has been published. In order to overcome this problem and to make their equation more generally useful, Ladanyi and Archambault carried out a large number of shear tests on prepared rough surfaces and, on the basis of these tests, proposed the following empirical relationships:

$$\dot{v} = \left(1 - \frac{\sigma}{\sigma_c}\right)^k \tan i \quad (23)$$

$$a_s = 1 - \left(1 - \frac{\sigma}{\sigma_c}\right)^L \quad (24)$$



Patton's measurement of i angles for first and second order projections on rough rock surfaces.

dered when attempting to understand the behavior of actual rock surfaces.

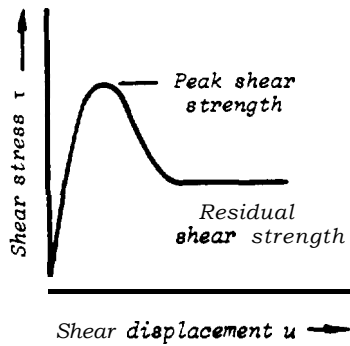
Surface roughness

The discussion on the previous page has been simplified because Patton found that, in order to obtain reasonable agreement between his field observations on the dip of unstable bedding planes and the sum of the roughness angle i and the basic friction angle ϕ , it was necessary to measure only the first order roughness of the surfaces. This is defined in the margin sketch which shows that the first order projections are those which correspond to the major undulations on the bedding surfaces. The small bumps and ripples on the surface have much higher i values and Patton called these the second order projections.

Later studies by Barton (82) show that Patton's results were related to the normal stress acting across the bedding planes in the slopes which he observed. At very low normal stresses, the second order projections come into play and Barton quotes a number of values of $(\phi + i)$ which were measured at extremely low normal stresses. These values are summarized in the following table:

Type of surface	Normal stress ($\phi + i$) σ kg/cm ²		Tested by
Limestone, slightly rough bedding surfaces	1.57	77°	Goodman (39)
	2.09	73°	
	6.00	71°	
Limestone, rough bedding surfaces	3.05	66°	Goodman (39)
	6.80	72°	
Shale, closely jointed sea in limestone	0.21	71°	Goodman (39)
	0.21	71°	
Quartzite, gneiss and amphibolite discontinuities - beneath natural slopes		80°	Paulding (83)
		75°	
Granite, rough undulating artificial tension fractures	1.5	72°	Rengers (84)
	3.5	69°	

Assuming a basic friction angle of 30°, these results show that the effective roughness angle i varies between 40° and 50° for these very low normal stress levels. In fact, one can assume that almost no fracturing of the very small second order projections takes place at these low normal stress levels and that these steep-sided projections control the shearing process. As the normal stress increases, the second order projections are sheared off and the first order projections take over as the controlling factor. One can imagine that, as the normal stress increases even further, the first order projections will be sheared off and a situation will eventually be reached where shearing takes place through the intact rock material which makes up the projections and the effective roughness angle i is reduced to zero.



level, results in the type of curve illustrated in the upper margin sketch. At very small displacements, the specimen behaves elastically and the shear stress increases linearly with displacement. As the forces resisting movement are overcome, the curve becomes non-linear and then reaches a peak at which the shear stress reaches its maximum value. Thereafter the shear stress required to cause further shear displacement drops rapidly and then levels out at a constant value called the residual shear strength.

If the peak shear strength values obtained from tests carried out at different normal stress levels are plotted, a curve such as that illustrated in the center margin sketch results. This curve will be approximately linear, within the accuracy of the experimental results, with a slope equal to the peak friction angle ϕ_p and an intercept on the shear stress axis of c_p , the cohesive strength of the cementing material. This cohesive component of the total shear strength is independent of the normal stress but the frictional component increases with the increasing normal stress as shown in the sketch. The peak shear strength is defined by the equation

$$\tau = c_p + \sigma \tan \phi_p \quad (15)$$

which, with the exception of the subscripts, is identical to equation 1 on page 2.5.

Plotting the residual shear strength against the normal stress gives a linear relationship defined by the equation

$$\tau = \sigma \tan \phi_r \quad (16)$$

which shows that all the cohesive strength of the cementing material has been lost. The residual friction angle ϕ_r is usually lower than the peak friction angle ϕ_p .

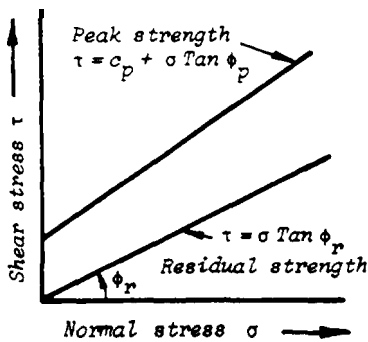
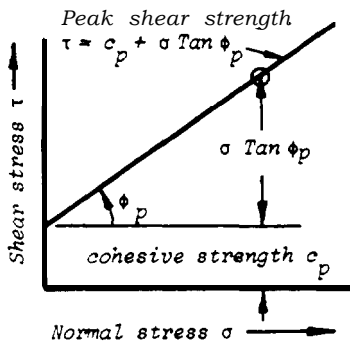
Influence of water on shear strength of planar discontinuities

The most important influence of the presence of water in a discontinuity in rock is a reduction of shear strength due to a reduction of the effective normal stress as a result of water pressure. Equation 10 on page 2.8 shows that this normal stress reduction can be incorporated into the shear strength equation in the following manner:

$$\tau = c + (\sigma - u) \tan \phi \quad (10)$$

where u is the water pressure within the discontinuity and c is either equal to c_p or zero and ϕ either ϕ_p or ϕ_r , depending upon whether one is concerned with peak or residual strength.

As discussed on pages 2.8 and 2.9, the influence of water upon the cohesive and frictional properties of the rock discontinuity depends upon the nature of the filling or cementing material. In most hard rocks and in many sandy soils and gravels, these properties are not significantly altered by water but many clays, shales, mudstones and similar materials will exhibit significant changes as a result of changes in moisture content. It is important, therefore, that shear tests should be carried out on samples which are as close as possible to the in situ moisture content of the rock.



Chapter 5 Shear strength of rock.

Introduction

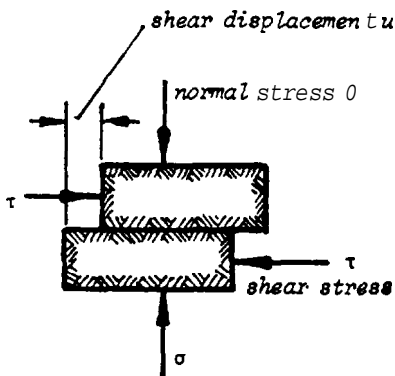
In analyzing the stability of a rock slope, the most important factor to be considered is the geometry of the rock mass behind the slope face. As discussed in Chapter 3, the geometrical relationship between the discontinuities in the rock mass and the slope and orientation of the excavated face will determine whether parts of the rock mass are free to slide or fall.

The next most important factor is the shear strength of the potential failure surface which may consist of a single discontinuity plane or a complex path following several discontinuities and involving some fracture of the intact rock material. Determination of reliable shear strength values is a critical part of a slope design because, as will be shown in later chapters, relatively small changes in shear strength can result in significant changes in the safe height or angle of a slope. The choice of appropriate shear strength values depends not only upon the availability of test data but also upon a careful interpretation of these data in the light of the behavior of the rock mass which makes up the full scale slope. While it may be possible to use the test results obtained from a shear test on a rock joint in designing a slope in which failure is likely to occur along a single joint surface, similar to the one tested, these shear test results could not be used directly in designing a slope in which a complex failure process involving several joints and some intact rock failure is anticipated. In the latter case, some modification would have to be made to the shear strength data to account for the difference between the shearing process in the test and that anticipated in the rock mass. In addition, differences in the shear strength of rock surfaces can occur because of the influence of weathering, surface roughness, the presence of water under pressure and because of differences in scale between the surface tested and that upon which slope failure is likely to occur.

From this discussion it will be clear that the choice of appropriate shear strength values for use in a rock slope design depends upon a sound understanding of the basic mechanics of shear failure and of the influence of various factors which can alter the shear strength characteristics of a rock mass. It is the aim of this chapter to provide this understanding and to encourage the reader to explore further in the literature on this subject.

Shear strength of planar discontinuities

Supposing that one were to obtain a number of samples of rock, each of which had been cored from the same block of rock which contains a through-going discontinuity such as a bedding plane. This bedding plane is still cemented, in other words, a tensile force would have to be applied to the two halves of the specimen on either side of the discontinuity in order to separate them. The bedding plane is absolutely planar, having no surface undulations or roughness. Each specimen is subjected to a normal stress σ , applied across the discontinuity surface as illustrated in the margin sketch, and the shear stress τ required to cause a displacement u is measured.



Plotting the shear stress level at various shear displacements, for one of the tests carried out at a constant normal stress



70. MOYE, D.C. Diamond drilling for foundation exploration. *Civil Engineering Transactions, Institution of Engineers of Australia*. Vol. CE9, 1967, pages 95-100.
71. KEHPE, W.F. Core orientation. *Proc. 12th Exploration Drilling Symposium*, University of Minnesota, 1967.
72. ROCHA, H. A method of integral sampling of rock masses. *Rock Mechanics*, Vol. 3, No. 1, 1967. pages 1-12.
73. KREBS, E. Optical surveying with a borehole periscope. *Mining Magazine*, Vol. 116, 1967, pages 390-399.
74. BURWELL, E.B. and NESBITT, R.H. The NX borehole camera. *Transactions American Inst. Mining Engineers*, Vol. 194. 1954, pages 805-808.
75. HOEK, E. and PENTZ, D.L. Review of the role of rock mechanics research in the design of opencast mines. *Proc. 9th Commonwealth Mining and Metallurgical Congress*, London, 1969, paper No. 4.
76. BALTOSSER, R.W. and LAWRENCE, H.W. Application of well logging techniques in metallic mineral mining. *Geophysics*, Vol. 35. 1970. pages 143-192.
77. TIXIER, H.P. and ALGER, R.P. Log evaluation of non-metallic mineral deposits. *Geophysics*, Vol. 35, 1970, pages 124-142.
78. ZEMANEK, J. The borehole televiewer - a new logging concept for fracture location and other types of borehole inspection. *Society of Petroleum Engineers*, Houston, Texas, September 1968. 14 pages.
79. GEOLOGICAL SOCIETY. LONDON ENGINEERING GROUP. The logging of rock cores for engineering purposes. *Quarterly Journal of Engineering Geology*, Vol. 3, No. 1, 1970, 25 pages.
60. ROYAL DUTCH SHELL COMPANY. Standard *Legend*, Internal Shell Report, The Hague, 1958. 200 pages. (A very comprehensive report on logging and geological data presentation).
61. LONDE, P. The role of rock mechanics in the reconnaissance of rock foundations, water seepage in rock slopes and the analysis of the stability of rock slopes. *Quarterly Journal of Engineering Geology*. Vol. 5, 1973, pages 57-127.

Add reference

- 81A Call, R.D., Savelly, J.P. and Pakalnis, R., "A Simple Core Orientation Technique" in *Stability in Surface Mining* (C.O. Brawner, Ed.), SME, AIME, Vol. 3, pp. 465 - 481, New York. 1982.
- 81B Wood, O.F., *Clay Imprint Core Orientator*, Golder Associates' Field Manual, 1987.

Chapter 4 references.

Selected references on geological data collection

56. MILLER, V.C. *Photogeology*. International Series on Earth Sciences. McGraw Hill Book Co., New York, 1961. 240 pages.
57. BROADBENT, C.D. and RIPPERS, K.H. Fracture studies at the Kimberley Pit. *Proc. Symposium on Planning Open Pit Mines*, Johannesburg, 1970. Published by A.A. Balkema, Amsterdam, 1971, pages 171-179.
58. WEAVER, R. and CALL, R.D. Computer estimation of oriented fracture set intensity. *Symposium on Computers in Mining and Exploration*. University of Arizona, Tucson, 1965. 17 pages. (Unpublished paper available from University of Arizona.)
59. HALSTEAD, P.N., CALL, R.D. and RIPPERS, K.H. Geological structural analysis for open pit slope design, Kimberley pit, Ely, Nevada. *A.I.M.E. Preprint 68AM-65*, 1968. Unpublished paper available from A.I.M.E., New York.
60. DA SILVEIRA, A.F., RODRIGUES, F.P., GROSSMAN, N.F. and HENDES, F. Qualitative characterization of the geometric parameters of jointing in rock masses. *Proc. 1st Congress of the International Society of Rock Mechanics*, Lisbon 1966, Vol. 1, pages 225-233.
61. TERZAGHI, R.D. Sources of error in joint surveys. *Geotechnique*, Vol. 15, 1965, pages 287-304.
62. MOFFIT, F.R. *Photogrammetry*. International Textbook Company, Scranton, Pennsylvania, 1967.
63. CALDER, P.N., BAUER, A. and HACDOUGALL, A.R. Stereo-photography and open pit mine design. *Canadian Inst. Min. Metall. Bulletin*, Vol. 63, No. 695. 1970, page 285.
64. ROSS-BROWN, D.M. and ATKINSON, K.B. Terrestrial photogrammetry in open pits. *Proc. Inst. Min. Metall. London*, Vol. 81, 1972, pages A205 - A214.
65. WILLIAMS, J.C.C. *Simple photogrammetry*. Academic Press, London, 1969, 211 pages.
66. FECKER, E. and RENGERS, N. Measurement of large scale roughness of rock planes by means of profilograph and geological compass. *Proc. Symposium on Rock Fracture*, Nancy, France, 1971. Paper 1-18.
67. ROSENGREN, K.J. Diamond drilling for structural purposes at Mount Isa. *Industrial Diamond Review*. Vol. 30, No. 359, 1970, pages 388-395.
68. JEFFERS, J.P. Core barrels designed for maximum core recovery and drilling performance. *Proc. Diamond Drilling Symposium*, Adelaide, August, 1966.
69. HUGHES, M.D. Diamond drilling for rock mechanics investigations. *Rock Mechanics Symposium*, University Sydney, Australia, 1969, pages 135-139.

A final word to engineers - we sometimes believe ourselves capable of quantifying a subject to a much greater extent than is actually possible. The geologist is frequently blamed for poor quality data and yet - if he did provide us with precise information on all the parameters listed above, would we really know what to do with it? How do you decide on the mechanical properties of a rock mass? The real answer is that we do not know but it is very convenient to have someone to blame for our lack of knowledge. In the final analysis, the best we can do is make an informed guess and the more information we have available at that time the better. This information must include a personal assessment of the rock conditions so that the geologist's reports can be read against a background appreciation of the actual site conditions. This imposes an obligation on the rock engineer to devote a little less time to his calculations and a little more to field observations. This obligation was summed up by Londe in a lecture on the design of rock foundations when he said "The time has come for us to consult not only the experts but the rock as well" (81).

from a 2,201 ft. 8 inch diameter borehole, only 37 ft. was successfully oriented with the aid of a borehole television camera. The authors' personal experiences with these devices have almost persuaded them that it would have been more profitable to invest in the provision of geology courses for leprechauns (who are reputedly small enough to fit down a borehole of reasonable size). However, it must be admitted that, in the hands of special 1st operators, these instruments can provide very valuable information. It seems more than likely that, with developments in the field of electronics, better and more reliable instruments of this type will become available in the years to come.

The mining and civil engineering industries have a great deal to learn from the oil industry in this area of borehole interpretation and well logging devices such as the Televiwer are bound to find greater applications in site investigation in years to come(76,77,78).

Presentation of geological information

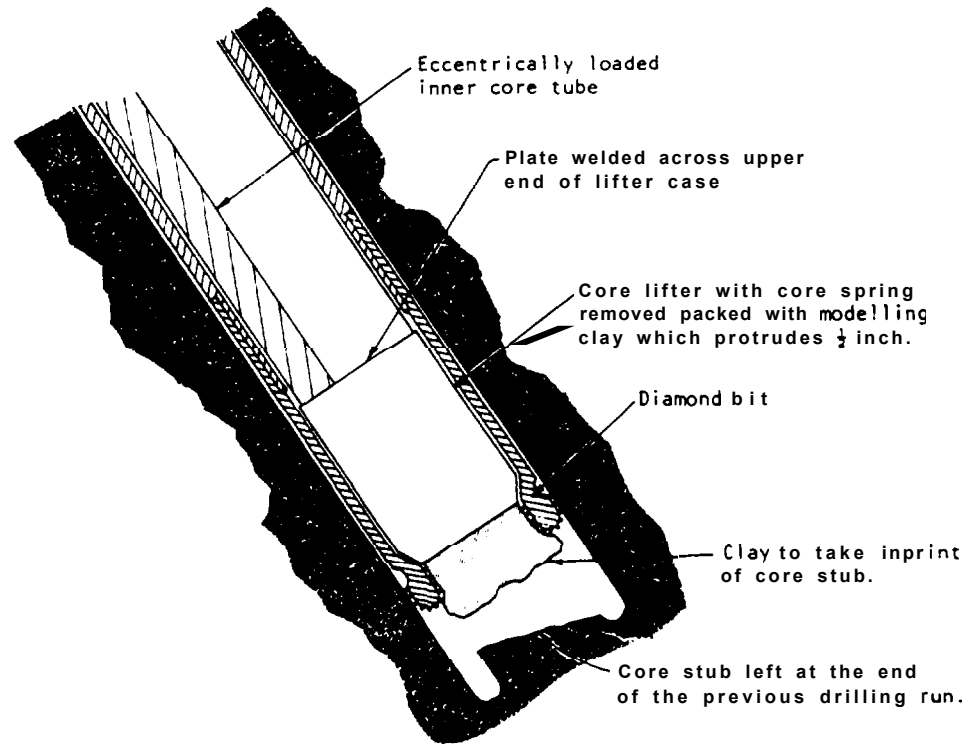
The collection of structural geological data is a difficult enough problem. Communication of this data to everyone concerned in the design of a highway is even more difficult. In the previous chapter it was suggested that the dips and dip directions of discontinuities are most conveniently presented on equal-area stereoplots. This information, in itself, is not adequate for the design of a rock slope since the strength of the rock mass is also required.

Ideally, the following information is required for each significant discontinuity.

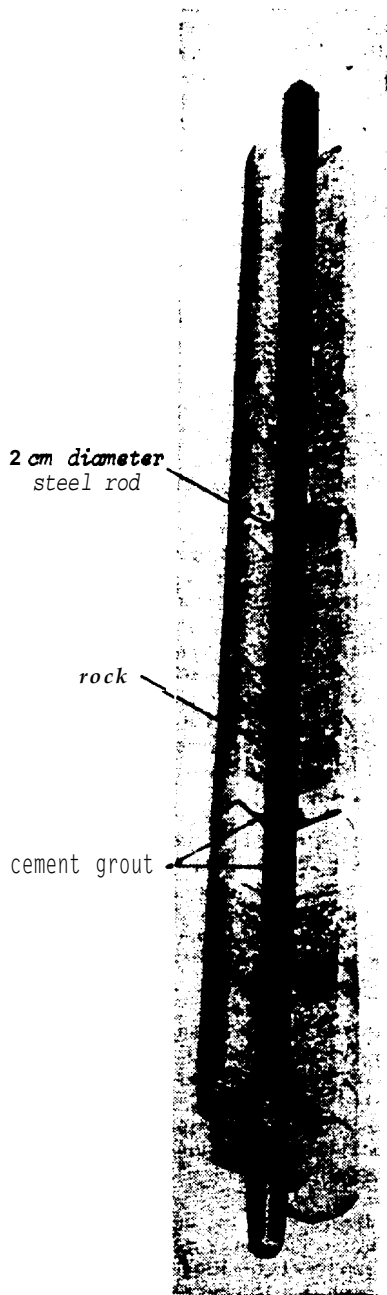
- a) Location in relation to map references
- b) Depth below reference datum
- c) Dip
- d) Dip direction
- e) Frequency or spacing between adjacent discontinuities
- f) Continuity or extent of discontinuity
- g) Width or opening of discontinuity
- h) Gouge or infilling between faces of discontinuity
- i) Surface roughness of faces of discontinuity
- j) Waviness or curvature of discontinuity surface
- k) Description and properties of intact rock between discontinuities.

Much of this information cannot be used quantitatively in a stability calculation but it all assists the engineer or geologist in deciding upon the most probable failure mode and in assigning reasonable strength properties to the rock mass. Consequently it is important that it should be recorded and presented in such a way that the maximum amount of relevant information is conveyed to those who were not involved in the logging itself.

Although standard methods of data presentation have been suggested(79,80), many geologists prefer to work out their own systems to suit their particular requirements. In the authors' opinion, it does not matter what system is used provided that it conveys the required information. If it does not serve this purpose then the geologist should have the courage to change it.



Core orientation device using clay to take inprint of core stub on end of drill hole.



A reinforced core, sectioned to show the rod grouted into the coaxial pilot hole. Note that the top end of the rod is square in order that it can be oriented. (Photograph reproduced with permission of Dr. M. Rocha.)

then retrieved with the wire-line and a conventional barrel is lowered to continue coring. The recovered core is fitted together and a straight reference line is transferred from the oriented barrel to the reconstructed core using the imprint match between the clay and the uphole core stub. Extreme hole inclinations for this technique range from about 45 to 70 degrees with optimum inclinations in the range of 60 to 65 degrees. Verification imprints should be taken frequently on each core run if possible to confirm the correct operation of the system. The method of use of the clay imprint orientor is shown on Page 4.15.

An alternative method, used in the Christensen-Hugel core barrel, is to scribe a reference mark on the core. The reference mark is oriented by a magnetic borehole survey instrument mounted in the core-barrel (71).

Rosengren (67) describes a simple device for core orientation in inclined holes. A short dummy barrel holding a marking pen and a mercury orienting switch is lowered down the hole on lightweight rods. The device is rotated until the mercury switch operates at a known orientation and the marker pen is then pushed onto the bottom of the hole, marking the core stub in this known position. Another system used by Rosengren for core orientation in inclined holes is to break a small container of paint against the end of the hole. The paint will run down the face of the core stub, thereby marking its orientation with respect to the vertical.

The most elaborate system of core orientation is to drill a small diameter hole at the end of the parent hole and to bond a compass of an oriented rod into this hole (69). This scheme has been taken further by Rocha (72) in order to recover intact an oriented core. Rocha describes drilling a pilot hole along the axis of a core and grouting an oriented rod into this hole. Overcoring this reinforced material gives an intact stick of oriented core in the worst types of material.

Walton of the National Coal Board in England has used a similar technique in which a wireline tool containing a bomb of polyester resin is lowered down a hole in which a pilot hole has been drilled. The resin charge is released and flows into the hole, carrying with it a floating compass. Resin reinforced cores have been successfully recovered from depths of 125 m (410 ft.) in coal measures but there are many practical difficulties associated with keeping the pilot hole in position and preventing caving in poor quality rock.

Examination of borehole walls

Because of the practical problems involved in orientation of core, another approach is to examine the walls of the borehole in an effort to map traces of structural features.

A borehole periscope, consisting of a rigid tube which supports a system of lenses and prisms, is probably the most successful instrument for borehole examination. A major advantage of this device is that it is oriented from outside the hole but a disadvantage is that it is only effective to borehole depths of approximately 100 ft. (73).

Various types of borehole cameras have been developed (74,75) and small diameter television cameras have also been used for the examination of borehole walls. Broadbent and Ripper (57) report rather sadly that out of 1,116 ft. of core recovered



A 48 inch diameter Calyx core recovered by the Hydroelectric Commission of Tasmania during site investigations for a dam.

diameter core barrels for structural drilling. The most common size used at present is NX (2-1/8 inch or 56 mm) but cores of 3 inch, 4 inch and 6 inch are favoured by some. Rosengren(67) describes the use of large diameter thin walled drilling equipment for underground hard rock drilling at Mt. Isa, Australia. The National Coal Board in England frequently uses 4-1/2 inch diameter double-barrel drills with air-flushing for exploration of potential opencast sites.

An extreme example, illustrated opposite, is a 48 inch diameter Calyx core from a dam-site investigation in Tasmania. This type of drilling would obviously only be justified in very special circumstances which the authors could not visualize occurring on highways.

Core orientation

It should have become obvious, from previous chapters, that the dip and dip direction of discontinuities are most important in slope stability evaluations. Consequently, however successful a drilling program has been in terms of core recovery, the most valuable information of all will have been lost if no effort has been made to orient the core.

One approach to this problem is to use inclined boreholes to check or to deduce the orientation of structural features. For example, if surface mapping suggests a strong concentration of planes dipping at 30° in a dip direction of 130° , a hole drilled in the direction of the normal to these planes, i.e. dipping at 60° in a dip direction of 310° , will intersect these planes at right angles and the accuracy of the surface mapping prediction can be checked. This approach is useful for checking the dip and dip direction of critical planes such as those in the slates on the eastern side of the hypothetical highway cut shown in Figure 3.10.

Alternatively, if two or more non-parallel boreholes have been drilled in a rock mass in which there are recognizable marker horizons, the orientation and inclination of these horizons can be deduced using graphical techniques. This approach is extensively discussed in published literature and is usefully summarized by Phillips(42). Where no recognizable marker horizons are present, this technique is of little value.

A second approach is to attempt to orient the core itself and, while the techniques available abound with practical difficulties which are the despair of many drillers, these methods do provide some of the best results currently obtainable. In fact the greatest possible service which could be rendered to the rock engineer by the manufacturers of drilling equipment would be the production of simple core orientation systems.

A simple core orientation technique was presented by Call, Savely and Pakalnis in 1981 (81A), which utilizes a modified inner core barrel for use with conventional wire-line diamond drilling equipment. The method has been field tested, and improved in subsequent years by Colder Associates (81B). The barrel is eccentrically weighted with lead and lowered into an inclined, fluid-filled borehole so that its orientation relative to vertical is known. Modelling clay protrudes from the downhole end of the inner barrel such that it will also extend through the drill bit when the inner and outer barrels are engaged. The barrel assembly is lowered to the hole bottom which causes the clay to take an imprint of the core stub left from the previous core run. The inner barrel is

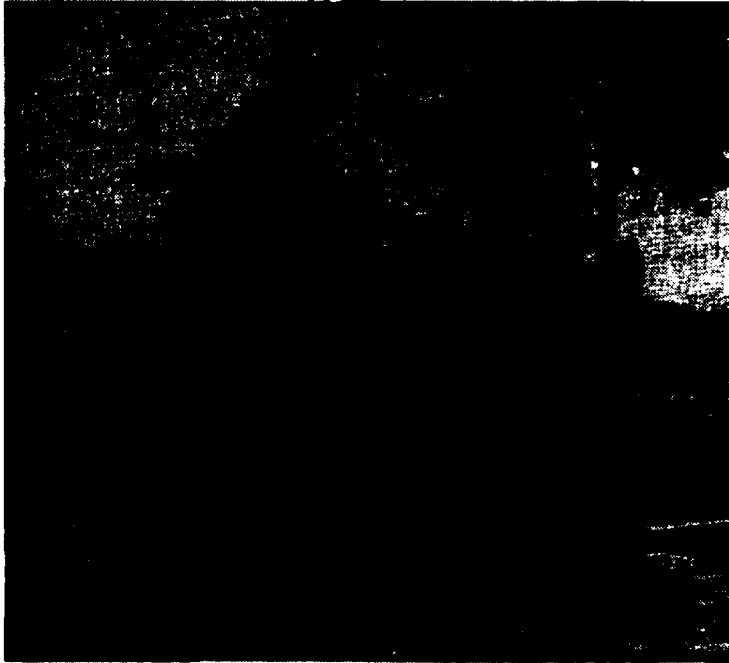


Figure 4.5a:
A typical hydraulic thrust diamond drilling machine being used for exploration drilling. High quality core recovery can be achieved with such a machine.
(Photograph reproduced with permission of Atlas Copco, Sweden)

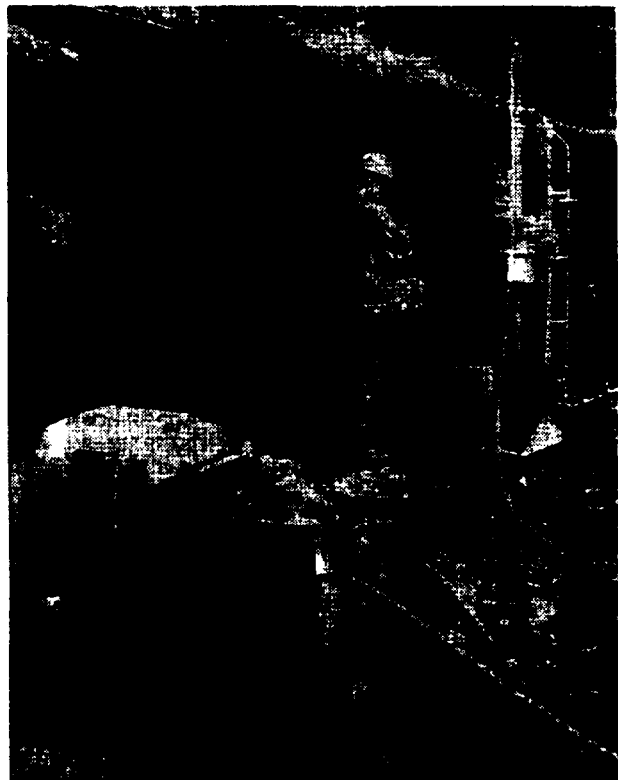


Figure 4.5b:
Atlas Copco Diamec 250 drilling machine set up for structural drilling in a difficult location on a quarry bench. The machine illustrated has been modified to allow drilling with core barrels of up to 3 inches (76 mm) outer diameter.

Drilling machines

Good core recovery in fractured ground depends upon the application of the correct thrust onto the rotating drill bit. The fixed rate of advance provided by a screw-feed machine will mean high bit pressures in hard formations. In soft formations, the bit pressure will be very low but the slow progress of the bit will allow the soft material to be eroded by the flushing water. In contrast, a hydraulic feed machine will maintain the same thrust and will allow the drill to move rapidly through soft formations, thereby minimizing the erosion.

Machines such as that illustrated in Figure 4.5a are widely used for exploration drilling and are ideal for structural drilling. Their one disadvantage is that they tend to be bulky and it is difficult to set them up on very rough sites which may be of particular interest to the rock engineer. On the other hand, the machine illustrated in Figure 4.5b can easily be rigged in very difficult locations and it can be operated as much as 100 ft. away from the prime mover and hydraulic pump unit. Hydraulic chucks on this machine allow easy rod changing and permit one man operations once the machine has been set up. Although this machine will not drill to the same depths as larger machines, it does provide adequate capacity for structural drilling for cut slopes where holes longer than about 200 ft. are not generally required.

Core barrels

The aim of structural drilling is to recover undisturbed core upon which measurements of structural features can be made. This can be achieved by the use of multiple-tube core barrels or by the use of large diameter barrels.

In a triple-tube core barrel, the inner tube or tubes are mounted on a bearing so that they remain stationary while the outer barrel, which carries the diamond bit, rotates. The core, cut out by the bit, is transferred into the non-rotating inner barrel where it remains undisturbed until the barrel is removed from the hole.

Removing the core from the barrel is the most critical part of the operation. More than once the authors have seen core removed from an expensive double-tube core barrel by thumping the outer barrel with a 4 lb. hammer - a process guaranteed to disturb any undisturbed core which may be in the barrel. By far the most satisfactory system is to use a split inner-barrel which is removed from the core barrel assembly with the core inside it and then split to reveal the undisturbed core. Sometimes a thin plastic or metal barrel is fitted inside the non-rotating barrel in order to provide the support for the core when it is transferred into the core-box.

Detailed literature on double and triple tube core barrels is available from a number of manufacturers and the reader who is unfamiliar with structural drilling is advised to consult this literature. More general information on drilling can be obtained from some of the references listed at the end of this chapter (67-70).

Experience has shown that core recovery increases with increasing core diameter and there is a tendency to use larger

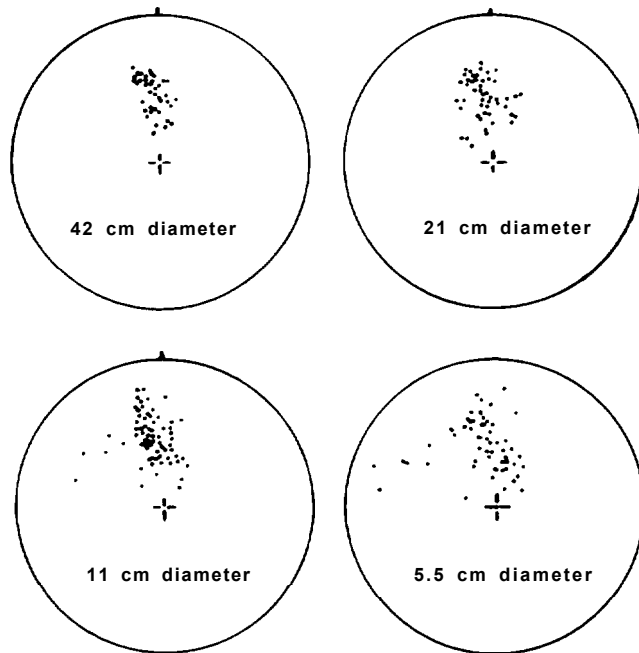


Figure 4.4d: Stereoplots of poles from measurements on rough rock surface using measuring plates of different diameters. The average dip of the plane is 35° and its dip direction is 170° .

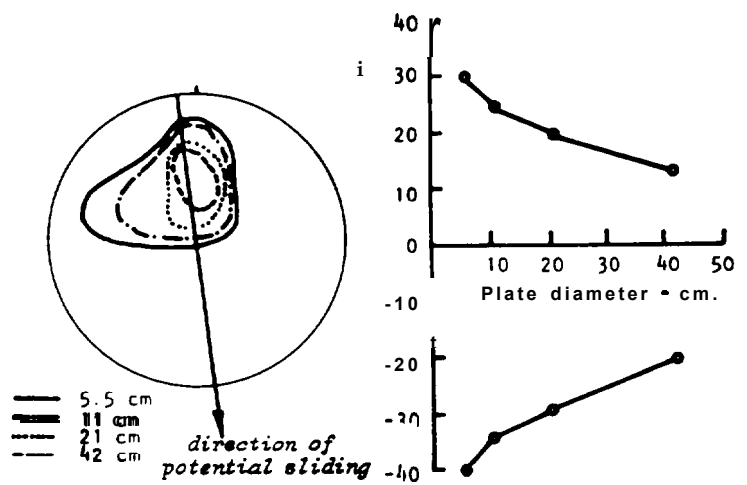


Figure 4.4e: Contours of maximum scatter for different base diameters and plot of affective roughness angle i along direction of potential sliding. Example adapted from paper by Fecker and Rengers⁶⁶.

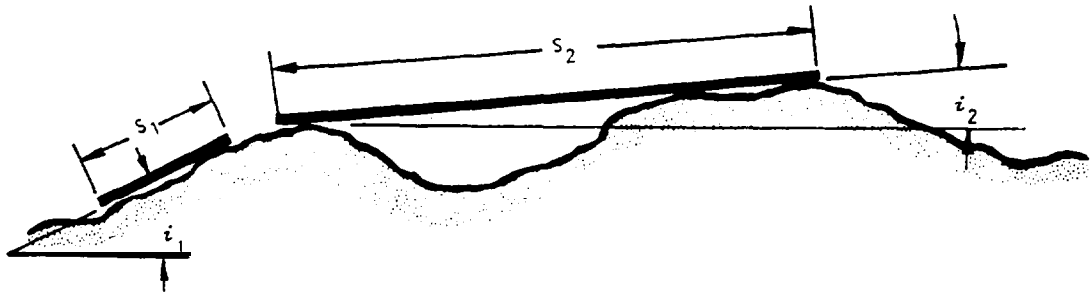


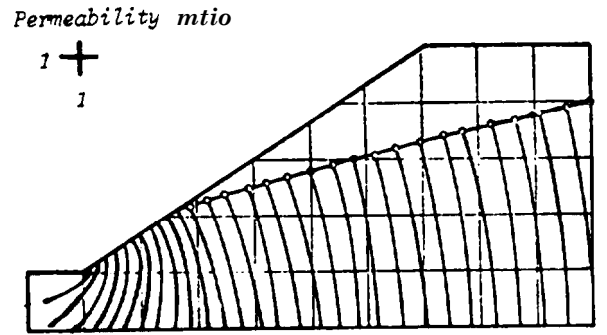
Figure 4.4a: Measurement of surface roughness with different base lengths. Short base length gives high values for the effective roughness angle while long bases give smaller angles.



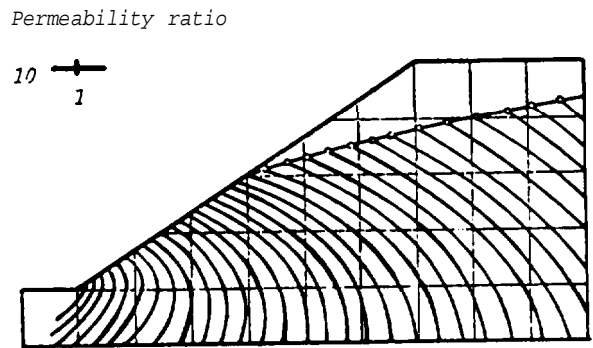
Figure 4.4b:
5.5 cm diameter measuring plate fitted to a Breithaupt geological compass.
Photographs reproduced with permission of Dr. N. Rengers from a paper by Fecker and Rengers⁶⁶.



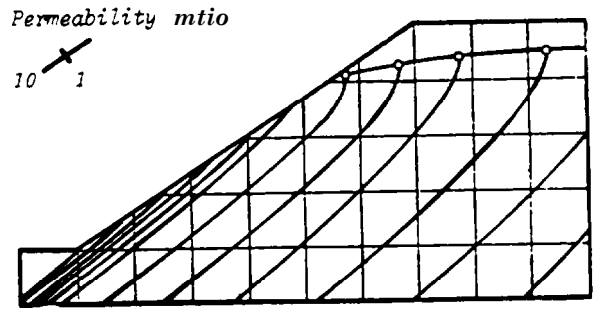
Figure 4.4c:
42 cm diameter measuring plate fitted to a Breithaupt geological compass for surface roughness measurement.



a) Isotropic rock slope



b) Anisotropic rock mass - horizontally bedded strata.



c) Anisotropic rock mass - strata dipping parallel to slope.

Figure 6.9 : Equipotential distributions in slopes with various permeability configurations.

The coefficient of permeability k is calculated from falling head and constant head tests in saturated ground (test section below water table) as follows.

$$\text{Falling head: } k = \frac{A}{F(t_2 - t_1)} \cdot \log_e \frac{H_1}{H_2} \quad (35)$$

$$\text{Constant head: } k = \frac{q}{F H_c} \quad (36)$$

where A is the cross-section area of the water column. $A = 1/4 \pi d^2$ where d is the inside diameter of the casing in a vertical borehole. For an inclined hole, A must be corrected to account for the elliptical shape of the horizontal water surface in the casing.

F is a shape factor which depends upon the conditions at the bottom of the hole. Shape factors for typical situations are given in Figure 6.10.

H_1 and H_2 are water levels in the borehole measured from the rest water level, at times t_1 and t_2 , respectively.

q is the flow rate, and

H_c is the water level, measured from the rest water level, maintained during a constant head test.

(Note that Napierian logarithms are used in these equations and that $\text{Log}_e = 2.3026 \text{Log}_{10}$).

Consider an example of a falling head test carried out in a borehole of 7.6 cm diameter with a casing of 6.0 cm diameter. The borehole is extended a distance of 100 cm beyond the end of the casing and the material in which the test is carried out is assumed to have a ratio of horizontal to vertical permeability $k_h/k_v = 5$.

The first step in this analysis is to calculate the shape factor F from the equation given for the 4th case in Figure 6.10. The value of $m = \sqrt{5} = 2.24$ and substituting $D = 7.6$ cm and $L = 100$ cm,

$$F = \frac{2\pi L}{\text{Log}_e(2mL/D)} = \frac{628}{\text{Log}_e 58.19} = 154$$

Measurement of water levels at different times for the falling head test give the following values:

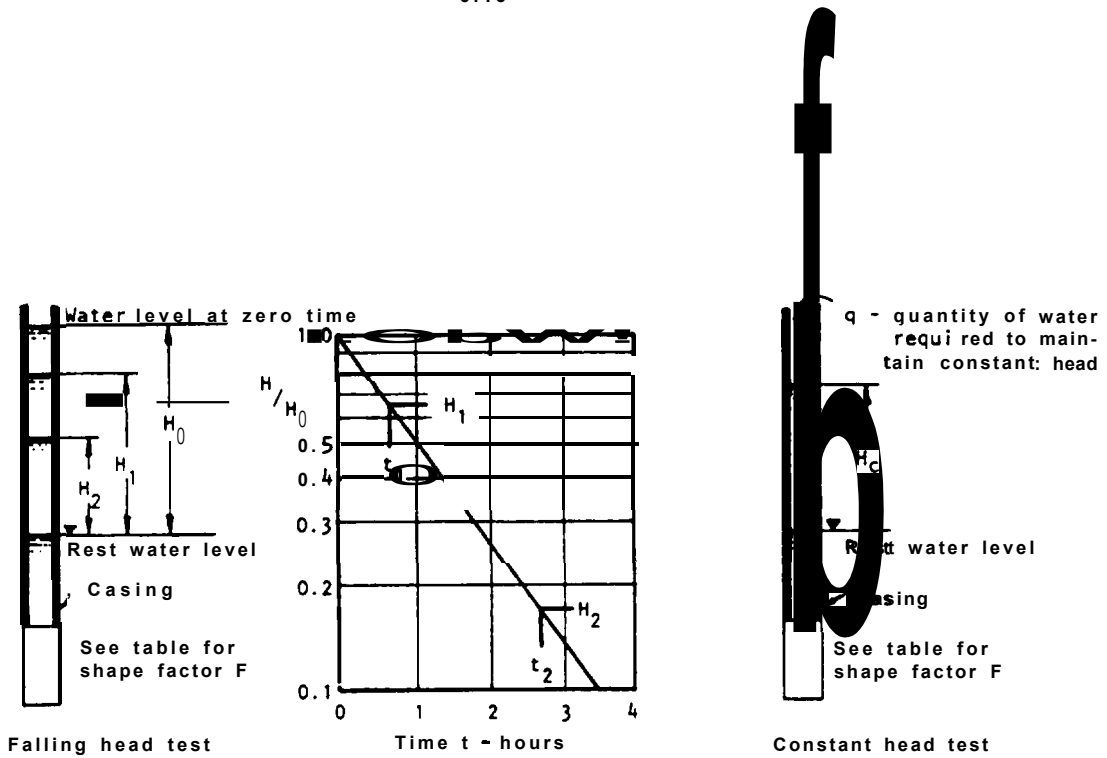
$$\begin{aligned} H_1 &= 10 \text{ meters at } t_1 = 30 \text{ seconds} \\ H_2 &= 5 \text{ meters at } t_2 = 150 \text{ seconds} \end{aligned}$$

The cross-sectional area A of the water column is

$$A = \frac{1}{4} \pi (6)^2 = 28.3 \text{ cm}^2$$

Substituting in equation (35), the horizontal permeability k_h is given by

$$k_h = \frac{28.3 \log_e 2}{154 (150 - 30)} = 1.06 \times 10^{-3} \text{ cm./sec.}$$



End conditions	Shape factor F
<p>Casing flush with end of borehole in soil or rock of uniform permeability. Inside diameter of casing is d cms.</p>	$F = 2.75d$
<p>Casing flush with boundary between impermeable and permeable strata. Inside diameter of casing is d cms.</p>	$F = 2.0d$
<p>Borehole extended a distance L beyond the end of the casing. Borehole diameter is D.</p>	$F = \frac{2\pi L}{\text{Log}_e (2L/D)}$ <p>for $L > 4D$</p>
<p>Borehole extended a distance L beyond the end of the casing in a stratified soil or rock mass with different horizontal and vertical permeabilities.</p>	<p>For determination of k_h:</p> $F = \frac{2\pi L}{\text{Log}_e (2m L/D)}$ <p>where $m = (k_h/k_v)^{1/2}$, $L > 4D$</p>
<p>Borehole extended a distance L beyond the end of the casing which is flush with an impermeable boundary.</p>	$F = \frac{2\pi L}{\text{Log}_e (4L/D)}$ <p>for $L > 4D$</p>

Figure 6.10 : Details of falling head and constant head tests for permeability measurement in soil and rock masses with shape factors for borehole end conditions.

Since the ratio of horizontal to vertical permeability has been estimated, from examination of the core, as $k_h/k_v = 5$, $k_v = 2.12 \times 10^{-4}$ cm/sec.

Laboratory tests on core samples are useful in checking this ratio of horizontal to vertical permeability but, because of the disturbance to the sample, it is unlikely that the absolute values of permeability measured in the laboratory will be as reliable as those determined by the borehole tests described. Laboratory methods for permeability testing are described in standard texts such as that by Lambe (180).

Pumping tests in boreholes

In a rock mass in which the groundwater flow is concentrated within regular joint sets, the permeability will be highly directional. If the joint opening e could be measured in situ, the permeability in the direction of each joint set could be calculated directly from equation (33). Unfortunately such measurements are not possible under field conditions and the permeability must therefore be determined by pumping tests.

A pumping test for the measurement of the permeability in the direction of a particular set of discontinuities such as joints involves drilling a borehole perpendicular to these discontinuities as shown in Figure 6.11. It is assumed that most of the flow is concentrated within this one joint set and that cross-flow through other joint sets, past the packers and through the intact rock surrounding the hole is negligible. A section of the borehole is isolated between packers or a single packer is used to isolate a length at the end of the hole and water is pumped into or out of this cavity.

A variety of borehole packers are available commercially (181) but the authors consider that many of these packers are too short to eliminate leakage. Leakage past packers is one of the most serious sources of error in pumping tests and every effort should be made to ensure that an effective seal has been achieved before measurements are commenced. A simple, inexpensive and highly effective packer has been described by Harper and Ross-Brown (182) and the principal features are illustrated in Figure 6.12. This packer is manufactured from rubber hosing which is normally used in the building industry for forming voids in concrete. It consists of inner and outer rubber tubes enclosing a diagonally braided cotton core and this arrangement allows an increase in diameter of approximately 20% when the hose is inflated. Because of its low cost and simplicity, long packers can be used and packer lengths of 10 ft. (3 m) have proved extremely effective in pumping tests in 3 inch (7.6 cm) diameter boreholes.

The permeability of the discontinuities perpendicular to the borehole is calculated as follows:

$$k = \frac{q \log_e (2R/d)}{2\pi L (H_1 - H_2)} \quad (37)$$

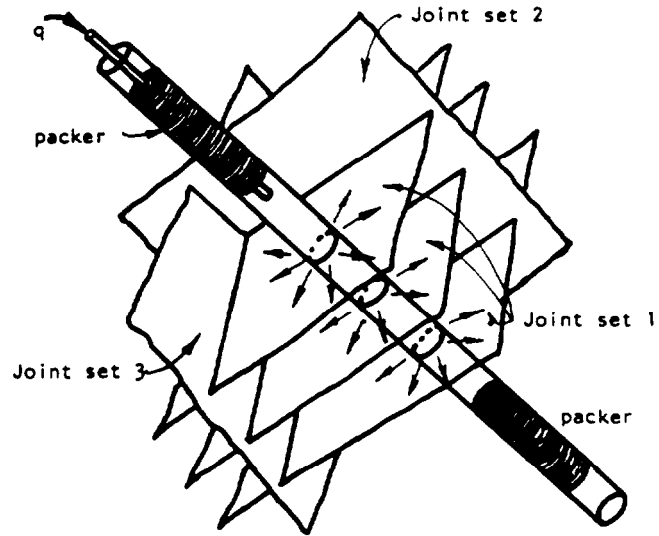


Figure 6.11: Pumping test in regularly jointed rock. The borehole is drilled at right angles to the joint set in which the permeability is to be measured.

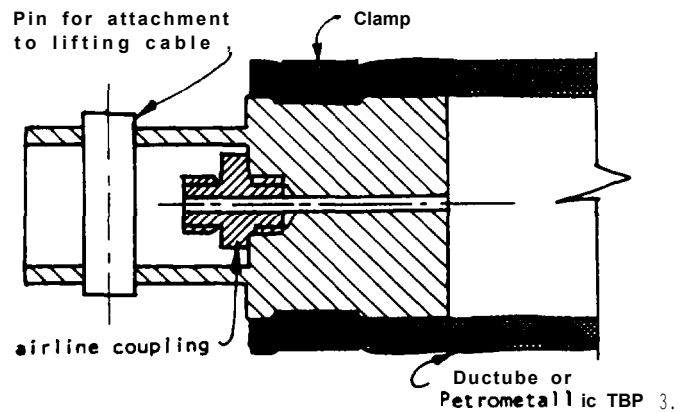


Figure 6.12 : Section through the end of a packer for sealing the bottom end of a pumping test cavity. The upper packer end has additional fittings for pressure inlet and piezo-meter cables.

where q is the pumping rate required to maintain a constant pressure in the test cavity
 L is the length of the test cavity
 H_1 is the total head in the test cavity
 D is the borehole diameter
 H_2 is the total head measured at a distance R from the borehole.

The most satisfactory means of obtaining the value of H_2 is to measure it in a borehole parallel to and at a distance R from the test hole. Where a pattern of boreholes is available, as the result of an investigation program, this does not present serious problems. Techniques for water pressure measurement are dealt with in the following section of this chapter.

When only one borehole is available, an approximate solution to equation (37) can be obtained by using the shape factor F for a stratified system (Figure 6.10). Substituting this value into equation (36) gives

$$k = \frac{q \cdot \text{Log}_e (2mL/D)}{2\pi L H_c} \quad (38)$$

where, in this case, $m = (k/k_p)^{\frac{1}{2}}$

k is the permeability at right angles to the borehole (quantity required)

k_p is the permeability parallel to the borehole which, if cross-flow is neglected, is equal to the permeability of the intact rock

H_c is the constant head above the original groundwater level in the borehole.

The value of the term $\text{Log}_e (2mL/D)$ in this equation does not have a major influence upon the value of k and hence a crude estimate of m is adequate. Consider the example where $L = 4D$; the values of $\text{Log}_e (2mL/D)$ are as follows:

k/k_p	1.0	10^2	10^4	10^6	10^8	10^{10}	10^{12}
m	1.0	10^1	10^2	10^3	10^4	10^5	10^6
$\text{Log}_e (2mL/D)$	2.1	4.4	6.7	9.0	11.3	13.6	15.9

A reasonable value of k for most practical applications is given by assuming $k/k_p = 10^6$, $m = 10^3$ which gives

$$k = \frac{1.4q}{L H_c} \quad (39)$$

In deriving equation (39), it has been assumed that the test cavity of length L intersects a large number of discontinuities (say 100) and that the value k represents a reasonable average permeability for the rock mass (in the direction at right angles to the borehole). When the discontinuity spacing varies

along the length of the hole, water flow will be concentrated in zones of closely spaced discontinuities and the use of an average permeability value can give misleading results. Under these circumstances, it is preferable to express the permeability in terms of the permeability k_j of individual discontinuities where

$$k_j = \frac{k}{n} \quad (40)$$

n is the number of discontinuities which intersect the test cavity of length L .

The value of n can be estimated from the borehole core log and, assuming that the discontinuity opening (e in equation 33) remains constant, the variation in permeability along the borehole can then be estimated.

Before leaving this question of permeability testing it must be pointed out that the discussion which has been presented has been grossly simplified. This has been done deliberately since the literature dealing with this subject is copious, complex and confusing. A number of techniques, more sophisticated than those which have been described here, are available for the evaluation of permeability but the authors believe that these are best left in the hands of experienced specialist consultants. The simple tests which have been described are generally adequate for highway stability and drainage studies.

Measurement of water pressure

The importance of water pressure in relation to the stability of slopes has been emphasized in several of the previous chapters. If a reliable estimate of stability is to be obtained or if the stability of a slope is to be controlled by drainage, it is essential that water pressures within the slope should be measured. Such measurements are most conveniently carried out by piezometers installed in boreholes.

A variety of piezometer types is available and the choice of the type to be used for a particular installation depends upon a number of practical considerations. A detailed discussion on this matter has been given by Terzaghi and Peck (1953) and only the most important considerations will be summarized here.

The most important factor to be considered in choosing a piezometer is the time lag of the complete installation. This is the time taken for the pressure in the system to reach equilibrium after a pressure change and it depends upon the permeability of the ground and the volume change associated with the pressure change. Open holes can be used for pressure measurement when the permeability is greater than 10^{-4} cm/sec. but, for less permeable ground, the time lag is too long. In order to overcome this problem, a pressure measuring device or piezometer is installed in a sealed section of the borehole. The volume change within this sealed section, caused by the operation of the piezometer should be very small in order that the response of the complete installation to pressure changes in the surrounding rock should be rapid. If a device which requires a large volume change for its operation is used, the change in pressure induced by this change in volume may give rise to significant errors in measurement.

Some of the common types of piezometer are briefly discussed below:

a) Open piezometers or observation wells

As discussed above, open ended cased holes can be used to measure water pressure in rock or soil in which the permeability is greater than about 10^{-4} cm/sec. All that is required for these measurements is a device for measuring water level in the borehole. A very simple probe consisting of a pair of electrical contacts housed in a brass weight is illustrated in the margin sketch. When the contacts touch the water, the resistance of the electrical circuit drops and this can be measured on a standard "Avometer" or similar instrument. The depth of water below the collar of the hole is measured by the length of cable and it is convenient to mark the cable in feet or meters for this purpose. Portable water level indicators, consisting of a probe, a marked cable and a small resistance measuring instrument, are available from Solitest Inc., 2205 Lee Street, Evanston, Illinois 60202, U.S.A.

b) Standpipe piezometers

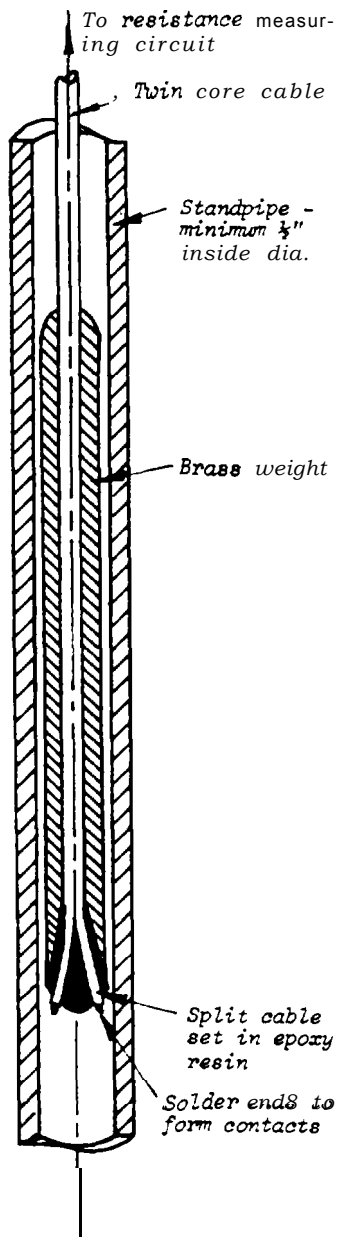
When the permeability of the ground in which water pressure is to be measured is less than 10^{-4} cm/sec., the time lag involved in using an open hole will be unacceptable and a standpipe piezometer such as that illustrated in Figure 6.13 should be used. This device consists of a perforated tip which is sealed into a section of borehole as shown. A small diameter standpipe passing through the seals allows the water level to be measured by means of the same type of water level indicator as described above under open hole piezometers. Because the volume of water within the standpipe is small, the response time of this piezometer installation will be adequate for most applications likely to be encountered on a highway.

An advantage of the standpipe piezometer is that, because of the small diameter of the standpipe, a number can be installed in the same hole. Hence different sections can be sealed off along the length of the borehole and the water pressure within each section monitored. This type of installation is important when it is suspected that water flow is confined to certain layers within a rock mass.

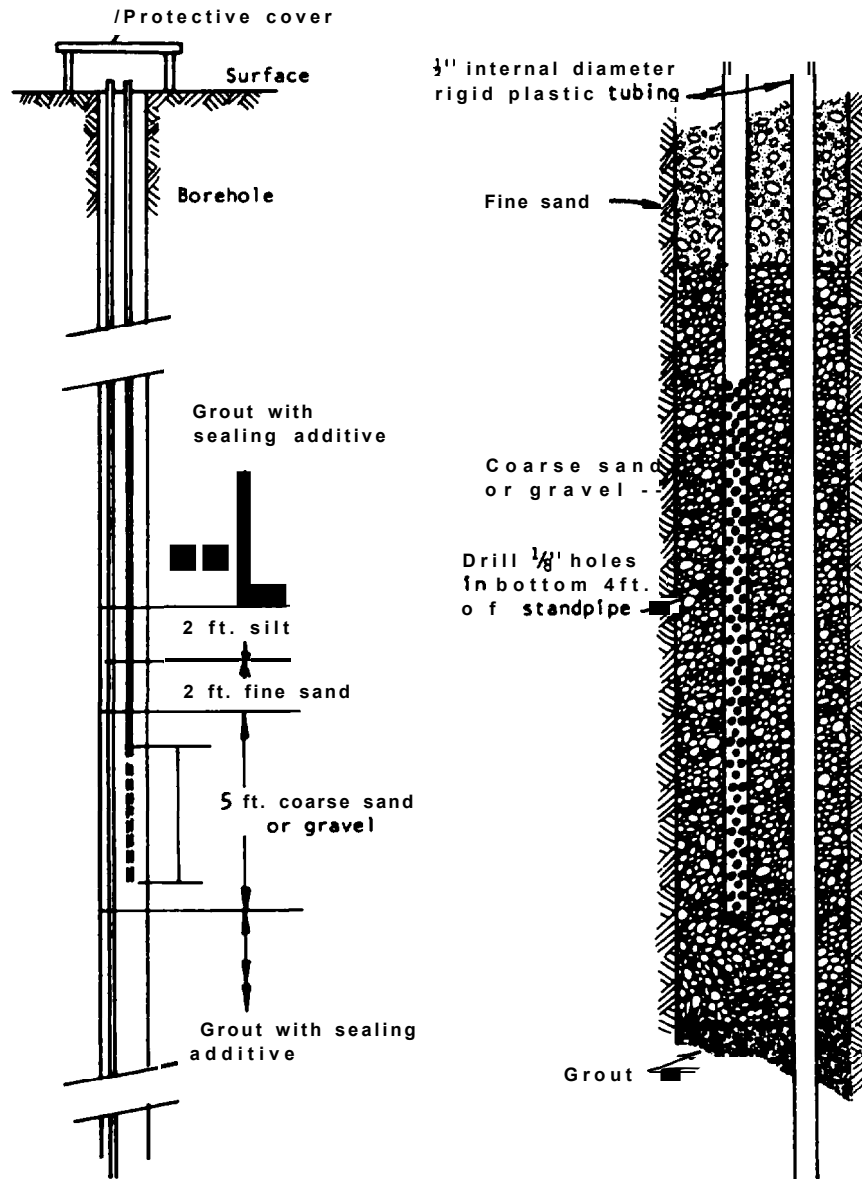
c) Closed hydraulic piezometers

When the permeability of the ground falls below about 10^{-6} cm/sec., the time lag of open ended boreholes or standpipe piezometers becomes unacceptable. For example, approximately 5 days would be required for a typical standpipe piezometer to reach an acceptable state of equilibrium after a change of water pressure in a rock or soil mass having a permeability of 10^{-7} cm/sec.

An improved time lag can be obtained by using a closed hydraulic piezometer such as that described by Bishop, et al (184). This type of piezometer is completely filled with de-aired water and is suitable for measurement of small water pressures. Such piezometers are generally used for pore pressure measurement during construction of embankments or dams where they can be installed during construction and left in place.



A simple probe for water level detection.



Note : The two sealing layers of fine sand and silt above the piezometer section can be replaced by bentonite pellets which form a gel in contact with water and form an effective seal . Pelletized bentonite is available commercially as "Peltonite" from Rocktest Ltd., Lambert, Quebec, Canada.

Figure 6.13 : Typical standpipe piezometer installation details .



Installation of a plastic tube standpipe piezometer in a drill hole.

d) Air actuated piezometers

A very rapid response time can be achieved by use of air actuated piezometers in which the water pressure is measured by a balancing air pressure acting against a diaphragm. As shown in Figure 6.14, an air valve allows air to escape when the air and water pressures on either side of the diaphragm are equal (185). A commercially available air piezometer is illustrated in Figure 6.15. Similar types of instrument are available from other suppliers and these devices are playing an increasingly important role in slope stability studies.

e) Electrically indicating piezometer

An almost instantaneous response time is obtained from piezometers in which the deflection of a diaphragm as a result of water pressure is measured electrically by means of some form of strain gauge attached to the diaphragm. A wide variety of such devices is available commercially and they are ideal for measuring the water pressure within the test cavity during a pumping test (172). Because of their relatively high cost and because of the possibility of electrical faults, these piezometers are less satisfactory for permanent installation in boreholes.

General comments

A frequent mistake made by engineers or geologists in examining rock or soil slopes is to assume that groundwater is not present if no seepage appears on the slope face. In many cases, the seepage rate may be lower than the evaporation rate and hence the slope surface may appear completely dry and yet there may be water at significant pressure within the rock mass. Remember that it is water pressure and not rate of flow which is responsible for instability in slopes and it is essential that measurement or calculation of this water pressure should form part of site investigation for stability studies. Drainage, which is discussed in Chapter 12, is one of the most effective and most economical means available for improving the stability of highway slopes. Rational design of drainage systems is only possible if the water flow pattern within the rock mass is understood and measurement of permeability and water pressure provides the key to this understanding.

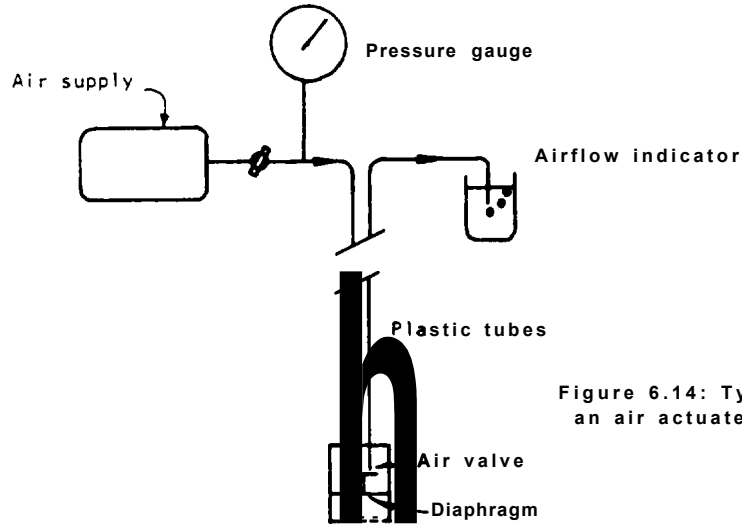


Figure 6.14: Typical circuit for an air actuated piezometer.

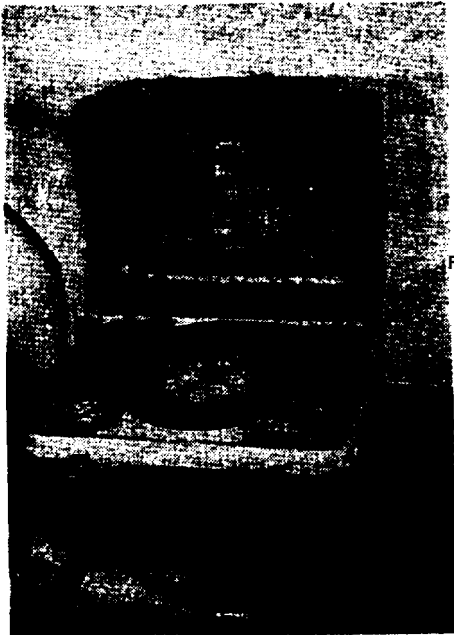


Figure 6.15: Model P-100 Pneumatic Piezometer and Model C-102 read-out unit manufactured by Thor Instrument Company Inc., Seattle.

Piezometer measures $\frac{1}{2}$ " x $2\frac{1}{2}$ " (12mm x 62mm).

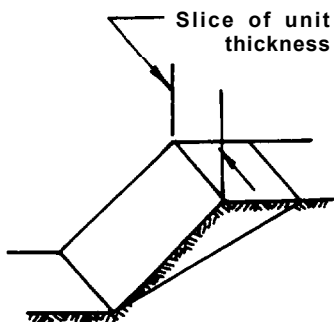
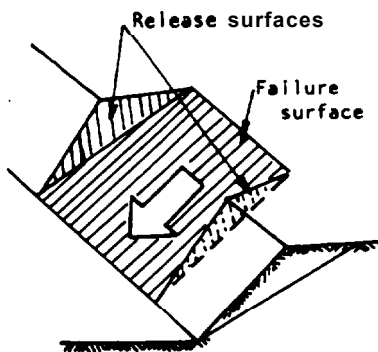
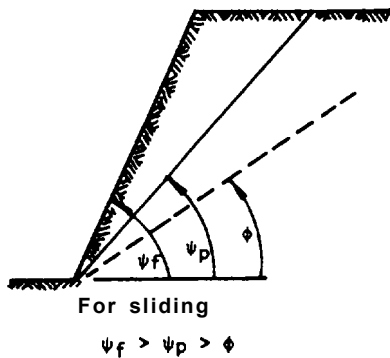
Chapter 6 references

Selected references on permeability and water pressure measurement.

159. **BRAWNER, C.O.** The influence and control of groundwater in open pit mining. *Proc. 5th Canadian Symposium on Rock Mechanics*, Toronto, 1968.
160. **DOBRY, R. and ALVAREZ, L.** Seismic failures of Chilean tailings dams. *Proc. American Society of Civil Engineers*. Vol. 93, No. SM6, 1967.
161. **CASACRANOE, L. and MACIVER, B.N.** Design and construction of tailings dams. *Proc. 1st Symposium on Stability for Open Pit Mining*, Vancouver, 1970.
162. **SEED, H.B. and LEE, K.L.** Liquefaction of saturated sands during cyclic loading. *Journal Soil Mechanics and Foundation Div. Proc. ASCE*. Vol. 92, No. SM6, 1966, pages 105-134.
163. **DAVIS, S.N. and DE WIEST, R.J.N.** *Hydrogeology*. John Wiley & Sons, New York & London, 1966, 463 pages.
164. **MORCENSTERN, N.R.** The influence of groundwater on stability. *Proc. 1st Symposium on Stability of Open Pit Mining*, Vancouver, 1970. Published by AIME, New York, 1971.
165. **SCHEIDEGGER, A.E.** *The physics of flow through porous media*. MacMillan, New York, 1960.
166. **CEOERGREN, H.R.** *Seepage, drainage and flow nets*. John Wiley and Sons, New York, 1967.
167. **DAVIS, S.N.** Porosity and permeability of natural materials, in *Flow through porous media*, edited by R. de Wiest, Academic Press, London, 1969, pages 54-89.
168. **HUITT, J.L.** Fluid flow in simulated fracture. *Journal American Inst. Chemical Eng.* Vol. 2, 1956, pages 259-264.
169. **SNOW, D.T.** Rock fracture spacings, openings and porosities. *Journal Soil. Mech. Foundation Div. Proc. ASCE*. Vol. 94, 1968, pages 73-91.
170. **LOUIS, c.** A study of groundwater flow in jointed rock and its influence on the stability of rock masses. Doctorate thesis, University of Karlsruhe. 1967, (in German). English translation *Imperial College Rock Mechanics Research Report* No. 10, September, 1969. 90 pages.
171. **SHARP, J.C.** Fluid flow through fissured media. *Ph.D. Thesis, University of London (Imperial College)*, 1970.
172. **MAINI, Y.N.** In situ parameters in jointed rock - their measurement and interpretation. *Ph.D. Thesis, University of London (Imperial College)*, 1971.
173. **HAAR, M.E.** *Groundwater and Seepage*, McGraw Hill Co., New York, 1962.

174. TAYLOR, D.U. *Fundamentals of Soil Mechanics*. John Wiley & Sons, New York, 1948.
175. KARPLUS, W.J. *Analog Simulation. Solution of Field Problems*. McGraw Hill Co., New York, 1968.
176. MEEHAN, R.L. and MORGENSTERN, N.R. The approximate solution of seepage problems by a simple electrical analogue method. *Civil Engineering and Public Works Review*. Vol. 63. 1968, pages 65-70.
177. ZIENKIEWICZ, O.C., MAYER, P. and CHEUNG, Y.K. Solution of anisotropic seepage by finite elements. *Journal Eng. Mech. Div., ASCE*, Vol. 92, EM1, 1966, pages 111-120.
178. SHARP, J.C., MAINI, Y.N. and HARPER, T.R. Influence of groundwater on the stability of rock masses. *Trans. Institute Mining and Metallurgy*, London. Vol. 81, Bulletin No. 782, 1972, pages A13 - 20.
79. HORSLEV, M.S. Time lag and soil permeability in groundwater measurements. *U.S. Corps of Engineers Waterways Experiment Station, Bulletin No. 36, 1951, 50 pages.*
180. LAMBE, T.V. *Soil testing for engineers*. John Wiley & Sons, New York, 1951.
181. MUIR WOOD, A.H. In-situ testing for the Channel Tunnel. *Proc. Conference on in-situ investigations in soils and rocks*, London, 1969. Published by the Institution of Civil Engineers, London, 1969. pages 79-86.
182. HARPER, T.R. and ROSS-BROWN, D.H. An inexpensive durable borehole packer. *Imperial College Rock Mechanics Research Report No. D24, 1972, 5 pages.*
183. TERZAGHI, K. and PECK, R. *Soil Mechanics in Engineering Practice*. John Wiley & Sons inc., New York, 1967, 729 pages.
184. BISHOP, A.W., KENNARD, M.F. and PENMAN, A.D.H. Pore-pressure observations at Selsset Dam. *Proc. Conference on Pore Pressure and Suction in Soils*. Butterworth, London, 1960, pages 91-102.
185. WARLAM, A.A. and THOMAS, E.U. Measurement of hydrostatic uplift pressure on spillway weir with air piezometers. *Instruments and apparatus for soil and rock mechanics*. American Society for Testing and Materials Special Technical Publication No. 392, 1965, pages 143-151.

Chapter 7 Plane failure.



Introduction

A plane failure is a comparatively rare sight in rock slopes because it is only occasionally that all the geometrical conditions required to produce such a failure occur in an actual slope. The wedge type of failure, considered in Chapter 8, is a much more general case and many rock slope engineers treat the plane failure as a special case of the more general wedge failure analysis.

While this is probably the correct approach for the experienced slope designer who has a wide range of design tools at his disposal, it would not be right to ignore the two-dimensional case in this general discussion on slope failure. There are many valuable lessons to be learned from a consideration of the mechanics of this simple failure mode and it is particularly useful for demonstrating the sensitivity of the slope to changes in shear strength and groundwater conditions - changes which are less obvious when dealing with the more complex mechanics of a three-dimensional slope failure.

General conditions for plane failure

In order that sliding should occur on a single plane, the following geometrical conditions must be satisfied:

- The plane on which sliding occurs must strike parallel or nearly parallel (within approximately $\pm 20^\circ$) to the slope face.
- The failure plane must "daylight" in the slope face. This means that its dip must be smaller than the dip of the slope face, i.e. $\psi_f > \psi_p$.
- The dip of the failure plane must be greater than the angle of friction of this plane, i.e. $\psi_p > \phi$.
- Release surfaces which provide negligible resistance to sliding must be present in the rock mass to define the lateral boundaries of the slide. Alternatively, failure can occur on a failure plane passing through the convex "nose" of a slope.

In analyzing two-dimensional slope problems, it is usual to consider a slice of unit thickness taken at right angles to the slope face. This means that the area of the sliding surface can be represented by the length of the surface visible on a vertical section through the slope and the volume of the sliding block is represented by the area of the figure representing this block on the vertical section.

Plane failure analysis

The geometry of the slope considered in this analysis is defined in Figure 7.1. Note that two cases must be considered.

- A slope having a tension crack in its upper surface.
- A slope with a tension crack in its face.

The transition from one case to another occurs when the tension crack coincides with the slope crest, i.e. when

$$z/H = (1 - \cot \psi_f \cdot \tan \psi_p) \quad (41)$$

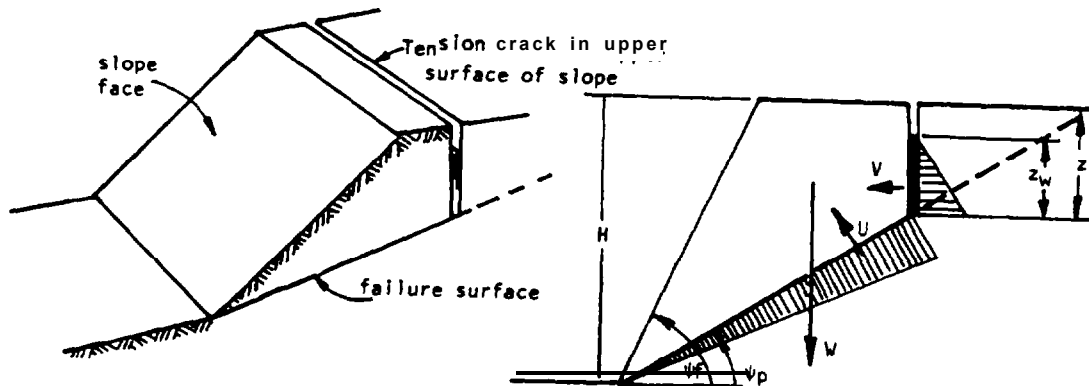


Figure 7.1a : Geometry of slope with tension crack in upper slope surface.

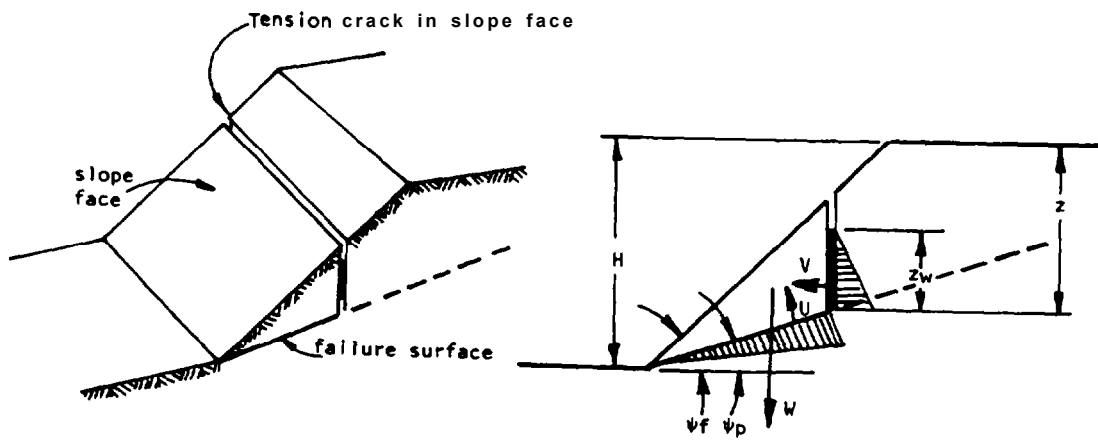


Figure 7.1b : Geometry of slope with tension crack in slope face.

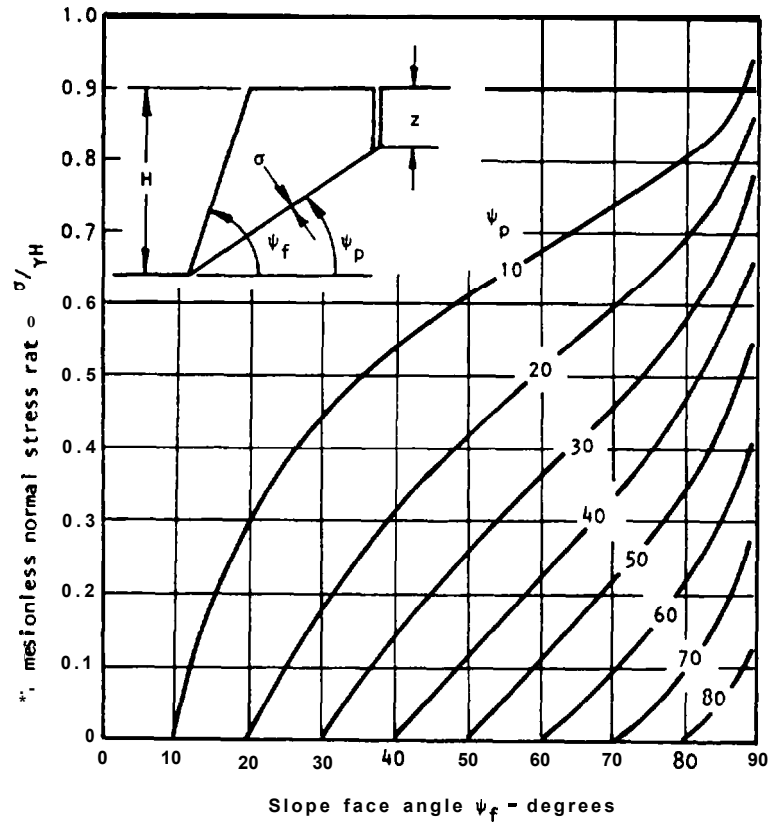
The following assumptions are made in this analysis:

- a. Both sliding surface and tension crack strike parallel to the slope surface.
- b. The tension crack is vertical and is filled with water to a depth Z_w .
- c. Water enters the sliding surface along the base of the tension crack and seeps along the sliding surface, escaping at atmospheric pressure where the sliding surface daylight in the slope face. The pressure distribution induced by the presence of water in the tension crack and along the sliding surface is illustrated in Figure 7.1.
- d. The forces W (the weight of the sliding block), U (uplift force due to water pressure on the sliding surface) and V (force due to water pressure in the tension crack) all act through the centroid of the sliding mass. In other words, it is assumed that there are no moments which would tend to cause rotation of the block and hence failure is by sliding only. While this assumption may not be strictly true for actual slopes, the errors introduced by ignoring moments are small enough to neglect. However, in steep slopes with steeply dipping discontinuities, the possibility that toppling failure may occur should be kept in mind.
- e. The shear strength of the sliding surface is defined by cohesion c and a friction angle ϕ which are related by the equation $\tau = c + \sigma \tan \phi$ as discussed on page 2.4. In the case of a rough surface having a curvilinear shear strength curve, the apparent cohesion and apparent friction angle, defined by a tangent to the curve are used. This tangent should touch the curve at a normal stress value which corresponds to the normal stress acting on the failure plane. In this case, the analysis is only valid for the slope height used to determine the normal stress level. The normal stress acting on a failure surface can be determined from the graph given in Figure 7.2.
- f. A slice of unit thickness is considered and it is assumed that release surfaces are present so that there is no resistance to sliding at the lateral boundaries of the failure.

The factor of safety of this slope is calculated in the same way as that for the block on an inclined plane considered on page 2.9. In this case the factor of safety, given by the total force resisting sliding to the total force tending to induce sliding, is

$$F = \frac{cA + (W \cos \psi_p - U - V \sin \psi_p) \tan \phi}{W \sin \psi_p + V \cos \psi_p} \quad (42)$$

where, from Figure 7.1:



$$\frac{\sigma}{\gamma H} = \frac{((1 - (z/H)^2) \cot \psi_p - \cot \psi_f) \sin \psi_p}{2(1 - z/H)}$$

where $z/H = 1 - \sqrt{\cot \psi_f \cdot \tan \psi_p}$ (see page 7.12)

Figure 7.2 Normal stress acting on the failure plane in a rock slope.

$$A = (H - z) \cdot \text{Cosec } \psi_p \quad (43)$$

$$U = \frac{1}{2} \gamma_w \cdot z_w (H - z) \cdot \text{Cosec } \psi_p \quad (44)$$

$$V = \frac{1}{2} \gamma_w \cdot z^2_w \quad (45)$$

For the tension crack in the upper slope surface (Figure 7.1a)

$$W = \frac{1}{2} \gamma H^2 \left((1 - (z/H)^2) \cot \psi_p - \cot \psi_f \right) \quad (46)$$

and, for the tension crack in the slope face (Figure 7.1b)

$$W = \frac{1}{2} \gamma H^2 \left((1 - z/H)^2 \cot \psi_p (\cot \psi_p \cdot \tan \psi_f - 1) \right) \quad (47)$$

When the geometry of the slope and the depth of water in the tension crack are known, the calculation of a factor of safety is a simple enough matter. However, it is sometimes necessary to compare a range of slope geometries, water depths and the influence of different shear strengths. In such cases, the solution of equations (42) to (47) can become rather tedious. In order to simplify the calculations, equation (42) can be rearranged in the following dimensionless form:

$$F = \frac{(2c/\gamma H) \cdot P + (Q \cdot \cot \psi_p - R(P+S)) \tan \phi}{Q + R \cdot S \cot \psi_p} \quad (48)$$

where

$$P = (1 - z/H) \cdot \text{Cosec } \psi_p \quad (49)$$

When the tension crack is in the upper slope surface:

$$Q = \left((1 - (z/H)^2) \cot \psi_p - \cot \psi_f \right) \sin \psi_p \quad (50)$$

When the tension crack is in the slope face:

$$Q = \left((1 - z/H)^2 \cot \psi_p (\cot \psi_p \cdot \tan \psi_f - 1) \right) \quad (51)$$

$$R = \frac{\gamma_w \cdot z_w \cdot z}{\gamma \cdot z \cdot H} \quad (52)$$

$$S = \frac{z_w \cdot z}{z \cdot H} \sin \psi_p \quad (53)$$

The ratios P, Q, R and S are all dimensionless which means that they depend upon the geometry but not upon the size of the slope. Hence, in cases where the cohesion $c = 0$, the factor of safety is independent of the size of the slope. The important principle of dimensionless grouping, illustrated in these equations, is a useful tool in rock engineering and extensive use will be made of this principle in the study of wedge and circular failures.

In order to facilitate the application of these equations to practical problems, values for the ratios P, Q and S, for a range of slope geometries, are presented in graphical form in Figure 7.3. Note that both tension crack positions are included in the graphs for the ratio Q and hence the values of Q may be determined for any slope configuration without having first to check on the tension crack position.

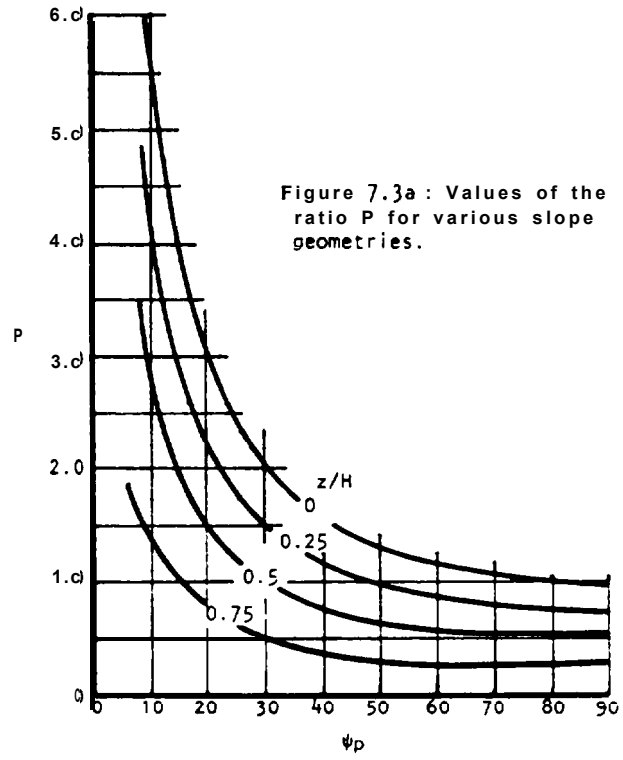
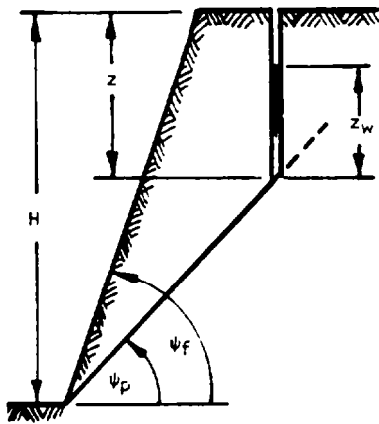


Figure 7.3a: Values of the ratio P for various slope geometries.

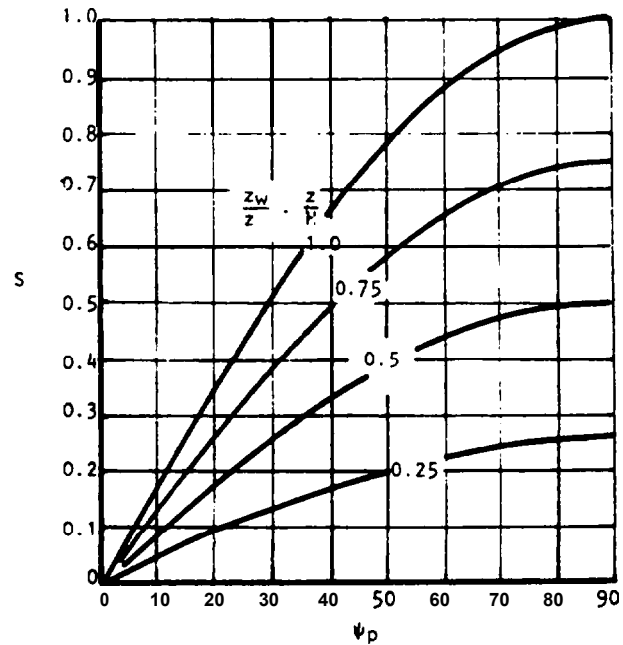


Figure 7.3b: Values of the ratio S for various geometries.

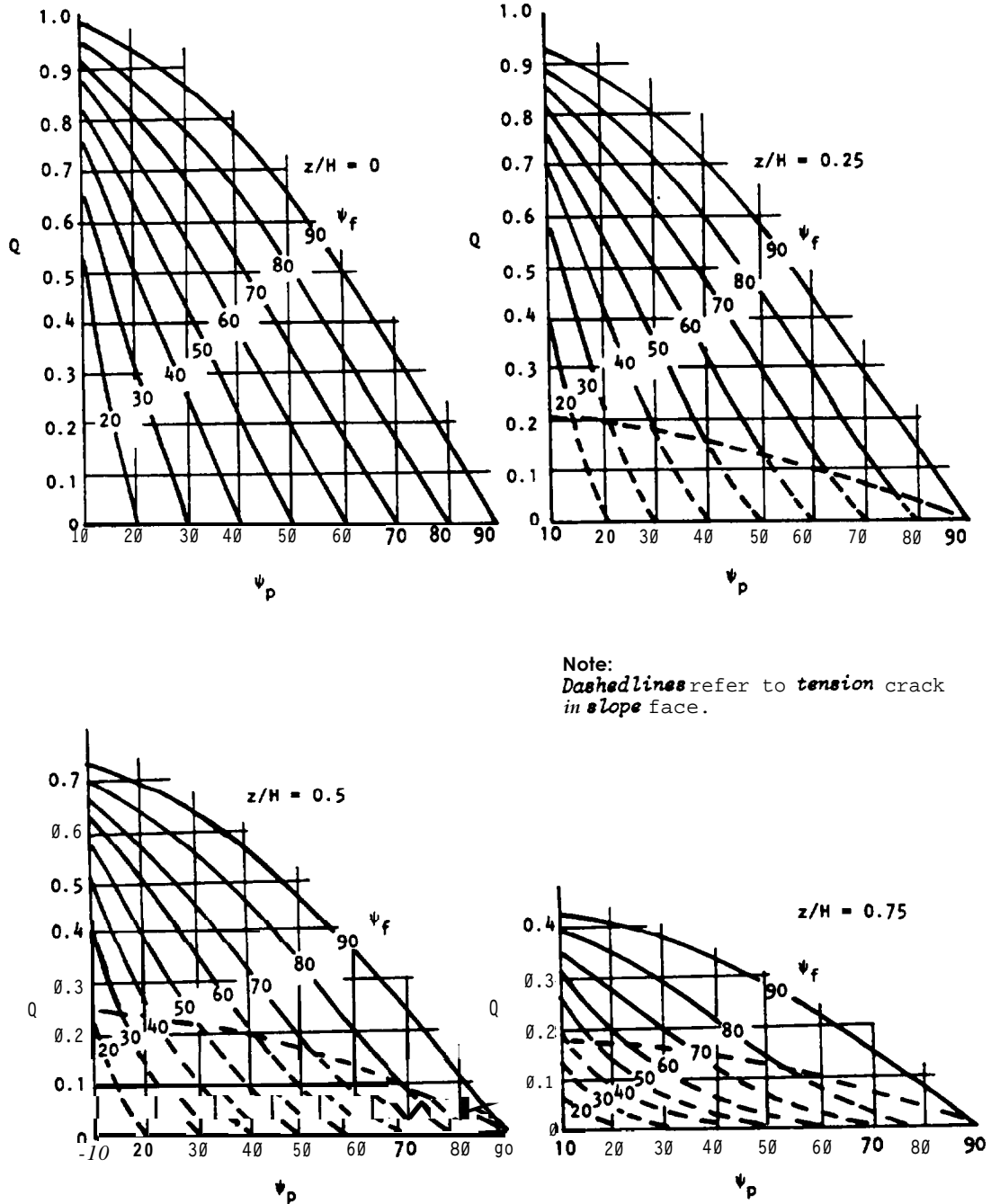
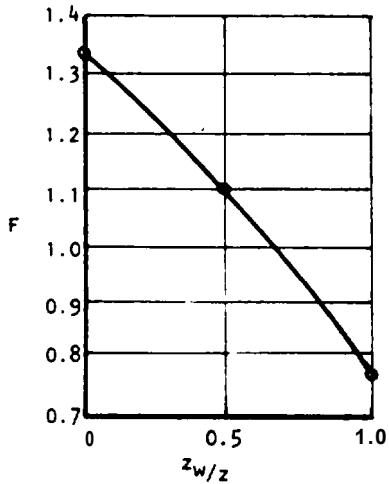


Figure 7.3c : Value of the ratio Q for various slope geometries.



One point to keep in mind when using these graphs is that the depth of the tension crack is always measured from the top of the slope as illustrated in Figure 7.1b.

Consider the example in which a 100 ft. high slope with a face angle $\psi_f = 60^\circ$ is found to have a bedding plane running through it at a dip $\psi_p = 30^\circ$. A tension crack occurs 29 ft. behind the crest of the slope and, from an accurately drawn cross-section of the slope, the tension crack is found to have a depth of 50 ft. The unit weight of rock $\gamma = 160 \text{ lb/ft.}^3$, that of water is $\gamma_w = 62.5 \text{ lb/ft.}^3$. Assuming that the cohesive strength of the bedding plane $c = 1,000 \text{ lb/ft.}^2$ and the friction angle $\phi = 30^\circ$, find the influence of water depth z_w upon the factor of safety of the slope.

The values of P and Q are found from Figure 7.3, for $z/H = 0.5$ to be:

$$P = 1.0 \text{ and } Q = 0.36$$

The values of R (from equation 52) and S (from Figure 7.3b), for a range of values of z_w/z , are:

z_w/z	1.0	0.5	0
R	0.195	0.098	0
S	0.26	0.13	0

The value of $2c/\gamma H = 0.125$

Hence, the factor of safety for different depths of water in the tension crack, from equation 48, varies as follows:

z_w/z	1.0	0.5	0
F	0.77	1.10	1.34

These values are plotted in the graph in the margin and the sensitivity of the slope to water in the tension crack is obvious. Simple analyses of this sort, varying one parameter at a time, can be carried out in a few minutes and are useful aids to decision making. In the example considered, it would be obviously worth taking steps to prevent water from entering the top of the tension crack. In other cases, it may be found that the presence of water in the tension crack does not have a significant influence upon stability and that other factors are more important.

Graphical analysis of stability

As an alternative to the analytical method presented above, some readers may prefer the following graphical method:

- From an accurately drawn cross-section of the slope, scale the lengths H, X, D, A, z and z_w shown in Figure 7.4s.
- Calculate the forces W, V and U from these dimensions by means of the equations given in Figure 7.4a. Also calculate the magnitude of the cohesive force A.c.
- Construct the force diagram illustrated in Figure 7.4b as follows:

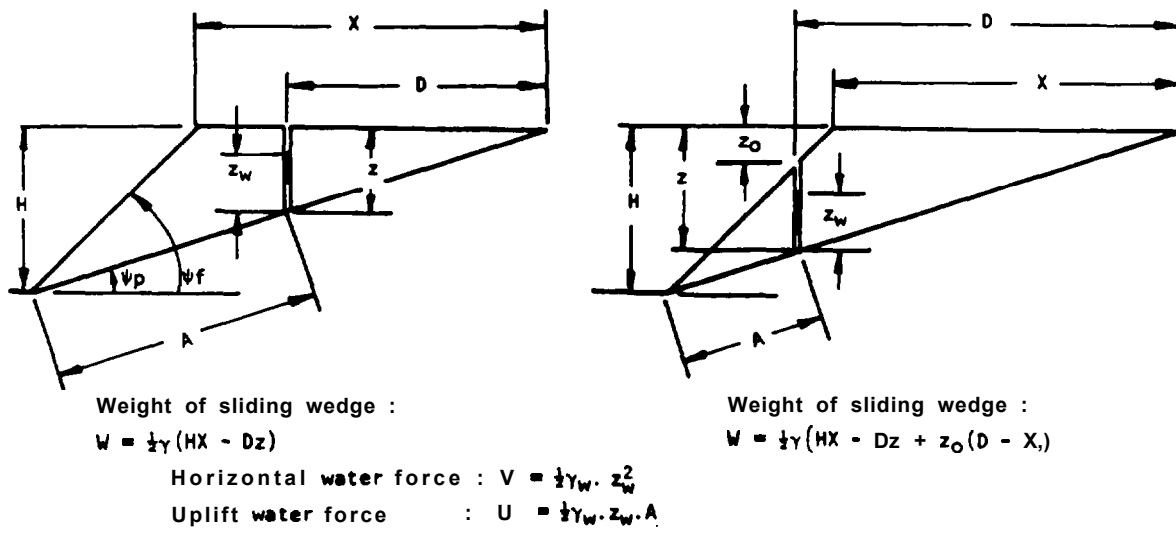


Figure 7.4a : Slope geometry and equations for calculating forces acting on slope.

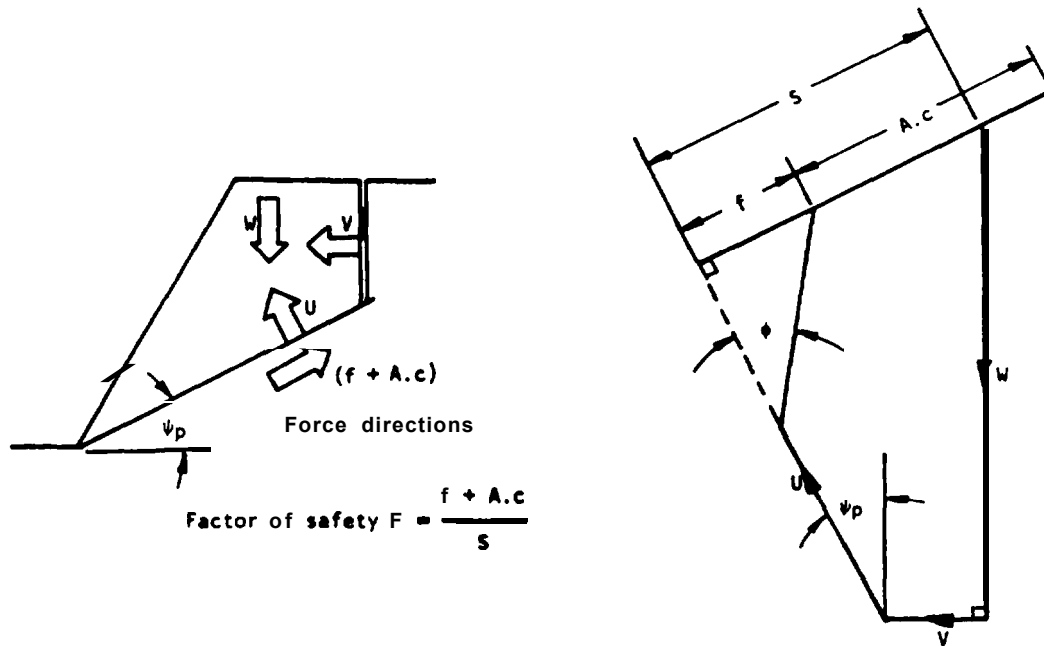


Figure 7.4b : Force diagram for two-dimensional slope stability analysis.

- i) Draw a vertical line to represent the weight W of the sliding wedge. The scale should be chosen to suit the size of the drawing board used.
- ii) At right angles to the line representing W , draw a line to represent the force V due to water pressure in the tension crack.
- iii) Measure the angle ψ/p as shown in Figure 7.4b and draw a line to represent the uplift force U due to water-pressure on the sliding surface.
- iv) Project the line representing U (shown dashed in Figure 7.4b) and, from the upper extremity of the line representing W , construct a perpendicular to the projection of the U line.
- v) From the upper extremity of the U line, draw a line at an angle ϕ to intersect the line from W to the projection for the U line.
- vi) The length f in Figure 7.4b represents the frictional force which resists sliding along the failure plane.
- vii) The cohesive resisting force $A.c$ can be drawn parallel to f . Although this step is not essential, drawing $A.c$ on the force diagrams ensures that there is no error in converting to and from the various scales which may have been used in this analysis since it provides a visual check of the magnitude of $A.c$.
- viii) The length of the line marked S on the force diagram represents the total force tending to induce sliding down the plane.
- ix) The factor of safety F of the slope is given by the ratio of the lengths $(f + A.c)$ to S .

An example of the application of this graphical technique will be given later in this chapter.

Influence of groundwater on stability

In the preceding discussion it has been assumed that it is only the water present in the tension crack and that along the failure surface which influences the stability of the slope. This is equivalent to assuming that the rest of the rock mass is impermeable, an assumption which is certainly not always justified. Consideration must, therefore, be given to water pressure distribution other than that upon which the analysis so far presented is based.

The current state of knowledge in rock engineering does not permit a precise definition of the groundwater flow patterns in a rock mass. Consequently, the only possibility open to the slope designer is to consider a number of realistic extremes in an attempt to bracket the range of possible factors of safety and to assess the sensitivity of the slope to variations in groundwater conditions.

a. Dry slopes

The simplest case which can be considered is that in which the slope is assumed to be completely drained. In practical terms, this means that there is no water pressure in the tension crack or along the sliding surface. Note that there may be moisture in the slope but, as long as no pressure is generated, it will not influence the stability of the slope.

Under these conditions, the forces V and U are both zero and equation (42) reduces to:

$$F = \frac{c \cdot A}{W \cdot \sin \psi_p} + \cot \psi_p \cdot \tan \phi \quad (54)$$

Alternatively, equation (48) reduces to:

$$F = \frac{2c}{\gamma H} \cdot \frac{P}{Q} + \cot \psi_p \cdot \tan \phi \quad (55)$$

b. Water in tension crack only

A heavy rain storm after a long dry spell can result in the rapid build-up of water pressure in the tension crack which will offer little resistance to the entry of surface flood water unless effective surface drainage has been provided. Assuming that the remainder of the rock mass is relatively impermeable, the only water pressure which will be generated during and immediately after the rain will be that due to water in the tension crack. In other words, the uplift force $U = 0$.

The uplift force U could also be reduced to zero or nearly zero if the failure surface was impermeable as a result of clay filling. In either case, the factor of safety of the slope is given by

$$F = \frac{c \cdot A + (W \cdot \cos \psi_p - V \cdot \sin \psi_p) \tan \phi}{W \cdot \sin \psi_p + V \cdot \cos \psi_p} \quad (56)$$

or, alternatively

$$F = \frac{2c/\gamma H \cdot P + (Q \cdot \cot \psi_p - RS) \tan \phi}{Q + RS \cdot \cot \psi_p} \quad (57)$$

c. Water in tension crack and on sliding surface

These are the conditions which were assumed in deriving the general solution presented on the preceding pages. The pressure distribution along the sliding surface has been assumed to decrease linearly from the base of the tension crack to the intersection of the failure surface and the slope face. This water pressure distribution is probably very much simpler than that which occurs in an actual slope but, since the actual pressure distribution is unknown, this assumed distribution is as reasonable as any other which could be made.

It is possible that a more dangerous water pressure distribution could exist if the face of the slope became frozen in winter so that, instead of the zero pressure condition which has been assumed at the face, the water pressure at the face would be that due to the full head of water in the slope. Such extreme water pressure conditions may occur from time to time and the slope designer should keep this possibility in mind. However, for general slope design, the use of this water pressure distribution would result in an excessively conservative

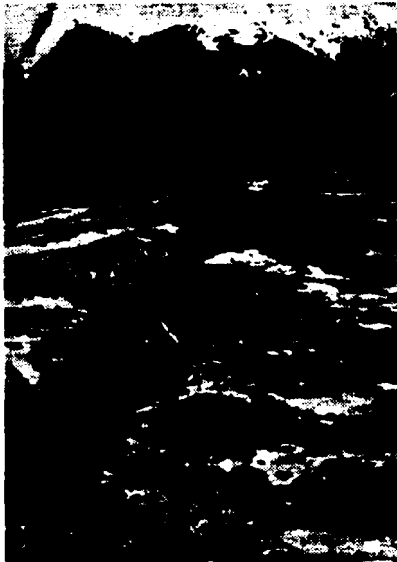
slope and hence the triangular pressure distribution used in the general analysis is presented as the basis for normal slope design.

d. Saturated slope with heavy recharge

If the rock mass is heavily fractured so that it becomes relatively permeable, a groundwater flow pattern similar to that which would develop in a porous system could occur (see Figure 6.9 on page 6.11). The most dangerous conditions which would develop in this case would be those given by prolonged heavy rain.

Flow nets for saturated slopes with heavy surface recharge have been constructed and the water pressure distributions obtained from these flow nets have been used to calculate the factors of safety of a variety of slopes. The process involved is too tedious to include in this chapter but the results can be summarized in a general form. It has been found that the factor of safety for a permeable slope, saturated by heavy rain and subjected to surface recharge by continued rain, can be approximated by equation (42) (or 48), assuming that the tension crack is water-filled, i.e. $z_w = z$.

In view of the uncertainties associated with the actual water pressure distributions which could occur in rock slopes subjected to these conditions, there seems little point in attempting to refine this analysis any further.



A mountain top tension crack above a large landslide.

Critical tension crack depth

In the analysis which has been presented, it has been assumed that the position of the tension crack is known from its visible trace on the upper surface or on the face of the slope and that its depth can be established by constructing an accurate cross-section of the slope. When the tension crack position is unknown, due for example, to the presence of soil on the top of the slope, it becomes necessary to consider the most probable position of a tension crack.

The influence of tension crack depth and of the depth of water in the tension crack upon the factor of safety of a typical slope is illustrated in Figure 7.5 (based on the example considered on page 7.8).

When the slope is dry or nearly dry, the factor of safety reaches a minimum value which, in the case of the example considered, corresponds to a tension crack depth of $0.42H$. This critical tension crack depth for a dry slope can be found by minimizing the right hand side of equation (54) with respect to z/H . This gives the critical tension crack depth as:

$$z_c/H = 1 - \sqrt{\cot \psi_f \cdot \tan \psi_p} \quad (58)$$

From the geometry of the slope, the corresponding position of the tension crack is:

$$b_c/H = \sqrt{\cot \psi_f \cdot \cot \psi_p} - \cot \psi_f \quad (59)$$

Critical tension crack depths and locations for a range of dry slopes are plotted in Figure 7.6.

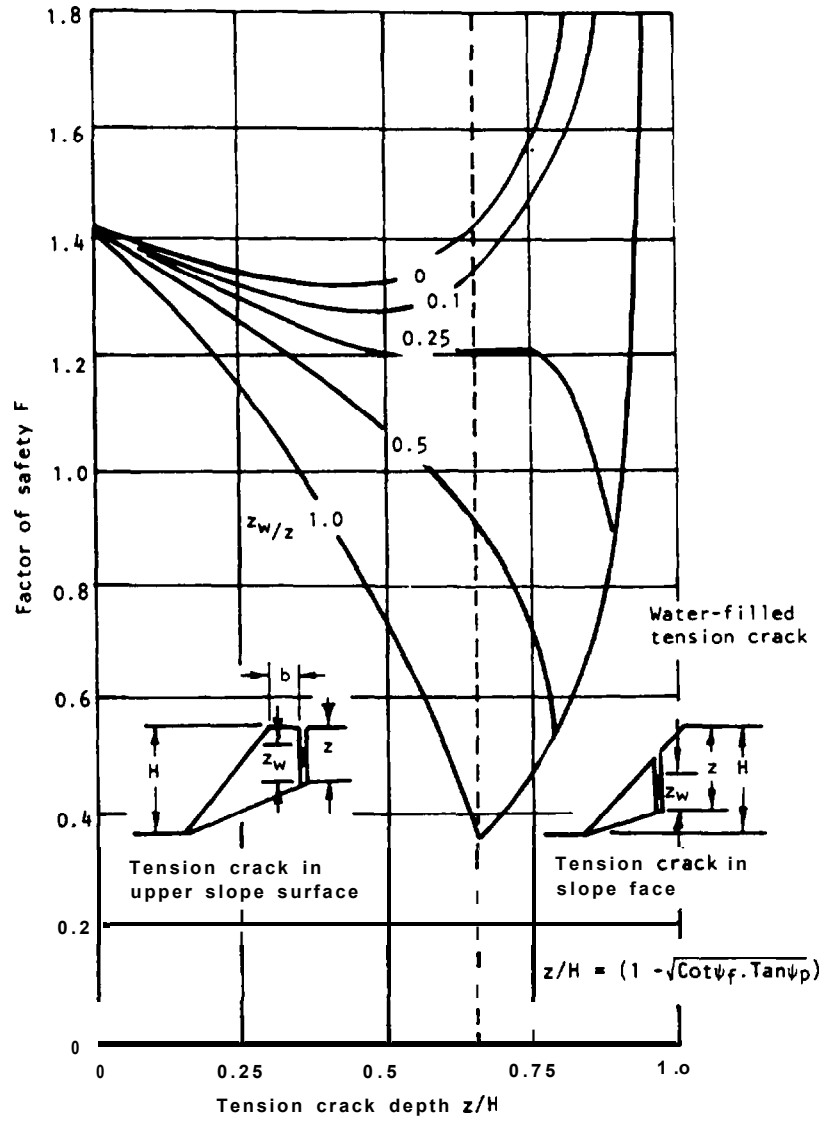


Figure 7.5 influence of tension crack depth and of depth of water in the tension crack upon the factor of safety of a slope. (Slope geometry and material properties as for example on page 7.8).

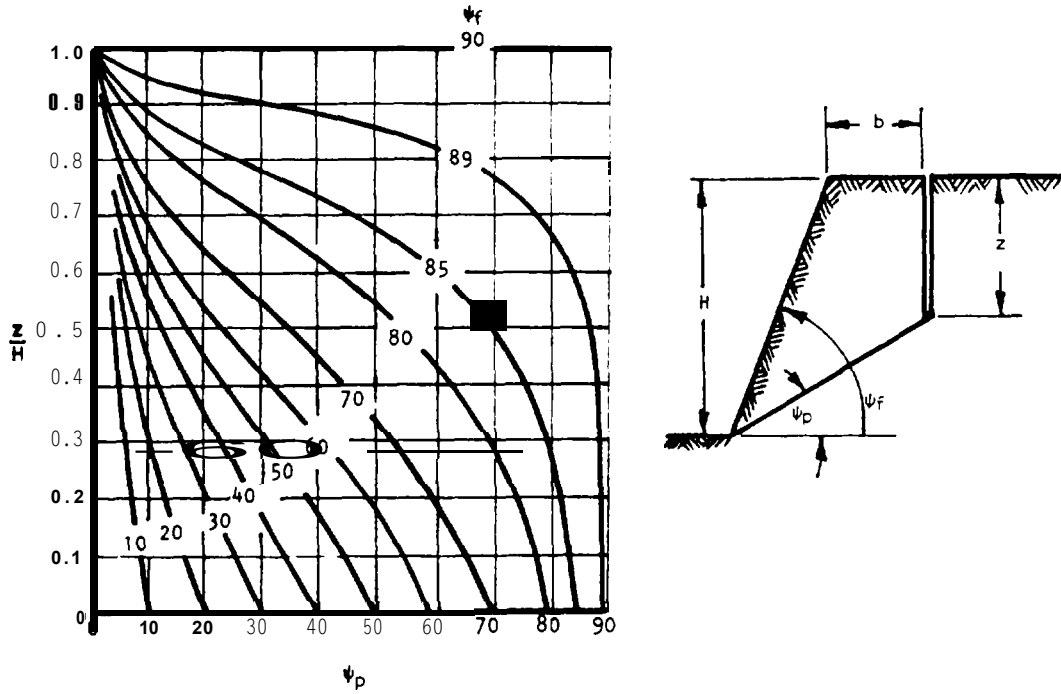


Figure 7.6a: Critical tension crack depth for a dry slope.

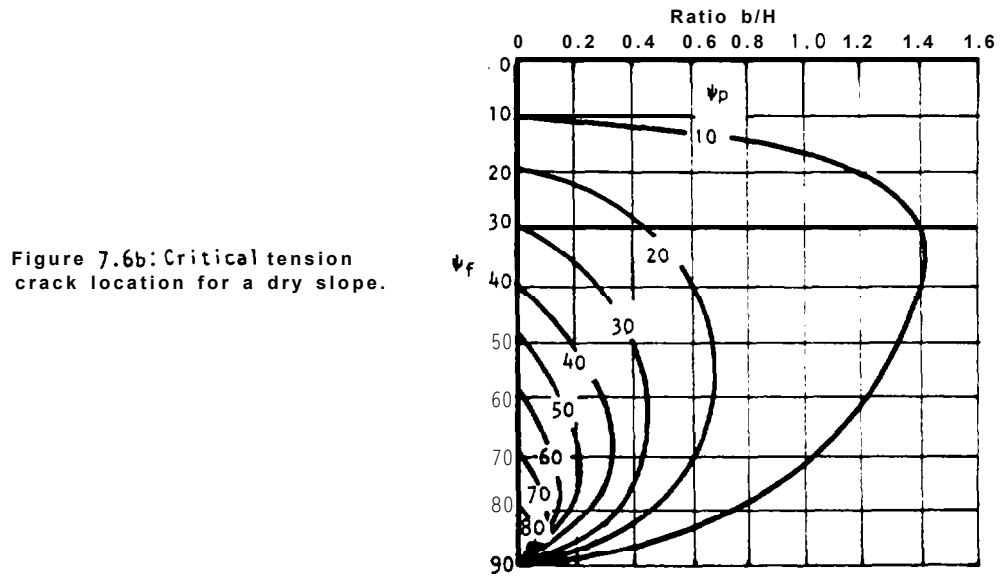
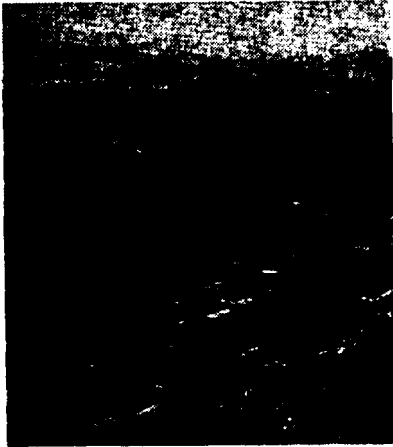


Figure 7.6b: Critical tension crack location for a dry slope.



A small tension crack on the bench of a slate quarry indicating the onset of instability.

Photograph by Dr. R. E. Goodman.



A large tension crack on an open pit mine bench in which considerable horizontal and vertical movement has occurred.

Figure 7.5 shows that, once the water level Z_w exceeds about one quarter of the tension crack depth, the factor of safety of the slope does not reach a minimum until the tension crack is water-filled. In this case, the minimum factor of safety is given by a water-filled tension crack which is coincident with the crest of the slope ($b = 0$).

It is most important, when considering the influence of water in a tension crack, to consider the sequence of tension crack formation and water filling. Field observations suggest that tension cracks usually occur behind the crest of a slope and, from Figure 7.5, it must be concluded that these tension cracks occur as a result of movement in a dry or nearly dry slope. If this tension crack becomes water-filled as a result of a subsequent rain storm, the influence of the water pressure will be in accordance with the rules laid down earlier in this chapter. The depth and location of the tension crack are, however, independent of the groundwater conditions and are defined by equations (58) and (59).

If the tension crack forms during heavy rain or if it is located on a pre-existing geological feature such as a vertical joint, equations (58) and (59) no longer apply. In these circumstances, when the tension crack position and depth are unknown, the only reasonable procedure is to assume that the tension crack is coincident with the slope crest and that it is water-filled.

The tension crack as an indicator of instability

Anyone who has examined excavated rock slopes cannot have failed to notice the frequent occurrences of tension cracks in the upper surfaces of these slopes. Some of these cracks have been visible for tens of years and, in many cases, do not appear to have had any adverse influence upon the stability of the slope. It is, therefore, interesting to consider how such cracks are formed and whether they can give any indication of slope instability.

In a series of very detailed model studies on the failure of slopes in jointed rocks, Barton (91) found that the tension crack was generated as a result of small shear movements within the rock mass. Although these individual movements were very small, their cumulative effect was a significant displacement of the slope surfaces - sufficient to cause separation of vertical joints behind the slope crest and to form "tension" cracks. The fact that the tension crack is caused by shear movements in the slope is important because it suggests that, when a tension crack becomes visible in the surface of a slope, it must be assumed that shear failure has initiated within the rock mass.

It is impossible to quantify the seriousness of this failure since it is only the start of a very complex progressive failure process about which very little is known. It is quite probable that, in some cases, the improved drainage resulting from the opening up of the rock structure and the interlocking of individual blocks within the rock mass could give rise to an increase in stability. In other cases, the initiation of failure could be followed by a very rapid decrease in stability with a consequent failure of the slope.

In summary, the authors recommend that the presence of a tension crack should be taken as an indication of potential instability and that, in the case of an important slope, this should signal the need for detailed investigation into the stability of that particular slope.

Critical failure plane inclination

When a through-going discontinuity such as a bedding plane exists in a slope and the inclination of this discontinuity is such that it satisfies the conditions for plane failure defined on page 7.1, the failure of the slope will be controlled by this feature. However, when no such feature exists and when a failure surface, if it were to occur, would follow minor geological features and, in some places, would pass through intact material, how could the inclination of such a failure path be determined?

The first assumption which must be made concerns the shape of the failure surface. In a soft rock slope or a soil slope with a relatively flat slope face ($\psi_f < 45^\circ$), the failure surface would have a circular shape. The analysis of such failure surfaces will be dealt with in Chapter 9.

In steep rock slopes, the failure surface is almost planar and the inclination of such a plane can be found by partial differentiation of equation (42) with respect to ψ_p and by equating the resulting differential to zero. For dry slopes this gives the critical failure plane inclination ψ_{pc} as

$$\psi_{pc} = \frac{1}{2} (\psi_f + \phi) \quad (60)$$

The presence of water in the tension crack will cause the failure plane inclination to be reduced by up to 10% and, in view of the uncertainties associated with this failure surface, the added complication of including the influence of groundwater is not considered justified. Consequently, equation (60) can be used to obtain an estimate of the critical failure plane inclination in steep slopes which do not contain through-going discontinuity surfaces. An example of the application of this equation in the case of chalk cliff failure will be given later in this chapter.

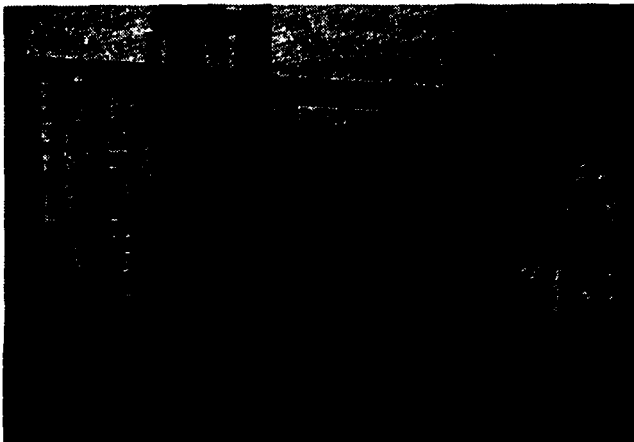
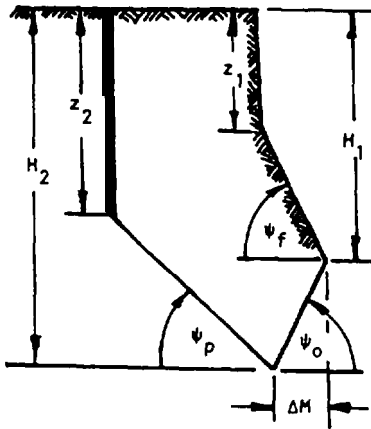


Figure 7.7: Two-dimensional model used by Barton (91) for the study of slope failure in jointed rock masses.

Influence of undercutting the toe of a slope

It is not unusual for the toe of a slope to be undercut, either intentionally by excavation or by natural agencies such as the weathering of underlying strata or, in the case of sea cliffs, by the action of waves. The influence of such undercutting on the stability of a slope is important in many practical situations and an analysis of this stability is presented here.



Geometry of under-cut slope

In order to provide as general a solution as possible, it is assumed that the geometry of the slope is that illustrated in the margin sketch. A previous failure is assumed to have left a face inclined at ψ_f and a vertical tension crack depth z_1 . As a result of an undercut of ΔM , inclined at an angle ψ_0 , a new failure occurs on a plane inclined at ψ_p and involves the formation of a new tension crack of depth z_2 .

The factor of safety of this slope is given by equation (42) but it is necessary to modify the expression for the weight terms as follows:

$$W = \frac{1}{2} \gamma [(H_2^2 - z_2^2) \cot \psi_p - (H_1^2 - z_1^2) \cot \psi_f + (H_1 + H_2) \Delta M] \quad (61)$$

Note that, for $\psi_0 > 0$,

$$\Delta M = (H_2 - H_1) \cot \psi_0 \quad (62)$$

The critical tension crack depth, for a dry undercut slope, is given by

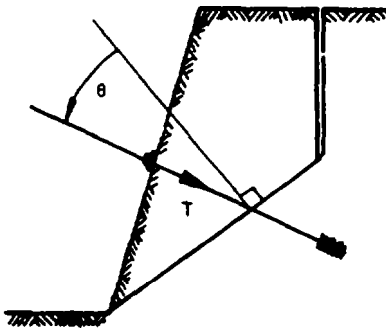
$$z_2 = \frac{c \cdot \cos \phi}{\gamma \cos \psi_p \cdot \sin (\psi_p - \phi)} \quad (63)$$

The critical failure plane inclination is

$$\psi_p = \frac{1}{2} \left(\phi + \arctan \frac{H_2^2 - z_2^2}{(H_1^2 - z_1^2) \cot \psi_f - (H_1 + H_2) \Delta M} \right) \quad (64)$$

The application of this analysis to an actual slope problem is presented at the end of this chapter.

Reinforcement of a slope



Reinforcement of a slope

When it has been established that a particular slope is unstable, it becomes necessary to consider whether it is possible to stabilize the slope by drainage or by the application of external loads. Such external loads may be applied by the installation of rock bolts or cables anchored into the rock mass behind the failure surface or by the construction of a waste rock berm to support the toe of the slope.

The factor of safety of a slope with external loading of magnitude T , inclined at an angle θ to the failure plane as shown in the sketch opposite, is approximated by:

$$F = \frac{cA + (W \cdot \cos \psi_p - U - V \cdot \sin \psi_p + T \cdot \cos \theta) \tan \phi}{W \cdot \sin \psi_p + V \cdot \cos \psi_p - T \cdot \sin \theta} \quad (65)$$

This equation is correct for the condition of limiting equilibrium ($F = 1$) but there are certain theoretical problems in using it for other values of F . These problems are discussed fully in Appendix 3 at the end of this book,

Analysis of failure on a rough plane

As discussed in Chapter 5, most rock surfaces exhibit a non-linear relationship between shear strength and effective normal stress. This relationship may be defined by Ladanyi and Archambault's equation (2) on page 5.5) or by Barton's equation (26 on page 5.7). In order to apply either of these equations to the analysis of failure on a rough surface plane it is necessary to know the effective normal stress σ acting on this plane.

Consider the slope geometry illustrated in Figure 7.1. The effective normal stress acting on the failure surface can be determined from equations (43) to (47) and is given by:

$$\sigma = \frac{W \cdot \cos \psi_p - U - V \cdot \sin \psi_p}{A} \quad (66)$$

Alternatively, from equations (49) to (53)

$$\sigma = \frac{\gamma H}{zP} (Q \cot \psi_p - R(P+S)) \quad (67)$$

Having determined the value of σ , the shear strength τ of the failure surface is calculated from equation (21) or (26). The factor of safety of the slope is given by modifying equations (42) and (48) as follows:

$$F = \frac{\tau \cdot A}{W \cdot \sin \psi_p + V \cdot \cos \psi_p} \quad (68)$$

or

$$F = \frac{zP \cdot \tau}{\gamma H (Q + R \cdot S \cdot \cot \psi_p)} \quad (69)$$

The application of these equations is best illustrated by means of a practical example. Consider a slope defined by $H = 100$ ft., $z = 50$ ft., $\psi_s = 60^\circ$ and $\psi_p = 30^\circ$. The unit weight of the rock $\gamma = 160$ lb/ft.³ and that of water $\gamma_w = 62.5$ lb/ft.³. Two cases will be considered:

Case 1: A drained slope in which $z_M = 0$

Case 2: A slope with a water filled tension crack defined by $z_M = z$.

The values given by substitution in equations (43) to (46) and (49), (50), (52) and (53) are as follows:

Case 1: $A = 100 \text{ ft.}^2/\text{ft.}$, $U = 0$, $V = 0$, $W = 571350 \text{ lb/ft.}$
 $P = 1.00$, $Q = 0.36$, $R = 0$ and $S = 0$.

Case 2: $A = 100 \text{ ft.}^2/\text{ft.}$, $U = 156250 \text{ lb/ft.}$, $V = 76125 \text{ lb/ft.}$,
 $W = 577350 \text{ lb/ft.}$, $P = 1.00$, $Q = 0.36$, $R = 0.195$ and $S = 0.25$

Substitution in equations (66) and (67) gives the effective normal stress on the failure plane as $\sigma = 5,000 \text{ lb/ft.}^2$ for Case 1 and $\sigma = 3,049 \text{ lb/ft.}^2$ for Car. 2.

Assume that the shear strength of the surface is defined by Barton's equation (26 on page 5.7) with $\phi = 30^\circ$, $JRC = 10$ and $\sigma_j = 720,000 \text{ lb/ft.}^2$. Substitution of these values gives $\tau = 6,305 \text{ lb/ft.}^2$ for Case 1 and $\tau = 4,155 \text{ lb/ft.}^2$ for Case 2. Substituting these values of τ into equations (68) or (69) gives:

Case 1: $F = 2.16$

Case 2: $F = 1.17$

The application of this analysis to a practical example will be discussed later in this chapter.

Practical example number 1

Stability of porphyry slopes in a Spanish open pit mine

In order to assist the mine planning engineers in designing an extension to the Atalaya open pit operated by Rio Tinto Espanola in southern Spain, an analysis was carried out on the stability of porphyry slopes forming the northern side of the pit (left hand side of the pit in the photograph reproduced in Figure 7.8). A summary of this analysis is presented in this example.

At the time of this design study (1969), the Atalaya pit was 260 m deep and the porphyry slopes, inclined at an overall angle of approximately 45° as shown in Figure 7.9 appeared to be stable. The proposed mine plan called for deepening the pit to in excess of 300 m and required that, if at all possible, the porphyry slopes should be left untouched. The problem, therefore, was to decide whether these slopes would remain stable at the proposed mining depth.

Since no slope failure had taken place in the porphyry slopes of the Atalaya pit, deciding upon the factor of safety of the existing slopes posed a difficult problem. Geological mapping and shear testing of discontinuities in the porphyry provided a useful guide to the possible failure modes and the range was too wide to permit the factor of safety to be determined with a reasonable degree of confidence.

Consequently, it was decided to use a technique similar to that employed by Salamon and Munro (1966) for the analysis of coal pillar failures in South Africa. This method involved collecting data on slope heights and slope angles for both stable and unstable slopes in porphyry in order to establish a pattern of slope behaviour based upon full scale slopes. The data on unstable slopes had to be collected from other open pit mines in the Rio Tinto area in which failures had occurred in porphyry judged to be similar to those in the Atalaya pit. The collected slope height versus slope angle data are plotted in Figure 7.10.



Figure 7.8: Rio Tinto Espanola's Atalaya open pit mine.

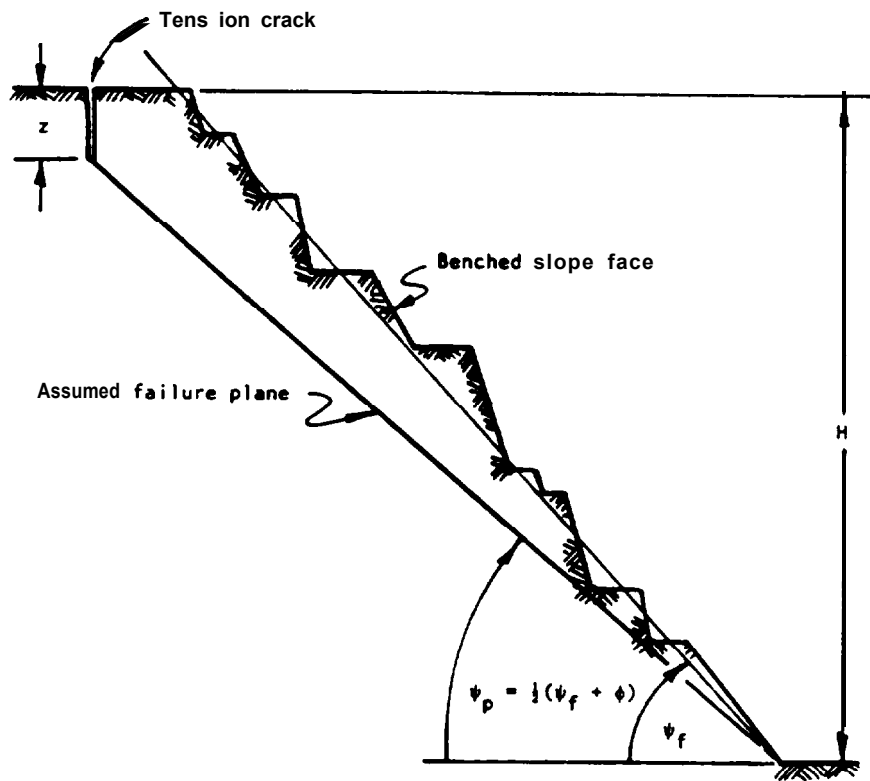


Figure 7.9: Section through a typical porphyry slope in the Atalaya open pit at Rio Tinto in Spain.

In order to establish the theoretical relationship between slope height and slope angle, the following assumptions are made:

- a. Because the geological mapping had failed to reveal any dominant through-going structures which could control the stability of the slopes in question but had revealed the presence of a number of intersecting joint sets, it was assumed that failure, if it were to occur, would be on a composite planar surface inclined at $\psi_p = 1/2 (\psi_f + \phi)$ as defined by equation (60) on page 7.16.
- b. From the shear strength data a friction angle $\phi = 35^\circ$ was chosen as the starting point for this analysis.
- c. Because of the presence of underground workings, the porphyry slopes were assumed to be fully drained and it was assumed that tension cracks would occur in accordance with the critical conditions defined in equation (58) on page 7.12. It was assumed that these tension cracks would occur in all slopes, including those with factors of safety in excess of unity, and the typical failure geometry is illustrated in Figure 7.9.

The factor of safety for a dry slope is defined by equation (55) on page 7.10 which, for the purposes of this analysis, can be rearranged in the following form:

$$H = \frac{2c \cdot P}{\gamma Q (F - \cot \psi_p \cdot \tan \phi)} \quad (70)$$

Solving equations (60), (58), (49) and (50) for a range of slope angles, assuming $\gamma = 2.95$ tonnes/m³, gives:

ψ_f	ψ_p	z/H	P	Q	H
85	60.0	0.610	0.450	0.238	1.28c/(F = 0.404)
80	57.5	0.474	0.624	0.268	1.58c/(F = 0.446)
70	52.5	0.311	0.668	0.261	2.25c/(F = 0.537)
60	47.5	0.206	1.077	0.221	3.30c/(F = 0.641)
50	42.5	0.123	1.300	0.159	5.54c/(F = 0.764)
40	37.5	0.044	1.572	0.007	152c/(F = 0.913)

The problem now is to find a value for the cohesion c which gives the best fit for a limiting curve ($F = 1$) passing through the slope height/slope angle points for unstable slopes. The two points at $\psi_f = 61^\circ$ and 66° and $H = 40$ m and 35 m respectively are ignored in this curve fitting since they were identified as individual bench failures on through-going discontinuities and they would not, therefore, belong to the same family as the other slopes.

A number of trial calculations showed that the best fit for the $F = 1$ curve to the seven failure points shown in Figure 7.10 is given by a cohesive strength $c = 14$ tonnes/m².

The shear strength relationship defined by $c = 14$ tonnes/m² and $\phi = 35^\circ$ has been plotted in Figure 7.11 which also shows peak and residual strength values determined by shear testing at Imperial College. Note that the shear strength relationship determined by back analysis appears to fall between the peak and residual shear strength values determined in the laboratory.

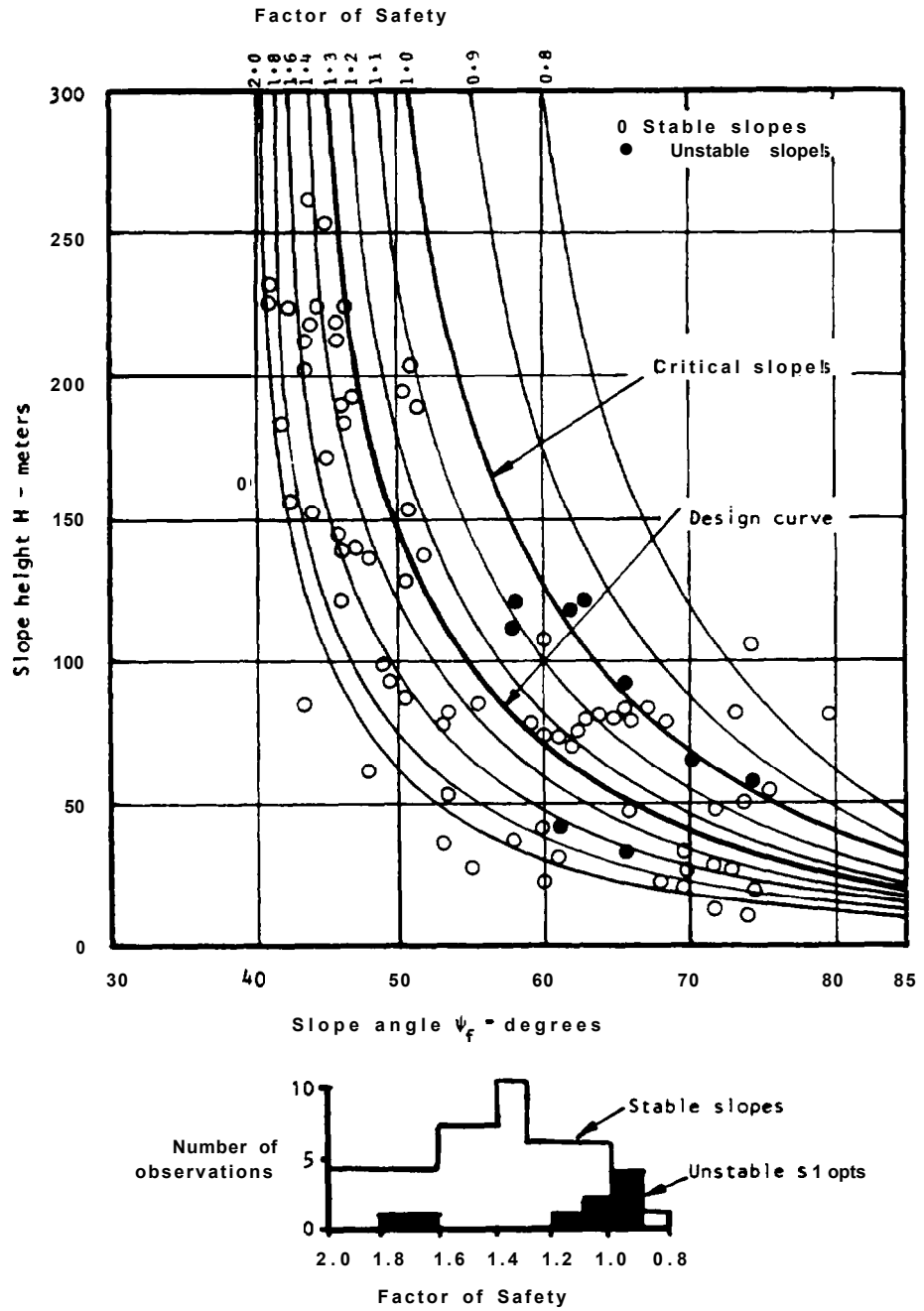


Figure 7.10: Relationship between slope heights and slope angles for porphyry slopes in the Rio Tinto area, Spain.

Care should, however, be exercised not to draw too many conclusions from this figure since the range of normal stresses in the slope failures which were back analyzed was approximately 20 to 50 tonnes/m². The scatter of test results in this stress range is too large to allow a more detailed analysis of the results to be carried out.

Figure 7.11 illustrates an important historical point in slope stability analysis since it reflects the shear testing philosophy of the late 1960s. The importance of testing at very low normal stress levels and of the non-linearity of the shear strength curve had not been recognized at that time and shear tests were frequently carried out at stress levels which were several times higher than the normal stresses acting in actual slopes. This philosophy was carried over from underground rock mechanics and from studies of intact rock fracture in which testing was usually carried out at high normal stresses. As discussed in Chapter 5, studies by Patton, Barton, Ladanyi and Archambault and others have contributed greatly to our understanding of shear strength behavior at low normal stresses and there is no doubt that the Rio Tinto analysis, presented on the preceding pages, would follow slightly different lines if it were to be reported today. An example of an analysis using a curvilinear shear strength relationship is given later in this chapter. Incidentally, the authors feel that, in spite of the crude analysis carried out on the Rio Tinto slopes, the engineering decisions summarized in Figure 7.10 are still sound and the overall approach is still valid.

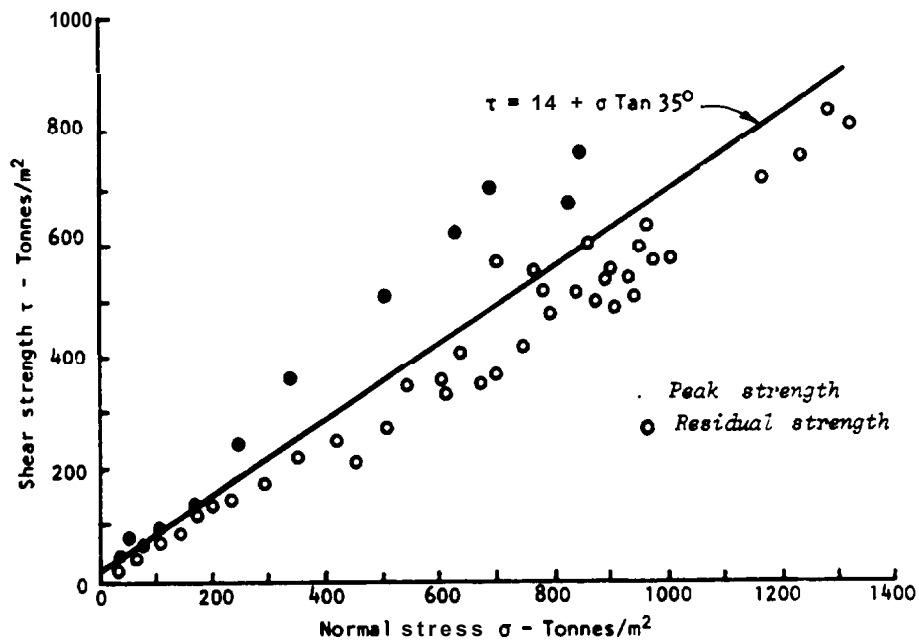


Figure 7.11: Shear strength characteristics of porphyry from Rio Tinto.



Figure 7.12: Small scale failures of individual benches are not usually significant in open pit mining unless they cause disruption of haul roads.



Figure 7.13: The open pit designer is concerned primarily with minimising the risk of overall slope failure. (Kennecott Copper photograph published by Broadbent & Armstrong¹⁸⁷).

Substitution of the value of $c = 14 \text{ tonnes/m}^2$ into the relationships for the slope height H , listed after equation (70), gives the curves for different factors of safety which have been plotted in Figure 7.10. By counting the number of points falling between factor of safety increments, it is possible to construct the histogram reproduced in the lower part of Figure 7.10. This histogram confirms that the seven unstable slopes are clustered around a factor of safety $F = 1$ while the stable slopes show a peak between 1.3 and 1.4.

From a general consideration of the anticipated working life of the slope and of the possible consequences of slope failure during the mining operations, it was concluded that a factor of safety of 1.3 would be acceptable for the porphyry slopes in the Atalaya pit and, hence, the design curve presented to the mine planning engineers is that shown as a heavy line in Figure 7.10. This curve shows that, for the slope heights in excess of 250 m under consideration, the factor of safety changes very little for a change in slope angle. It was, therefore, concluded that the proposed deepening of the pit would not decrease the overall stability of the porphyry slopes, provided that no major changes in rock mass properties or drainage conditions were encountered in this deepening process.

Before leaving this example it is important to point out that this analysis deals with the stability of the overall pit slope and not with possible failures of individual benches. In a large pit such as the Atalaya pit, it would be totally uneconomic to attempt to analyze the stability of each bench and, in any case, small bench failures are not particularly important in large pits provided that they do not influence haul roads. On the other hand, a failure of the wedge illustrated in Figure 7.13, involving approximately 20,000 tonnes/meter of face (from equation (46) assuming $\gamma = 2.95 \text{ tonnes/m}^3$) would obviously represent a very serious problem which has to be avoided.

Practical example number 2

Investigation of the stability of a limestone quarry face

Figure 7.14 shows a hillside limestone quarry in the Mendip Hills in England, owned and operated by the Amalgamated Roadstone Corporation*. This photograph was taken in 1968 after a slope failure had occurred during a period of exceptionally heavy rain.

In 1970, it was decided to expand the quarry facilities and this involved the installation of new plant on the floor of the quarry. In view of the large horizontal movements of material which had occurred in the 1968 slope failure (as shown in Figure 7.14), it was considered that an investigation of the stability of the remainder of the slope was necessary. This example gives a summary of the most important aspects of this stability study, full details of which have been published by Roberts and Hoek (148).

The 1968 failure occurred after a week or more of steady soaking rain had saturated the area. This was followed by an exceptionally heavy downpour which flooded the upper quarry

*Now Hney Roadstone Corporation

floor, filling an existing tension crack in the slope crest. The geometry of the failure is illustrated in Figure 7.15. As seen in Figure 7.14, the failure is basically two-dimensional, the sliding surface being a bedding plane striking parallel to the slope crest and dipping into the excavation at 20° . A vertical tension crack existed 41 ft. behind the slope crest at the time of the failure.

In order to provide shear strength data for the analysis of the stability of the slope under which the new plant was to be installed, it was decided to analyze the 1968 failure by means of the graphical method described in Figure 7.4 on page 7.9. Because the dimensions of the proposed slope were reasonably similar to those of the 1968 failure, it was assumed that a linear shear strength relationship, defined by a cohesive strength and angle of friction, would be sufficiently accurate for this analysis.

Assuming a rock density of 0.08 tons/ft.^3 (160 lb/ft.^3) and a water density of 0.031 tons/ft.^3 (62.4 lb/ft.^3);

Weight of sliding mass $W = 1/2\gamma(XH - Dz) = 404.8 \text{ tons/ft.}$

Horizontal water force $V = 1/2\gamma_w \cdot z_w^2 = 65.5 \text{ tons/ft.}$

Uplift of water force $U = 1/2\gamma_w \cdot z_w \cdot A = 110.8 \text{ tons/ft.}$

From the force diagram, Figure 7.16(a), the shear strength mobilized in the 1968 failure can be determined and this is plotted in Figure 7.16(b).

From an examination of the surface upon which failure had taken place in 1968, it was concluded that the friction angle was probably $20^\circ + 5^\circ$. This range of friction angles and the associated cohesive strengths, shown in Figure 7.16(b) are used to determine the stability of the overall slopes in this illustrative example.

Having established the range of shear strengths mobilized in the 1968 failure, these values were now used to check the stability of the 210 ft. high slopes under which the new plant was to be installed. The geometry of the slope analyzed is illustrated in Figure 7.17 which shows that, in order to provide for the worst possible combination of circumstances, it was assumed that the bedding plane on which the 1968 slide had occurred daylighted in the toe of the slope.

Figure 7.18 shows typical force diagrams for dry and saturated slopes, assuming a slope face angle $\beta = 50^\circ$ and a friction angle $\phi = 25^\circ$. A range of such force diagrams was constructed and the factors of safety determined from these constructions are plotted in Figure 7.19. In this figure the full lines are for a friction angle $\phi = 20^\circ$, considered the most probable value, while the dashed lines define the influence of a 5° variation on either side of this angle.

It is clear from Figure 7.19 that 58° slopes are unstable under the heavy rainfall conditions which caused the slopes to become saturated in 1968. Drainage of the slope, particularly the control of surface water which could enter the top of an open tension crack, is very beneficial but, since it cannot be guaranteed that such drainage could be fully effective, it was recom-



Figure 7.14: Air photograph of Amalgamated Roadstone Corporation's **Batts Combe** limestone quarry in Somerset, England, showing details of the 1968 slope failure (Roberts and Hoek¹⁴⁸).

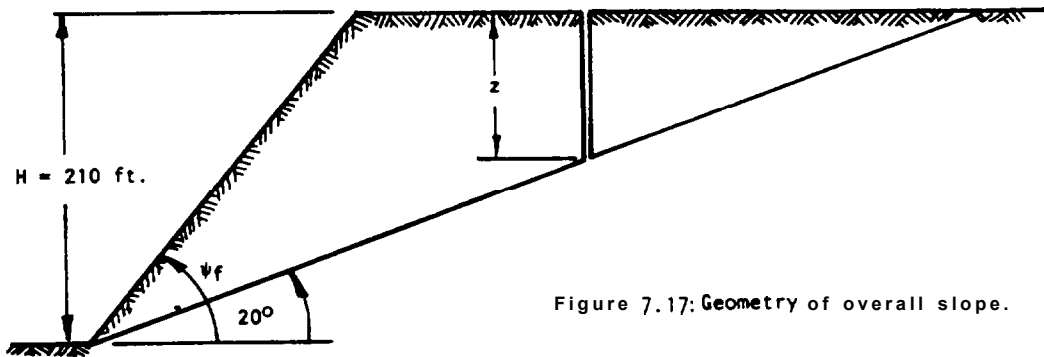


Figure 7.17: Geometry of overall slope.

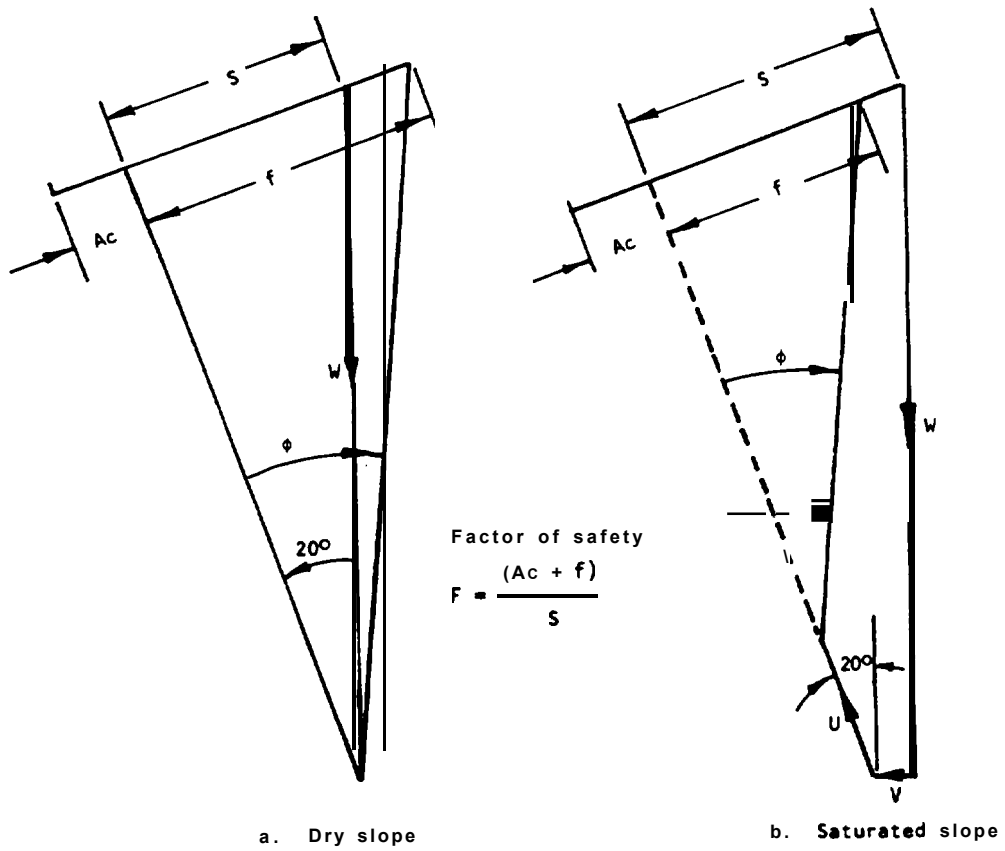


Figure 7.18: Force diagrams for design of overall quarry slopes.

mended that the slope should also be benched back to an overall angle of 45° .

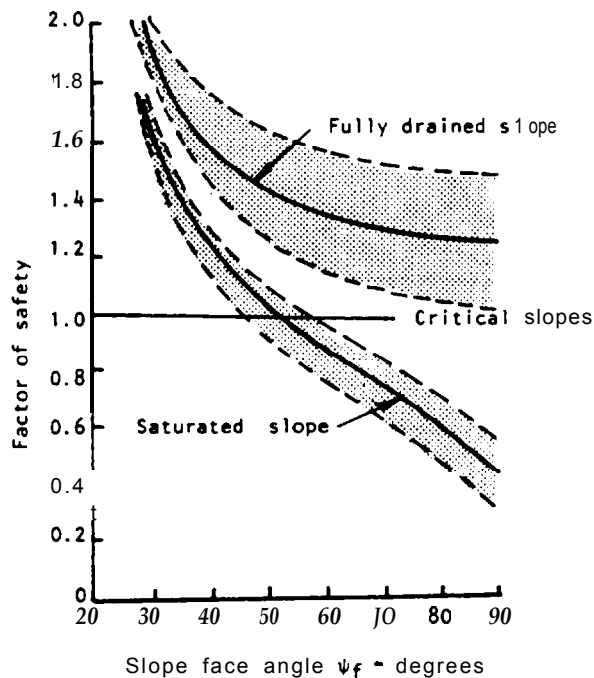


Figure 7.19: Factor of safety for dry and saturated slopes with different face angles.

Practical example number 3

Choice of remedial measures for critical slopes

When a slope above an important highway or railroad or above a civil engineering structure such as a dam is found to be **potentially** unstable, an urgent decision on the **effective** and economical **remedial** measures which can be employed is frequently required. The **following** example illustrates one of the methods **which** may be adopted in **arriving** at such a decision. Although this example is **hypothetical**, it is based upon a number of actual problems **with** which the authors have been concerned.

The first stage in the analysis is obviously to check that the slope is actually unstable and whether any remedial measures are **required**. **Sometimes** it is obvious that a potential failure **problem exists** because failures of limited extent have already taken place in part of the slope - this was the case in the quarry stability problem **discussed** in practical example 2. In other cases, a suspicion may have been created by **failures** of adjacent slopes or even by the fact that the **engineer** in charge of the slope has recently attended a conference on slope **stability** and has become alarmed about the **stability** of the slopes in his charge. Whatever the cause, once a doubt has been cast upon the **stability** of an important slope, it is essential that

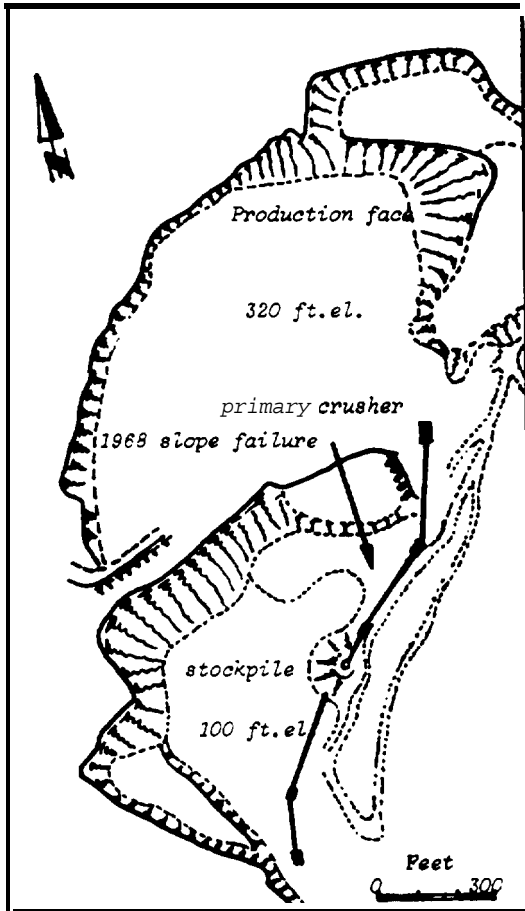


Figure 7.20a : Batts Combe quarry plan in 1970 showing the location of the 1968 slope failure which destroyed part of the conveyor system (see Figure 7.14).

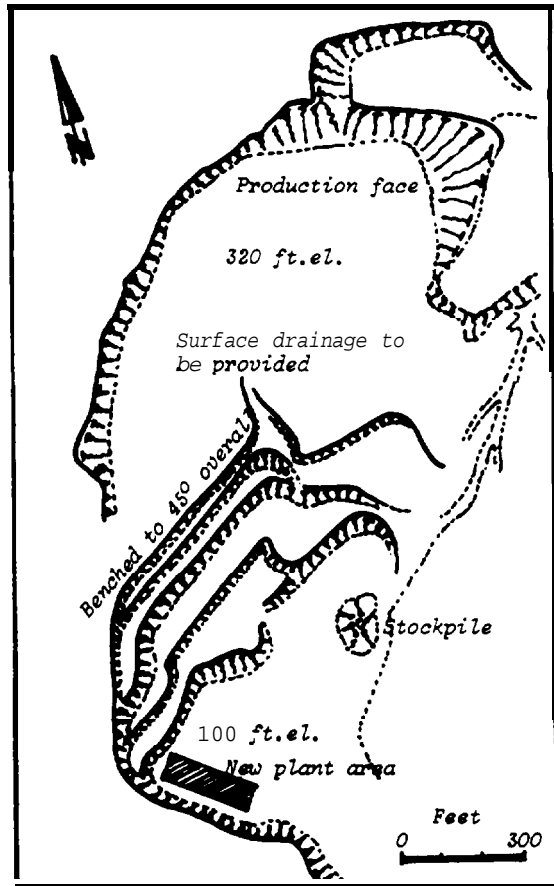


Figure 7.20b : Plan of proposed benching of lower slopes in Batts Combe quarry. Slopes are to be benched back to an overall slope of 45° with pre-splitting of final faces. Surface drainage on upper quarry floor and provision of horizontal drain holes in bench faces if piezometers indicate high sub-surface water levels.

Its overall stability should be investigated and that appropriate remedial measures should be implemented if these are found to be necessary.

Consider the following examples:

A 60 m high slope has an overall face angle of 50° , made up from three 20 m benches with 70° faces. The slope is in reasonably fresh granite but several sets of steeply dipping joints are visible and sheet jointing similar to that described by Terzaghi (17) is evident. The slope is in an area of high rainfall intensity and low seismicity. An acceleration of 0.08 g has been suggested as the maximum to which this slope is likely to be subjected. A small slide in a nearby slope has caused attention to be focused onto this particular slope and concern has been expressed in case a major slide could occur and could result in serious damage to an important civil engineering structure at the foot of the slope. The rock slope engineer called in to examine the problem is required to assess both the short and the long term stability of the slope and to recommend appropriate remedial measures, should these prove necessary. No previous geological or engineering studies have been carried out on this slope and no boreholes are known to exist in the area.

Faced with this problem and having no geological or engineering data from which to work, the first task of the rock slope engineer is to obtain a representative sample of structural geology data in order that the most likely failure mode can be established. Time would not usually allow a drilling program to be mounted, even if drilling equipment and operators of the required standard were readily available in the area. Consequently, the collection of structural data would have to be based upon surface mapping as described in Chapter 4, page 4.1. In some circumstances, this mapping can be carried out using the photogrammetric techniques described on page 4.5.

It is assumed that structural mapping is carried out and that the following geometrical and structural features have been identified:

Feature	dip $^\circ$	dip direction $^\circ$
Overall slope face	50	200
Individual benches	70	200
Sheet joint	35	190
Joint set J1	80	233
Joint set J2	80	040
Joint set J3	70	325

The stereoplot of this data is given in Figure 7.21 and a friction circle of 30° is included on this plot. Note that, although the three joint sets provide a number of steep release surfaces which would allow blocks to separate from the rock mass, none of their lines of intersection, ringed in Figure 7.21, fall within the zone designated as potentially unstable. On the other hand, the sheet joint great circle passes through the zone of potential instability and, since its dip direction is close to that of the slope face, it can be concluded that the most likely failure mode is that involving a planar slide on the sheet joint surface in the direction indicated in Figure 7.21.

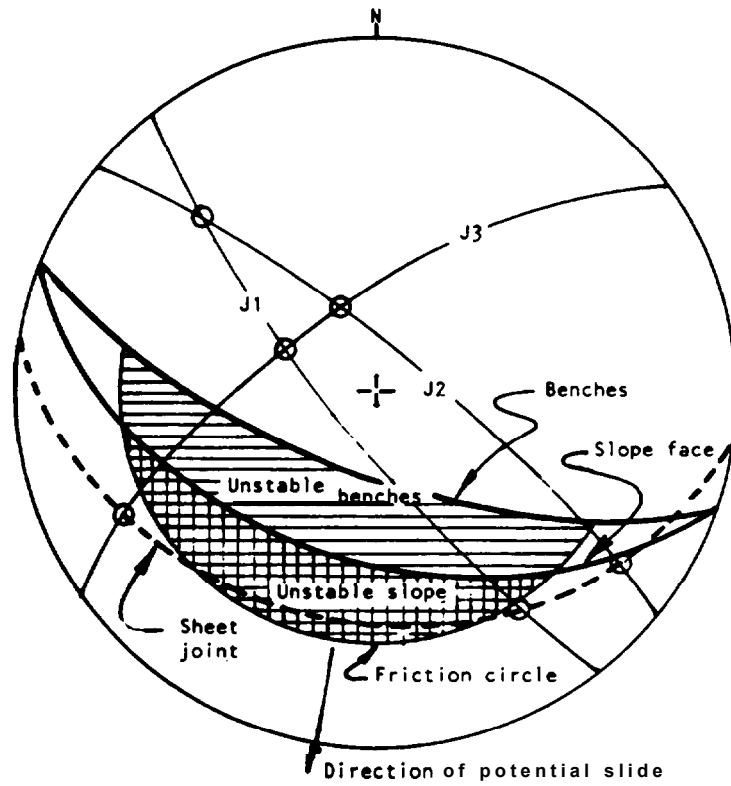


Figure 7.21: Stereoplot of geometrical and geological data for example number 3.

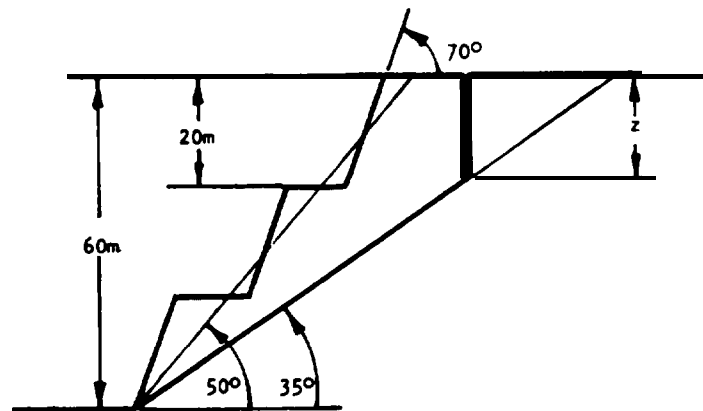


Figure 7.22: Geometry assumed for two-dimensional analysis of the slope defined in Figure 7.21.

The stability check carried out in Figure 7.21 suggests that both the **overall** slope and the individual benches are potentially unstable and it is therefore clearly necessary to carry out further checks on both.

Because of the presence of the three steeply **dipping joint** sets, the possibility of a tension **crack** forming in the upper surface of the slope must be regarded as high. One possible failure **mode** is that illustrated as Model I in Figure 7.23. This theoretical model assumes that a tension crack occurs in the dry state in the most **critical** position and that this crack is filled to **depth** z_w with water during a period of **exceptionally heavy rain**. A **simultaneous** earthquake subjects the slope to an acceleration of 0.08 g. The factor of **safety** of this slope is given by **equation (71)** in Figure 7.23 derived from **equation (42)** on page 7.3 with provision for the earthquake loading.

In deriving equation (71), it has been assumed that the acceleration induced by an earthquake can be replaced by an **equivalent** static force of αW . This is almost certainly a gross over-simplification of the actual loading to which the slope is subjected during an **earthquake (188, 189)** but it is probable that it tends to over-estimate the loading and hence it errs on the **side of safety**. In view of the poor **quality** of the other input **data** in this problem, there is no justification for attempting to carry out a **more detailed** analysis of earthquake loading.

Since no boreholes exist on this hypothetical site, the subsurface groundwater conditions are totally unknown. To allow for the possibility that substantial subsurface water may be present, an alternative theoretical model is proposed. This is illustrated as Model II in Figure 7.23 and, again **this** model includes the effect of earthquake loading.

Having decided upon the most likely **failure** mode and having proposed one or more theoretical models to represent this failure mode, the rock engineer is now in a **position** to substitute a range of possible values into the factor of safety equations in order to determine the sensitivity of the slope to the different **conditions** to which it is likely to be subjected.

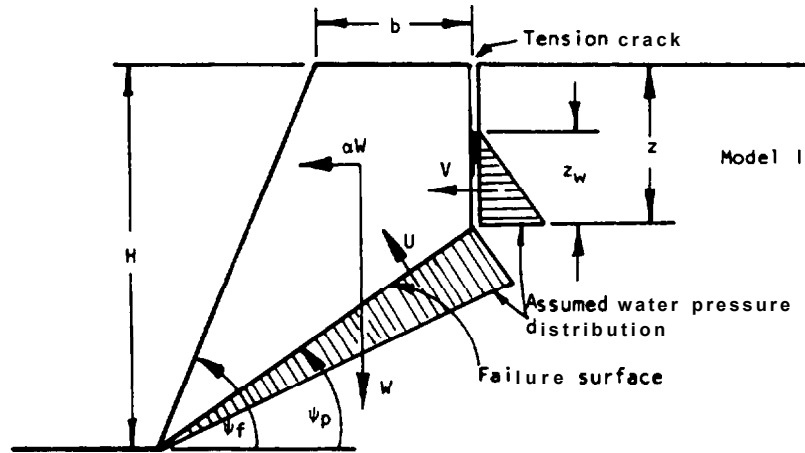
Summarizing the available input data:

Slope height	H = 60 m
Overall slope angle	$\psi_t = 50^\circ$
Bench face angle	$\psi_t = 70^\circ$
Bench height	H = 20 m
Failure plane angle	$\psi_D = 35^\circ$
Rock density	$\gamma = 2.6 \text{ tonnes/m}^3$
Water density	$\gamma_w = 1.0 \text{ tonnes/m}^3$
Earthquake acceleration	a = 0.08 g

Substituting in equations (71) and (72):

Overall slopes **Model I**

$$F = \frac{80.2c + (1850 - 40.1z_w - 0.287z_w^2) \tan \phi}{1529 + 0.410z_w^2} \quad (74)$$



$$F = \frac{cA + (W(\cos\psi_p - a\sin\psi_p) - U - V \sin\psi_p)\tan\phi}{W(\sin\psi_p + a\cos\psi_p) + v \cos\psi_p} \quad (71)$$

Where

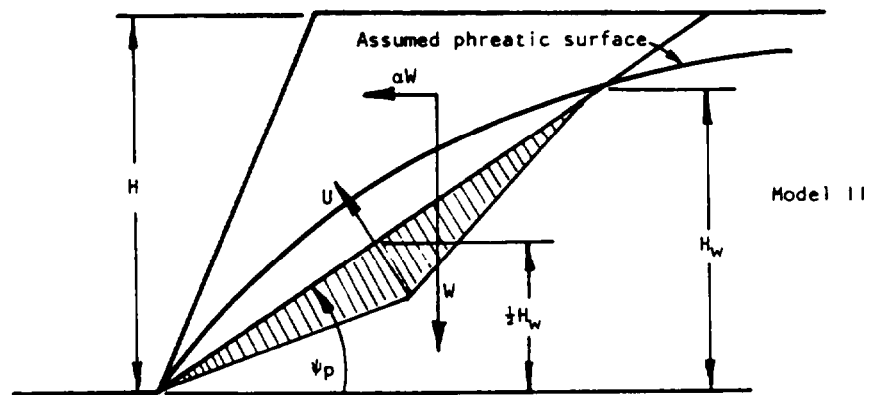
$$z = H(1 - \sqrt{\cot\psi_f \cdot \tan\psi_p}) \quad (58)$$

$$A = (H - z) \operatorname{Cosec}\psi_p \quad (43)$$

$$W = \frac{1}{2}\gamma H^2 \left((1 - (z/H)^2) \cot\psi_p - \cot\psi_f \right) \quad (46)$$

$$U = \frac{1}{2}\gamma_w \cdot z_w \cdot A \quad (44)$$

$$V = \frac{1}{2}\gamma_w \cdot z_w^2 \quad (45)$$



$$F = \frac{cA + (W(\cos\psi_p - a\sin\psi_p) - U)\tan\phi}{W(\sin\psi_p + a\cos\psi_p)} \quad (72)$$

Where

$$U = \frac{1}{4}\gamma_w \cdot H_w^2 \operatorname{Cosec}\psi_p \quad (73)$$

Figure 7.23: Theoretical models for example number 3.

Overall slopes Model II

$$F = \frac{104.6c + (2132 - 0.436H_W^2) \tan \phi}{1762} \quad (75)$$

Individual benches Model I

$$F = \frac{17.6c + (287.1 - 8.8z_W - 0.287z_W^2) \tan \phi}{237.3 + 0.410z_W^2} \quad (76)$$

Individual benches Model II

$$F = \frac{34.9c + (428.0 - 0.436H_W^2) \tan \phi}{953.7} \quad (77)$$

One of the most useful studies which can be carried out with the aid of equations (74) to (77) is to find the shear strength which would have to be mobilized for failure of the overall slope or for the individual benches. Figure 7.24 gives the results of such a study and the numbered lines on this plot represents the following conditions:

- 1 - Overall slope, Model I, dry, $Z_W = 0$.
- 2 - Overall slope, Model I, saturated, $Z_W = z = 14$ m.
- 3 - Overall slope, Model I I, dry, $H_W = 0$.
- 4 - Overall slope, Model I I, saturated, $H_W = H = 60$ m.
- 5 - Individual bench, Model I, dry, $Z_W = 0$.
- 6 - Individual bench, Model I, saturated, $Z_W = z = 9.9$ m.
- 7 - Individual bench, Model I I, dry, $H_W = 0$.
- 8 - Individual bench, Model II, saturated, $H = 20$ m.

The reader may feel that a consideration of all these possibilities is unnecessary but it is only coincidental that, because of the geometry of this particular slope, the shear strength values found happen to fall reasonably close together. In other cases, one of the conditions may be very much more critical than the others and it would take a very experienced slope engineer to detect this condition without going through the calculations required to produce Figure 7.24. In any case, these calculations should only take about one hour with the aid of a calculator and this is a very reasonable investment of time when lives and property may be in danger.

The elliptical figure in Figure 7.24 surrounds the range of shear strengths which the authors consider to be reasonable for partially weathered granite. These values are based on the plot given in Figure 5.17 on page 5.32 and on experience from working with granites. Note that a high range of friction angles has been chosen because experience suggests that even heavily mobilized granites (point 11 in Figure 5.17) exhibit high friction values because of the angular nature of the mineral grains.

It is clear from Figure 7.24 that simultaneous heavy rain and earthquake loading could cause the shear strength required to maintain stability to rise to a dangerous level. Considering the rapidity with which granite weathers, particularly in tropical environments, with a consequent reduction in available cohesive strength, these results suggest that the slope is un-

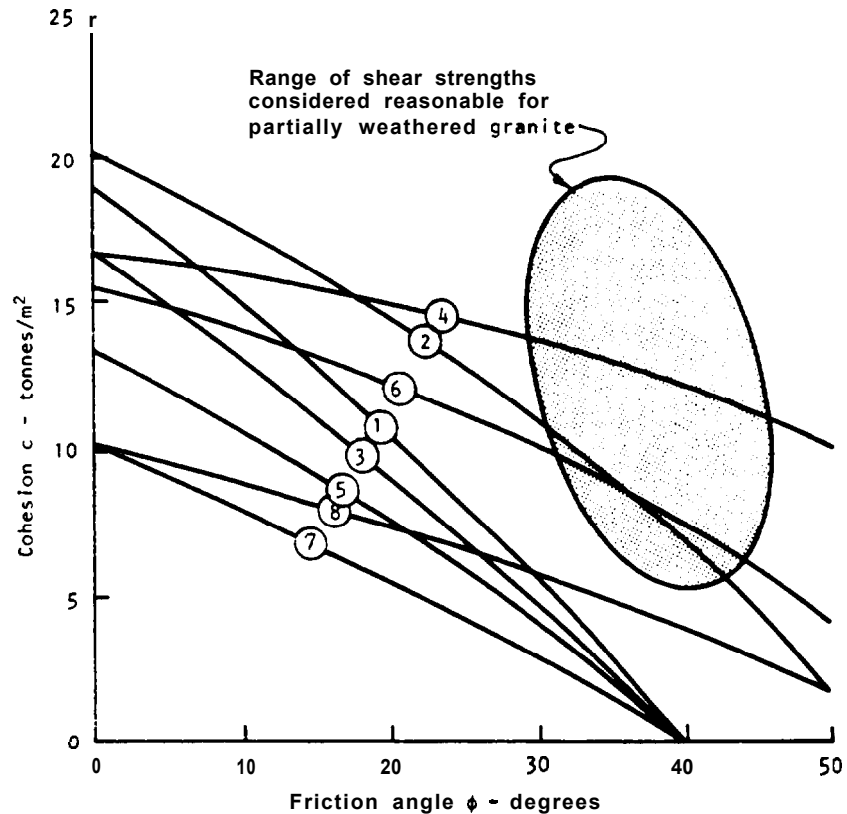


Figure 7.24: Shear strength mobilized for failure of slope considered in practical example number 3.

safe and that steps should be taken to increase its stability.

Four basic methods for improving the stability of the slope can be considered. These methods are the following:

- a. Reduction of slope height.
- b. Reduction of slope face inclination.
- c. Drainage of slope.
4. Reinforcement of slope with bolts and cables.

In order to compare the effectiveness of these different methods, it is assumed that the sheet joint surface has a cohesive strength of 10 tonnes/m² and a friction angle of 35°. The increase in factor of safety for a reduction in slope height, slope angle and water level can be found by altering one of these variables at a time in equations (71) and (72). The influence of reinforcing the slope is obtained by modifying these equations as in equations (78) and (79) on page 7.39.

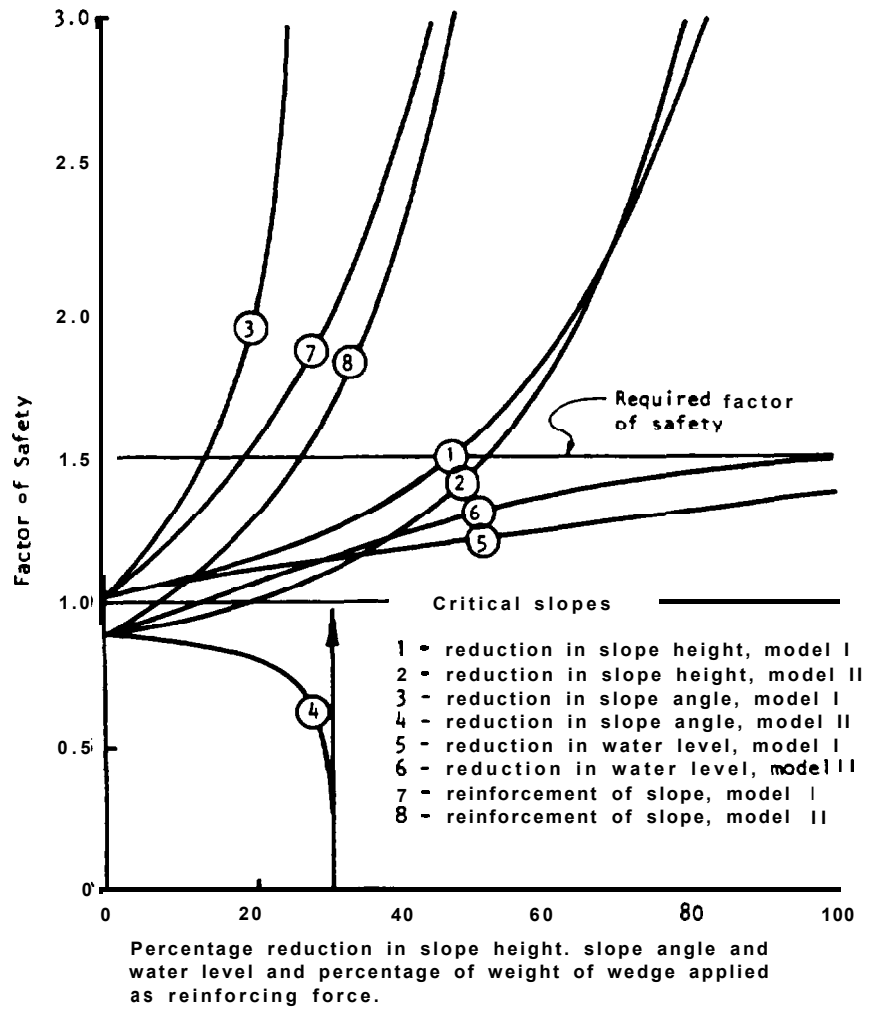


Figure 7.25: Comparison between alternative methods of increasing stability of overall slope considered in example 3.

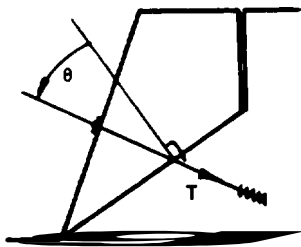
Model I

$$F = \frac{cA + (W(\cos \psi_p - \alpha \sin \psi_p) - U - V \sin \psi_p + T \cos \theta) \tan \phi}{W(\sin \psi_p + \alpha \cos \psi_p) + V \cos \psi_p - T \sin \theta} \quad (78)$$

Model II

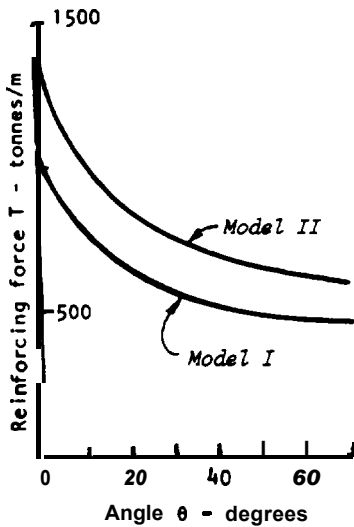
$$F = \frac{cA + (W(\cos \psi_p - \alpha \sin \psi_p) - U + T \cos \theta) \tan \phi}{W(\sin \psi_p + \alpha \cos \psi_p) - T \sin \theta} \quad (79)$$

Where T is the total reinforcing force applied by bolts or cables and θ is the inclination of this force to the normal to the failure surface, as illustrated in the sketch opposite.



Slope reinforcement

Figure 7.25 gives the results of the comparison between the different methods which could be considered for increasing the stability of the overall slope. In each case, the change is expressed as a percentage of the total range of the variable (H = 60 m, $\psi_p = 50^\circ$, $z_w/z = 1$, $H_w = 60$ m) except for the reinforcing load. This is expressed as a percentage of the weight of the wedge of rock being supported. In calculating the effect of the reinforcement, it has been assumed that the cables or bolts are installed horizontally, i.e. $\theta = 55^\circ$. The influence of the inclination θ upon the reinforcing load required to produce a factor of safety of 1.5 is shown in the graph given in the margin.



Total reinforcing force required for a factor of safety of 1.5.

Figure 7.25 shows that reduction in slope height (lines 1 and 2) only begins to show significant benefits once the height reduction exceeds about 40%. In many practical situations, a height reduction of this magnitude may be totally impossible, particularly when the slope has been cut into a mountainside. In any case, once one has reduced the slope height by 40%, more than 60% of the mass of the material forming the unstable wedge will have been removed and it would then be worth removing the rest of the wedge and the remains of the problem. Obviously, this solution would be very expensive but it does have the merit of providing a permanent solution to the problem.

Reducing the angle of the slope face can be very effective, as shown by line 3, but it can also be very dangerous as shown by line 4. This wide variation in response to what is normally regarded as a standard method for improving the stability of a slope raises a very interesting problem which deserves more detailed examination.

Equations (58) and (46) (Figure 7.23) both contain the term $\cot \psi_p$ and hence both z and W are decreased as the slope face angle ψ_p is reduced. A reduction in tension crack depth reduces both water forces U and V and the final result is a dramatic increase in factor of safety for a decrease in slope face inclination. Note that, if the tension crack occurs before the slope is flattened, the tension crack z will remain unaltered at 14 m and the water forces U and V will remain at their maximum values. Under these conditions the factor of safety will still be increased for a reduction in slope face inclination but not to the same extent as shown by line 3 in Figure 7.25.

In the case of Model II in Figure 7.23, it is only the weight term which is altered by the reduction in slope angle and,

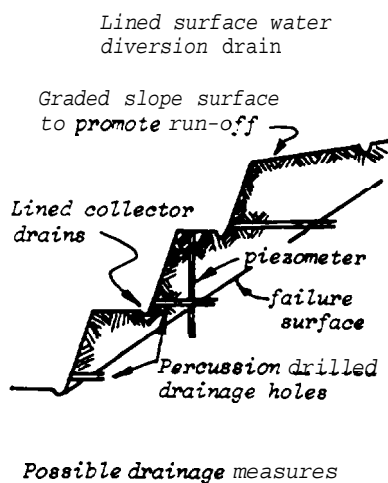
because the uplift force term $U \tan \phi$ is greater than the cohesive force cA , the factor of safety actually reduces as the slope face is flattened. As the slope face angle approaches the failure plane angle, the thin sliver of material resting on the failure plane will be floated off by the excess water force U . Although many practical arguments could be put forward to show that this extreme behavior would be very unlikely, the example does illustrate the danger of indiscriminate alteration of the slope geometry without having first considered the possible consequences. The practical conclusion to be drawn from this discussion is that, if Model II in Figure 7.23 is representative of the conditions which exist in an actual slope, partial flattening of the slope would achieve no useful purpose. The wedge of rock resting on the failure plane would have to be removed entirely if it was decided that flattening the slope was the only means to be used for increasing the stability.

Drainage of the slope is probably the cheapest remedial measure which can be employed and, as shown in Figure 7.25, complete drainage, if this could be achieved, would increase the factor of safety to very nearly the required value. Unfortunately, complete drainage can never be achieved and hence, in this particular slope, drainage would have to be supplemented by some other remedial measure such as bolting in order to produce an acceptable level of safety. In any event, nothing would be lost by the provision of some drainage and the authors would recommend careful consideration of surface water control and also the drilling of horizontal drain holes to intersect the potential failure surface.

Reinforcing the slope by means of bolts or cables may create a useful illusion of safety but unless the job is done properly, the result could be little more than an illusion. In order to achieve a factor of safety of 1.5, assuming the bolts or cables to be installed in a horizontal plane, the total force required amounts to about 500 tonnes per meter of slope length. In other words, the complete reinforcement of a 100 m face would require the installation of 500 one tonne capacity cables. Simultaneous drainage of the slope, even if only partially successful, would reduce this number by about half but reinforcing a slope of this size would obviously be a very costly process.

Considering all the facts now available, the authors would offer the following suggestions to the engineer responsible for the hypothetical slope which has been under discussion in this example:

- a. Immediate steps should be taken to have a series of standpipe piezometers installed in vertical drill holes from the upper slope surface or from one of the benches. The importance of groundwater has been clearly demonstrated in the calculations which have been presented and it is essential that further information on possible groundwater flow patterns should be obtained.
- b. If diamond drilling equipment of reasonable quality is readily available, the vertical holes for the piezometers should be cored. A geologist should be present during this drilling program and should log the core immediately upon removal from the core barrel. Parti-



cular attention should be given to establishing the exact position of the sheet joint or joints so that an accurate cross-section of the slope can be constructed. If adequate diamond drilling equipment is not available, the piezometer holes may be percussion drilled.

- c. As soon as the piezometers are in position and it has been demonstrated that groundwater is present in the slope, horizontal drain holes should be percussion drilled into the bench face to intersect the sheet joints. These holes can be drilled at an initial spacing of about 10 m and their effectiveness checked by means of the piezometers. The hole spacing can be increased or decreased according to the water level changes observed in the piezometers.
- d. During this groundwater control program, a careful examination of the upper surface of the slope should be carried out to determine whether open tension cracks are present and whether any recent movements have taken place in the slope. Such movements would be detected by cracks in concrete or plaster or by displacements of vertical markers such as telephone poles. If the upper surface of the slope is covered by overburden soil, it may be very difficult to detect cracks and it may be necessary to rely upon the reports of persons resident on or close to the top of the slope.
- e. Depending upon the findings of this examination of the upper slope surface, a decision could then be made on what surface drainage measures should be taken. If open tension cracks are found, these should be filled with gravel and capped with an impermeable material such as clay. The existence of such cracks should be taken as evidence of severe danger and serious consideration should be given to remedial measures in addition to drainage.
- f. Further geological mapping to confirm the geological structure of the slope, together with evidence on groundwater and tension cracks, would provide information for a review of the situation to decide upon the best means of permanent stabilization, in addition to the drainage measures which have already been implemented.

Practical example number 4

Chalk cliff failure induced by undercutting

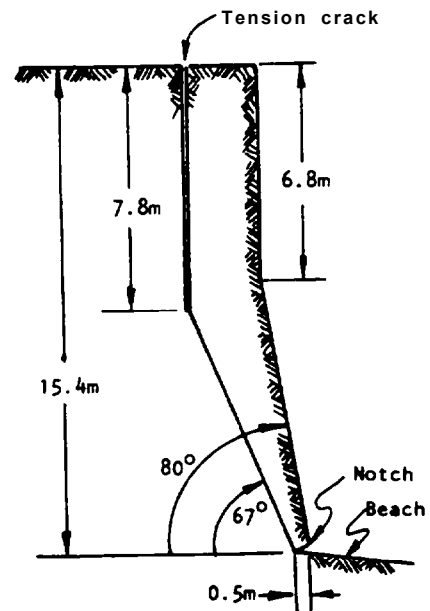
Hutchinson(156) has described the details of a chalk cliff failure at Joss Bay on the Isle of Thanet in England. This failure, induced by the undercutting action of the sea, provides an interesting illustration of the analysis of undercutting on page 7.17 and Hutchinson's data is reanalyzed on the following pages.

The failure is illustrated in the photograph reproduced in Figure 7.26 and a cross-section, reconstructed from the paper by Hutchinson, is given in Figure 7.27. Apart from a thin capping of overburden and the presence of a few flint bands, the chalk



Figure 7.26: Chalk cliff failure at Joss Bay, Isle of Thanet, England.
(Photograph reproduced with permission of Dr. J.N.Hutchinson, Imperial College, London.)

Figure 7.27: Cross section of chalk cliff failure at Joss Bay.



is reasonably uniform. Bedding is within one degree of horizontal and two major joint sets, both almost vertical, are present. The cliff is parallel to one of these joint sets.

Measurement of water levels in wells near the coast together with the lack of face seepage caused Hutchinson to conclude that the chalk mass in which the failure occurred could be taken as fully drained. Since the failure does not appear to have been associated with a period of exceptionally heavy rain, as was the case of the quarry failure discussed in example number 2, the possibility of a water-filled tension crack is considered to be remote and will not be included in this analysis. The interested reader is left to check the influence of various water pressure distributions upon the behavior of this slope.

Laboratory tests on samples taken from the cliff face gave a density of 1.9 tonnes/m³ and a friction angle of about 42° for the peak strength and 30° for the residual strength. The cohesive strength ranged from 13.5 tonnes/m² for the peak strength to zero for the residual strength. Since this failure can be classed as a fall in which relatively little movement may have taken place before failure, as opposed to a slide in which the shear strength on the failure plane is reduced to its residual value by movements before the actual failure, there is considerable justification for regarding the peak strength of the chalk as relevant for this analysis. The purpose of this analysis is to determine the shear strength mobilized in the actual failure and to compare this with the laboratory values.

Summarizing the available input data:

H - slope height ($H_1 = H_2$)	15.4 m
Z_1 - original tension crack depth	6.8 m
Z_2 - new tension crack depth	7.8 m
AM - depth of undercut	0.5 m
ψ_0 - inclination of undercut	0°
ψ_1 - slope face angle	80°
ψ_p - failure plane angle	67°

The effective friction angle of the chalk mass can be determined by rearranging equation (64) on page 7.17.

$$\phi = 2\psi_p - \text{Arctan} \frac{H_2^2 - Z_2^2}{(H_1^2 - Z_1^2) \cot \psi_p - (H_1 + H_2) AM} \quad (80)$$

Substitution gives $\phi = 49.9^\circ$.

This value is significantly higher than the friction angle of 42° measured on laboratory specimens but the influence of the roughness of the actual failure surface must be taken into account in comparing the results. The photograph reproduced in Figure 7.26 shows this surface is very rough indeed and the difference between the laboratory value and the friction angle mobilized in the failure is not surprising.

The cohesion mobilized at failure can be estimated by rearranging equation (63) on page 7.17:

$$c = \frac{\gamma Z_2 \cos \psi_p \cdot \sin(\psi_p - \phi)}{\cos \phi} \quad (81)$$

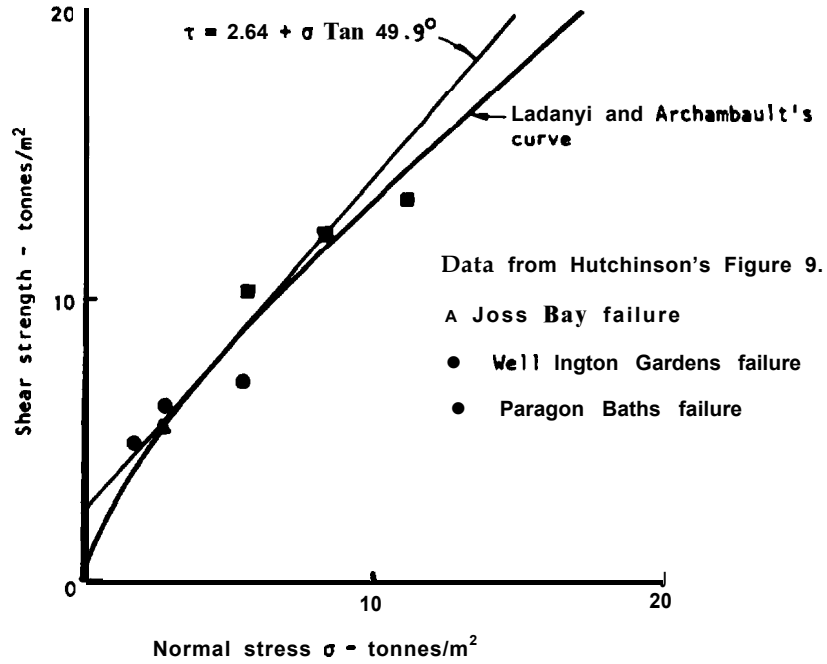


Figure 7.28: Relationship between shear strength and normal stress for chalk cliff failures analysed by Hutchinson¹⁵⁶.

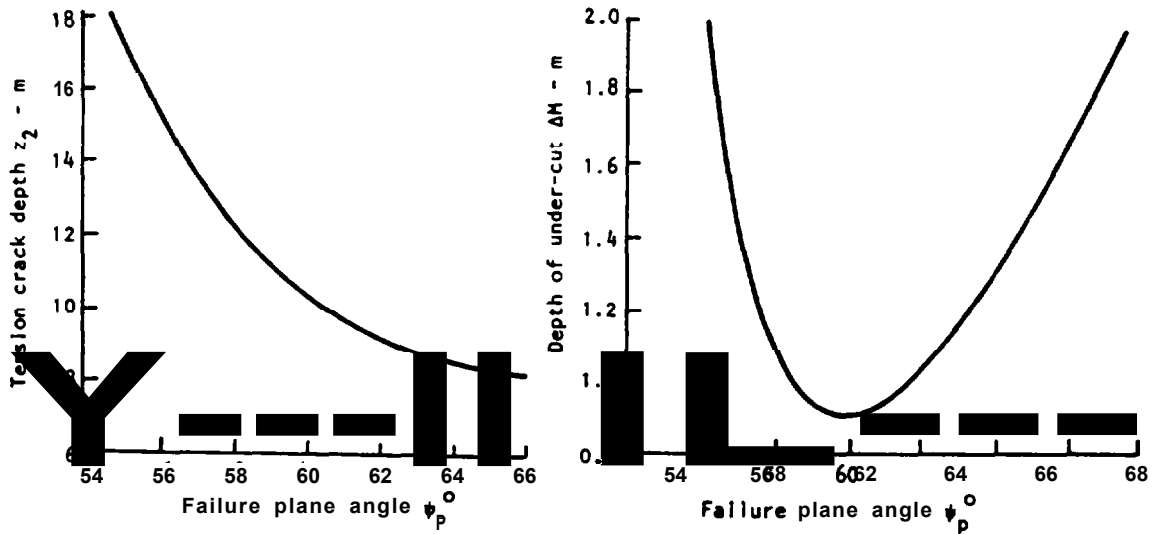


Figure 7.29: Tension crack depths and under-cut depths required for failure for different failure plane inclinations.

Substituting $z_2 = 7.8$ m, $\psi_p = 67^\circ$ and $\phi = 49.9^\circ$ gives $c = 2.64$ tonnes/m². As would be expected, this value is considerably lower than the value of $c = 13.3$ tonnes/m² determined by laboratory shear tests on intact chalk.

Hutchinson's paper (Figure 9) contains further data on the shear strength mobilized in chalk cliff failures at Wellington Gardens and Paragon Baths and this data is reproduced in Figure 7.28. The dashed curve, calculated from Ladanyi and Archambault's equation (28 on page 5.22) is a good fit to this rock mass strength data and it will be seen that the line defined by $c = 2.64 + \sigma \tan 49.9^\circ$ is a tangent to the dashed curve. The evidence presented in Figure 7.28 suggests that the values of cohesion and friction angle determined from the failure geometry illustrated in Figure 7.27 are reasonable.

Before leaving this example, it is instructive to consider what will happen to the Joss Bay cliff as the sea continues to undercut its toe. The input data for the next step in the failure process is now as follows:

H = slope height ($H_1 = H_2$)	15.4 m
z_1 = original tension crack depth	7.8 m
ψ_f = slope face angle	67°
c = cohesive strength of chalk mass	2.65 tonnes/m ²
ϕ = friction angle of chalk	49.9°

The unknowns in this analysis are

z_2 = new tension crack depth
ψ_p = failure plane angle
ΔM = depth of undercut

Since there are three unknowns and only two equations (63 and 64) the solution to this problem is obtained in the following manner:

- From equation (63), the depth of the tension crack z_2 is calculated for a range of possible failure plane angles (ψ_p). The results of this calculation are plotted in Figure 7.29. Since z_2 must lie between z_1 and H , Figure 7.29 shows that the angle of the failure plane ψ_p must lie between 67° and 56° .
- Rearranging equation (64) gives:

$$\Delta M = \frac{(H^2 - z_1^2) \cot \psi_f}{2H} - \frac{H^2 - z_2^2}{2H \tan(2\psi_p - \phi)} \quad (62)$$

Solving for a range of corresponding values of ψ_p and z_2 gives the depth of the undercut shown in Figure 7.31.

It is clear, from this figure, that a further cliff failure will occur when the undercut reaches a depth of approximately 0.9 m and that the corresponding failure plane angle will be $\psi_p = 60^\circ$ and the new tension crack depth will be $z_2 = 10.2$ m. This new failure geometry is illustrated in Figure 7.30.

The consequence of the cliff failure illustrated in Figure 7.30 is serious for property owners on the cliff-top and, hence, the problem of stabilization of the cliff face must be considered.

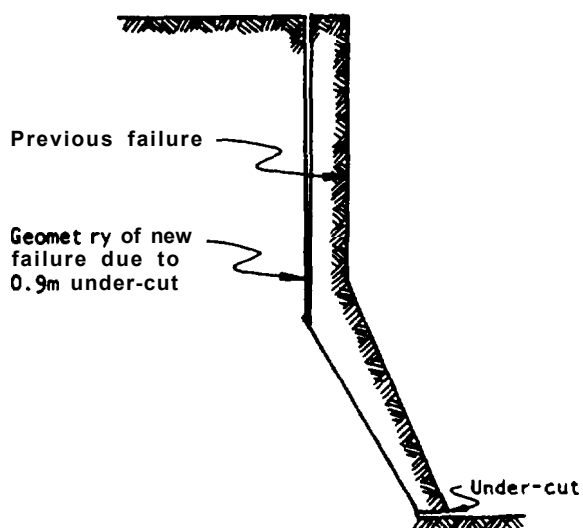


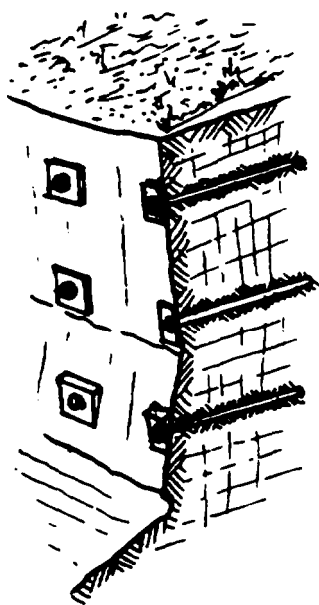
Figure 7.30: Predicted geometry of next cliff failure due to undercutting.

In the analysis which has been presented on the previous pages, it has been assumed that the chalk mass is dry. The presence of groundwater in the cliff, and particularly in the tension crack, would result in a serious reduction of face stability. Consequently, the first step in stabilizing the slope is to ensure that it remains completely drained. Attention to surface water to ensure that pools cannot collect near the slope crest is important and, if possible, horizontal drains should be drilled into the face to allow free drainage of any water which does find its way into the rock mass which would be involved in a further failure.

In view of the fact that the stability of this slope is so sensitive to undercutting, it is tempting to suggest that this undercutting should be prevented by the provision of a concrete wall along the toe of the cliff. In some cases this may be a practical solution but, in others, it may be impossible to provide a secure foundation for such a wall.

Assuming that the protection of the toe of the cliff illustrated in Figure 7.50 is not possible, the only remaining alternative is to stabilize the cliff face by reinforcement. Since the mass of material involved in any further failure will be relatively small - say 50 tonnes per meter of slope - the stabilizing force need not be very large.

Because of the dilatant nature of the failure process, it is suggested that the most effective reinforcement would be provided by fully grouted bolts or cables lightly tensioned to ensure that all contacts were closed. The onset of failure would induce tension in this reinforcement which would inhibit further failure. It is suggested that the load capacity of these bolts or cables should be approximately 25% of the mass



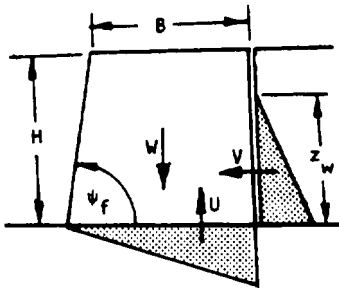
Suggested reinforcement of cliff face with 5m x 5m pattern of 5m long bolts.

of the material which could fall and hence a pattern of 20 tonne bolts or cables, each 5 m long, installed in a 5 m grid, should provide adequate reinforcement for this slope. If the chalk mass is closely jointed so that there is a danger of raveling between washers, the pattern can be changed to a closer grid of lower capacity bolts or, alternatively, corrosion resistant wire mesh can be clamped beneath the washers to reinforce the chalk surface.

Practical example number 5

Block sliding on clay layers

In a slope cut in a horizontal bedded sandstone/shale sequence, sliding of blocks of material on clay seams occurs during periods of high rainfall. The clay seams have a high montmorillonite content and have been slickensided by previous shear displacements, consequently very low residual shear strength values of $c = 0$ and $\phi = 10^\circ$ are considered appropriate for the analysis of failures (114).



Geometry of failure and water pressure distribution

The geometry of the block is illustrated in the margin sketch and it is assumed that the clay seam is horizontal.

- H is the height of the block
- ψ_f is the angle of the face of the block
- B is the distance of a vertical crack behind the crest of the slope
- z_w is the depth of water in the tension crack
- W is the weight of the block
- V is the horizontal force due to water in the tension crack
- U is the uplift force due to water pressure on the base

The factor of safety of the block is given by:

$$F = \frac{(W - U) \tan \phi}{V} \quad (83)$$

Where $W = \gamma BH - 1/2 \gamma H^2 \cot \psi_f$

$$U = 1/2 \gamma_w z_w (B + H \cot \psi_f)$$

$$V = 1/2 \gamma_w z_w^2$$

γ is the density of the rock

γ_w is the density of water

Hence

$$F = \frac{[(2B/H - \cot \psi_f) - \gamma_w/\gamma \cdot z_w/H \cdot B/H(1 + \cot \psi_f)] \tan \phi}{\gamma_w/\gamma \cdot (z_w/H)^2} \quad (84)$$

This equation has been solved for a range of values of B/H and z_w/H , assuming $\psi_f = 80^\circ$, $\gamma_w/\gamma = 0.4$ and $\phi = 10^\circ$, and the results are plotted in Figure 7.31.

The extreme sensitivity of the factor of safety to changes in water level depth in the tension crack is evident in this figure. This means that drainage, even if it is not very efficient, should do a great deal to improve the stability of the

slope. Horizontal holes through the base of the block may be the most economical drainage system and the effectiveness of such drain holes can be checked by monitoring the movement across a tension crack before and after drilling of the hole.

It must be emphasized that it is not the quantity of water which is important in this case but the pressure of water in the tension crack. Hence, in a low permeability rock mass, the drain may only produce a trickle of water but, if it has reduced the water pressure in the tension crack, it will stabilize the slope.

As the ratio B/H decreases, the weight of the block W decreases and hence the factor of safety of the slope decreases, as shown in Figure 7.31. This is a factor over which there is no control but it would be interesting to relate the ratio B/H to the frequency of observed block failures.

An increase in the block face angle ψ results in an increase in the weight of the block and improvement in slope stability. This suggests that, for this type of failure, the face angle should be kept as steep as possible.

In some cases of block failure on clay seams, the blocks have been observed to move up-hill on seams dipping into the rock mass. This requires a combination of a very low friction angle in the clay and a relatively high water level in the tension crack. Since the shear strength of the clay cannot be altered, drainage is the obvious remedial measure in such cases.

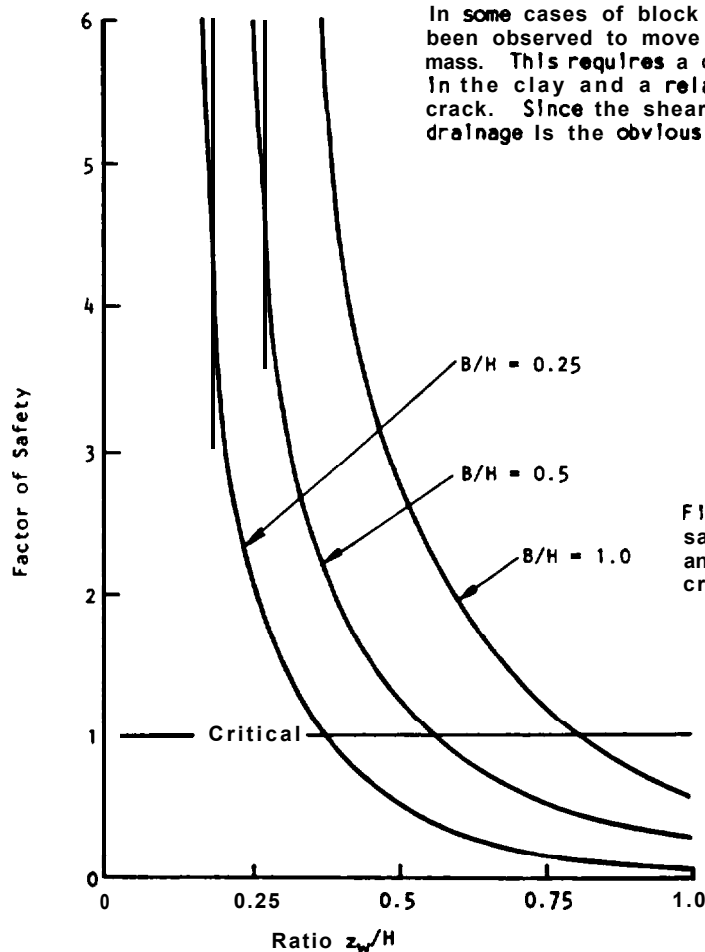


Figure 7.31 : Sensitivity of factor of safety to depth of water in tension crack and distance of tension crack behind slope crest.

Chapter 7 references

186. SALAHON, M.D.G. and MUNRO, A.H. A study of the strength of coal pillars. *J. South African Inst. Min. Metall.* Vol.68, 1967, pages 55-67.
187. BROADBENT, C.D. and ARMSTRONG, C.W. Design and application of microseismic devices. *Proc. 5th Canadian Symposium on Rock Mechanics.* 1968.
188. IDRIS, I.H. and SEED, H.B. The response of earth banks during earthquakes. *Report Soil Mech. and Bituminous Materials Lab. University of California. Berkley.* April 1966.
189. FINN. W.D.L. Static and dynamic stresses in slopes *Proc. 1st Congress, Intl. Soc. Rock Mechanics,* Lisbon. 1966. Vol. 2. page 167.

Chapter 8 Wedge failure.

Introduction

The previous chapter was concerned with slope failure resulting from sliding on a single planar surface dipping into the excavation and striking parallel or nearly parallel to the slope face. It was stated that the plane failure analysis is valid provided that the strike of the failure plane is within $\pm 20^\circ$ of the strike of the slope face. This chapter is concerned with the failure of slopes in which structural features upon which sliding can occur strike across the slope crest and where sliding takes place along the line of intersection of two such planes.

This problem has been extensively discussed in geotechnical literature and the authors have drawn heavily upon the work of Londe, John, Wittke, Goodman and others listed in references 190-200 at the end of this chapter. The reader who has examined this literature may have been confused by some of the mathematics which have been presented. It must, however, be appreciated that our understanding of the subject has grown rapidly over the past decade and that many of the simplifications which are now clear were not at all obvious when some of these papers were written. The basic mechanics of failure are very simple but, because of the large number of variables involved, the mathematical treatment of the mechanics can become very complex unless a very strict sequence is adhered to in the development of the equations.

In this chapter, the basic mechanics of failure involving the sliding of a wedge along the line of intersection of two planar discontinuities are presented in a form which the non-specialist reader should find easy to follow. Unfortunately the very simple equations which are presented to illustrate the mechanics are of limited practical value because the variables used to define the wedge geometry cannot easily be measured in the field. Consequently, the second part of the chapter deals with the stability analysis in terms of the dips and dip directions of the planes and the slope face. In the transformation of the equations which is necessary in order to accommodate this information the basic mechanics becomes obscure but it is hoped that the reader should be able to follow the logic involved in the development of these equations.

In the chapter itself, the discussion is limited to the case of the sliding of a simple wedge such as that illustrated in Figure 8.1, acted upon by friction, cohesion and water pressure. The influence of a tension crack and of external forces due to bolts, cables or seismic accelerations results in a significant increase in the complexity of the equations and, since it would only be necessary to consider these influences on the fairly rare occasions when the critical slopes are being examined, the complex solution to the problem has been presented in Appendix 2 at the end of the manual. The analytical treatment of this problem, given in Appendix 2, has been designed for use on a computer or a programmable calculator. Once the reader has understood the basic mechanics of the problem, he or she should have no difficulty in using the complete solution given in Appendix 2.

Figure 8.1 : A typical wedge failure involving sliding along the line of intersection of two planar discontinuities.

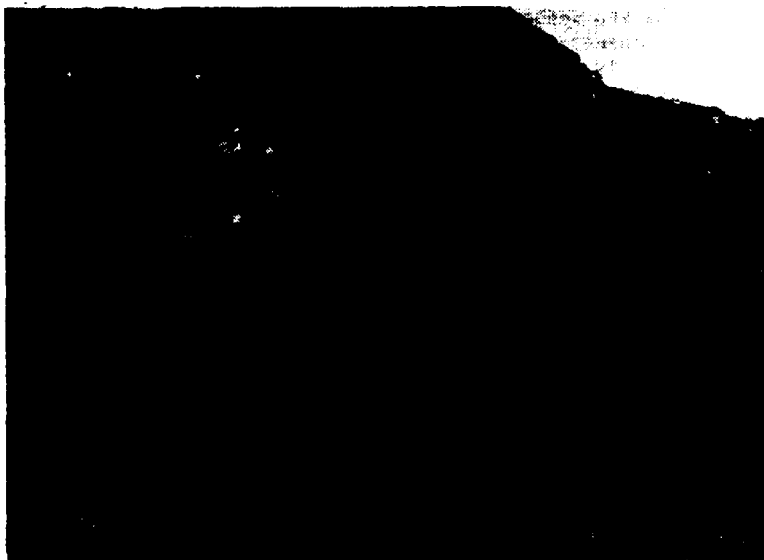
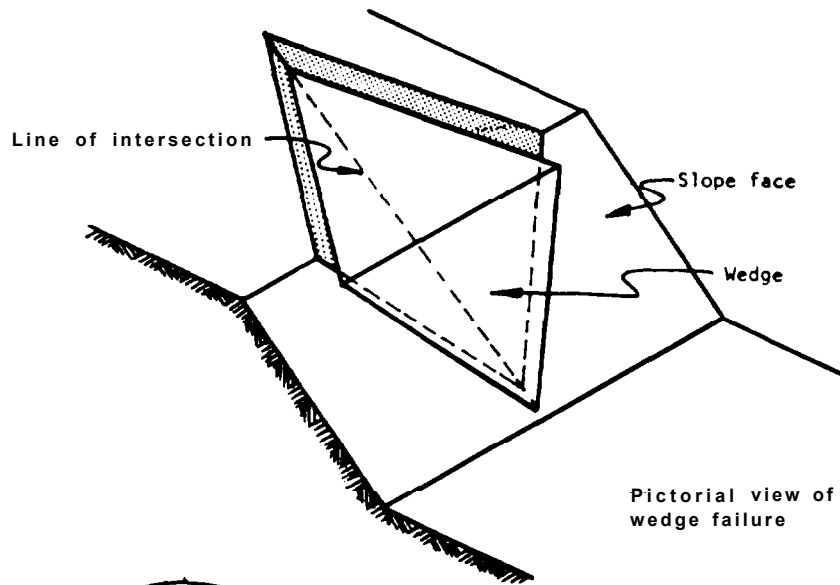
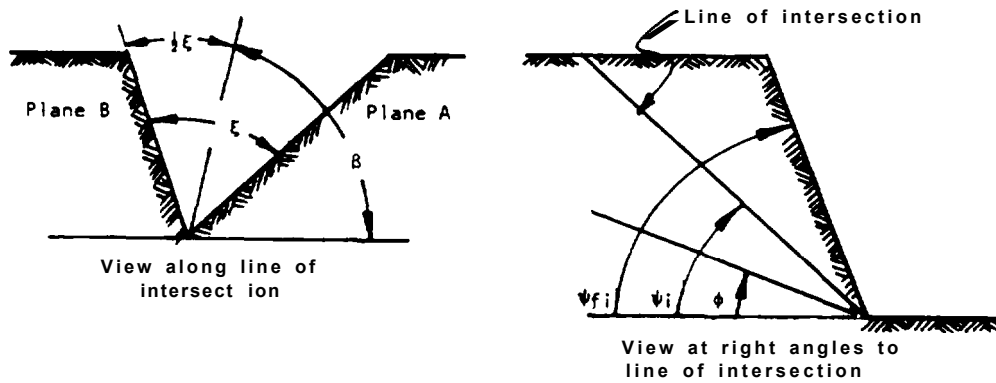


Figure 8.2 : Sets of intersecting discontinuities can sometimes give rise to the formation of families of wedge failures.

(Photograph reproduced with permission of Hr. K.M. Pare)



Note : The convention adopted in this analysis is that the plane with the flatter of the two dips is always referred to as Plane A,

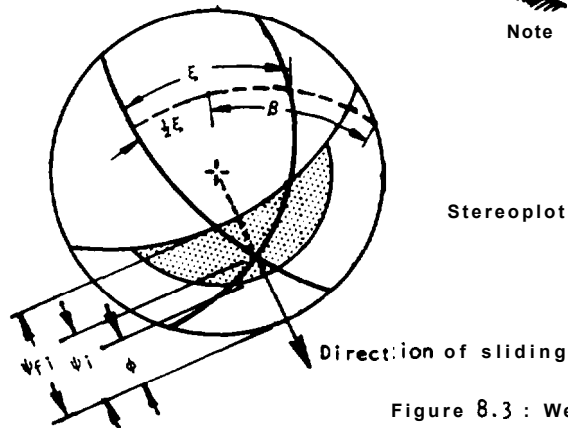
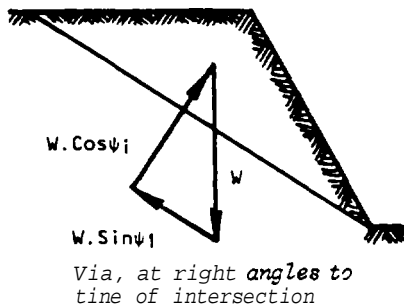


Figure 8.3 : Wedge failure geometry.

Definition of wedge geometry

Typical wedge failures are illustrated in Figures 8.1 and 8.2 which show, in the one case, the through-going planar discontinuities which are normally assumed for the analytical treatment of this problem and, in the other case, the wedge formed by sets of closely spaced structural features. In the latter case, the analytical treatment would still be based upon the assumption of through-going planar features although it would have to be realized that the definition of the dips and dip directions and the locations of these planes may present practical difficulties. The failure illustrated in Figure 8.2 would probably have involved the fairly gradual raveling of small loose blocks or rock and it is unlikely that this failure was associated with any violence. On the other hand, the failure illustrated in Figure 8.1 probably involved a fairly sudden fall of a single wedge which would only have broken up on impact and which would, therefore, constitute a threat to anyone working at the toe of the slope.



The geometry of the wedge, for the purpose of analyzing the basic mechanics of sliding, is defined in Figure 8.3. Note that, throughout this manual, the flatter of the two planes is called Plane A while the steeper plane is called Plane B.

As in the case of plane failure, a condition of sliding is defined by $\psi_{fi} > \phi$, where ψ_{fi} is the inclination of the slope face, measured in the view at right angles to the line of intersection, and ψ_i is the dip of the line of intersection. Note the ψ_{fi} would only be the same as the true dip of the slope face, if the dip direction of the line of intersection was the same as the dip direction of the slope face.

Analysis of wedge failure

The factor of safety of the wedge defined in Figure 8.3, assuming that sliding is resisted by friction only and that the friction angle ϕ is the same for both planes, is given by

$$F = \frac{(R_A + R_B) \tan \phi}{W \sin \psi_i} \quad (85)$$

where R_A and R_B are the normal reactions provided by planes A and B as illustrated in the sketch opposite.

In order to find R_A and R_B , resolve horizontally and vertically in the view along the line of intersection:

$$R_A \sin(\beta - \frac{1}{2} \epsilon) = R_B \sin(\beta + \frac{1}{2} \epsilon) \quad (86)$$

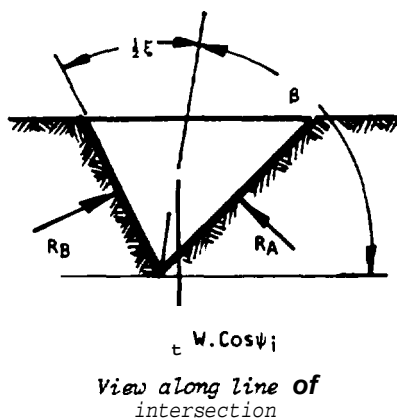
$$R_A \cos(\beta - \frac{1}{2} \epsilon) - R_B \cos(\beta + \frac{1}{2} \epsilon) = W \cos \psi_i \quad (87)$$

Solving for R_A and R_B and adding:

$$R_A + R_B = \frac{W \cos \psi_i \cdot \sin \beta}{\sin \frac{1}{2} \epsilon} \quad (88)$$

Hence

$$F = \frac{\sin \beta}{\sin \frac{1}{2} \epsilon} \cdot \frac{\tan \phi}{\tan \psi_i} \quad (89)$$



In other words:

$$F_W = K \cdot F_p \quad (90)$$

where F_W is the factor of safety of a wedge supported by friction only. F_p is the factor of safety of a plane failure in which the slope face is inclined at ψ_i and the failure plane is inclined at ψ_j .

K is the wedge factor which, as shown by equation (89), depends upon the included angle of the wedge and upon the angle of tilt of the wedge. Values for the wedge factor K , for a range of values of β and ϵ are plotted in Figure 8.4.

As shown in the stereoplot given in Figure 8.3, measurement of the angles β and ϵ can be carried out on the great circle, the pole of which is the point representing the line of intersection of the two planes. Hence, a stereoplot of the features which define the slope and the wedge geometry can provide all the information required for the determination of the factor of safety. It should, however, be remembered that the case which has been dealt with is very simple and that, when different friction angles and the influence of cohesion and water pressure are allowed for, the equations become more complex. Rather than develop these equations in terms of the angles β and ϵ , which cannot be measured directly in the field, the more complete analysis is presented in terms of directly measurable dips and dip directions.

Before leaving this simple analysis, the reader's attention is drawn to the important influence of the wedging action as the included angle of the wedge decreases below 90° . The increase by a factor of 2 or 3 on the factor of safety determined by plane failure analysis is of great practical importance. Some authors have suggested that a plane failure analysis is acceptable for all rock slopes because it provides a lower bound solution which has the merit of being conservative. Figure 8.4 shows that this solution is so conservative as to be totally uneconomic for most practical slope designs. It is therefore recommended that, where the structural features which are likely to control the stability of a rock slope do not strike parallel to the slope face, the stability analysis should be carried out by means of the three-dimensional methods presented in this book or published by the authors listed in references 190 to 202 at the end of this chapter.

Wedge analysis including cohesion and water pressure

Figure 8.5 shows the geometry of the wedge which will be considered in the following analysis. Note that the upper slope surface in this analysis can be obliquely inclined with respect to the slope face, thereby removing a restriction which has been present in all the stability analyses which have been discussed so far in this book. The total height of the slope, defined in Figure 8.5, is the total difference in vertical elevation between the upper and lower extremities of the line of intersection along which sliding is assumed to occur.

The water pressure distribution assumed for this analysis is based upon the hypothesis that the wedge itself is impermeable and that water enters the top of the wedge along lines of intersection 3 and 4 and leaks from the slope face along lines of

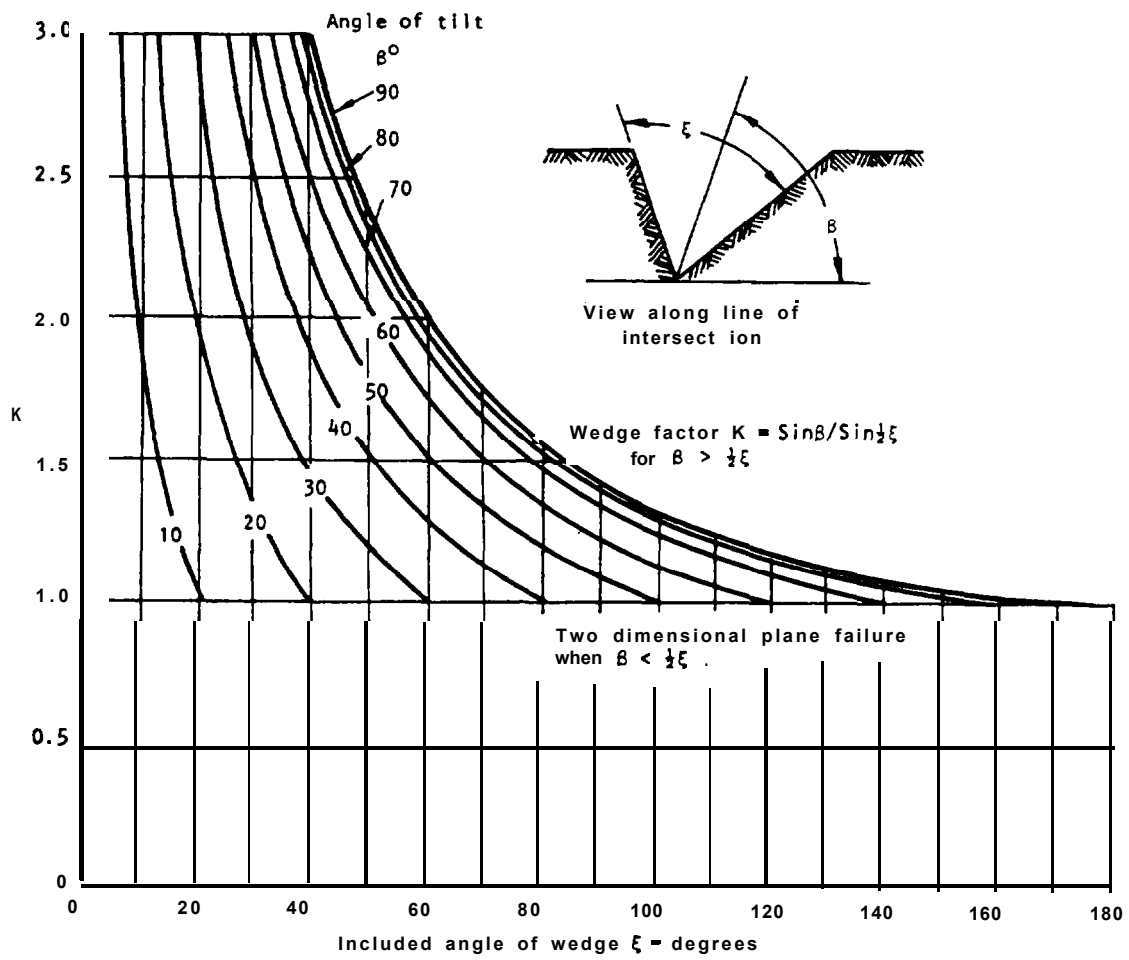
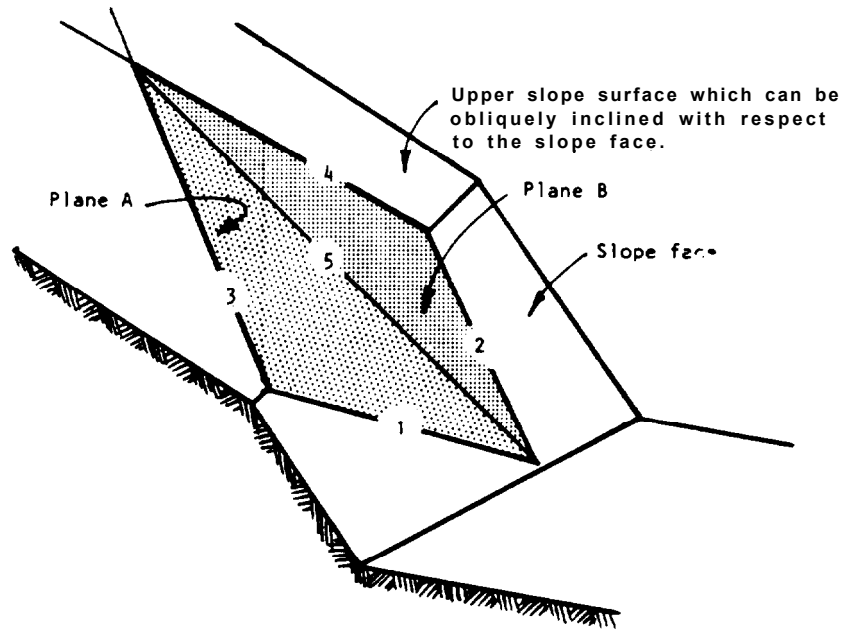
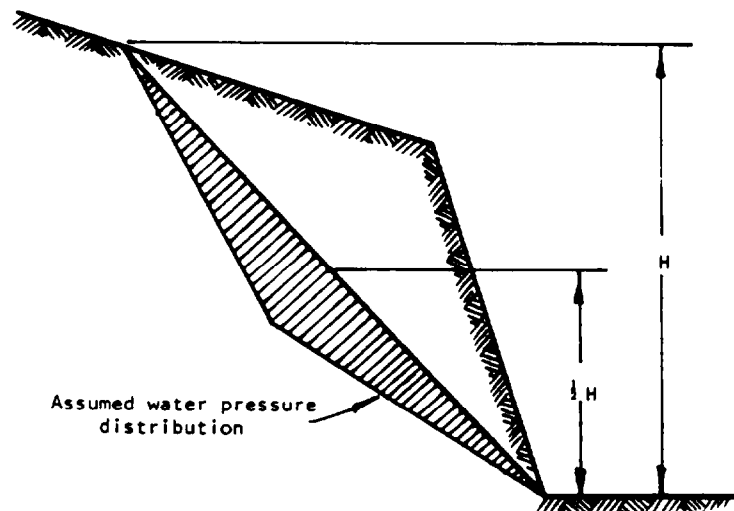


Figure 8.4 : Wedge factor K as a function of wedge geometry.



a) Pictorial view of wedge showing the numbering of intersection lines and planes.



b) View normal to the line of intersection 5 showing the total wedge height and the water pressure distribution.

figure 8.5 : Geometry of wedge used for stability analysis including the influence of cohesion and of water pressure on the failure surfaces.

Intersection 1 and 2. The resulting pressure distribution is shown in Figure 8.5b - the maximum pressure occurring along the line of intersection 5 and the pressure being zero along lines 1, 2, 3 and 4. This water pressure distribution is believed to be representative of the extreme conditions which could occur during very heavy rain.

The numbering of the lines of Intersection of the various planes involved in this problem is of extreme importance since total confusion can arise in the analysis if these numbers are mixed-up. The numbering used throughout this book is as follows:

- 1 - Intersection of plane A with the slope face
- 2 - Intersection of plane B with the slope face
- 3 - Intersection of plane A with upper slope surface
- 4 - Intersection of plane B with upper slope surface
- 5 - Intersection of planes A and B

It is assumed that sliding of the wedge always takes place along the line of Intersection numbered 5.

The factor of safety of this slope is derived from the detailed analysis of this problem published by Hoek, Bray and Boyd (201).

$$F = \frac{3}{\gamma H} (c_A \cdot X + c_B \cdot Y) + \left(A - \frac{\gamma_w}{\gamma} \cdot X \right) \tan \phi_A + \left(B - \frac{\gamma_w}{\gamma} \cdot Y \right) \tan \phi_B \quad (91)$$

where

c_A and c_B are the cohesive strengths of planes A and B

ϕ_A and ϕ_B are the angles of friction on planes A and B

γ is the unit weight of the rock

γ_w is the unit weight of water

H is the total height of the wedge (see Figure 8.5)

X, Y, A, and B are dimensionless factors which depend upon the geometry of the wedge.

$$X = \frac{\sin \theta_{24}}{\sin \theta_{45} \cdot \cos \theta_{21a}} \quad (92)$$

$$Y = \frac{\sin \theta_{13}}{\sin \theta_{35} \cdot \cos \theta_{1nb}} \quad (93)$$

$$A = \frac{\cos \psi_a - \cos \psi_b \cdot \cos \theta_{1a} \cdot nb}{\sin \psi_5 \cdot \sin^2 \theta_{1a} \cdot nb} \quad (94)$$

$$B = \frac{\cos \psi_b - \cos \psi_a \cdot \cos \theta_{1a} \cdot nb}{\sin \psi_5 \cdot \sin^2 \theta_{1a} \cdot nb} \quad (95)$$

where ψ_a and ψ_b are the dips of planes A and B respectively and ψ_5 is the dip of the line of intersection 5.

The angles required for the solution of these equations can most conveniently be measured on a stereoplot of the data which defines the geometry of the wedge and the slope.

Consider the following example:

Plane	dip°	dip direction°	Properties
A	45	105	$\phi_A = 20^\circ, C_A = 500 \text{ lb/ft}^2$ $\phi_B = 30^\circ, C_B = 1000 \text{ lb/ft}^2$ $\gamma = 160 \text{ lb/ft}^3$ $\gamma_w = 62.5 \text{ lb/ft}^3$
B	70	235	
Slope face	65	185	
Upper surface	12	195	

The total height of the wedge $H = 130 \text{ ft}$.

The stereoplot of the great circles representing the four planes involved in this problem is presented in Figure 8.6 and all the angles required for the solution of equations (92) to (95) are marked in this figure.

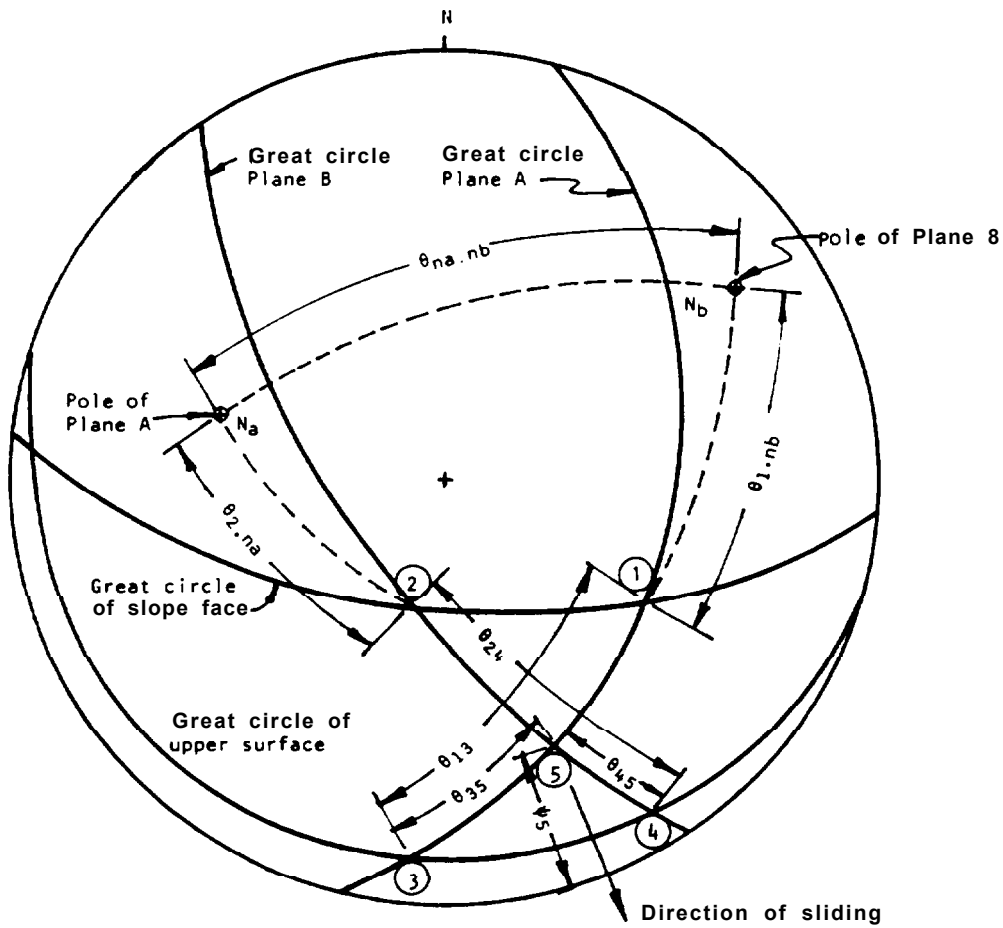


Figure 8.6: Stereoplot of data required for wedge stability analysis.

WEDGE STABILITY CALCULATION SHEET

INPUT DATA	FUNCTION VALUE	CALCULATED ANSWER
$\psi_a = 45^\circ$ $\psi_b = 70^\circ$ $\psi_5 = 31.20$ $\theta_{na.nb} = 101^\circ$	$\cos \psi_a = 0.7071$ $\cos \psi_b = 0.3420$ $\sin \psi_5 = 0.5180$ $\cos \theta_{na.nb} = -0.191$ $\sin \theta_{na.nb} = 0.982$	$A = \frac{\cos \psi_a - \cos \psi_b \cdot \cos \theta_{na.nb}}{\sin \psi_5 \cdot \sin^2 \theta_{na.nb}} * \frac{0.7071 + 0.342 \times 0.191}{0.5180 \times 0.9636} = 1.5475$ $B = \frac{\cos \psi_b - \cos \psi_a \cdot \cos \theta_{na.nb}}{\sin \psi_5 \cdot \sin^2 \theta_{na.nb}} * \frac{0.3420 + 0.7071 \times 0.191}{0.5180 \times 0.9636} = 0.9557$
$\theta_{24} = 65^\circ$ $\theta_{45} = 25^\circ$ $\theta_{2.na} = 50^\circ$	$\sin \theta_{24} = 0.9063$ $\sin \theta_{45} = 0.4226$ $\cos \theta_{2.na} = 0.6428$	$x = \frac{\sin \theta_{24}}{\sin \theta_{45} \cdot \cos \theta_{2.na}} * \frac{0.9063}{0.4226 \times 0.6428} = 3.3363$
$\theta_{13} = 62^\circ$ $\theta_{35} = 31^\circ$ $\theta_{1.nb} = 60^\circ$	$\sin \theta_{13} = 0.8829$ $\sin \theta_{35} = 0.5150$ $\cos \theta_{1.nb} = 0.5000$	$Y = \frac{\sin \theta_{13}}{\sin \theta_{35} \cdot \cos \theta_{1.nb}} * \frac{0.8829}{0.5150 \times 0.5000} = 3.4287$
$\phi_A = 30^\circ$ $\phi_B = 20^\circ$ $\gamma = 160 \text{ lb/ft}^3$ $\gamma_w = 62.5 \text{ lb/ft}^3$ $c_A = 500 \text{ lb/ft}^2$ $c_B = 1000 \text{ lb/ft}^2$ $H = 130 \text{ ft}$	$\tan \phi_A = 0.5773$ $\tan \phi_B = 0.3640$ $\gamma_w / 2\gamma = 0.1953$ $3c_A / \gamma H = 0.0721$ $3c_B / \gamma H = 0.1442$	$F = \frac{3c_A}{\gamma H} X + \frac{3c_B}{\gamma H} Y + (A - \frac{\gamma_w}{2\gamma} \cdot X) \tan \phi_A + (B - \frac{\gamma_w}{2\gamma} \cdot Y) \tan \phi_B$ $F = 0.2405 + 0.4944 + 0.6934 - 0.3762 + 0.3476 - 0.2437 = 1.3562$

Determination of the factor of safety is most conveniently carried out on a calculation sheet such as that presented on page 8.10. Setting the calculations out in this manner not only enables the user to check all the data but it also shows how each variable contributes to the overall factor of safety. Hence, if it is required to check the influence of the cohesion on both planes falling to zero, this can be done by setting the two groups containing the cohesion values C_A and C_B to zero, giving a factor of safety of 0.62. Alternatively, the effect of drainage can be checked by putting the two water pressure terms (i.e. those containing T_w) to zero, giving $F = 1.98$.

As has been emphasized in previous chapters, this ability to check the sensitivity of the factor of safety to changes in material properties or in slope loading is probably as important as the ability to calculate the factor of safety itself.

Wedge stability charts for friction only

If the cohesive strength of the planes A and B is zero and the slope is fully drained, equation (77) reduces to

$$F = A \cdot \tan \phi_A + B \cdot \tan \phi_B \quad (96)$$

The dimensionless factors A and B are found to depend upon the dips and dip directions of the two planes and values of these two factors have been computed for a range of wedge geometries and the results are presented as a series of charts on the following pages.

In order to illustrate the use of these charts, consider the following example:

	dip°	dip direction°	friction angle°
Plane A	40	165	35
Plane B	<u>70</u>	<u>285</u>	20
Differences	30	120	

Hence, turning to the charts headed "Dip difference 30°" and reading off the values of A and B for a difference in dip direction of 120°, one finds that

$$A = 1.5 \text{ and } B = 0.7$$

Substitution in equation (96) gives the factor of safety as $F = 1.30$. The values of A and B give a direct indication of the contribution which each of the planes makes to the total factor of safety.

Note that the factor of safety calculated from equation 96 is independent of the slope height, the angle of the slope face and the inclination of the upper slope surface. This rather surprising result arises because the weight of the wedge occurs in both the numerator and denominator of the factor of safety equation and, for the friction only case, this term cancels out, leaving a dimensionless ratio which defines the factor of safety (see equation (89) on page 8.4). This simplification is very useful in that it enables the user of these charts to carry out a very quick check on the stability of a slope on the

basis of the dips and dip directions of the discontinuities in the rock mass into which the slope has been cut. An example of such an analysis is presented later in this chapter.

Many trial calculations have shown that a wedge having a factor of safety in excess of 2.0, as obtained from the friction only stability charts, is unlikely to fail under even the most severe combination of conditions to which the slope is likely to be subjected. Consider the example discussed on pages 8.9 to 8.11 in which the factor of safety for the worst conditions (zero cohesion and maximum water pressure) is 0.62. This is 50% of the factor of safety of 1.24 for the friction only case. Hence, had the factor of safety for the worst conditions been 2.0, the factor of safety for the worst conditions would have been 1.0, assuming that the ratio of the factors of safety for the two cases remains constant.

On the basis of such trial calculations, the authors suggest that the friction only stability charts can be used to define those slopes which are adequately stable and which can be ignored in subsequent analyses. Such slopes, having a factor of safety in excess of 2.0, pass into the stable category in the chart presented in Figure 1.5 (page 1.8). Slopes with a factor of safety, based upon friction only, of less than 2.0 must be regarded as in the potentially unstable category of Figure 1.5, i.e. these slopes require further detailed examination.

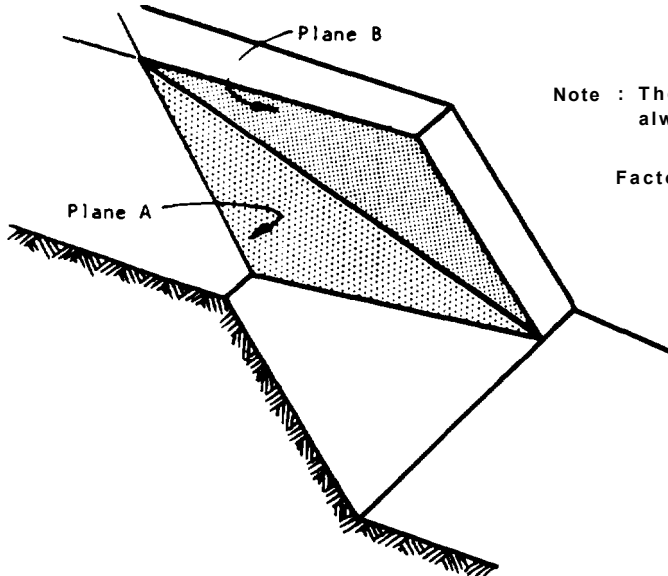
In many practical problems involving the design of the cut slopes for a highway, it will be found that these friction only stability charts provide all the information which is required. It is frequently possible, having identified a potentially dangerous slope, to eliminate the problem by a slight re-alignment of the benches or of the road alignment. Such a solution is clearly only feasible if the potential danger is recognized before excavation of the slope is started and the main use of the charts is during the site investigation and preliminary planning stage of a slope project.

Once a slope has been excavated, these charts will be of limited use since it will be fairly obvious if the slope is unstable. Under these conditions, a more detailed study of the slope will be required and use would then have to be made of the method described on pages 8.5 to 8.10 or of the analytical solution presented in Appendix 2. In the authors' experience relatively few slopes require this detailed analysis and the reader should beware of wasting time on such an analysis when the simpler methods presented in this chapter would be adequate. A full stability analysis may look very impressive in a report but, unless it has enabled the slope engineer to take positive remedial measures, it may have served no useful purpose.

Practical example of wedge analysis

During the route location study for a proposed highway, the engineer responsible for the highway layout has requested guidance on the maximum safe angles which may be used for the design of the slopes. Extensive geological mapping of outcrops on the site together with a certain amount of core logging has established that there are five sets of geological discontinuities in the rock mass through which the road will pass. The dips and dip directions of these discontinuities are as follows:

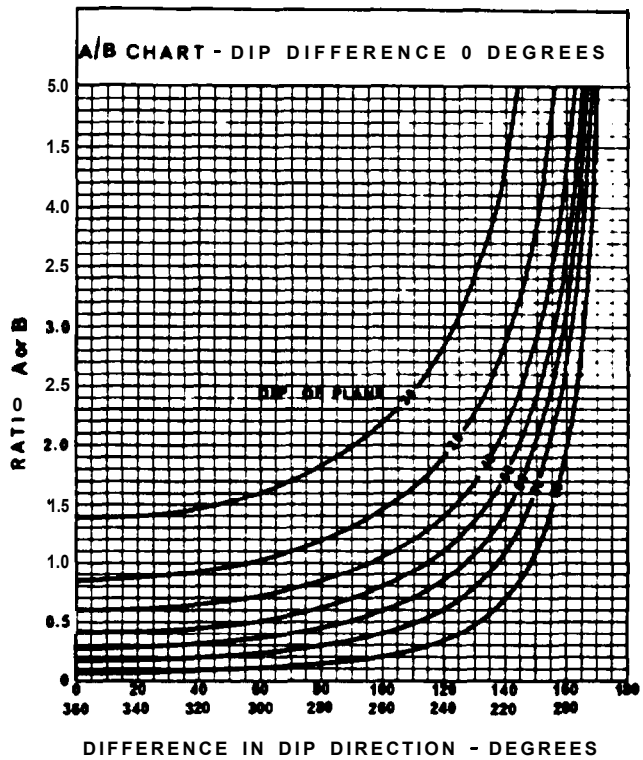
WEDGE STABILITY CHARTS FOR FRICTION ONLY

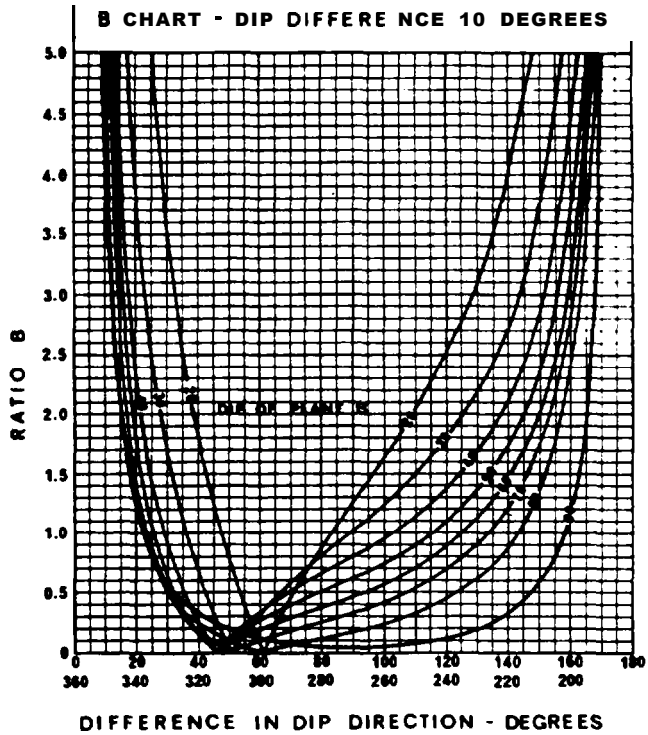
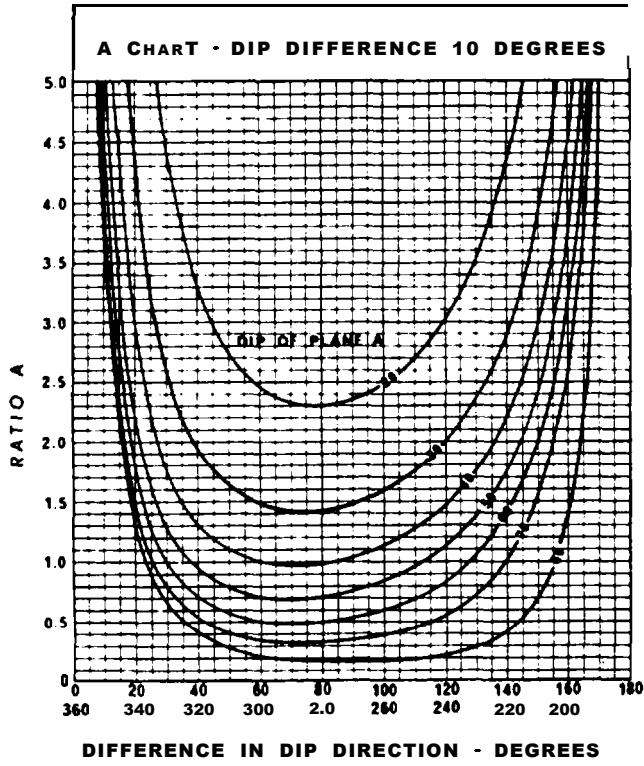


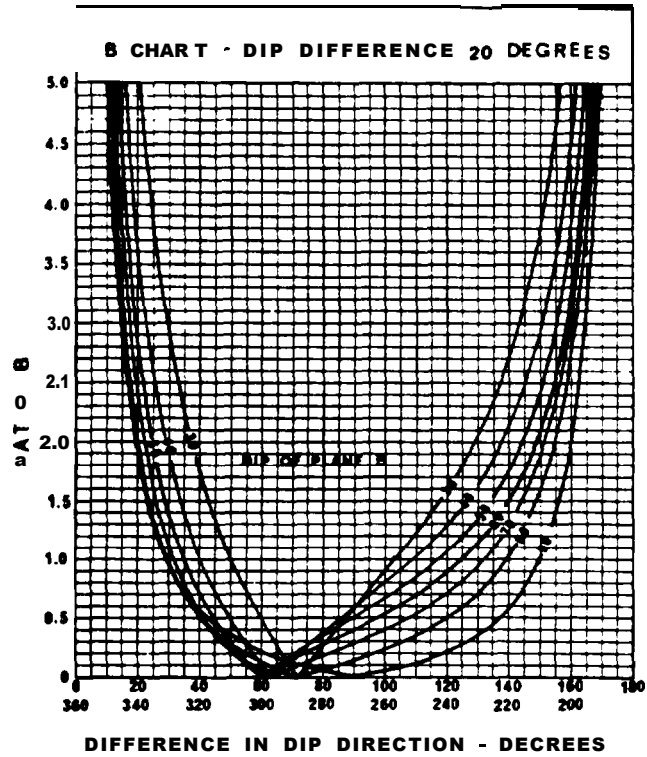
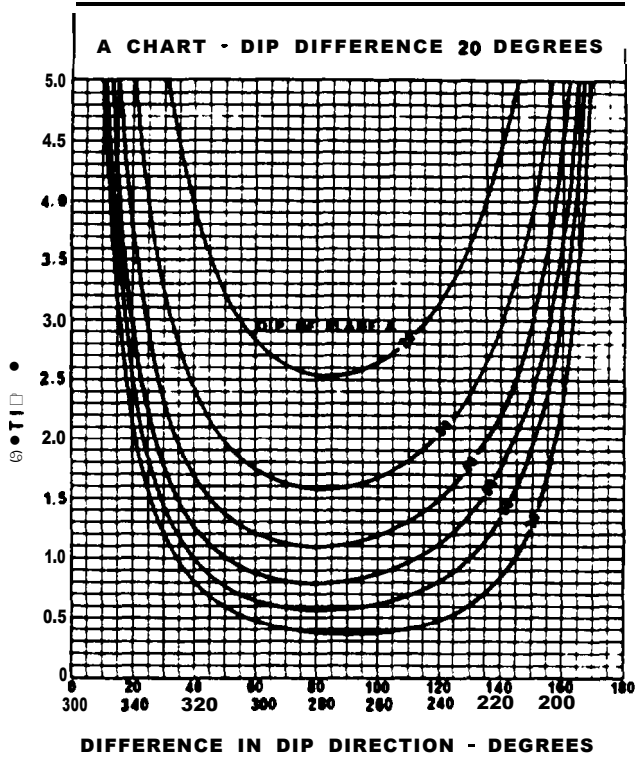
Note : The flatter of the two planes is always called plane A.

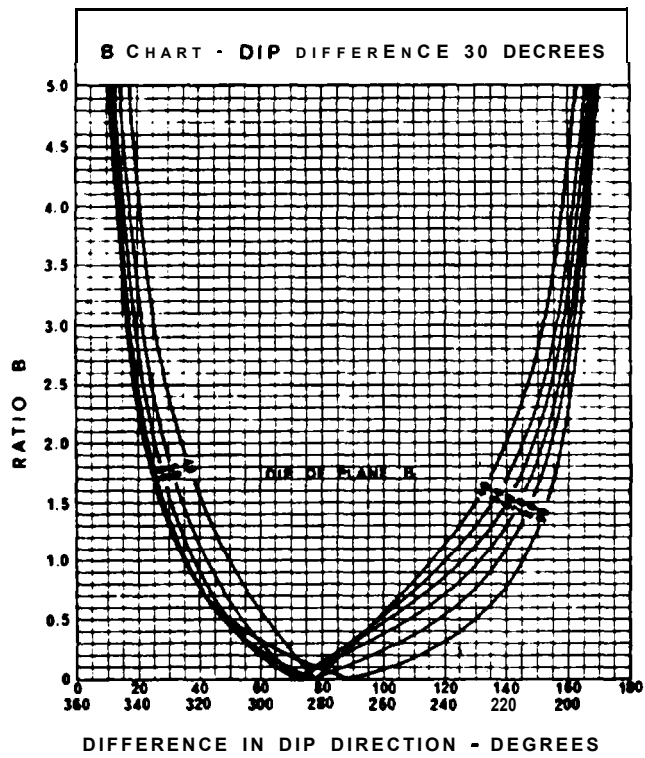
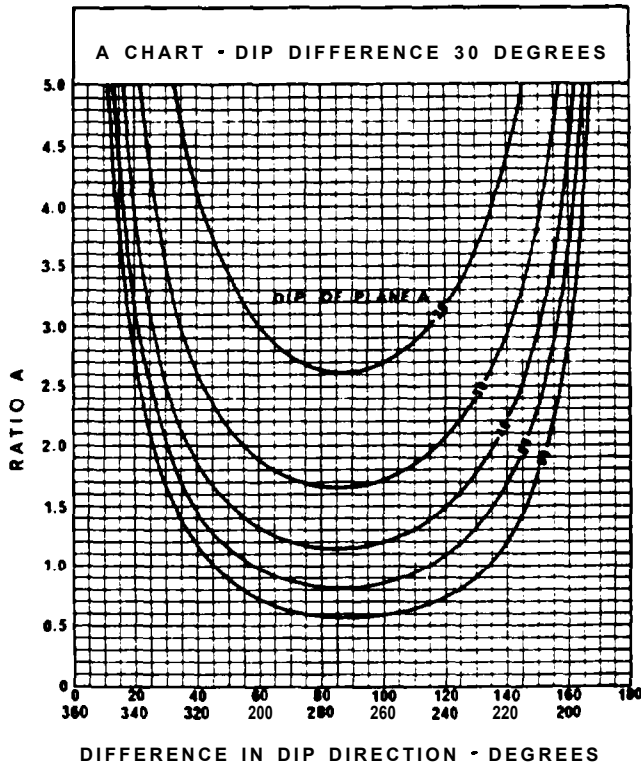
Factor of Safety

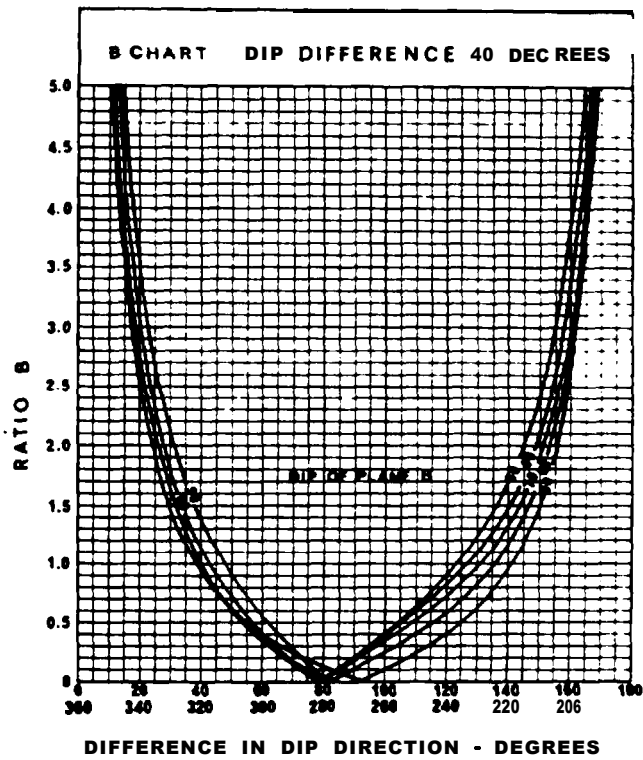
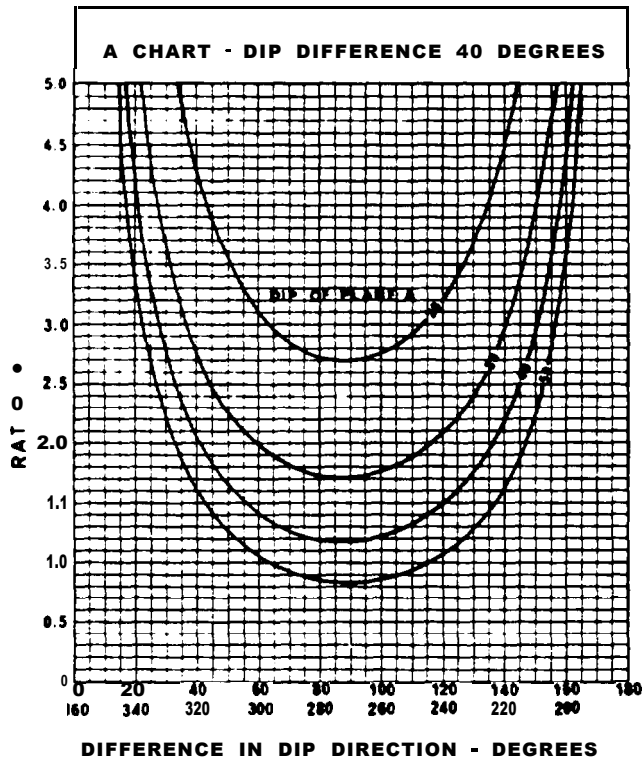
$$F = A.Tan\phi_A + B.Tan\phi_B$$

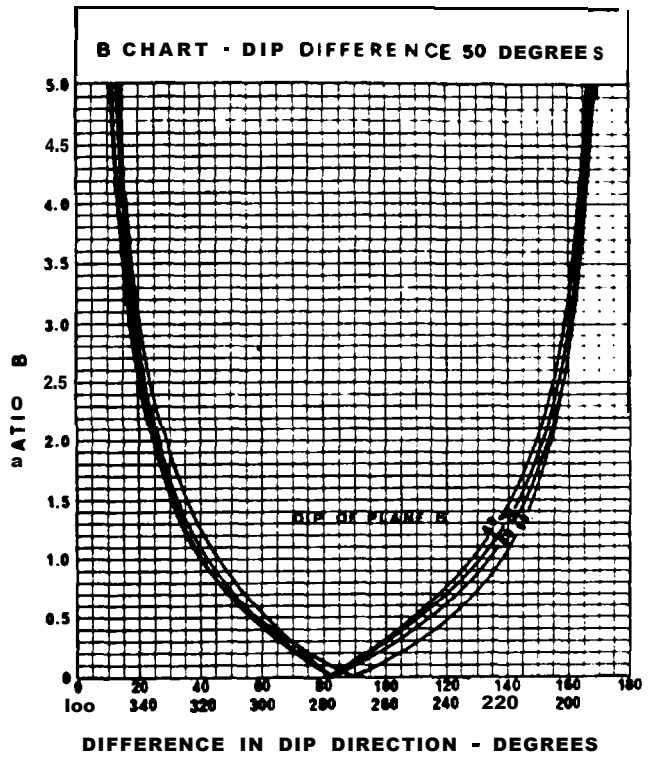
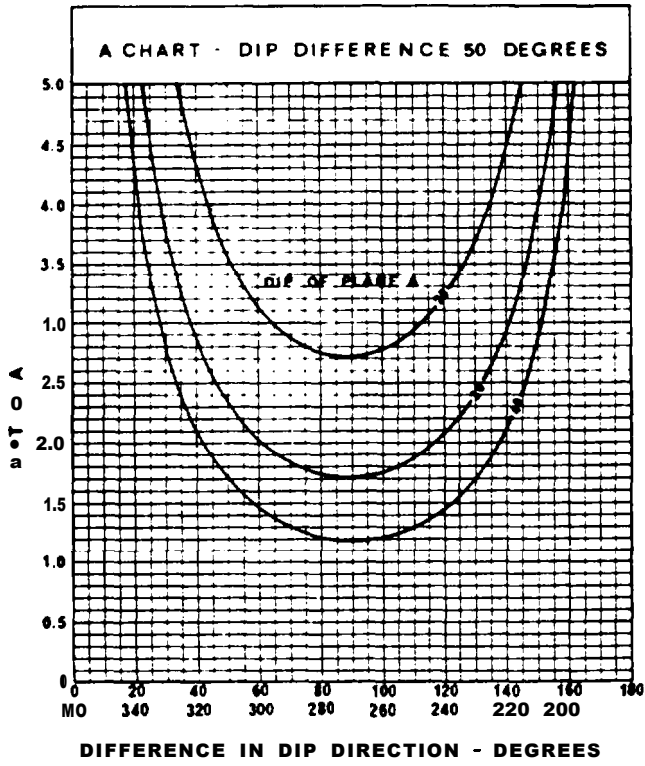


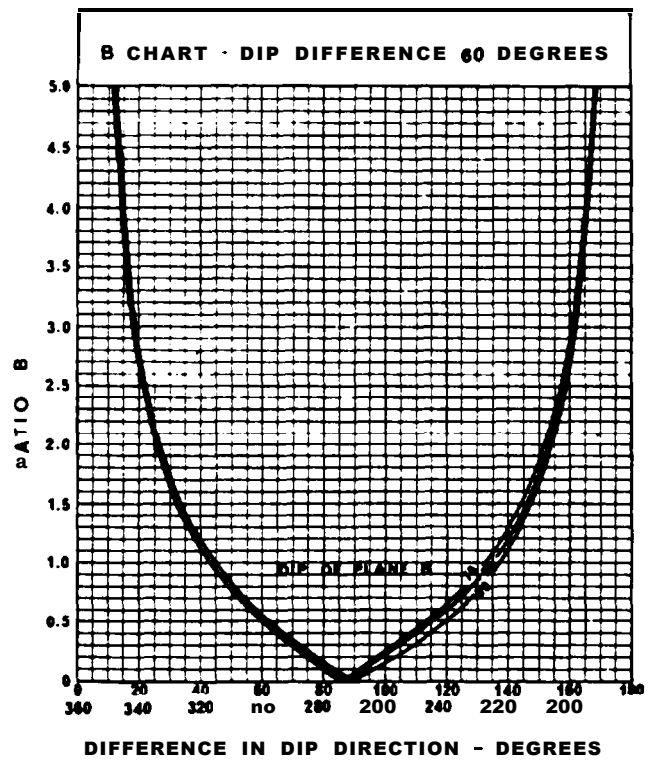
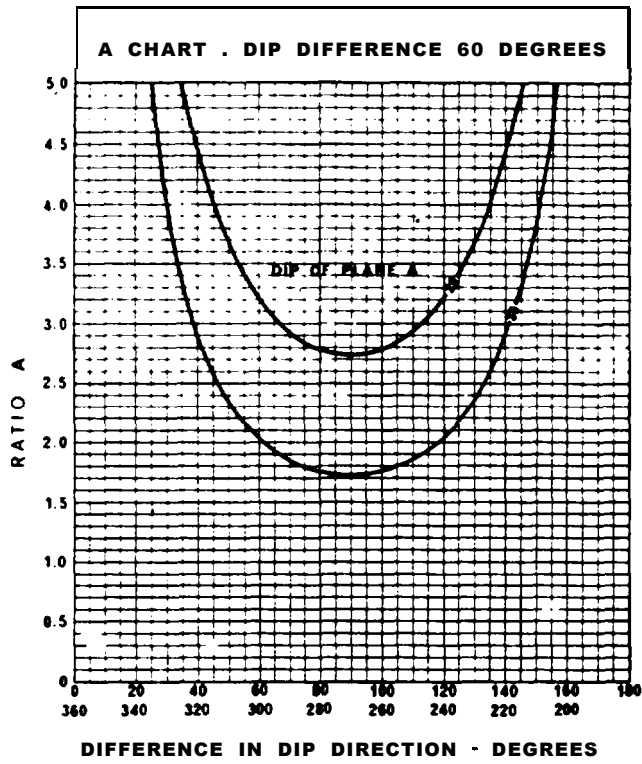


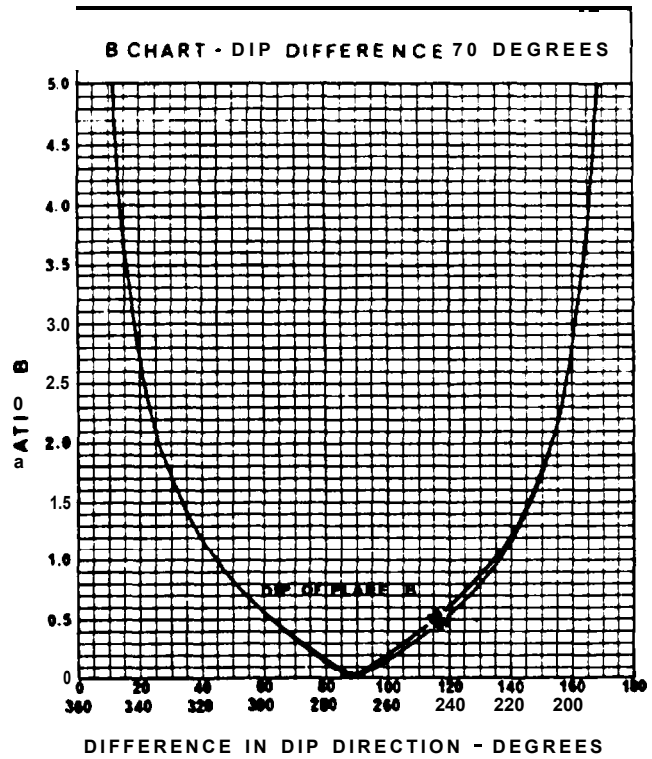
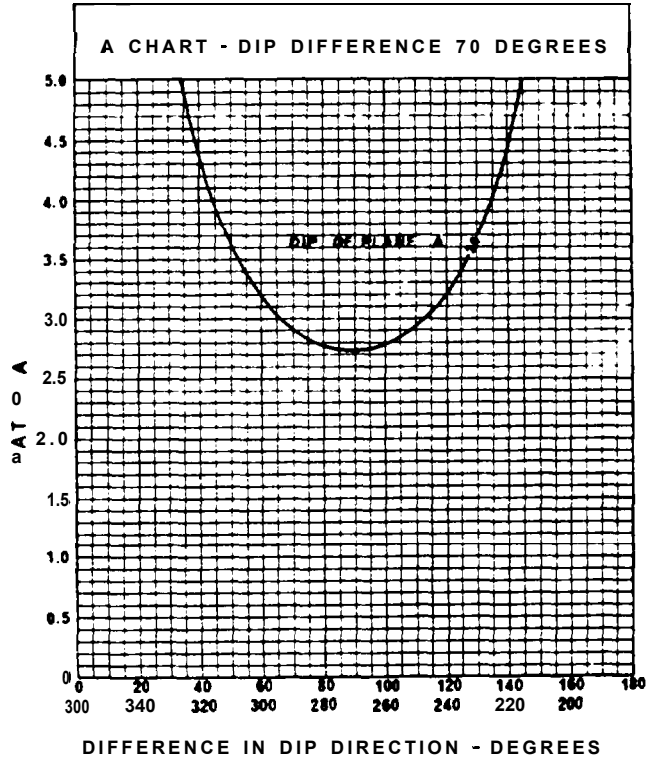












Discontinuity set	dip"	dip direction"
1	66 + 2	298 + 2
2	68 + 6	320 + 15
3	60.5 + 1.6	360 + 10
4	58 + 6	76 + 6
5	54 + 4	118 + 2

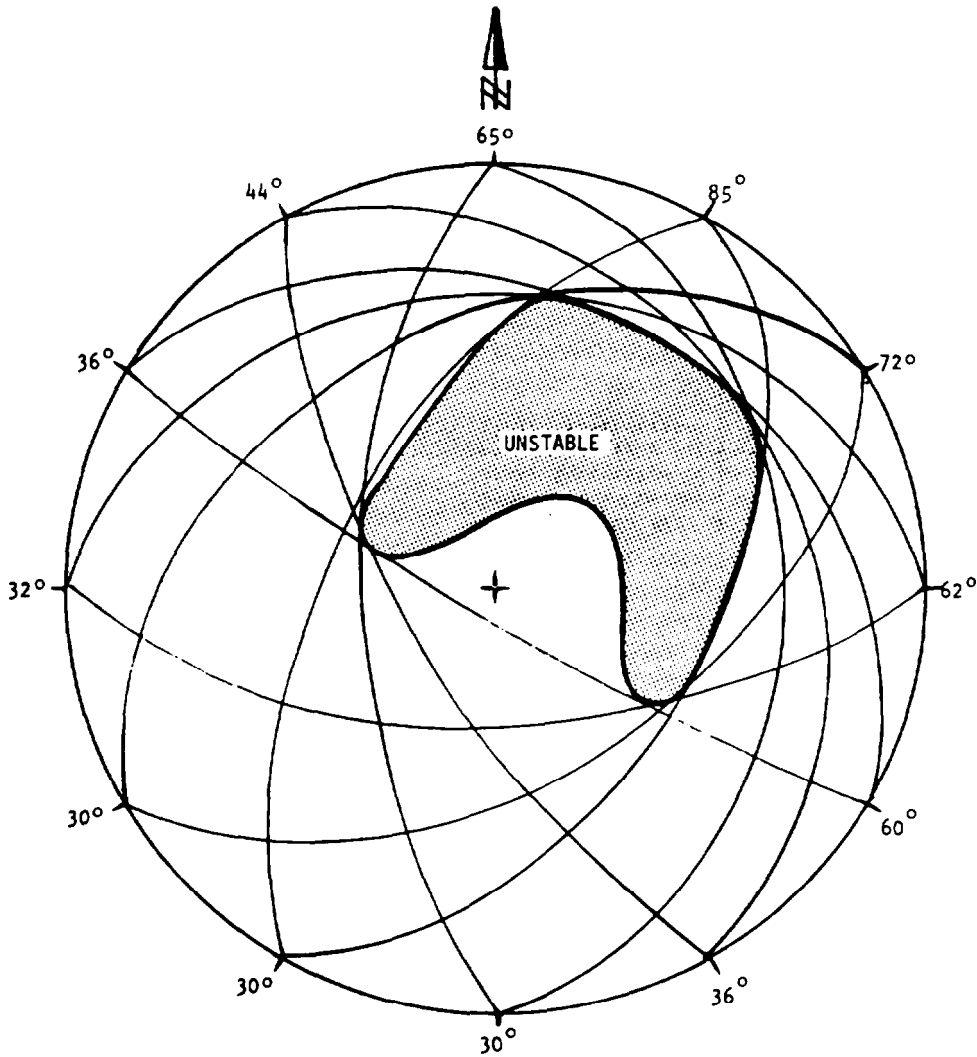
Note that, because this mapping covers the entire site which extends over several acres, the scatter in the dip and dip direction measurements is considerable and must be taken into account in the analysis. This scatter can be reduced by more detailed mapping in specific locations, for example, Figure 3.10 on page 3.25, but this may not be possible because of shortage of time or because suitable outcrops are not available.

Figure 8.7 shows the pole locations for these five sets of discontinuities. Also shown on this figure are the extent of the scatter in the pole measurements and the great circles corresponding to the most probable pole positions. The dashed figure surrounding the great circle intersections is obtained by rotating the stereoplot to find the extent to which the intersection point is influenced by the scatter around the pole points. The technique described on page 3.11 is used to define this dashed figure. The intersection of great circles 2 and 5 has been excluded from the dashed figure because it defines a line of intersection dipping at less than 20° and this is considered to be less than the angle of friction.

The factors of safety for each of the discontinuity intersections is determined from the wedge charts (some interpolation is necessary) and the values are given in the circles over the intersection points. Because all of the planes are relatively steep, some of the factors of safety are dangerously low (assuming a friction angle of 30°). Since it is unlikely that slopes with a factor of safety of less than 0.5 could be economically stabilized, the only practical solution is to cut the slopes in these regions to a flat enough overall angle to eliminate the problem.

The construction given in Figure 8.8 is that which is used to find the maximum safe slope angle for the slopes on either side of the highway. This construction involves positioning the great circle representing the slope face for a particular dip direction in such a way that the unstable region (shaded) is avoided. The maximum safe slope angles are marked around the perimeter of this figure and their positions correspond to the orientation of the slope.

Figure 8.9 shows the suggested slope angles as presented to the highway engineer by the rock slope engineer. The slopes on the east side can be cut at 72° but on the west side, it is necessary to cut them back to 30° . Note that as the highway continues to curve in the direction shown in the diagram, it will be necessary to flatten the east slope because more unstable wedges will become adversely oriented on the slope as shown in Figure 8.8.



Note: Figures around the perimeter are the recommended stable slope angles for the corresponding position on the slope.

Figure 8.8: Stereoplot of great circles representing stable slopes above the highway in a rock mass containing the five sets of discontinuities defined in Figure 8.7.

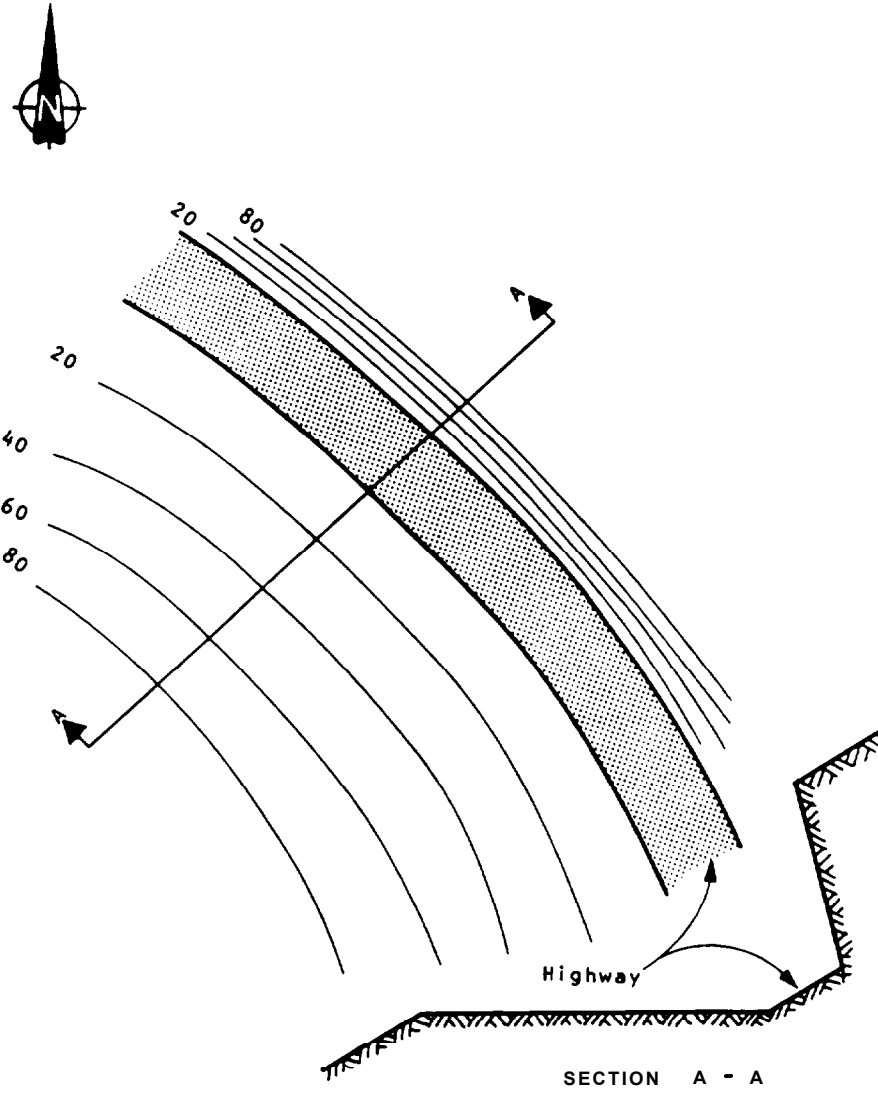


Figure 8.9: Design of highway slopes according to safe angles defined in Figure 8.8.

Chapter 8 references

190. LONDE, P. Une méthode d'analyse à trois dimensions de la stabilité d'une rive rocheuse. *Annales des Ponts et Chaussées*. Paris. 1965, pages 37-60.
191. LONDE, P., VIGIER, G. and VORHERINGER, R. The stability of rock slopes, a three-dimensional study. *J. Soil Mech. and Foundation Div.* ASCE. Vol. 95, No. SM 1, 1969, ptgts 235-262.
192. LONDE, P., VIGIER, G. and VORHERINGER, R. Stability of slopes - graphical methods. *J. Soil Mech. and Foundation Div.* ASCE. vol. 96, NO. SM 4, 1970, ptgts 1411-1434.
193. JOHN, K.W. Engineering analysis of three-dimensional stability problems utilising the reference hemisphere. *Proc. 2nd Congress. Intl. Soc. Rock Mech.* Belgrade. 1970, Vol. 2, ptgts 314-321.
194. WITTKÉ, W.W. Method to analyse the stability of rock slopes with and without additional loading. (In German) *Felsmechanik und Ingenieurgeologie*. Supp. 11, Vol. 30, 1965, pages 52-79.
English translation in Imperial College Rock Mechanics Research Report No. 6, July 1971.
195. GOODMAN, R.E. The resolution of stresses in rock using stereographic projection. *Intl. J. Rock Mech. Mining Sci.* vol. 1, 1964, pages 93-103.
196. GOODMAN, R.E. and TAYLOR, R.L. Methods of analysis of rock slopes and embankments: a review of recent developments. in *Failure and Breakage of Rocks*. Edited by C. Fairhurst. AIME, 1967, pages 303-320.
197. HEUZE, F.E. and GOODMAN, R.E. Three-dimensional approach for the design of cuts in jointed rock. *Proc. 23th Sympos. Rock Mech.* Urbana, Illinois. 1971.
198. HENDRON, A.J., CORDING, E.J. and AIYER, A.K. Analytical and graphic methods for the analysis of slopes in rock masses. *U.S. Army Engineering Nuclear Cratering Group*. Tech. Rep. No. 36, 1971. 168 pages.
199. SRIVASTAVA, L.S. Stability of rock slopes and excavations. *J. Eng. Geology*. Indian Soc. Engineering Geology. Vol. 1/1, 1966. ptgts 57-72.
200. SAVKOV, L.V. Considerations of fracture in the calculation of rock slope stability. *Soviet Mining Science* 1967, ptgts 1-6.
201. HOEK, E., BRAY, J.W. and BOYD, J.H. The stability of a rock slope containing a wedge resting on two intersecting discontinuities. *Quarterly J. Engineering Geology*. Vol. 6, No. 1, 1973.
202. HOEK, E. Methods for the rapid assessment of the stability of three-dimensional rock slopes. *Quarterly J. Engineering Geology*. Vol. 6, No. 3, 1973.

203. TAYLOR, C.L. Geometric analysis of geological separation for slope stability Investigations. *Butt. Ass. Engineering Geologists*. Vol. VI 1, Nos.1 b 2, 1970, pages 76-85.
204. TAYLOR, C.E. Geometric analysis of rock slopes. *Proc. 21st Annual Highway Geology Symposium*. University Kansas, April, 1970.
205. WILSON, S.D. The application of soil mechanics to the stability of open pit mines. *Colorado School of Mines Quarterly*. Vol. 54, No.3, 1959, pages 95-113.
206. HULLER, L. The European approach to slope stability problems in open-pit mines. *Colorado School of Mines Quarterly*. Vol.54, No.3, 1999. pages 117-133.
207. HULLER, L. and JOHN, K.W. Recent developments of stability studies of steep rock slopes In Europe. *Trans. Soc. Min. Engineers, AIME*. Vol.226. No. 3. 1963, pages 326-332.
208. HULLER, L. Application of rock mechanics in the design of rock slopes. *Intnl. Conf. State Of Stress in the Earth's Crust*. Santa Monica. 1963. Elsevier, New York. 1964.
209. PETZNY, H. On the stability of rock slopes (in German) *Felsmechanik und Ingenieurgeologie*. Suppl. III, 1967.

Chapter 9 Circular failure.

Introduction

Although this book is concerned primarily with the stability of rock slopes, the reader will occasionally be faced with a slope problem involving soft materials such as highly weathered rock or rock fills. In such materials, failure occurs along a surface which approaches a circular shape and this chapter is devoted to a brief discussion on how stability problems involving these materials are dealt with.

In a review on the historical development of slope stability theories, Golder(210) has traced the subject back almost 3 hundred years. During the past half century, a vast body of literature on this subject has accumulated and no attempt will be made to summarize this material in this chapter. Standard soil mechanics text books such as those by Taylor(174), Terzaghi(211) and Lambe and Whitman(212) all contain excellent chapters on the stability of soil slopes and it is suggested that at least one of these books should occupy a prominent place on the bookshelf of anyone who is concerned with slope stability. In addition to these books a number of important papers dealing with specific aspects of soil slope stability have been published and a selected list of these is given under references 213 to 233 at the end of this chapter.

The approach adopted in this chapter is to present a series of the slope stability charts for circular failure. These charts enable the user to carry out a very rapid check on the factor of safety of a slope or upon the sensitivity of the factor of safety to changes in groundwater conditions or slope profile. These charts should only be used for the analysis of circular failure in materials where the properties do not vary through the soil or waste rock mass and where the conditions assumed in deriving the charts, discussed in the next section, apply. A more elaborate form of analysis is presented at the end of this chapter for use in cases where the material properties vary within the slope or where part of the slide surface is at a soil/rock interface and the shape of the failure surface differs significantly from a simple circular arc.

Conditions for circular failure

In the previous chapters it has been assumed that the failure of rock slopes is controlled by geological features such as bedding planes and joints which divide the rock body up into a discontinuous mass. Under these conditions, the failure path is normally defined by one or more of the discontinuities. In the case of a soil, a strongly defined structural pattern no longer exists and the failure surface is free to find the line of least resistance through the slope. Observations of slope failures in soils suggests that this failure surface generally takes the form of a circle and most stability theories are based upon this observation.

The conditions under which circular failure will occur arise when the individual particles in a soil or rock mass are very small as compared with the size of the slope and when these particles are not interlocked as result of their shape. Hence, broken rock in a large fill will tend to behave as a "soil" and large failures will occur in a circular mode. Alternatively, soil consisting of sand, silt and smaller particle sizes will exhibit circular failure surfaces, even in slopes of only a few

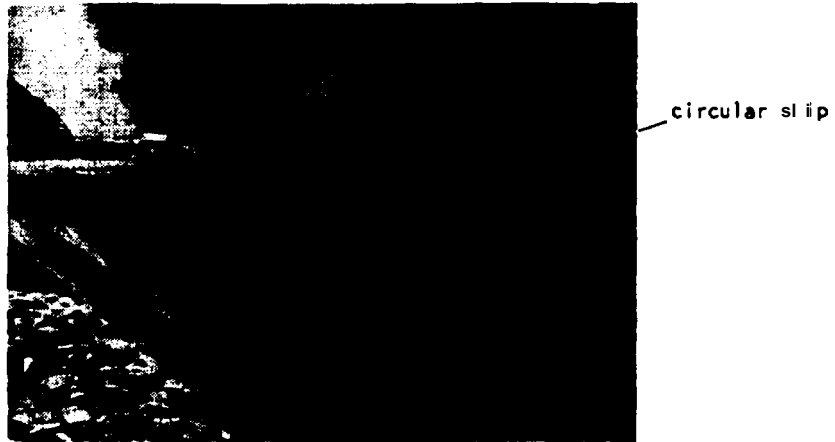


Figure 9.1 : Shallow surface failure in large waste dumps are generally of a circular type.

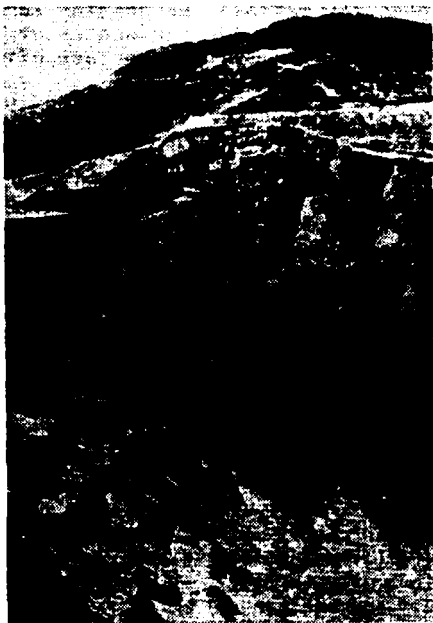


Figure 9.2 : Circular failure in the highly altered and weathered rock forming the upper benches of an open pit mine.

feet in height. Highly altered and weathered rocks will also tend to fail in this manner and it is appropriate to design the soil slopes on the crest of rock cuts on the assumption that failure would be by a circular failure process.

Derivation of circular failure chart

The following assumptions are made in deriving the stability charts presented in this chapter:

NOTE:

Circular failure charts are optimized for density of 120 pcf. Densities higher than this give high factors of safety, densities lower than this give low factors of safety. Detailed circular analysis may be required for slopes in which the material density is significantly different from 120 pcf.

- a) The material forming the slope is assumed to be homogeneous, i.e. its mechanical properties do not vary with direction of loading.
- b) The shear strength of the material is characterized by a cohesion c and a friction angle ϕ which are related by the equation $\tau = c + \sigma \cdot \tan \phi$.
- c) Failure is assumed to occur on a circular failure surface which passes through the toe of the slope*.
- d) A vertical tension crack is assumed to occur in the upper surface of the face of the slope.
- e) The locations of the tension crack and of the failure surface are such that the factor of safety of the slope is a minimum for the slope geometry and groundwater conditions considered.
- f) A range of groundwater conditions, varying from a dry slope to a fully saturated slope under heavy recharge, are considered in the analysis. These conditions are defined later in this chapter.

Defining the factor of safety of the slope as

$$F = \frac{\text{shear strength available to resist sliding}}{\text{shear stress mobilized along failure surface}}$$

and rearranging this equation, we obtain

$$\tau_{mb} = \frac{c}{F} + \frac{\sigma \cdot \tan \phi}{F} \quad (97)$$

where τ_{mb} is the shear stress mobilized along the failure surface.

Since the shear strength available to resist sliding is dependent upon the distribution of the normal stress σ along this surface and, since this normal stress distribution is unknown, the problem is statically indeterminate. In order to obtain a solution it is necessary to assume a specific normal stress distribution and then to check whether this distribution gives meaningful practical results.

● Terzaghi (1944), page 170, shows that the toe failure assumed for this analysis gives the lowest factor of safety provided that $\phi > 5^\circ$. The $\phi = 0$ analysis, involving failure below the toe of the slope through the base material has been discussed by Skempton (1954) and by Bishop and Bjerrum (1960) and is applicable to failures which occur during or after the rapid construction of a slope.

The influence of various normal stress distributions upon the factor of safety of soil slopes has been examined by Frohlich(216) who found that a lower bound for all factors of safety which satisfy statics is given by the assumption that the normal stress is concentrated at a single point on the failure surface. Similarly, the upper bound is obtained by assuming that the normal load is concentrated at the two end points of the failure arc.

The unreal nature of these stress distributions is of no consequence since the object of the exercise, up to this point, is simply to determine the extremes between which the actual factor of safety of the slope must lie. In an example considered by Lamb and Whitman(212), the upper and lower bounds for the factor of safety of a particular slope corresponded to 1.62 and 1.27 respectively. Analysis of the same problem by Bishop's simplified method of slices gives a factor of safety of 1.30 which suggests that the actual factor of safety may lie reasonably close to the lower bound solution.

Further evidence that the lower bound solution is also a meaningful practical solution is provided by an examination of the analysis which assumed that the failure surface has the form of a logarithmic spiral(227). In this case, the factor of safety is independent of the normal stress distribution and the upper and lower bounds coincide. Taylor(174) compared the results from a number of logarithmic spiral analyses with results of lower bound solutions* and found that the difference is negligible. On the basis of this comparison, Taylor concluded that the lower bound solution provides a value of the factor of safety which is sufficiently accurate for most practical problems involving simple circular failure of homogeneous slopes.

The authors have carried out similar checks to those carried out by Taylor and have reached the same conclusions. Hence, the charts presented in this chapter correspond to the lower bound solution for the factor of safety, obtained by assuming that the normal load is concentrated at a single point on the failure surface. These charts differ from those published by Taylor in 1948 in that they include the influence of a critical tension crack and of groundwater in the slope.

Groundwater flow assumptions

In order to calculate the uplift force due to water pressure acting on the failure surface and the force due to water in the tension crack, it is necessary to assume a set of groundwater flow patterns which coincide as closely as possible with those conditions which are believed to exist in the field.

In the analysis of rock slope failures, discussed in Chapters 7 and 8, it was assumed that most of the water flow took place in discontinuities in the rock and that the rock itself was practically impermeable. In the case of slopes in soil or waste rock, the permeability of the mass of material is generally

*The lower bound solution discussed in this chapter is usually known as the Friction Circle Method and was used by Taylor(174) for the derivation of his stability charts.

several orders of magnitude higher than that of intact rock and, hence, a general flow pattern will develop in the material behind the slope.

Figure 6.9s on page 6.11 shows that, within the soil mass, the equipotentials are approximately perpendicular to the phreatic surface. Consequently, the flow lines will be approximately parallel to the phreatic surface for the condition of steady state drawdown. Figure 9.3s shows that this approximation has been used for the analysis of the water pressure distribution in a slope under conditions of normal drawdown. Note that the phreatic surface is assumed to coincide with ground surface at a distance X , measured in multiples of the slope height, behind the toe of the slope. This may correspond to the position of a surface water source such as a river or dam or it may simply be the point where the phreatic surface is judged to intersect the ground surface.

The phreatic surface itself has been obtained, for the range of slope angles and values of X considered, by a computer solution of the equations proposed by L. Casagrande (236), discussed in the text book by Taylor (174).

For the case of a saturated slope subjected to heavy surface recharge, the equipotentials and the associated flow lines used in the stability analysis are based upon the work of Han (237) who used an electrical resistance analogue method for the study of groundwater flow patterns in isotropic slopes.

Production of circular failure charts

The circular failure charts presented in this chapter were produced by means of a Hewlett-Packard 9100 B calculator with graph plotting facilities. This machine was programmed to seek out the most critical combination of failure surface and tension crack for each of a range of slope geometries and groundwater conditions. Provision was made for the tension crack to be located in either the upper surface of the slope or in the face of the slope. Detailed checks were carried out in the region surrounding the toe of the slope where the curvature of the equipotentials results in local flow which differs from that illustrated in Figure 9.3a.

The charts are numbered 1 to 5 to correspond with the groundwater conditions defined in the table presented on page 9.6.

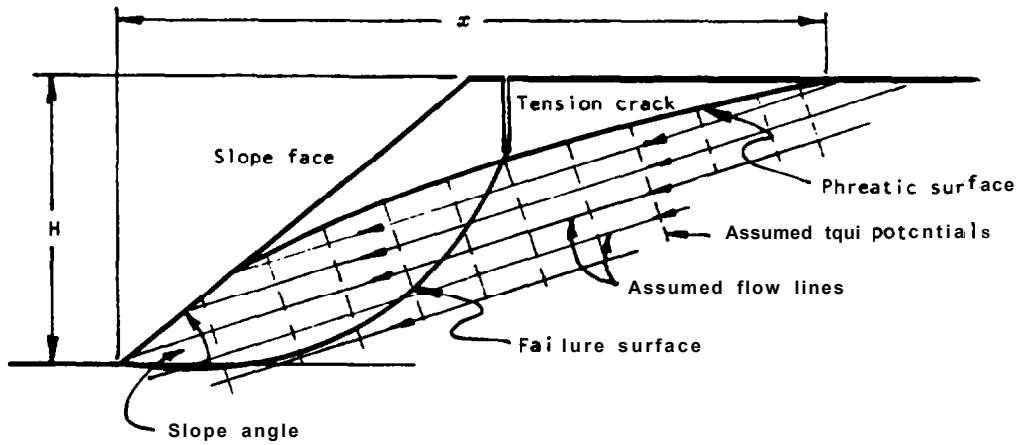
Use of the circular failure charts

In order to use the charts to determine the factor of safety of a particular slope, the steps outlined below and shown in Figure 9.4 should be followed.

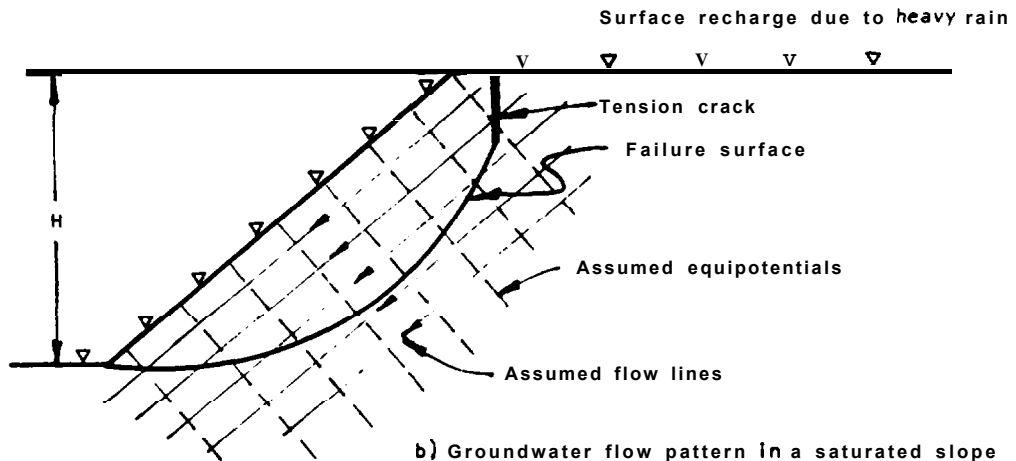
Step 1: Decide upon the groundwater conditions which are believed to exist in the slope and choose the chart which is closest to these conditions, using the table presented on page 9.6.

Step 2: Calculate the value of the dimensionless ratio

$$\frac{c}{\gamma H \cdot \tan \phi}$$



a) Groundwater flow pattern under steady state drawdown conditions where the phreatic surface coincides with the ground surface at a distance x behind the toe of the slope. The distance x is measured in multiples of the slope height H .



b) Groundwater flow pattern in a saturated slope subjected to heavy surface recharge by heavy rain.

Figure 9.3 : Definition of groundwater flow patterns used in circular failure analysis of soil and waste rock slopes.

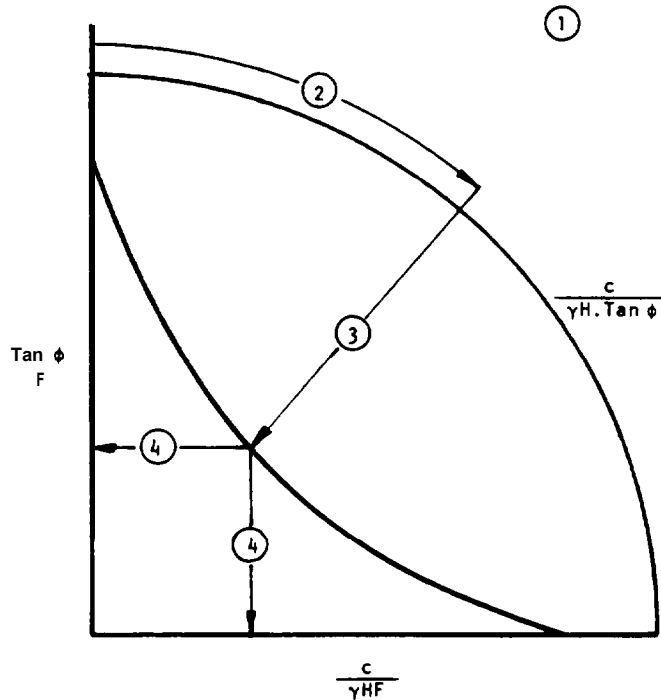


Figure 9.4 : Sequence of steps involved in using circular failure charts to find the factor of safety of a slope.

Find this value on the outer circular scale of the chart.

step 3: Follow the radial line from the value found in step 2 to its intersection with the curve which corresponds to the slope angle under consideration.

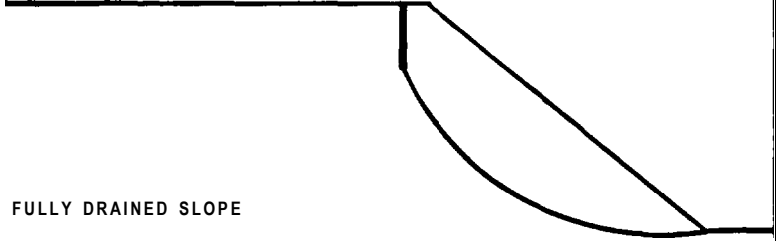
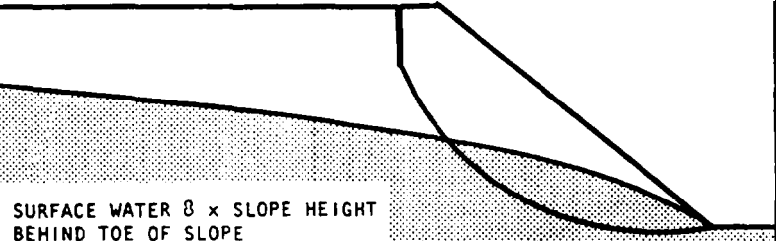
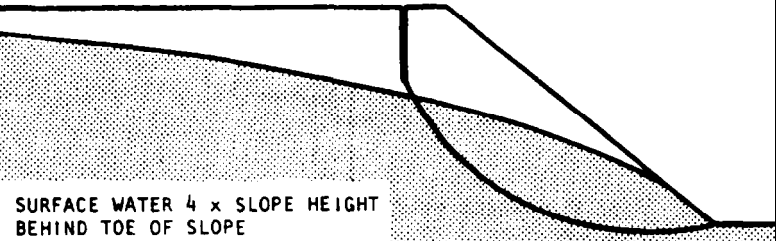
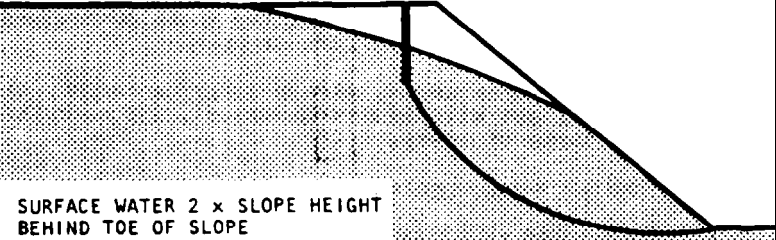
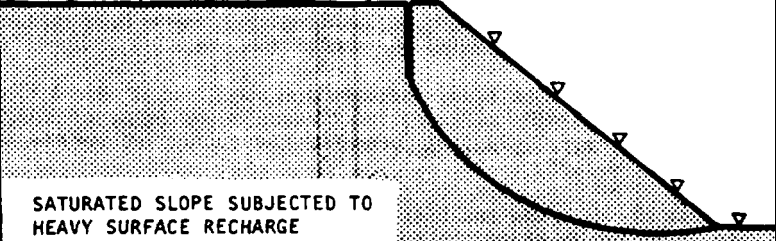
Step 4: Find the corresponding value of $\text{Tan}\phi/F$ or $c/\gamma HF$, depending upon which is more convenient, and calculate the factor of safety.

Consider the following example:

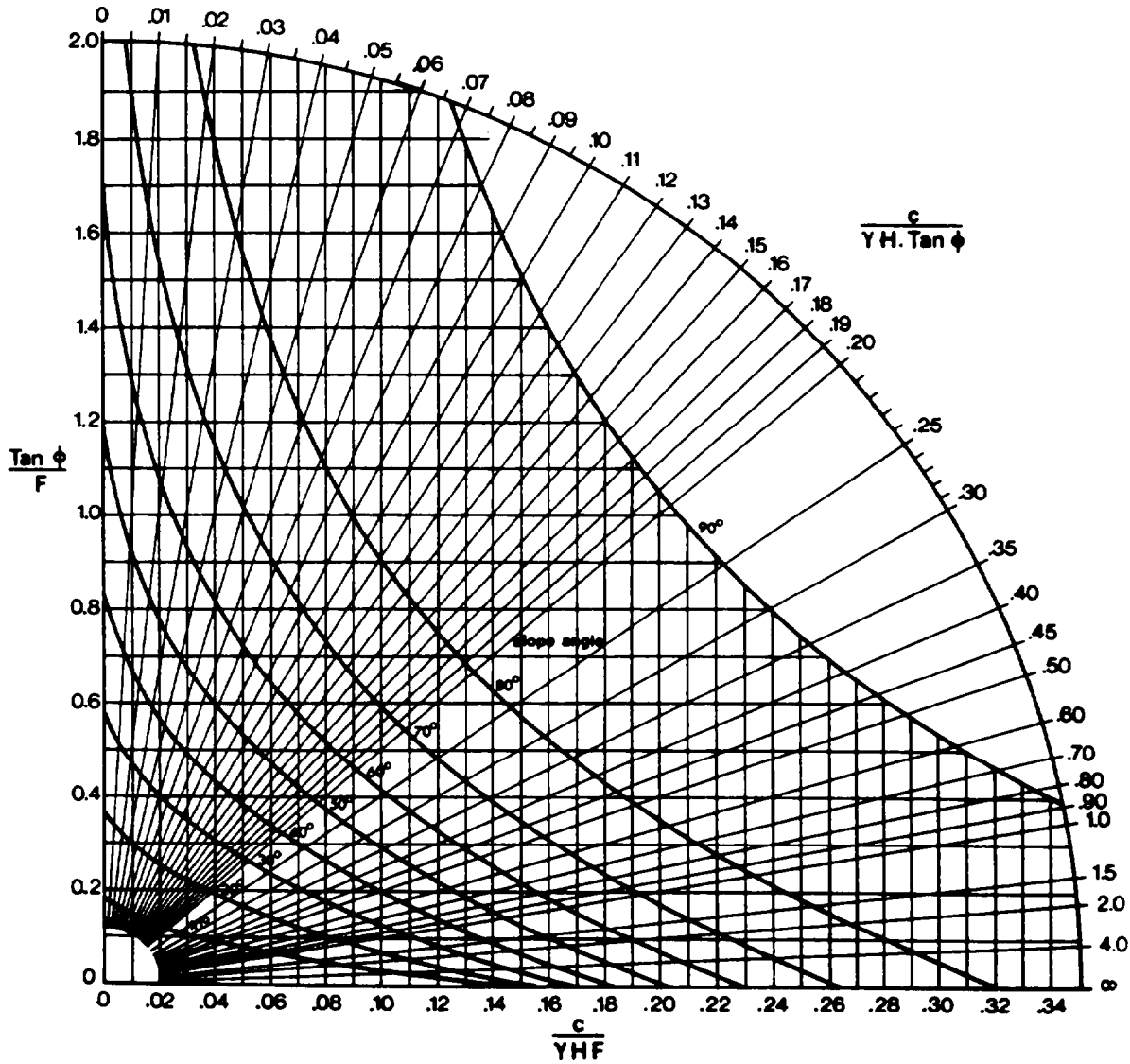
A 50 ft. high slope with a face angle of 40° is to be excavated in overburden soil with a density $\gamma = 100 \text{ lb/ft}^3$, a cohesive strength of 800 lb/ft^2 and a friction angle of 30° . Find the factor of safety of the slope, assuming that there is a surface water source 200 ft. behind the toe of the slope.

The groundwater conditions indicate the use of chart No. 3. The value of $c/\gamma H \cdot \text{Tan}\phi = 0.28$ and the corresponding value of $\text{Tan}\phi/F$, for a 40° slope, is 0.32. Hence, the factor of safety of the slope is 1.80.

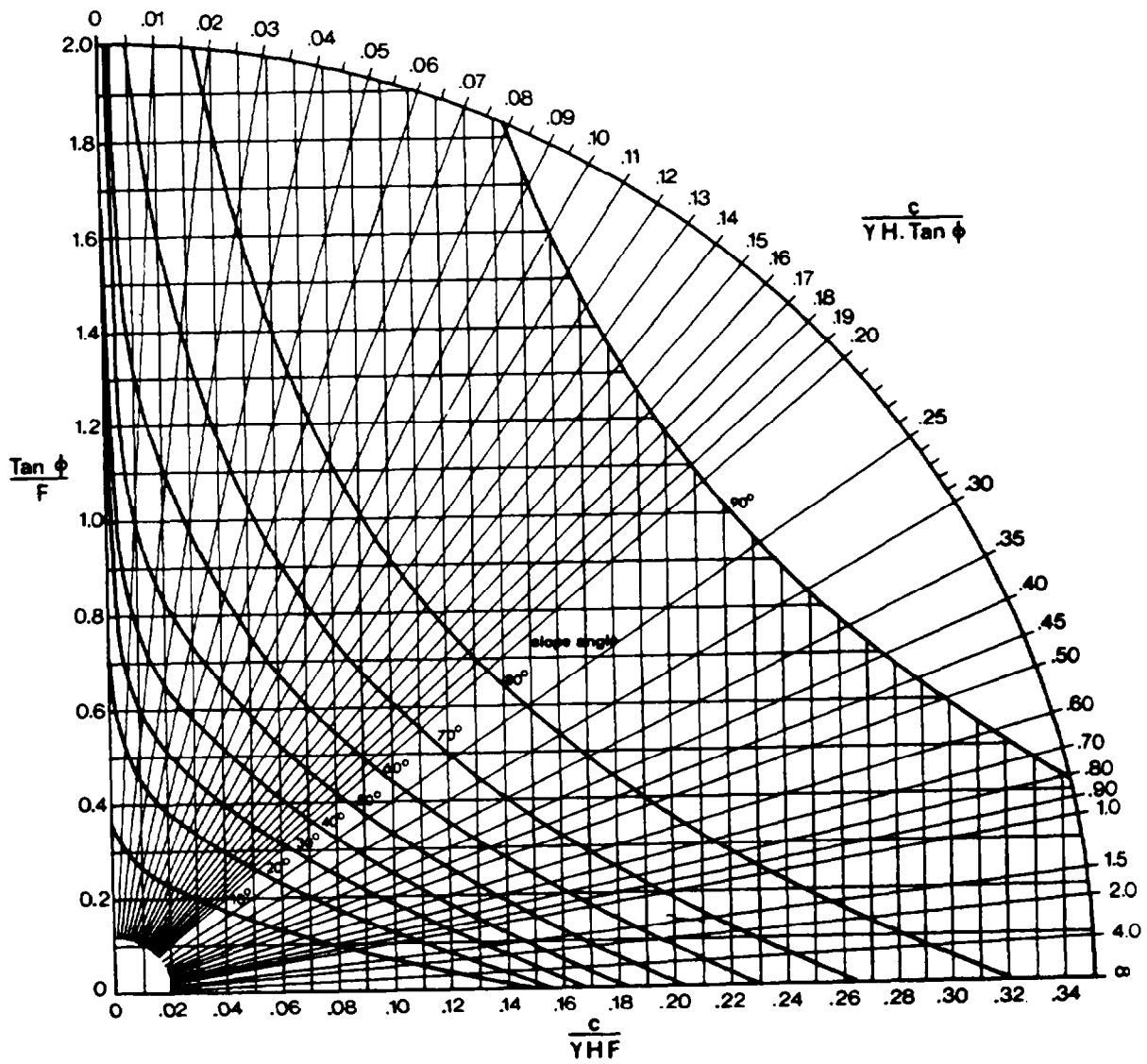
Because of the speed and simplicity of using these charts, they are ideal for checking the sensitivity of the factor of safety of a slope to a wide range of conditions and the authors suggest that this should be their main use.

GROUNDWATER FLOW CONDITIONS	CHART NUMBER
 <p>FULLY DRAINED SLOPE</p>	<p>1</p>
 <p>SURFACE WATER 8 x SLOPE HEIGHT BEHIND TOE OF SLOPE</p>	<p>2</p>
 <p>SURFACE WATER 4 x SLOPE HEIGHT BEHIND TOE OF SLOPE</p>	<p>3</p>
 <p>SURFACE WATER 2 x SLOPE HEIGHT BEHIND TOE OF SLOPE</p>	<p>4</p>
 <p>SATURATED SLOPE SUBJECTED TO HEAVY SURFACE RECHARGE</p>	<p>5</p>

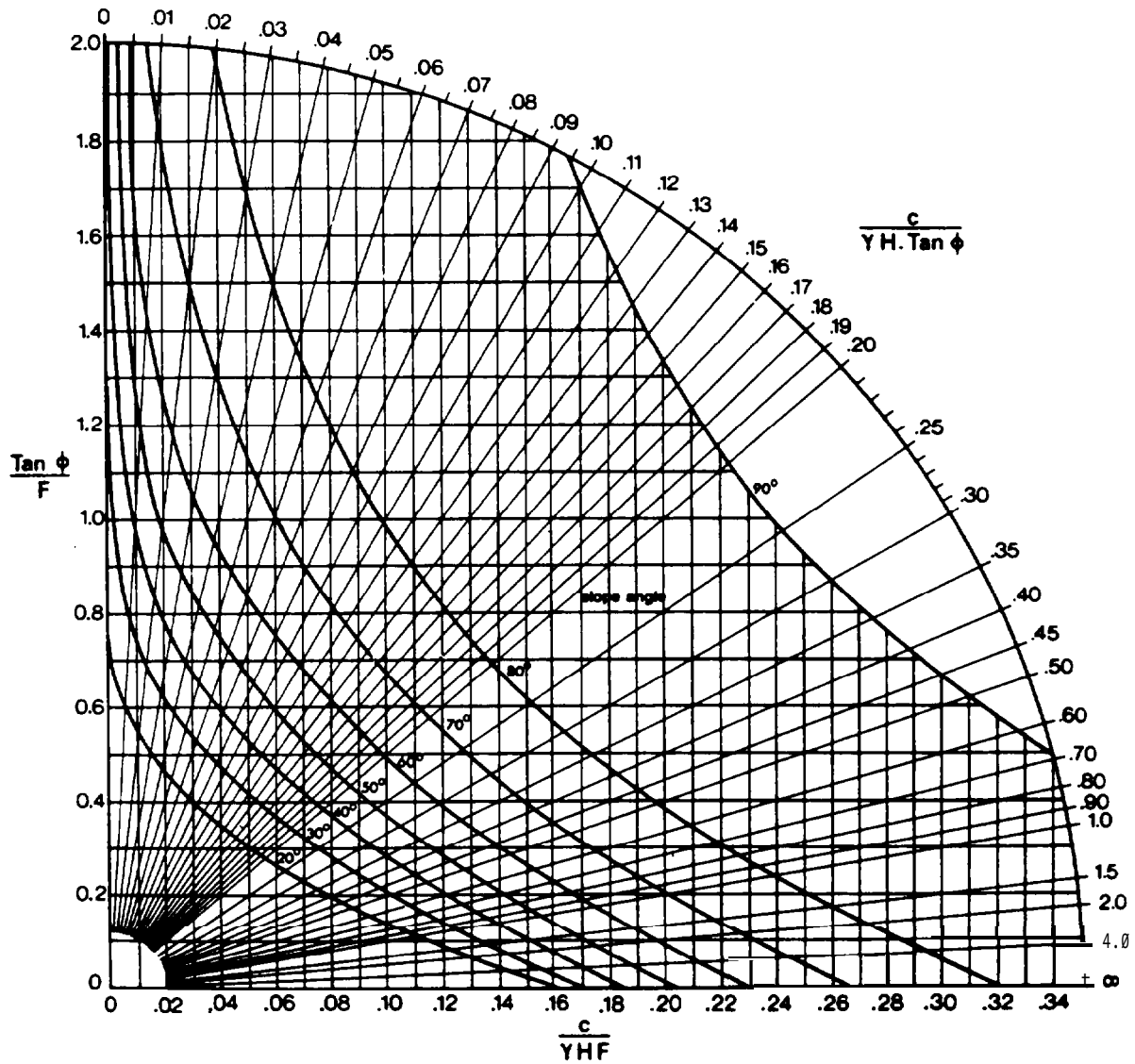
CIRCULAR FAILURE CHART NUMBER 1



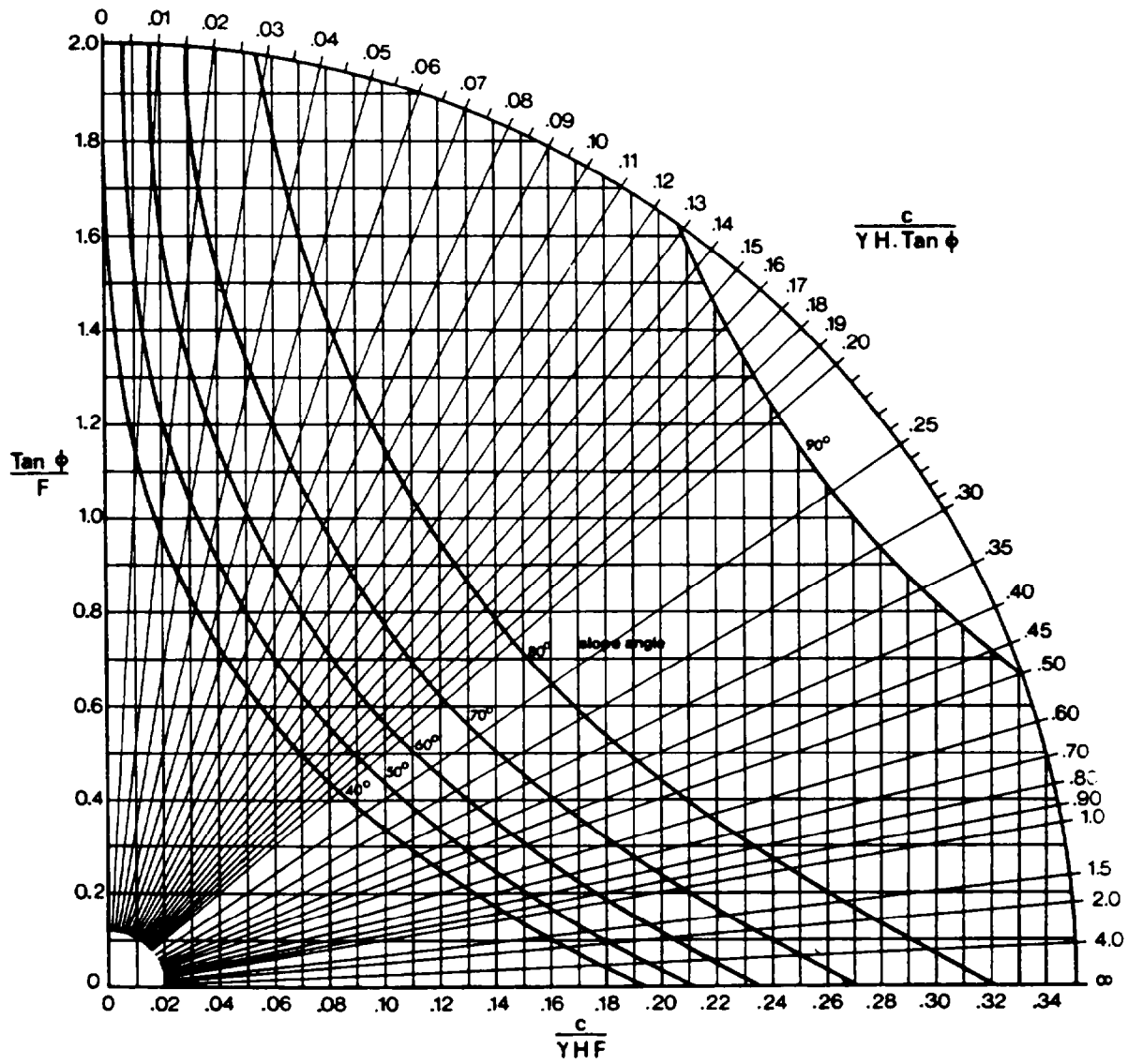
CIRCULAR FAILURE CHART NUMBER 2



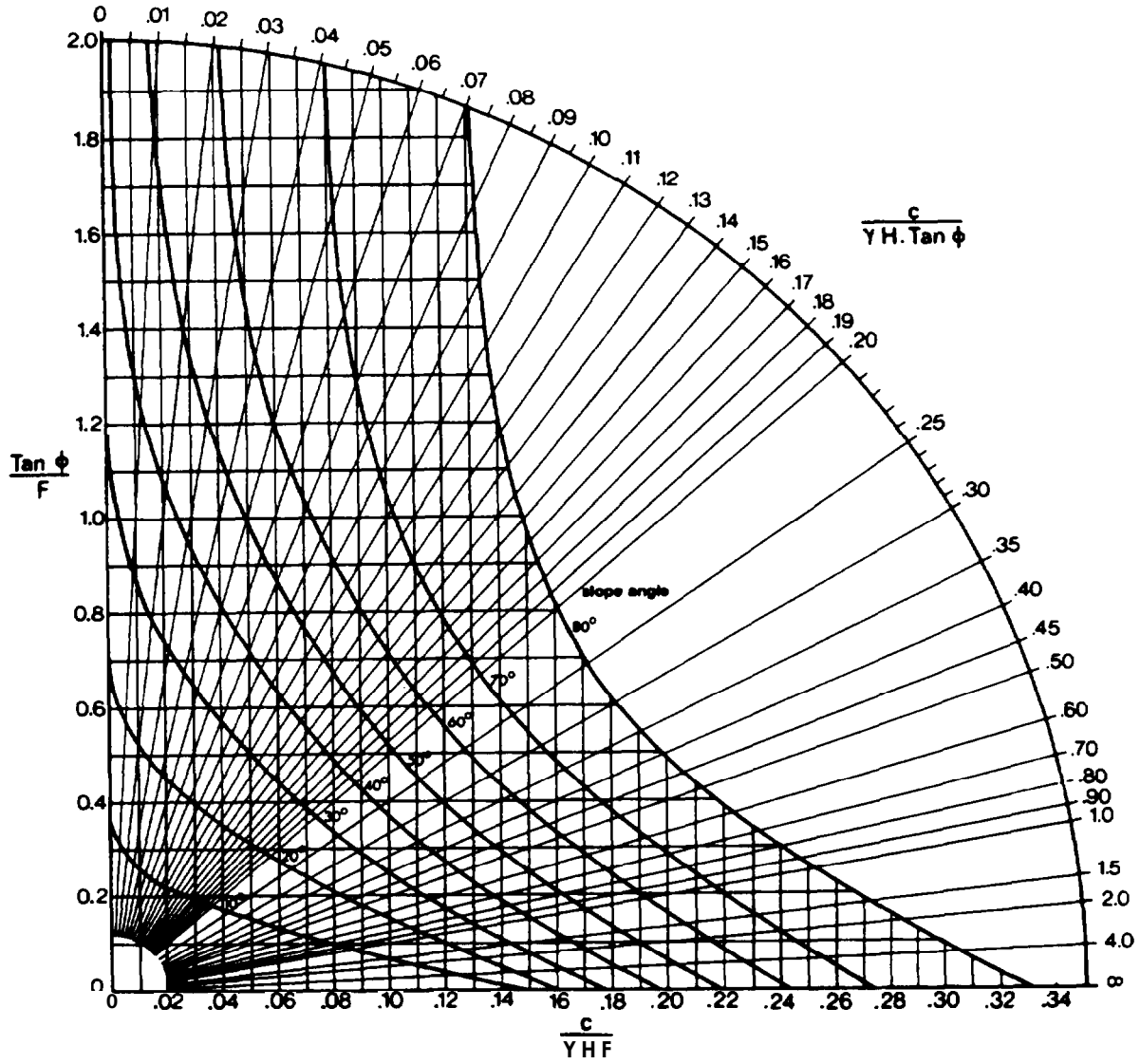
CIRCULAR FAILURE CHART NUMBER 3



CIRCULAR FAILURE CHART NUMBER 4



CIRCULAR FAILURE CHART NUMBER 5



Location of critical failure circle and tension crack

During the production of the circular failure charts, presented on the previous pages, the locations of both the critical failure circle and the critical tension crack for limiting equilibrium ($F = 1$) were determined for each slope analyzed. These locations are presented, in the form of charts, in Figures 9.5a and 9.5b.

It was found that, once groundwater is present in the slope, the locations of the critical circle and the tension crack are not particularly sensitive to the position of the phreatic surface and hence only one case, that for chart No. 3, has been plotted. It will be noted that the location of the critical circle centre given in Figure 9.5b differs significantly from that for the drained slope plotted in Figure 9.5a.

These charts are useful for the construction of drawings of potential slides and also for estimating the friction angle when back-analyzing existing circular slides. They also provide a start for a more sophisticated circular failure analysis in which the location of the circular failure surface having the lowest factor of safety is found by iterative methods.

As an example of the application of these charts, consider the case of a slope having a face angle of 30° in a drained soil with a friction angle of 20° . Figure 9.5a shows that the critical failure circle centre is located at $X = 0.2H$ and $Y = 1.85H$ and that the critical tension crack is at a distance $b = 0.1H$ behind the crest of the slope. These dimensions are shown in Figure 9.6 below.

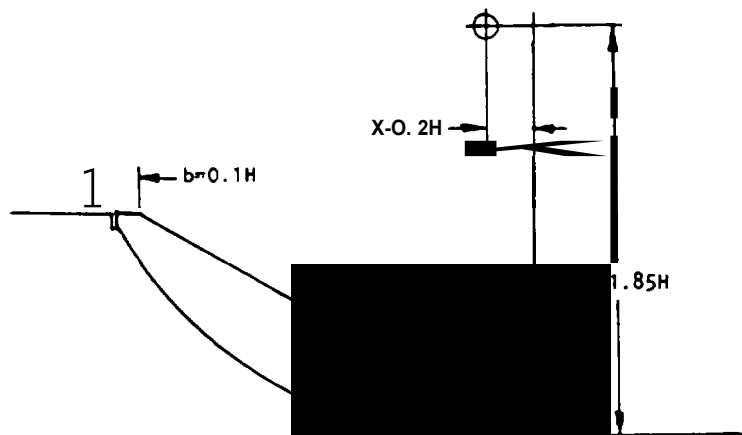
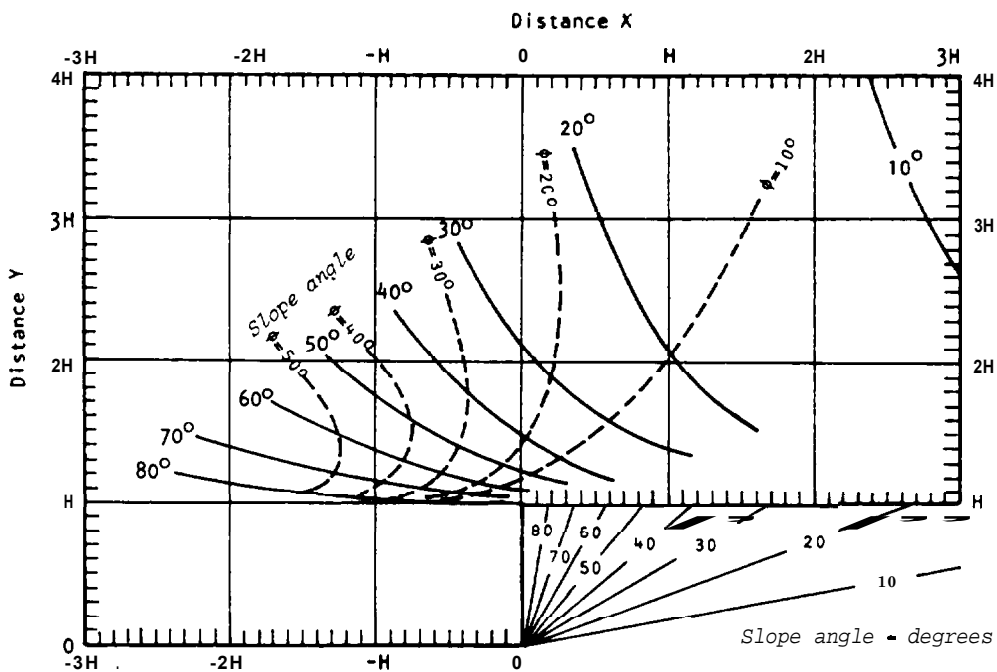
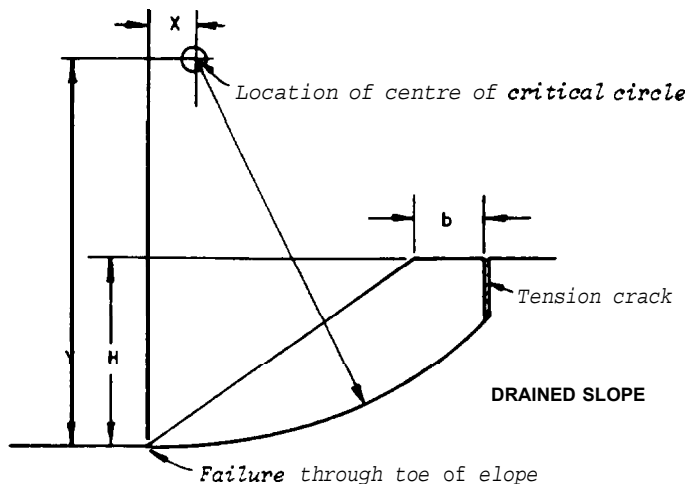
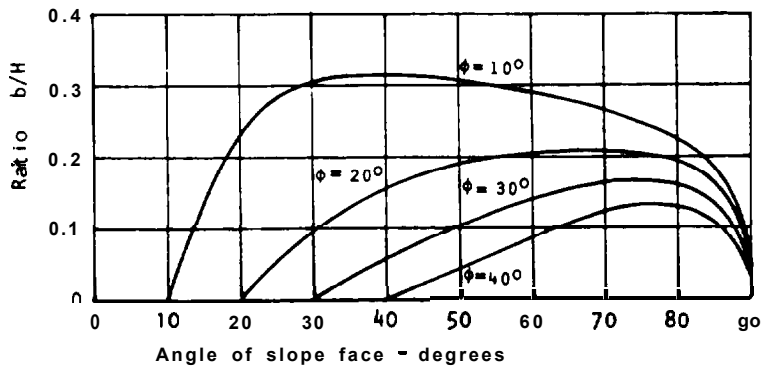


Figure 9.6 : Location of critical failure surface and critical tension crack for a 30° slope in drained soil with a friction angle of 20° .



Location of centre of critical circle for failure through toe



Location of critical tension crack position

Figure 9.5a : Location of critical failure surface and critical tension crack for drained slopes.

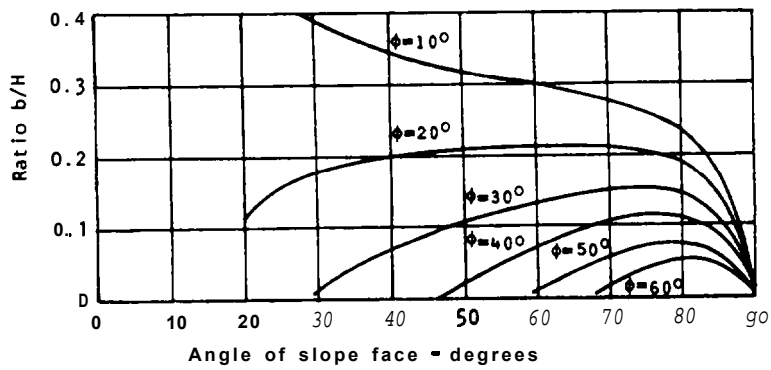
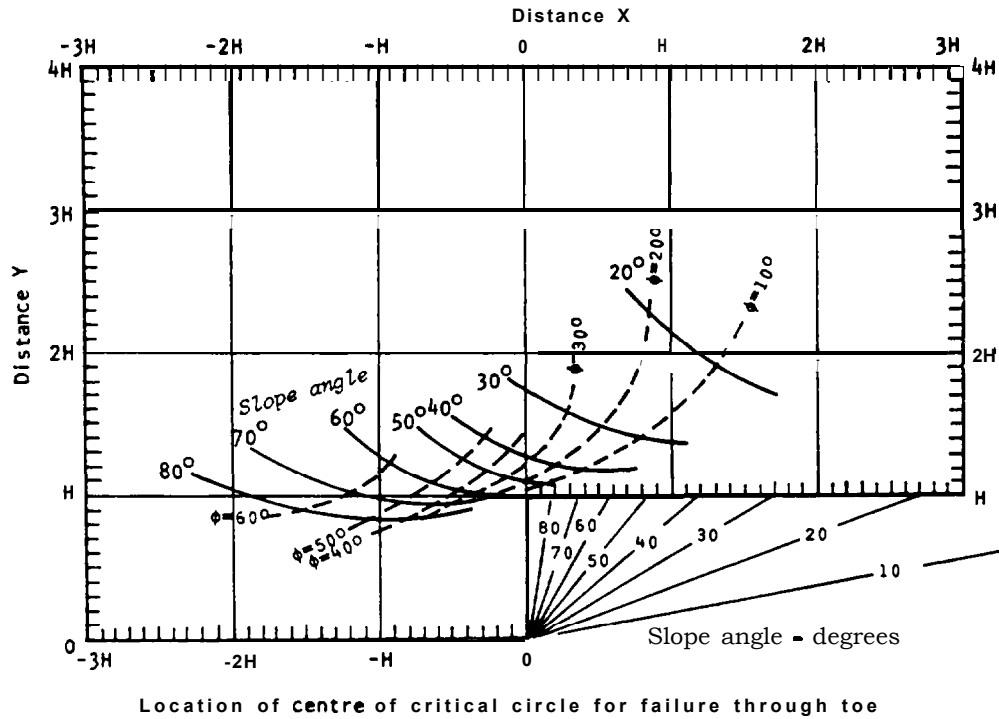
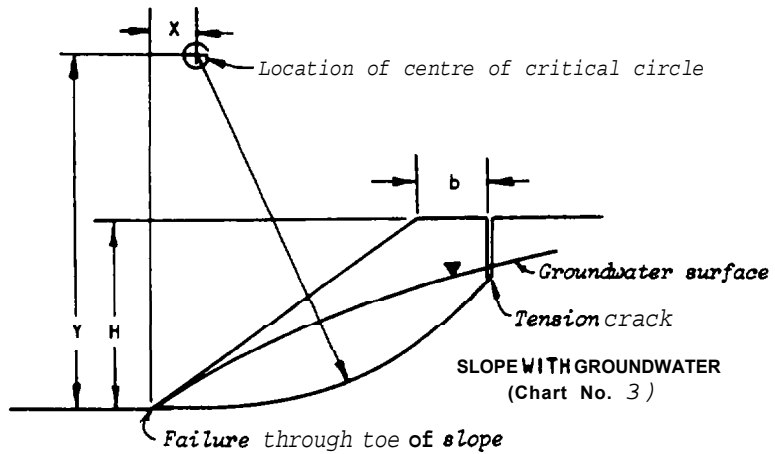


Figure 9.5b : Location of critical failure surface and critical **tension crack** for slopes with groundwater present.

Practical example number 1

China clay pit slope

Ley (1953) has investigated the stability of a China clay pit slope which was considered to be potentially unstable. The slope profile is illustrated in Figure 9.7 below and the input data used for the analysis is included in this figure. The material, a heavily kaolinized granite, was carefully tested by Ley and the friction angle and cohesive strength are considered reliable for this particular slope.

Two piezometers in the slope and a known water source some distance behind the slope enabled Ley to postulate the phreatic surface shown in Figure 9.7. The chart which corresponds most closely to these groundwater conditions is considered to be chart number 2.

From the information given in Figure 9.7, the value of the ratio $c/H \cdot \tan \phi = 0.0056$ and the corresponding value of $\tan \phi/F$, from chart number 2, is 0.76. Hence, the factor of safety of the slope is 1.01.

Ley also carried out a number of trial calculations using Janbu's method (238) and, for the critical slip circle shown in Figure 9.7, found a factor of safety of 1.03.

These factors of safety indicated that the stability of the slope was inadequate under the assumed conditions and steps were taken to deal with the problem.

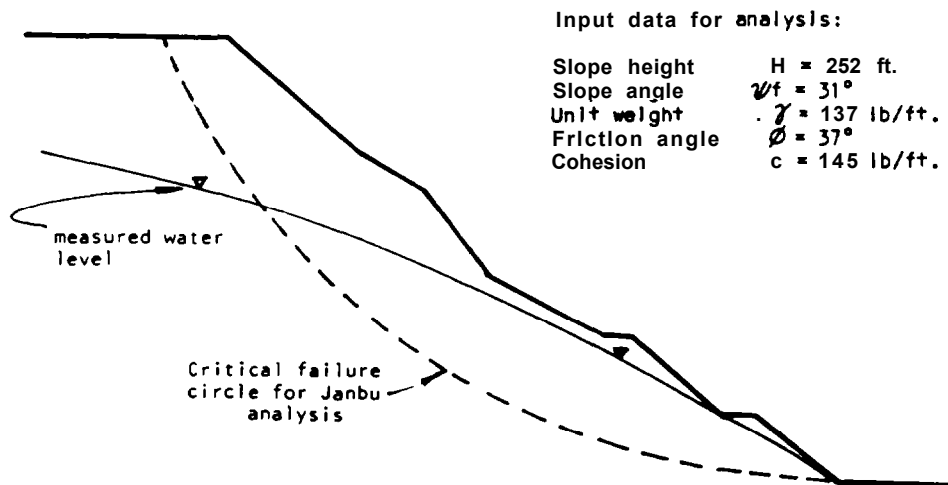


Figure 9.7 : Slope profile of China clay pit slope considered in example number 1.

Practical example number 2

Projected highway slope

A highway plan calls for a slope on one side of the highway to have an angle of 42° . The total height of the slope will be 200 ft. when completed and it is required to check whether the slope will be stable. A site visit enables the slope engineer to assess that the slope is in weathered and altered material and that failure, if it occurs, will be of a circular type. Insufficient time is available for groundwater levels to be accurately established or for shear tests to be carried out. The stability analysis is carried out as follows:

For the condition of limiting equilibrium, $F = 1$ and $\tan\phi/F = \tan\phi$. For a range of friction angles, the values of $\tan\phi$ are used to find the values of $c/H \cdot \tan\phi$, for 42° , by reversing the procedure outlined in Figure 9.4. The value of the cohesion c which is mobilized at failure, for a given friction angle, can then be calculated. This analysis is carried out for dry slopes, using chart number 1, and for saturated slopes, using chart number 5. The resulting range of friction angles and cohesive strengths which would be mobilized at failure are plotted in Figure 9.6.

The shaded circle included in Figure 9.8 indicates the range of shear strengths which are considered probable for the material under consideration, based upon the data presented in Figure 5.17 on page 5.32. It is clear from this figure that the available shear strength may not be adequate to maintain stability in this slope, particularly when the slope is saturated. Consequently, the slope engineer would have to recommend that, either the slope should be flattened or, that investigations into the groundwater conditions and material properties should be undertaken in order to establish whether the analysis presented in Figure 9.8 is too pessimistic.

The effect of flattening the slope can be checked very quickly by finding the value of $c/H \cdot \tan\phi$ for a flatter slope, say 30° , in the same way as it was found for the 42° slope. The dashed line in Figure 9.8 indicates the shear strength which would be mobilized in a dry slope with a face angle of 30° .

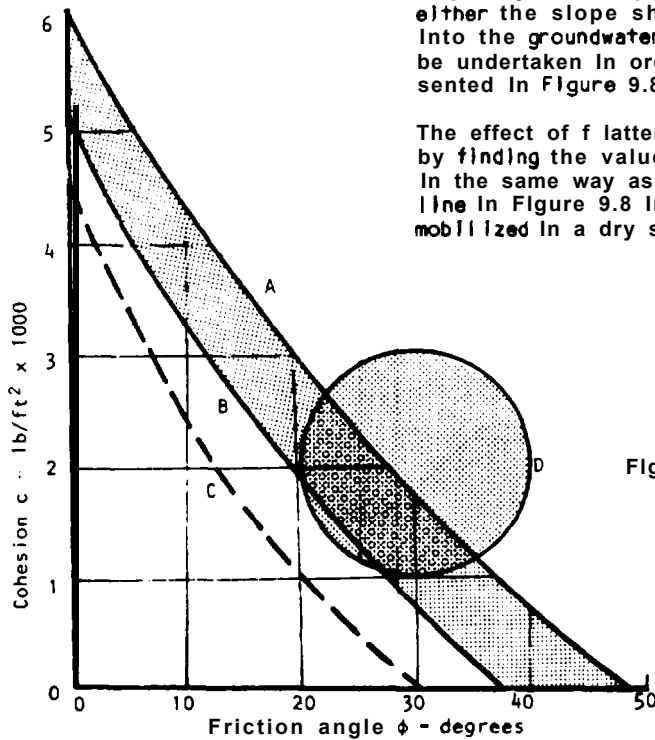


Figure 9.8: Comparison between shear strength mobilized and shear strength available for slope considered in example number 2.

- A - saturated 42° slope.
- B - dry 42° slope.
- C - dry 30° slope.
- D - probable shear strength range for material in which slope is cut.

Practical example number 3

Stability of waste dumps

As a result of the catastrophic slide in colliery waste material at Aberfan in Wales on October 22nd 1966, attention was focused on the potential danger associated with large dumps of waste material from mining operations(239). Since 1966, a number of excellent papers and handbooks dealing with waste dump stability and with the disposal of finely ground waste have become available(241-243) and the authors do not feel that a detailed discussion on this subject would be justified in this book. The purpose of this example is to illustrate the application of the design charts for circular failure, presented earlier in this chapter, to waste dump stability problems.

McKechnie Thapson and Rodin(240) have shown that the relationship between shear strength and normal stress for colliery waste material is usually non-linear as shown in Figure 9.9. In view of the discussion on shear strength presented in chapter 5, this finding is not particularly surprising and the authors suspect that most waste materials exhibit this non-linearity to a greater or lesser degree. Consequently, the methods used in this example, although applied specifically to colliery waste, are believed to be equally applicable to most rock waste dumps.

In order to apply the circular failure charts presented earlier in this chapter to the failure of a material which exhibits non-linear failure characteristics, it is necessary to determine a number of instantaneous friction angles and cohesive strengths for different effective normal stress levels. This is done by drawing a series of tangents to the Mohr envelope, each tangent touching the envelope at the normal stress level at which c_i and ϕ_i are to be found.

In the case of the failure curve for colliery waste, shown in Figure 9.9, the instantaneous cohesion and the friction angles given by the three tangents are as follows:

Tangent number	Cohesion kN/m	Friction angle degrees
1	0	38
2	20	26
3	40	22

The relationship between slope height and slope angle for the condition of limiting equilibrium, $F = 1$, will be investigated for a dry dump (using chart No. 1) and for a dump with some groundwater flow (using chart No. 3).

Tangent number 1

Since the cohesion intercept is zero for this tangent, the value of the dimensionless ratio $c/H \cdot \tan \phi = 0$ and hence, the slope angle at which the face would repose is given by the slope angle corresponding to the value of $\tan 38^\circ = 0.78$ on the $\tan \phi/F$ axis (noting that $F = 1$). From chart No. 1, this intercept is $38'$ and for chart No. 3 it is approximately $25'$.

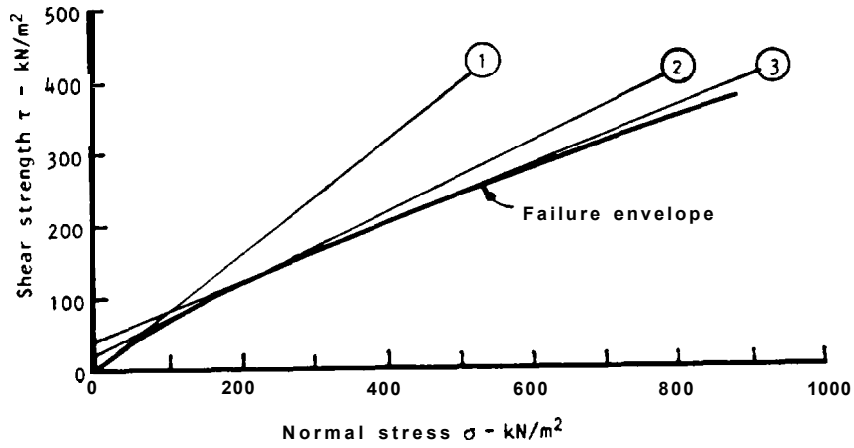


Figure 9.9 : Shear strength of typical colliery waste material.

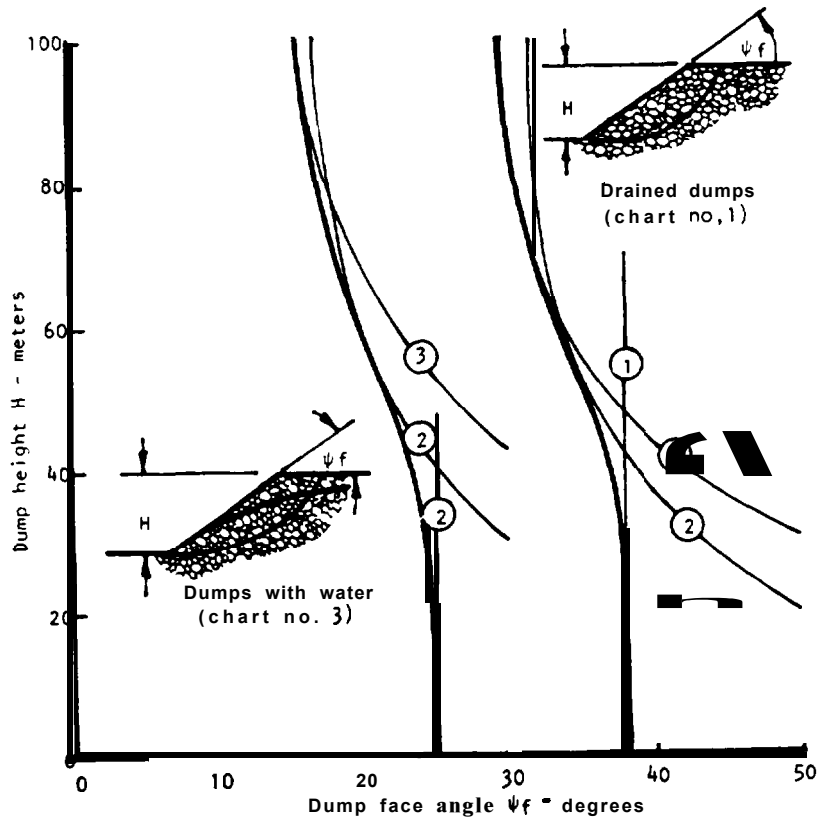


Figure 9.10 : Relationship between slope height and slope angle for a typical colliery waste dump with different water conditions.

Note that, for zero cohesion, the dump face angle would be independent of the slope height. It is normally assumed that the angle of repose of a waste dump is independent of the height of the dump and is equal to the angle of friction of the material. Figure 9.10 shows that this assumption is only correct for a dry slope of limited height. Any build-up of water pressure within the dump causes a serious reduction in the stable face angle and, once the normal stress across the potential failure surface becomes high enough for the next tangent to become operative, the high initial friction angle no longer applies and the dump face assumes a flatter angle.

Tangent number 2

For $c = 20 \text{ kN/m}^2$, $\gamma = 18 \text{ kN/m}^3$ and $\phi = 26^\circ$,

$$\frac{c}{\gamma H \cdot \tan \phi} = \frac{20}{18 \cdot \tan 26^\circ \cdot H} = \frac{2.28}{H}$$

$$\text{and } \tan \phi / F = \tan 26^\circ = 0.49$$

Hence	H meters	$\frac{c}{\gamma H \cdot \tan \phi}$	Slope angle°	
			Chart 1	Chart 3
	20	0.114	50	39
	40	0.057	39	25
	60	0.038	34	20
	80	0.029	32	18
	100	0.023	31	17

Plotting these values on Figure 9.10 gives the curves numbered 2 for the drained and the wet dumps.

Tangent number 3

$c = 40 \text{ kN/m}^2$, $\gamma = 18 \text{ kN/m}^3$ and $\phi = 22^\circ$, hence
 $\frac{c}{\gamma H \cdot \tan \phi} = 5.5/H$ and $\tan \phi / F = 0.4$

H meters	$\frac{c}{\gamma H \cdot \tan \phi}$	Slope angle°	
		Chart 1	Chart 3
20	0.215	61	56
40	0.138	34	31
60	0.092	31	22
80	0.069		18
100	0.055	30	16

The relationships between dump face angle and dump height, for both drained and wet dumps, are given by the envelopes of the curves derived from tangents 1, 2 and 3. These envelopes, shown in Figure 9.10, illustrate the danger in continuing to increase the height of a dump on the assumption that it will remain stable at an angle of repose equal to the friction angle. The dangers associated with poor dump drainage are also evident in this figure.

The reader who attempts this type of analysis for himself, and it is strongly recommended that he should, will find that the slope height versus slope angle relationship is extremely sensitive to the shape of the shear failure curve. This emphasizes the need for reliable in situ shear test methods such as those

described by McKechnie Thompson and Rodin(240) and Schultze and Horn(244) to be further developed for application to waste dump problems.

Bishop's and Janbu's methods of slices

The circular failure charts presented earlier in this chapter are based upon the assumptions that the material forming the slope has uniform properties throughout the slope and that failure occurs along a circular failure path passing through the toe of the slope. When these conditions are not satisfied it is necessary to use one of the methods of slices published by Bishop(213), Janbu(217), Nonveiller(224), Spencer(228), Morgenstern and Price(222) or others. With the wide availability of programmable calculators and computers, the iterative procedure required in obtaining a factor of safety by one of these methods of slices is no longer as tedious as it once was and there is no excuse for not using one of these methods if it is appropriate for the problem under consideration.

The slope and failure surface geometries and the equations for the determination of the factor of safety by the Bishop simplified method of slices(213) and the Janbu modified method of slices(217) are given in Figures 9.11 and 9.12 respectively. Bishop's method assumes a circular failure surface while that of Janbu assumes that the failure surface can be of a general shape. As pointed out by Nonveiller(224), Janbu's method gives reasonable factors of safety when applied to shallow slip surfaces (which are typical in rocks with an angle of friction in excess of 30°) but it is seriously in error and should not be used for deep slip surfaces in materials with low friction angles.

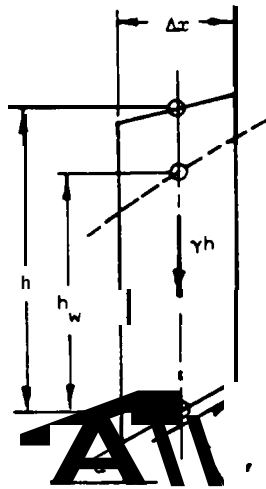
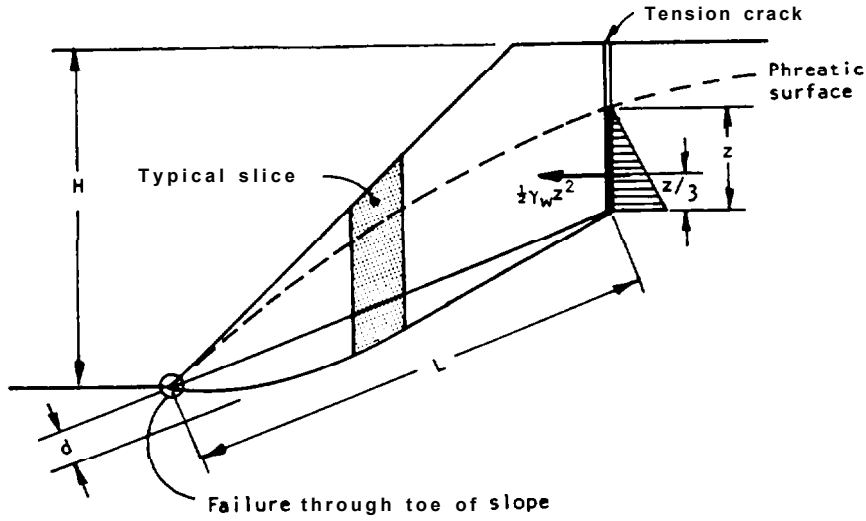
The procedures for using Bishop's and Janbu's methods of slices are very similar and it is convenient to discuss them together. Note that the form of the equations given in Figures 9.11 and 9.12 has been designed to facilitate programming on a calculator such as a Hewlett-Packard 67.

Step 1: Slope and failure surface geometry

The geometry of the slope is defined by the actual or the designed profile as seen in a vertical section through the slope. This profile should be reproduced as accurately as possible on a drawing to a conveniently large scale. In the case of a circular failure, the charts given in figures 9.5a and b can be used to estimate the center of the circle with the lowest factor of safety. In the Janbu analysis, the failure surface may be defined by known structural features or weak zones within the rock or soil mass or it may be estimated in the same way as that for the Bishop analysis. In either case, the failure surface assumed for the first analysis may not give the lowest factor of safety and the user should be prepared to repeat the entire calculation a number of times in order to find the failure surface with the lowest factor of safety.

Step 2: Slice parameters

The sliding mass assumed in slice 1 is divided into a number of slices. Generally, a minimum of five slices should be used for very simple cases. For complex slope profiles or a large number of different materials in the rock or



Note : Angle α is negative when sliding is uphill.

Factor of Safety :

$$F = \frac{f_0 \sum \frac{X}{(1 + Y/F)}}{\sum Z + Q}$$

where

$$X = (c' + (\gamma h - \gamma_w h_w) \tan \phi') (1 + \tan^2 \alpha) \Delta x$$

$$Y = \tan \alpha \tan \phi'$$

$$Z = \gamma h \Delta x \tan \alpha$$

$$Q = \frac{1}{2} \gamma_w z^2$$

Approximate correction factor f_0

$$f_0 = 1 + K \left(\frac{d}{L} - 1.4 \left(\frac{d}{L} \right)^2 \right)$$

for $c' = 0$; $K = 0.31$,

$c' > 0, \phi' > 0$; $K = 0.50$

Figure 9.12 : Janbu's modified method of slices for the analysis of non-circular failure in slopes cut into materials in which failure is defined by the Mohr-Coulomb failure criterion.

soil mass, a larger number of slices may be required in order adequately to define the problem. The parameters which have to be defined for each slice are the angle α of the base of the slice, the vertical stress on the base of the slice given by the product of the vertical height h and the unit weight γ of the rock or soil, the uplift water pressure given by the product of the height h_w to the phreatic surface and the unit weight of water and the width of the slice Δx .

Step 3: Shear strength parameters

The shear strength acting on the base of each slice is required for the stability calculation. In the case of a uniform material in which the failure criterion is assumed to be that of Mohr-Coulomb (equation (10) on page 5.2), the shear strength parameters c' and ϕ' will be the same on the base of each slice. When the slope is cut into a rock or soil mass made up of a number of materials, the shear strength parameters for each slice must be chosen according to the material in which it lies. When the shear strengths of the materials forming the slope are defined by non-linear failure criteria such as that given by equation (30) on page 5.25 it is necessary to determine an instantaneous cohesion c_i and an instantaneous friction angle ϕ_i for each slice. This determination requires a knowledge of the effective normal stress acting on the base of each slice and this problem will be discussed later in this chapter.

Step 4: Factor of safety iteration

When the slice parameters and the shear strength parameters have been defined, the values of X , Y , and Z are calculated for each slice. The water force Q is added to ΣZ , the sum of the components of the weight of each slice acting parallel to the failure surface. An initial estimate of $F \approx 1.00$ for the factor of safety is used in the solution of the factor of safety equations given in Figures 9.11 and 9.12. If the difference between the calculated and the assumed factors of safety is greater than 0.001, the calculated factor of safety is used as a second estimate of F for a new factor of safety calculation. This process is repeated until the difference between successive factors of safety is less than 0.001. For both the Bishop and the Janbu methods, approximately 7 iteration cycles will be required to achieve this result for most slope and failure surface geometries.

Step 5: Conditions and corrections

Figure 9.11 lists two conditions which must be satisfied for each slice in the Bishop analysis. The first condition ensures that the effective normal stress on the base of each slice is always positive. If this condition is not met for any slice, the inclusion of a tension crack into the analysis should be considered. If it is impossible to satisfy this condition by readjustment on the groundwater conditions or the introduction of a tension crack, the analysis as presented in Figure 9.11 should be abandoned and a more elaborate form of analysis, to be described later, adopted.

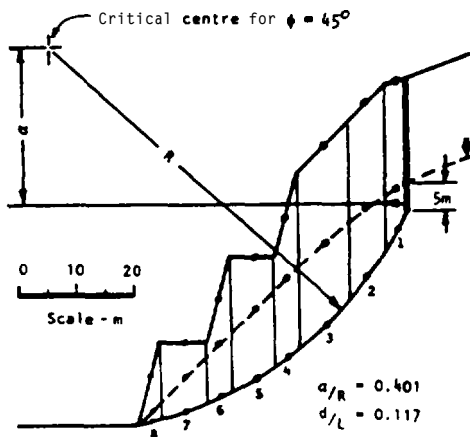
Condition 2 in Figure 9.11 was suggested by Whitman and Bailey(233) and it ensures that the analysis is not invalidated by conditions which can sometimes occur near the toe of a slope in which a deep failure surface has been assumed. If this condition is not satisfied by all slices, the slice dimensions should be changed and, if this fails to resolve the problem, the analysis should be abandoned.

Figure 9.12 gives a correction factor which is used in calculating the factor of safety by means of the Janbu method. This factor allows for interslice forces resulting from the shape of the failure surface assumed in the Janbu analysis. The equation for f_0 given in Figure 9.12 has been derived by the authors from the curves published in Janbu(217).

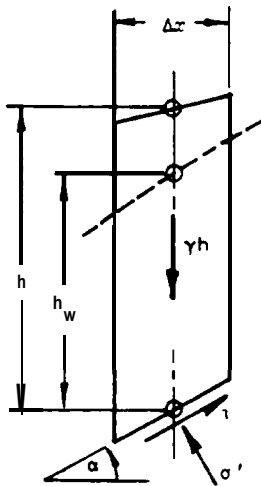
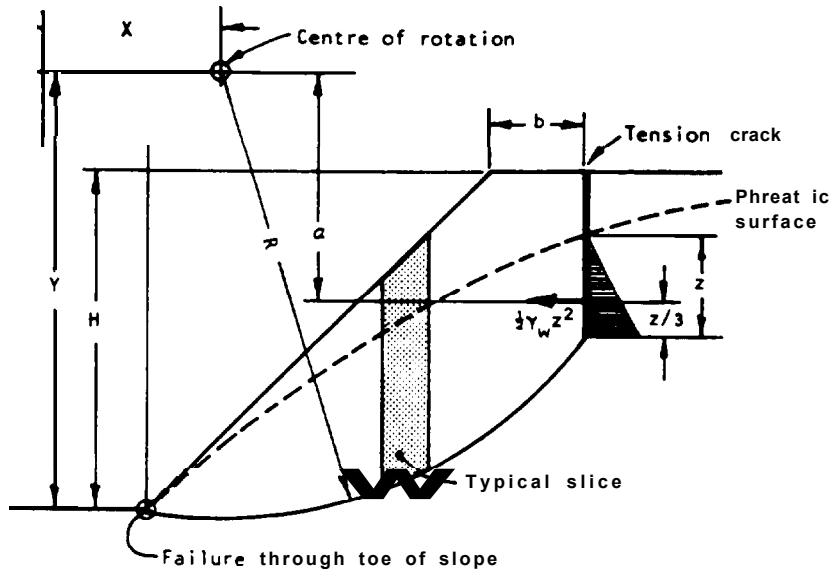
Use of non-linear failure criterion

When the material in which the slope is cut obeys the non-linear failure criterion defined by equation(30) on page 5.25 the Bishop simplified method of slices as outlined in figure 9.13 can be used to calculate the factor of safety. The following procedure is used, once the slice parameters have been defined as described earlier for the Bishop and Janbu analyses:

- 1) Calculate the effective normal stress σ' acting on the base of each slice by means of the Fel enius equation given in Figure 9.13.
- 2) Using this value of σ' , calculate $\tan \phi_i'$ and c_i' from the equations given in Figure 9.13.
- 3) Substitute these values of $\tan \phi_i'$ and c_i' into the factor of safety equation in order to obtain the first estimate of the factor of safety.
- 4) Use this estimate of F to calculate a new value of σ' on the base of each slice, using the Bishop equation given in Figure 9.13.
- 5) On the basis of this new value of σ' , calculate new values for $\tan \phi_i'$ and c_i' .
- 6) Check that conditions 1 and 2 (Figure 9.13) are satisfied for each slice.
- 7) Calculate a new factor of safety for the new values of $\tan \phi_i'$ and c_i' .
- 8) If the difference between the first and second factors of safety is greater than 0.001, return to step 4 and repeat the analysis, using the second factor of safety as input. Repeat this procedure until the difference between successive factors of safety is less than 0.001.



Generally, about ten iterations will be required to achieve the required accuracy in the calculated factor of safety.



Note : Angle α is negative when sliding is uphill.

Factor of Safety :

$$F = \frac{\sum (c_i' + \sigma' \tan \phi_i') \cos \alpha}{\sum \gamma h \Delta x \sin \alpha + \frac{1}{2} \gamma_w z^2 \cdot \frac{\Delta x}{R}}$$

where

$$\sigma' = \gamma h \cos^2 \alpha - \gamma_w h_w \quad (\text{Fellenius solution})$$

and

$$\alpha' = \frac{\gamma h - \gamma_w h_w - \frac{c_i' \tan \alpha}{F}}{1 + \frac{\tan \phi_i' \tan \alpha}{F}} \quad (\text{Bishop solution})$$

The instantaneous friction angle ϕ_i' and the instantaneous cohesion c_i' are given by :

$$\tan \phi_i' = AB (\sigma' / \sigma_c - T)^{B-1}$$

$$c_i' = A \sigma_c (\sigma' / \sigma_c - T)^B - \sigma' \tan \phi_i'$$

The conditions which must be satisfied for arch slice are :

1) $\sigma' > 0$, where σ' is calculated by Bishop's method

2) $\cos \alpha (1 + \tan \alpha \tan \phi_i' / F) > 0.2$

Figure 9.13 : Bishop's simplified method of slices for the analysis of circular failure in slopes cut into materials in which failure is defined by the non-linear failure criterion given in equation (30) on page 5.25.

Example of the use of Bishop's and Janbu's methods of analysis

A slope is to be excavated in a highly weathered granitic rock mass. The slope, illustrated in the margin drawing on page 9.26, is to consist of three 15 m high benches with two 8 m wide berms. The bench faces are inclined at 75° to the horizontal and the top of the slope is cut at 45° from the top of the third bench to the natural ground surface.

A classification of the rock mass and the use of the resulting Index to estimate the material properties from Table IV on page 5.26 gives the following values for the constants defined in equation (30) on page 5.25:

$$A = 0.203, B = 0.686 \text{ and } T = -0.00008.$$

The uniaxial compressive strength σ_c of the intact rock pieces is estimated at 150 MPa from point load testing. The unit weight of the rock mass is assumed to be $\gamma = 0.025 \text{ MN/m}^3$ and the unit weight of water $\gamma_w = 0.010 \text{ MN/m}^3$.

In order to estimate the position of the critical failure surface and to carry out a Bishop and Janbu analysis, a tangent to the curved Mohr envelope is drawn at a normal stress level estimated from the slope geometry. This tangent is defined by a friction angle $\phi = 45^\circ$ and a cohesive strength $c = 0.14 \text{ MPa}$.

Slice parameters for all cases					Mohr-Coulomb values for Bishop & Janbu analyses		Non-linear failure criterion values for Bishop analysis (8th iteration)		
Slice number	Angle α degrees	Vertical stress γh MPa	Uplift $\gamma_w h_w$ MPa	Slice width Δx m	Friction angle ϕ' degs.	Cohesion c' MPa	Normal stress σ'_i MPa	Inst. Frict. ϕ'_i °	Inst. Cohesion c'_i MPa
1	62	0.663	0.075	4.0	45	0.14	0.176	48.6	0.111
2	55	0.769	0.125	6.5	45	0.14	0.251	45.6	0.135
3	44	0.794	0.150	8.5	45	0.14	0.327	43.3	0.158
4	36	0.625	0.140	4.0	45				
5	31	0.544	0.125	8.0	45	0.14 0.14	0.273 0.253	44.9 45.6	0.142 0.136
6	25	0.438	0.095	4.0	45	0.14	0.224	46.6	0.127
7	20	0.313	0.060	8.0	45	0.14	0.174	48.7	0.111
8	12	0.188	0.002	4.0	45	0.14	0.145	50.2	0.101

Using the slice parameters and shear strength values tabulated above, the factor of safety for the slope under consideration have been calculated by three methods. The successive factor of safety estimates are:

Bishop simplified method of slices for Mohr-Coulomb failure

1.000, 1.237, 1.353, 1.402, 1.421, 1.428, 1.430, 1.431

Janbu modified method of slices for Mohr-Coulomb failure

1.000, 1.207, 1.315, 1.364, 1.385, 1.393, 1.397, 1.398, 1.399

Bishop simplified method of slices for non-linear failure

1.271, 1.353, 1.396, 1.413, 1.420, 1.422, 1.423, 1.423

Of these three analyses, the last which utilizes the non-linear failure criterion, is regarded as correct for this particular application.

Chapter 9 references

210. COLDER, H.Q. The stability of natural and man-made slopes in soil and rock. Cootechnical Practice for *Stability in Open Pit Mining*. Editors Brawner, C.O. and Milligan, V. AIME, New York, 1972. pages 79-85.
211. TERZAGHI, K. *Theoretical Soil Mechanics*. Wiley, New York, 1943.
212. LAMBE, W.T. and WHITMAN, R.V. *Soil Mechanics*. Wiley, New York, 1969, 553 pages.
213. BISHOP, A.W. The use of the slip circle in the stability analysis of earth slopes. *Geotechnique*. Vol.5, 1955. pages 7-17.
214. BISHOP, A.W. and HORGENSTERN, N. Stability coefficients for earth slopes. *Geotechnique*. Vol.10, 1960. pages 29-150.
215. FELLENIUS, W. Calculation of the stability of earth dams. *Trans. 2nd Congress on Large Dams*. Washington, Vol.4, 1936. page 445.
216. FROMLICH, O.K. General theory of the stability of slopes. *Geotechnique*. Vol.5, 1955. pages 37-47.
217. JANBU, N. Application of composite slip circles for stability analysis. *Proc. European Conference a Stability of Earth Slopes*. Stockholm, Vol.3, 1954, pages 43-49.
218. JANBU, N. Stability analysis of slopes with dimensionless parameters. *D.Sc. Thesis. Harvard Soil Mechanics Series. No.46, 1954. 81 pages.*
219. LOWE, J. Stability analysis of embankments. *J. Soil Mech. Foundation Div. ASCE. Vol.93, No.SM4, 1967, pages 286-299.*
220. HEYERHOF, C.G. The mechanism of flow slides in cohesive soils. *Geotechnique*. Vol.7, 1961, pages 21-31.
221. MENCL, V. The influence of the stiffness of a sliding mass on the stability of slopes. *Rock Mechanics and Engineering Geology*. Vol.4, 1966. pages 127-131.
222. HORGENSTERN, N.R. and PRICE, V.E. The analysis of the stability of general slip surfaces. *Geotechnique*. Vol.15, 1965. pages 79-93.
223. HORGENSTERN, N.R. Stability charts for earth slopes during rapid drawdown. *Geotechnique*. Vol.13, 1963. pages 121-131.
224. NONVEILLER, E. The stability analysis of slopes with a slip surface of general shape. *Proc. 6th Intl. Conf. Soil Mech. Foundation Engg, Montreal. Vol.2, 1965, page 522.*
225. PECK, R.B. Stability of natural slopes. *Proc. ASCE. Vol.93, No.SM 4. 1967, pages 403-417.*

226. RODRIGUEZ, A. Analysis of slope stability. *Proc. 5th Intl. Conf. Soil Mech. Foundation Engg.* Paris. 1961, Vol.2, page 709.
227. SPENCER, E. Circular and logarithmic spiral slip surfaces. *J. Soil Mech. Foundation Div. ASCE.* Vol.95. No.SM 1, 1969, pages 227-234.
228. SPENCER, E. A method of analysis of the stability of embankments assuming parallel inter-slice forces. *Ceotechnique.* Vol.17, 1967, pages 11-26.
229. TAYLOR, D.W. Stability of earth slopes. *J. Boston Soc. Civil Engineers.* Vol.24, 1937, page 197.
230. TERZAGHI, K. Critical height and factor of safety of slopes against sliding. *Proc. Intl. Conf. Soil Mechanics.* Cambridge, Mass. 1936, Vol.1, pages 156-161.
231. VERGHESE, P.C. Investigations of a new procedure for analysing the stability of slopes. *M.Sc. Thesis,* Harvard University. 1949.
232. VISHNER, D. Use of moment planimeter for analysis of slope stability. (in German). *Schwerz. Bauztg.* Vol.81, No. 12, 1963, pages 183-187.
233. WHITMAN, R.V. and BAILEY, W.A. The use of computers for slope stability analysis. *J. Soil Mech. Foundation Engg., ASCE.* Vol.93, No.SM 4, 1967. pages 475-498.
234. SKEHPTDN. A.W. The $\phi = 0$ analysis for stability and its theoretical basis. *Proc. 2nd Intl. Conf. Soil Mech. Foundation Engg.* Rotterdam. Vol.1, 1948, page 72.
235. BISHOP, A.W. and BJERRUM. L. The relevance of the triaxial test to the solution of stability problems. *Proc. ASCE Conf. on shear strength of cohesive soils.* Boulder, Colorado. 1960, pages 437-501.
236. CASAGRANDE, L. Nihierungsverfahren zur Ermittlung der Sickerung in geschütteten Dämmen auf unterchlässiger Sohle, *Die Bautechnik.* Heft 15, 1934.
237. HAN. C. The technique for obtaining equipotential lines of groundwater flow in slopes using electrically conducting paper. *M.Sc. Thesis,* London University (Imperial College), 1972.
238. JANBU, N., BJERRUM. L and KJAERNSLI, B. Soil mechanics applied to some engineering problems. (in Norwegian with an English summary). *Norwegian Ceotechnical Inst. Publ. 16,* 1956.
239. Report of the tribunal appointed to enquire into the disaster at Aberfan on October 21st, 1966. Her Majesty's Stationery Office, London. 1968.
240. MCKECHNIE THOMPSON, G. and RODIN, S. *Colliery spoil tips - after Aberfan.* Inst. Civil Engineers, London. 1972. Paper 7522. 60 pages.

241. NATIONAL COAL BOARD. *Technical handbook on spoil heap8 and lagoons*. National Coal Board Mining Department. London. Final Draft 1970, 233 pages.
242. CHINA CLAY ASSOCIATION. *China Clay industry technical handbook for the disposal of waste materials*. China Clay Association. St. Austell, Cornwall, 1971, 82 pages.
243. CANADIAN DEPARTMENT OF ENERGY, MINES AND RESOURCES. *Tentative deesign guide for mine waste embankments in Canada*. Mining Research Centre, Canadian Department of Energy, Hines and Resources. Ottawa. Final Draft. May, 1971, 185 pages.
244. SCHULTZE, E. and HORN, A. The base friction for horizontally loaded footings in sand and gravel. *Ceotechnique*. Vol.17, 1967, pages 329-347.

Chapter 10: Toppling failure

Introduction

The failure modes discussed in previous Chapters of this book are all related to the sliding of a rock or soil mass along an existing or an induced failure surface. On page 2.13 brief mention was made of a different failure mode - that of toppling. Toppling failure involves rotation of columns or blocks of rock about ~~some~~ fixed base and the simple geometrical conditions governing the toppling of a single block on an inclined surface were defined in Figure 2.5 on page 2.14.

Toppling failures in hard rock slopes have only been described in literature during the past few years. One of the earliest references is by Muller(245) who suggested that block rotation or toppling may have been a contributory factor in the failure of the north face of the Vajont slide. Hofmann(246) carried out a number of model studies under Muller's direction to investigate block rotation. Similar model studies were carried out under the authors' direction at Imperial College by Ashby(247), Soto(248) and Whyte(249) while Cundall(250) made one of the earliest attempts to study the problem numerically. Burman(251), Byrne(252), and Hammett(253), all of the James Cook University of North Queensland in Australia, made significant contributions to the understanding of this problem and to the incorporation of rotational failure modes into computer analysis of rock mass behavior. An excellent descriptive paper on toppling failures in the United Kingdom by de Freitas and Watters(254) is recommended reading and Wylie(255) has discussed examples of toppling associated with railroads. Most of the discussion which follows in this chapter is based on a paper by Goodman and Bray(256) in which a formal mathematical solution to a simple toppling problem is attempted. This solution, which is reproduced here, is believed to represent a basis for the development of methods for designing rock slopes in which toppling is present. Several years of development work will be necessary before these methods can be used with the same degree of confidence as other methods of stability analyses described in this book.

Types of toppling failure

Goodman and Bray have described a number of different types of toppling failures which may be encountered in the field and each of these types is discussed briefly on the following pages.

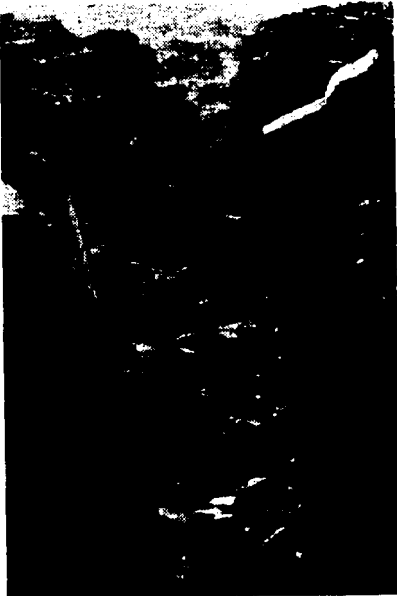
Flexural toppling

The process of flexural toppling is illustrated in Figure 10.1 which shows that continuous columns of rock, which are separated by well developed steeply dipping discontinuities, break in flexure as they bend forward. An example of this type of failure is illustrated in the photograph in the margin on page 2.13 which shows a large flexural topple in the Dinorwic slate quarry in North Wales. The example illustrated in Figure 10.1 is in the Penn Rynn slate quarry in North Wales.

Sliding, undermining or erosion of the toe of the slope allows the toppling process to start and it retrogresses backwards into the rock mass with the formation of deep, wide tension cracks. The lower portion of the slope is covered with dis-



Suggested toppling failure mechanism of the north face of the Vajont slide. After Muller²⁴⁵.



Deep wide tension cracks are associated with toppling failure in hard rock slopes. Photograph by R. E. Goodman.

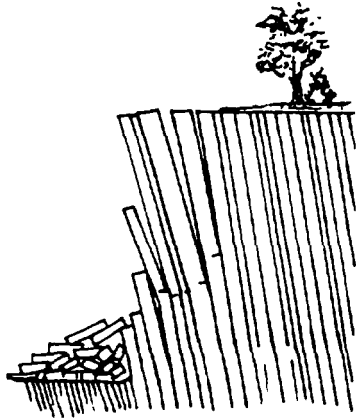


Figure 10.1 : Flexural toppling occurs in hard rock slopes with well developed steeply dipping discontinuities. Photograph by R.E.Goodman.

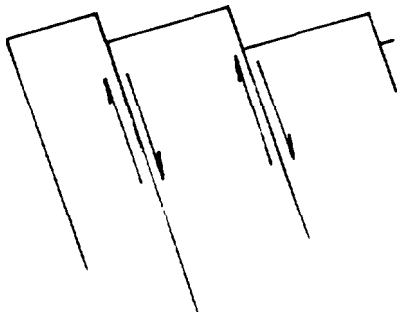
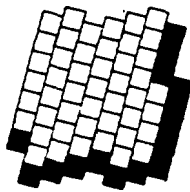


Figure 10.2 : Interlayer sliding between toppling columns results in a series of back facing or obsequent scarps in the upper surface of the rock slope. Photograph by R.E.Goodman.

oriented and disordered blocks and it is sometimes very difficult to recognize a toppling failure from the bottom of the slope.

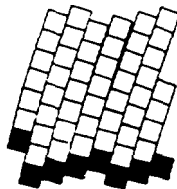
The outward movement of each cantilevered column produces an interlayer slip and a portion of the upper surface of each plane is exposed in a series of back facing or obsequent scarps such as those illustrated in Figure 10.2.

Block toppling



As illustrated in Figure 10.3, block toppling occurs when individual columns of hard rock are divided by widely spaced orthogonal joints. The short columns forming the toe of the slope are pushed forward by the loads from the longer overturning columns behind and this sliding of the toe allows further toppling to develop higher up the slope. The base of the failure is better defined than that in a flexural topple and it generally consists of a stairway rising from one cross joint to the next.

Block-flexure toppling



As shown in Figure 10.4 this type of toppling failure is characterized by pseudo-continuous flexure along long columns which are divided by numerous cross joints. Instead of the flexural failure of continuous columns, resulting in flexural toppling, the toppling of the columns in this case results from accumulated displacements on the cross joints. Because of the large number of small movements in this type of topple, there are fewer tension cracks than in flexural toppling and fewer edge-to-face contacts and voids than in block toppling.

SECONDARY TOPPLING MODES

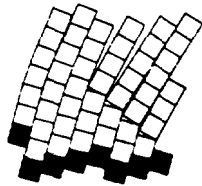
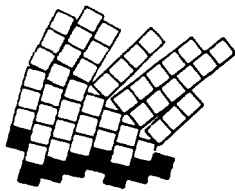


Figure 10.5 illustrates a number of possible secondary toppling mechanisms suggested by Goodman and Bray. In general, these failures are initiated by some undercutting of the toe of the slope, either by natural agencies such as erosion or weathering or by the activities of man. In all cases, the primary failure mode involves sliding or physical breakdown of the rock and toppling is induced in some part of the slope as a result of this primary failure.

ANALYSIS OF TOPPLING FAILURE



Computer generated model of toppling failure by Cundall²⁵⁰. Solid blocks are fixed in space.

Goodman⁽²⁴⁾ has published a detailed discussion on the base friction modelling technique which is an ideal tool for simple physical model studies of toppling phenomena. As illustrated in Figure 10.6, the apparatus consists of a base and frame to hold a pair of wide rollers over which a sanding belt runs. This sanding belt applies a friction force to the underside of the model resting on the belt and, if the base of the model is prevented from moving, the base friction forces will simulate the gravitational loads of the individual blocks which make up the model. Block toppling in models made from cork, plaster, plastic blocks or wooden blocks can be studied by means of this technique and the type of behavior illustrated in the computer generated margin drawing can be simulated very easily.

While this method is ideal for demonstration and teaching purposes, its value as a design tool for rock slope engineering

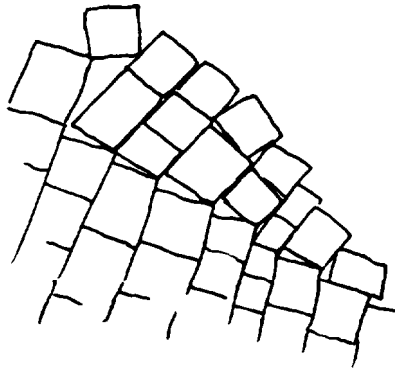


Figure 10.3 : Block toppling can occur in a hard rock mass with widely spaced orthogonal joints.
 Photograph by R.E.Goodman.

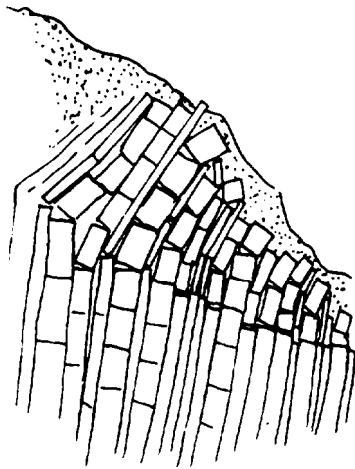


Figure 10.4 : Block flexure toppling is characterised by pseudo-continuous flexure of long columns through accumulated motions along numerous cross joints.
 Photograph by R.E.Goodman.

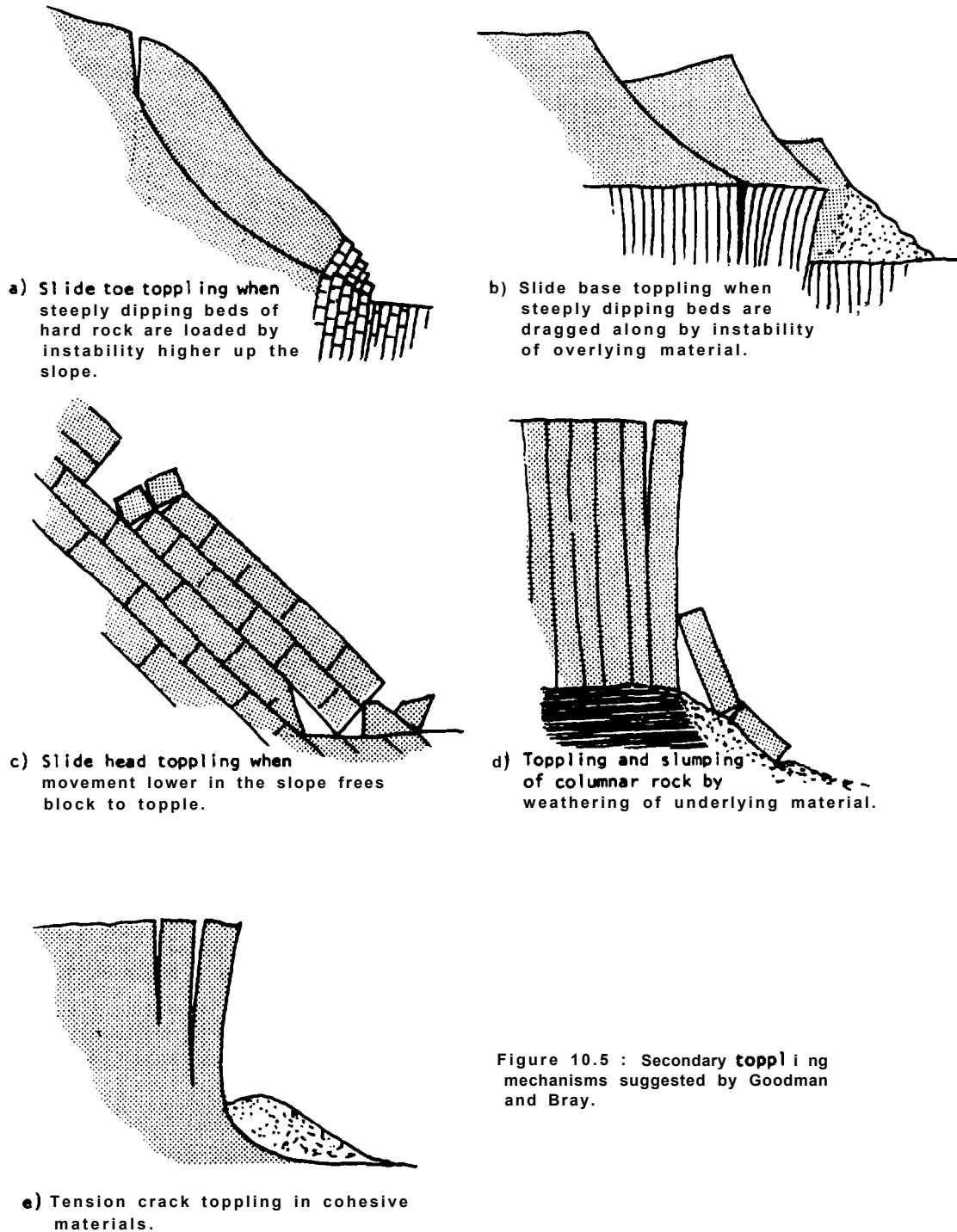


Figure 10.5 : Secondary toppling mechanisms suggested by Goodman and Bray.

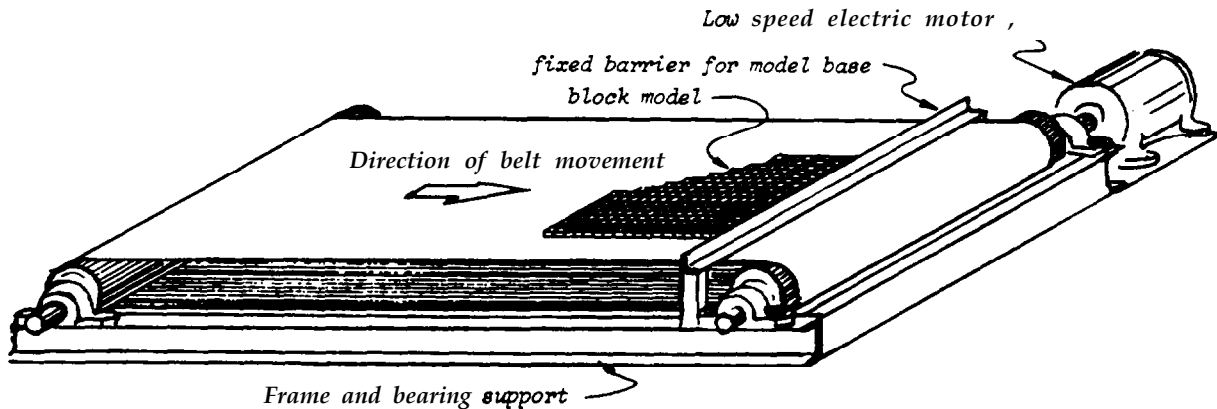


Figure 10.6 : Base friction model apparatus which can be used for demonstrating toppling effects in block models.

Is limited because studies on the sensitivity of the slope to small changes in geometry become very tedious. In addition, the range of physical properties which can be incorporated into the model is limited by available modelling materials.

Attempts to overcome these problems by modelling toppling processes numerically have been made by Cundall(250), Byrne(252) and Hammett(253) and, while the results of these studies have been very promising, the numerical techniques are demanding on computer storage and time and these methods are not yet suitable for general engineering use. The authors believe that these numerical methods will eventually become practical design tools, particularly the computer graphics techniques being explored by Cundall at the University of Minnesota.

The method of analysis described below utilizes the same principles of limiting equilibrium which have been used throughout the remainder of this book and, while the solution is limited to a few simple cases of toppling failure, it should provide the reader with a basic understanding of the factors which are important in toppling situations.

Limit equilibrium analysis of toppling on a stepped base

Consider the regular system of blocks shown in Figure 10.7 in which a slope angle θ is excavated in a rock mass with layers dipping at $90-\alpha$. The base is stepped upwards with an overall inclination β . The constants a_1, a_2 and b shown in the figure are given by

$$a_1 = 5x \cdot \tan(\theta - \alpha) \tag{98}$$

$$a_2 = 5x \cdot \tan \alpha \tag{99}$$

$$b = Ax \cdot \tan(\beta - \alpha) \tag{100}$$

where Δx is the width of each block.

In this idealized model, the height of the n th block in a position below the crest of the slope is

$$y_n = n(a_1 - b) \tag{101}$$



Incipient toppling failure in a steeply jointed hard rock slope. Photograph by R. E. Goodman.

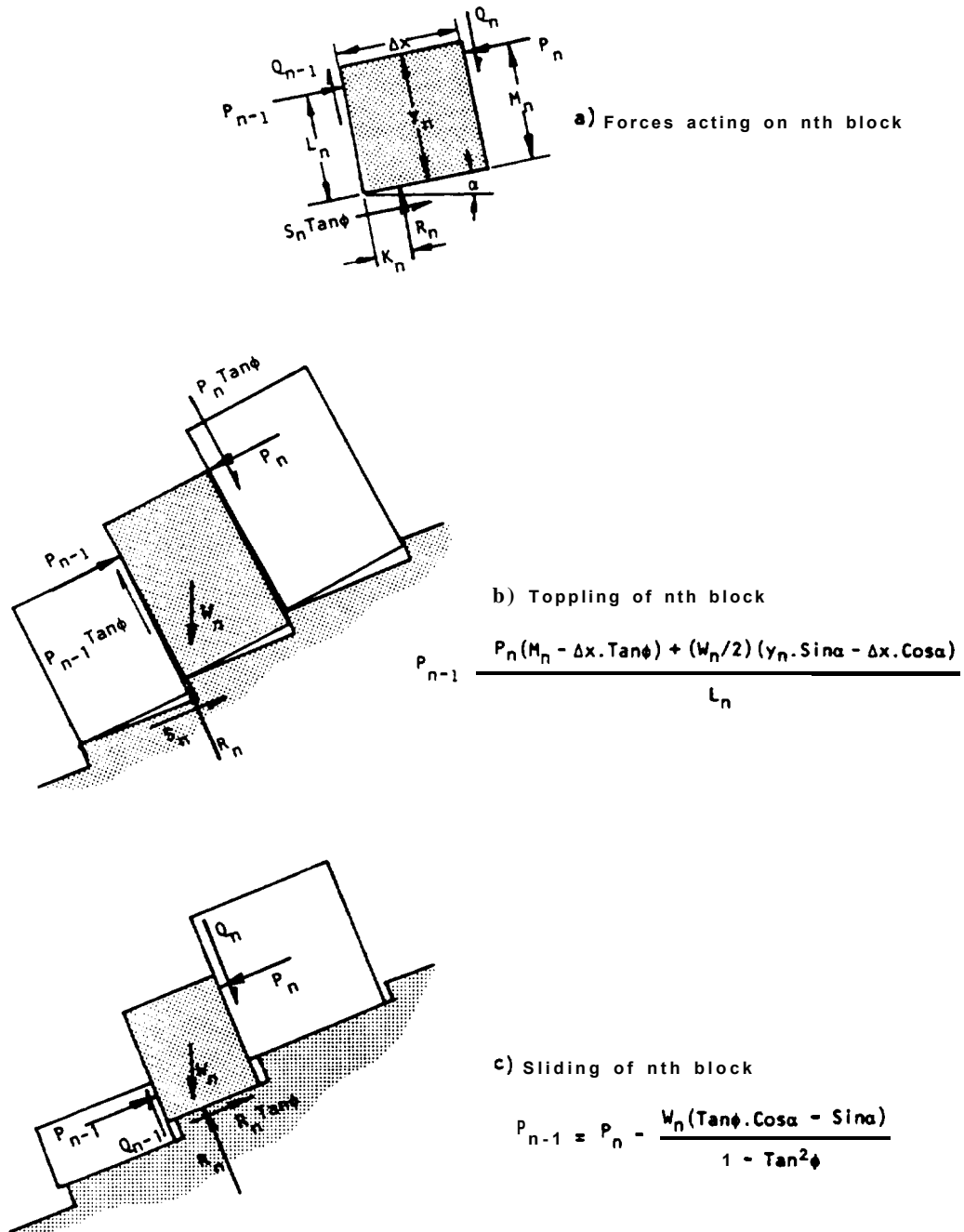


Figure 10.8 : Limiting equilibrium conditions for toppling and for sliding of the nth block.

If the n th block is the crest block:

$$M_n = y_n - a_2 \quad (105)$$

$$L_n = y_n - a_1 \quad (106)$$

If the n th block is above the slope crest:

$$M_n = y_n - a_2 \quad (107)$$

$$L_n = y_n \quad (108)$$

In all cases $K_n = 0$

For an irregular array of blocks, y_n , L_n and M_n can be determined graphically.

For limiting friction on the sides of the block:

$$Q_n = P_n \cdot \tan \phi$$

$$Q_{n-1} = P_{n-1} \cdot \tan \phi$$

By resolving perpendicular and parallel to the base,

$$R_n = W_n \cdot \cos \alpha + (P_n - P_{n-1}) \tan \phi \quad (110)$$

$$S_n = W_n \cdot \sin \alpha + (P_n - P_{n-1}) \quad (111)$$

Considering rotational equilibrium, it is found that the force P_{n-1} which is just sufficient to prevent toppling has the value

$$P_{n-1,t} = \frac{P_n(M_n - \Delta x \cdot \tan \phi) + (W_n/2)(y_n \cdot \sin \alpha - \Delta x \cdot \cos \alpha)}{L_n} \quad (112)$$

When the block under consideration is one of the sliding set,

$$S_n = R_n \cdot \tan \phi \quad (113)$$

However, the magnitudes and points of application of all the forces applied to the sides and base of the block are unknown. The procedure suggested here is to assume that, as in the toppling case, conditions of limiting equilibrium are established on the side faces so that equations (110) and (111) apply. Taken in conjunction with (113), these show that the force P_{n-1} which is just sufficient to prevent sliding has the value

$$P_{n-1,s} = P_n - \frac{W_n (\tan \phi \cdot \cos \alpha - \sin \alpha)}{1 - \tan^2 \phi} \quad (114)$$

The assumption introduced here is quite arbitrary, but a little consideration will show that it has no effect on calculations of the overall stability of the slope. Any other reasonable assumption would produce the same results.

Calculation procedure

Let n_1 = uppermost block of the toppling set,
 n_2 = uppermost block of the sliding set.

a) To determine the value of ϕ for limiting equilibrium.

1) Assume a reasonable value of ϕ , such that $\phi > \alpha$.

- 2) Establish n_1 by determining the uppermost block of the whole group which satisfies the condition

$$y_n / \Delta x > \cot \alpha$$

- 3) Starting with this block, determine the lateral forces $P_{n-1,t}$ required to prevent toppling and $P_{n-1,s}$ to prevent sliding.

If $P_{n-1,t} > P_{n-1,s}$, the block is on the point of toppling and P_{n-1} is set equal to $P_{n-1,t}$.

If $P_{n-1,s} > P_{n-1,t}$, the block is on the point of sliding and P_{n-1} is set equal to $P_{n-1,s}$.

For this particular block, and all other tall blocks of the system, it will be found that the toppling mode is critical, and this check is purely a matter of routine. It is required at a later stage to determine n_2 which defines the upper limit of the sliding section. Further checks should be carried out to ensure that

$$R_n > 0 \\ |S_n| < R_n \cdot \tan \phi$$

- 4) The next lower block ($n_1 - 1$) and all the lower blocks are treated in succession, using the same procedure.
- 5) Eventually a block may be reached for which $P_{n-1,s} > P_{n-1,t}$. This establishes block n_2 , and for this and all lower blocks, the critical state is one of sliding. If the condition $P_{n-1,s} > P_{n-1,t}$ is not met for any of the blocks, the sliding set is absent and toppling extends down to block 1.
- 6) Considering the toe block 1:

If $P_0 > 0$, the slope is unstable for the assumed value of ϕ . It is necessary to repeat the calculations for an increased value of ϕ .

If $P_0 < 0$, repeat the calculations with a reduced value of ϕ .

When P_0 is sufficiently small, the corresponding value of ϕ can be taken as that for limiting equilibrium.

- b) To determine the cable force required to stabilise a slope.

Suppose that a cable is installed through block 1 at a distance L_1 above its base. The cable is inclined at an angle δ degrees below horizontal and anchored a safe distance below the base. The tension in the cable required to prevent toppling of block 1 is

$$T_t = \frac{(W_1/2)(y_1 \cdot \sin \alpha - \Delta x \cdot \cos \alpha) + P_1(y_1 - \Delta x \cdot \tan \phi)}{L_1 \cdot \cos(\alpha + \delta)} \quad (115)$$

while the tension in the cable to prevent sliding is

$$T_s = \frac{P_1(1 - \tan^2 \phi) - W_1(\tan \phi \cdot \cos \alpha - \sin \alpha)}{\tan \phi \cdot \sin(\alpha + \delta) + \cos(\alpha + \delta)} \quad (116)$$

The normal and shear force on the base of the block are respectively:

$$R_1 = P_1 \cdot \tan \phi + T \cdot \sin(\alpha + \delta) + W_1 \cdot \cos \alpha \quad (117)$$

$$S_1 = P_1 - T \cdot \cos(\alpha + \delta) + W_1 \cdot \sin \alpha \quad (118)$$

The procedure in this case is identical to that described above apart from the calculations relating to block 1. The required tension is the greater of T_f and T_s defined by equations (115) and (116).

EXAMPLE

An idealized example is illustrated in Figure 10.9. A rock slope 92.5 m high is cut on a 56.6' slope in a layered rock mass dipping at 60° into the hill. A regular system of 16 blocks is shown on a base stepped at 1m in every 5 (angle $\beta - \alpha = 5.8^\circ$). The constants are $a_1 = 5.0$ m, $a_2 = 5.2$ m, $b = 1.0$ m, $\Delta x = 10.0$ m and $\gamma = 25$ kN/m³. Block 10 is at the crest which rises 4° above the horizontal. Since $\cot \alpha = 1.78$, blocks 16, 15 and 14 comprise a stable zone for all cases in which $\phi > 30^\circ$ ($\tan \phi > 0.577$).

In this example, $\tan \phi$ is set as 0.7855, P_{13} is then equal to 0 and P_{12} calculated as the greater of $P_{12,t}$ and $P_{12,s}$ given by equations (112) and (114) respectively. As shown in the table given on page 10.12, $P_{n-1,t}$ turns out to be the larger until a value of $n = 3$, whereupon $P_{n-1,s}$ remains larger. Thus blocks 4 to 13 constitute the potential toppling zone and blocks 1 to 3 constitute a sliding zone.

The force required to prevent sliding in block 1 tends to zero which indicates that the slope is very close to limiting equilibrium. The installed tension required to stabilize block 1 is 0.5 kN per meter of slope crest length, as compared with the maximum value of P (in block 5) equal to 4837 kN/m.

If $\tan \phi$ is reduced to 0.650, it will be found that blocks 1 to 4 in the toe region will slide while blocks 5 to 13 will topple. The tension in a bolt or cable installed horizontally through block 1, required to restore equilibrium, is found to be 2013 kN/meter of slope crest. This is not a large number, demonstrating that support of the "keystone" is remarkably effective in increasing the degree of stability. Conversely, removing or weakening the keystone of a slope near failure as a result of toppling can have serious consequences. The support force required to stabilize a slope from which the first n toe blocks have been removed can be calculated from equations (115) and (116), substituting P_{n+1} for P_1 .

Now that the distribution of P forces has been defined in the toppling region, the forces R_n and S_n on the base of the columns can be calculated using equations (110) and (111); and assuming $Q_{n-1} = P_{n-1} \cdot \tan \phi$, R_n and S_n can also be calculated for the sliding region. Figure 10.9 shows the distribution of these forces throughout the slope. The conditions defined by $R_n > 0$ and $|S_n| < R_n \cdot \tan \phi$ are satisfied everywhere.

The limitations of pre-shearing are that it is difficult to determine results until primary excavation is complete to the finished wall. Since pre-shearing is done before primary blasts are made, it is not possible to take advantage of the knowledge of local rock conditions that is gained in the primary blasts. Also, the hole spacings in cushion blasting can usually be greater than in pre-shearing, thus reducing drilling costs.

Buffer Blasting

The following description of buffer blasting is taken verbatim from the Pit Slope Manual(272).

Buffer blasting, possibly the most simple method of control blasting involves a modification to the last row of the main blast pattern. Modifications are limited to reduced burden, spacings, and explosive loads.

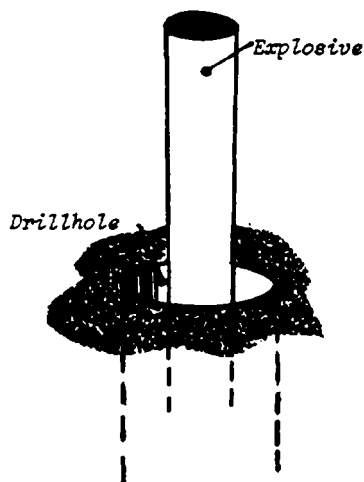
The aim is to limit the load of ground shock from the blast. The method is usually employed in conjunction with some other control blasting technique, such as pre-shearing, and its results are quite economical. Buffer blasting can only be used by itself when the ground is fairly competent. It may produce minor crest fracturing or backbreak. However, the amount of damage is still less than that which would be produced by the main production blast if no control blasting was used at all.

Buffer blasting is the cheapest form of control blasting. The powder factor is essentially the same as for production blasting so explosives costs are the same. Drilling costs in buffer blasting are slightly higher because of the reduced burden and spacing which is used. Coupled charges produce high borehole pressures (usually greater than 300,000 psi) but breaking of the rock is desirable for buffer blasting.

CONTROLLED BLASTING: CONSTRUCTION PRACTICES AND ECONOMICS

Controlled blasting has been used on a wide range of construction projects and this experience has been used to draw some conclusions on the type of construction problems that may be encountered, and the cost savings that may be achieved(273, 274, 275). The following is a summary of these conclusions.

- 1) Typical blasting problems, their probable causes and solutions are listed on Table IX.
- 2) Borehole pressure, and hence backbreak, can be reduced by decoupling or decking charges. Charges are decoupled when they do not touch the borehole wall (see margin sketch). The ratio of the charge radius to the hole radius is a measure of the decoupling of the charge.
- 3) The comments earlier in this chapter relating to the correct burden dimensions and delay sequencing for the main blast, are equally applicable to controlled blasting.
- 4) Doubling the hole diameter doubles the rupture radius (assuming that the coupling ratio, $D_{\text{explos}}/D_{\text{hole}}$, is kept constant). Hence, small diameter drill holes will create less damage to final walls than larger holes.



Centering a pre-split charge in a drillhole

TABLE IX
SOLUTIONS TO CONTROLLED BLASTING PROBLEMS
(after Pit Slope Manual (Chap. 1), 1976)

<u>Problem</u>	<u>Probable Cause</u>	<u>Solutions</u>
backbreak throughout wall (no boreholes showing)	a) buffer row overloaded or too close b) control blast may be overloaded	a) move buffer row further from excavation limit, reduce borehole pressure of buffer charge, use 15 msec. delay between buffer charges (if not already being done) b) increase hole spacing or decrease powder load (by decoupling or decking) of cushion or presplit holes
backbreak around boreholes	borehole pressure greater than in situ dynamic compressive rock strength	decouple or deck charges
backbreak between boreholes	buffer holes too close	increase spacing, decouple or deck charges
jointing interferes between blast holes	a) spacing too great b) burden insufficient c) delays between perimeter holes too large	a) reduce spacing and powder load b) make burden larger than spacing c) detonate holes on perimeter row simultaneously
Very poor fragmentation at excavation limit, or blast fails to break to presplit line	buffer row too far from excavation limit	decrease the distance from buffer row to presplit or line drilled holes
crest fracture	stemming insufficient or rock exceptionally weak (e.g. weathered) at crest	increase the height of collar, eliminate subgrade in drilled holes overlying the crest of a berm, use spacers in the upper portion of the explosive column, drill small diameter guide holes.

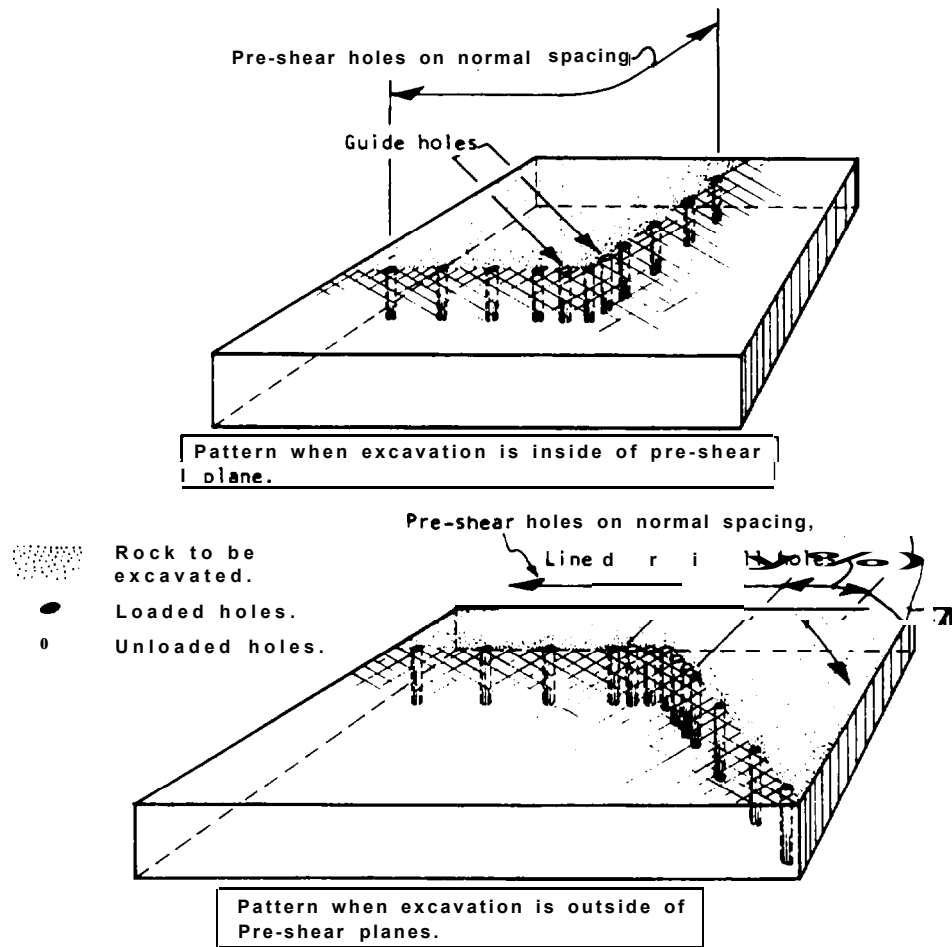


Figure 11.14: Pre-shearing non-linear faces.

All loaded **pre-shear** holes should be stemmed completely around and between charges to prevent gas venting if weak strata are present. However, like cushion blasting, in more solid homogeneous formations it is preferable to have decoupled charges and to only place stemming in the top 2 or 3 ft. of the hole. Also, like cushion blasting, it is desirable to increase the charge in the first few feet of hole to about **two** or three times that used in the upper portion. This promotes shearing at the bottom where it is more difficult to break the rock.

Pre-shearing loads are placed and detonated in the same manner as described for **cushion** blasting. The staggering of charges in adjacent holes is also recommended for pre-shearing to give better overall load distribution.

The depth that can be pre-sheared at one time is again dependent upon the ability to maintain good hole alignment. Deviation greater than 6 inches from the desired plane of shear will give inferior results. Generally, 50 ft. is the maximum depth that can be used for 2 to 3-1/2 inch diameter holes without significant deviation of alignment.

Theoretically, the length of a pre-shear shot is unlimited. In practice, however, shooting far in advance of primary excavation can be troublesome if the rock characteristics change and the load causes excessive shatter in the weaker areas. By carrying the pre-shear only one-half shot in advance of the primary blasting (see Figure 11.121, the knowledge gained from the primary blasts regarding the rock can be applied to subsequent **pre-shear** shots. In other words, the loads can be modified if necessary, and less risk is involved as compared to shooting the full length of the neat excavation line before progressing with the primary blasts.

Pre-shearing can be accomplished during the primary blast by delaying the primary holes so that the pre-shear holes will fire ahead of them (see Figure 11.13).

In many cases, especially when shooting non-linear cuts, **pre-shearing** in combination with **line** drilling will give good results. For example, when it is desirable to maintain a corner of solid rock, line drilling the corner may be used to prevent breakage across it (see Figure 11.14). Guide holes to promote shear along the desired plane are as advantageous in **pre-shearing** as they are in cushion blasting.

When **pre-shearing** in **unconsolidated** formations and **line** drilling between the normally spaced holes, the **line** drilled holes may vary in depth from the top few feet to the full depth of the pre-shear holes. Backbreak is more likely at the top of a bench or lift; consequently, **line** drilling between pre-shear holes for the top few feet reduces the chance of over-break in all types of formations. In very unconsolidated material, the explosive **loads/ft.** in the upper portion of the hole should be reduced by 50 percent to minimize overbreak at the crest of the finished wall.

The main advantage of pre-shearing is that it is not necessary to return to blast the remaining portion of the cut after primary excavation.

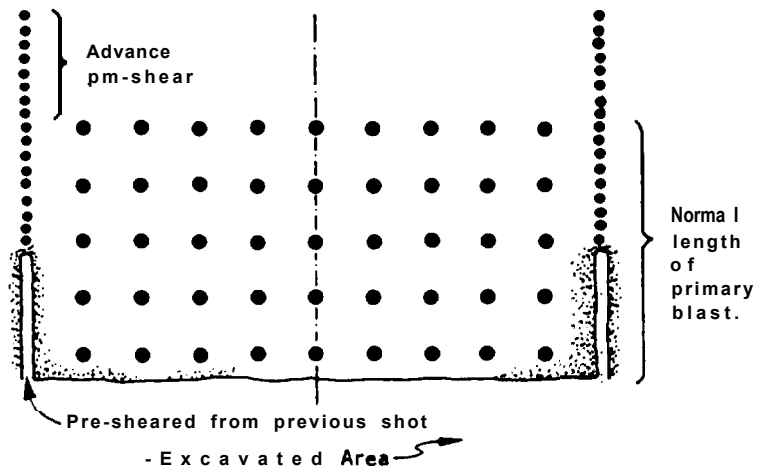


Figure 11.12: Recommended drilling pattern for pro-shearing.

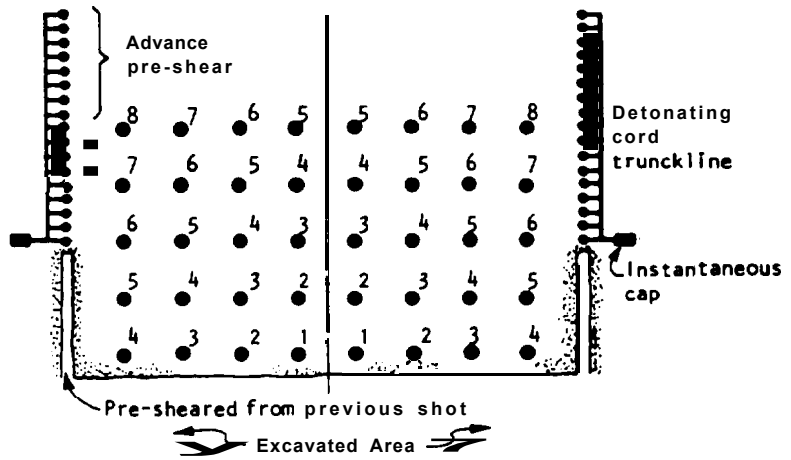


Figure 11.13: Delay sequence for pro-shearing during primary blast.

The theory of pre-shearing is that when two charges are shot simultaneously in adjoining holes, collision of the shock waves between holes places the web in tension and causes cracking that gives a sheared zone between the holes. With proper spacing and charge, the fractured zone between the holes will be a narrow sheared area to which the subsequent primary blasts can break. This results in a smooth wall with little or no overbreak.

The pre-sheared plane reflects some of the shock waves from the primary blasts that follow preventing them from being transmitted into the finished wall, minimizing shattering and overbreak. However, the pre-sheared plane does not reduce vibrations from the primary blast in the surrounding rock.

Description

Pre-shear holes are loaded similarly to cushion blast holes; that is, either heavy core load detonating cord or string loads of full or partial cartridges of 1 to 1-1/2 inch diameter by 8 inches long, spaced at 1 to 2 ft. centers.

Like cushion blasting, holes are usually fired simultaneously using a detonating cord trunkline. If excessively long lines are shot, portions can be delayed with MS Delays.

In extremely unconsolidated rock, results are improved by using guide or relief holes between loaded holes to promote shear along the desired plane. Even in harder formations, guide holes between loaded holes give better results than increasing the explosive charge per hole.

The average spacings and charges per foot of hole are given in Table VIII. These loads are for normal rock conditions and can be obtained using partial or whole conventional cartridges of dynamite spaced on detonating cord downlines. In an extremely unconsolidated formation, poor results were obtained until the load was reduced to a column of 400 grain detonating cord in holes drilled on 12 inch centers. There is also a case on record where it was necessary to reduce the column load to 2 strands of 50 grain detonating cord in order to prevent excessive shatter into a very unconsolidated finished wall. Therefore, the loads and spacings given in Table VIII can only be used as a guide.

TABLE VIII

PRE-SHEAR BLASTING

Hole Diameter Inches	Spacing* ft.	Explosive Charge** lb/ft.
1-1/2 to 1-3/4	1-1/2	0.08 - 0.25
2 to 2-1/2	1-1/2 to 2	0.08 - 0.25
3 to 3-1/2	1-1/2 to 3	0.13 - 0.50
4	2 to 4	0.25 - 0.75

- Dependent upon formation being shot. Figures given are an average as provided by Du Pont of Canada (1964).
- * Ideally, dynamite cartridge diameter should be no longer than 1/2 the diameter of the hole.

Where only the top of the formation is weathered, the guide holes need be drilled only to that depth and not to the full depth of the cushion holes. This procedure is common on the first lift or bench, since backbreak is more probable there than on lower benches.

Satisfactory results have been obtained in homogeneous formations by stemming only the top 2 or 3 ft. of the hole and not between charges. In this case, the air between the charges and the borehole wall serves as the protective "cushion." When stemming is not used between charges, the gases formed by the explosion can find any weak zone in the formation and tend to vent before the desired shear between holes is obtained. Similarly, the gases may find areas of weakness back into the finished wall and produce overbreak. If the formation is weak, highly fractured, or contains faults, complete stemming between and around individual charges is recommended. Also, though not generally practiced in the field, staggering of discrete charges between holes as shown in Figure 11.11 improves powder distribution and gives better results.

Advantages and Limitations

Cushion blasting offers certain advantages including:

- Increased hole spacings to reduce drilling costs.
- Better results in unconsolidated formations.
- Possible to take full advantage of geological information gained from shooting the main cuts when loading cushion holes -less guesswork.
- Results can be observed on first shot, which permits adjustment of loads if necessary before proceeding.
- Better hole alignment with large diameter holes permits deeper holes.

There are situations where cushion blasting should not be considered. Among these are:

- Not practical for cutting 90 degree corners without also using Line Drilling or Pre-shearing.
- Sometimes overbreak from primary blasts completely or partially removes berm to be cushion blasted, thus requiring several load adjustments for different holes.

PRE-SHEAR BLASTING

Basic Principles

Pre-shearing, sometimes referred to as pre-splitting, involves a single row of holes drilled along the neat excavation line. The holes are usually the same diameter (2 to 4 inches) as the main blast holes, and in most cases are loaded. Pre-shearing differs from line drilling and cushion blasting in that the holes are fired before any adjoining main excavation area is blasted.

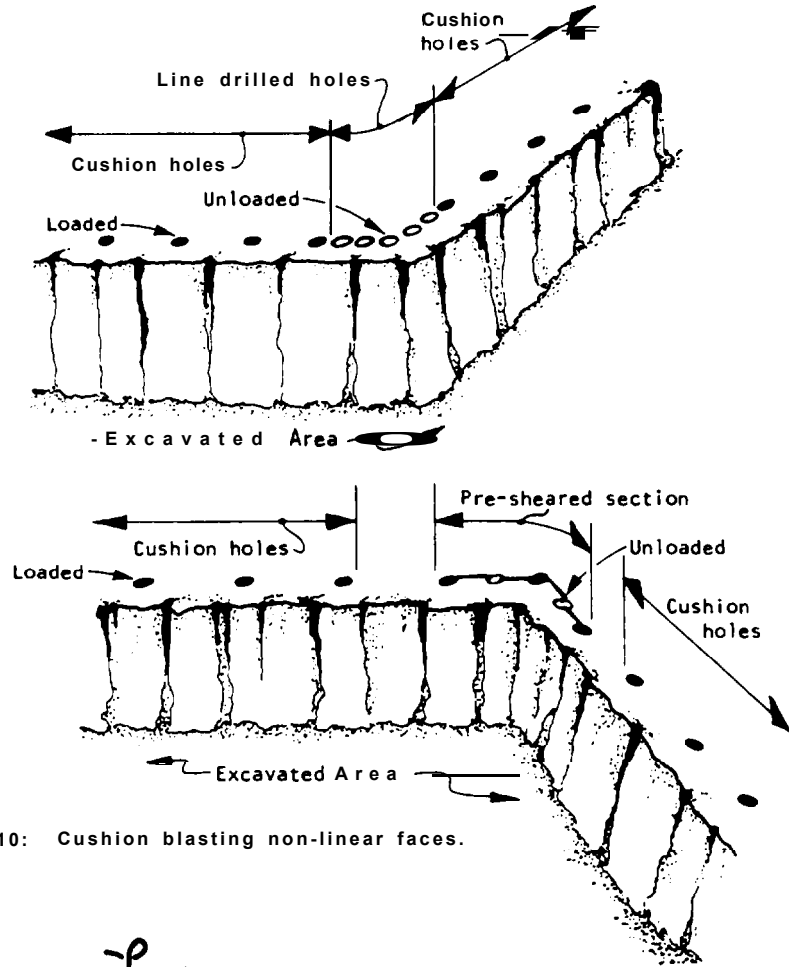


Figure 11.10: Cushion blasting non-linear faces.

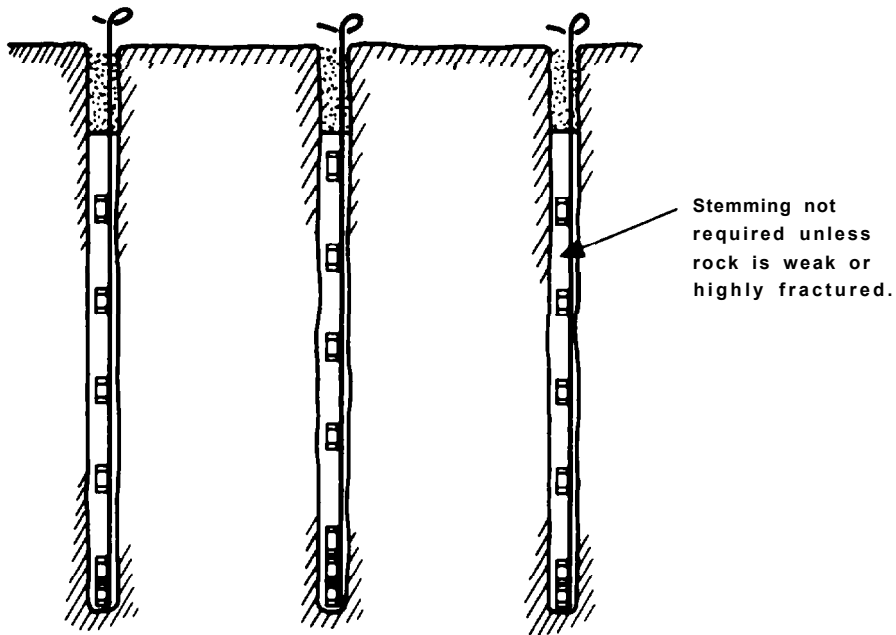


Figure 11.11: Staggered spacing of discrete charges for optimum powder distribution.

spacing must always be less than the width of the berm being removed as indicated in Table VII.

TABLE VII
TYPICAL LOADS AND ROLE PATTERNS

Role Diameter Inches	Spacing* ft.	Burden* ft.	Explosive Charge** lb/ft.
2 - 2 1/2	3	4	0.08 to 0.25
3 - 3 1/2	4	5	0.13 to 0.50
4 - 4 1/2	5	6	0.25 to 0.75
5 - 5 1/2	6	7	0.75 to 1.00
6 - 6 1/2	7	9	1.00 to 1.50

• Dependent upon formation being shot. Figures given are an average as by Du Pont of Canada (1964).

• * Ideally, dynamite cartridge diameter should be no larger than 1/2 the diameter of the hole.

Cushion blasting can be practiced by benching or by pre-drilling the cushion holes to full depth of the excavation. When benching is used, a minimum 1 ft. offset per bench is usually left since it is impossible to position the drill flush to the wall of the upper bench.

The maximum depth that can be successfully cushion blasted depends on the accuracy of the hole alignment. With larger diameter holes better hole alignment can be maintained for greater depths. Deviations of more than 6 inches from the plane of the holes generally gives poor results. Holes 90 ft. deep have been successfully cushion blasted. The penetration rates of the drill should also be considered when determining the depth to be cushion blasted. If, for example, the penetration beyond a given depth becomes excessively slow, it may be more economical to bench in order to keep penetration rates and drilling costs at acceptable levels.

When cushion blasting around curved areas or corners, closer spacings are required than when blasting a straight section. Also, guide holes can be used to advantage when blasting nonlinear faces. On 90 degree corners, a combination of controlled blasting techniques will give better results than cushion blasting alone (see Figure 11.10).

In very unconsolidated sedimentary formations where it is difficult to hold a smooth wall, unloaded guide holes between cushion holes are recommended. Generally, small diameter guide holes are employed to reduce drilling costs.

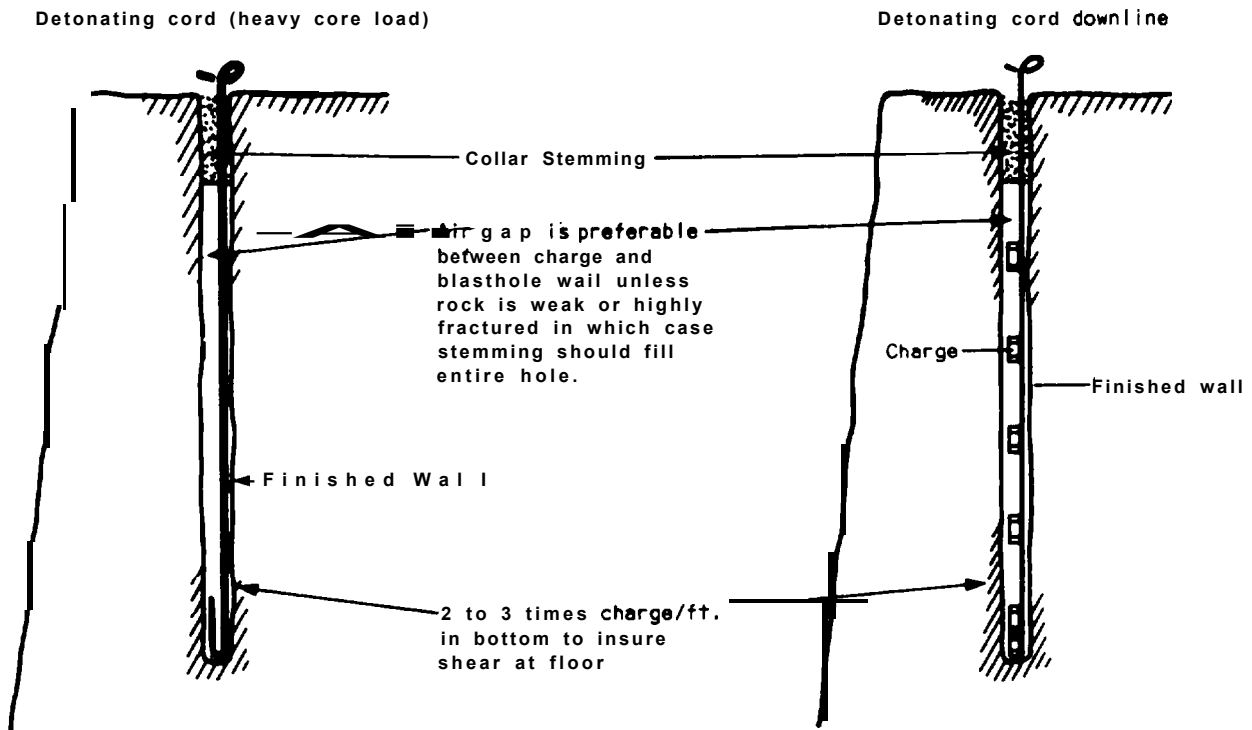


Figure 11.9: Alternative charge placements for cushion blasting.

CUSHIONBLASTING

Basic Principles

Cushion Blasting, sometimes referred to as trimming, smooth wall or slashing, is similar to line drilling in that it involves a single row of holes along the neat excavation line. Although cushion blasting as originally practiced involved holes of 4 to 6-1/2 inches diameter, this technique is also used with smaller diameter holes of 2 to 3-1/2 inches. Cushion blast holes are loaded with light, well-distributed charges and fired after the main excavation is removed. The stemming or air-gap "cushions" the shock from the finished wall as the berm is blasted thus minimizing fracturing and stressing of the finished wall. By firing the cushion holes with minimum delay between holes, the detonation tends to shear the rock web between holes giving a smooth wall with minimum overbreak. Obviously, the larger the hole diameter the more "cushioning" effect realized.

Description

In cushion blasting, the main cut area is removed, leaving a minimum buffer or berm zone in front of the neat excavation line. The cushion holes can be drilled prior to the primary blasting in that area.

The burden and spacing will vary with the hole diameter being used. Table VII provides a guide for patterns and loads for different hole diameters. Note that the numbers shown are an average range because of variations experienced with the type of formation being shot.

Alternative blasting agents for cushion blasting include heavy core load detonating cord extended the full hole depth or dynamite cartridges (full or partial) spaced along a detonating cord downline (see Figure 11.9). To promote shearing at the bottom of the hole, a bottom charge 2 to 3 times that used in the upper portion of the hole is generally employed. For maximum "cushioning," the charges should be decoupled; that is an air-gap should be present between the charge and the wall of the blasthole. If cartridges are used, they can be taped to the detonating cord at a spacing of 1 to 2 ft. The top 2 or 3 ft. of the hole is completely stemmed and not loaded. The length of top stemming required varies with the formation being shot.

Minimum delay between cushion holes gives best shearing action from hole to hole; therefore, detonating core trunklines are normally employed. Where noise and vibration control are critical, good results can be obtained with millisecond (MS) delay caps.

The burden-t-spacing relationship will vary with different formations but, to obtain maximum shearing between holes, the

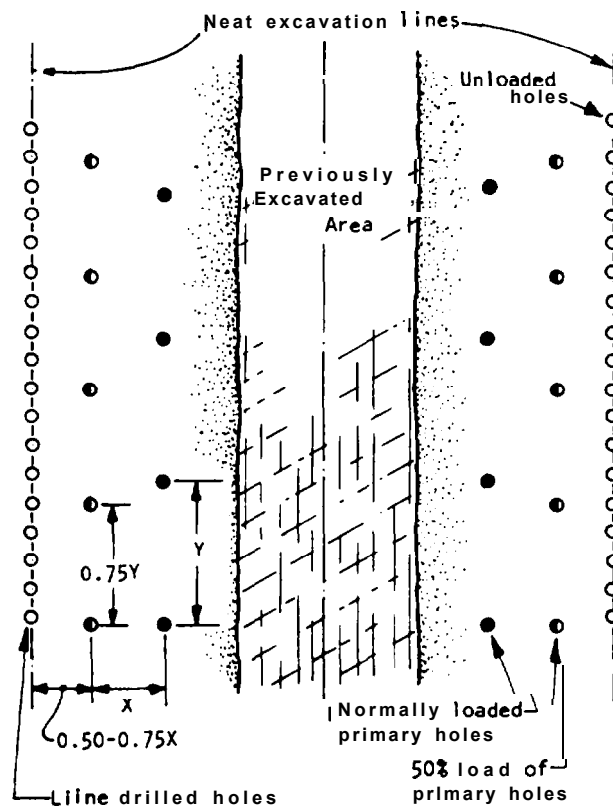


Figure 11.8: Typical pattern and procedure for line drilling (plan view).

the normal burden. A common practice is to reduce the spacings of the adjacent blast holes the same amount with a 50 percent reduction in explosive load. The explosives should be well distributed in the hole using decks and Primacord downlines.

Best results with line drilling are obtained in homogeneous formations where bedding planes, joints and seams are at a minimum. These irregularities are natural planes of weakness that tend to promote shear through the line drilled holes into the finished wall. Therefore, thin-bedded sedimentary and more unconsolidated metamorphic formations are not well suited to line drilling for overbreak control unless drilling can be done perpendicular to the strike of the formation. This, however, is not practical in most excavation work.

Figure 11.8 shows a typical pattern and procedure for line drilling in open work. Best results are obtained when the primary excavation is removed to within 1 to 3 rows of the neat excavation line. The last two rows of holes are then stepped away from the line drill holes using delay caps or "Primacord" connectors. This procedure gives maximum relief in front of the finished wall, allowing the rock to move forward thus creating less back pressures which could cause overbreak beyond the line drilling. As indicated in Figure 11.8, reduced spacing and burden are used on the row next to the excavation line.

In thin-bedded sedimentary and unconsolidated metamorphic formations, results with line drilling can usually be improved by light loading some of the line drill holes. This procedure led to the development of Cushion Blasting. Also, it was found that line drilling results could be improved in some formations by light loading and firing the line drill holes in advance of the primary blast, and this led to the introduction of the technique known as Pre-Shearing or Pre-Splitting. These modifications of line drilling also promoted additional weakness along the neat excavation line by using explosive force to shear the rock between the holes.

Advantages and Limitations

Line drilling is applicable in areas where even the light explosive loads associated with other controlled blasting techniques may cause damage beyond the excavation limit.

When used with other controlled blasting techniques, line drilling between the loaded holes promotes shearing to improve results.

There are a number of limitations of line drilling which must be recognized:

- Line drilling is rather unpredictable except in the most homogeneous formations.
- Due to the close spacings required, drilling costs are high.
- Because line drilling requires a large number of holes on rather close spacings, drilling becomes tedious and results are often unsatisfactory due to poor hole alignment.



An 18m high rock face created by pre-split blasting. Note the clean fracture running between parallel holes in the face, in spite of the variability of the rock through which these holes have been drilled.

Photograph reproduced with permission of Atlas Copco. Sweden.

Slopes excavated after pre-splitting the final faces on a site for a hydro-electric project in Austria.

Photograph reproduced with permission of Atlas Copco. Sweden.



Figure 11.7: Examples of controlled blasting.

- e) Delays should be used to control the maximum instantaneous charge to ensure that rock breakage does not occur in the rock mass which is supposed to remain intact (see Figure 11.16).
- f) Back row holes should be drilled at an optimum distance from the final digline to permit free digging and yet minimize damage to the wall. Experience can be used to adjust the back row positions and charges to achieve this result.

Controlled Blasting

On permanent slopes where even small slope failures are not acceptable, the use of controlled blasting methods is often economically justified. The principle behind all these methods is that closely spaced holes are loaded with a relatively light charge so that this charge is well distributed on the final face. The detonation of these holes, often on a single delay, tends to shear the rock between the holes while doing little damage to the surrounding rock. The following is a discussion on various methods of controlled blasting, and their advantages and disadvantages, which is taken from a publication by du Pont (273). Examples of controlled blasting are shown in Figure 11.7.

A general comment on the design of controlled blasts is that it is often necessary to carry out a number of trial blasts at the start of a project to determine the optimum hole layout and explosive charge. This requires flexibility on the part of the contractor and the specifications. It is also advisable to have the program under the direction of an engineer experienced in controlled blasting.

Line Drilling

Line Drilling requires a single row of closely spaced, unloaded, small-diameter holes along the neat excavation line. This provides a plane of weakness to which the primary blast can break. It also causes some of the shock waves created by the blast to be reflected which reduces shattering and stressing of the finished wall.

Description

Line drill holes are generally 2 to 3 inches in diameter and are spaced from 2 to 4 times the hole diameter apart along the excavation line. Holes larger than 3 inches are seldom used in line drilling since the higher drilling costs cannot be offset by increased spacings.

The depth of line drill holes is dependent upon how accurately the alignment of the holes can be maintained. For good results, the holes must be on the same plane; any wander or drift by attempting to drill too deep will have an adverse effect on results. For holes of 2 to 3 inches diameter, depths greater than 30 ft. are seldom satisfactory.

The blast holes directly adjacent to the line drill holes are generally loaded lighter and are more closely spaced than the other holes. The distance between the line drill holes and the directly adjacent blast holes is usually 50 to 75 percent of

Similar test sequences could be carried for each of the other factors which are relevant in a particular situation.

- a) **Rationalization** - Document present powder factors on an **equivalent energy basis** using the weight of the **explosive** in current use. **Weight** strength data should be obtained from the **explosives** manufacturer if these are not already **available**.
- b) **Evaluation** - For a blast with the **explosive** currently in use, document the behavior of the blast **during initiation** and the **condition** of the resulting muck pile.
- c) Document rate and **conditions** of digging.
- d) Document **fragmentation** based upon the ratio of **oversized material requiring** secondary blasting to the total blast tonnage.
- e) **Document drilling** and blasting costs.
- f) **Experimentation** - Select a similar area of ground and carry out a blast **with a higher** powder factor which is obtained by **using a higher energy explosive**.
- g) **Evaluation** - Document the results as for steps (b) to (e).
- h) Carry out a **cost-benefit** study.

Repeat the **experiment** to **determine its validity**.

II CONTROLLED BLASTING TO **IMPROVE** STABILITY

Based upon the **assumption** that the damage caused by a blast increases in proportion to the weight of explosive used, it follows that any reduction in **explosive consumption** will lead to a reduction in damage to the rock. **Slope instability** is often related to blast damage to the rock **which** can be minimized by **optimization** of the production blast as well as using controlled blasting methods such as line drilling, buffer, pre-split, and **cushion blasting**.

The following conditions should be satisfied if the production blast is to be **optimized** and damage to the rock **behind** the face **minimized**.

- a) Choke blasting into **excessive** burden or broken muck piles should be avoided.
- b) The front row charge should be adequately designed to move the front row burden.
- c) The **main** charge and blasthole pattern should be **optimized** to **give** the best **possible** fragmentation and **digging** conditions for the minimum powder factor.
- d) Adequate delays should be used to ensure good **movement** towards free faces and the creation of new free faces for following rows.

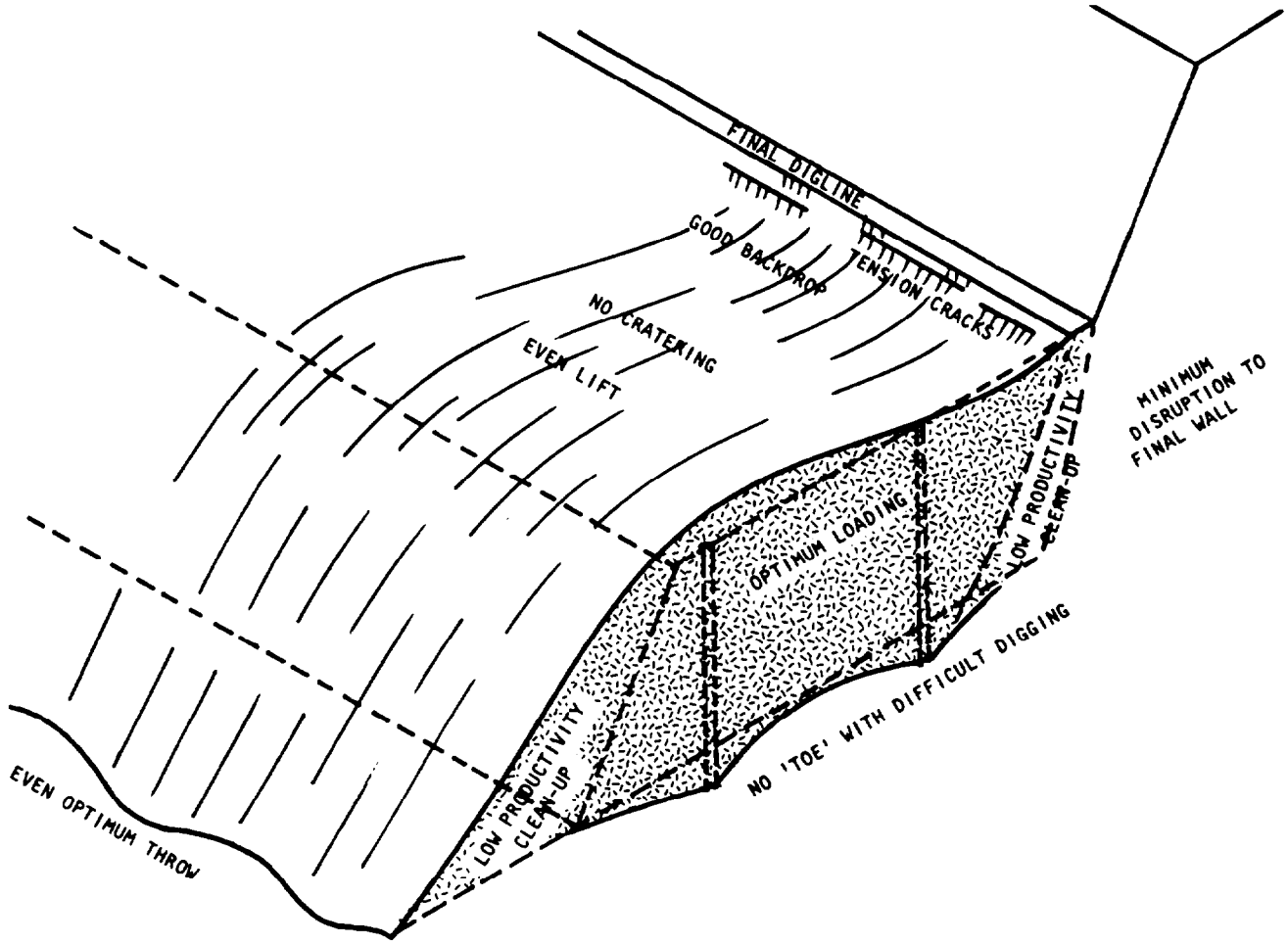


Figure 11.6 : Features of a satisfactory production blast.

Evaluation of a blast

Once the dust has settled and the fumes have dispersed after a blast, an inspection of the area should be carried out. The main features of a satisfactory blast are illustrated in Figure 11.6.

The front row should have moved out evenly but not too far. Excessive throw is unnecessary and very expensive to clean up. The heights of most benches are designed for efficient loader operation; low muck piles, due to excessive front row movement, represent low loader productivity.

The main charge should have lifted evenly and cratering should, at worst, be an occasional occurrence. Flat or wrinkled areas are indicative of misfires or poor delaying.

The back of the blast should be characterized by a drop, indicating a good forward movement of the free face. Tension cracks should be visible in front of the final diglines. Excessive cracking behind the final digline represents damage to the slopes and wastage of powder.

The quality of a blast has a significant effect on components of the rock excavation cost such as secondary drilling and blasting of oversize boulders, digging rate, the condition of the haul roads, and loader and truck maintenance. Therefore, careful evaluation of the blast to determine how improvements could be made to the design are usually worthwhile.

Oversized fragments, hard toes, tight areas and low muck piles (caused by excessive throw) have the most significant detrimental effect on the digging rate and digging conditions. A study of loader performance and of complaints from loader operators helps to maintain an awareness of these problems among blasting personnel. An attempt should be made to measure digging rate by noting the time required to fill trucks or by comparing average daily production rates. Similarly, loader wear and tear should be noted since this may reflect difficult digging conditions.

Poor fragmentation of the toe due to an excessive toe burden can lead to poor digging and uneven haul road condition. Uneven haul roads lead to suspension wear on the trucks and also spillage which can give rise to high tire wear. An attempt to correct this problem by additional subdrilling rather than by correcting the front row charge can lead to excessive sub-break which can give rise to blast hole instability and also to poor bench crest conditions if a deeper bench is to be removed.

Modification of Blasting Methods

When it is evident that unsatisfactory results are being obtained from a particular blasting method and that the method should be modified, the engineer may have to embark on a series of trials in order to arrive at an optimum design. As with any trials, careful documentation of each blast is essential and, whenever possible, only one variable at a time should be changed. The following sequence of test work is an illustration of the type of experiment which would be carried out to evaluate the cost effectiveness of using a higher energy explosive.

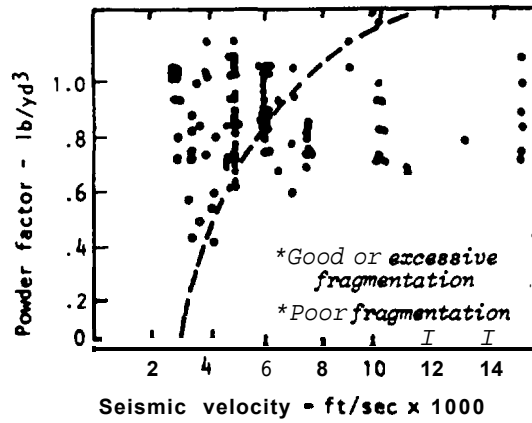


Figure 11.4 : Correlation between in situ seismic velocity and required powder factor . After Broadbent²⁷¹.

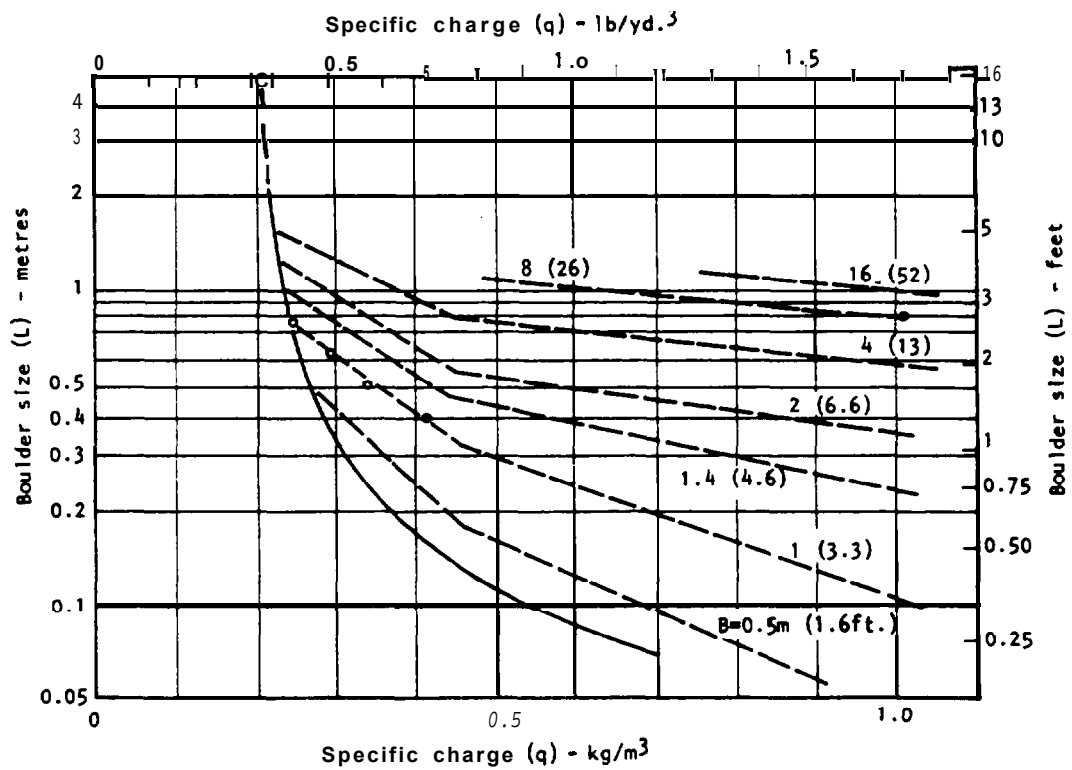


Figure 11.5: Relationship between boulder size L, specific charge q and burden B in bench blasting.

grounds to support this suggestion and the optimum blasting direction is usually established by carefully controlled trials.

The importance of blasting to a free face has already been stressed and it is equally important to plan the blast so that suitable free faces are created for the next blast. When free faces are not available, e.g. when the face changes direction, there is a danger that the blast may become choked and it may be necessary to use delays in order to work in such a situation. A typical firing sequence for a choked blast situation is illustrated in Figure 11.3 (iv).

The use of delays in a blast is one of the most powerful weapons in the fight against excessive blast damage and slope instability. This subject will be discussed more fully in a later section of this chapter.

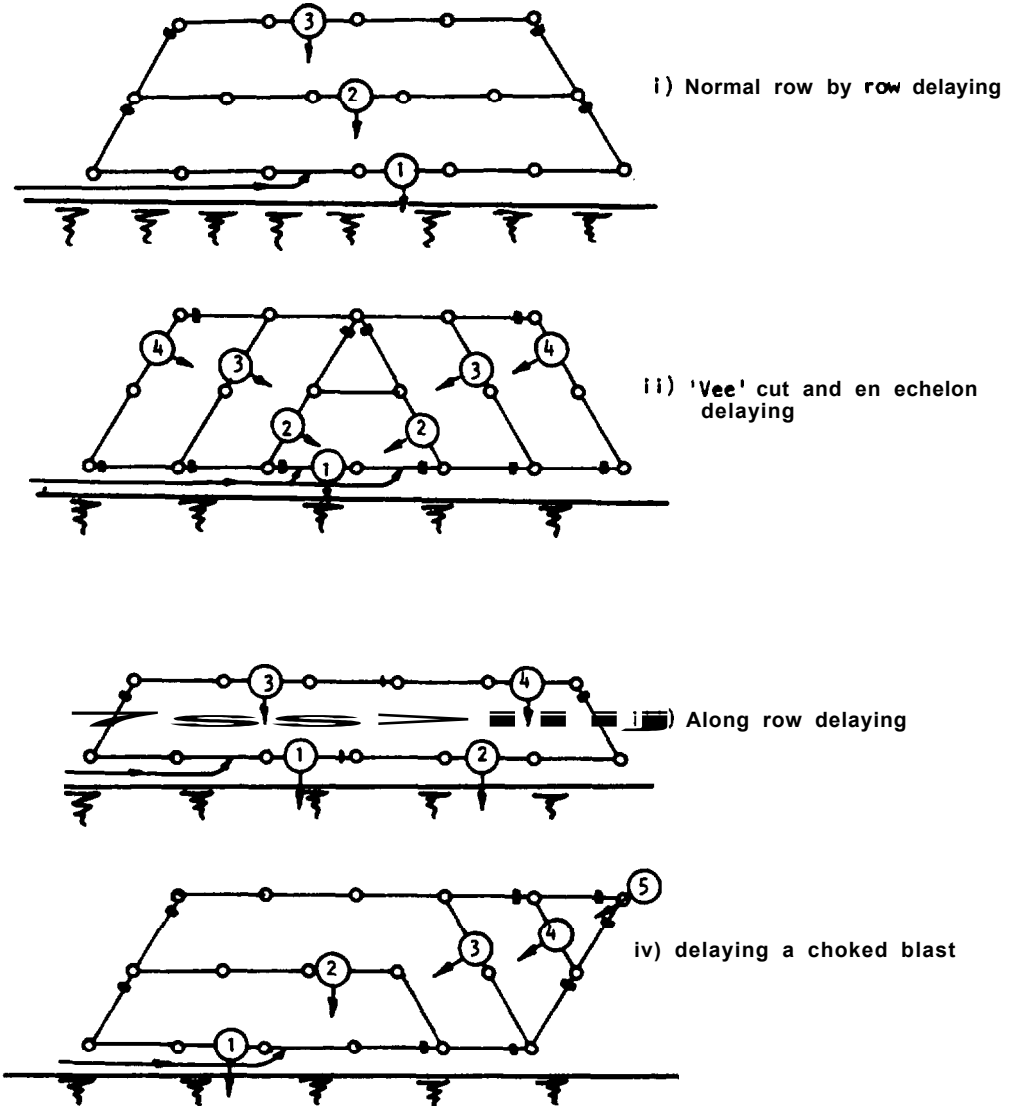
Blast Design

Nine factors which influence the effectiveness of a blast have been discussed on the preceding pages. In order to design a blast it is necessary to select values for all these parameters and determine the optimum explosive load. Usually the hole diameter is decided by the size of available drills and the bench height by the dimensions of the cut. The bench height should not exceed 20 to 30 ft. since it becomes difficult to control hole deviation at depths greater than this. The bench height should not exceed the vertical reach of the loading equipment by more than about 5 ft. This gives the operator protection from sudden collapses of the face.

The basic parameter for measuring explosive charge is the "powder factor" which is the weight of explosive required to break a unit volume of rock, e.g. lb/yd.³ or kg/m³. It is also necessary to relate the powder factor to the type of explosive used because the amount of energy for a given weight of explosive varies with the explosive type (see Table VI). The selection of an appropriate powder factor and drill hole pattern, because these two factors are directly related, is usually based on the blasters' experience. However, this experience has been used to draw up some guidelines to determine powder factors. For example, Broadbent relates the powder factor to the seismic velocity of the rock (Figure 11.4) and this may be useful information in highway construction when seismic studies have been carried out to determine overburden thickness.

An alternative approach is to use theoretical equations which have been developed, and extensively tested in the field, by Langefors and Kihlstrom(257) and others. These equations take into account all parameters governing blast design and could serve as a starting point in blast design.

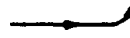
Blast design charts are included in Chapter 2 of Langefors and Kihlstrom's book. One of these design charts is shown in Figure 11.5 which relates the powder factor (q) to the burden and the boulder size (sieve size through which 95 percent of the blast will pass). The unbroken lines represent the powder factor to just loosen the rock. This chart may be useful in designing a blast to produce rock of a certain size for riprap, for example. Other equations, using a different approach have been developed by Bauer(272).



Symbols :



Firing sequence and direction of rock movement



Initiating line

—●— 35 millisecond delay

—+— 17 millisecond delay

Note - safety lines are omitted for clarity.

Figure 11.3 : Typical firing sequences.

locating a small "pocket" charge centrally within the stemming(269).

(8) Initiation Sequence for Detonation of Explosives

Having drilled and charged a blast it is then necessary to tie up the pattern. This involves laying out detonating cord along the "rows" to form trunk lines which are then tied to the downline of each charge. The rows are normally parallel to the free face but, as shown in the margin sketch on page 11.6, may be inclined to it. Safety lines are used in large patterns to ensure complete detonation and reduce the risk of cut-offs. A perimeter or "ring" line is then tied around the pattern to provide a further safeguard.

The firing or initiating line will normally be connected to the middle of the front row trunk line. Other firing sequences are illustrated in Figure 11.5. The blasting sequence, after the initiation of the first row, is controlled by the use of delays as discussed in the next section.

(9) Delays Between Successive Hole or Row Firing

A typical blast for a highway cut may contain as many as 100 blast holes which in total contain several thousand pounds of explosives. Simultaneous detonation of this quantity of explosive would not only produce very poorly fragmented rock, but would also damage the rock in the walls of the excavation and create large vibrations in any nearby structures. In order to overcome this situation, the blast is broken down into a number of sequential detonations by means of delays.

Recent research(270) has shown that there can be considerable error in the timing of delays. This can produce incorrect sequencing of blast holes and poor blasting results. If this problem is suspected the performance of the detonator should be checked with the manufacturer.

When the front row is detonated and moves away from the rock mass to create a new free face, it is important that time should be allowed for this new face to be established before the next row is detonated. Typically, delay intervals of 1 to 2 milliseconds per ft. of burden are used. A typical blast with a burden of 10 ft. would have about 15 msec. delays between rows.

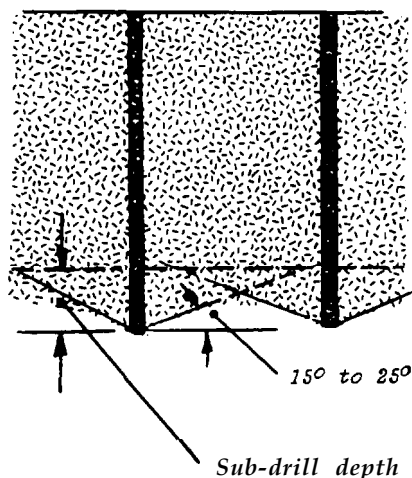
Normal row by row delaying is the simplest and generally the most satisfactory firing sequence. Delay patterns can become quite complex and should be planned and checked carefully. The number of rows should not exceed 4 to 6 as choking occurs with deeper blasts and vertical craters may be formed above the back rows which do not have sufficient room to move laterally.

An alternative is to use an echelon delaying and to initiate the firing sequence with a vee cut to create the first free face. This type of firing sequence can be useful when blasting in strongly jointed rock where near vertical joints strike across the bench at an angle to the face. Some blasting engineers suggest that the row line should bisect the angle between the strike of the joints and the face or the strike of two joint sets. There does not appear to be very strong theoretical

should exercise caution in applying this pattern since its success depends upon rock of good quality. Joints running across a line of holes in a row could allow explosive gases to vent and reduce the effectiveness of the blast.

(5) Subdrill Depth

Subdrilling or drilling to a depth below the required grade, is necessary in order to break the rock on the floor of the cut. Poor fragmentation at this level will form a series of hard "toes" which can lead to expensive loader operation due to difficult digging conditions and breakdowns. Excessive fragmentation probably means that the rock behind the face and below the grade is damaged and this means a reduction in stability.



Rock breakage at the bottom of a blasthole

As illustrated in the margin sketch, breakage of the rock usually projects from the base of the bottom load in the form of an inverted cone with sides inclined at 15 degrees to 25 degrees to the horizontal, depending upon the strength and structure of the rock. In multi-row blasting, the breakage cones interact and link up to give a reasonably even transition from broken to undamaged rock. Experience has shown that a subdrill depth of 0.2 to 0.3 times the distance between adjacent blast holes is usually adequate to ensure effective digging to grade. It is particularly important that subdrill depths should not be exceeded in the front and back rows otherwise unstable crest and toe conditions can be created in the new bench. In fact, there is good justification for reducing or even eliminating subdrilling in the front and back rows if bench stability is critical.

(6) Blast Hole Inclination

As pointed out in the discussion on burden, the front row burden varies with depth if vertical blast holes are used and the bench faces are inclined. Inclined blast holes are obviously advantageous for the front row and, by drilling the blast holes parallel to the bench face, a constant front row burden is achieved. In order to maintain a constant burden with depth for the remainder of the blast, it follows that all the blast holes should be inclined. Some blasting engineers would argue that the use of blast holes drilled at between 10 degrees and 30 degrees to the vertical will give better fragmentation (268), greater displacement and reduced back-break problems (269).

(7) Stemming

The use of stemming consisting of drill cuttings is a generally accepted procedure for directing explosive effort into the rock mass. The same arguments as were used in the discussion on burden apply in the case of stemming. Too little stemming will allow the explosion gases to vent and will generate flyrock and air blast problems as well as reducing the effectiveness of the blast. Too much stemming will give poor fragmentation of the rock above the top load.

The optimum stemming length depends upon the properties of the rock and can vary between 0.67 and 2 times the burden. If unacceptably large blocks are obtained from the top of the bench, even when the minimum stemming column consistent with flyrock and airblast problems is used, fragmentation can be improved by

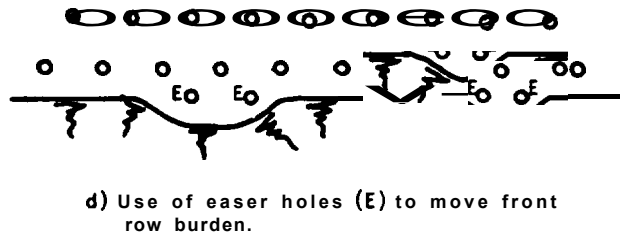
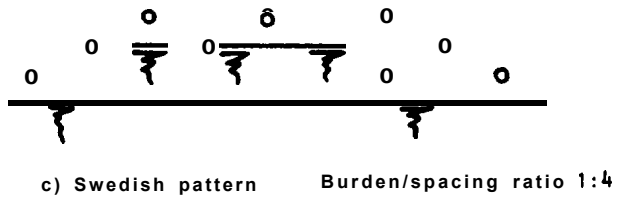
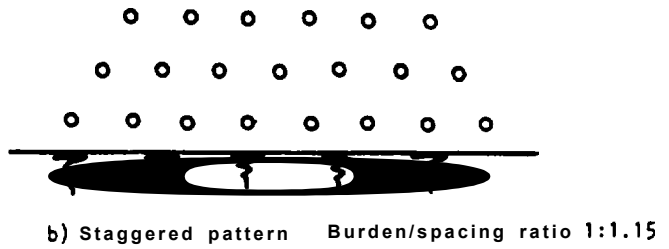
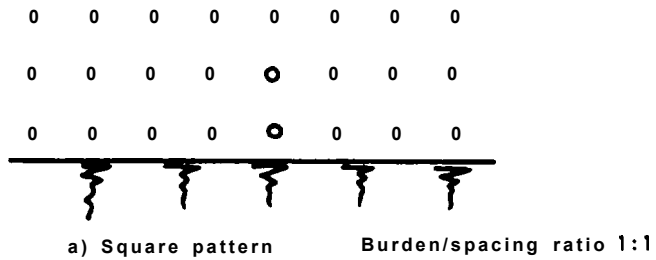
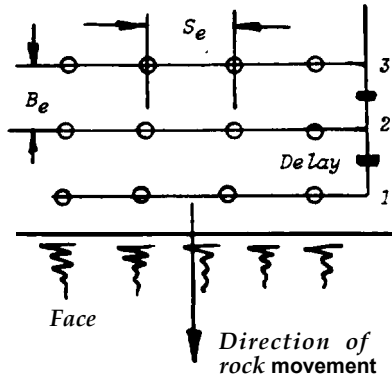
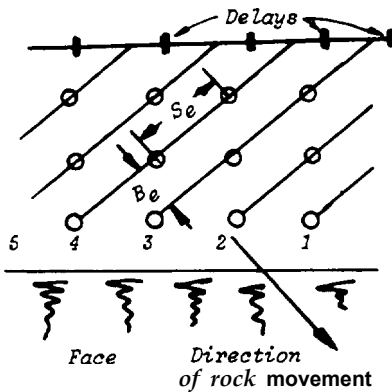


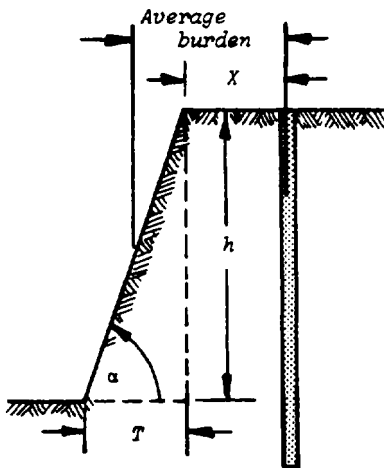
Figure 11.2 : Various blasthole patterns used in open pit production blasting.



Effective burden and spacing for a square blasting pattern



Effective burden and spacing for an echelon blasting pattern



Average front row burden =
 $X + \frac{1}{2}T = X + \frac{1}{2}h \cdot \cot \alpha$

Too small a burden will allow the radial cracks to extend to the free face end this will give rise to venting of the explosion gases with a consequent loss of efficiency and the generation of flyrock and air blast problems. Too large a burden will choke the blast and will give rise to very poor fragmentation and a general loss of efficiency. Experience has shown that the explosive charge is most efficient when the burden is equal to approximately 40 times the hole diameter.

The effective burden B_e and the effective spacing S_e depend not only upon the blast hole pattern but also upon the sequence of firing. As illustrated in the margin sketch, a square blast hole pattern which is fired row by row from the face gives an effective burden equal to the spacing between successive rows parallel to the face. On the other hand, an identical pattern of blast holes can be fired in echelon resulting in completely different burdens and spacings as shown in the margin sketch.

One of the most important questions to be considered in designing a blast is the choice of the front row burden. If vertical blast holes are used and the bench face is inclined as a result of the digging angle of the loader in clearing the previous blast, the front row burden will not be constant but will vary with depth as illustrated in the margin sketch. Allowance can be made for this variation by using a higher energy bottom load in the front row of holes. Alternatively, the blast hole can be inclined to give a more uniform burden as will be discussed later in this section. When the free face is uneven, the use of easer holes to reduce the burden to acceptable limits is advisable (see Figure 11.2d).

Since the effectiveness of the fragmentation process depends upon the creation of a free face from which a tensile strain wave can be generated and to which the burden rock can move, the design of the front row blast is critical. Once this row has been detonated and effectively broken, a new free face is created for the next row and so on until the last row is fired.

(4) Effective Spacing

When cracks are opened parallel to the free face as a result of the reflected tensile strain wave, gas pressure entering these cracks exerts an outward force which fragments the rock and heaves it onto the muck pile. Obviously, the lateral extent to which this gas can penetrate is limited by the size of the crack and the volume of gas available and a stage will be reached when the force generated is no longer large enough to fragment and move the rock. If the effect of a single blast hole is reinforced by holes on either side at an effective spacing S_e , the total force acting on the strip of burden material will be evened out and uniform fragmentation of this rock will result.

Experience suggests that an effective spacing of 1.25 times the effective burden gives good results. However, work by Lundborg of Nitro Nobel in Sweden, mentioned in the paper by Persson(267) shows that improved fragmentation may be obtained by increasing the spacing to burden ratio to as much as 4, 6 or even 8. This finding has been incorporated into the "Swedish" blast hole pattern illustrated in Figure 11.2c. The reader

TABLE VI'
PROPERTIES OF EXPLOSIVES'

<u>Explosive</u>	<u>Grade</u>	<u>Strength'</u>	<u>Velocity of Detonation (ft/sec)</u>	<u>Specific Gravity</u>	<u>Water Resistance</u>
Atlas Power Primer	--	75% c	17,000 - 18,000	1.36	Excel lent
Atlas Powerdyn	--	52% c	10,000 - 14,000	1.29	Fair
Atlas Gelodyn	No. 1	52% c	10,000 - 14,000	1.29	Fair
	No. 5	35% c	10,000 - 12,000	1.03	Fair
Hercules Hercomix	--	65% w	10,700 - 15,750	0.80 - 0.95	Very Poor
Hercules Gelamite	1, 1-x	67% w	11,500	1.3	Good
	5, 5-x	62% w	10,000	0.95	Fair
	D	70% w	15,000	1.4	Very Good
Dupont ³ Dynamite	A	70%	10,700	1.21	Fair
	B	40%	11,000	1.55	Good
	B	75%	15,700	1.40	Good
Dupont Tovex	2000 SD-A	--	14,800	1.15	Fair
	5000 SD	--	14,200 - 14,700	1.15	Fair
C.I.L. Forcite	--	40%	to.200	1.49	Good
	--	80%	17,700	1.30	Good

Notes:

1. Information on selected explosives obtained from manufacturer's product information.
2. c = cartridge strength; w = weight strength as indicated by manufacturer.
3. Dupont products now supplied by Explosives Technologies International Inc.

dynamites are rated according to the percentage by weight of nitroglycerin they contain. However, the relative strengths are not proportional to the relative amounts of nitroglycerin because this is not the only energy-producing ingredient in the formulation. For example, 60 percent dynamite is not twice as strong as 30 percent dynamite.

One measure of the strength of an explosive is its velocity of detonation; the higher the velocity the greater the shattering effect. However, the strength, density and degree of confinement are also factors that should be considered in selecting an explosive for a specific purpose. Table VI lists the velocity of detonation, specific gravity and water resistance of some common Dupont(261) and C.I.L. explosives(263).

Explosive strength is also defined by weight and bulk strengths. Weight strengths are useful when comparing blast designs in which explosives of different strengths are used, and also when comparing the cost of explosives because explosives are sold by weight. The bulk (or volume) strength is related to the weight strength by the specific gravity, and this figure is important in calculating the volume of blast hole required to contain a given amount of explosive energy. A higher bulk strength requires less blast hole capacity to contain a required charge.

The sensitivity of an explosive is a characteristic which determines the method by which a charge is detonated, the minimum diameter of the charge and the safety with which the explosive can be handled. Highly sensitive explosives will detonate when used in smaller diameter charges and as the sensitivity of the explosive is decreased, the diameter of the charge must be increased.

(2) Blast Hole Diameter

Blast hole diameter on highway construction work ranges from about 1-1/2 inches for hand held-drills to 2-1/2 inches and 4 inches for "air-trac" and wagon drills. All these drills are rotary percussive and are powered with compressed air.

Persson(267) shows that the cost of drilling and blasting decreases as the hole size increases. This is because the hole volume per foot of hole increases with the square of hole size so that the same volume of explosive can be loaded into fewer holes. This cost saving is offset by the greater shattering of the rock that is produced by the more highly concentrated explosive which can result in less stable slopes.

(3) Effective Burden

In order to understand the influence of the effective burden (the distance between the row of holes under consideration and the nearest free face) it is necessary to understand the mechanism of rock fracture described earlier in the chapter.

The blast is most efficient when the shock wave is reflected in tension from a free face so that the rock is broken and displaced to form a well-fragmented muck pile. This efficiency depends to a large extent on having the correct burden.

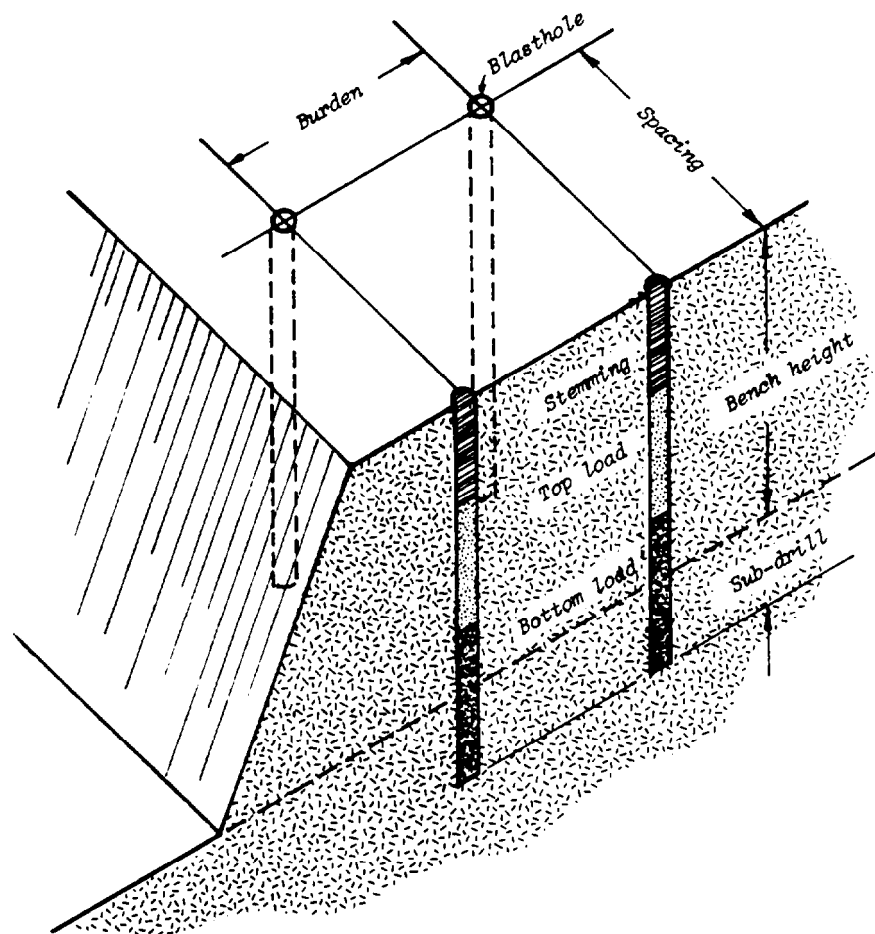
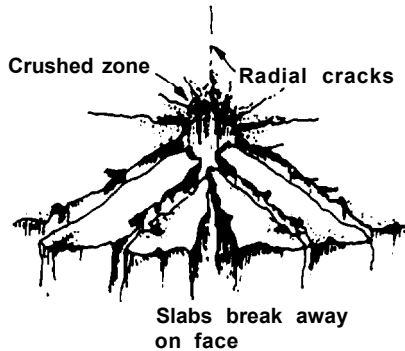


Figure 11.1 : Definition of bench blasting terms.



Mechanism of rock fracture by explosive.

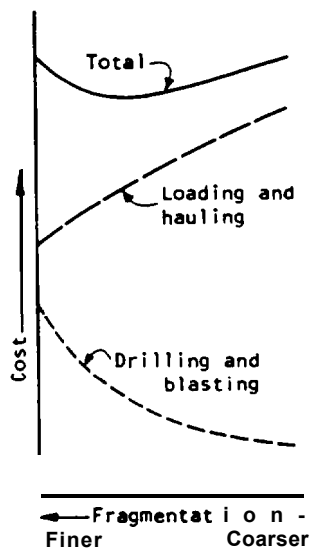
Within about one borehole radius, the pressure exerted by the shock wave is sufficient to shatter the rock and form a crushed zone around the hole. As the wave moves outwards, the tangential stress becomes tensile. Because rock is much weaker in tension than compression, the rock breaks to form a pattern of radial cracks around the hole. When the shock wave reaches a free face, the rock is able to expand and slabs of rock break from the face. The shock wave is also reflected from the face in tension and this aids in rock breakage.

From this description, it can be seen that explosives will break rock at distances of between 10 and 20 hole diameters from the point of detonation. To prevent damage to rock behind the face, the zone of crushed rock and radial cracking around the holes in the final row is controlled by reducing the explosive charge in the holes. As the shock wave travels beyond the limit of rock breakage into the surrounding rock, it sets up vibrations both within the rock and at the ground surface. Structures through which these vibration waves pass will be subjected to a twisting and rocking motion which may be sufficient to cause damage. Allowable levels of vibration for different structures, and methods of controlling vibrations, are discussed later in this chapter.

Production Blasting

The basic economics of rock excavation using explosives is shown in the margin sketch which is taken from a paper by Harries and Mercer (266). The production of a well-fragmented and loosely decked muck pile that has not been scattered around the excavation area facilitates loading and hauling operations. This condition is at the minimum total cost point on the graph. However, close to the final face, drilling and blasting costs will increase because more closely spaced and carefully loaded holes will be required. In order to achieve the optimum results under both conditions, a thorough understanding of the following parameters is required:

- 1) Type, weight, distribution of explosive
- 2) Blast hole diameter
- 3) Effective burden
- 4) Effective spacing
- 5) Subdrill depth
- 6) Blast hole inclination
- 7) Stemming
- 8) Initiation sequence for detonation of explosives
- 9) Delays between successive hole or row firing.



Effect of fragmentation on the cost of drilling, blasting, loading and hauling.

Factors 2 to 7 are introduced in Figure 11.1 and are described in the following sections.

Each of the factors listed above will be considered in relation to its influence upon the effectiveness of the blast and its influence upon the amount of damage inflicted upon the remaining rock.

(1) Type, Weight and Distribution of Explosive

The strength of an explosive is a measure of the work done by a certain weight or volume of explosive. This strength can be expressed in absolute units, or as a ratio relative to a standard explosive such as dynamite. Thus nitroglycerin or straight

Chapter 11 Blasting.

Introduction

The excavation of rock slopes usually involves blasting and it is appropriate that the subject receive attention in this manual on rock slope engineering. The fragmentation of rock by means of explosives is a major subject in its own right and the fundamentals have been dealt with in a number of excellent text books (257-260), while most of the practical aspects have been described in handbooks published by manufacturers of drilling equipment and explosives (261-264). The first part of this chapter reviews the principles of production blasting and discusses methods of evaluating the results.

Detailed design of blasting operations are usually the responsibility of the contractor, while the principle duty of the owner's representative is to ensure that the desired results are being produced. This requires that the owner understands blasting methods so that he can review alternative procedures and propose modifications if necessary. The owner should also ensure that accurate records are kept of each blast so that the results obtained can be related to the method used. The records are also useful for cost control purposes.

Rock excavation for highway construction often requires the formation of a slope that will be stable for many years, and that will also be as steep as possible to minimize excavation volume and land use. While these two requirements are contradictory, the stability of slopes will be enhanced, and the maximum safe slope angle increased, by using a blasting method that does the least possible damage to the rock behind the final face. The second part of the chapter describes proven methods of minimizing blasting damage which are included in the general term "controlled blasting". The techniques are described in some detail because they may not be standard practice for the contractor and the design engineer is often involved with writing the specifications and supervising the work.

The third part of the chapter describes methods of controlling structural damage due to blast vibrations and minimizing hazards of flyrock, airblast and noise. A glossary of blasting and excavation terms is included in the Appendix 5.

I PRINCIPLES OF BLASTING

Mechanism of Rock Failure by Explosive

The mechanism by which rock is fractured by explosives is fundamental to the design of blasting patterns, whether for production or controlled blasting. It also relates to the damage to surrounding structures and disturbance to people living in the vicinity. The following is a description of this mechanism (265).

When an explosive is detonated, it is converted in a few thousandths of a second from a solid into a high temperature gas. If the explosive is confined in a drill hole, this very rapid reaction causes the gas to exert pressure in the rock immediately around the hole. This pressure can exceed 100,000 atmospheres, and the energy is dissipated into the surrounding rock in the form of a shock wave that travels with a velocity of several thousand feet per second. It is the passage of this shock wave that breaks rock by the mechanisms shown in the margin sketch.

Chapter 10 references

245. MULLER, L. New considerations of the Vajont slide. *Felsmechanik und ingenieurgeologie*. Vol. 6. No. 1, 1968, pages 1-91.
246. HOFMANN, H. Kinematische Modellstudien zum Boshungsproblem in regelmässig geklüfteten Medien. *Veröffentlichungen des Institutes für Bodenmechanik und Felsmechanik*. Karlsruhe, Heft 54, 1972.
247. ASHBY, J. Sliding and toppling modes of failure in models and jointed rock slopes. *M.Sc Thesis*. London University, Imperial College, 1971.
248. SOTO, C. A comparative study of slope modelling techniques for fractured ground. *M.Sc Thesis*. London University, Imperial College, 1974.
249. WHYTE, R.J. A study of progressive hanging wall caving at Chambishi copper mine in Zambia using the base friction model concept. *M.Sc Thesis*. London University, Imperial College, 1973.
250. CUNDALL, P. A computer model for simulating progressive, large scale movements in blocky rock systems. *Proc. Internl. Symposium on Rock Fracture*. Nancy, France, 1971, Paper 11-8.
251. BURMAN, B.C. Some aspects of the mechanics of slope and discontinuous media. *Ph.D Thesis*. James Cook University of North Queensland, Australia, 1971.
252. BYRNE, R.J. Physical and numerical models in rock and soil slope stability. *Ph.D Thesis*. James Cook University of North Queensland, Australia, 1974.
253. HAMMETT, R.D. A study of the behaviour of discontinuous rock masses. *Ph.D Thesis*. James Cook University of North Queensland, Australia, 1974.
254. DE FREITAS, M.H and WATTERS, R.J. Some field examples of toppling failure. *Ceotechnique*. Vol. 23. No. 4, 1973. pages 495-514.
255. WYLLIE, D.C. Toppling rock slope failures, examples of analysis and stabilization. *Rock Mechanics* 13, 89-98 (1980).
256. GOODMAN, R.E and BRAY, J.W. Toppling of rock slopes. *Proc. Speciality Conference on Rock Engineering for Foundations and Slopes*. Boulder, Colorado, ASCE, Vol.2, 1976.

FACTOR OF SAFETY FOR LIMITING EQUILIBRIUM ANALYSIS OF TOPPLING FAILURES

The factor of safety for toppling can be defined by dividing the tangent of the friction angle believed to apply to the rock layers ($Tan\phi_{available}$) by the tangent of the friction angle required for equilibrium with a given support force T ($Tan\phi_{required}$)

$$F = \frac{Tan\phi_{available}}{Tan\phi_{required}} \quad (119)$$

If, for example, the best estimate of $Tan\phi$ is 0.800 for the rock surfaces sliding on one another, the factor of safety in the example, with $Tan\phi_{required} = 0.7855$ and with a 0.5 kN support force in block 1, is equal to $0.800/0.7855 = 1.02$. With $Tan\phi_{required} = 0.650$ and a support force of 2013 kN, the factor of safety is $0.800/0.650 = 1.23$.

Once a column overturns by a small amount, the friction required to prevent further rotation increases. Hence, a slope just at limiting equilibrium is meta-stable. However, rotation equal to $2(\beta - \alpha)$ will convert the edge to face contacts along the sides of the columns into continuous face contacts and the friction angle required to prevent further rotation will drop sharply, possibly even below that required for initial equilibrium. The choice of factor of safety, therefore, depends on whether or not some deformation can be tolerated.

The restoration of continuous face-to-face contact of toppled columns of rock is probably a very important arrest mechanism in large scale toppling failures. In many cases in the field, large surface displacements and tension crack formation can be observed and yet the volumes of rock which detach themselves from the rock mass are relatively modest.

GENERAL COMMENTS ON TOPPLING FAILURE

The analyses presented on the preceding pages can be applied to a few special cases of toppling failure and it is obviously not a rock slope design tool at this stage of development. However, the basic principles which have been included in this analysis are generally true and, with suitable additions, will probably provide a basis for further developments of toppling failure analysis.

The reader is strongly advised to work through the example given for himself and to try examples of his own since this can be a very instructive exercise. The calculations are relatively simple to program on a desk top calculator or a computer and the availability of such a program will enable the user to explore a number of possibilities, thereby gaining a better understanding of the sensitivity of the toppling process to changes in geometry and material properties.

CALCULATION OF FORCES FOR EXAHPLE SHOWN IN FIGURE 10.9											
n	Y_n	$y_n/\Delta x$	M_n	L_n	$P_{n,t}$	$P_{n,s}$	P_n	R_n	S_n	S_n/R_n	Mode
16	4.0	0.4			0	0	0	866	500	0.577	
15	10.0	1.0			0	0	0	2165	1250	0.577	STABLE
14	16.0	1.6			0	0	0	3463	2000	0.577	
13	22.0	2.2	17	22	0	0	0	4533.4	2457.5	0.542	
12	28.0	2.8	23	28	292.5	-2588.7	292.5	5643.3	2966.8	0.526	
11	34.0	3.4	29	34	825.7	-3003.2	825.7	6787.6	3520.0	0.519	T
10	40.0	4.0	35	35	1556.0	-3175.0	1556.0	7662.1	3729.3	0.487	0
9	36.0	3.6	36	31	2826.7	-3150.8	2826.7	6933.8	3404.6	0.491	P
8	32.0	3.2	32	27	3922.1	-1409.4	3922.1	6399.8	3327.3	0.520	P
7	28.0	2.8	28	23	4594.0	156.8	4594.8	5872.0	3257.8	0.555	L
6	24.0	2.4	24	19	4837.0	1300.1	4037.0	5352.9	3199.5	0.598	I
5	20.0	2.0	20	15	4637.5	2013.0	4637.5	4848.1	3159.4	0.652	N
4	16.0	1.6	16	11	3978.1	2284.1	3978.1	4369.4	3152.5	0.722	G
3	12.0	1.2	12	7	2825.6	2095.4	2825.6	3707.3	2912.1	0.7855	
2	8.0	0.8	8	3	1103.1	1413.5	1413.5	2471.4	1941.3	0.7855	SLIDING
1	4.0	0.4	4	-	-1485.1	472.2	472.2	1237.1	971.8	0.7855	

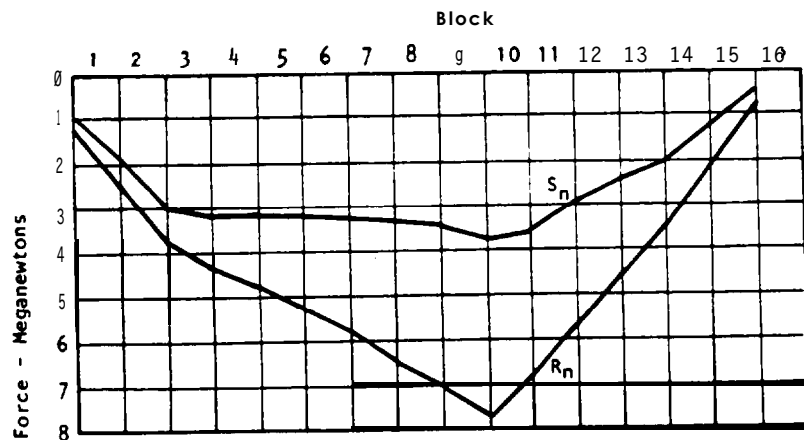
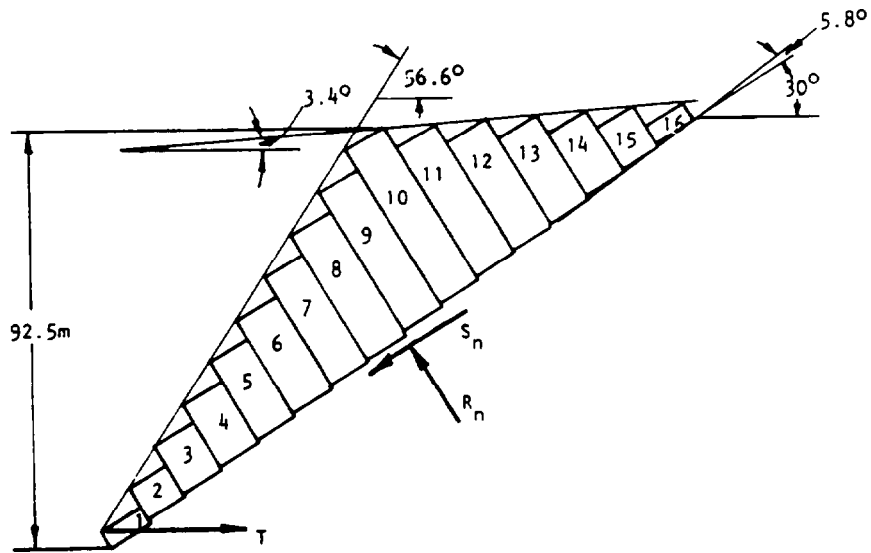


Figure 10.9 : Limiting equilibrium of a toppling slope with $\text{Tan}\phi = 0.7855$.

The use of small diameter blast holes also means using smaller hole spacings. However, small holes are more subject to wander, or to caving in incompetent ground.

- 5) The concentration of charge at the wall should be as low as possible by using a closer hole spacing and loading density than for normal production blasting. Use of a larger number of smaller charges decreases the radius of fracture around blast holes. This lessens the likelihood that large volumes of explosive gases from a single charge will be channelled into a joint or fracture, causing serious backbreak.
- 6) Accurate drilling is important in controlled blasting to ensure an even distribution of the charge on the face. Some applications require that holes be drilled at an angle corresponding to that of the final wall. Hence, some form of equipment which can drill back under itself (e.g., small diameter percussive drilling) would probably be required.
- 7) Depth of subgrade drilling and stemming both affect crest fracturing. Crest fracturing can be caused directly by the natural tendency of an explosive column to crater or break out towards the free surface. The depth of stemming varies from 30 times the charge diameter for hard competent rock to 60 times the charge diameter for soft incompetent rock. Subgrade drilling may fracture the rock at the toe of the slope as well as the crest of an underlying bench, thereby, weakening it and making it susceptible to rock falls.
- 8) Specifications should always contain provision for experimentation to determine the correct combination of hole diameter, burden and charge for each project and each change of rock type.

Because the design of the production blast has an effect on the performance of the controlled blast, the following aspects of production blasting should be considered.

- 1) Charge the upper half of the last few lines of production blast holes lighter than normal to prevent excessive damage beyond the preshear line.
- 2) Besides offering safer working conditions, inclined drilling of production blast holes leads to less backbreak near the collar of the hole and resistance of the rock to blasting appears to be reduced.
- 3) Reduce the shock transmitted to the back slope, by reducing the delay period between the next to last and last rows of production holes by about 40 to 50 milliseconds.
- 4) Reduce backbreak by having proportionally fewer production blast holes exposed to the final slope face. This can be achieved by adopting an elongated drilling pattern, i.e. the spacing of the blast holes is much greater than the burden.

- 5) Drill the last line of production blast holes about half the normal burden from the preshear line to ensure the production blast holes backbreak to the preshear.

The cost savings achieved by controlled blasting cannot be measured directly but it is generally accepted(275) that these savings are greater than the extra cost of drilling closely spaced, carefully aligned holes and loading them with special charges. The savings that are achieved are the result of being able to cut steeper slopes and reduce excavation volume. This in turn means that less land adjacent to the highway is disturbed. It is also found that less time is spent scaling loose rock from the face after the blast and the resulting face is more stable and requires less maintenance in the future. From an aesthetic point of view, steep cuts have a smaller exposed area than flat slopes. However, some people may find the trace of drill holes on the face to be objectionable, even if the rock is less highly fractured than would be the case in conventional blasting.

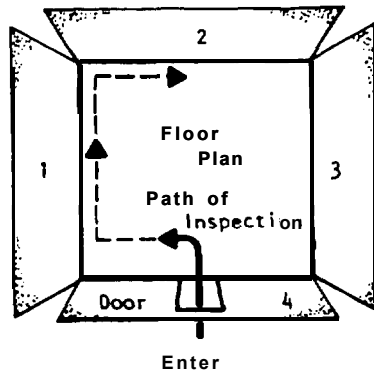
III BLAST DAMAGE AND ITS CONTROL

Highway construction is often carried out in populated areas and in these cases blasting operations must be controlled to ensure that damage and disturbance is minimized. Four types of damage caused by blasting are as follows(267):

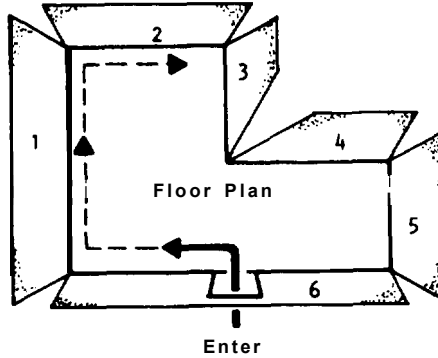
- 1) Structural damage due to vibrations induced in the rock mass.
- 2) Damage due to fly rock or boulders ejected from the blast area.
- 3) Damage due to air blast.
- 4) Damage due to noise.

Further consideration is that ground vibrations are perceptible well outside the zone within which the vibrations may cause damage. This can cause people living in the area to complain about the vibration and possibly put in claims for damages not caused by vibrations. This problem can often be overcome by informing people before blasting starts about the vibrations that they will feel. Within the zone where damage may possibly occur, a survey should be carried out to record all existing cracks, with photographs where possible. The Office of Surface Mining(277) has drawn up a standardized system of recording structural damage that helps to accurately survey buildings, an example of which is shown in Figure 11.15. Finally, vibrations should be measured, at least during the initial blasts, to ensure that vibration levels are within allowable limits and to determine the maximum explosive weights that can be detonated per delay. If these precautions are followed, it is unlikely that a successful claim for blast damage will be made.

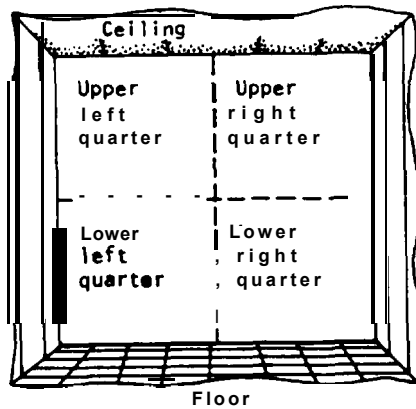
The following is a discussion on the types of damage and what steps can be taken in designing the blast to prevent damage from occurring. A complete review of blast damage mechanisms is beyond the scope of this manual and the interested reader is referred to the excellent literature on the subject(257, 258, 260, 276-289).



(a) Wall identification procedure.



(b) Multi-wall identification procedure.



(c) Field wall identification procedure.

Figure 11 .15: Example of Office of Surface Mining method of making damage surveys.

Structural Damage

The fragmentation of rock by detonation of an explosive charge depends upon the effects of both strain induced in the rock and upon the gas pressure generated by the burning of the explosive. Structural damage resulting from vibration is dependent upon the strains induced in the rock.

When an explosive charge is detonated near a free surface, two body waves and one surface wave are generated as a result of the elastic response of the rock. The faster of the two waves propagated within the rock is called the primary or P wave, while the **slower** type is known as the secondary or S wave. The surface wave, which is slower than **either** the P or S wave, is named after **Rayleigh** who proved its existence and is known as the R wave. Ladegaard-Pedersen and Dally (276) suggest that, in terms of vibration damage, the R wave is the most important since it propagates along the surface of the earth and because its amplitude decays more slowly with distance travelled than the P or S waves. While this may be true for damage to surface structures, rock remaining in the **final** slopes is also of concern and hence the effects of all three waves should be considered.

In the review by Ladegaard-Pedersen and Dally it is concluded that the wide variations in geometrical and geological conditions on **typical** blasting sites preclude the solution of ground vibration problems by means of elastodynamic equations and that the most reliable predictions are given by empirical relationships developed as a result of observations of actual blasts. Of the many empirical relationships which have been postulated, the most **reliable** appears to be that relating particle velocity to scaled distance.

The scaled distance is defined by the function R/\sqrt{W} where R is the radial **distance** from the point of detonation and W is the weight of explosive detonated per delay. The U.S. Bureau of Mines has established that the maximum particle velocity V is related to the scaled distance by following relationship:

$$V = k(R/\sqrt{W})^{\beta} \quad (124)$$

where k and β are constants which have to be determined by measurements on each particular blasting site.

Equation 124 plots as a straight line on log-log paper and the value of k is given by the V intercept at a scaled distance of unity while the constant β is given by the slope of the line. A hypothetical example of such a plot is given in Figure 11.16.

In order to obtain data from the construction of a plot such as that given in Figure 11.16, **some** form of vibration measuring instrument must be **available**. Typical **specifications** for seismographs and geophones, with which to measure vibration levels, are summarized in Tables X and XI.

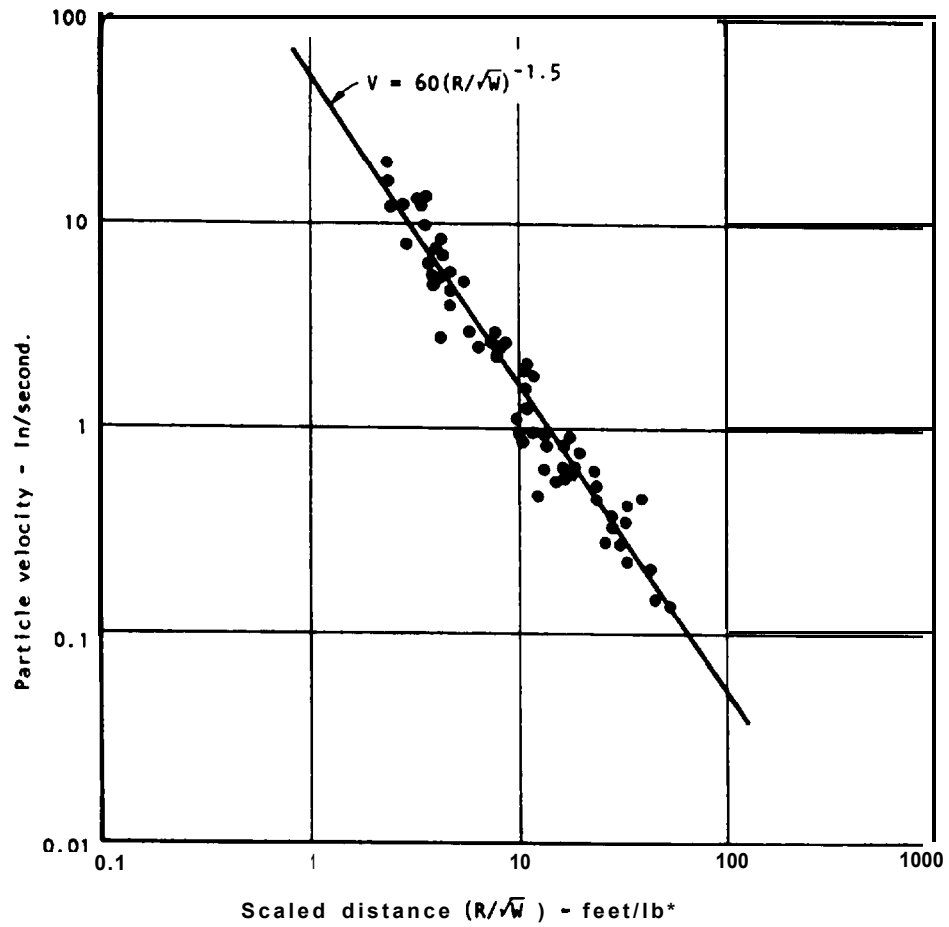


Figure 11.16 : Hypothetical plot of measured particle velocity versus scaled distance from blast.

Typical values of k and β quoted by Orland²⁸⁴ are :

Down hole blasting : $k = 26$ to 260 , $\beta = -1.6$

Coyote blasting : $k = 5$ to 20 , $\beta = -1.1$

Pre-splitting : $k = 800$, $\beta = -1.6$

TABLE X
TYPICAL SPECIFICATIONS FOR SEISMOGRAPHS*

<u>Property</u>	<u>Unit</u>	<u>Range</u>
Frequency response	HZ	2 - 250
Ranges :		
0 Seismic Particle Velocity	in/sec	0.5 - 8
0 Sound overpressure	dB	100 - 140
Trigger Levels		
0 Seismic	in/sec	.04 - 2
0 Sound	dB	110 - 123
Record Times	sec	1 to 7
Total Weight of Instrument	lb	<40

- From InstanTel Inc. product specifications.

TABLE XI
TYPICAL SPECIFICATIONS FOR GEOPHONES*

Standard Natural Frequency	10 Hz \pm .5 Hz
Maintains Specifications	Up to 20°C
Clean Band Pass	To 25 x Natural Frequency
Standard Coil Resistance @ 20°C	395 ohms \pm 5%
Intrinsic Voltage Sensitivity with 395 ohm coil	.70 V/in/sec
Sensitivity at 70% damping	.50 V/in/sec
Normalized Transduction Constant (V/in/sec)	.035 $\sqrt{R_c}$
Moving Mass	.388 oz
Typical Case to Coil Motion P-P	.06 in
Harmonic Distortion with driving velocity of .7 in/sec P-P	.2% or less at 12 Hz

- From Geo Space Corporation product specifications.

Langetors and Kihlstrom(257), Duval and Fogelson(283) and others(272) have examined the relationship between maximum particle velocity and structural damage and the following threshold values have been suggested:

\dot{u} in/sec	Damage
0.08-0.2	Vibrations Perceptible
0.5	Rigidly mounted mercury switches trip out
1.0	Maximum vibration for green concrete*
1.5-2.00	Vibrations Objections ¹
2	Limit below which risk of damage to structures, even old buildings, is very slight (less than 5 percent)
5	Minor damage, cracking of plaster, serious complaints
9	Cracks in concrete blocks
12	Rock falls in unlined tunnel
15	Horizontal offset in cased drill holes
25	Onset of cracking of rock
40	Shafts misaligned in pumps, compressors
60	Prefabricated metal buildings on concrete pads: metal twisted and concrete cracked
100	Breakage of rock

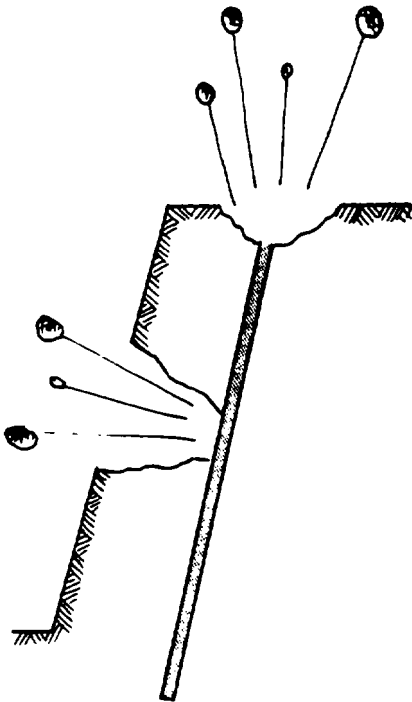
- * Varies with strength gain of concrete, see Konya and Walter(290)

A range of these threshold values have been plotted in Figure 11.17 for different combinations of distance R and weight of explosive charge W . In plotting this figure, values of $k = 200$ and $\beta = -1.5$ have been used in solving equation 124. These values are based upon an average range derived from a paper by Oriard(289) and this plot should only be used for very general guidance. When damage is a serious problem, values of k and β should be determined from a plot of measured particle velocities, such as that presented in Figure 11.16 plotted for these values.

Figure 11.17 shows that 1000 lb. of explosive detonated per delay will cause minor cracking of plaster in houses at distances less than 500 ft. from the blast, while the vibrations will be felt at distances of about one mile. Halving of the weight of explosive detonated per delay will reduce these distances to 300 ft. and 1/2 mile respectively. Thus, the use of delays to limit the weight of explosive detonated per delay is a very important method of controlling both damage and reactions by the public to the blasting operations.

Control of Flyrock

When the front row burden is inadequate or when the stemming column is too short, a crater is formed as illustrated in the margin sketch. Under these conditions, rock is ejected from the crater and it may be thrown a considerable distance. In a



Flyrock problems are caused by cratering as a result of inadequate stemming or too small a front row burden.

Typical vibration record.

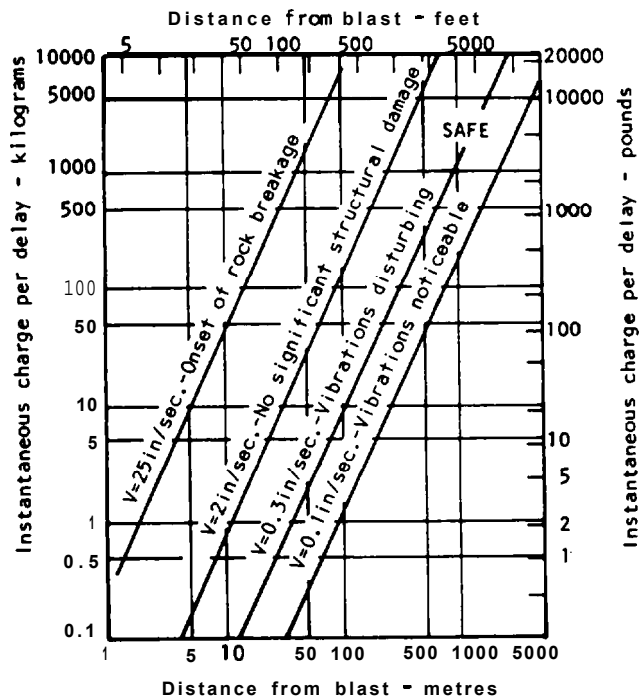
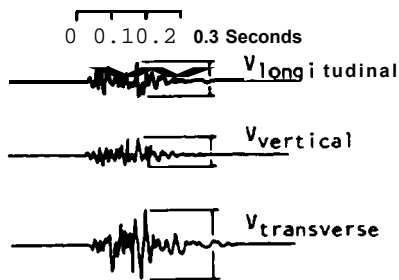


Figure 11.17: Plot of particle velocities induced at given distances by particular charges.

study by the Swedish Detonic Research Foundation(287), the maximum distance which boulders were thrown was studied for a range of powder factors and the results are plotted in Figure 11.18. This plot shows that, for the particular rock mass and blasting geometry tested, the flyrock problem could be eliminated by reducing the powder factor to 0.2 kg/m³. A low powder factor such as that required to eliminate flyrock may not give adequate fragmentation and hence blasting mats would have to be used to cover the blast.

An alternative to changing the powder factor would be to increase the front row burden and/or the length of the stemming column but, as pointed out earlier in this chapter, this could give rise to choking the blast and to poor fragmentation of the rock above the top load. A stemming column length of 40 blast hole diameters is recommended by the Swedish Detonic Research Foundation for the control of flyrock and this is in line with the optimum stemming column length of 0.67 to 2 times the burden which is recommended by Hagan(269).

A relationship between the blast hole diameter and the throw distance for a boulder of given size was established by the Swedish Detonic Research Foundation(287) and is plotted in Figure 11.19. From this figure it can be seen that a 1 m granite boulder would be thrown 40 m (130 ft.) by the cratering of a 50 mm (2 inches) diameter charge. This result should provide ample inducement for the blasting engineer to either do something about controlling flyrock or else stand a long way from the blast.

Airblast and Noise Problems Associated with Production Blasts

These two problems are taken together because they both stem from the same cause. Airblast, which occurs close to the blast itself, can cause structural damage such as the breaking of windows. Noise, into which the airblast degenerates with distance from the blast, can cause discomfort and will almost certainly give rise to complaints from those living close to the construction site.

Factors contributing to the development of an airblast and noise include overcharged blast holes, poor stemming, uncovered detonating cord, venting of developing cracks in the rock and the use of inadequate burdens giving rise to cratering. The propagation of the pressure wave depends upon atmospheric conditions including temperature, wind and the pressure-altitude relationship. Cloud cover can also cause reflection of the pressure wave back to ground level at some distance from the blast.

Figure 11.20 gives a useful guide to the response of structures and humans to sound pressure level. Legislation in the USA now restricts blast noise to 140 dB which corresponds to the "no damage" threshold shown in Figure 11.20.

The decrease of sound pressure level with distance can be predicted by means of cube root scaling. The scaling factor with distance K_R is given by:

$$K_R = R/\sqrt[3]{W} \quad (125)$$

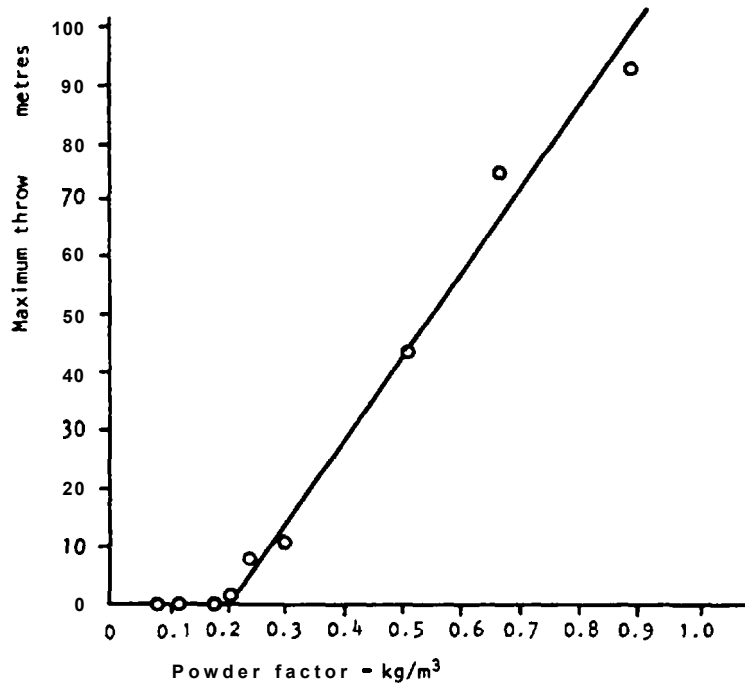


Figure 11.18 : Maximum throw of flyrock as a function of powder factor in tests by Swedish Detonic Research Foundation.

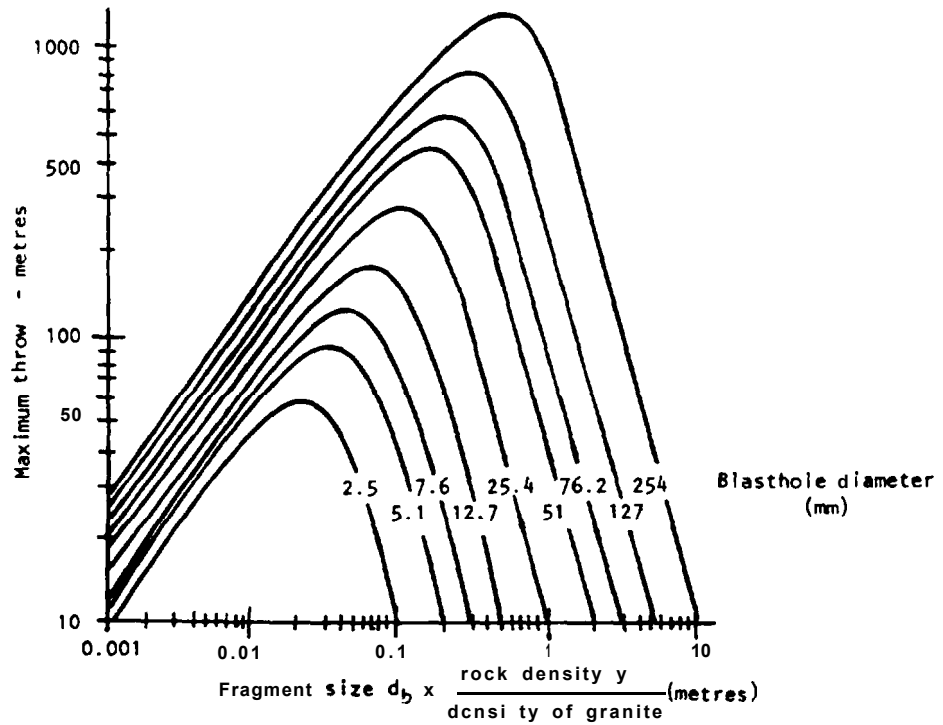
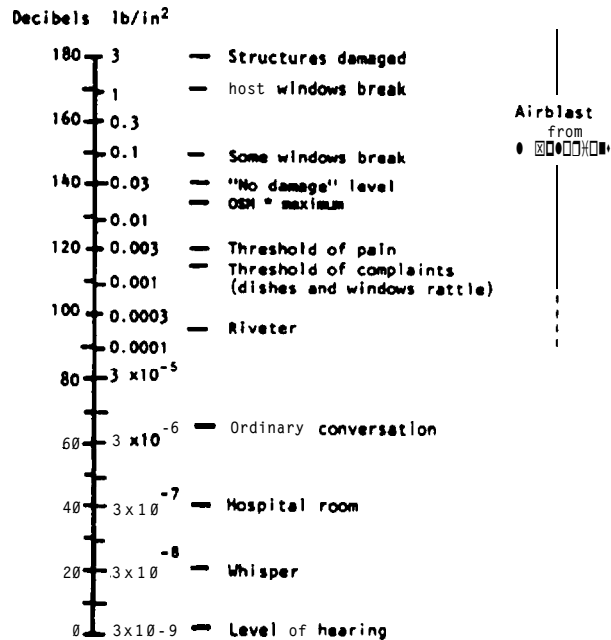


Figure 11.19 : Relationship between fragment size and maximum throw established by Swedish Detonic Research Foundation.



• OSM = Office of Surface Mining Reclamation and Enforcement,, see Skelly and Loy (291)

Figure 11.20: Human and structural response to sound pressure level. After Ladegaard-Pedersen and Dally 272.

where R is the radial distance from the explosion
W is the weight of charge detonated

Figure 11.21 gives the results of pressure measurements carried out by the U.S. Bureau of Mines in a number of quarries (reported by Ladegaard-Pedersen and Dally(276)). The burden B was varied and the length of stemming was 2.6 ft. per inch diameter of borehole. For example, if a 1,000 lb. charge is detonated with a burden of 10 ft., then the over-pressure at a distance of 500 ft. is found as follows:

$$\begin{aligned}
 R/\sqrt[3]{W} &= 500/\sqrt[3]{1000} \\
 &= 50 \\
 B/\sqrt[3]{W} &= 10/\sqrt[3]{1000} \\
 &= 1
 \end{aligned}$$

From Figure 11.21, over-pressure equals about 0.006 psi.

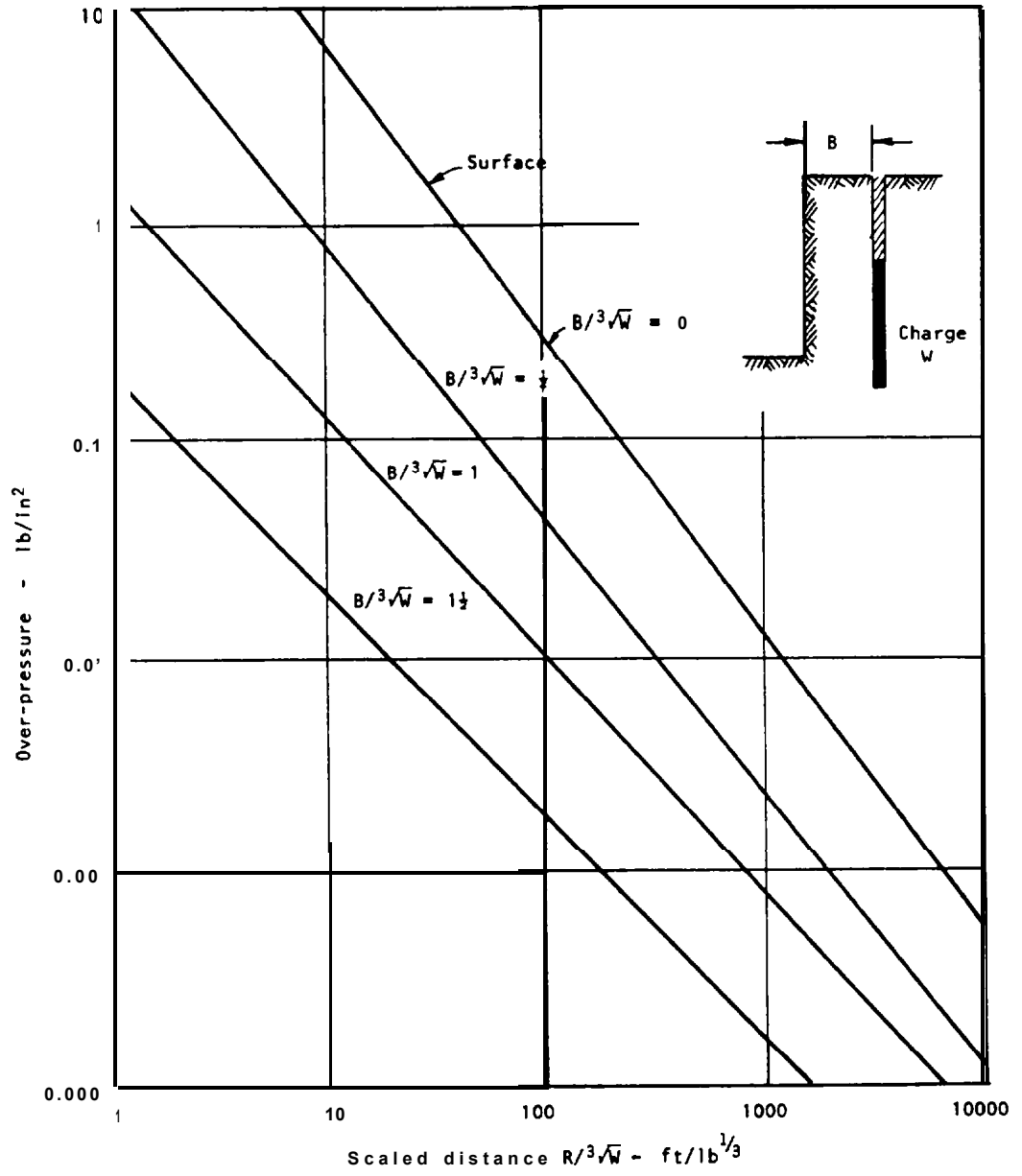


Figure 11.21: Over-pressure as a function of scaled distance for bench blasting.

Chapter 11 references

257. LANGEFRS, U., and KIHLMSTROM, B. The modern technique of rock blasting. John Wiley and Sons, New York, Second edition, 1973, 405 pages.
258. GUSTAFSSON, R. Swedish blasting technique. Published by SPI, Gothenburg, Sweden, 1973, 378 pages.
259. COOK, M.A. The science of high explosives. Reinhold Book Corp., New York, 1958.
260. JOHANSSON, C.H., and PERSSON, P.A. Detonics of high explosives. Academic Press, London, 1970.
261. DU PONT DE MEMOURS & CO. INC. Blaster's Handbook. Du Pont, Wilmington, Delaware, 15th edition, 1966.
262. FRAENKEL, K.H. Manual on rock blasting. Atlas Copco AB and Sandvikens Jernverks AB, Stockholm, Sweden, Second edition, 1963.
263. C.I.L. Blaster's handbook. Canadian Industries Limited, Montreal, Quebec, 1959.
264. I.C.I. Blaster's Practice. Imperial Chemical Industries Limited, Glasgow, 1975.
265. MCINTYRE, J.S., and HAGAN, T.N. The design of overburden blasts to promote highwall stability at a large strip mine. Proc. 11th Canadian Rock Mechanics Symposium. Vancouver, October 1976.
266. HARRIES, G., and HERCER, J.K. The science of blasting and its use to minimize costs. Proc. Australian Inst. Min. Metall. Annual Conf. Adelaide, Part B, 1975, pages 387-399.
267. PERSSON, P.A. Bench drilling - An important first step in the rock fragmentation process. Atlas Copco Bench Drilling Symposium, Stockholm, 1975.
268. ANTILL, J.M. Modern Blasting Techniques for Construction Engineering. Australian Civil Engineering and Construction. November 1964, page 17.
269. HAGAN, T.N. Blasting Physics - What the operator can use in 1975. Proc. Australian Inst. Min. Metall. Annual Conf. Adelaide. Part B. 1975, pages 369-386.
270. WINZER, S.R., and RITTER, A., A field test of Du Pont new technology MS delay electric blasting caps. Martin Marietta Laboratories MML TR 79-44C, 1979.
271. BORADBENT, C.D. Predictable blasting with in situ seismic surveys. Mining Engineering. S.M.E., April 1974, pages 37-41.
272. PIT SLOPE MANUAL (CHAPTER 7), Perimeter blasting. Canada Centre for Mineral and Energy Technology; Energy Mines and Resources, 65 pages.
273. DU PONT OF CANADA. Controlled blasting. Booklet by du Pont of Canada Ltd., 1964.

274. **MCCAULEY, M.L., HOOVER, T.P. FORSHYTH, R.A.** Presplitting. California Division of Highways, Research Report DA-DOT-TL-2955-4-74-32, 1974.
275. **BUREAU OF PUBLIC ROADS.** Presplitting - A controlled blasting technique for rock cuts. U.S. Dept. of Commerce, Washington, D.C., 1966, 36 pages.
276. **LADEGAARD-PEDERSEN, A., and DALLY, J.W.** A review of factors effecting damage in blasting. Report to the National Science Foundation. Mechanical Engineering Department, University of Maryland. January 1975, 170 pages.
277. **U.S. OFFICE OF SURFACE MINING REGULATIONS.** Section 816-62.
278. **BOLLINGER, G.A.** Blast vibration analysis. Feffer and Slnons, Inc. Lodong and Amsterdam, 1971.
279. **CRANDELL, F.J.** Ground vibrations due to blasting and its effects upon structures. J. Boston Civil Engineers. Vol. 36, No. 2 1949, pages 222-245.
280. **DEVINE, J.F., BECK, R.H., MEYER, A.V.C., and DUVALL, W.I.** Vibration levels transmitted across presplit failure plane. U.S. Bureau of Mines Report of Investigations. 6695, 1966, 29 pages.
281. **DEVINE, J.F., BECK, R.H., MEYER, A.V.C. and DUVALL, W.I.** Effect of charge weight on the vibration levels in quarry blasting. U.S. Bureau of Mines Report of Investigations. 6774, 1966, 37 pages.
282. **DUVALL, W.I., DEVINE, J.F., JOHNSON, C.F., and MEYER, A.V.C.** Vibration from blasting at Iowa Limestone quarries. U.S. Bureau of Mines Report of Investigations. 6270, 1963, 28 pages.
283. **DUVALL, W.I., and FOGELSON, D.E.** Review of Criteria for estimating damage to residences from blasting vibrations. U.S. Bureau of Mines Report of investigations 5968, 1962, 19 pages.
284. **DUVALL, W.I., JOHNSON, C.F., MEYER, A.V.C., and DEVINE, J.F.** Vibrations from Instantaneous and millisecond-delayed quarry blasts. U.S. Bureau of Mines Report of Investigations. 6151, 1963, 34 pages.
285. **EDWARDS, A.T. and NORTHWOOD, T.D.** Experimental Studies of the effects of blasting on structures. The Engineer. Vol. 210, September 30th, 1960, pages 538-546.
286. **LEET, L.D.** Vibrations from blasting rock. Harvard University Press. Cambridge, Mass., IWO.
287. **LUNDBORG, N., PERSSON, A., LADEGAARD-PEDERSEN, A and HOLMBERG, R.** Keeping the lid on flyrock in open pit blasting. Engineering and Mining Journal. May 1975, Pages 95-100.

288. **DUVALL, W. I.** Design requirements for instrumentation to record vibrations produced by blasting. U.S. Bureau of Mines Report of Investigations, 6387, 1965. 5 pages.
289. **ORIARD, L.L.** Blasting effects and their control in open pit mining. **Proc. 2nd Intl. Cont. on Stability in Open Pit Mining.** Vancouver 1971. Published by **AIME**, New York, 1972, pages 197-222.
290. **KONYA, C.J., and WALTER, E.J.** Rock Blasting. U.S. Department of Transportation Technical Report, **May 1985**, 355 pages.
291. **SKELLY and LOY.** A **Compliance Manual - Methods for Meeting OSM Requirements.** **Published** by McGraw Hill, Inc., 1979.

Chapter 12 Stabilization and protection measures

Introduction

Expenditure of funds for slope stabilization programs is often justified because unstable slopes can rarely be tolerated on highways, and because weathering of the rock tends to cause deterioration of slopes with time. This chapter describes alternative stabilization methods and the conditions in which they can be used. Design of the stabilization work is carried out by the methods described in Chapters 7 through 10 for the appropriate type of slope failure; references to these design methods are included with each of the stabilization procedures. Note that each design method is particular to the type of slope failure, i.e. planar, wedge, circular or toppling, and it is essential that the type and cause of failure be identified.

The first step in planning a stabilization program is to identify potentially hazardous slopes which usually requires accurate observations of slope stability conditions and the maintenance of records over a considerable time period. These records, which can be kept by maintenance personnel, should contain the following information.

- Location of slope.
- Weather conditions, particularly during 24 hours preceding failure.
- Volume of failed material and height of fall.
- Time taken to clear rock and stabilize slope.
- Belays to traffic and damage to highway and vehicles.
- Stabilization work carried out with time and costs.
- Warning received of failure from prior falls, or movement monitoring instruments (see Chapter 13).

These reports should be supplemented with photographs to record changes in conditions of the slope and the progress of stabilization work. Photographs in stereo pair are particularly useful for planning stabilization work. They can be taken with a regular 35 mm camera by taking two photographs from positions which are separated by a distance equal to about 2 to 5 percent of the distance of the camera from the slope. For more detailed work, terrestrial or oblique aerial photogrammetry can be used from which contour maps and cross-sections can be drawn up. This information is usually required in making detailed stability studies and calculation of excavation volumes. High altitude aerial photographs rarely provide information sufficiently detailed for rock slope engineering.

By relating these records to the geological data contained on stability assessment sheets (11) discussed previously (see Figure 1.6), information will soon be developed on the most hazardous areas and the consequences of the failure. This can then be used to schedule stabilization work, keeping in mind that slopes that have already failed are likely to be more stable than similar slopes that have not yet failed.

The selection of an appropriate stabilization method depends not only on the technical feasibility, but also costs and the

ease of installation. For example, the least expensive construction cost for rock bolt installation may be to use a crane to put in a few, high capacity anchors. However, if the use of the crane will disrupt traffic because the shoulder is too narrow to accommodate the crane, then it would be preferable to have men on ropes drilling holes for a greater number of smaller anchors because they can work independently of the traffic. Another consideration is that stabilization work should be effective over a long time period and corners should not be cut to save costs. For example, anchors should be protected against corrosion, and blasting should be controlled to ensure that the rock in the new face is not fractured by the explosives.

The design of stabilization work should be carried out by experienced personnel who can draw on their knowledge of previous failures to estimate such factors as rock strength and groundwater conditions. They will also know which stabilization methods are best suited to the physical constraints at the site. Highway personnel with geological engineering training who are familiar with local conditions should be assigned to both the design and construction supervision tasks so they obtain feedback on the application of their designs. Consultants who specialize in rock slope engineering may also be required, on occasion, to assist highway personnel with unusual problems.



Installing rock bolts from a crane and basket.

Rock slope stabilization work should usually be carried out by specialist contractors who have experienced men and appropriate equipment. For scaling and rock bolt installation, equipment would include compressors, hand-held percussion drills, a loader to clear broken rock from the highway and assorted ropes, hoses, pipes, drill steel and grout pumps. The men will either use climbing ropes to access the face or work off an air-winch operated platform ("spider"). For larger excavation jobs, cranes and track-mounted drills and dozers may be required. Rock work that requires men to climb on steep slopes is hazardous when snow and ice cover the slope so these projects should not be scheduled for the winter in areas where such climatic conditions exist. However, rock excavation work using heavy equipment can proceed in almost all weathers. The types of contracts which are suitable for rock excavation and stabilization work are discussed in Chapter 14.

STABILIZATION METHODS

Slope stabilization methods can be divided into three categories as follows:

- I Methods which reduce or eliminate the driving forces, e.g., reduction in water pressure or excavation.
- II Methods which increase the resisting force, e.g., installation of support.
- III Methods which protect the highway from rock falls, or warn of hazardous conditions, e.g., rock sheds, warning fences.

The following sections of this chapter describe these stabilization methods, and the conditions in which they are applicable.

I STABILIZATION METHODS THAT REDUCE DRIVING FORCES

Drainage

As discussed in Chapter 6, groundwater pressures usually have a significant effect on stability. This is shown by the great number of slope failures that occur after heavy rainfall, during snow-melt periods and during the winter when the face freezes and water pressures increase. Consequently, stability conditions can often be improved by reducing water pressures, if they exist, by installing drainage systems. Furthermore, drainage is often an inexpensive method of stabilization.

The installation of drainage, as the primary stabilization method, should only proceed after careful investigation because one must be certain that water pressures are the primary cause of instability. Also, it can be difficult to produce effective drainage of the slope, and ensure that the drainage system is effective over the full life of the slope. To overcome these problems, piezometers should first be installed to measure the actual pressure in the slope and calculate its effect on stability. These piezometers can be used in the future to monitor the drawdown produced by the drains. Another problem is that the water is contained in the fractures in the rock so that the drains will only be effective if they intersect these water carrying fractures. Also, the drains may eventually become blocked with ice or silt and the pressures will increase.

If the stability studies show that drainage is the best stabilization method to use, then there are a number of alternatives from which to select (see Figure 12.1). This influence of water pressure on plane failures is calculated using the design charts in Figure 7.31 and similar calculations can be carried out for circular failures using the design charts on page 9.8 through 9.13. Appendix 3 shows the analysis method for wedge failures.

Surface drains: If water is flowing down the slope and into tension cracks, ditches can be dug along the crest to divert the water and prevent ponding, and the tension crack can be covered with clay or plastic sheets. If plastic sheets are used, they should be as strong as possible and covered with sand to prevent damage from wind and vandalism. The sides of ditches can be reinforced with burlap bags filled with a sand/cement mixture, and if it is suspected that water is leaking from the ditch, it could be lined with shotcrete, asphalt, or other means.

Horizontal drains: If there is no surface water to remove, then, it is necessary to drill holes to drain the subsurface water. The simplest method is to drill horizontal holes into the face to intercept the water table behind the potential failure surface, with a minimum depth of about 1/3 of the slope height. The spacing between holes depends upon the permeability of the rock, with closer spacing required in less permeable rock. Spacing may range from 20 to 100 ft. The direction of the holes should be chosen so that the maximum number of water carrying fractures are intercepted, and they are usually inclined slightly above the horizontal. If there is any danger that the holes will cave, then they should be lined with a perforated plastic pipe with the discharge in the ditch so that the flowing water does not erode the face.

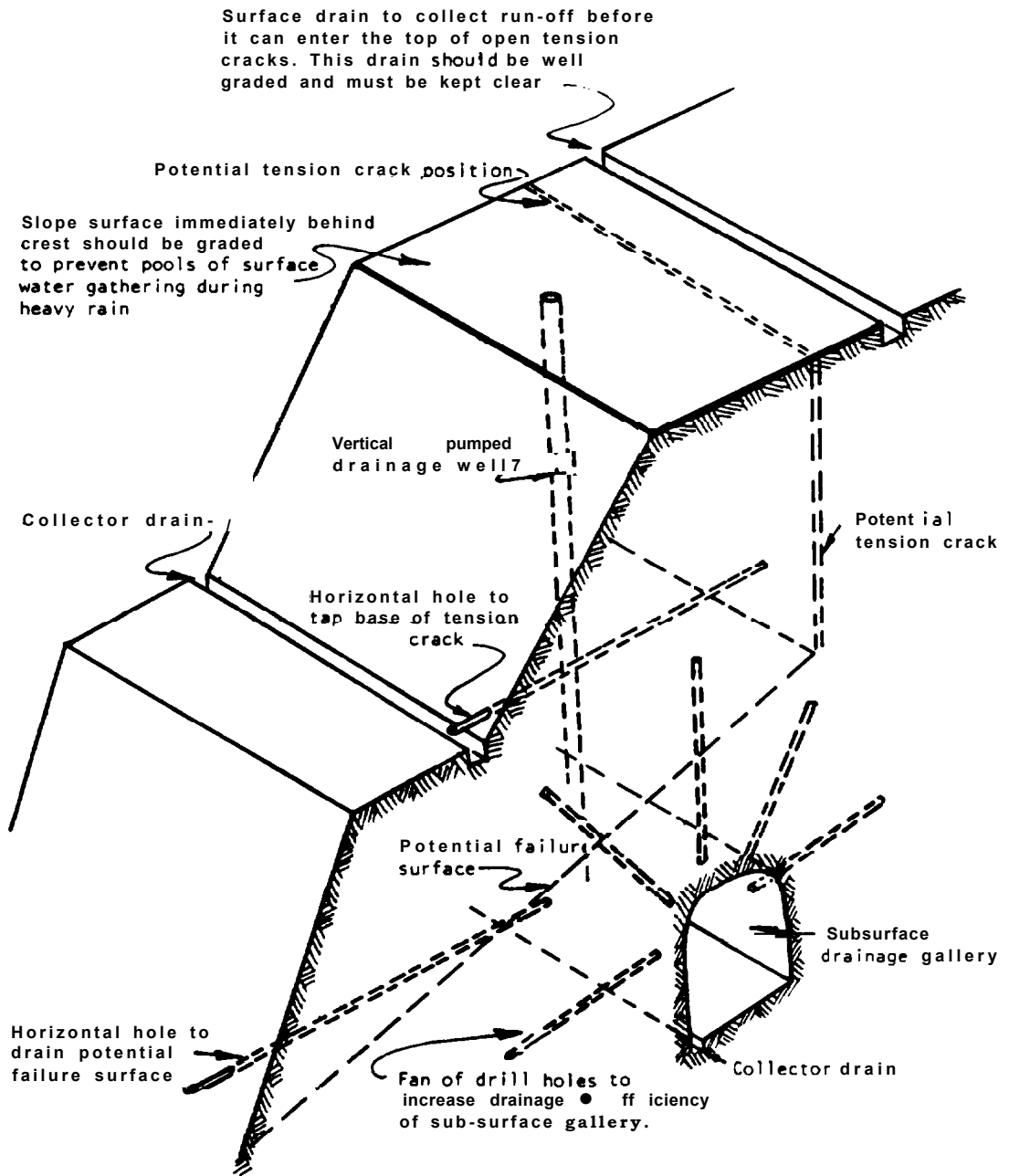
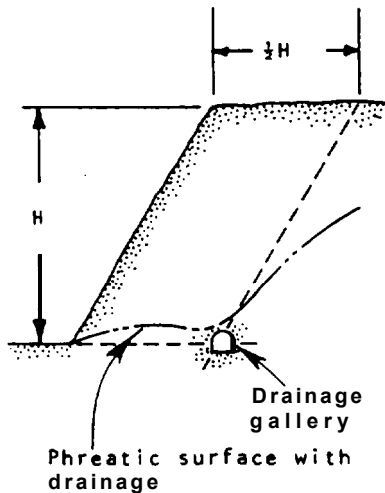


Figure 12.1: Slope drainage and depressurization measures.

Drain holes can be drilled with a standard track-mounted drill, and holes can be fanned out from one location to save moving and setting up time. Drill cuttings should be thoroughly cleaned from the hole to ensure that these fine particles do not inhibit drainage. In particularly soft ground, an Aardvark drill can be used which carries the casing into the hole as it is drilled. When the hole is complete, the bit is dropped off and the rods are removed from inside the casing.

It should be kept in mind that the volume of water contained in the fractures can be very small so that the drains may be producing effective drawdown in the slope despite there being a very low discharge. In fact, no water may be visible at all if it evaporates as it reaches the face. This shows the importance of monitoring drawdown with piezometers.

Pumped wells: pumped wells consist of vertical drill holes about 6 inches in diameter, lined with a perforated casing and with a submersible electric pump at the bottom. The diameter of the cone of drawdown produced by the pump increases as the permeability increases and the wells should be spaced accordingly (294).



Optimum location for subsurface drainage gallery in a slope.

It is unlikely that pumped wells would be a permanent stabilization measure because of the necessity of supplying power and maintaining the pumps. However, they could be used as a temporary measure, or during construction, to stabilize the slope while horizontal drains or anchors are being installed.

Drainage galleries: drainage galleries can be the most effective, but most expensive method of draining a slope. The effective diameter of this gallery can be increased by drilling fans of drill holes around the gallery; holes may also be required to pierce layers of low permeability rock which are inhibiting downward flow of the groundwater (295).

Drainage galleries are usually only justified to stabilize large failures where the forces involved are so great that it is uneconomical to unload the slope by excavating material from the crest. The gallery can be driven without interrupting traffic on the highway, and the cost of excavation may be lower than that of a large excavation project, unless the rock is very soft and extensive support is required. The margin sketch shows the optimum position for a gallery (296).

Excavation

The principle of stabilization by excavation is that removal of material from the upper portion of the slope reduces the driving force. Alternatively, in the case of small failures, the entire loose rock is removed. The following is a description of alternative excavation stabilization measures.

Scaling and Trimming

Loose, overhanging or protruding rock on the face of the slope can be removed by scaling or trimming (see Figure 12.2 a,b). Scaling involves the use of hand scaling bars, hydraulic splitters or light explosives to remove isolated pieces of loose rock, while trimming involves the removal of overhanging and potentially unstable rock. These operations are usually carried

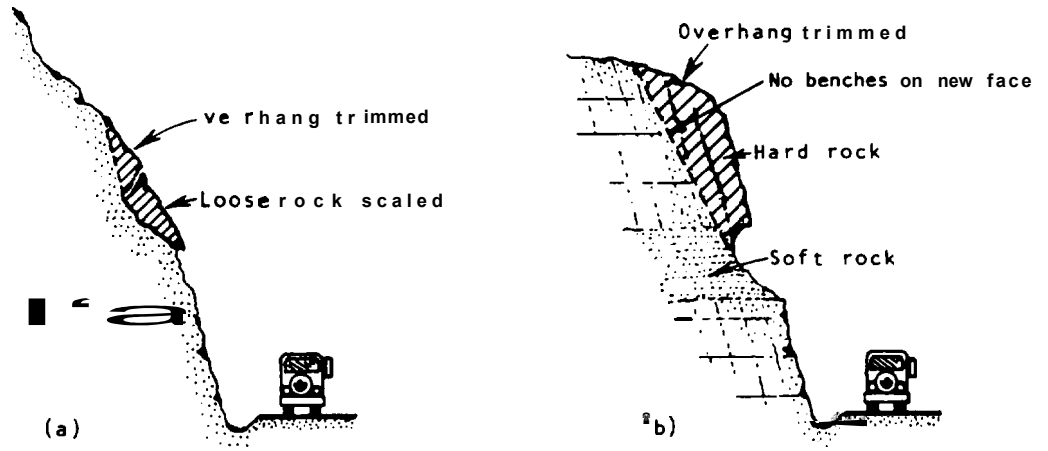


Figure 12.2: Scaling and trimming.

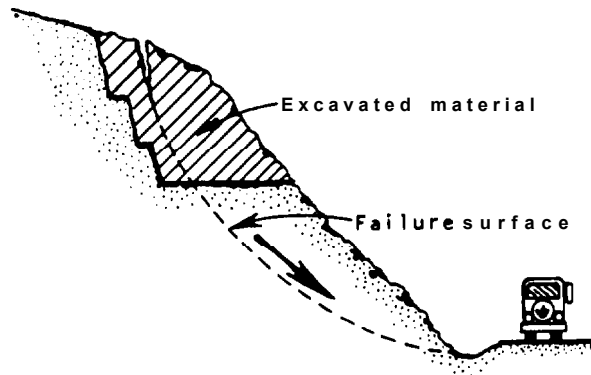


Figure 12.3: Unloading

out, for high slopes, by men working from ropes or on cable suspended platforms ("spiders") and, for lower slopes, from cranes or hydraulic booms. If a crane is used the basket must be tied to the slope to prevent it from swinging away from the face. Scaling and trimming are slow operations because moving on the face is slow and only light, hand-held equipment can be used.

Careful inspections of all scaling operations should be carried out to determine the rock to be removed and ensure that the new face is stable. For example, in Figure 12.2(a) hand scaling of the loose rock will form an overhang that will have to be trimmed with light blasting. All blasting that is carried out should be of sufficient strength to break the rock and not damage the remaining slope. This requires the drilling of carefully aligned, closely spaced holes and the use of light charges. See Chapter 11 for details of controlled blasting procedures.

The frequency of scaling may vary between 2 and 20 years and depends upon the rate at which the rock weathers and the influence of such factors as ice-jacking, root growth and traffic use.

The trimming operation shown in Figure 12.2(b) has created a uniform slope face without benches. It is the recommendation of the writers that intermediate benches on slope faces should be avoided because they rarely have the width to act as effective rock catchment areas; it is preferable to form a wide ditch at the toe of the slope. The actual width of benches is usually less than the design width due to loss of rock along the crest and failure to remove rock at the toe of the upper cut. Furthermore, small rock falls that do accumulate on the benches, further reduce their width and eventually form "ski jumps" which project falling rocks outwards to the highway. Cleaning of accumulated rock falls on benches is rarely carried out because of the danger of working on high rock faces, and is impossible if a substantial fall cuts the access on to the bench.

Intermediate benches may be effective if they have widths of at least 30 ft. as shown in Figure 12.3, where the crest of the slope has been raved. The required width of the bench should be checked on the ditch design chart (Figure 12.10a) which shows the required width and depth for the slope dimensions. If the width is insufficient, a berm or gabion should be constructed along the outside edge to trap rolling rock, but only if the crest is stable.

Unloading

Where overall failure of the slope is occurring, rather than falls of individual blocks of rock, stabilization can be achieved by excavating (unloading) the crest to reduce the driving force (Figure 12.3). The volume of material to be removed is determined by stability analysis methods described earlier in the manual. The procedure for a back analysis is as follows. The position of the failure surface is estimated from the position of the tension crack, the geology, and possibly drilling.

12.8

The type of slope failure and the causes of failure are identified and a stability analysis is carried out using a factor of safety of 1.0 to determine the rock strength parameters. Then, using the same strength parameters and groundwater level, additional analyses are carried out to determine how much material must be unloaded to increase the factor of safety to an acceptable level. Stability of all four types of slope failures - planar, wedge, circular and **toppling** - depend upon the slope height, which is reduced by unloading.

Since it may be necessary to unload as much as 1/3 of the failure in order to stabilize it, this work will have to be done with earth-moving equipment except in the case of minor slides. For this equipment to have sufficient working space, the cut will have to be at least 20 ft. wide and preferably 30 to 40 ft. wide. If blasting is required, vibrations should be kept to a minimum by reducing the charge weight per delay as much as possible (see Chapter 11), because large vibrations may be sufficient to cause the slope to fail. If the slope is moving during excavation, movement monitoring systems (Chapter 13) should be set up to provide a warning of deteriorating stability conditions. This will ensure, if failure were to occur, that men and equipment will have time to evacuate the slope.

Resloping

This stabilization method is applied in similar conditions to the unloading method when overall slope failure is occurring. If it appears doubtful that unloading will achieve long-term stability because extensive movement and rock breakage have occurred, then it would be necessary to excavate the slope at a flatter slope angle - "resloping" (see Figure 12.4). Much the same design and excavation methods and precautions are applicable in both unloading and resloping. The new slope should have a face angle that produces a satisfactory factor of safety based on the strength and groundwater values determined from back analysis. In designing the cut dimensions, sufficient space must be left at the toe of the slope for equipment to operate which means that a triangular shaped excavation (in section) cannot be made. Intermediate benches should not be incorporated in the slope design unless a significant width, say 30 ft., can be accommodated.

In both unloading and resloping, additional practical matters to consider are property ownership of the land along the crest and available areas for the disposal of the excavated material. Long hauls may be expensive, although there is always the possibility that the material could be used for fill elsewhere at some cost savings over quarried material. Finally, controlled blasting should be used to minimize rock damage.

II REINFORCEMENT AND SUPPORT STABILIZATION METHODS

The following is a description of stabilization methods in which the forces resisting failure are increased by installing either reinforcement or support.

Reinforcement consists of installing bolts or cables across the failure surface to increase its strength, while support consists of installing dowels, walls, gabions or buttresses at the toe of the failure. Usually, reinforcement is used for smaller failures where the forces are not great and the tension that can be applied to the anchors is sufficient to produce a significant increase in the factor of safety. However, very high

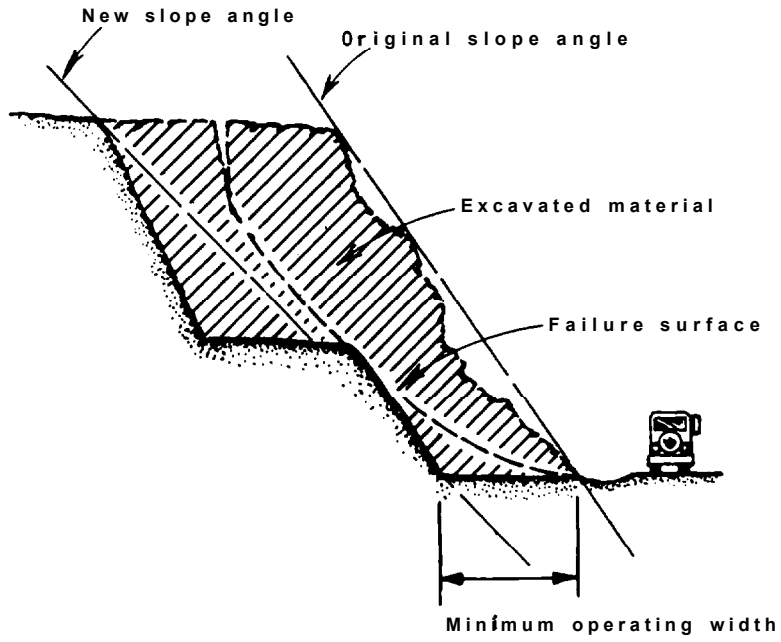


Figure 12.4: Resloping.

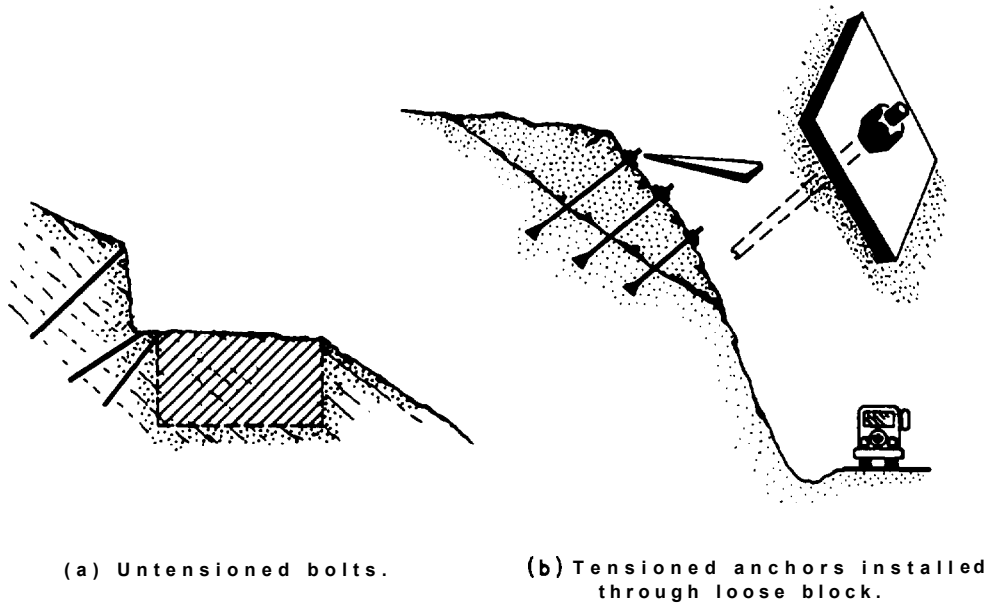


Figure 12.5: Rock bolt installations.

capacity, multistrand cables are available to reinforce large rock masses.

Support ranges from dowels to hold small blocks in place, to buttresses that provide monolithic support under large unstable blocks. The following is a description of the alternative stabilization measures.

Rock Bolts and Cables

If there is potential for a block to slide down a plane, the resistance forces can be increased by increasing the normal load on the plane. This can be achieved by installing rock bolts or cables, anchored in stable rock behind the failure surface, and applying a tension (see Figure 12.5). The reactions within the rock to this tension are normal and shear forces acting across the failure plane, the relative magnitude of which depend upon the orientation of the bolt with respect to the failure plane. These forces have a much greater influence on increasing stability than the shear strength of the steel across the failure plane. Anchors can be used to stabilize both individual blocks and slopes ranging in height from about 10 ft. to several hundred feet. Detail of design methods for anchor support are given in Chapter 7 (page 7.17) by Littlejohn and Bruce(297), the Post Tensioning Institute(298) and other authors(299-303). Different types of rock anchors are discussed below.

Rock Bolts

Rock bolts are rigid steel rods ranging in size from about 5/8 inch to 2 inches in diameter and up to about 100 ft. in length; long bolts are usually coupled together in 20 ft. sections. The surface of the bar is often corrugated, like reinforcing steel, to improve the steel/grout shear strength. Rock bolts are either grouted into the hole without tensioning and subsequent movement of the rock tensions the bolt (Figure 12.5(a)), or they are tensioned at the time of installation (Figure 12.5(b)).

Untensioned bolts (sometimes referred to as dowels) can be installed from the floor of a bench so that subsequent removal of this bench and slight movement of the rock will activate the support provided by the steel. If the bolt was tensioned, movement of the rock as a result of excavation may overstress the bolt. The technique shown in Figure 12.5(a) should be used whenever possible because, by minimizing movement of the rock on the failure planes, the maximum rock strength is retained. Also the cost of installing the bolts is much less than installing tensioned bolts when the excavation is complete and a crane would be required for drilling. Untensioned bolts are installed by drilling a hole to the required depth, partially filling it with cement or epoxy grout, and pushing in the anchor so that it is grouted over its full length. Sufficient time should be allowed for the grout to set before setting off the next blast, and vibrations in the reinforced wall should be kept to acceptable levels (see Chapter 11).

Tensioned bolts are installed in blocks and slopes which are already showing signs of instability and immediate support is required. Any additional movement of the rock may decrease the

shear strength of the failure surface. Methods of installing and tensioning these bolts are discussed below:

Tensioned bolts are made from high tensile strength steel and have threads on the exposed end for a bearing plate and nut. The different types of anchors that can be used include mechanical expansion shells, cement grout and epoxy grout. Both mechanical and epoxy grouts allow tensioning to be carried out soon after installation which is an advantage if access to the site is difficult. Mechanical anchors are usually some form of wedge which is expanded by turning or driving the bolt. Two component epoxy resins are packaged in plastic tubes and are mixed by rapidly rotating the bolt. By using resin with different setting times, the anchor will set in a few minutes and the remainder will set after the bolt has been tensioned.

Cement or epoxy grout is usually used in soft rock where mechanical anchors could slip, and cement grout is used for all high capacity, permanent anchors. Cement grout should have a non-shrink agent added, and high-early strength cement should not be used because it is brittle and sometimes contains reagents that accelerate corrosion. The length of the anchor zone is calculated using the assumption that the shear stress is uniformly distributed along the periphery of the hole. Therefore, the required bond length (L) is calculated from the following equation:

$$L = \frac{T}{(\pi d) \tau}$$

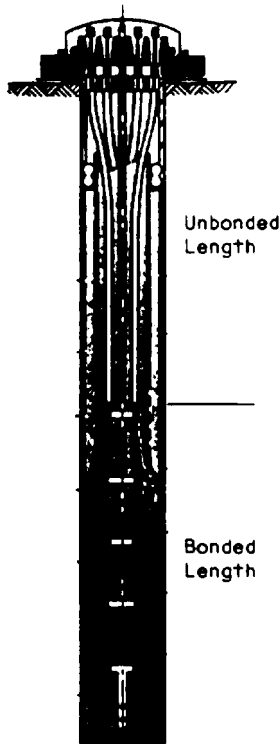
where T is the applied tension and d is the hole diameter. The working rock/grout interface shear strengths (τ) used for design varies from about 50 psi in weak rock to 200 psi in strong rock. In general, the working bond strength is about 1/20 to 1/30 of the uniaxial compressive strength of the rock. It is also found that the steel/grout shear strength is usually greater than the rock/grout shear strength.

Tensioning is carried out by pulling on the bolt with a hydraulic jack to a load of about 50 percent of the yield load and locking in this tension by tightening the nut. Alternatively, a torque wrench can be used for tensioning, but this is likely to be less reliable than using a hydraulic jack.

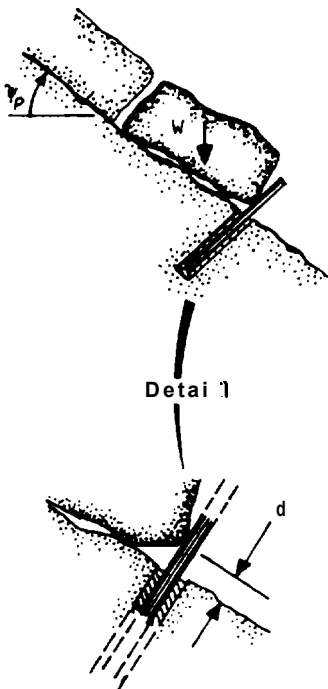
After tensioning, all bolts should be fully grouted to provide corrosion protection and to "lock in" the tension. Mechanical anchors should only be considered temporary means of maintaining tension because corrosion of the anchor and creep in the highly stressed rock around the anchor can lead to loss of load. The bolt manufacturers' recommended installation procedure should be carefully followed.

Cables

Cables can be used to reinforce rock slopes in a similar manner to rigid bolts as described above. However, cables have a greater strength than rigid bolts of the same diameter and so can be used to stabilize particularly large rock



Dywidag corrosion protected cable anchor



Dowel installation to support sliding block.

masses (304-306). For example, a 1 inch diameter rigid bolt may have a working tensile strength of 25,000 lb. while a 1/2 inch, 7-wire strand cable has strength of 40,000 lb. If greater strengths are required, then bundles of as many as 50 cables can be used. A further advantage of cables is that their flexibility allows them to be coiled which facilitates installation where space is limited and rigid bars could only be used if they were coupled together in short lengths. Cables can be either tensioned or untensioned in identical applications to rigid bolts and the same design methods (see Chapter 7) are applicable.

Because of the high tension on cables, cement grout anchorage is usually used which must be allowed to set for several days before tensioning. Before installation begins, the hole should be tested to see if fractures have been intersected through which grout could flow out of the hole and prevent full embedment. If the hole cannot be filled with water, then it should be filled with a low slump grout to seal the fractures and re-drilled when the cement is partially set (299).

The anchor is formed by pumping grout down a grout line so that the hole is filled from the bottom, with particular attention being paid to ensuring that the head is fully protected from corrosion with grout and anti-corrosion agents. When the grout has set, the tension is applied with a hydraulic jack using load/deformation monitoring procedures as specified by the Post Tensionary Institute (298). The applied tension is maintained by securing the cables with tapered wedges which are pushed into tapered holes in the bearing plate. When the grout has set, the tension is applied with a hydraulic jack. The applied tension is maintained by securing it at the collar with tapered wedges by using a bearing block with a tapered hole through which the cable passes. The pair of tapered wedges are fitted around the cable and pushed into the tapered hole so that they grip the cable and hold the tension. The size of the bearing plate should be sufficient to distribute the load without fracturing the rock under the plate.

Dowels

Dowels are lengths of reinforcing bars, or blocks of reinforced concrete, installed at the toe of potentially unstable blocks to provide passive support against sliding (see Figure 12.6). This support is provided by the shear and bending strength of the reinforcing steel, or the shear strength of the reinforced concrete. The number of dowels required to support a block is calculated as follows (see margin sketch).

$$\text{Factor of Safety, } F = \frac{W \cos \psi_0 + T \tan \phi + R}{W \sin \psi_0} \quad (126)$$

- where: W = weight of block
- ψ_0 = inclination of sliding plane
- ϕ = sliding plane friction angle
- R = support provided by dowel

The design methods described in Chapter 7 can be used to develop equations which include the effects of cohesion and water pressure.

The support provided by the dowel is the lesser of either its bending strength or its shear strength, as follows:

$$\text{Bending, } R_b = \frac{\sigma_t \cdot I}{r \cdot d} \quad (127)$$

$$\text{Shear, } R_s = \tau \cdot \pi \cdot r^2 \quad (128)$$

where: σ_t = tensile strength of steel
 I = moment of inertia of bar
 r = radius of bar
 d = moment arm of load on dowel
 τ = shear strength of steel.

These equations show that the support is increased by increasing the diameter of the bar, and that the bending resistance is decreased by having the block load the dowel above the embedment point in the rock. This illustrates the importance of installing the dowel tight against the face of the block.

If extra shear resistance is required, then a number of dowels can be placed in a group which is then encased in concrete poured against the rock face.

Commonly, dowels are 1 inch to 1-3/8 inch diameter reinforcing bar. Holes for this size dowel can be readily drilled with hand-held equipment. The depth of embedment is between 1 and 2 ft. depending on the quality of the rock. The dowel is fully grouted into the hole and a concrete cap can be cast over the dowel to protect it against corrosion and make sure the support is in contact with the rock. If it is not possible to drill the hole at the toe of the block, then the dowel can be bent against the face after installation.

Trial calculations of dowel support using equations (126) to (128) and typical rock slope parameters show that a 1-3/8 inch diameter bar will hold a block with a volume of about 5 to 15 cu.yd. Therefore, dowels should only be used to support small, isolated blocks where scaling would not produce permanent stabilization and bolting would be more expensive. As noted above, stronger dowels can be constructed from blocks of reinforced concrete.

Buttresses and Retaining Walls

Buttresses and retaining walls are usually reinforced concrete structures constructed at the toe of slopes, or beneath overhanging pieces of rock to provide support and resistance to sliding (see Figure 12.7(a)). Concrete buttresses are used to support overhangs that are difficult to remove because of access problems, or the danger that more rock higher up the slope may become unstable. The concrete buttress should have sufficient mass and strength to resist the weight of rock and also be securely tied to the face with reinforcing tie-backs grouted into holes drilled in the rock. The tie-backs will ensure that the buttress does not tilt outwards if the force applied by the rock is not coincident with the axis of the buttress.

The required strength of the buttress is the difference between the component of the weight down the failure plane and the re-

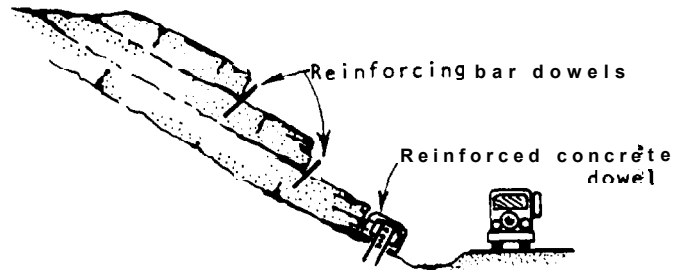


Figure 12.6: Dowels to support sliding blocks.

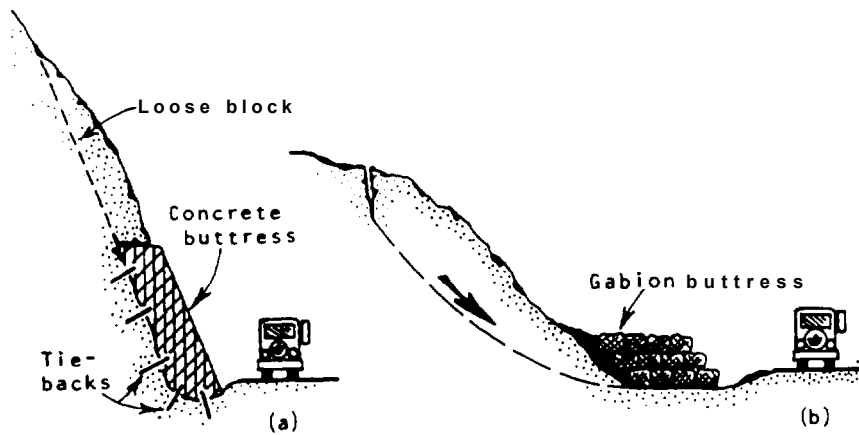


figure 12.7: Support at toe of unstable slopes.

sistence produced by the strength of this plane, with an appropriate factor of safety applied. The actual design used will depend upon the type of failure.

The top of the buttress must be in continuous contact with the underside of the block to prevent movement from occurring before the support becomes effective. In some cases, it may be necessary to use a nonshrinking agent in the last concrete pour to ensure good rock/concrete contact. To prevent build-up of water pressure behind the buttress, drain holes should be let through the concrete.

An alternative form of buttress to stabilize a sliding failure is to place a sufficient mass at the toe to support the slope (see Figure 12.7(b)). This can often be achieved by placing piles of free-draining rock, or installing gablons. Gablons are rock-filled wire baskets that can be jointed together to form walls that are strong and less expensive to construct than reinforced concrete. The dimensions of the baskets are usually cubes with 3 ft. side lengths. An advantage of a toe buttress is that the slope can be stabilized without providing access to the crest of the slope. A disadvantage of gablons is that they can be readily damaged by vandals.

Toe buttresses can usually only be used to stabilize small slides because the quantity of rock required can be substantial which requires considerable space between the toe of the slope and the highway. However, some relocation may provide sufficient space for a toe buttress.

Retaining walls are another means of stabilizing sliding slopes. They are usually concrete, or sometimes timber, structures designed to resist the inclined thrust of the slope. Methods of designing gravity type walls are described in the soils mechanics literature (307) and will not be discussed further here. In stabilizing rock slopes, particularly where there is little space between the highway and the toe of the slope, it is usually necessary to use tie-backs to prevent overturning. Tie-backs are rock bolts or cables that are anchored in stable rock behind the failure surface. The concrete wall is then built so that it forms a large reaction block to the tension generated in the anchors. The foundation of the wall should also be securely attached to sound rock with dowels to increase its resistance to sliding. Drain holes should be let through the concrete to prevent build-up of water pressures.

In some cases, a series of concrete pillars, instead of a continuous wall, may provide sufficient support and save on the quantity of concrete required.

Cable Lashing

Isolated blocks of loose rock that cannot be removed, can be secured in place with cables tensioned across the face of the block and anchored in sound rock on either side (see Figure 12.8). Tension can be applied by means of turn-buckles or "come-a-long" winches and then cable clamps are used to hold the tension. Care should be taken to ensure that each component of the system, i.e., cables, clamps, eye-bolts and rock anchors are equally strong and can withstand some impact loading in the event of sudden failure. Where the cable is in contact with

Design methods that quantify the impact loads of rock falls and avalanches are not well developed. However, recent work on snow avalanches using fluid mechanics principles can be applied to the design of rock sheds(314).

Tunnels are the most positive method of protection from rock falls. The cost of driving and supporting a tunnel may be less than the cost of constructing a shed, depending on how much support is required(315).

Relocation

In cases where a large landslide is occurring, it may be more economical to relocate the highway rather than to try and stabilize the slide. The feasibility of relocation will depend on such factors as property ownership and alignment, and care should be taken to ensure that the new location is on stable ground and not an extension of the original slide.

EXAMPLE OF SLOPE STABILIZATION PROJECT

The following is a description of a project that was undertaken to reduce a rock fall hazard on a railway and highway. It involves blasting for a ditch excavation, control of blasting damage and rock bolting.

Site Description

The railroad and highway are located on benches cut in a 250 ft. high, 40 degree slope above a river in 3,000 ft. deep canyon (see Figure 12.15). In constructing the bench for the railroad, it had been necessary to construct about 100 ft. of retaining wall and cut a slope that was about 900 ft. long and varied in height from 20 ft. at either end to about 100 ft. at the center. A slope had also been excavated for the construction of the highway.

A hazard to traffic had developed due to rock falls from the upper slope and it became necessary that some remedial work be carried out. This hazard was particularly acute because the track curvature restricted visibility and trains did not have sufficient time to stop in the event of a rock fall. Furthermore, even a minor derailment could cause rail cars to fall onto the highway below. The rock falls varied in size from less than 1 cu.yd. to as much as 10 cu.yds. and were most likely to occur in the spring and fall during freeze-thaw cycles when ice formed in cracks and loosened blocks of rock on the face. During the winter, the temperatures can drop to -30°F and ice can be a problem despite the area being semi-arid with a rainfall as low as 6 inches annually.

The rock falls were occurring because, although the intact rock was moderately strong, it was intersected by a number of fracture planes (joints) with continuous lengths of several tens of feet. The length, orientation and spacing of these fractures controlled stability conditions and the size of the rock falls. Figure 12.16 illustrates that these fractures occur in three sets which were oriented such that they formed roughly cubic shaped blocks. The two near vertical sets would form the sides of blocks, which would slide if the third fracture was inclined out of the slope. Weathering of the rock on these joint sur-

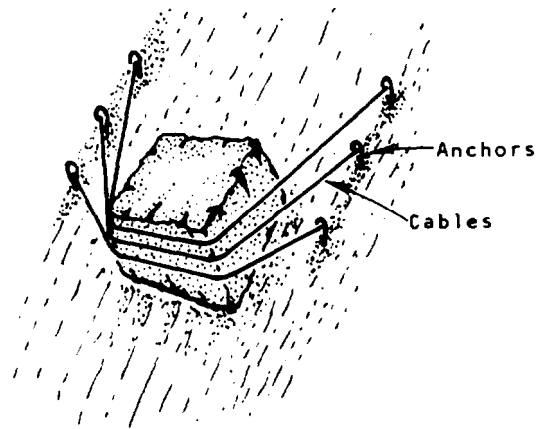


Figure 12.8: Cable lashing to hold loose block.

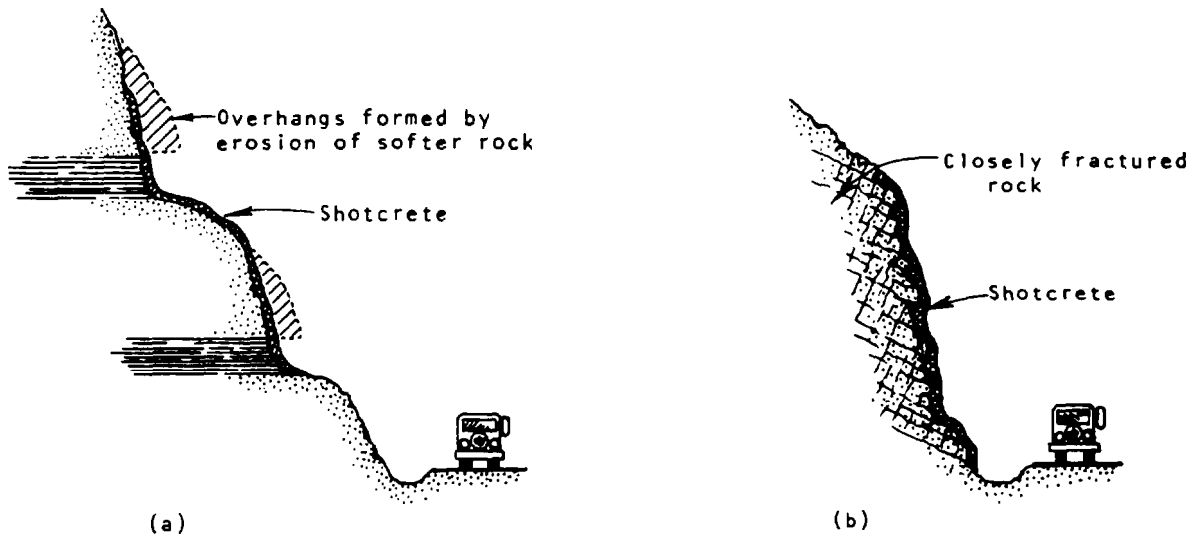


Figure 12.9: Shotcrete.

row weathered zones should be deepened so that there is some sound rock on either side to which the shotcrete can adhere. It is also important that water and ice pressures do not build up behind the shotcrete. Drainage can be achieved by drilling holes into cracks in the rock, putting a drainpipe in the hole and applying the shotcrete around the pipe. Alternatively, insulated drains can collect seepage water behind the shotcrete and discharge it in a sump(310).

The strength of the shotcrete is improved, and the amount of rebound reduced, by pre-moisturizing dry-mix shotcrete to about 3 per cent to 6 per cent moisture before it reaches the nozzle. The maximum distance that shotcrete can be pumped is about 500 ft. horizontally and 100 ft. vertically depending upon the equipment available. Dry-mix shotcrete, i.e. the water is added at the nozzle, can be pumped further than wet mix shotcrete.

Control of shotcrete thickness is difficult on irregular rock surfaces. Probably the most practical control method is to measure the area of the face covered and the volume used and ensure that the material is being evenly applied, keeping in mind that the amount of rebound may vary between 50 and 100 percent. Some coring with a small diamond drill may be carried out after the shotcrete has set to check thickness and cement/rock bond, and obtain samples for testing. Another thickness test is to probe the shotcrete before it sets.

Details of shotcrete practice and specifications have been drawn up by the American Concrete Institute(311). Sample specifications are provided in Chapter 14.

III PROTECTION MEASURES

Conditions may exist where stabilization of a slope is either so expensive, or disruptive to traffic, that it is more economical to protect the highway from rock falls. Protective measures could also be used where it is difficult to achieve permanent stabilization and continual maintenance will be required in the future. A number of different protection methods are discussed below.

Ditches

Ditches at the toe of slopes are an effective means of catching falling rock and they can often be excavated at relatively low cost compared to the cost of stabilization. The required width and depth of a ditch depends upon the angle and height of the slope, and the design chart in Figure 12.10(a) shows the relationship between these four factors(312). The chart shows that the ditch dimensions are minimized where the slope angle is steep because rocks tend to fall vertically rather than bounce outwards off the face (Figure 12.10(b)). The effectiveness of the ditch is also improved by having a vertical, rather than rounded slope on the highway side. This can be achieved by careful blasting of this slope if the rock is competent, or by constructing a concrete or gabion wall. A gabion wall has the advantages over a concrete wall of being better able to withstand the impact of falling rock because of its flexibility, and being less expensive to construct and repair. However, it can easily be damaged by vandalism.

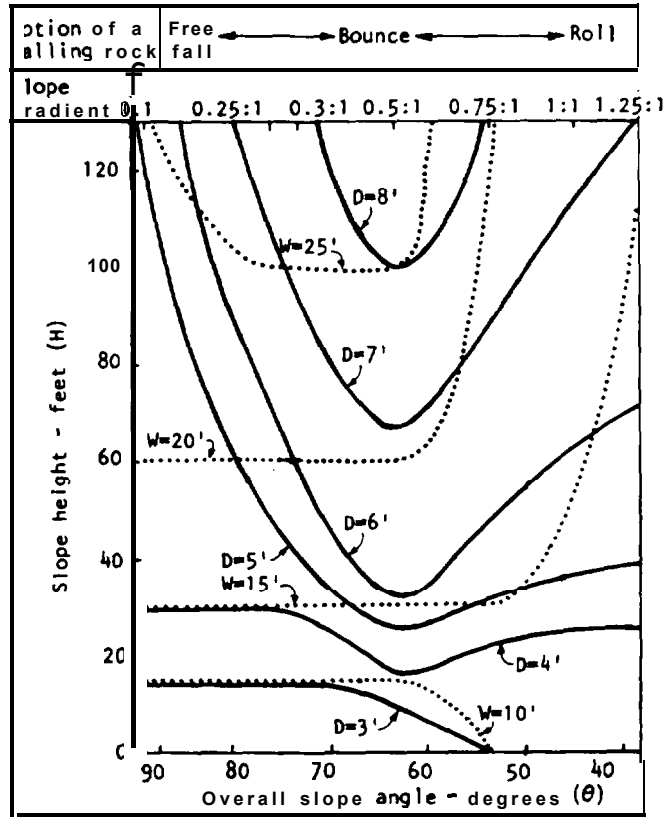


Figure 12.10(a): Ditch design chart.

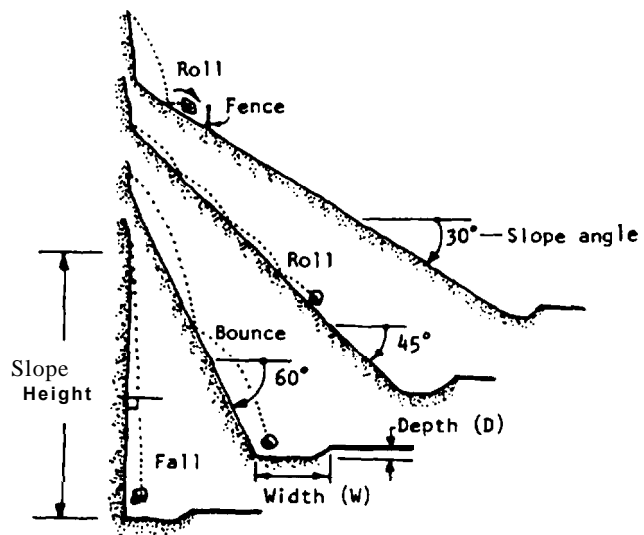


Figure 12.10(b): Rock falls on slopes.

The effective depth of the ditch can be increased by constructing walls along the outside edge rather than excavating material from the base of the ditch. Where possible, the base of the ditch should be covered with loose gravel or sand to reduce the tendency of rocks to bounce. Also, access should be left for equipment to clean fallen rock that has accumulated in the ditch and reduced its effectiveness.

An important aspect of ditch design is to ensure that excavation at the toe of the slope for the ditch does not oversteepen the slope and cause it to fail.

Fences

Fences can be used to intercept rocks rolling down slopes with angles less than about 40 degrees, i.e. talus slopes. On slopes steeper than this, rolling rocks tend to accelerate as they fall and a more substantial structure is required. Fences can also be used in narrow gullies where the path of the falling rock is well defined.

Fences can consist of wire mesh or interlaced wire rope suspended from cables anchored to pins or posts in the rock face. The fence should be flexible so that it can absorb the impact of falling rock, and have the bottom open so that rocks do not accumulate in it. Fences of this type are unlikely to stop boulders larger than about 1 ft. across.

Fences have been used extensively on slopes above railroads in Japan (313). To stop boulders less than about 3 ft. in diameter, piles are sunk into the slope and 1 inch diameter steep cables are strung horizontally between the piles. The height of the fence is about 10 ft. (see Figure 12.11). To stop larger boulders 10 ft. diameter reinforced concrete piles are cast into the slope and very strong mesh is placed between the piles. Some of these piles are protected from the impact of falling rock by 18 ft. diameter corrugated steel sheathing with the annular space filled with rock.

Mesh

Wire mesh suspended down the face of a slope will intercept falling rock and direct it into a ditch or catchment area. It is usually suspended from pins and cables on the crest of the slope and draped down the face (see Figure 12.12). The mesh can consist of 9 or 11 gauge galvanized chain-link mesh or gablon wire mesh. Gablon mesh has the advantage that it has a double twist hexagonal weave which does not unravel, like chain-link mesh, when it is broken. The bottom of the mesh blanket should be left open so that falling rock does not catch in the mesh.

Mesh is not suitable where the boulder size is greater than about 1 ft. diameter and the slope is steeper than about 40 degrees. On these slopes, the impact of rolling boulders may be sufficient to break the mesh. This can be overcome by securing the larger boulders with rock bolts and anchoring the mesh to the face with pins so that rocks are prevented from gaining momentum when they come loose. However, eventually these rocks may accumulate behind the mesh and have sufficient weight to break it.

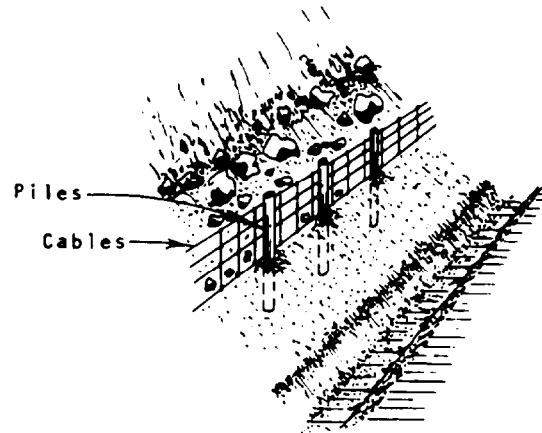


Figure 12.11: Fence to catch rolling rock.

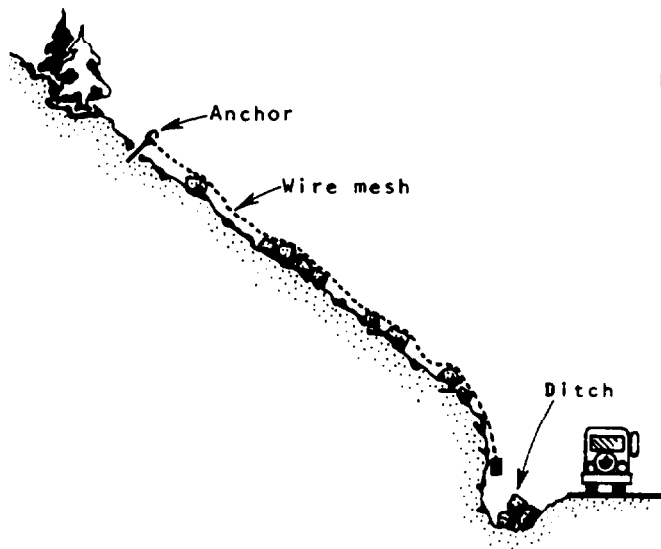


Figure 12.12: Wire mesh on slope to trap falling rock.



Photograph courtesy of Canadian Pacific Railway.

Figure 12.13: Rock slide protection fence

Warning Fences

Where the cost of stabilization is very high and rock falls are infrequent, warning fences can be constructed. These fences contain wires that, when broken by a rock fall, activate stop lights on the highway. Warning fences are often used on railroads where the warning lights are incorporated into the signal system. The fences consist of a row of poles at the toe of the slope with horizontal wires stretched between them at a vertical spacing of between 1 and 2 ft. Overhead wires, which are supported on members cantilevered out from the top of the pole, are often required where the face is steep and close to the right-of-way (see Figure 12.13).

Disadvantages of warning fences are that false alarms, due to minor rock falls or vandalism, can seriously disrupt traffic. Also in cold climates, icicles and minor snow slides can set off the warning lights. It may be possible to overcome these problems by modifying the location and spacing of the wires to suit particular conditions. Another problem is that rock falls can occur after a car has passed the stop light so the driver will obtain no warning of the fall.

Rock Patrols

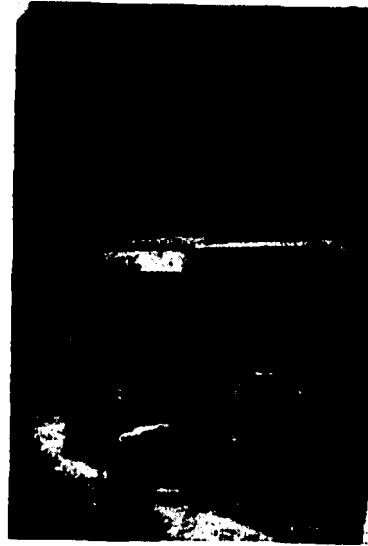
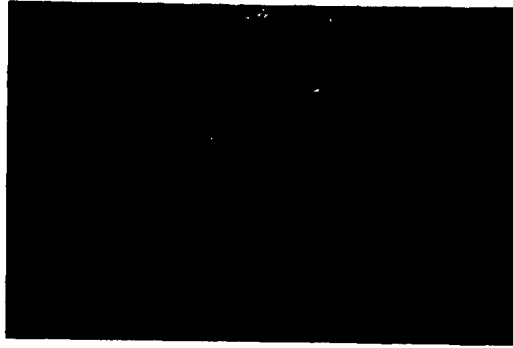
Another warning method that can be used where the cost of stabilization is high, is to use rock patrols along dangerous sections. Patrols have the advantages of reliability and flexibility since their frequency can be adjusted to the demands of traffic and weather conditions. The frequency of patrols should be increased after heavy rainfall and during the spring and fall in climates where frost action will loosen rocks on the face. Patrols do have the disadvantage that they cannot give 100 percent coverage and falls can occur between patrols. Also, there is the continuing cost of the patrols and the requirement to find reliable personnel who are willing to work in isolated and sometimes hazardous conditions.

The patrolmen should have some means of removing minor rock falls and have radio contact with maintenance crews in the event of a large fall.

Rock Sheds and Tunnels

In cases where the hazard from rock falls is high and stabilization is not feasible, it may be necessary to construct a concrete shed over the highway, or to relocate the highway into a tunnel (Figure 12.14). While the construction cost of both these protection measures can be significant, maintenance costs are likely to be minimal.

Concrete sheds should be designed with the roof inclined so that rocks roll across the shed with minimum impact. The concrete should also be protected with a layer of gravel, particularly if the slope is so steep that rocks can land directly on the roof. Much of the impact load will be taken in the columns on the outer side of the shed. On steep mountainsides, it may be difficult to found the columns on sound rock in which case it may be necessary to sink piles, install reinforcement or, if no adequate foundations exist, to construct a cantilevered shed. Wing walls will often be required about the portals to prevent falls spilling onto the highway.



Rock sheds.

Photographs courtesy of
Canadian National Railway

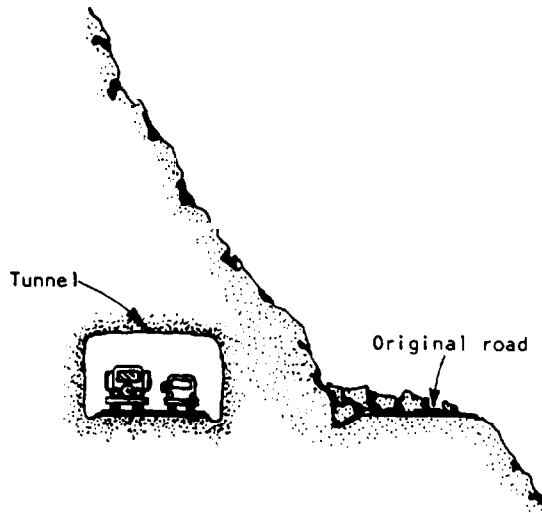


Figure 12.14: Rock sheds and tunnels.

Design methods that quantify the impact loads of rock falls and avalanches are not well developed. However, recent work on snow avalanches using fluid mechanics principles can be applied to the design of rock sheds(314).

Tunnels are the most positive method of protection from rock falls. The cost of driving and supporting a tunnel may be less than the cost of constructing a shed, depending on how much support is required(315).

Relocation

In cases where a large landslide is occurring, it may be more economical to relocate the highway rather than to try and stabilize the slide. The feasibility of relocation will depend on such factors as property ownership and alignment, and care should be taken to ensure that the new location is on stable ground and not an extension of the original slide.

EXAMPLE OF SLOPE STABILIZATION PROJECT

The following is a description of a project that was undertaken to reduce a rock fall hazard on a railway and highway. It involves blasting for a ditch excavation, control of blasting damage and rock bolting.

Site Description

The railroad and highway are located on benches cut in a 250 ft. high, 40 degree slope above a river in 3,000 ft. deep canyon (see Figure 12.15). In constructing the bench for the railroad, it had been necessary to construct about 100 ft. of retaining wall and cut a slope that was about 900 ft. long and varied in height from 20 ft. at either end to about 100 ft. at the center. A slope had also been excavated for the construction of the highway.

A hazard to traffic had developed due to rock falls from the upper slope and it became necessary that some remedial work be carried out. This hazard was particularly acute because the track curvature restricted visibility and trains did not have sufficient time to stop in the event of a rock fall. Furthermore, even a minor derailment could cause rail cars to fall onto the highway below. The rock falls varied in size from less than 1 cu.yd. to as much as 10 cu.yds. and were most likely to occur in the spring and fall during freeze-thaw cycles when ice formed in cracks and loosened blocks of rock on the face. During the winter, the temperatures can drop to -30°F and ice can be a problem despite the area being semi-arid with a rainfall as low as 6 inches annually.

The rock falls were occurring because, although the intact rock was moderately strong, it was intersected by a number of fracture planes (joints) with continuous lengths of several tens of feet. The length, orientation and spacing of these fractures controlled stability conditions and the size of the rock falls. Figure 12.16 illustrates that these fractures occur in three sets which were oriented such that they formed roughly cubic shaped blocks. The two near vertical sets would form the sides of blocks, which would slide if the third fracture was inclined out of the slope. Weathering of the rock on these joint sur-

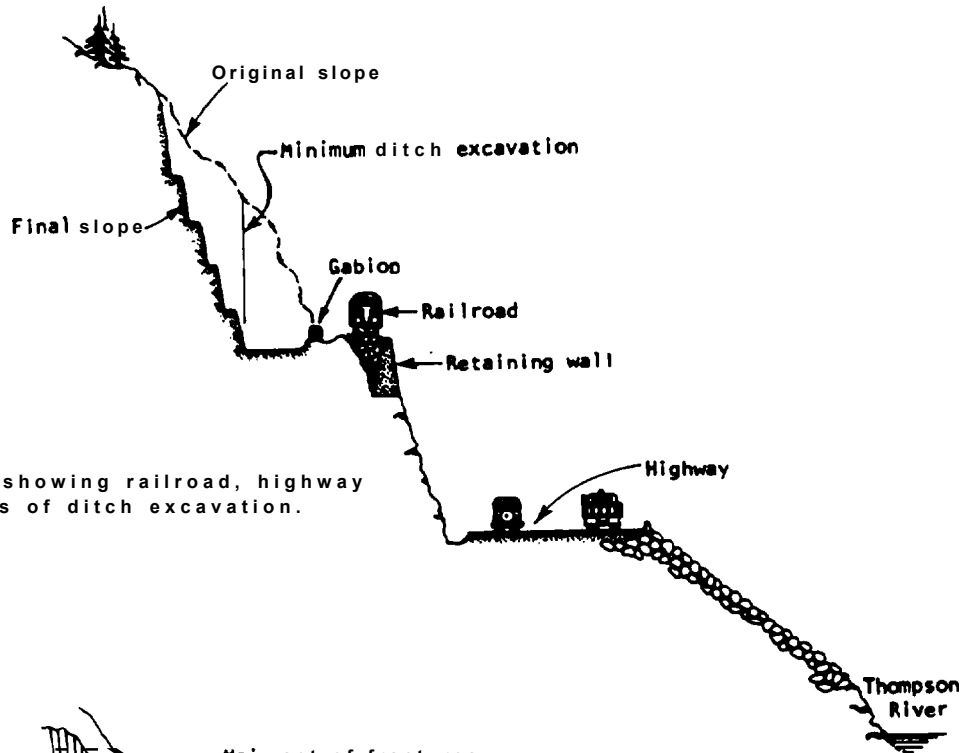


Figure 12.15:
Cross-section showing railroad, highway
and dimensions of ditch excavation.

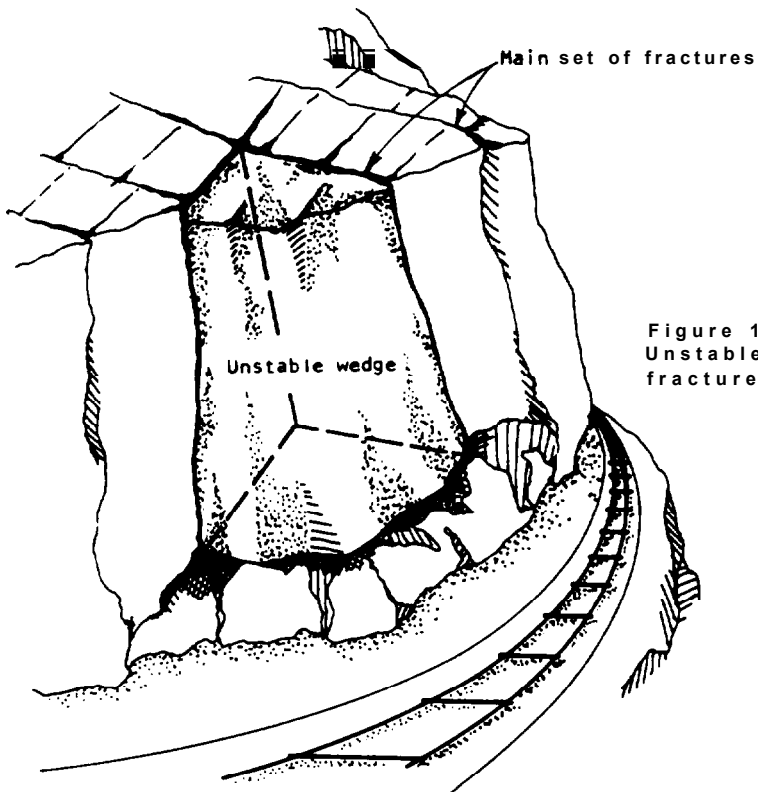


Figure 12.16:
Unstable rock wedge formed by intersecting
fractures.

faces, infilling with soil, and root growth had accelerated loosening of the blocks. However, the intact rock itself was sufficiently strong that it did not usually break up on impact with the track.

Alternative stabilization methods

The first method used to attempt to control the rock falls was to use hand scaling and light explosives to remove the loosest rock from the face, and to secure other potentially loose rocks in place with the rock bolts. However, frost action on the slope continued to produce occasional rock falls and it was decided that a more extensive and longer term stabilization program, than periodic scaling and bolting, was required. The following alternatives were considered:

- a) Install rock bolts on a regular pattern to reinforce the rock, and then cover the face with wire mesh and apply shotcrete to reduce the rate at which the rock was weathering. This alternative was rejected because it was believed that frost action and continued weathering of the rock behind the face would soon cause the shotcrete to deteriorate. Furthermore, it would have been expensive to install rock bolts sufficiently long to ensure that they were anchored in sound rock.
- b) Relocate the railroad in a through-cut behind the face. This would have the advantages of being able to excavate slopes in less weathered rock, and to work continuously with little interruption to traffic. However, the disadvantages were that the volume of excavated rock would be substantial, the maximum slope height would have approached 200 ft. and snow removal in through-cuts tends to be difficult.
- c) The stabilization program adopted was to excavate rock to form a ditch at the toe of the slope that would be of sufficient size to catch rock falls. Rock bolts would be installed, as required, to secure potentially unstable rock. The major disadvantage of this alternative was that excavation work would be restricted to a few hours a day to minimize interruptions to both rail and highway traffic.

Ditch design

The required depth and width of a ditch that will be effective in catching rock falls depends upon both the height and angle of the slope; the principles of designing an effective ditch are illustrated in Figure 12.10(b). This diagram shows that the dimensions of an effective ditch are minimized if the slope is cut as steep as possible. Of course a steep slope also minimizes the excavation volume, although care should be taken to ensure that the excavation does not over-steepen the slope and cause it to fail.

The relationship between the required ditch dimensions and the height and angle of the slope are shown in Figure 12.10(a). This information was used to design a ditch, the dimensions of which vary along the slope as the slope height increased from 20 ft. at either end to 100 ft. at the center. Thus the minimum

width and depth were 13 ft. and 4 ft. respectively while at the center, the ditch had to be 7 ft. deep and 23 ft. wide. In order to achieve this maximum depth, it was found that the most economical design was to excavate a ditch to a 4 ft. depth and then erect a 3 ft. high gablon barrier along the outside of the edge of the ditch. This saved the excavation of an extra 3 ft. thickness of rock over the full 23 ft. width. An advantage of the gablon, which is a box shaped, wire basket filled with loose rock, is that it formed a vertical face which helps to prevent falling rock from rolling out of the ditch and reaching the track. The gablon is also flexible so that it can withstand impact from falling rock and can be readily repaired if damaged. It is also less expensive to construct than a concrete wall.

The plans required for the design, and survey control during excavation, were obtained by terrestrial photogrammetry from a pair of survey stations on the opposite side of the river. From these photographs, a topographic plan and cross-sections were prepared. The dimensions of the ditch were defined by offsets from the centerline of the track at 20 ft. section intervals along the slope.

Excavation method

The two important objectives of the excavation program which had to be achieved by the contractor were as follows:

- a) Steep slopes had to be cut in this moderately weathered rock. This required the use of very carefully controlled blasting to ensure that the explosive loads were just strong enough to break the rock but not damage the rock behind the face.
- b) There had to be minimal interruptions to traffic both on the highway and the railroad. This required the use of a blasting method that would not damage either the rail or the retaining walls, and would also minimize the amount of rock thrown onto the railroad and highway so that clean-up times would be minimized. The traffic closure schedule that was drawn up allowed a five hour closure on the railway and a 45 minute closure in every hour on the highway.

The excavation method adopted by the contractor was as follows. The minimum ditch excavation was too narrow at the top of the cut to allow equipment access, so a 20 ft. wide bench was first developed along the entire length of the slope just below the slope crest. This access bench was developed by working a face at both ends of the cut, drilling horizontal holes parallel to the face with tank and air-track drills. A dozer then pushed the blasted rock onto the track. Prior to each blast, the length of track under the blast was protected with about a 4 ft. thickness of reject ballast. Once the top bench had been developed across the full length of the slope, it was then possible to excavate the remaining benches in 15 ft. lifts using vertical holes. By cutting each bench vertically and drilling the back row of holes 4 ft. from the toe of the previous bench, an overall slope angle of about 75 degrees was achieved.

A number of trial blasts were required to determine the optimum drill pattern and explosive load required to minimize damage to the rock behind the face. The blasting method finally adopted was as follows:

Production Holes - hole pattern = 5 ft. x 5 ft.
 hole diameter = 2-1/2 inches
 explosive load = 9 lb/hole, 0.5 lb/yd.³

Holes on face - hole spacing = 2 ft.
 explosive load = 3 lb/hole, 0.04 lb/ft.²

Wooden spacers 18 inches long were used between 5 inch long explosive sticks to distribute the load evenly in the rock.

The delay sequence was set up with each row perpendicular to the face so as to minimize the volume of rock that was thrown onto the track. The row of closely spaced holes along the bench face was fired last in sequence to ensure that they had a free-face to which to break. Figure 12.17 shows the completed slope with drilling in progress for the excavation of the ditch.

Control of blast damage

As the excavation approached track level, the blast vibrations had to be controlled to ensure that there was no damage to either the structure, or to the retaining walls outside the track. Damage to structures from blast vibrations is related to the peak particle velocity of these vibrations. Experience has shown that masonry retaining walls such as the ones at this site were unlikely to be damaged if the peak particle velocity does not exceed 4 inches per second. The magnitude of these vibrations depends upon the maximum charge weight detonated per delay. In order to determine what weight of explosive could be detonated per delay, a number of vibration measurements were taken for the initial blast and from these measurements a blast control chart was drawn up (see Figure 12.18). This chart relates the distance of the blast to the maximum permissible charge weight that can be detonated on a single delay. By keeping within these guidelines, the excavation was completed without damaging the walls.

When the excavation had been completed, selective rock bolting was carried out where natural fractures were or tended to form potentially unstable blocks. The drilling and bolt installation was carried out in a basket suspended from a crane located in the ditch. This method was adapted instead of installing bolts from each bench as the excavation proceeded, because use of the wagon drill for bolting would have slowed the excavation program. Also the blast vibrations may have damaged the grout around the bolts. The bolts used were 1 inch diameter hollow bolts either 8 ft. or 14 ft. long. Each was tensioned to 25,000 lbs. and fully grouted to both lock in the tension, and to protect the bolt from corrosion.

The final step in the excavation program was to construct a 3 ft. square gabion, 500 ft. long on the outside edge of the ditch where a 7 ft. depth was required. Figure 12.19 shows a photograph of this gabion and the completed ditch.



Figure 12.17: Completed slope with drilling in progress for ditch excavation.

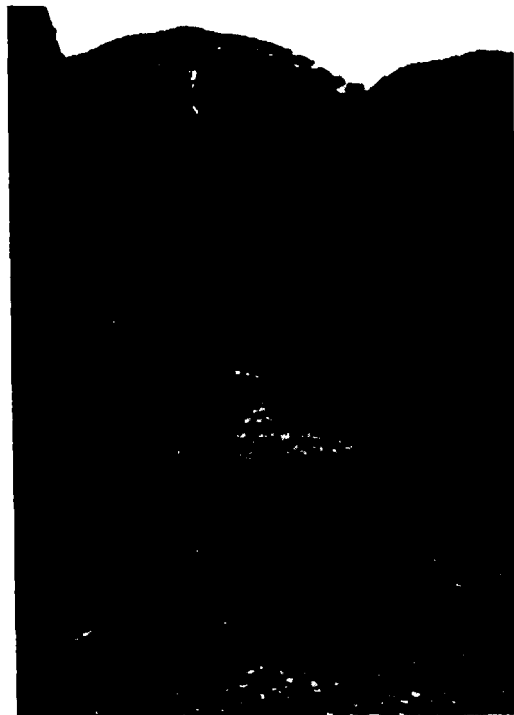


Figure 12.19: Ditch after construction of gabion.

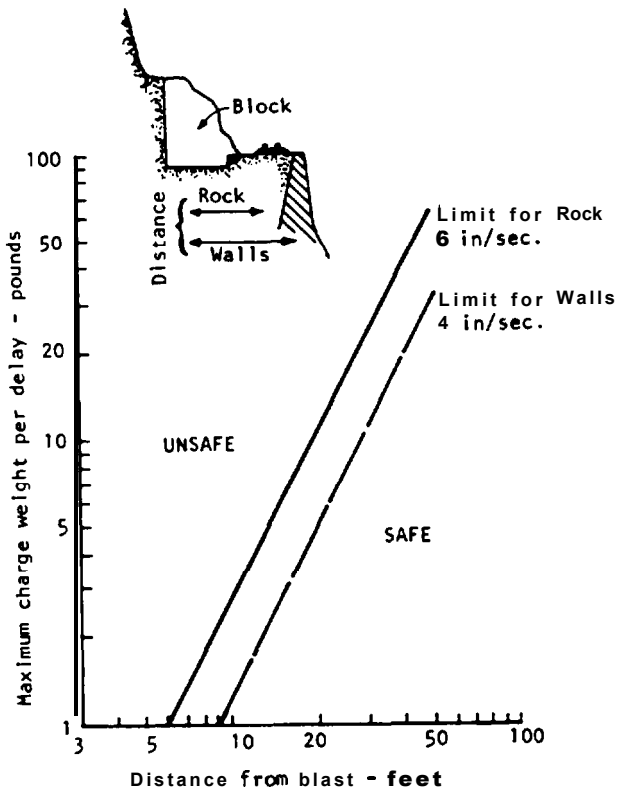


Figure 12.18: Blast damage control chart.

Contracts

A target type contract was used for this project to give the contractor incentive to control costs, while providing flexibility in the event of changed quantities or more traffic interruptions than set out in the contract. Each bidder supplied the owner with an Original Target Estimate based upon the design value of rock to be excavated, and a lump sum price for access construction. This estimate was adjusted upon job completion, for changes in quantities or work type, to become the Final Target Estimate. A penalty clause for over excavation beyond the design line was also included to encourage the contractor to reduce over-break from blasting and to excavate the minimum amount of rock. Since payments to the contractor were based upon actual costs, each bidder was requested to supply lists of rates for labour and equipment, and to provide back-up calculations for the Original Target Estimate.

The fee or profit to the contractor was quoted separately in the tender and could be adjusted to reflect the difference in the Final and Original Target Estimates. To provide an incentive, the fee was on a sliding scale: if the actual cost of the work was greater than the Final Target Estimate then the fee payable would be reduced by x percent of the difference; if it were less than the Final Target Estimate then the fee would be increased by y percent of the difference. Both these percentages were bid items and were 10 percent and 40 percent respectively.

Several contract problems developed during the course of the project; the following are suggestions on how they might be avoided.

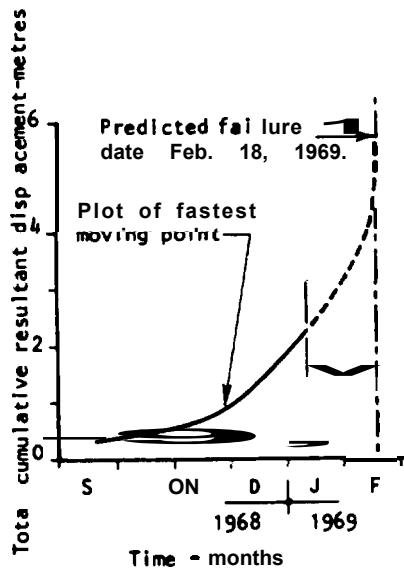
- a) A lump sum payment was to be made for all access construction and rock excavated outside the ditch design lines. This matter was discussed at the pre-bid site meeting, but later disagreements arose over the definition of rock that was to be paid for in the lump sum payment, and that which was to be paid at cost. It is suggested that these two classes of rock be very clearly defined and that records of pre-bid meetings be included in the contract.
- b) Trains delayed work on 50 percent of the working days, interrupting the coordinated railway-highway closure schedule. Production losses due to delays should be estimated and spelled out in the contract so that the contractor can include this item in his bid calculation.
- c) The bids should be analyzed to ensure that the contractor is not "low-balling" his bid and that his quoted rates are out-of-pocket costs and do not include profit.
- d) The contract should include an "upset price" to ensure that the contractor does not prolong the job for which he is paid cost plus the minimum fee.

Chapter 12 references

290. BEHR, H., KLENGEL, K.J. Stability of rock slopes on the German State Railway. Deutsche Eisenbahntechnik, Germany, pp. 324-328, 1966.
291. BAKER, R.F., MARSHALL, H.C. Control and correction, landslides and engineering practice, HRB Special Report 29, Publ. 544, 1958, pp. 150-187.
292. ZARUBA, Q., MNCL, V. Landslides and their control. Elsevier, Amsterdam, 1969.
293. PITEAU, D.R., PECKOVER, F.L. Rock slope engineering. Book on Landslides: analysis and control, Chapter 9, Transportation Research Board, Washington, D.C., 1977.
294. CEDERGREN, H.R. Seepage, drainage and flownets, J. Wiley and Sons, New York, 460 p., 1967.
- 2%. SHARP, J.C. Fluid flow through fissured media, Ph.D. Thesis, University of London (Imperial College), 1970.
- 2%. SHARP, J.C., HOEK, E., BRAUNER, C.O. Influence of groundwater on the stability of rock masses - drainage systems for increasing the stability of slopes. Trans. Inst. Mining and Metallurgy, London. Section A, Vol. 80, No. 788, 1972, pp. 113-120.
297. LITTLEJOHN, G.S., BRUCE, D.A. Rock anchors - state of the art (3 parts). Ground Engineering. May, July 1975, May 1976.
- 2%. POST TENSIONING INSTITUTE. Recommendations for Prestressed Rock and Soil Anchors.
299. HOEK, E., LONDE, P. Surface workings in rock. Advances in rock mechanics, 3rd International Congress on rock mechanics, Denver, Vol. 1, Part A, pp. 613-654, September 1974.
300. WYLLIE, D.C. Bridge piers stabilized under traffic. Railway Track and Structures, July 1979.
301. LANG, T.A. Rock reinforcement. Bull. Assoc. Eng. Geol., Vol. IX, No. 3, pp. 215-239, 1972.
302. RAWLINGS, G.E. Stabilization of potential rock slides in folded quartzite in Northwestern Tasmania. Eng. Geol. Vol. 12, No. 5, pp. 283-292, 1968.
303. REDLINGER, J.F., DDDSDN, E.L. Rock anchor design, 1st International Congress of Rock Mechanics, Lisbon, September 1966.
304. SEEGMILLER, B.L. Artificial stabilization in open pit mines: a new concept to achieve slope stability. AIME Meeting, Vail, CO, August 1975.
305. ECKERT, O. Consolidation de massifs rocheaux per ancrage de cables (Consolidation of rock masses by cable anchors). Paris, Sols, Vol. 5, No. 18, pp. 33-40, 1966.

306. BARRON, K., COATES, O.F., GYENGE, M. Artificial support of rock slopes. Mining Research Centre, Mines Branch, Ottawa Research Report, R. 228, 145 p., 1971.
307. SOWERS, G.B., SOWERS, G.F. Introductory soil mechanics and foundation engineering. Third edition, McMillan Publishing Co. Inc., New York, 556 p.
308. VAN RYSWYK R., Tunnel repairs. Construction West, pp. 10-1 1, September 1979.
309. RIAMAKRISHNAN, V., COYLE, W.V., FOWLER, L.J. A comparative evaluation of fibre shotcretes. South Dakota School of Mines and Technology, Report SDSM-T-CBS 7902, August 1979.
310. BREKKE, T.L. Shotcrete in hard rock tunneling. Bul. I. Assoc. Eng. Geol., Vol. IX, No. 3, pp. 241-264, 1972.
311. AMERICAN CONCRETE INSTITUTE. Shotcreting. ACI Committee 506, ACI SP-14, Detroit, 1966.
312. RITCHIE, A.M. Evaluation of rock fall and its control. Highway Research Board, Record 17, Washington, D.C. pp. 13-28, 1963.
313. FUKUOKA, S. Personal communication.
314. MEARS, A.I. Personal communication.
315. HOEK, E., BROWN, E.T. Underground excavations in rock. IMM London, England, 1981.

Chapter 13 Slope movement monitoring.



Typical plot of cumulative displacement against time showing acceleration period before failure.

Introduction

Circumstances can arise when it is not possible to stabilize potentially hazardous slopes and it is necessary that some method of detecting deteriorating stability conditions be installed. Stabilization of a slope may not be possible when weather conditions such as ice and snow make work hazardous for scalers, or when funds are not available. Other circumstances could be where a potential slope failure is identified but it is uncertain as to how close it is to failure, or when stabilization work is unlikely to produce long-term improvement in stability.

Warning of deteriorating stability conditions can be obtained by measuring the rate at which the slope is moving and detecting the period of accelerating movement which always precedes failure. A typical movement/time plot of a failing slope is shown in the margin sketch. This chapter describes methods of monitoring slope movement, and recording and interpreting the results. These methods have been used successfully to predict the time of failure of a number of slopes (316-318), and they are presently widely used to monitor slopes adjacent to highways and railways. Details of installation methods are available from the equipment suppliers and equipment originally developed for soil slopes is usually suitable for rock slopes.

Movement monitoring can be used in a wide range of conditions; for example, on large slides which are moving at rates as great as several feet a month, on individual blocks which are susceptible to sliding or toppling, and on bridge abutments where it is important that very small movements be detected. The method of monitoring depends upon such factors as the type and size of the failure, the magnitude and rate of movement and the warning system employed. In general, the successful application of movement monitoring depends upon carrying out three important steps:

- 1) Recognizing the type of failure and the probable causes of failure.
- 2) Making accurate and unambiguous movement measurements.
- 3) Correctly interpreting the results to determine when acceleration occurs.

The following is a discussion of these factors.

1. Type and cause of failure

The four types of slope failure discussed in Chapters 7 through 10 have a particular direction in which movement occurs and this should be considered when designing a monitoring system. Thus, planar and wedge type failures slide in a direction parallel to the inclination of the failure plane, circular failures show tension cracks and slumping at the crest and heaving at the toe, and toppling failures show horizontal movement at the crest with little movement at the toe (see margin sketch). The monitoring system that is installed should be able to detect movement in the direction which it is most likely to occur. Conversely, the measured direction of movement will provide information on the type of failure that is occurring. De-

termining the cause of failure is important in order to obtain the earliest possible warning of failure. For example, if high groundwater pressures are the main cause of instability, then the installation of piezometers to monitor increases in pressures will provide an earlier warning of failure than measuring movement. Other possible causes of failure are vibrations from nearby blasts(319) and excavation at the toe of the slope for road or ditch widening.

2. Accurate and unambiguous measurements

The monitoring system installed should be sufficiently accurate to detect movements that are significant to stability. For example, a circular failure with a height of a hundred feet may move several feet before collapsing. Therefore, a monitoring system that can detect movements of 1/2 inch to 1 inch is probably sufficiently accurate. However, on a bridge abutment, movements as small as 1/2 inch may have a significant effect on stability so the monitoring system should be able to detect movements as small as 0.1 inch. In making these measurements, one should be sure that the survey results are an accurate representation of the movement of the slope. In this way, one can draw confident conclusions as to whether or not hazardous conditions exist.

3. Interpretation of results

Rapid and reliable interpretation of the results is important to ensure that one is able to identify movement conditions that are indicative of potential failure. The first step is to plot the measurements as graphs of movement against time because these graphs will much more readily show any change in the rate of movement than lists of figures. Also, the graphs should be brought up to date as soon as the measurements are made. Other methods of recording data, such as acceleration time plots, vectors and velocity contours, which assist in interpreting results, are discussed later in this chapter.

METHODS OF MEASURING SLOPE MOVEMENTS

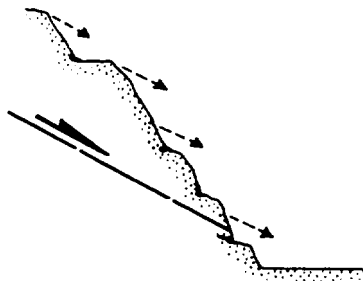
Methods of measuring slope movement can be divided into two general classes:

- 1) Surface methods - surveying, crack width measurements, tiltmeters.
- 2) Subsurface methods - "sonds", inclinometers, extensometers, shear strips, strain gauges.

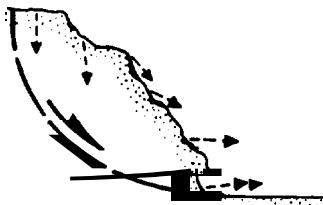
Information on instrumentation systems is provided by manufacturers and such publications as Highway Focus(320).

The selection of the most appropriate method will depend upon such factors as:

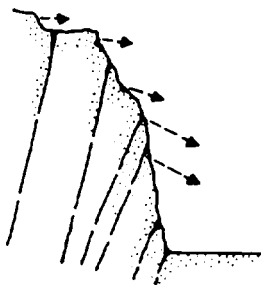
Access to the slope - some slopes may be too steep or too hazardous for personnel to climb in order to make measurements, in which case remote methods of measurement are required.



(a) Plane or wedge failure.



(b) Circular failure.



(c) Toppling failure.

Characteristic direction of movement of three common types of slope failure.

Size of failure - on large failures it is preferable to use surveying methods to measure long distances rather than measure widths of individual cracks which may not be opening at the same rate at which the overall slide is moving.

Magnitude and rate of movement - slopes that are moving slowly need a more precise monitoring system than slopes which are moving fast.

Frequency of readings - the frequency at which readings are taken depends upon the rate of movement and the consequence of failure. The frequency should be increased as the slope starts to accelerate, particularly if the road has not been closed to traffic. If readings are made more frequently than about once a week over extended periods, then it may be preferable to install an automatic system of recording the measurements, rather than a manual system, in order to save on manpower time and costs.

Warning systems - In particularly hazardous conditions, it may be necessary to install an automatic warning system that closes the highway if sudden movements occur. Extensometers are particularly well suited for incorporation with warning systems.

Weather conditions - If measurements have to be made at night and in poor weather conditions, then surveying methods which rely on good visibility would not be suitable. Under these conditions, extensometers, inclinometers or tiltmeters would be more appropriate.

Vandalism - all movement monitoring systems can be the object of vandalism unless access is particularly difficult. It might be necessary to install secure protective housings if vandalism becomes a problem.

Data handling - If there are only a few stations which are infrequently measured, the movement graphs can be plotted by hand. However, if there are many stations which are frequently read, then automatic methods of recording the results and updating graphs should be considered.

In general, the measuring system used should be free of operator bias and capable of producing consistently reliable results over the full time period in which it is likely to be in operation.

The following is a description of methods of monitoring slope movements.

SURFACE METHODS

Crack Width Measurements

In almost all slides, the opening of tension cracks on the crest of the slope is the first sign of instability. Measurement of the width of these cracks will often be representative of the movement of the slide itself.

The simplest means of measuring crack width is to set pairs of steel pins, one on either side of the crack, and measure the distance between the pins with a steel tape or rule as shown in Figure 13.1. The advantages of this system are that the equipment is readily available and can be set up quickly, and that readings can be made and results analyzed immediately. The disadvantages are that the movement measured is not absolute because it is difficult to locate the back pin on stable ground; this limits the system to small failures. Furthermore, vertical movement is not readily measured. Also, safe access to the crest of the slope must be possible in order to make measurements, and this will probably become dangerous when the width of the crack is several feet.

Extensometers

As the slide becomes larger and it is no longer possible to use pairs of pins across the cracks, tensioned wire extensometers can be used to measure movement over a greater distance as shown in Figure 13.2. In this method, a wire is stretched across the tension cracks between a measurement station established on stable ground and an anchor is secured on the crest. Relative movement between the station and the anchor is indicated by an adjustable block threaded on the wire which moves along a steel rule. This type of equipment can readily be manufactured from pieces of scrap metal and need not take the exact form shown in Figure 13.2.

Wire extensometers have much the same advantages and disadvantages as crack width measurements. The main advantage is that it is easier to measure movement over longer distances so that the measurement station can be established some distance behind the tension cracks. In addition, the wire can be extended over the crest so that movement of the toe of the slope can also be measured. However, if this is done, corrections for thermal expansion and contraction of the wire may have to be made. The accuracy of this system is of the order of ± 0.25 inches.

Another feature of the wire extensometer is that it can incorporate an alarm device that can close the highway in the event of sudden movement of the slope. In Figure 13.2, the alarm device shown consists of a switch mounted on the measurement station which is tripped by the movement of a second block threaded on the tensioned wire. In order to prevent false alarms when the slope is moving slowly and steadily, it is necessary that the trip block be set back from the trip switch at regular intervals. The set-back distance should be carefully selected to prevent false alarms and to ensure that adequate warning of failure is obtained. A set-back distance of about 3 to 4 times the movement that is occurring between readings could be used as a guideline when setting up the initial system and this can be modified as movement data is collected.

Where more precise movement measurements are required, it may be necessary to purchase commercial instruments. For example, a tape extensometer consists of a steel tape with fittings at the ends which allow the tape to be attached to reference points on either side of the tension crack (see Figure 13.3). The tape is tensioned to the same tension every time a reading is made by means of a proving ring. The accuracy of a tape extensometer is about ± 0.003 inches.

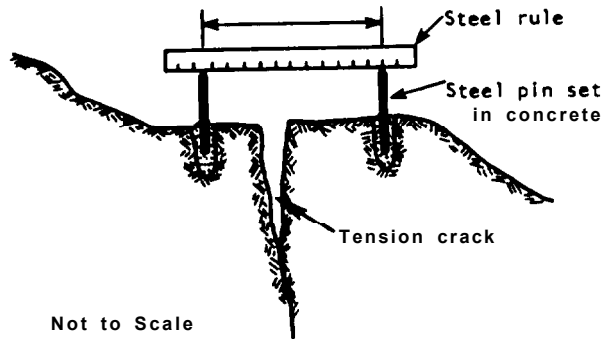


Figure 13.1: Crack width measurements show movement of crest of failure.

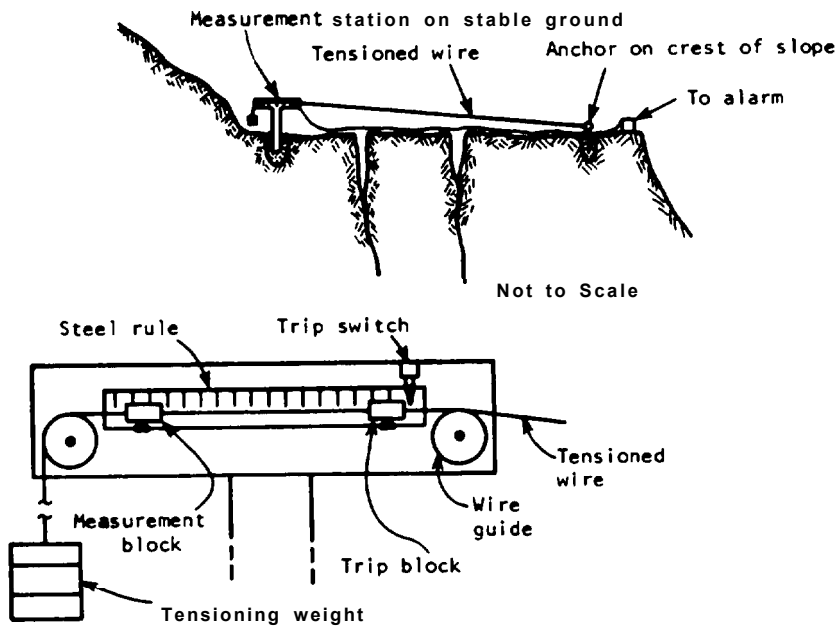


Figure 13.2: Wire extensometer on crest of slope.



Figure 13.4: Tape extensometer.
Photograph courtesy of Slope Indicator Company

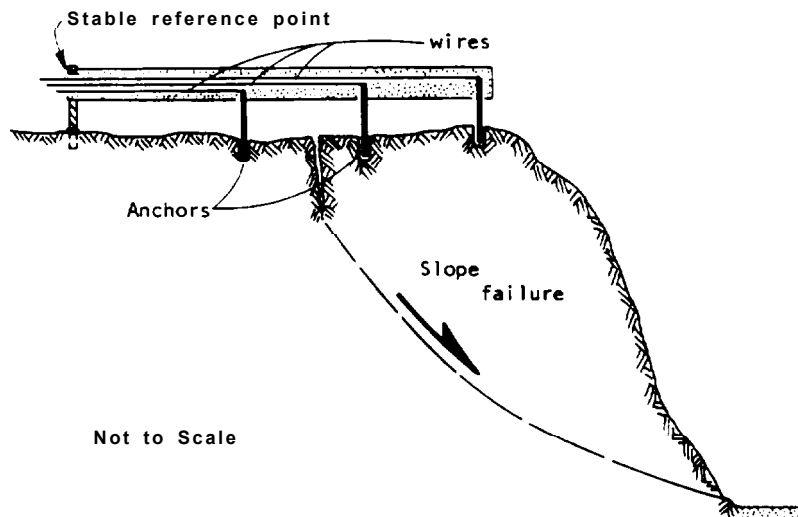


Figure 13.4: Sketch illustrating principles of wire extensometer.

Where precise, continuous monitoring of a slope crest is required, a multiwire extensometer can be installed. This consists of a number of wires of different lengths with one end of each attached to an anchor grouted into the slope (see Figure 13.4). The other ends of the wires pass through a reference point so that movement can be measured between the anchor and the reference point. Measurements can be made either with a micrometer or, if continuous, remote readings are required, a linear potentiometer is used. The readings from the potentiometers can be transmitted to a central recording station so that a number of extensometers can be monitored simultaneously. Methods of transmitting the data from the monitoring instrument to the recording station include electrical cable, radio transmitters and telephone lines(321).

Surveying

As the slide becomes larger, crack width measurements will probably not be possible because a stable reference point will be difficult to find. Therefore, remote measurement using standard surveying techniques will be required. The selection of the most appropriate method will depend upon the degree of accuracy required and the physical constraints at the site.

The general principles of any surveying technique are shown in Figure 13.5. Instrument stations are established below the slide, and their positions are determined from a reference station on stable ground some distance from the slope. It is essential that the position of the instrument stations be checked against the reference, because the slope beneath the instrument stations may also be moving. Monitoring points are established on the slide and by regularly determining their positions, the movement of the whole slide can be found. These points should also be established behind and to either side of the expected extent of failure, so that the limits of instability, as well as any increase in its size, can be determined.

The different surveying methods that can be used for slope monitoring are described below.

Electronic Distance Measurement

Electronic distance measurement (EDM) equipment can measure displacement to an accuracy of better than 1/2 inch over slight distances of more than one mile. The measurements are made in a few seconds so that an almost continuous record of movement can be obtained. The instruments also have built-in corrections for variations in temperature and barometric pressure, and can be used at night if targets are illuminated. The targets themselves consist of reflector prisms costing about \$150 each and can be mounted on pieces of reinforcing bar driven into the ground or grouted into drill holes. Most instruments employed in surveying work use an infrared beam which is adequate for most applications. Over extreme distances, a laser instrument may be required. One disadvantage of the surveying technique is that it is not possible to make readings during heavy rainstorms or snowstorms, or when clouds obscure the targets, and thus a back-up system of extensometers may be useful during extended periods of poor weather. Access to the slope to inspect prisms or change their orientations is also desirable.

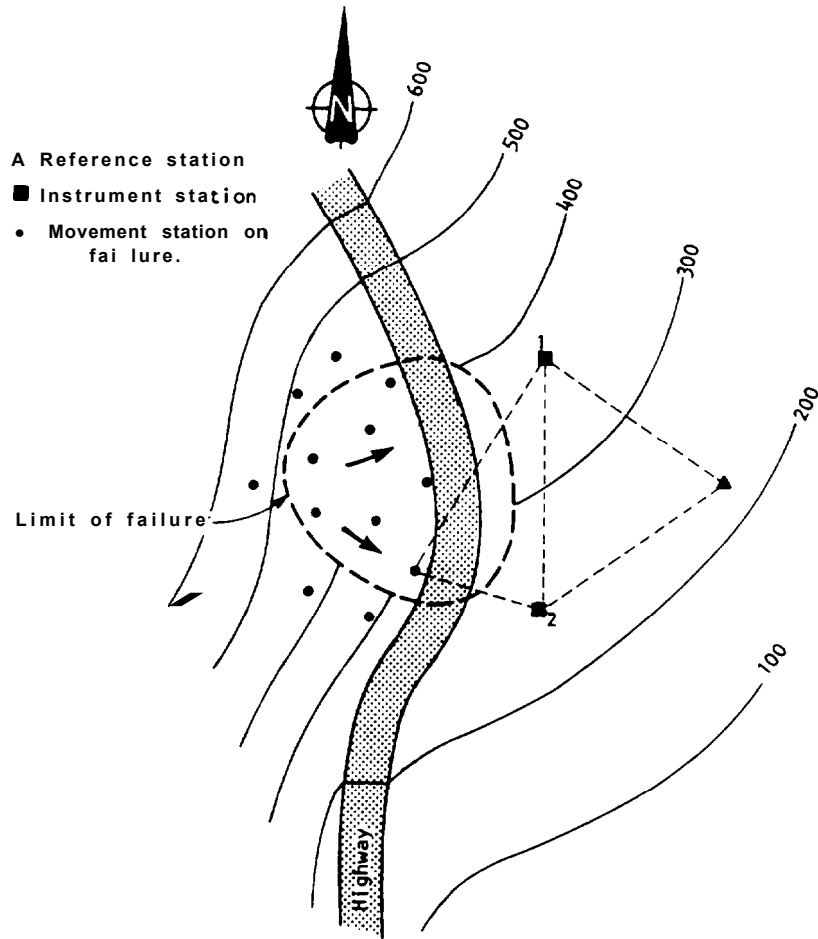
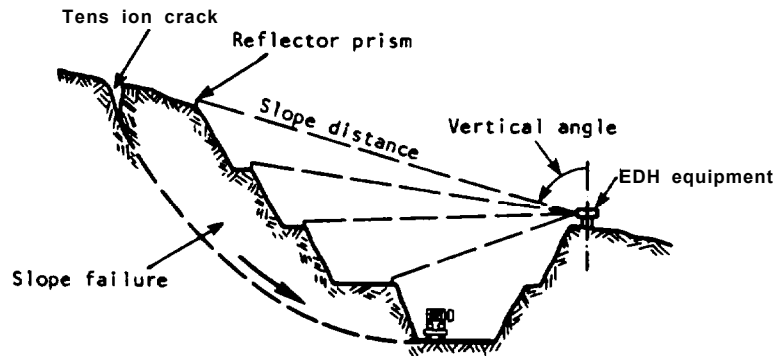


Figure 13.5: Surveying of slope movement.



Not to Scale

Figure 13.6: Slope distance measurement with EDH equipment.

The simplest method of surveying involves measuring the distance between the instrument station and prisms on the slope, as can be seen in Figure 13.6. For this method to be accurate, it is essential that measurements be made parallel to the expected direction of movements otherwise only a component of the movement will be measured. This is illustrated in Figure 13.5 where the northern half of the slide, which is moving northeast, is monitored from station 1 and the southern part, which is moving southeast, is measured from station 2. Information on the approximate vertical movement can be obtained by measuring the vertical angle to each station as well as the slope distance. This will give an indication of the mode of failure, as discussed on page 13.1.

Triangulation, Offsets, Trilateration

More precise information on the direction of movement and the failure mechanism can be obtained by finding the coordinates and elevation of each station, from which vectors of movement between successive readings can be calculated. A number of ways in which this can be done are illustrated in Figure 13.5. If there is only one instrument station, angles can be turned from the reference station to each prism, and the distance measured with EDM equipment (offsets). If there are two instrument stations, the position of each prism can be determined either by triangulation, or by trilateration using EDM equipment. Best results are obtained if the three points form an equilateral triangle, and this should be taken into account when setting out the baselines between the instrument stations.

Another alternative, which does not require the measurement of any angles, is to determine the distance of the prisms from three stations forming a tetrahedron(322).

EDM measurements are rapid and accurate, and surveying is useful in that it gives the three-dimensional position of each prism. Surveying does have the disadvantage that the measurements and the calculations are time-consuming and results are not immediately available. Triangulation, under ideal conditions, using a 1 second theodolite with all angles doubled, and an EDM measuring to ± 0.05 inch over slight distances of 1,000 ft. can give errors in coordinate positions of as little as 0.12 inches(323). However, it is likely that highway surveyors doing routine measurements in all weather conditions using equipment in less than perfect adjustment will obtain average errors of ± 4 inches to ± 6 inches. For this reason, coordinate determinations should only be carried out when the expected movement distance between readings is greater than the magnitude of error.

Leveling

Information on the rate and extent of subsidence of an area can be obtained by making leveling measurements of a network of stations on the crest of the slope. This method is only applicable where access to the slope crest is possible and where the terrain permits reasonably long sight distances. Of course, it is also important that a stable reference station be available. Leveling can be used in conjunction with EDM transit measurements to determine coordinate positions where the terrain does not allow set-up of instrument stations below the slide as shown in Figure 13.5.

Tiltmeters

Tiltmeters are instruments that, when mounted on a ceramic plate rigidly attached to the ground, record the angular tilt of the plate. Changes in tilt of the plate of about ± 10 seconds can be measured by the tiltmeter and the readings are highly reproducible. This instrument can either be left in place to continuously record tilting or can be carried around the site and set up on each plate each time a set of readings is made. The unit weighs about 6 lbs. and is easily portable on rough terrain.

Tiltmeters should only be used when it is certain that measurement of tilt will be an accurate representation of slope movement. Usually, tiltmeters would be used in conjunction with other monitoring methods. One possible application for tiltmeters would be on bridge abutments and piers where continuous and precise measurement of tilting is required.

Photogrammetry

On some large slides where it is not possible to survey the whole moving area, the use of photogrammetry may be considered. It is likely that the minimum error in coordinate position that can be obtained with this method is 6 inches. While wide coverage will be obtained, results will not be available for several days or even weeks, and photographs can only be taken on cloud-free days.

SUBSURFACE SURVEYING METHODS

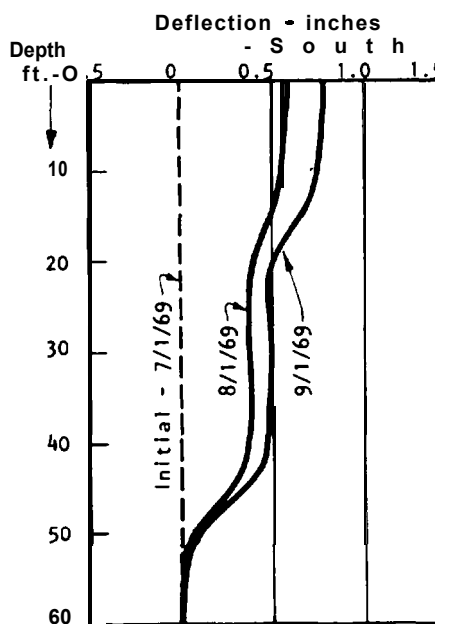
It is often useful to know the position of the failure surface, if it is not clearly defined by the geological structure, so that the volume of the sliding mass can be calculated, the type of failure identified, and stability analyses carried out. All the methods of obtaining this information require drill holes and remote readings cannot be made as readily as they can with surface measurements. The following is a description of methods that could be used on transportation routes.

Sond

The "sond" method consists of drilling a hole to below the expected depth of the failure, casing the hole, and then lowering a length of steel on a piece of rope down the hole. As the slope moves, the casing will be bent, and eventually it will not be possible to pull the steel past the distortion. This will indicate the base of the failure plane. In a similar manner, a sond lowered from the surface will show the top of the failure (see margin sketch).

Inclinometers

If the positions of several failure surfaces and the rate of movement is required, an inclinometer can be used. This instrument precisely measures small movements over the length of the hole and also gives the plan direction of movement. However, if the movement rate is great, the casing will bend at the failure surface, and the instrument may be lost in the hole.



Plot of inclinometer data.

The instrument operates in an identical manner to the tiltmeter described previously in that it makes precise measurements of the tilt of the borehole. By making measurements at fixed intervals up the casing, a plot of the inclination of the borehole is obtained (see margin sketch). The casing has grooves cut in the walls to prevent the instrument from rotating as it is pulled up the hole. This enables the direction of movement to be determined. The casing is a special item that must be purchased from the manufacturer of the inclinometer.

Borehole Extensometer

The multiwire extensometer described previously (see Figure 13.4) can readily be installed in a borehole (hole diameter 2-1/2 to 3 inches) with the wires anchored at different positions down the hole. The relative movement of the rock between anchor positions and the collar of the borehole is indicated by movement of the ends of the wires at the collar. The longest wire should extend beyond the failure surface so that it forms a stable reference point as the collar moves.

Most types of extensometers require that the wires be tensioned to a standard tension each time readings are made. This requires the use of a special tensioning/reading instrument that must be kept in good adjustment and that careful measurements be made by qualified personnel. However, extensometers are now available in which the wires consist of 1/4 inch diameter strands that are sufficiently rigid not to require tensioning. Measurements can be made with a standard dial gauge which is not as subject to error as the tensioning instrument.

When designing an extensometer system one should be sure that the instrument is installed parallel to the direction of movement because it can only register tension or compression. Therefore, extensometers are ideal for measuring the depth of movement in a toppling failure. In a circular failure where shear displacements are occurring on the failure surface, a "shear strip" movement indicator is more appropriate. This instrument consists of a strip of electrical conductor that is broken by movement on the failure surface; this will show the depth down the borehole of the surface, but not the rate of movement.

Rock Bolt Load Cells

In conditions where rock bolts are a critical part of a stabilization program, it may be required that the tension in the bolt be monitored to determine if creep, or loss of anchorage is occurring. Tension can be measured by placing a load cell between the nut and the plate on the face of the slope, or by attaching strain gauges to the bolt. If strain gauges are used, it is useful to have access to the gauge after installation in the event that the gauge has to be replaced. If a load cell is used, this may require the design of a special nut and plate arrangement to avoid untensioning the bolt in the event that it is necessary to change the cell.

INTERPRETING MOVEMENT RESULTS

In order to use monitoring to successfully decide whether traffic may, or may not, continue to travel below a falling slope, the movement data must be correctly and rapidly interpreted.

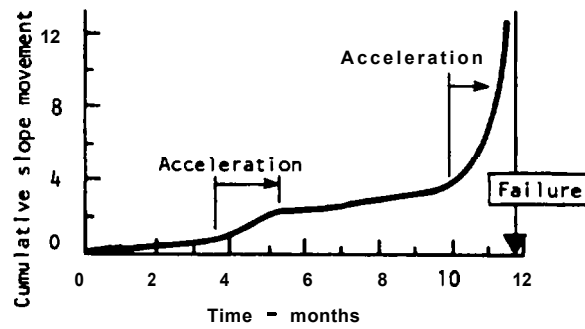


Figure 13.7: Typical shape of movement/time plot preceding failure.

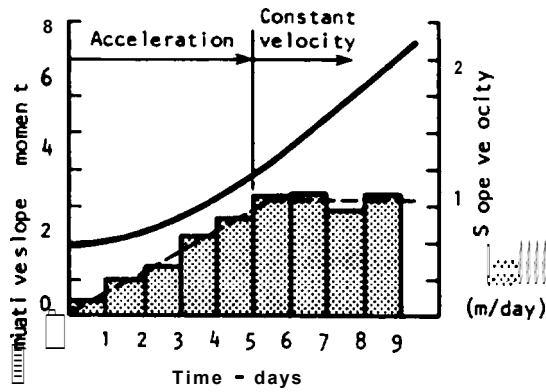


Figure 13.8: Velocity/time plot highlights changes in movement rate.

The most useful method of displaying movement data is to plot cumulative slope movement against time as illustrated in Figure 13.7. This graph will readily show any increase in the rate of movement that is indicative of deteriorating stability conditions. Since the appearance of the graph is dependent on the scales chosen for the axes, these dimensions should be carefully selected to ensure that acceleration is clearly identifiable. This means that monitoring should start when instability first becomes apparent so that the steady rate of movement can be established.

The frequency of measurements will depend upon traffic conditions. On low volume roads monthly readings may be sufficient, but on major highways hourly readings may be necessary if rapid movement is occurring. Figure 13.7 shows that sometimes several cycles of acceleration may occur before failure and that the total displacement is usually substantial. Also, the acceleration period will often have a duration of several days or weeks, thus producing an adequate warning of failure. However, it should be noted that planar type failures may occur with much less warning.

Further information on stability can be obtained by plotting movement velocity against time, where the gradient of the graph indicates the acceleration of the slope (see Figure 13.8). In this figure, the slope accelerated for the first five days and then moved at a constant velocity. If it were necessary to halt traffic during the acceleration period, it may be possible to reopen the road if the slope continues to move with zero acceleration. Frequent monitoring would be required under these circumstances.

Monitoring data can also provide information on aerial extent, mechanism, and depth of failure. In Figure 13.9, contours of slope velocity plotted on plan show the size of the slide and the fastest moving areas. These contours can be used to decide how stabilization work should be scheduled to minimize traffic closures. For example, for the slope failure shown in Figure 13.9, stabilization should start in the south end of the slide which is the fastest moving area.

Plan plots of displacement vectors obtained from triangulation will show the direction of movement. Also vectors plotted on section often have dip angles parallel to the failure surface beneath them, which may indicate the geometry and mechanism of failure, as illustrated in Figure 13.10. Thus, in a circular failure, prisms near the crest will tend to have movement vectors with steep dip angles, while prisms at the toe will move approximately horizontally, or even slightly upwards.

If monitoring of a large slide continues for some time, a considerable amount of data will soon be accumulated and the plotting of movements and vector will become most time-consuming. In fact, it may become difficult, in circumstances that require a rapid assessment of stability conditions, to make quick reliable interpretations of large volumes of data. Fortunately, storage of survey data, calculation of vectors, and plotting of movement graphs is an ideal application for computers. In this way, movement plots of many stations over any time span can be prepared in a few minutes.

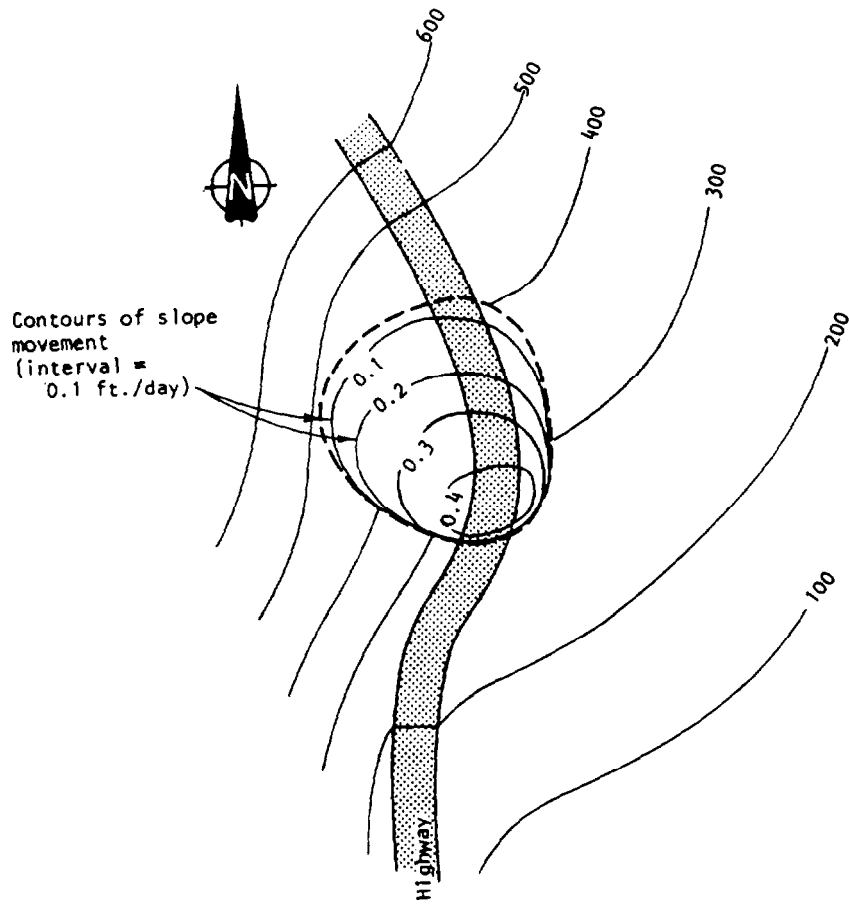


Figure 13.9: Contours of slope movement show extent and relative movement rates of slide.

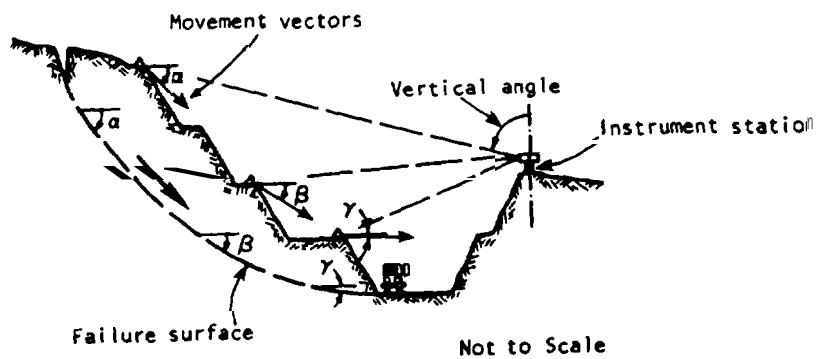


Figure 13.10: Dip angle of movement vectors shows approximate depth of failure.

Chapter 13 : References

316. WYLLIE, D.C., and MUNN, F.J. The use of movement monitoring to minimize production losses due to pit slope failures. 1st International Conference on Stability in Coal Mining, Vancouver, B.C. 1978.
317. KENNEDY, B.A. Some methods of monitoring open pit slopes. 13th Symposium on Rock Mechanics, Urbana, Illinois, 1971.
318. BRAWNER, C.O., STACEY, P.F. and STARK R. A successful application of mining with pit wall movement. Canadian Inst. of Mining and Metallurgy Bulletin, April 1976.
319. ORIARD, L.L. Blasting effects and their control in open pit mining. Second International Conference on Stability in Open Pit Mining, Vancouver, Canada, 1971.
320. HIGHWAY FOCUS. Compilation of papers on instrumentation from various sources - principle authors J.P. Gould, C.J. Dunniff. Vol. 4, No. 2, June 1972.
321. PIT SLOPE MANUAL, CHAPTER 8 MONITORING. Mining Research Laboratories, Canada Center for Mineral and Energy Technology, Ottawa, Canada, 1977.
322. HEDLEY, D.G.F. Triangulation and trilateration methods of measuring slope movement. Canadian Department of Energy Mines and Resources, Mines Branch, Mining Research Center, Internal Report 72/69.
323. YU, Y.S., HEDLEY, D.G.F. A trial of monitoring slope wall movement at Hilton Mines using a high precision theodolite. Canadian Department of Energy Mines and Resources, Mines Branch, Mining Research Center, Internal Report 73/18.

Chapter 14 Construction contracts and specifications.

Introduction

Contracts between owners and contractors are legal documents and must comply with federal and state laws. Standard general provisions are usually available to the owner, and federal and state agencies have well established procedures. Many sources are available to assist in contract preparation, including references 261 and 324 through 328. This chapter will concentrate on the types of construction contracts and the writing of specifications for rock slope engineering.

SELECTING THE TYPE OF CONSTRUCTION CONTRACT

Many types of construction contracts are used for rock excavation and stabilization on highways, and we can look to the United States highway construction requirements as a broad class of contracts for this type of work. The Federal Procurement Regulations (324) describe all the types of contracts and point out that contracting can be done either by formal advertisement or negotiation. Since most highway work has many potential contractors and enough lead time to allow for formal advertising, this is the preferred method of contracting. This is very fair because cost is the selection criteria and the government (owner) has the work accomplished for the least cost.

In drawing up any type of contract for rock work, it is important that some flexibility in quantities, timing and methods be incorporated in the specifications. This is necessary because it is rarely possible to precisely define the scope of work, especially on a slope stabilization program where the exact nature of the problem may only become apparent when access has been provided to the slope face and work has started. Because of the possibility of these "changed conditions" occurring, some flexibility should also be allowed in the budget allocations so that more or less money can be spent at each location. In general, this can be handled by obtaining bid prices on unit quantities (e.g. cu.yd. of rock, linear foot of rock bolt) and having provision for changing the estimated quantities as conditions demand.

Much rock excavation and stabilization work requires special skills such as controlled blasting, high scaling and rock bolt installation. Therefore, it is advantageous if both the contractor, and the engineer supervising the work, have experience in the procedures involved. If bids are invited from all contractors and the lowest bidder is accepted, then it is possible that the work will not be carried out to the required standards. This can be overcome by sending bid documents to selected, experienced contractors only, or by specifying the type of experience that the successful bidder must have obtained on previous projects. If there are no experienced contractors or inspectors available, then full-time supervision and "tight" specifications are required.

As discussed previously in Chapter 12 on slope stabilization methods, the supervising engineer should be involved with both the design and construction programs so that he obtains feedback on the success and applicability of his designs under different conditions. Because it may take several years to acquire this experience, and because methods used in one geological

environment may not be applicable in another, it is usually worthwhile to maintain an in-house staff of experienced rock work engineers. If they are not available, or are overcommitted, then specialist consulting services can be hired.

SELECTING THE TYPE OF CONSTRUCTION CONTRACT

The following is a description of the various types of contracts that can be used on rock slope work, and typical conditions in which they may be applicable. Any particular contract may be a combination of the types discussed.

Table XII summarizes the content of these discussions and gives examples of the uses of the types of contracts for rock slope engineering. Keep in mind that most U.S. highway requirements will be performed under advertised unit price contracts.

Unit Price Contract

The most frequently used contract in the United States highway system is the advertised "unit-price" contract. The terms of this contract provide that the owner will pay to the contractor a specified amount of money for each unit of work completed in a project. The units of work may be any items whose quantities can be determined, such as cubic yards of rock. Payments are usually made by the owner to the contractor at specified intervals during the period of construction, with the amount of each payment depending on the value of the work completed during the prior period of time. The Federal Procurement Regulations call this a fixed-price contract with adjustable unit prices. It is most frequently used for rock slope engineering because often neither the exact amount of common or rock excavation, nor the amount of required rock support is known.

The types of work that can be specified as unit quantities are as follows:

- mobilization/demobilization
- access road construction
- cubic yards of soil
- cubic yards of rock
- linear feet of rock bolts
- square feet of pre-shear face
- scaling manhours
- equipment rental, standby and operating
- *standby time for highway openings when no work is possible
- cubic yards of shotcrete

The specifications should give an estimate of the quantities involved so that the contractor knows the magnitude of the project. It should also be clear that the quantities may be changed during the course of the work. Figure 14.1 shows a typical specification sheet for a unit price stabilization contract.

This type of contract would be used for slope stabilization work where the full extent of the work required is usually only determined as the work progresses. For example, the estimated number of bolts may decrease if it is decided that loose rock should be scaled down rather than bolted.

Lump Sum Contract

If the owner (government) knows exactly the quantities of work to be accomplished, it will advertise a "Lump Sum" contract. The terms of this contract provide that the owner will pay to the contractor a specified sum of money for the completion of a project conforming to the plans and specifications furnished by the engineer. It is common practice for the owner to pay to the contractor a portion of this money at specified intervals, such as monthly, with the amount of each payment depending on the value of the work completed during the period of time, or according to some other schedule.

Lump sum contracts can be used on routine excavation projects where the volumes are clearly specified by accurately surveyed cross-sections and the owner has confidence in stability of the designed slope angles. Controlled blasting on final slopes is usually specified and the contract should state that the contractor pay for all excavation outside the design lines. The lump sum bid by the contractor may include the installation of slope stabilization measures such as rock bolts, or these may be bid on a unit price basis if the quantities cannot be defined until the excavation is made.

Lump sum contracts can also be used on stabilization work when the quantities are well defined, e.g. the construction of a retaining wall or concrete buttress.

Fixed Price with Escalation Contract

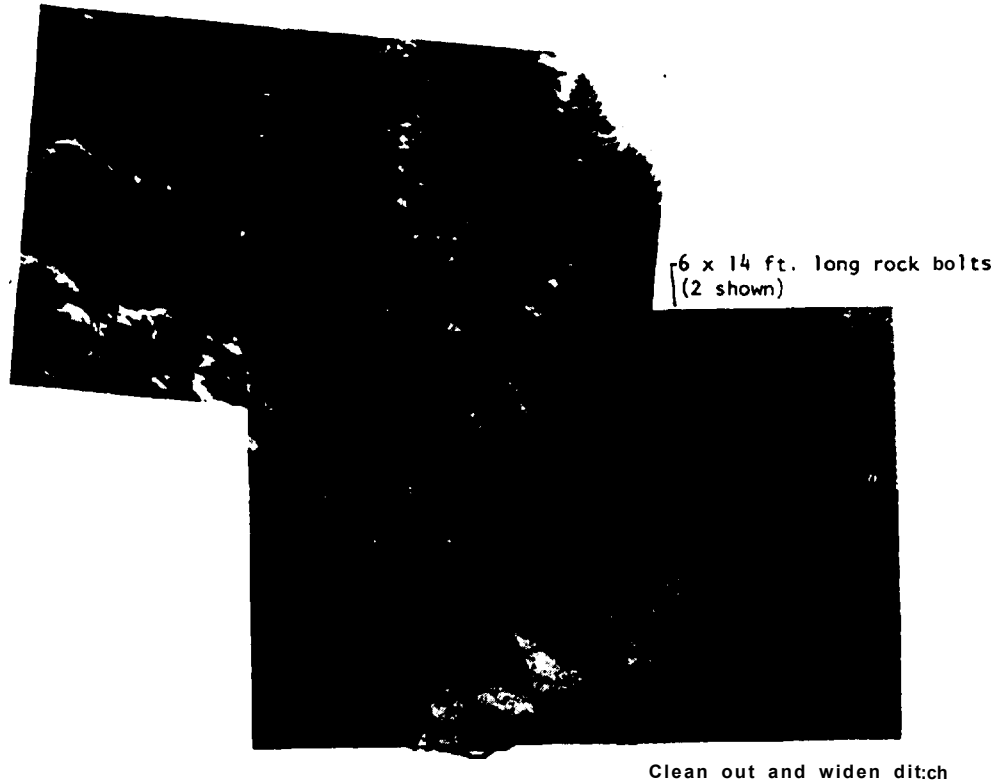
A minor variation of the fixed-price contract used for contracts of long duration are advertised fixed-price contracts with escalation. An example would be for the owner to agree to pay for any increases in fuel costs that the contractor must pay. This can allow for a lower bid price, thus a savings to the taxpayer, because the contractor is free of the risk of oil price increases and does not need to add a margin to his price.

Indefinite Delivery Type Contract

If the exact time of delivery is not known at the time of the contracting, the government can use several forms of what the Federal Procurement Regulations call indefinite delivery type contracts. These are sometimes called "open-ended" contracts or "day-rate" contracts and can be in force for up to a year to do such work as clearing ditches or scaling rock on a day-by-day, or as-required basis. These contracts are sometimes used to allow work to be done by small, local contractors and are suited to small budgets where it is not worthwhile setting up another type of contract.

Cost-Plus-A-Fixed-Fee Contract

If for some reason, such as emergency, the government cannot advertise, they may negotiate any of the above type of contracts. Alternatively, they may award a cost-reimbursement type contract of several forms, the most common of which is the cost-plus-a-fixed-fee contract. Under the terms of this contract the owner agrees to reimburse the contractor for specified costs, usually on-site costs, incurred by the contractor in carrying out the work, plus an additional fee. The fee is a profit plus a management fee to reimburse the contractor for



STABILIZATION REQUIRED

1. Scale loose rock from slope to a height of about 80 ft. Only blocks of rock larger than 0.25 cu.yd. should be removed. There are at least three loose blocks with volumes up to 6 cu.yd. Remove trees and apply weed killer to stumps.
2. Install 6 x 14 ft. long rock bolts in loose block at east end at a height of about 30 ft. above track level. Other bolts to be installed as directed by the Engineer.
Estimated total bolt footage = 130 ft.
3. Excavate a 180 ft. long, ditch at toe of slope; some blasting required at west end. Approximate back line shown on photograph.

Figure 14.1 : Typical specification sheet for slope stabilization work.

the costs incurred at his head office resulting from the construction of the project. Items of expense covered by the fee include, but are not limited to, salaries, rent, taxes, insurance, interest on money borrowed to finance the project, the cost of trips made by persons to the project, expediting the delivery of materials to the project, etc.

Emergency situations where cost-plus-fixed-fee contracts could be used would be where a rock fall has blocked the highway and men and equipment are needed immediately to clear the rock and stabilize the slope.

Cost-Plus Converted to Lump Sum

In some emergency situations, it may become apparent after work has started that the required remedial work can be clearly defined so that the contractor can make a firm bid on the total project. The previously negotiated cost-plus contract can then be converted to a lump sum payment to cover all the required work. This provides the owner with protection against overruns which is not the case with cost-plus contracts.

In order to avoid delays in the start of emergency work because the owner and contractor cannot agree on the fee for the job, it is worthwhile making some prior arrangements with local contractors in the event of an emergency call-out. These arrangements would include equipment availabilities, mobilization times and fee scales.

Guaranteed Maximum Cost

Just as a contractor approaches a lump-sum agreement with many misgivings, so too will most owners contemplate any cost-plus arrangement. Indeed, many owners feel, perhaps not entirely unreasonably, that an unlimited cost-plus agreement destroys any real incentive to hold costs down and usually results in a large increase in the cost of construction. The issue can, of course, be debated, but the fact that this feeling is prevalent cannot be denied. To combat this threat, owners will often insist that the contractor agree to a guaranteed maximum price. Typically, this type of provision will fix a maximum amount, often referred to as an upset price. The contractor agrees that he is to be reimbursed by the owner for all the costs of the work up to a fixed amount, and the contractor further agrees that any cost of the work beyond that fixed amount will be his responsibility. The Federal Procurement Regulations call this a cost-plus-incentive-fee contract.

Shared-Savings Provisions

This type of agreement provides flexibility to cope with changed conditions, but also provides the owner with some protection against overruns by giving the contractor an incentive to control costs. It is, in one way, the reverse of the maximum price provision. Here, an amount is fixed by the agreement, often referred to as the "target" price. This target price is made up of the actual cost to the contractor for doing the job plus a variable fee for head office, related business expenses and profit. This fee varies according to whether the final cost is over or under the target estimate cost. That is, if the cost is greater than the target the fee is reduced, and if

the cost is less than the target the fee is increased. The factor by which the profit is varied is a bid item.

An example of a target price contract is as follows:

Target estimate = \$550,000
 Fee = \$110,000
 Reduction in fee for overruns = 5% of overrun
 Increase in fee for underrun = 20% of underrun

Case a) If actual price is \$680,000, then total cost to owner is:

Actual cost	= \$680,000
+ Fee	= 510,000
- Decrease in Fee = $(\$680,000 - 550,000) \times 5\%$	= 6,500
Total Cost	<u>\$783,500</u>

Case b) If actual cost is \$500,000, then the total cost to the owner is:

Actual cost	= 150,000
+ Fee	= 110,000
+ Increase in Fee = $(\$550,000 - 500,000) \times 20\%$	= 10,000
Total Cost	<u>\$670,000</u>

The Federal Procurement Regulations call this a contract with performance incentives.

In some cases, a maximum and minimum fee can be specified so that there is some control on the range of costs which may be incurred. It is also worthwhile putting in an upset price clause to ensure that costs do not exceed this limit. Otherwise, the contractor can exceed the target estimate by a wide margin and although his fee is minimal, he will still generate revenue while keeping his men and equipment busy and have little incentive to finish the job. In this respect, one should keep in mind that the target estimate may bear little relationship to the actual cost.

Target estimate contracts are suited to projects where the exact scope of the work is uncertain. This makes it difficult for the contractor to bid on a lump sum basis, while the owner wants to avoid a cost-plus contract in which there will be little incentive to control costs. An example of such a project would be excavation work where it is necessary to halt work at frequent intervals to allow traffic through. If the closure times cannot be precisely defined then the contractor cannot calculate his costs accurately. An example of this type of contract is described in Chapter 12.

WRITINGSPECIFICATIONS

The basic rule of writing specifications is for the owner to tell the contractor what he wants, not how to do the work, while protecting the interest of the owner. Protection of the owner's interest requires judgement and experience. An important rule is that each job is different and the type of contract selected, based on the factors discussed above, influences the specifications and method of payment. Standard or typical specifications can be helpful in the early stages of con-

tract preparation, but should never be used in a contract without careful review to determine applicability. The choice of an appropriate type of contract and the preparation of specifications will depend upon such factors as:

- Size of project
- Degree of owner supervision
- Degree of detail in design
- Project location, i.e. urban or rural
- Geological conditions, i.e. strong, competent rock or weak weathered rock

For example, specifications for blasting must ensure that an excavation is produced that meets the design requirements as to slope angle and long-term stability, and that no blasting damage is done to any surrounding structures. It must also allow flexibility to ensure that the best method is used to suit changing rock conditions and excavation requirements. However, it should also be kept in mind that restrictive specifications may result in the blasting operation being very expensive. It is good practice to require trial blasts at the start of the work to determine the optimum technique. Thus, specifications should provide general guidelines and required results with the choice of the actual methods being left to the contractor. This method is usually satisfactory if the contractor is experienced. The engineer should still have the authority to review the methods and results and request changes if necessary.

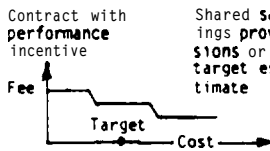
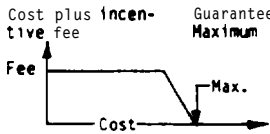
The following typical specifications cover many of the areas that need to be included in contracts that involve rock slope excavation.

TYPICAL SPECIFICATIONS*

*These specifications are for illustration purposes only; specific specifications should be prepared for each project to suit conditions. Dimensions (e.g. rock bolt lengths and diameters) should be determined from design calculations.

TABLE XII
TYPES OF CONTRACT

TYPE OF CONTRACT		GOVERNMENT (OWNER) VIEWPOINT		CONTRACTOR VIEWPOINT		EXAMPLES
Name	Common Name	Advantages	Disadvantages	Advantages	Disadvantages	
Fedcrd1 Procurement Regulations Cost plus a fixed fee	cost plus a fixed fee	Good owner/contractor team work. Quick start. Easy to make changes.	Higher costs. Lacks contractor initiative . No budget control.	No risk on costs . Higher chance of profit.	Low fee and profit.	Emergency work or projects not well defined such as repairing existing retaining walls.
Letter Contract	cost plus converted to lump sum	Immediate start. Easy to administer after conversion to lump sum.	Potential overruns.	Can negotiate Job after conditions known. In a strong negotiating position.		Emergency work (flood damage, rock falls, bridge failure, etc.).
Cost plus incentive fee	Guaranteed Maximum	Contractor will try to reduce costs through initiative to gain larger fee. Calling price fixed. Good owner/contractor team work.	Claims possible.	Good selling point for good contractor.	Risk on contractor for total cost.	Can be used if owner is using new construction techniques .
Contract with performance incentive	Shared savings provisions or target estimate	Contractor will try to reduce costs through initiative to gain larger fee. Good owner/contractor term work.	Possibility of serious overrun.	Good selling point for good contractor . Risk/profit shared by owner and contractor.	Low fee if costs high.	For larger Jobs where quantities are not precisely known but incentive is required to contain costs .
Fixed Price with Adjustable Unit Prices	Unit Price	Easy to make adjustments . Easy to determine final price. Low cost - pay for what you get.	Unbalancing, i.e. contractor puts high cost on items it expects will increase. Disputes and claims on quantities performed.	Easy estimating . Eliminates loss due to quantity variation.	Units may not be in relation to costs. Potential unbalancing .	Highway Jobs where excavation or rock support quantities are not exactly known, i.e. cubic yards of rock • x-caution; dowels; rock bolts; shotcrete ; linear yards of ditching.
Fin Fixed Price	Lump Sum	Fixed price good for budgeting, financing.	Claim if contractor runs into problems. Contractor may cut costs and do low quality job. Adversary status between contractor and owner.	Good profit. Clean cut, easy book-keeping.	High risk if conditions change such as poor weather, unstable slopes .	Excavation where quantities are well defined, slope can be cut to specified angle, quantities of support well specified. Construction of concrete buttress where anchoring, reinforcement quantities are well defined.
Fixed Price with Escalation	Unit Price or Lump sum with Escalation	Same plus possible lower costs because of reduced contractor risk.	Same plus increased administration.	Same plus less risk of loss due to uncontrollable costs.	Same plus increased administration.	Large job requiring long periods of time.
Indefinite Delivery Type Contract	Open ended or Day rate	Can award contract prior to requirement. Easy to control costs. Responsive to quick requirements.	Higher cost.	Good fill in between jobs.	Difficult to schedule.	used for small jobs that can be started or stopped readily such as ditching, sealing, clean-up of rock falls, etc.



1.0 LIMITS OF EXCAVATION

All excavation shall be to the lines and grades shown in the drawings. Any excavation beyond these lines and grades, which is performed by the Contractor for any reason whatsoever, shall be at the expense of the Contractor. Surveying during excavation, for excavation control purposes, shall be the responsibility of the Contractor.

All quantities shall be measured and classified in place to the lines shown on the drawings. Surveying for the purpose of payment shall be the responsibility of the Engineer.

2.0 CLASSIFICATION OF MATERIALS

Except as otherwise provided in these specifications, material will be classified for payment as follows.

2.1 Rock Excavation

For purposes of classification of excavation, rock is defined as sound and solid masses, layers, or ledges of mineral matter in place and of such hardness and texture that:

- 1) It cannot be effectively loosened or broken down by ripping in a single pass with a late model tractor-mounted hydraulic ripper equipped with one digging point of standard manufacturer's design adequately sized for use with, and propelled by a crawler-type tractor with a net flywheel power rating between 210 and 240 horsepower, operating in low gear.

or

- 2) In areas where it is impracticable to classify by use of the ripper described above, rock excavation is defined as sound material of such hardness and texture that it cannot be loosened or broken down by a 6 lb. drifting pick. The drifting pick shall be Class D, Federal Specification CCC-H-506d with a handle not less than 34 inches in length.

All boulders or detached pieces of solid rock more than 1 cubic yard in volume will be classified as rock excavation.

2.2 Common Excavation

Common excavation includes all material other than rock excavation. All boulders or detached pieces of solid rock less than 1 cubic yard in volume will be classified as common excavation (328).

3.0 ROCK EXCAVATION SPECIFICATIONS

In order to excavate the site to the required elevations, rock blasting will be necessary.

The stability of the final cut slopes and foundations will depend to some degree upon the existing jointing and crack system in the rock, and will be influenced greatly by the procedures of blasting that are used. Consequently, the Contractor shall

14.10

carefully control all blasting by limiting the size and type of the charges in accordance with these specifications, varying the size and spacing of drill holes, using delays, and such other controls as may be reasonably required by the circumstances in order to preserve the rock strength beyond the required minimum lines and grades in the soundest possible conditions.

Trial blasts shall be conducted as required by the Engineer at the start of the work, and at other times when the rock and/or the dimensions of the blasts change, to determine the optimum drill hole layout, explosive loads and delay sequences. The specifications below shall be used as a guideline in determining the optimum procedure.

3.1 Experience of Contractor

The foreman who provides on-site supervision of the work described in this Contract shall have a minimum of two years experience in controlled blasting. Before starting operations the Contractor shall submit to the Engineer a resume of the qualifications and experience of the foreman.

3.2 Alterations by Contractor

Not later than three (3) days prior to commencing excavation in the specified areas, and at any time the Contractor proposes to alter his methods of excavation, he shall submit to the Engineer for review full details of the drilling and blasting patterns and controls he proposes to use in the specified areas. The Contractor shall not commence excavation in the areas or change his method of excavation until his drilling and blasting patterns, controls, and his methods have been reviewed by the Engineer.

If, in the opinion of the Engineer, the methods of excavation adopted by the Contractor are unsatisfactory in that they result in an excessive amount of excavation and/or rock damage beyond the minimum lines and grades or that they fail to satisfy the requirements specified elsewhere in these specifications, then, notwithstanding the Engineer's prior review of such methods, the Contractor shall adopt such revised methods, techniques and procedures as are necessary to achieve the required results.

3.3 Excavation Of Slopes

To ensure that final slopes are stable, controlled blasting shall be used to minimize the damage to the rock behind the faces. The following specifications describe the general method of blasting to be used on final slopes. The optimum procedure, which may vary at different locations on the site, shall be determined from trial blasts.

The maximum bench height when excavating on the final slopes shall be (for bench heights see Chapter 111; this is to ensure control over drill hole direction so that the holes on the final slopes are evenly spaced.

Controlled Blasting Terminology

These specifications, in part, provide for the use of final line holes, buffer holes, production holes, maximum charges

and blasting delays to achieve the specified blasting control for the slopes. Explanation Of tk888 terms are as follows:

3.3.1 Final Line Blasting

- 1) Blast holes and timing in detonation sequence - "Controlled Blasting" is the technique of carefully drilling the final line of holes on the plane of the final cut slope required. Each hole of the final line is loaded with an explosive charge "decoupled" from the blast hole wall with a centering sleeve. The holes are fired simultaneously, and first or last in the delay sequence to create a crack along the plane of the final rock surface.
- 2) Alignment and depth of holes in the final line - The final line of holes shall be on tk8 line of the final face and the spacing shall be as uniform as possible, and the diameter of these holes shall not be greater than (for hole diameters 884 Chapter 11). The bottom8 Of final line holes shall not be positioned at a higher elevation than tk8 bottom8 of adjacent production blast holes. The depth of tk8 final line holes shall be limited to (for hole lengths 888 Chapter 11).
- 3) Explosives - The hole spacing and amount of explosive in the final line of holes may require adjusting, depending on surface quality and integrity of the exposed rock surface and conditions encountered during the progress of the work. Water resistant explosives may be required for some of the work.

3.3.2 Buffer Row

- 1) Buffer holes and charges - The line of buffer holes shall be parallel to the final line of holes and shall be the same diameter as in the holes of the final line. The amount of explosives per hole shall be less than the explosive used per production hole contained in the main pattern. The purpose of the88 holes is to protect the final face by more uniformly distributing the explosive within the rock adjacent to the face.

3.3.3 Production Holes

- 2) Hole pattern and loading - The main production blasting shall use (for hole diameters see Chapter 11) diameter holes laid out to detonate in a delay sequence employing the criteria of loading and maximum charge per detonation given in Maximum Charges and Delays, Section 3.3.4, following. Detonation shall be toward a free face.

3.3.4 Maximum Charges and Delays

- 1) Maximum charges - Vibrations generated by detonation of charges for both the final line and main pattern blasting shall be controlled by use of delays to minimize damage to the surrounding rock. The Contractor shall advise the Engineer in sufficient time prior to each blast to provide the Engineer with an opportunity to monitor the vibrations from the blast if desired.

- 21 Design of delays - Delay sequencing for multiple shots may be accomplished through the use of short period delays of the type appropriate to the method of fusing adopted.

3.4 CONTROL OF FLYROCK

Precautions shall be taken to ensure that flyrock from the blasting operations does not reach the locations designated on the drawings.

3.5 SCALING

The objective of scaling shall be to remove loose blocks of rock and to ensure that the new face is stable.

3.5.1 Method

Scaling shall be conducted under the supervision of the Engineer who shall determine the areas to be scaled, the scaling method to be employed, and shall inspect the new faces. Hand scaling shall be employed except where other means, such as hydraulic splitters or light blasting is approved by the Engineer. Scaling shall start at the top of the slope and work downwards, to roadbed level. After scaling, the new face shall be inspected by the Engineer to determine whether or not scaling is complete.

3.5.2 Blasting

When blasting is required, the force shall be sufficient to remove the block but not damage the surrounding rock. If a crack exists between the loose block and the slope, the explosive can be placed in this crack.

3.5.3 Drilling

If drilling is required, the holes shall be parallel, drilled in straight lines, and have the spacing equal to about 10 times the hole diameter. They shall be loaded with sufficient explosive to break the rock between the holes but not damage the new face. All blasting shall be conducted by an experienced powder man, with blasting patterns subject to review by the Engineer.

3.6 Ditching of Hook Slopes

The excavation of ditches along the toe of certain slopes is required to prevent falling rock from reaching the roadbed.

3.6.1 The areas to be ditched shall be specified by the Engineer.

3.6.2 Near vertical slopes close to the roadbed shall not be ditched where the Engineer determines that excessive rock excavation will result.

3.6.3 The dimensions of ditches are specified on the drawings; care shall be taken to ensure that the excavation does not undercut the roadbed.

3.6.4 The ditch shall have vertical sides and a horizontal base to ensure that rocks fall vertically and do not bounce outwards towards the roadbed. If possible, a 6 inch thick layer of fine, broken rock, or sand, shall be left in the bottom of the ditch to absorb the impact of falling rock.

3.6.5 Trim blasting techniques shall be used such that permanent vertical slopes are produced and that damage to the rock behind the face is minimized. Any excavation beyond the minimum lines specified by the Engineer, which is performed by the Contractor for any purpose whatsoever, shall be at the expense of the Contractor, unless it has received the prior approval of the Engineer. The Contractor is cautioned to ensure that the final line drill holes conform with the planned excavation limits.

3.6.6 The holes for the trim line shall be parallel to each other and to the side of the ditch. Hole spacing shall be about 10 times the hole diameter.

3.6.7 The explosive load in the back line shall be sufficient to break the rock along the minimum excavation line and shall be equivalent to about (for explosive loads see Chapter 11). The trim line shall be detonated on a single delay.

3.6.8 The broken rock shall be removed from the ditch with loading equipment working in the excavation, pushing the material to one point for disposal. Care is to ensure that the toe of the cut slope is as near vertical as possible and to minimize damage to the pavement from loading equipment. Care shall also be exercised not to undermine the roadbed.

3.6.9 The ditch shall be graded such that drainage will occur and water does not collect at low points.

3.6.10 At the completion of excavation, the cut slopes shall be inspected by the Engineer and rock bolts and dowels shall be installed as required to stabilize potentially unstable rock.

4.0 SUPPORT OF ROCK SLOPES

4.1 Dowels

Natural fractures in the rock slope may produce potentially unstable blocks of rock that must be supported. Locations on the slope that require support will be determined by the Engineer. Dowels consisting of reinforcing steel (for length and diameter see Chapter 12) fully grouted into holes drilled into the face. The grout shall be Type I Portland cement. Plates and nuts on the face of the slope shall not be required. The dowels shall be installed during excavation from the current working bench.

4.2 Rock Bolts

The function of rock bolts is to exert permanent normal force across potential failure planes. This time, the frictional force and resists sliding.

4.2.1 All rock bolts to be installed in this work shall be products of a manufacturer regularly engaged in the manufacture of rock bolts. Bolts shall be fabricated from deformed bars and tensionable. Permissible types are:

- 1) A mechanically-anchored, hollow, groutable bolt.
- 2) A 2-stage-setting resin-embedded bolt.
- 3) A plastic-covered bolt (approved by the Engineer) with grout anchor.

4.2.2 The length of each bolt to be installed shall be determined from measurements to be made at the time of stabilization. Unless specified herein, the length of each bolt in the rock shall be approximately twice the thickness of the slab or block to be stabilized.

4.2.3 Rock bolts shall be fully corrosion-protected. All parts of the bolt, bearing plate, and nut on the surface of the cut, shall either be encased in shotcrete or painted with a corrosion protective paint.

4.2.4 The cement grout used for rock bolt types (1) or (3) described above shall be a non-shrink type grout and achieve a strength of 3,000 pounds per square inch in not more than 4 days. Portland cement shall not be used. Resin may be epoxy or polyester in bulk or cartridge form, but shall be a make approved by the Engineer.

4.2.5 When the end of the bolt is anchored in place (either mechanically or chemically), each bolt shall be tensioned to (for required tension see Chapter 7) with a hollow-ram hydraulic jack. Load/extension measurements shall be made during tensioning. If the load cannot be maintained for 10 minutes, or the extension (after shell tightening) exceeds the elastic strain of the bolt by 20 percent, the bolt shall be replaced or a further bolt installed in a separate hole.

4.2.6 After tensioning and approval by the Engineer, the full length of the bolt shall then be grouted with non-shrink grout to ensure that tension is maintained permanently along the length of the bolt. One or more representative rock bolts shall be pulltested to failure if so requested by the Engineer.

4.2.7 The hydraulic jack and pressure gauge used for tensioning shall be calibrated by a registered calibration agency, a maximum of 1 month prior to the tensioning operation, and a copy of the calibration certificate shall be shown to the Engineer before tensioning begins.

4.2.8 A bearing plate, a hardened flat washer and a nut shall be used to transfer the tension in the bolt to the rock. The plate shall be in uniform contact with the rock surface. If the rock face is not perpendicular to the axis of the bolt, or the rock under the bearing plate is not sound, a bearing pad approved by the Engineer shall be constructed so that the bolt is not bent when the tension is applied. Bevelled washers may also be used to level a bearing plate. Where the rock surface is generally weak or weathered, extra large bearing plates (such as 8 inch square) shall be used.

4.2.9 The installation of the corrosion protection, the installation method and the tensioning, should all be carried out according to the manufacturer's specifications.

4.3 Shotcrete

The function of shotcrete is to eliminate erosion effects, prevent blocks on the face from becoming loose, and to hold in place blocks that can slide on adversely oriented joint or fault surfaces.

4.3.1 Personnel

The foreman shall have good personal experience, including not less than two years as a shotcrete nozzleman. The nozzleman shall have worked at least six months applying a similar application and shall be able to demonstrate by testing his ability to perform satisfactorily his duties and to gun shotcrete of the required quality.

4.3.2 Materials

Materials used shall be a pre-mix shotcrete product manufactured by a manufacturer regularly engaged in the manufacture of concrete products. Class "A" aggregate shall be used which shall conform to ACI Standards for fine aggregate. The water used for mixing and curing shall be clean and free from substances which might be deleterious or corrosive to concrete or steel, and shall be furnished by the Contractor. The Contractor, if so requested by the Engineer, shall submit reports of tests made by a competent laboratory, on samples of the water which he proposes to use or is using.

Admixtures such as accelerators, air entraining admixtures or retarders, if used, shall be approved by the Engineer.

4.3.3 Strength

The shotcrete shall achieve a minimum 28-day strength of 3,500 pounds per square inch.

The responsibility for the design of all mixes for the mortar and for the quality of the mortar placed in the work shall rest with the Contractor.

No cement/sand mixture shall be used if allowed to stand for 45 minutes or more before use.

4.3.4 Equipment Requirements

The mixing equipment shall be capable of thoroughly mixing the specified materials in sufficient quantity to maintain continuous placing.

In order to ensure that the cement/sand premix will flow at a uniform rate (without slugs) through the main hopper, delivery hose, and dry-mix nozzle to form uniform shotcrete (free of dry pockets) on the rock surface, pre-dampening (also referred to as pre-moisturizing) equipment shall be used to bring the moisture content from essentially zero, in sealed transporting bags, to within the range of three percent to six percent. Pre-dampening shall be carried out prior to flow into the main hopper, and immediately after flow out of the bags.

The air compressor shall be capable of supplying clean air adequate for maintaining sufficient nozzle velocity throughout all

phases of the work, as well as for the simultaneous operation of a blow pipe for clearing away rebound.

4.3.5 Quality Control

In order to satisfy himself as to the quality of the mortar being placed in the Work, the Engineer will inspect all aspects of the manufacture and placement of mortar and carry out such tests on the mortar and its constituent materials as he may deem necessary. The Contractor shall cooperate fully and provide all necessary assistance to enable the Engineer to carry out such inspections and tests.

Test cylinders of mortar shall be shot with the same air pressure, nozzle tip, and hydration as the mortar being placed at the point in the Work where the cylinders are taken.

4.3.6 Surface Preparation

Prior to the application of mortar, all mud, loose, shattered and rebound material, and all other objectionable matter shall be removed from the surface against which the mortar is to be placed. Sand blasting procedure shall be used to effect the necessary cleaning of the surface against which the mortar is to be placed, as and where directed by the Engineer. The surface shall be washed clean immediately prior to shotcreting, using alternate jets of air and water. Care shall be taken that key blocks are not removed.

4.3.7 Mesh Reinforcement

Areas that are to be covered with mesh reinforcement shall be determined by the Engineer. The mesh shall consist of welded wire mesh 4 inches by 4 inches opening size which shall be securely attached to the rock surface with pins grouted into holes not less than 12 inches deep at a minimum spacing of 5 ft. The exposed portion of the pins shall be threaded so that a nut and washer can be used to place the mesh in contact with the surface. The location of mesh pins shall be approved by the Engineer. At all splices the wire fabric shall be lapped a minimum of 8 inches.

4.3.8 Application

The area of each rock face to be shotcreted shall be determined by the Engineer. On competent rock slopes where only cracks are to be covered, the shotcrete shall extend at least 12 inches on either side of the crack. A minimum thickness of 1-1/2 inches and an average thickness of three inches shall be applied, and reinforcing mesh shall be completely encased. The shotcrete shall be applied from the bottom of the slope upward so that rebound does not accumulate on rock that has still to be covered. Surfaces to be shot shall be damp but have no free standing water. No shotcrete shall be placed on dry, dusty or frosty surfaces. The nozzle shall be held at a distance and at an angle from the perpendicular to the working face so that rebound material will be minimal and compaction will be maximal; this distance is usually between two and five feet.

A nozzleman's helper equipped with an air blow-out jet shall attend the nozzleman, at all times during the placement of mortar, to keep the working area free from rebound.

Mortar shall emerge from the nozzle in a steady, uninterrupted flow. When for any reason the flow becomes intermittent, the nozzle shall be diverted from the work until steady flow resumes.

Where a layer of shotcrete is to be covered by a succeeding layer, it shall first be allowed to take its initial set. Then all laitance, loose material and rebound shall be removed by brooming. In addition, the surface should be thoroughly sounded with a hammer for drummy areas resulting from rebound pockets or lack of bond. Drummy areas, age, or other defects shall be carefully cut out and replaced with a succeeding layer.

Rebound shall not be worked back into the construction by the nozzleman; if it does not fall clear of the work it must be removed. Nor shall the rebound be salvaged and included in later batches because of the danger of contamination.

Construction joints shall be tapered over a minimum distance of 12 inches to a thin edge, and the surface of such joints shall be thoroughly wetted before any adjacent action of mortar is placed. No square joints shall be permitted.

Shooting shall be temporarily suspended if:

- High wind prevents the nozzleman from proper application of the material.
- The temperature is below 35°F and the work cannot be protected.
- Rain occurs which may wash cement out of the freshly placed material and cause sloughs in the work.

4.3.9 Drainage

Drainage holes shall be provided so that water pressure does not build up behind the shotcrete. The drains shall be produced by driving wooden plugs into cracks designated by the Engineer prior to shotcreting. After the shotcrete has obtained its initial set, the plugs shall be removed.

4.3.10 curing

Either the shotcrete surface shall be kept continuously wet for at least seven days or membranes curing shall be used. The air in contact with shotcrete surfaces shall be maintained at temperature above freezing for a minimum of seven days.

4.3.11 Testing

At each site and for each new batch of shotcrete, small, unreinforced test panels at least one foot square and three inches thick shall be gunned, if required by the Engineer. These panels will be inspected by the Engineer and periodically cured for testing purposes.

Chapter 14 : References

324. OFFICE OF THE FEDERAL REGISTER, NATIONAL ARCHIVES AND RECORDS SERVICE, GENERAL SERVICES ADMINISTRATION, Code of Federal Regulations 41, Public Contracts and Property Management, Chapters 1 and 2, as of July 1st, 1977 (41CFR 1-1 Federal Procurement Regulation).
325. PEURITTOY, R.L. Construction Planning, Equipment and Methods, 2nd Ed. McGraw-Hill Book Company, New York, 1970.
326. CRIMMINS, R., SAMUELS, R., AND MONAHAN, B.P. Construction Rock Work Guide, Wiley-Interscience, New York, 1972.
327. BERMAN, T. AND CROSSLAND, S.H. Selecting the Appropriate Construction Contract, Chapter 14 of Construction Business Handbook, McGraw-Hill Book Co., New York, 1972.
328. GOODMAN, R. Methods of Geological Engineering, West Publishing Company, St. Paul, 1976.

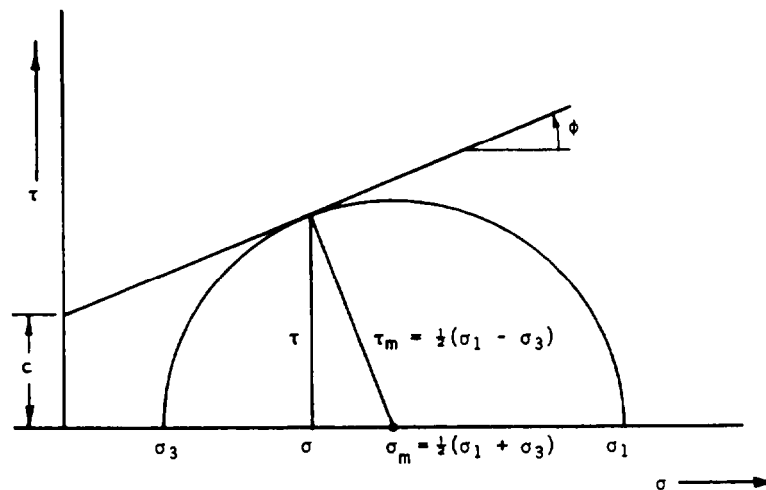
Appendix 1 : Analysis of laboratory strength test data

Introduction

The choice of the shear strength of a failure surface or zone is a critical part of any slope stability analysis. Consequently, the analysis of laboratory strength test data is an important component of any slope design.

This appendix presents a number of simple statistical regression analyses which can be used to determine the angle of friction and the cohesive strength or the constants which define the non-linear failure characteristics of rock or soil. These analyses are presented in □ form which is designed to facilitate programming on a programmable calculator or computer.

Determination of the angle of friction and cohesive strength for a Mohr-Coulomb failure criterion



The Mohr-Coulomb failure criterion may be expressed in the following forms :

$$\tau = c + \sigma \tan \phi \quad 1$$

$$\tau_m = c \cdot \cos \phi + \sigma_m \cdot \sin \phi \quad 2$$

$$\sigma_1 = \frac{2c \cdot \cos \phi}{1 - \sin \phi} + \sigma_3 \frac{1 + \sin \phi}{1 - \sin \phi} \quad 3$$

These equations may be expressed in the general form :

$$y = a + bx \quad 4$$

The constants a and b and the coefficient of determination r^2 can be determined by linear regression analysis as follows:

$$b = \frac{\sum xy - \frac{\sum x \sum y}{n}}{\sum x^2 - \frac{(\sum x)^2}{n}} \quad 5$$

$$a = \left(\frac{\sum y}{n} - b \cdot \frac{\sum x}{n} \right) \quad 6$$

$$r^2 = \frac{(\sum xy - \sum x \sum y / n)^2}{(\sum x^2 - (\sum x)^2 / n) (\sum y^2 - (\sum y)^2 / n)} \quad 7$$

where x , y are successive data pairs and n is the total number of such pairs.

The angle of friction ϕ and the cohesive strength c are calculated as follows :

a. For input $x = \tau$ and $y = \sigma$

$$\phi = \text{Arctan } b \quad 8$$

$$c = a \quad 9$$

b. For input $x = \tau_m$ and $y = \sigma_m$

$$\phi = \text{Arcsin } b \quad 10$$

$$c = a / \cos \phi \quad 11$$

c. For input $x = \sigma_1$ and $y = \sigma_3$

$$\phi = \text{Arcsin } \frac{b - 1}{b + 1} \quad 12$$

$$c = \frac{a \cdot (1 - \sin \phi)}{2 \cos \phi} \quad 13$$

Determination of material constants defining non-linear failure criterion

The non-linear failure criterion defined by equation 29:

$$\sigma_1 = \sigma_3 + \sqrt{m \sigma_c \sigma_3 + s \sigma_c^2} \quad 29$$

may be rewritten as :

$$y = m \sigma_c x + s \sigma_c^2 \quad 14$$

where $y = (\sigma_1 - \sigma_3)^2$ and $x = \sigma_3$

Intact rock

For intact rock, $s = 1$ and the uniaxial compressive strength σ_c and the material constant m are given by :

$$\sigma_c^2 = \frac{\sum y}{n} - \left[\frac{\sum xy - \frac{\sum x \sum y}{n}}{\sum x^2 - \frac{(\sum x)^2}{n}} \right] \frac{\sum x}{n} \quad 15$$

$$m = \frac{1}{\sigma_c} \left[\frac{\sum xy - \frac{\sum x \sum y}{n}}{\sum x^2 - \frac{(\sum x)^2}{n}} \right] \quad 16$$

The coefficient of determination r^2 is determined from equation 7 above. The closer the value of r^2 is to 1.00, the better the fit of the empirical equation to the triaxial test data.

Broken or heavily jointed rock

For a broken or heavily jointed rock mass, the strength of the intact pieces of rock is determined from the analysis presented on the previous page. The value of m for the broken or heavily jointed rock is found from equation 16 and the value of the constant s is given by :

$$s = \frac{1}{\sigma_c^2} \left[\frac{\sum y}{n} - m \sigma_c \frac{\sum x}{n} \right] \quad 17$$

The coefficient of determination r^2 is found from equation 7.

When the value of the constant s is very close to zero, equation 17 will sometimes give a small negative value. In such cases, put $s = 0$ and calculate m as follows :

$$m = \frac{\sum y}{\sigma_c \sum x} \quad 18$$

When equation 18 is used, the coefficient of determination r^2 cannot be calculated from equation 7.

Mohr envelope

The relationships between the shear strength τ and the normal stress σ and the principal stresses σ_1 and σ_3 are defined by the following equations * :

$$\sigma = \sigma_3 + \frac{\tau_m^2}{\tau_m + m\sigma_c/8} \quad 19$$

$$\tau = (\sigma - \sigma_3) \sqrt{1 + m\sigma_c/4\tau_m} \quad 20$$

By substituting successive pairs of σ_1 and σ_3 values into equations 19 and 20, a complete Mohr envelope can be generated. While this process is convenient for some applications, it is not convenient in slope stability calculations in which the shear strength is required for specified normal stress values. A more useful expression for the Mohr envelope is given by equation 30 on page 107 :

$$\tau = A\sigma_c \left(\sigma/\sigma_c - T \right)^B \quad 30$$

where A and B are empirical constants which are determined as follows :

Rewriting equation 30 :

$$y = ax + b \quad 31$$

where

$$\begin{aligned} y &= \log \tau / \sigma_c \\ x &= \log (\sigma / \sigma_c - T) \\ a &= B \\ b &= \log A \\ T &= \frac{1}{2} (m + \sqrt{m^2 + 4s}) \end{aligned}$$

* BALMER, G. A general analytical solution for Mohr's envelope. *Amer. Soc. Testing Materials*, Vol. 52, 1952, pages 1260-1271.

The values of the constants A and B are given by :

$$B = \frac{\frac{\sum \tau \tau}{n} - \frac{(\sum \tau)^2}{n^2}}{\frac{\sum \sigma^2}{n} - \frac{(\sum \sigma)^2}{n^2}} \quad 32$$

$$\log A = \frac{\sum \tau}{n} - B \frac{\sum \sigma}{n} \quad 33$$

Values of A and B are calculated for values of σ and τ given by substituting the following values of σ_3 into equations 29, 19 and 20 :

$$\sigma_{3m}, \sigma_{3m}/2, \sigma_{3m}/4, \sigma_{3m}/8, \sigma_{3m}/16, \sigma_{3m}/32, \sigma_{3m}/64, \sigma_{3m}/128, \\ \sigma_{3m}/256, T/4, T/2, 3T/4 \text{ and } T$$

where σ_{3m} is the maximum value of σ_3 for the data set being analysed and $T = \frac{1}{2}(m - \sqrt{m^2 + 4s})$.

The instantaneous friction angle ϕ_i and the instantaneous cohesive strength c_i for a given value of the normal stress σ are given by :

$$\phi_i = \text{Arctan } AB(\sigma/\sigma_c - T)^{B-1} \quad 34$$

$$c_i = \tau - \sigma \tan \phi_i \quad 35$$

Practical *example* of non-linear analysis

The following set of data was obtained from a series of triaxial tests on intact samples of andesite :

σ_1 (MPa)	269.0	206.7	503.5	586.5	683.3
σ_3 (MPa)	0	6.9	27.6	31.0	69.0

Analysis of the data, using $\sigma_{3m} = 69$ MPa, gave

$\sigma_c = 265.5$ MPa, $m = 18.84$, $s = 1$, $r^2 = 0.85$, $A = 1.115$ and $B = 0.698$.

Carefully drilled 154mm diameter cores of heavily jointed andesite were tested triaxially and gave the following set of data :

σ_1 (MPa)	1.24	6.07	8.96	12.07	12.82	19.31	20.00
σ_3 (MPa)	0	0.35	0.69	1.24	1.38	3.45	3.45

Analysis of these data, using $\sigma_{3m} = 3.45$ MPa, gave

$m = 0.277$, $s = 0.0002$, $T = -0.00072$, $r^2 = 0.99$, $A = 0.316$ and $B = 0.700$.

Appendix 2 : Wedge solution for rapid computation

Introduction

The solution of the wedge problem presented in reference 201 was designed for teaching purposes rather than for convenience of calculation. In this appendix, two solutions designed for maximum speed and efficiency of calculation are given. These solutions are :

1. A short solution for a wedge with a horizontal slope crest and with no tension crack. Each plane may have a different friction angle and cohesive strength and the influence of water pressure on each plane is included in the solution. The influence of an external force is not included in this solution.
2. A comprehensive solution which included the effects of a superimposed load, a tension crack and an external force such as that applied by a tensioned cable.

The short solution is suitable for programming on a pocket calculator such as a Hewlett-Packard 67 or a Texas Instruments SR52. It can also be used with a non-programmable calculator such as a Hewlett-Packard 21 and a typical problem would require about 30 minutes of calculation on such a machine.

The comprehensive solution is 4 to 5 times longer than the short solution and would normally be programmed on a desk top calculator or in a computer.

SHORT SOLUTION

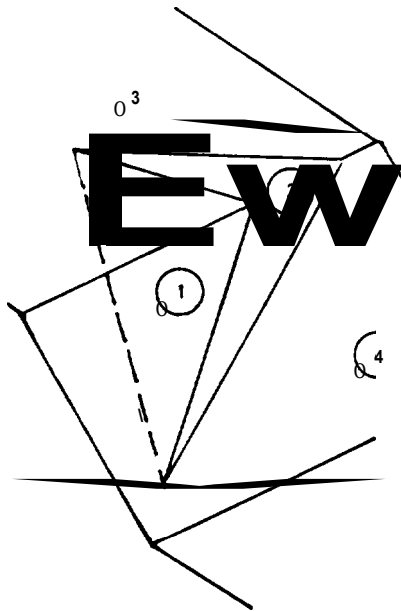
Scope of solution

The solution presented is for the computation of the factor of safety for translational slip of a tetrahedral wedge formed in a rock slope by two intersecting discontinuities, the slope face and the upper ground surface. It does not take account of rotational slip or toppling, nor does it include a consideration of those cases in which more than two intersecting discontinuities isolate tetrahedral or tapered wedges of rock. In other words, the influence of a tension crack is not considered in this solution.

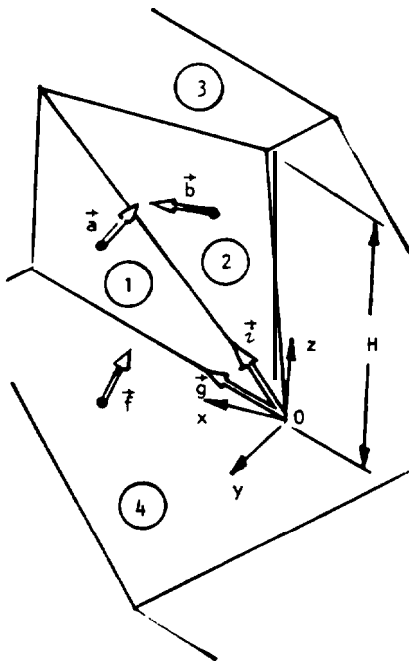
The solution allows for different strength parameters and water pressures on the two planes of weakness. It is assumed that the slope crest is horizontal, i.e. the upper ground surface is either horizontal or dips in the same direction as the slope face or at 180° to this direction.

When a pair of discontinuities are selected at random from a set of field data, it is not known whether :

- a) the planes could form a wedge (the line of intersection may plunge too steeply to daylight in the slope face or it may be too flat to intersect the upper ground surface).



Plane 1 overlies plane 2



b) one of the planes overlies the other (this affects the calculation of the normal reactions on the planes)

c) one of the planes lies to the right or the left of the other plane when viewed from the bottom of the slope.

In order to resolve these uncertainties, the solution has been derived in such a way that either of the planes may be labelled 1 (or 2) and allowance has been made for one plane overlying the other. In addition, a check on whether the two planes do form a wedge is included in the solution at an early stage. Depending upon the geometry of the wedge and the magnitude of the water pressure acting on each plane, contact may be lost on either plane and this contingency is provided for in the solution.

Notation

The geometry of the problem is illustrated in the margin sketch. The discontinuities are denoted by 1 and 2, the upper ground surface by 3 and the slope face by 4. The data required for the solution of the problem are the unit weight of the rock γ , the height H of the crest of the slope above the intersection O , the dip ψ and dip direction α of each plane, the cohesion c and the friction angle ϕ for planes 1 and 2 and the average water pressure u on each of the planes 1 and 2*. If the slope face overhangs the toe of the slope, the index η is assigned the value of -1 ; if the slope does not overhang, $\eta = +1$.

Other terms used in the solution are :

F = factor of safety against wedge sliding calculated as the ratio of the resisting to the actuating shear forces

A = area of a face of the wedge

W = weight of the wedge

N = effective normal reaction on a plane

S = actuating shear force on a plane

x, y, z = co-ordinate axes with origin at O . The z axis is directed vertically upwards, the y axis is in the dip direction of plane 2

\vec{a} = unit vector in the direction of the normal to plane 1 with components (a_x, a_y, a_z)

\vec{b} = unit vector in the direction of the normal to plane 2 with components (b_x, b_y, b_z)

\vec{f} = unit vector in the direction of the normal to plane 4 with components (f_x, f_y, f_z)

\vec{g} = vector in the direction of the line of intersection of planes 1 and 4 with components (g_x, g_y, g_z)

\vec{z} = vector in the direction of the line of intersection of planes 1 and 2 with components (z_x, z_y, z_z)

* If it is assumed that the discontinuities are completely filled with water and that the water pressure varies from zero at the free faces to a maximum at some point on the line of intersection, then $u_1 = u_2 = \gamma_w H_w / 6$ where H_w is the overall height of the wedge.

$$i = -i_z$$

q = component of \vec{g} in the direction of \vec{b}

r = component of \vec{a} in the direction of \vec{b}

$$k = |\vec{i}|^2 = i_x^2 + i_y^2 + i_z^2$$

$$Z = W/A_2$$

$$p = A_1/A_2$$

$$n_1 = N_1/A_2$$

$$n_2 = N_2/A_2$$

$$|Zi|/\sqrt{k} = SA_2$$

} Assuming contact on both planes

$$m_1 = N_1/A_2$$

denominator of $F = S_1/A_2$ } contact on plane 1 only

$$m_2 = N_2/A_2$$

denominator of $F = S_2/A_2$ } contact on plane 2 only

Sequence of calculations

The factor of safety of a tetrahedral wedge against sliding along a line of intersection may be calculated as follows :

1. $(a_x, a_y, a_z) = \{\sin\psi_1 \cdot \sin(\alpha_1 - \alpha_2), \sin\psi_1 \cdot \cos(\alpha_1 - \alpha_2), \cos\psi_1\}$
2. $(f_x, f_y, f_z) = \{\sin\psi_4 \cdot \sin(\alpha_4 - \alpha_2), \sin\psi_4 \cdot \cos(\alpha_4 - \alpha_2), \cos\psi_4\}$
3. $b_y = \sin\psi_2$
4. $b_z = \cos\psi_2$
5. $i = a_x b_y$
6. $g_z = f_x a_y - f_y a_x$
7. $q = b_y (f_z a_x - f_x a_z) + b_z g_z$
8. If $\eta q/i > 0$, or if $\eta (f_z - q/i) \tan\psi_3 > \sqrt{a_x^2 + a_y^2}$ and $\sigma_3 = \alpha_4 \pm (1 - \eta) \pi/2$, no wedge is formed and the calculations should be terminated.
9. $r = a_y b_y + a_z b_z$
10. $k = 1 - r^2$
11. $Z = (\gamma H q) / (3 g_z)$
12. $p = -b_y f_x / g_z$
13. $n_1 = \{(Z/k) (a_x - r b_z) - p u_1\} \cdot p / |p|$
14. $n_2 = \{(Z/k) (b_z - r a_z) - u_2\}$
15. $m_1 = (Z a_z - r u_2 - p u_1) \cdot p / |p|$
16. $m_2 = (Z b_z - r p u_1 - u_2)$
17. a) If $n_1 > 0$ and $n_2 > 0$, there is contact on both planes and

$$F = (n_1 \cdot \tan\phi_1 + n_2 \cdot \tan\phi_2 + |p| c_1 + c_2) \sqrt{k} / |Zi|$$
- b) If $n_2 < 0$ and $m_1 > 0$, there is contact on plane 1

only and

$$F = \frac{m_1 \cdot \tan \phi_1 + |p| c_1}{\{Z^2(1 - a_z^2) + ku_2^2 + 2(ra_z - b_z)Zu_2\}^{\frac{1}{2}}}$$

c) If $n_1 < 0$ and $m_2 > 0$, there is contact on plane 2 only and

$$F = \frac{m_2 \cdot \tan \phi_2 + c_2}{\{Z^2 b_y^2 + kp^2 u_1^2 + 2(rb_z - a_z)pZu_1\}^{\frac{1}{2}}}$$

d) If $m_1 < 0$ and $m_2 < 0$, contact is lost on both planes and the wedge floats as a result of water pressure acting on planes 1 and 2. In this case, the factor of safety falls to zero.

Example

Calculate the factor of safety against wedge failure of a slope for which the following data applies :

Plane	1	2	3	4
ψ°	47	70	10	65
α°	052	018	045	045

$$\gamma = 25 \text{ kN/m}^3, H = 20\text{m}, c_1 = 25 \text{ kN/m}^2, c_2 = 0.$$

$$\phi_1 = 30^\circ, \phi_2 = 35^\circ, u_1 = u_2 = 30 \text{ kN/m}^2, \eta = +1$$

$$1. (a_x, a_y, a_z) = (0.40897, 0.60632, 0.68200)$$

$$2. (f_x, f_y, f_z) = (0.41146, 0.80753, 0.42262)$$

$$3. b_y = 0.93969$$

$$4. b_z = 0.34202$$

$$5. i = 0.38431$$

$$6. g_z = -0.08078$$

$$7. q = -0.12981$$

$$8. "q/i < 0; \eta(f_z - q/i) \tan \psi_3 - \sqrt{1 - f_z^2} < 0.$$

A wedge is formed. continue calculation sequence.

$$9. r = 0.80301$$

$$10. k = 0.35517$$

$$11. Z = 265.969$$

$$12. p = 4.78639$$

$$13. n_1 = 161.456$$

$$14. n_2 = -183.988$$

$$15. m_1 = 13.7089$$

$$16. m_2 = -54.3389$$

17. $n_2 < 0$ and $m_1 > 0$, hence there is contact on plane 1 only ;

c) gives $F = 0.626$ and hence the slope is unstable.

Note that water pressure acting on the planes has a significant influence upon the solution to this problem. If $u_1 = u_2 = 0$, $F = 1.154$.

COMPREHENSIVE SOLUTION

Scope of solution

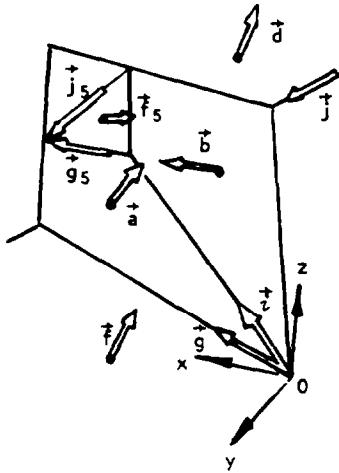
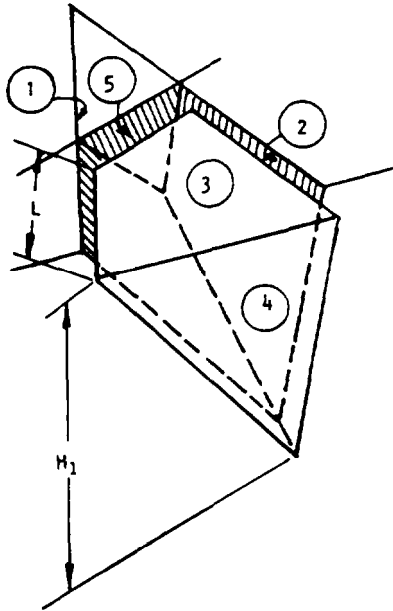
As in the previous solution, this solution is for computation of the factor of safety for translational slip of a tetrahedral wedge formed in a rock slope by two intersecting discontinuities, the slope face and the upper ground surface. In this case, the influence of a tension crack is included in the solution. The solution does not take account of rotational slip or toppling.

The solution allows for different strength parameters and water pressures on the two planes of weakness and for water pressure in the tension crack. There is no restriction on the inclination of the crest of the slope. The influence of an external load E and a cable tension T are included in the analysis and supplementary sections are provided for the examination of the minimum factor of safety for a given external load (eg a blast acceleration acting in a known direction) and for minimizing the cable force required for a given factor of safety.

Part of the input data is concerned with the average values of the water pressure on the failure planes (u_1 and u_2) and on the tension crack (u_5). These may be estimated from field data or by using some form of analysis. In the absence of precise information on the water bearing fissures, one cannot hope to make accurate predictions but two simple methods for obtaining approximate estimates were suggested in Appendix 1 of this book. In both methods it is assumed that extreme conditions of very heavy rainfall occur, and that in consequence the fissures are completely full of water. Again, in both methods, it is assumed that the pressure varies from zero at the free faces to a maximum value at some point on the line of intersection of the two failure planes. The first method treats the case where no tension crack exists and gives the result $u_1 = u_2 = \gamma_w H_w / 6$, where H_w is the total height of the wedge. The second method allows for the presence of a tension crack and gives $u_1 = u_2 = u_5 = \gamma_w H_{5w} / 3$, where H_{5w} is the depth of the bottom vertex of the tension crack below the upper ground surface.

As in the short solution, allowance is made for the following :

- a) interchange of planes 1 and 2
- b) the possibility of one of the planes overlying the other
- c) the situation where the crest overhangs the base of the slope (in which case $\eta = -1$)
- d) the possibility of contact being lost on either plane.



In addition to detecting whether or not a wedge can form, the solution also examines how the tension crack intersects the other planes and only accepts those cases where the tension crack truncates the wedge in the manner shown in the margin sketch.

Notation

The geometry of the problem is illustrated in the margin sketch. The failure surfaces are denoted by 1 and 2, the upper ground surface by 3, the slope face by 4 and the tension crack by 5. The following input data are required for the solution :

- ψ, α = dip and dip direction of plane or plunge and trend of force
- H_1 = slope height referred to plane 1
- L = distance of tension crack from crest, measured along the trace of plane 1
- u = average water pressure on face of wedge
- c = cohesive strength of each failure plane
- ϕ = angle of friction of each failure plane
- γ = unit weight of rock
- γ_w = unit weight of water
- T = cable or bolt tension
- E = external load
- n = -1 if slope is overhanging and +1 if slope does not overhang

Other terms used in the solution are

- F = factor of safety against sliding along the line of intersection or on plane 1 or plane 2
- A = area of face of wedge
- W = weight of wedge
- V = water thrust on tension crack face
- N_a = total normal force on plane 1
- S_a = shear force on plane 1
- Q_a = shear resistance on plane 1
- F_1 = factor of safety
- N_b = total normal force on plane 2
- S_b = shear force on plane 2
- Q_b = shear resistance on plane 2
- F_2 = factor of safety
- N_1, N_2 = effective normal reactions
- S = total shear force on 1,2
- Q = total shear resistance on 1,2
- F_3 = factor of safety

} when contact is maintained on plane 1 only

} when contact is maintained on plane 2 only

} when contact is maintained on both planes 1 and 2

- N_1', N_2' = values of N_1, N_2, S etc when $T = 0$
- S', ttc
- N_1'', N_2'' = values of N_1, N_2, S etc when $E = 0$
- S'', etc
- \vec{a} = unit normal vector for plane 1
- \vec{b} = unit normal vector for plane 2
- \vec{a} = unit normal vector for plant 3
- \vec{f} = unit normal vector for plant 4
- \vec{f}_5 = unit normal vector for plant 5
- \vec{g} = vector in direction of intersection lint of 1,4
- \vec{g}_5 = vector in direction of intersection lint of 1,5
- \vec{i} = vector in direction of intersection lint of 1,2
- \vec{j} = vector in direction of intersection lint of 3,4
- \vec{j}_5 = vector in direction of intersection lint of 3,5
- \vec{k} = vector in plane 2 normal to \vec{i}
- \vec{l} = vector in plane 1 normal to \vec{i}
- R = magnitude of vector \vec{l}
- G = square of magnitude of vector \vec{g}
- G_5 = square of magnitude of vector \vec{g}_5

Note 1 : The computed value of V is negative when the tension crack dips away from the toe of the slope but this does not indicate a tensile force.

2 : The expressions for $a_1, a_2, a_3, a_4, a_5, \alpha_1, \alpha_2$ & α_3 which occur later in the solution are normally evaluated by ATAN2 of Fortran, or by "Rectangular to Polar" operation on desk top calculators. For this reason, -v should not be cancelled out in equation 47 for α_2 .

Sequence of calculations

1. Calculation of factor of safety *when* the forces T and E are either **zero** or completely specified in magnitude and direction.

a. Components of unit vectors in directions of normals to plants 1 to 5, and of forces T and E.

- $(a_x, a_y, a_z) = (\sin\psi_1 \sin\alpha_1, \sin\psi_1 \cos\alpha_1, \cos\psi_1)$ 1
- $(b_x, b_y, b_z) = (\sin\psi_2 \sin\alpha_2, \sin\psi_2 \cos\alpha_2, \cos\psi_2)$ 2
- $(d_x, d_y, d_z) = (\sin\psi_3 \sin\alpha_3, \sin\psi_3 \cos\alpha_3, \cos\psi_3)$ 3
- $(f_x, f_y, f_z) = (\sin\psi_4 \sin\alpha_4, \sin\psi_4 \cos\alpha_4, \cos\psi_4)$ 4
- $(f_{5x}, f_{5y}, f_{5z}) = (\sin\psi_5 \sin\alpha_5, \sin\psi_5 \cos\alpha_5, \cos\psi_5)$ 5
- $(t_x, t_y, t_z) = (\cos\psi_t \sin\alpha_t, \cos\psi_t \cos\alpha_t, -\sin\psi_t)$ 6
- $(e_x, e_y, e_z) = (\cos\psi_e \sin\alpha_e, \cos\psi_e \cos\alpha_e, -\sin\psi_e)$ 7

b. Components of vectors in the direction of the lines of intersection of various planes .

$$(g_x, g_y, g_z) = (f_y a_z - f_z a_y), (f_z a_x - f_x a_z), (f_x a_y - f_y a_x) \quad 8$$

$$(g_{5x}, g_{5y}, g_{5z}) = (f_{5y} a_z - f_{5z} a_y), (f_{5z} a_x - f_{5x} a_z), (f_{5x} a_y - f_{5y} a_x) \quad 9$$

$$(i_x, i_y, i_z) = (b_y a_z - b_z a_y), (b_z a_x - b_x a_z), (b_x a_y - b_y a_x) \quad 10$$

$$(j_x, j_y, j_z) = (f_y d_z - f_z d_y), (f_z d_x - f_x d_z), (f_x d_y - f_y d_x) \quad 11$$

$$(j_{5x}, j_{5y}, j_{5z}) = (f_{5y} d_z - f_{5z} d_y), (f_{5z} d_x - f_{5x} d_z), (f_{5x} d_y - f_{5y} d_x) \quad 12$$

$$(k_x, k_y, k_z) = (i_y b_z - i_z b_y), (i_z b_x - i_x b_z), (i_x b_y - i_y b_x) \quad 13$$

$$(l_x, l_y, l_z) = (a_y i_z - a_z i_y), (a_z i_x - a_x i_z), (a_x i_y - a_y i_x) \quad 14$$

c. Numbers proportional to cosines of various angles

$$m = g_x d_x + g_y d_y + g_z d_z \quad 15$$

$$m_5 = g_{5x} d_x + g_{5y} d_y + g_{5z} d_z \quad 16$$

$$n = b_x j_x + b_y j_y + b_z j_z \quad 17$$

$$n_5 = b_x j_{5x} + b_y j_{5y} + b_z j_{5z} \quad 18$$

$$p = i_x d_x + i_y d_y + i_z d_z \quad 19$$

$$q = b_x g_x + b_y g_y + b_z g_z \quad 20$$

$$q_5 = b_x g_{5x} + b_y g_{5y} + b_z g_{5z} \quad 21$$

$$r = a_x b_x + a_y b_y + a_z b_z \quad 22$$

$$s = a_x t_x + a_y t_y + a_z t_z \quad 23$$

$$v = b_x t_x + b_y t_y + b_z t_z \quad 24$$

$$w = i_x t_x + i_y t_y + i_z t_z \quad 25$$

$$s_e = a_x e_x + a_y e_y + a_z e_z \quad 26$$

$$v_e = b_x e_x + b_y e_y + b_z e_z \quad 27$$

$$w_e = i_x e_x + i_y e_y + i_z e_z \quad 28$$

$$s_5 = a_x f_{5x} + a_y f_{5y} + a_z f_{5z} \quad 29$$

$$v_5 = b_x f_{5x} + b_y f_{5y} + b_z f_{5z} \quad 30$$

$$w_5 = i_x f_{5x} + i_y f_{5y} + i_z f_{5z} \quad 31$$

$$\lambda = i_x g_x + i_y g_y + i_z g_z \quad 32$$

$$\lambda_5 = i_x g_{5x} + i_y g_{5y} + i_z g_{5z} \quad 33$$

$$\epsilon = f_x f_{5x} + f_y f_{5y} + f_z f_{5z} \quad 34$$

d. Miscellaneous factors

$$R = \sqrt{1 - r^2} \quad 35$$

$$\rho = \frac{1}{R} \cdot \frac{nq}{|nq|} \quad 36$$

$$\mu = \frac{1}{R^2} \cdot \frac{mq}{|mq|} \quad 37$$

$$\nu = \frac{1}{R} \cdot \frac{p}{|p|} \quad 38$$

$$G = g_x^2 + g_y^2 + g_z^2 \quad 39$$

$$G_5 = g_{5x}^2 + g_{5y}^2 + g_{5z}^2 \quad 40$$

$$M = (G\rho^2 - 2\mu\rho\lambda + m^2 R^2)^{\frac{1}{2}} \quad 41$$

$$M_5 = (G_5 p^2 - 2 m_5 p \lambda_5 + m_5^2 R^2)^{\frac{1}{2}} \quad 42$$

$$h = M_1 / |g_z| \quad 43$$

$$h_5 = (Mh - |p|L) / M_5 \quad 44$$

$$B = (\tan^2 \phi_1 + \tan^2 \phi_2 - 2(\mu r / \rho) \tan \phi_1 \tan \phi_2) / R^2 \quad 45$$

e. Plunge and trend of line of intersection of planes 1 & 2

$$\psi_i = \text{Arcsin}(v i_z) \quad 46$$

$$\alpha_i = \text{Arctan}(-v i_x / -v i_y) \quad 47$$

f. Check on wedge geometry

$$\text{No wedge is formed,} \quad \left\{ \begin{array}{l} \text{if } p i_z < 0 \text{ or} \\ \text{terminate computation.} \quad \text{if } n q i_z < 0 \end{array} \right. \quad \begin{array}{l} 48 \\ 49 \end{array}$$

$$\left\{ \begin{array}{l} \text{if } \epsilon n q_5 i_z < 0, \text{ or} \\ \text{if } h_5 < 0, \text{ or} \end{array} \right. \quad \begin{array}{l} 50 \\ 51 \end{array}$$

$$\text{Tension crack invalid,} \quad \left\{ \begin{array}{l} \text{terminate computation.} \\ \text{if } \left| \frac{m_5 h_5}{m h} \right| > 1, \text{ or} \\ \text{if } \left| \frac{n q_5 m_5 h_5}{n_5 q m h} \right| > 1 \end{array} \right. \quad \begin{array}{l} 52 \\ 53 \end{array}$$

g. Areas of faces and weight of wedge

$$A_1 = (|mq|h^2 - |m_5 q_5| h_5^2) / 2 |p| \quad 54$$

$$A_2 = (|q/n|m^2 h^2 - |q_5/n_5|m_5^2 h_5^2) / 2 |p| \quad 55$$

$$A_5 = |m_5 q_5| h_5^2 / 2 |n_5| \quad 56$$

$$W = \gamma (q^2 m^2 h^3 / |n| - q_5^2 m_5^2 h_5^3 / |n_5|) / 6 |p| \quad 57$$

h. Water pressures

i) With no tension crack

$$u_1 = u_2 = \gamma_w h |m i_z| / 6 |p| \quad 58$$

ii) With tension crack

$$u_1 = u_2 = u_5 = \gamma_w h_5 |m_5| / 3 d_z \quad 59$$

$$V = u_5 A_5 n \epsilon / |\epsilon| \quad 60$$

i. Effective normal reactions on planes 1 and 2 assuming contact on both planes

$$N_1 = \rho \{ W k_z + T(rv - s) + E(rv_e - s_e) + V(rv_5 - s_5) \} - u_1 A_1 \quad 61$$

$$N_2 = \mu \{ W l_z + T(rs - v) + E(rs_e - v_e) + V(rs_5 - v_5) \} - u_2 A_2 \quad 62$$

j. Factor of safety when $N_1 < 0$ and $N_2 < 0$ (contact is lost on both planes)

$$F = 0 \quad 63$$

- k. If $N_1 > 0$ and $N_2 < 0$, contact is maintained on plane 1 only and the factor of safety is calculated as follows:

$$N_a = Wa_z - Ts - Es - Vs_5 - u_2 A_2 r \quad 64$$

$$S_x = -(Tt_x + Ee_x + N_a a_x + Vf_{5x} + u_2 A_2 b_x) \quad 65$$

$$S_y = -(Tt_y + Ee_y + N_a a_y + Vf_{5y} + u_2 A_2 b_y) \quad 66$$

$$S_z = -(Tt_z + Ee_z + N_a a_z + Vf_{5z} + u_2 A_2 b_z) + W \quad 67$$

$$S_a = (S_x^2 + S_y^2 + S_z^2)^{\frac{1}{2}} \quad 68$$

$$Q_a = (N_a - u_1 A_1) \tan \phi_1 + c_1 A_1 \quad 69$$

$$F_1 = Q_a / S_a \quad 70$$

- l. If $N_1 < 0$ and $N_2 > 0$, contact is maintained on plane 2 only and the factor of safety is calculated as follows:

$$N_b = Wb_z - Tv - Ev_e - Vv_5 - u_1 A_1 r \quad 71$$

$$S_x = -(Tt_x + Ee_x + N_b b_x + Vf_{5x} + u_1 A_1 a_x) \quad 72$$

$$S_y = -(Tt_y + Ee_y + N_b b_y + Vf_{5y} + u_1 A_1 a_y) \quad 73$$

$$S_z = -(Tt_z + Ee_z + N_b b_z + Vf_{5z} + u_1 A_1 a_z) + W \quad 74$$

$$S_b = (S_x^2 + S_y^2 + S_z^2)^{\frac{1}{2}} \quad 75$$

$$Q_b = (N_b - u_2 A_2) \tan \phi_2 + c_2 A_2 \quad 76$$

$$F_2 = Q_b / S_b \quad 77$$

- m. If $N_1 > 0$ and $N_2 > 0$, contact is maintained on both planes and the factor of safety is calculated as follows:

$$S = v(Wi_z - Tw - Ew_e - Vw_5) \quad 78$$

$$Q = N_1 \tan \phi_1 + N_2 \tan \phi_2 + c_1 A_1 + c_2 A_2 \quad 79$$

$$F_3 = Q/S \quad 80$$

2. *Minimum factor of safety produced when load E of given magnitude is applied in the worst direction.*

- a) Evaluate N_1'' , N_2'' , S'' , Q'' , F_3'' by use of equations 61, 62, 78, 79 and 80 with $E = 0$.

- b) If $N_1'' < 0$ and $N_2'' < 0$, even before E is applied, then $F = 0$, terminate computation.

$$c) D = \{ (N_1'')^2 + (N_2'')^2 + 2 \frac{mn}{|mn|} N_1'' N_2'' r \}^{\frac{1}{2}} \quad 81$$

$$\psi_e = \text{Arcsin} \left(-\frac{1}{G} \left(\frac{m}{|m|} \cdot N_1'' a_z + \frac{n}{|n|} \cdot N_2'' b_z \right) \right) \quad 82$$

$$\alpha_e = \text{Arctan} \left\{ \frac{\frac{m}{|m|} \cdot N_1'' a_x + \frac{n}{|n|} \cdot N_2'' b_x}{\frac{m}{|m|} \cdot N_1'' a_y + \frac{n}{|n|} \cdot N_2'' b_y} \right\} \quad 83$$

If $E > D$, and E is applied in the direction ψ_e , α_e , or within a certain range encompassing this direction, then contact is lost on both planes and $F = 0$.
Terminate computation.

- d) If $N_1'' > 0$ and $N_2'' < 0$, assume contact on plane 1 only after application of E.

Determine $S_x'', S_y'', S_z'', S_a'', Q_a'', F_1''$ from equations 65 to 70 with $E = 0$.

If $F_1'' < 1$, terminate computation.

If $F_1'' > 1$:

$$F_1 = \frac{S_a'' Q_a'' - E \{ (Q_a'')^2 + ((S_a'')^2 - E^2) \tan^2 \phi_1 \}^{\frac{1}{2}}}{(S_a'')^2 - E^2} \quad 84$$

$$\psi_{e1} = \text{Arcsin}(S_z''/S_a'') - \text{Arctan}(\tan \phi_1 / F_1) \quad a5$$

$$\alpha_{e1} = \text{Arctan}(S_x''/S_y'') + 180^\circ \quad 86$$

- e) If $N_1'' < 0$ and $N_2'' > 0$, assume contact on plane 2 only after application of E.

Determine $S_x'', S_y'', S_z'', S_b'', Q_b'', F_2''$ from equations 72 to 77 with $E = 0$.

If $F_2'' < 1$, terminate computation.

If $F_2'' > 1$:

$$F_2 = \frac{S_b'' Q_b'' - E \{ (Q_b'')^2 + ((S_b'')^2 - E^2) \tan^2 \phi_2 \}^{\frac{1}{2}}}{(S_b'')^2 - E^2} \quad a7$$

$$\psi_{e2} = \text{Arcsin}(S_z''/S_b'') - \text{Arctan}(\tan \phi_2 / F_2) \quad 88$$

$$\alpha_{e2} = \text{Arctan}(S_x''/S_y'') + 180^\circ \quad 89$$

- f) If $N_1'' > 0$ and $N_2'' > 0$, assume contact on both planes after application of E.

If $F_3'' < 1$, terminate computation.

If $F_3'' > 1$:

$$F_3 = \frac{S'' Q'' - E \{ (Q'')^2 + B((S'')^2 - E^2) \}^{\frac{1}{2}}}{(S'')^2 - E^2} \quad 90$$

$$\chi = \sqrt{B + F_3^2} \quad 91$$

$$e_x = -(F_3 v z_x - \rho k_x \tan \phi_1 - \mu l_x \tan \phi_2) / \chi \quad 92$$

$$e_y = -(F_3 v z_y - \rho k_y \tan \phi_1 - \mu l_y \tan \phi_2) / \chi \quad 93$$

$$e_z = -(F_3 v z_z - \rho k_z \tan \phi_1 - \mu l_z \tan \phi_2) / \chi \quad 94$$

$$\psi_{e3} = \text{Arcsin}(-e_z) \quad 95$$

$$\alpha_{e3} = \text{Arctan}(e_x/e_y) \quad 96$$

Compute s_e and v_e using equations 26 and 27

$$N_1 = N_1'' + E \rho (r v_e - s_e) \quad 97$$

$$N_2 = N_2'' + E \mu (r s_e - v_e) \quad 98$$

Check that $N_1 \geq 0$ and $N_2 \geq 0$

3. Minimum cable or bolt tension T_{min} required to raise the factor of safety to some specified value F .

- a). Evaluate N_1' , N_2' , S' , Q' by means of equations 61, 62, 78, 79 with $T = 0$.
- b) If $N_2' < 0$, contact is lost on plane 2 when $T = 0$. Assume contact on plane 1 only, after application of T . Evaluate S_x' , S_y' , S_z' , S_a' and Q_a' using equations 65 to 69 with $T = 0$.

$$T_1 = (FS_a' - Q_a') / \sqrt{F^2 + \tan^2 \phi_1} \quad 99$$

$$\psi_{t1} = \arctan(\tan \phi_1 / F) - \arcsin(S_z' / S_a') \quad 100$$

$$\alpha_{t1} = \arctan(S_x' / S_y') \quad 101$$

- c) If $N_1' < 0$, contact is lost on plane 1 when $T = 0$. Assume contact on plane 2 only, after application of T . Evaluate S_x' , S_y' , S_z' , S_b' and Q_b' using equations 72 to 76 with $T = 0$.

$$T_2 = (FS_b' - Q_b') / \sqrt{F^2 + \tan^2 \phi_2} \quad 102$$

$$\psi_{t2} = \arctan(\tan \phi_2 / F) - \arcsin(S_z' / S_b') \quad 103$$

$$\alpha_{t2} = \arctan(S_x' / S_y') \quad 104$$

- d) All cases. No restriction on values of N_1' and N_2' . Assume contact on both planes after application of T .

$$\chi = (F^2 + B)^{1/2} \quad 105$$

$$T_3 = (FS' - Q') / \chi \quad 106$$

$$t_x = (Fvz_x - \rho k_x \tan \phi_1 - \mu z_x \tan \phi_2) / \chi \quad 107$$

$$t_y = (Fvz_y - \rho k_y \tan \phi_1 - \mu z_y \tan \phi_2) / \chi \quad 108$$

$$t_z = (Fvz_z - \rho k_z \tan \phi_1 - \mu z_z \tan \phi_2) / \chi \quad 109$$

$$\psi_{t3} = \arcsin(-t_z) \quad 110$$

$$\alpha_{t3} = \arctan(t_x / t_y) \quad 111$$

Compute s and v using equations 23 and 24

$$N_1 = N_1' + T_3 \rho (rv - s) \quad 112$$

$$N_2 = N_2' + T_3 \mu (rs - v) \quad 113$$

If $N_1 < 0$ or $N_2 < 0$, ignore the results of this section

If $N_1' > 0$ and $N_2' > 0$, $T_{min} = T_3$

If $N_1' > 0$ and $N_2' < 0$, $T_{min} = \text{smallest of } T_1, T_3$

If $N_1' < 0$ and $N_2' > 0$, $T_{min} = \text{smallest of } T_2, T_3$

If $N_1' < 0$ and $N_2' < 0$, $T_{min} = \text{smallest of } T_1, T_2, T_3$

Example

Calculate the factor of safety for the following wedge :

	1			5	
Plane	45	70	32	45	70
a	105	235	195	185	165
					$n = +1$

$$H_1 = 100', L = 40', c_1 = 500 \text{ lb/ft}^2, c_2 = 1000 \text{ lb/ft}^2$$

$$\phi_1 = 20^\circ, \phi_2 = 30^\circ, \gamma = 160 \text{ lb/ft}^3.$$

1a) $T = 0$, $E = 0$, $u_1 = u_2 = u_5$ from equation 59.

$$(a_x, a_y, a_z) = (0.68301, -0.18301, 0.70711)$$

$$(b_x, b_y, b_z) = (-0.76975, -0.53899, 0.34202)$$

$$(d_x, d_y, d_z) = (-0.05381, -0.20083, 0.97815)$$

$$(f_x, f_y, f_z) = (-0.07899, -0.90286, 0.42262)$$

$$(f_{5x}, f_{5y}, f_{5z}) = (0.24321, -0.90767, 0.34202)$$

$$(g_x, g_y, g_z) = (-0.56107, 0.34451, 0.63112)$$

$$(g_{5x}, g_{5y}, g_{5z}) = (-0.57923, 0.061627, 0.57544)$$

$$(i_x, i_y, i_z) = (-0.31853, 0.77790, 0.50901)$$

$$(j_x, j_y, j_z) = (-0.79826, 0.05452, -0.03272)$$

$$(j_{5x}, j_{5y}, j_{5z}) = (-0.81915, -0.25630, -0.09769)$$

$$(k_x, k_y, k_z) = (0.54041, -0.28287, 0.77047)$$

$$(l_x, l_y, l_z) = (-0.64321, -0.57289, 0.47302)$$

$$m = 0.57833$$

$$m_5 = 0.58166$$

$$n = 0.57388$$

$$n_5 = 0.73527$$

$$P = 0.35880$$

$$q = 0.46206$$

$$q_5 = 0.60945$$

$$r = -0.18526$$

$$s_5 = 0.57407$$

$$s_5 = 0.41899$$

$$w_5 = -0.60945$$

$$\lambda = 0.76796$$

$$\lambda_5 = 0.52535$$

$$e = 0.94483$$

$$R = 0.98269$$

$$\rho = 1.03554$$

$$\mu = 1.03554$$

$$v = 1.01762$$

$$G = 0.83180$$

$$G_5 = 0.67044$$

$$M = 0.33371$$

$$M_5 = 0.44017$$

$$h = 158.45$$

$$h_5 = 87.521$$

$$B = 0.56299$$

$$\psi_i = 31.20^\circ$$

$$\alpha_i = 157.73^\circ$$

$$\left. \begin{array}{l}
 p_i z > 0 \\
 nq_i z > 0 \\
 \epsilon nq_5 i_z > 0 \\
 h_5 > 0 \\
 |m_5 h_5| / |mh| = 0.55554 < 1 \\
 |nq_5 m_5 h_5| / |n_5 qmh| = 0.57191 < 1
 \end{array} \right\} \begin{array}{l}
 \text{Wedge is formed} \\
 \\
 \\
 \\
 \\
 \\
 \end{array} \left. \vphantom{\begin{array}{l} p_i z > 0 \\ nq_i z > 0 \\ \epsilon nq_5 i_z > 0 \\ h_5 > 0 \\ |m_5 h_5| / |mh| = 0.55554 < 1 \\ |nq_5 m_5 h_5| / |n_5 qmh| = 0.57191 < 1 \end{array}} \right\} \text{Tension crack valid}$$

$$\begin{aligned}
 A_1 &= 5565.0 \text{ ft}^2 \\
 A_2 &= 6428.1 \text{ ft}^2 \\
 AS &= 1846.6 \text{ ft}^2 \\
 W &= 2.8272 \times 10^7 \text{ lb} \\
 u_1 &= u_2 = u_5 = 1084.3 \text{ lb/ft}^2 ; v = 2.0023 \times 10^6 \text{ lb} \\
 N_1 &= 1.5171 \times 10^7 \text{ lb} \\
 N_2 &= 5.7892 \times 10^6 \text{ lb} \\
 s &= 1.5886 \times 10^7 \text{ lb} \\
 Q &= 1.8075 \times 10^7 \text{ lb} \\
 F &= 1.1378 \quad \text{Factor of safety.}
 \end{aligned}$$

This value can be compared with the value of 1.10 obtained in case c of Appendix 1 - note that small differences in calculated areas and water pressures account for the difference in the factors of safety.

1 b) T - O, E = 0, dry slope, $u_1 = u_2 = u_5 = 0$.

As in 1a) except as follows:

$$\begin{aligned}
 V &= 0 \\
 N_1 &= 2.2565 \times 10^7 \text{ lb} \\
 N_2 &= 1.3853 \times 10^7 \text{ lb} \\
 s &= 1.4644 \times 10^7 \text{ lb} \\
 Q &= 2.5422 \times 10^7 \text{ lb} \\
 F_3 &= 1.7360 \quad \text{Factor of safety}
 \end{aligned}$$

Compare this value with the value of 1.73 obtained in case b of Appendix 1.

2) As in 1b) except E = 8×10^6 lb. Find the value of F_{\min} .

Values of N_1'' , N_2'' , S'' , Q'' , F_3'' as given in 1b),
 $N_1'' > 0$, $N_2'' > 0$, $F_3'' > 1$, continue calculation.

$$\begin{aligned}
 B &= 0.56299 \\
 F_3 &= 1.04 \quad F_{\min} \text{ (Minimum factor of safety)} \\
 x &= 1.2790 \\
 e_x &= 0.12128 \\
 e_y &= -0.99226 \\
 e_z &= 0.028243
 \end{aligned}$$

$\psi_{e3} = -1.62^\circ$ - Plunge of force (*upwards*)
 $\alpha_{e3} = 173.03^\circ$ - Trend of force
 $N_1 = 1.9517 \times 10^6$ lb Both positive therefore contact
 $N_2 = 9.6793 \times 10^6$ lb maintained on both planes.

3). As in 1a) except that the minimum cable tension T_{min} required to increase the factor of safety to 1.5 is to be determined.

N_1', N_2', S' and Q' - as given in 1a)
 $\chi = 1.6772$
 $T_3 = 3.4307 \times 10^6$ lb - T_{min} (Minimum cable tension)
 $t_x = -0.18205$
 $t_y = 0.97574$
 $t_z = 0.12148$
 $\psi_{t3} = -6.98^\circ$ - Plunge of cable (*upwards*)
 $\alpha_{t3} = 349.430$ - Trend of cable

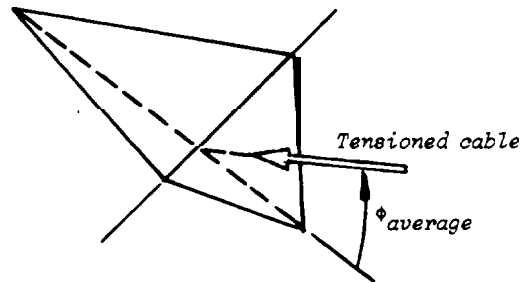
Note that the optimum plunge and trend of the cable are approximately :

$$\psi_{t3} = \psi_i + 180^\circ - \frac{1}{2}(\phi_1 + \phi_2) = 31.2 + 180 - 25 = -6.2^\circ \text{ (upwards)}$$

$$\text{and } \alpha_{t3} = \alpha_i \pm 180^\circ = 157.73 + 180 = 337.730$$

In other words, a practical rule of thumb for the best direction in which to install the cables to reinforce a wedge is :

The cable should be aligned with the line of intersection of the two planes, viewed from the bottom of the slope, and it should be inclined at the average friction angle to the line of intersection.



Optimum cable direction for reinforcement of a wedge.

Appendix 3: Factors of safety for reinforced rock slopes

Throughout this book, the factor of safety of a reinforced rock slope (for both plane and wedge failure) has been defined as :

$$F = \frac{\text{Resisting force}}{\text{Disturbing force} - T \cdot \sin \theta}$$

where T is the force applied to the rock by the reinforcing member.

In other words, the force T is assumed to act in such a manner as to *decrease* the *disturbing force*. Pierre Londe*, in a personal communication to the authors, suggested that a second definition is equally applicable :

$$F = \frac{\text{Resisting force} + T}{\text{Disturbing force}} \quad 2$$

In this definition, the force T *increases* the *resisting force*.

Which definition should be used ? Londe suggests that there is some justification for using equation 1 when T is an *active* force, i.e. the cable is tensioned *before* any movement of the rock block or wedge has taken place. On the other hand, if T is a *passive* force, applied by un-tensioned bars or cables, the resisting force can only be developed after some movement has taken place. In this case, Londe suggests that equation 2 is more appropriate.

In fact, since one never knows the exact sequence of loading and movement in a rock slope, the choice becomes arbitrary. However, in considering this problem, a second and more significant problem arises and this relates to the degree of confidence attached to the values of the shear strengths and water pressures used in the stability analysis. The method of solution described below, based upon a suggestion by Londe, is designed to overcome both of the problems raised here.

If, for the moment, it is assumed that the frictional and cohesive strengths of a rock surface are known with a high degree of precision and the water pressures have been measured by means of *piezometers*, one may be led to believe that a high degree of confidence can be attached to the calculated driving and resisting forces and hence the factor of safety of the slope. While this confidence would be justified in the case of an unreinforced slope, that same could not be said of a reinforced slope. This is because the response of the various elements to displacement in the slope is not the same. The development of the full frictional strength, due to ϕ , and the cohesive strength c require a finite displacement on the sliding surface and this displacement may be incompatible with that imposed by the application of the cable tension T. Similarly, water pressures in the fissures are *sensitive* to displacement and may increase or decrease, depending upon the *manner* in which the cables are installed. Consequently, it cannot be assumed that the cable tension T, the frictional strength due to ϕ , the cohesive strength c and the various water pressures are all fully *mobilised* at the same time.

* Technical director, Coyne & Bellier, Paris. France.

Londe suggests that, instead of using a single factor of safety to define the stability of the slope, different factors of safety should be used, depending upon the degree of confidence which the designer has in the particular parameter being considered. High factors of safety can be applied to ill-defined parameters (such as water pressures and cohesive strengths) while low factors of safety can be used for those quantities (such as the weight of a wedge) which are known with a greater degree of precision. For a typical problem, Londe suggests :

$$\begin{aligned} f_c &= 1.5 \text{ for cohesive strengths (c)} \\ f_\phi &= 1.2 \text{ for frictional strengths (\phi)} \\ f_U &= 2.0 \text{ for water pressures} \\ f_W &= 1.0 \text{ for weights and forces.} \end{aligned}$$

Using these values, the conditions of limiting equilibrium expressed in equation 12 on page 77, for a block sliding down a plane, can be expressed as :

$$W \cdot \sin\psi + 2V - T \cdot \cos\beta = \frac{cA}{1.5} + (W \cdot \cos\psi - 2U + T \cdot \sin\beta) \frac{\tan\phi}{1.2} \quad 3$$

Note that the factors of safety (given in italics) for the parameters corresponding to the resisting forces (c and ϕ) are decreasing factors while they are increasing factors for the driving forces (U and V).

Solving equation 3 for T gives :

$$T = \frac{W(\sin\psi - 0.83 \cdot \cos\psi \cdot \tan\phi) + 2V + 1.67U \tan\phi - 0.67cA}{0.83 \sin\beta \cdot \tan\phi + \cos\beta} \quad 4$$

This is the cable tension required to satisfy the factors of safety assigned to each of the components of the driving and resisting force terms.

Consider the practical example discussed in Case d) of Appendix 1 of this book. It was required to determine the cable tension T needed to increase the factor of safety of a rock wedge to 1.5. In this case, the factor of safety was applied uniformly to c_A , c_B , $\tan\phi_A$ and $\tan\phi_B$ while a factor of safety of 1 was applied to U_A , U_B , V and W. The required value of T was found to be 4.64×10^6 lb.

Using the alternative method proposed by Londe and substituting the factors of safety suggested by him, equation A49 of Appendix 1 can be rewritten as :

$$\begin{aligned} \frac{1}{1.5} (c_A A_A + c_B A_B) + (qW + 2rV + sT - 2U_A) \frac{\tan\phi_A}{1.2} \\ + (xW + 2yV + zT - 2U_B) \frac{\tan\phi_B}{1.2} = m_W W - 2m_V V - m_T T \quad 5 \end{aligned}$$

Solving for T, using the same values as in case d) of Appendix 1, gives $T = 9.8 \times 10^6$ lb.

This value is approximately twice that obtained by using a single value of $F = 1.5$ and Londe considers it to be more realistic in view of the uncertainties associated with the water pressures and the simultaneous mobilisation of T, c and ϕ . The reader should not be alarmed unduly by the discrepancy between the two calculated values of T since

```

550 IF LEN(WATER$)=0 THEN 520 ELSE WATER =VAL(WATER$)
560 IF WATER = 0 THEN FLAG2=1
570 FLAG3=0: LOCATE 13.12
580 INPUT "Are shear strengths uniform throughout slope (y/n) ? ",STRENGTH$
590 IF LEFT$(STRENGTH$,1)="q" OR LEFT$(STRENGTH$,1)="Q" THEN 6980
600 IF LEN(STRENGTH$)=0 THEN 570
610 IF LEFT$(STRENGTH$,1)="Y" OR LEFT$(STRENGTH$,1)="y" THEN FLAG3=1
620 N=NUM+1:GOTO 1950
630 '
640 ' Data entry from a disk file
650 '
660 CLS: LOCATE 8,1:PRINT STRING$(80,45)
670 PRINT:PRINT "Sarua data files on disk ";
680 PRINT:FILES "A:SARUA.DAT":PRINT:PRINT STRING$(80,45):PRINT
690 INPUT "Enter filename (without extension): ",FILE$
700 CLS:OPEN "A:"+FILE$+".DAT" FOR INPUT AS #1
710 LINK INPUT#1, TITLE$: INPUT#1,N: INPUT#1,WATER
720 RAD=3.141593/180:F=1:M=1:NUM=N-1
730 INPUT#1,FLAG2: INPUT#1,FLAG3:INPUT#1,FLAG4
740 FOR K = 1 TO N:FOR J=1 TO 39:INPUT#1,A(J,K):NEXT J:NEXT K
750 INPUT#1,ACC: INPUT#1,ACC(2): INPUT#1,FOS
760 CLOSE #1:F=1:FLAG6=1:STATUS="e":GOTO 1950
770 '
780 ' Display of data array
790 '
800 CLS: LOCATE 1,1:PRINT "Analysis no. ";TITLE$
810 LOCATE 3,1:COLOR 15,0:PRINT "Side number":COLOR 7,0
820 LOCATE 4,1:PRINT "coordinate xt"
830 LOCATE 5,1:PRINT "coordinate yt"
&O LOCATE 6,1:PRINT "coordinate xw"
850 LOCATE 7,1:PRINT "coordinate yw"
860 LOCATE 8,1:PRINT "coordinate xb"
870 LOCATE 9,1:PRINT "coordinate yb"
880 LOCATE 10,1:PRINT "friction angle"
890 LOCATE 11,1:PRINT "cohesion"
900 LOCATE 12,1:PRINT "unit weight of water = "
910 LOCATE 12,23:PRINT WATER
920 LOCATE 13,1:COLOR 15.0
930 PRINT "Slice number":COLOR 7.0
940 LOCATE 14,1:PRINT "rock unit weight"
950 LOCATE 15,1:PRINT "friction angle"
960 LOCATE 16,1:PRINT "cohesion"
970 LOCATE 17,1:PRINT "force T ":LOCATE 18.1
980 PRINT "angle theta"
990 GOSUB 1040
1000 IF STATUS="i" THEN GOSUB 1140:RETURN ELSE RETURN
1010 '
1020 ' Subroutine for slice number display
1030 '
1040 COLOR 15,0:LOCATE 3,22:PRINT M:LOCATE 13,27:PRINT M
1050 LOCATE 3,32:PRINT M+1:COLOR 7,0:IF N=M+1 THEN RETURN
1060 COLOR 15,0:LOCATE 13,37:PRINT M+1:LOCATE 3.42
1070 PRINT M+2:COLOR 7,0:IF N=M+2 THEN RETURN
1080 COLOR 15,0:LOCATE 13,47:PRINT M+2:LOCATE 3.52

```


Appendix 4 : Conversion factors

	Imperial	Metric	SI
Length	1 mile	1.609 km	1.609 km
	1 ft	0.3048 m	0.3048 m
	1 in	2.54 cm	25.40 mm
Area	1 mile ²	2.590 km ²	2.590 km ²
	1 acre	0.4047 hectare	4046.9 m ²
	1 ft ²	0.0929 m ²	0.0929 m ²
	1 in ²	6.452 cm ²	6.452 cm ²
Volume	1 yd ³	0.7646 m ³	0.7646 m ³
	1 ft ³	0.0283 m ³	0.0283 m ³
	1 ft ³	28.32 litres	0.0283 m ³
	1 Imperial gallon	4.546 litres	4546 cm ³
	1 US gallon	3.785 litres	3785 cm ³
	1 in ³	16.387 cm ³	16.387 cm ³
Mass	1 ton	1.016 tonne	1.016 Mg
	1 lb	0.4536 kg	0.4536 kg
	1 oz	28.352 gm	28.352 gm
Density	1 lb/ft ³	16.019 kg/m ³	16.019 kg/m ³
Unit weight	1 lbf/ft ³	16.019 kgf/m ³	0.1571 kN/m ³
Force	1 ton f	1.016 tonne f	9.964 kN
	1 lb f	0.4536 kg f	4.448 N
Pressure or stress	1 ton f/in ²	157.47 kg f/cm ²	15.44 MPa
	1 ton f/ft ²	10.936 tonne f/m ²	107.3 kPa
	1 lb f/in ²	0.0703 kg f/cm ²	6.895 kPa
	1 lb f/ft ²	4.882 kg f/m ²	0.04788 kPa
	1 standard atmosphere	1.033 kg f/m ²	101.325 kPa
	14.435 lb f/in ²	1.015 kg f/cm ²	1 bar
	1 ft water	0.0305 kg f/cm ²	2.989 kPa
1 in mercury	0.0345 kg f/cm ²	3.386 kPa	
Permeability	1 ft/year	0.9659 x 10 ⁻⁶ cm/s	0.9659 x 10 ⁻⁸ m/s
Flow rate	1 ft ³ /s	0.02832 m ³ /s	0.02832 m ³ /s
Moment	1 lbf ft	0.1383 kgf m	1.3558 Nm
Energy	1 ft lbf	1.3558 J	1.3558 J
Frequency	1 c/s	1 c/s	1 Hz

SI unit prefixes

Prefix	tera	giga	mega	kilo	milli	micro	nano	pico
Symbol	T	G	M	k	m	μ	n	p
Multiplier	10 ¹²	10 ⁹	10 ⁶	10 ³	10 ⁻³	10 ⁻⁶	10 ⁻⁹	10 ⁻¹²

SI symbols and definitions

N = Newton = kg m/s²

Pa = Pascal = N/m²

J = Joule = m.N

Appendix 5

GLOSSARY OF BLASTING AND EXCAVATION TERMS

Acoustical Impedance - The mathematical expression for characterizing a material as to its energy transfer properties (the product of its unit density and its sound velocity (ρV)).

Adit - A nearly horizontal passage from the surface by which an underground mine is entered, as opposed to a tunnel.

Air Gap - A blasting technique wherein a charge is suspended in a borehole, and the hole tightly stemmed so as to allow a time lapse between detonation and ultimate failure of the rock (no coupling realized).

Anfo - Ammonium Nitrate - Fuel Oil Mixture. Used as a blasting agent.

Astrolite - A family of two-component explosives, usually liquid, with variable detonating velocities.

Back - The roof or top of an underground opening. Also, used to specify the ore between a level and the surface, or that between two levels.

Back Break - Rock broken beyond the limits of the last row of holes.

Bench - The horizontal ledge in a face along which holes are drilled vertically. Benching is the process of excavating whereby terraces or ledges are worked in a stepped shape.

Blast - The operation of rending (breaking) rock by means of explosives. Shot is also used to mean blast.

Blasting Agent - Any material or mixture, consisting of a fuel and oxidizer, intended for blasting, not otherwise classified as an explosive and in which none of the ingredients are classified as an explosive, provided that the finished product, as mixed and packaged for use or shipment, cannot be detonated by means of a No. B test blasting cap when unconfined.

Blast Hole - A hole drilled in rock or other material for the placement of explosives.

Block Hole - A hole drilled into a boulder to allow the placement of a small charge to break the boulder.

Booster - A chemical compound used for intensifying an explosive reaction. A booster does not contain an initiating device but must be cap sensitive.

Boot-Leg - A situation in which the blast fails to cause total failure of the rock due to insufficient explosives for the amount of burden, or caused by incomplete detonation of the explosives. That portion of a borehole that remains relatively intact after having been charged with explosive and fired.

Bridging - Where the continuity of a column of explosives in a borehole is broken, either by improper placement, as in the case of slurries or poured blasting agents, or where some foreign matter has plugged the hole.

Bulk Strength - Refers to the strength of a cartridge of dynamite in relation to the same sized cartridge of straight Nitroglycerine dynamite.

Burden - generally considered the distance from an explosive charge to the nearest free or open face. Technically, there may be an apparent burden and a true burden, the latter being measured always in the direction in which displacement of broken rock will occur following firing of an explosive charge.

Centers - The distance measured between two or more adjacent blast holes without reference to hole locations as to row. The term has no association with the blast hole burdens.

Chambering - More commonly termed Springing. The process of enlarging a portion of a blast hole (usually the bottom) by firing a series of small explosive charges.

Collar - The mouth or opening of a borehole, drill steep, or shaft. Also, to collar in drilling means the act of starting a borehole.

Condenser-Discharge - A blasting machine which uses batteries to energize a series of condensers, whose stored energy is released into a blasting circuit.

Connecting Wire - Any wire used in a blasting circuit to extend the length of a leg wire or leading wire.

Connector - Refers to a device used to initiate a delay in a Primacord circuit, connecting one hole in the circuit with another, or one row of holes to other rows of holes.

Coupling - The act of connecting or joining two or more distinct parts. In blasting the reference concerns the transfer of energy from an explosive reaction into the surrounding rock and is considered perfect when there are no losses due to absorption or cushioning.

Coyote Blasting - The practice of drilling blast holes (tunnels), horizontally into a rock face at the foot of the shot. Used where it is impractical to drill vertically.

Cushion Blasting - The technique of firing of a single row of holes along a neat excavation line to shear the web between the closely drilled holes. Fired after production shooting has been accomplished.

cut - More strictly it is that portion of an excavation with more or less specific depth and width, and continued in like manner along or through the extreme limits of the excavation. A series of cuts are taken before complete removal of the excavated material is accomplished. The specific dimensions of any cut is closely related to the material's properties and required production levels.

Cut-Off - Where a portion of a column of explosives has failed to detonate due to bridging, or to a shifting of the rock formation due to an improper delay system.

Deck - In blasting a smaller charge or portion of a blast hole loaded with explosives that is separated from the main charge by stemming or air cushion.

Deflagration - An explosive reaction that consists of a burning ~~action at a~~ high rate of speed along which occur gaseous formation and pressure expansion.

Delay Element - That portion of a blasting cap which causes a ~~delay between~~ the instant of impressment of electrical energy on the cap and the time of detonation of the base charge of the cap.

Detonating Cord - A plastic covered core of high velocity explosives used to detonate charges of explosives in boreholes and under water, e.g. Primacord.

Detonation - An explosive reaction that consists of the propagation of a shock wave through the explosive accompanied by a chemical reaction that furnishes energy to sustain the shock-wave propagation in a stable manner, with gaseous formation and pressure expansion following shortly thereafter.

Dip - The angle at which strata, beds, or veins are inclined from the horizontal.

Drop Ball - known also as a Headache Ball. An iron or steel ~~weight~~ held on a wire rope that is dropped from a height onto large boulders for the purpose of breaking them into smaller fragments.

Explosion - A thermochemical process whereby mixtures of gases, ~~solids,~~ or liquids react with the almost instantaneous formation of gaseous pressures and near sudden heat release. There must always be a source of ignition and the proper temperature limit reached to initiate the reaction. Technically, a boiler can rupture but cannot explode.

Explosive - Any chemical mixture that reacts at high speed to ~~liberate~~ gas and heat and thus cause tremendous pressures. The distinctions between High and Low Explosives are twofold; the former are designed to detonate and contain at least one high explosive ingredient; the latter always deflagrate and contain no ingredients which by themselves can be exploded. Both High and Low Explosives can be initiated by a single No. 8 blasting cap as opposed to Blasting Agents which cannot be so initiated.

Face - The end of an excavation toward which work is progress- or that which was last done. It is also any rock surface exposed to air.

Fire - In blasting it is the act of initiating an explosive reaction.

Floor - The bottom horizontal, or nearly so, part of an excavation upon which haulage or walking is done.

Fragmentation - The extent to which rock is broken into small pieces by primary blasting.

Fracture - Literally, the breaking of rock without movement of the broken pieces.

Fuel - In explosive calculations it is the chemical compound used for purposes of combining with oxygen to form gaseous products and cause a release of heat.

Galvanic Action - Currents caused when dis-similar metals contact each other, or through a conductive medium. This action may create sufficient voltage to cause premature firing of an electric blasting circuit, particularly in the presence of salt water.

Galvanometer - A device containing a silver chloride cell which is used to measure resistance in an electric blasting circuit.

Grade - In excavation, it specifies the elevation of a roadbed, ~~road~~, foundation, etc. When given a value such as percent or degree grade it is the amount of fall or inclination compared to a unit horizontal distance for a ditch, road, etc. To grade means to level ground irregularities to a prescribed level.

Gram Atom - The unit used in chemistry to express the atomic weight of an element in terms of grams (weight).

Hardpan - Boulder clay, or layers of gravel found usually a few feet below the surface and so cemented together that it must be blasted or ripped in order to excavate.

Highwall - The bench, bluff, or ledge on the edge of a surface excavation and most usually used only in coal strip mining.

Initiation - The act of detonating a high explosive by means of a mechanical device or other means.

Joints - Planes within rock masses along which there is no resistance to separation and along which there has been no relative movement of the material on each side of the break. They occur in sets, the planes of which are generally mutually perpendicular. Joints, like stratification, are often called partings.

Jumbo - A machine designed to contain two or more mounted drilling units which may or may not be operated independently.

Lead Wire - The wires connecting the electrodes of an electric blasting machine with the final leg wires of a blasting circuit.

LEDC - Low Energy Detonating Cord. Used to initiate non-electric caps at the bottom of boreholes.

Leg Wires - Wires, leading from the top end of an electric blasting cap; used to couple caps into the circuit.

Mat - Used to cover a shot to hold down flying material; usually made of woven wire cable, tires or conveyor belt.

Millisecond Delay Caps - Delay electric caps which have a built-in delay element, usually 25/1000th of a second apart, consecutively. This timing may vary from manufacturer to manufacturer.

Misfire - A charge, or part of a charge, which for any reason has failed to fire as planned. All misfires are to be considered extremely dangerous until the cause of the misfire has been determined.

Mole - A unit in chemical technology equal to the molecular weight of a substance expressed in grams (weight).

Muck Pile - The pile of broken material or dirt in excavating that is to be loaded for removal.

Mud Cap - Referred to also as Adobe or Plaster Shot. A charge of explosive fired in contact with the surface of a rock after being covered with a quantity of mud, wet earth, or similar substance, no borehole being used.

Open Pit - A surface operation for the mining of metallic ores, coal, clay, etc.

Overbreak - Excessive breakage of rock beyond the desired excavation limit.

Overburden - The material lying on top of the rock to be shot; usually refers to dirt and gravel, but can mean another type of rock; e.g. shale over limestone.

Oxidizer - A supplier of oxygen.

Permissible - Explosives having been approved by the U.S. Bureau of Mines for non-toxic fumes, and allowed in underground work.

Powder - Any of various solid explosives.

Premature - A charge which detonates before it is intended to.

Presplitting - Stress relief involving a single row of holes, drilled along a neat excavation line, where detonation of explosives in the hole causes shearing of the web of rock between the holes. Presplit holes are fired in advance of the production holes.

Primary Blast - The main blast executed to sustain production.

Primer - An explosive unit containing a suitable firing device that is used for the initiation of an entire explosive charge.

Quarry - An open or surface mine used for the extraction of rock such as limestone, slate, building stone, etc.

Riprap - Coarse sized rocks used for river bank, dam, etc., stabilization to reduce erosion by water flow.

Round - A group or set of blast holes constituting a complete cut in underground headings, tunnels, etc.

Seam - A stratum or bed of mineral. Also, a stratification plane in a sedimentary rock deposit.

Secondary Blasting - Using explosives to break up larger masses of rock resulting from the primary blasts, the rocks of which are generally too large for easy handling.

Seismograph - An instrument that measures and supplies a permanent record of earthborne vibrations induced by earthquakes, blasting, etc.

Sensitizer - The ingredient used in explosive compounds to promote greater ease in initiation or propagation of the reactions.

Shot Firer - Also referred to as the Shooter or Blaster. The person who actually fires a blast. A Powderman, on the other hand, may charge or load blast holes with explosives but may not fire the blast.

Shunt - A piece of metal connecting two ends of leg wires to prevent stray currents from causing accidental detonation of the cap. The act of deliberately shorting any portion of an electrical blasting circuit.

Slope - Used to define the ratio of the vertical rise or height to horizontal distances in describing the angle a bank or bench face makes with the horizontal. For example, a 1-1/2 to 1 slope means there would be a 1-1/2 ft. rise to each 1 ft. or horizontal distance.

Snake Hole - A hole drilled or bored under a rock or tree stump for the placement of explosives.

Spacing - In blasting, the distance between boreholes or charges in a row.

Stemming - The inert material, such as drill cuttings, used in the collar portion (or elsewhere) of a blast hole so as to confine the gaseous products formed on explosion. Also, the length of blast hole left uncharged.

Strength - Refers to the energy content of an explosive in relation to an equal amount of nitroglycerine dynamite.

Stratification - Planes within sedimentary rock deposits formed by interruptions in the deposition of sediments.

Strike - The course or bearing of the outcrop of an inclined bed or geologic structure on a level surface.

Sub-Drill - To drill blast holes beyond the planned grade lines or below floor level.

Swell Factor - The ratio of the volume of a material in its solid state to that when broken.

- The process of compressing the stemming or explosive in a blast hole.

Toe - The burden or distance between the bottom of a borehole to the vertical free face of a bench in an excavation.

Velocity - The measure of the rate at which the detonation wave travels through an explosive.

Appendix 6 Geotechnical data collection manual

PART 1 - INTRODUCTION

A natural rock mass is never a continuous, homogeneous, isotropic material but is intersected by a great variety of **dis-**continuities such as faults, joints, bedding, foliation or cleavage. In addition, there may be a number of rock types, and these may be subjected to varying degrees of alteration by weathering. It is clear that the behavior of such a material, subjected to external loading, cannot be analyzed or predicted unless these structural features are taken into account.

When subjected *to* loading the rock mass will preferentially fail along the weak discontinuities rather than through stronger intact rock. In order to establish the mechanism by which movement may occur, and also the resistance to that movement, a geotechnical appraisal of the rock mass is required. Ideally a complete description should be obtained of the location and orientation of all discontinuities and also the nature of the intact rock which may affect the stability of the underground opening or slope under study. Such a complete study is rarely either technically possible and/or economically justifiable and a compromise is usually required.

Once the spatial relationship of the discontinuities has been approximately determined, a "model" can be formed. The analysis of these models, when the stress distribution and strength properties are also known, enables a prediction of the performance of the slope to be made.

Part 2 of this manual outlines the parameters **which** are considered important in structural analysis. Parts 3 and 4 detail the techniques for obtaining structural information from surface and underground exposures, and from boreholes, respectively. Parts 5, 6, and 7 describe associated techniques and equipment which are used to collect the geological and geotechnical data and provide additional information.

Attempts have been made to standardize mapping and logging methods and the format of the recording sheets. However, the diversity of site conditions and different uses of the data often require that some **modifications** be made to the methods to suit the needs of each project. The purpose of geological investigations for slope designs is to identify and make proper record of those parameters that are most likely to influence the stability of a particular slope. Experience is important in the identification of controlling parameters and the decision as to methodology must remain with the project engineer.

The end product of an investigation is the presentation of **data** in such a way that it graphically illustrates the field situation and contains data in a form compatible with any intended analytical procedures. Typically, this may **include** a set of maps or plans, a complete data listing with selected stereo plots, and drafted versions of some field sheets.

To this end, the investigation will always start on a reconnaissance basis, with the emphasis on observation and generalized sampling method; in short, rapid efficient development of a picture of general geological site conditions. Detailed sampling techniques including definitive joint mapping, in situ

materials testing, structural drilling, and hydrological testing can then be undertaken in places where specific information is required for analytical purposes.

It is, therefore, important to establish the objective of an investigation early in the program and direct all data collection toward that objective. This will lead to maximum utility of the data and will ensure that a minimum of time is spent detailing non-important characteristics.

PART 2 - PARAMETERS

The basic parameters to be considered when collecting structural geological data related to discontinuities for stability studies in rocks are:

- 1) Mapping location.
- 2) Classification of discontinuities by type.
- 3) Orientation of discontinuities, and division into "sets" having similar orientations.
- 4) Infilling of the discontinuities.
- 5) Surface properties.
- 6) Spacing of discontinuities within sets.
- 7) Persistence of fractures.
- 8) Rock mass parameters.

Parameters 4 and 5 define the strength properties of the **dis-**continuity while parameters 6 and 7 define the geometry of the blocks forming the rock mass. The following sections give details of coding notations to assist in filling out the forms and logs explained in parts 3 and 4 of this manual. Coding notations are used to simplify input to a variety of data handling and processing computer programs. Specific notations may be changed provided that a detailed record is kept of their meanings.

1) MAPPING LOCATION

The location of the area being mapped is recorded as Data Unit information and in columns 1 to 4 of the logging sheets shown in Figures 9 and 11 for surface mapping and core logging respectively. The data unit is the traverse or **borehole** number and the location is the distance along the unit at which the intersection of the discontinuity occurs.

2) CLASSIFICATION OF DISCONTINUITY TYPES

A discontinuity in the context of engineering geology can be defined as any natural fracture in the rock mass; in addition, it may be a plane marking the change in geological or **geotechnical** characteristics. The discontinuity type notation is placed in columns 5 to 7 on the logging **sheets** (Figures 9 and 11). **Common** types of discontinuity and their notations include:

Contact

The boundary between two distinct rock types. Contacts are not always regular and well defined, nor do they necessarily form the site of a discontinuity, particularly in metamorphic and igneous rocks. Notation C.

Fault or Shear

A fault or shear is a discontinuity along which movement can be demonstrated to have **occurred**, either by the relative displacement of marker horizons, or by the presence of slickensides or **gouge**. The magnitude and direction of movement may be **measurable**. The fault may be represented by a zone of **breccia/gouge**, rather than a single discontinuity surface, or shear plane. The

notations used are F for fault, and S for shear. In certain cases faults may be rehealed or cemented by subsequent geological processes.

Joint

A joint is a natural discontinuity which is generally not parallel to lithological variations and which shows no signs of shear displacement. Such features are often impermanent. Notation J.

A **group** of joints having the same general orientation is termed a **"set"**.

Bedding

Lithological layering in sedimentary rocks is very often a prominent weakness direction. Such features can be very persistent and be traced for hundreds of feet. Bedding features carry a B notation.

A bedding feature which is not separated is termed a "Bedding Plane Trace".

Flow Banding

Igneous equivalent of bedding; where directional movement of a fluid causes mineralogical or textural banding. Not necessarily a discontinuity. Equivalent to B for igneous rocks.

Foliation, Schistosity and Cleavage

Metamorphic layering which should be treated in the same way as bedding, and coded as L.

These features may be closely spaced, and may result from orientation of platy minerals, e.g. micas and hence represent a preferred direction of weakness.

Vein

A tabular feature of finite thickness composed of material which differs from the surrounding rock either in grain size or composition or both. Notation V.

"Healed" joints can be classified as veins, and as such are not necessarily planes of weakness.

3) ORIENTATION

The orientation of a planar discontinuity is a unique measurement. Figure 1 shows how the orientation of a plane may be described by a vector. The dip direction of the plane from a reference direction and the dip angle from a reference plane describe its orientation. In normal field circumstances the reference direction is True North and the reference plane is horizontal. These references may be changed when mapping in magnetic environments or when logging oriented core from inclined boreholes, see below.

Orientation data is placed in columns 8-12 of the logging sheets.

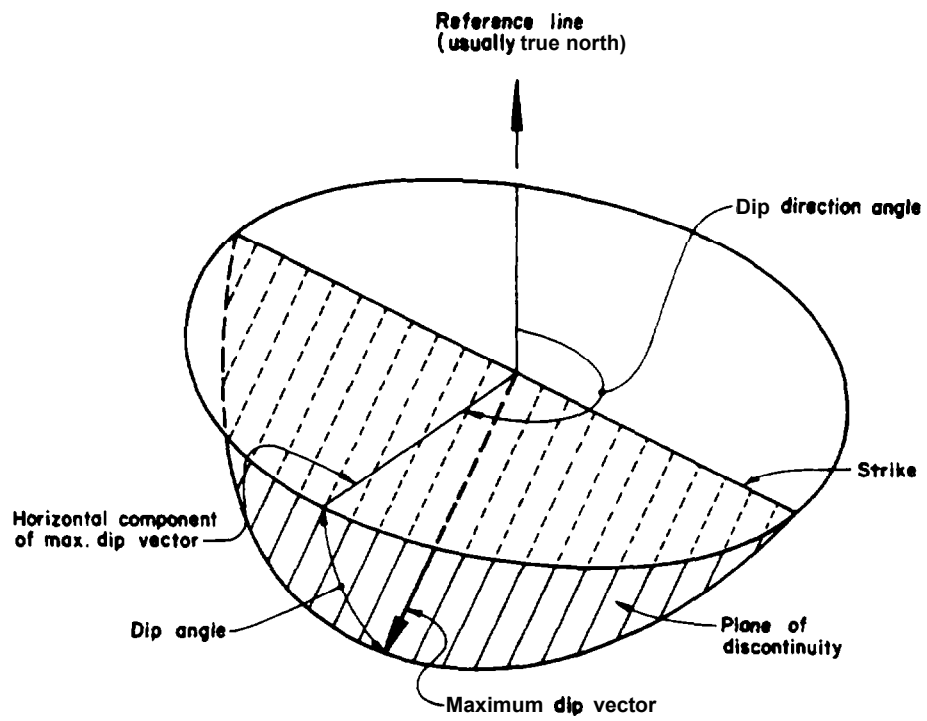


Figure 1: Orientation of a discontinuity.

Surface Mapping

Rock discontinuities are often not planar and the surfaces may be curved or irregular on a large or small scale. This factor causes inaccuracy in the determination of orientation.

A mean orientation can be established for a particular surface area by two methods:

- 1) A large number of individual measurements on a single surface may be located mathematically and a mean vector computed. This mean vector may then be regarded as the orientation of that discontinuity. Unfortunately this method may require more than 50 measurements per surface.
- 2) The estimation of a mean plane may be done by eye. This is the most practical method but can be of doubtful validity when only a small area of the joint surface is exposed.

Orientation in Magnetic Environment

Where there is a strongly magnetic environment it will not be possible to use a compass to measure the **spacial** azimuths (dip directions) of the geological discontinuities. It is therefore proposed that a tape be used, stretched out parallel to the bench face as the basic azimuth against which orientations are recorded. The true orientation of this tape should be surveyed and recorded.

All mapping should be performed in the same direction when facing the slope face, and the end of each tape traverse towards which mapping is progressing should be referred to as azimuth "000" for that unique tape traverse. It is suggested that all mapping proceed from left to right when facing the slope in which case the right hand end of the tape would have an arbitrary azimuth of "000" for each traverse.

Azimuths relative to the tape can be measured with a standard carpenter's rule.

Core Orientation

When logging oriented core the orientations recorded are shown on Figure 2 and described below.

The core dip **angle, α** , is between the discontinuity plane and the core axis, and can be measured with a core goniometer, see Figure 3.

Core dip **direction, β** , is the angle around the core from a reference line, usually top of core, to the lowest intersection of the discontinuity plane with the core. All measurements are made clockwise around the core when looking in a **downhole** direction using a linear protractor, see Figure 4.

Where the dip direction cannot be determined due to loss of orientation for the run, the dip angle with respect to the core axis is recorded, and "999" is noted as the dip direction on the form shown in Figure 11.

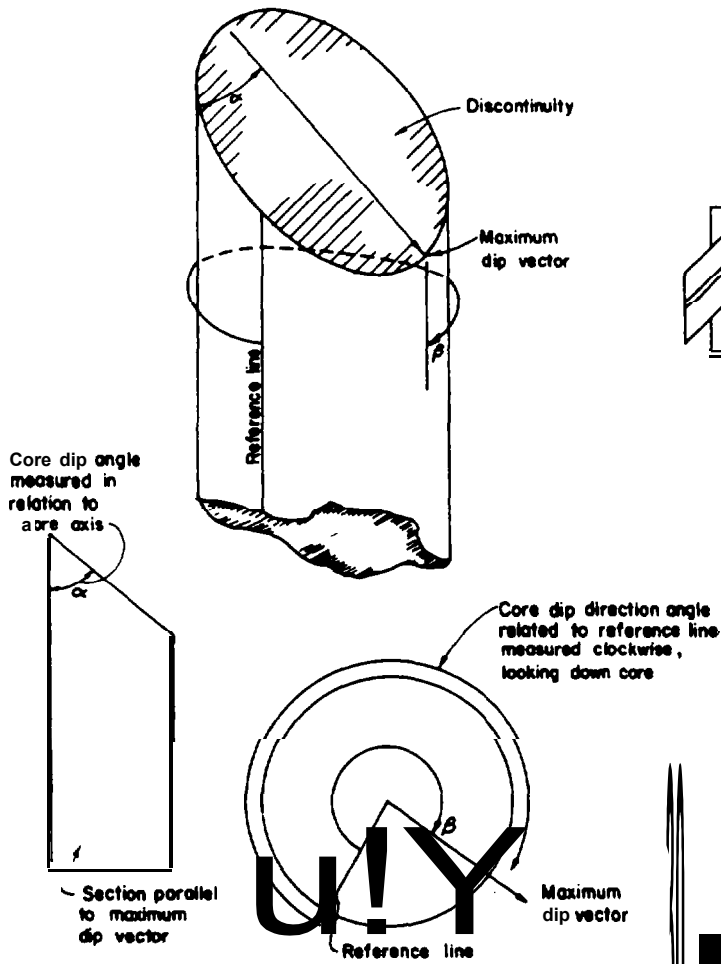


Figure 2: Core dip and dip direction angle.

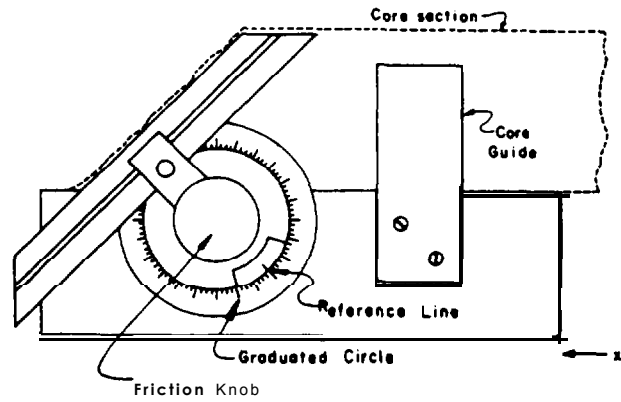


Figure 3: Core goniometer.

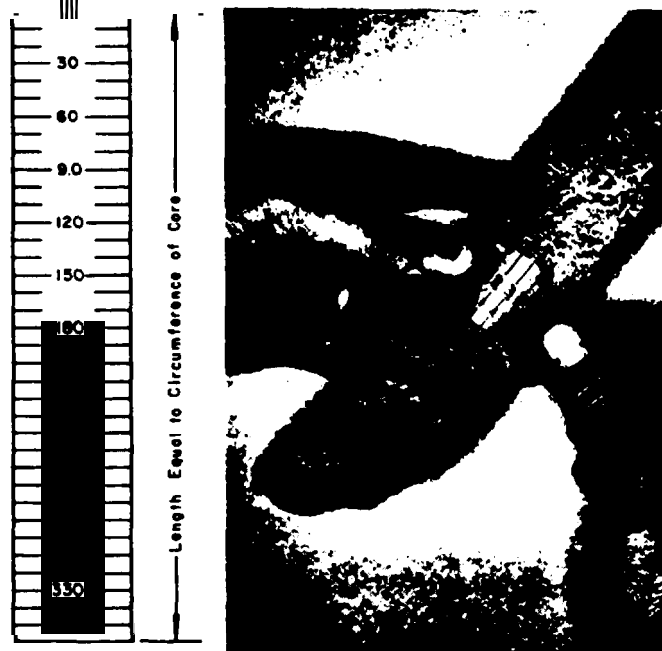


Figure 4: Linear protractor.

Orientation is generally lost across a broken or lost core intersection in the run. However, if the core contains a unique constant foliation orientation, e.g. bedding or banding, this can be used to continue the orientation if its orientation has already been ascertained.

4) DISCONTINUITY INFILLING

The nature and thickness of the infilling of faults and joints may give important information regarding groundwater conditions, e.g. preferential iron staining on particular joint sets will indicate directions of predominant water flow. Also a weak material infilling will indicate that the infilling and not the host rock will govern the shear strength of the discontinuity.

Common types of infilling with their notation symbols are:

- 1) Clay - montmorillonite, kaolin, etc; A
- 2) Iron minerals - limonite, etc; F
- 3) Calcite; W
- 4) Chlorite; K
- 5) Quartz; Q
- 6) Pyrite; P

This system can be expanded to suit the needs of specific projects, with a record being kept of the symbols used.

Clean discontinuities can be distinguished by C.

In some instances water may be seen issuing from a particular discontinuity and this should be noted separately. If more than one type of infilling is present each should be recorded in order of priority.

The type of infilling is placed in columns 13 to 15 of the logging sheet, the thickness code letter in column 16 and the presence of water by a W(wet) or D(dry) in column 17.

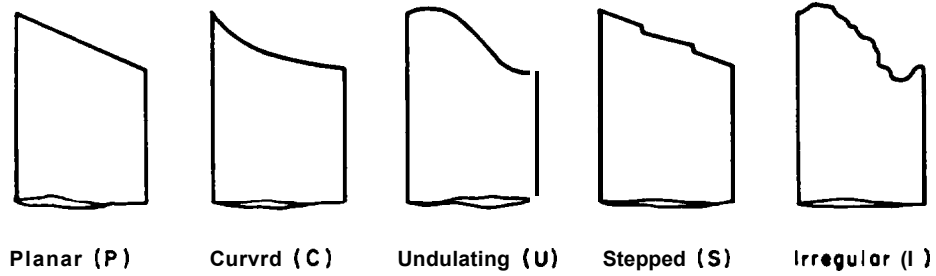
5) SURFACE PROPERTIES

The surface properties affect the shear strength of discontinuities, and should be assessed subjectively in the mapping program. The assessment may be divided into two factors: shape and roughness.

Shape	<u>Roughness</u>
P Planar	P Polished
C Curved	K Slickensided
U Undulating (Wavy)	S Smooth
S Stepped	R Rough
I Irregular	V Very Rough

Alternatively, the roughness can be classified according to the Joint Roughness Coefficient (JRC) described in Chapter 5 of the manual.

Figure 5 shows the distinguishing features of shape and roughness of joints as seen in drill core and in surface exposures. The code letters or numbers describing roughness are entered in columns 18 and 19.

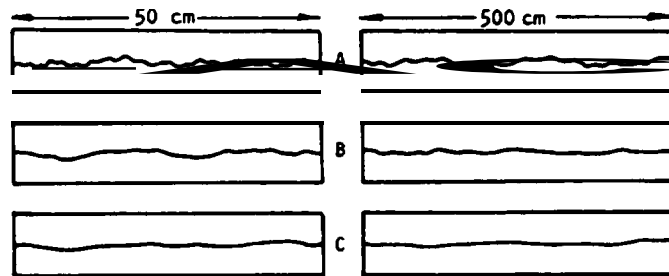


SHAPE



ROUGHNESS

EXAMPLES OF ROUGHNESS PROFILES



- A. Rough undulating - tension joints, rough sheeting, rough bedding. JRC = 20
- B. Smooth undulating - smooth sheeting, non-planar foliation, undulating bedding. JRC = 10
- C. Smooth nearly planar - planar shear joints, planar foliation, planar bedding. JRC = 5

Barton's definition of Joint Roughness Coefficient JRC.

Figure 5: Shape and roughness of joints in drl 11 core.

6) SPACING

The true spacing is the distance between discontinuities in a set, measured in the direction normal to the planes. Apparent spacing is the spacing between planes measured along a line or traverse at an angle to discontinuity sets. Traverses can be along boreholes, **adits**, bench faces or exposures. The relationship between true and apparent spacing is shown in Figure 6. The spacing between fractures can be recorded by the code letters shown on Figure 9 which is entered in column 20. The same system can be used to record the number of fractures which is entered in column 21.

7) PERSISTENCE

Persistence is the length or areal extent of a discontinuity which can be seen or inferred from mapping procedures. This is the most difficult to assess of all the parameters important to geotechnical mapping. Unfortunately persistence is often critical to the design of slopes and underground openings, since it provides an assessment of the amount of intact rock which separates joints of a similar set occurring down or up dip. The areas of intact rock are known as "rock bridges".

Exposure Flapping

Persistence may be simply assessed in up to four categories relating to each type of discontinuity when mapping exposed structures, and recorded as a suffix to the notation for discontinuity type (e.g. **J1, B2**, etc.). The categories are also related to the size of underground opening or exposure height as shown below, and in Figure 7.

<u>Category</u>	<u>Measurement</u>
1	Greater than 3 m in two directions
2	Greater than 3 m in one direction
3	Less than 3 m in one direction
4	Less than 1 m in one direction (normally only mapped in critical structures such as bridge abutments).
5	Healed discontinuity

In some instances it may be simpler to scale the measurements to the size of the underground opening or bench. This data is entered in column 22 of the logging sheet.

The other factor **which** is used to assess the **persistence** of discontinuities is the termination, i.e. the visibility of the ends of the fracture. The following three code numbers, which are entered in column 23, can be used to define termination.

- 0 - neither end of fracture visible
- 1 - one end visible
- 2 - both ends visible

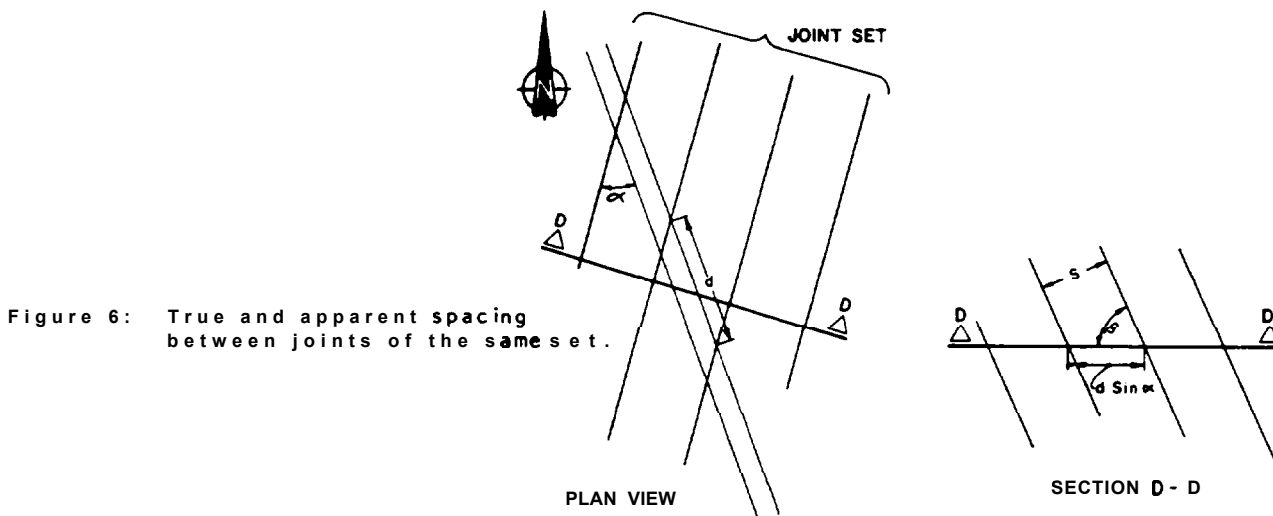


Figure 6: True and apparent spacing between joints of the same set.

LEGEND

- d Apparent spacing
- α Angle between strike of joint and adit direction.
- β True dip of joint
- S True spacing $d \sin \alpha \sin \beta$

EXAMPLE

- Joint set dipping $61^\circ / 105^\circ$
- Adit running
- d = 50 m
- $\alpha = 36^\circ$
- $\beta = 61^\circ$
- S = $50 \cdot \sin 36^\circ \cdot \sin 61^\circ$
- = 25 m

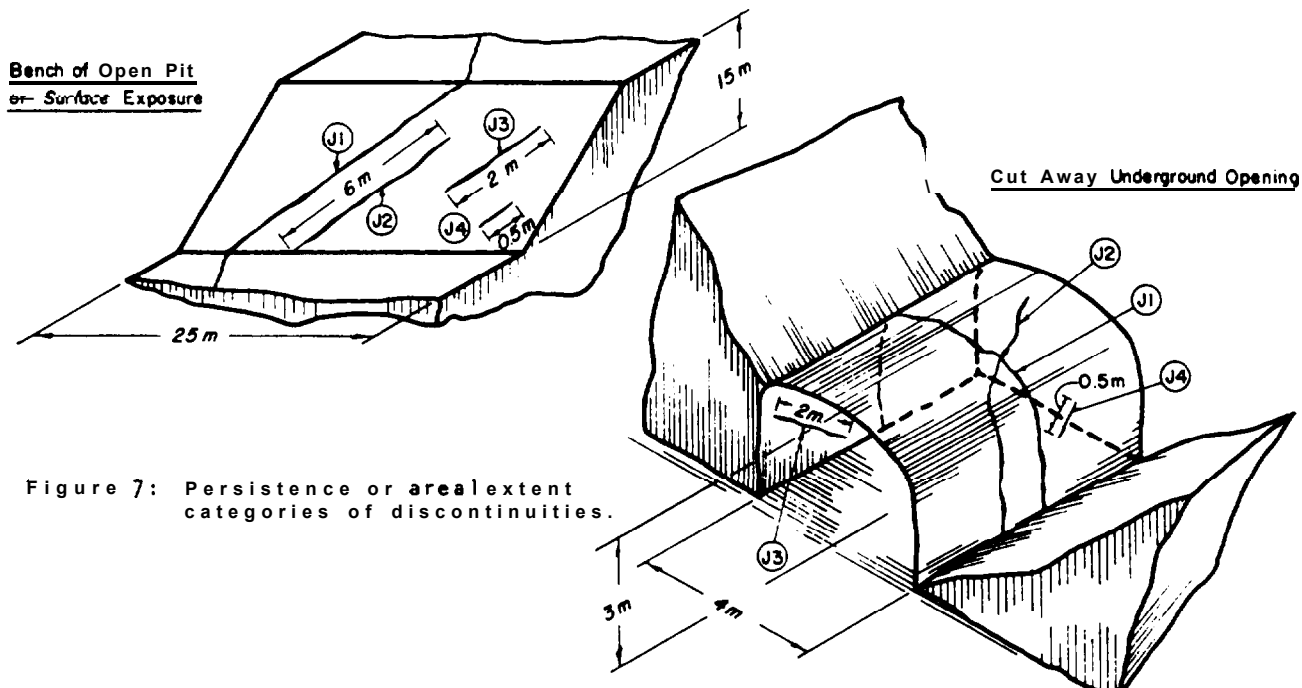


Figure 7: Persistence or areal extent categories of discontinuities.

Core Logging

Persistence cannot be measured from drill core but the relative importance of discontinuities may be estimated using the following scheme:

<u>Category</u>	<u>Measurement</u>
1	Pre-existing open fracture in rock mass which is continuous across the core.
2	A drilling induced fracture which occurs along a pre-existing plane of weakness in the rock.
3	A drilling induced fracture which is not related to any plane of weakness in the rock mass.
5	A pre-existing open fracture in the rock mass which is not continuous across the core or an intact feature which has been healed.
9	A trace of a geological feature which does not represent any inherent weakness in the rock mass.

A conservative approach would be to assume that a discontinuity is pre-existing if there is any doubt as to its origin.

8) OTHER PARAMETERS

The following are not quantitative measurements recorded directly from mapping or logging techniques on discrete discontinuities, but are used as indices to assess rock mass characteristics, derivations are described where not self-explanatory:

- 1) Rock Type
- 2) Weathering and Alteration
- 3) Strength or Hardness
- 4) Recovery or Loss of Core
- 5) **R.Q.D.**
- 6) Fracture Frequency or Index

This data is either recorded as back-up data to the structural mapping program, or in a drilling program, forms part of the core log shown in Figure 11.

Rock Type

Depending on the format chosen for geological data presentation different rock type descriptions are used. The codes used should be recorded during the field mapping program to ensure that maximum usage of the data is possible.

When using written descriptions in geological or engineering logs it has been found that the system described below presents a uniform approach, allowing continuity of description from location to location, and project to project. The following standard sequence of systematic description is proposed:

Weathered state, structure, colour, grain size, rock material strength, ROCK TYPE.

It is considered that the qualifications are **more** important in core descriptions than the actual rock name and, for this reason, the name is placed last. Such a system is appropriate to an engineering description where classification by mechanical properties is more significant than classification by mineralogy and texture. The following examples are provided for illustrative purposes:

- 1) Fresh, foliated, dark grey, coarse, very strong, hornblende GNEISS.
- 2) Moderately weathered, thickly bedded, cream, **medium-grained**, strong dolomitic LIMESTONE.
- 3) Completely weathered, thinly flow-banded, mid-grey, very coarse, porphyritic, kaolinized, weak tourmaline GRANITE.

Various of the qualifying types are detailed in sections below.

Weathering

The following system of weathering classification is proposed:

Fresh (FR)	no visible sign of weathering
Fresh jointed (FJ)	weathering limited to the surface of major discontinuities
Slightly weathered (SW)	penetrative weathering developed on open discontinuity surfaces but only slight weathering of rock material
Moderately weathered (MW)	weathering extends throughout the rock mass but the rock material is not friable
High weathered (HW)	weathering extends throughout rock mass and the rock material is partly friable
Completely weathered (CW)	rock is wholly decomposed and in a friable condition but the rock texture and structure are preserved.

It will be noted that this scheme is broadly based on that development for the Snowy Mountains Authority (Moye 1955), but has been adapted for a general range of rock types rather than simply for granitic rocks for which it was originally devised. In the case of weathered rocks with a significant clay content, the material may exhibit plasticity rather than friability; in consequence, some care may be required in assessing the weathering state of such rocks.

A comparative table of mineralogical, mechanical and appearance characteristics is included as Table 2.1, where it should be noted that various states of weathering are defined by the alteration products of primary constituents of the rock fabric.

Alteration and weathering are both included in the weakening assessment.

Strength

The rock strength classifications used, either by code or term, have been derived from a number of sources and are presented with reference to simple field hardness tests shown in Table 2.2. Different mapping and logging requirements will dictate which method of presentation will be used, and the uniaxial compressive strengths appear as a guide for order of magnitude analyses only.

Core Recovery or Loss

This index should be recorded on all core logging forms either as recovery or loss depending on the requirements of the project. Core recovery is determined as the ratio of core recovered to the total drilled run length expressed as a percentage; the value may be recorded on a run by run basis or over a normalized core length. Occasionally core loss is plotted in order to highlight zones of weaker core. From the point of view of most geotechnical drilling it is the core that is hardest to recover which will indicate most clearly the weakest parts of the rock fabric.

R.Q.D.

A refinement of the core recovery system is proposed following the work of Deere et al (1967). It defines the fraction of solid core recovered greater than 4 inches in length as the Rock Quality Designation. It is calculated as the ratio of the sum of the length of core fragments longer than 4 inches to the total drilled footage per run. **expressed** as a percentage. The core is measured along the centerline from fracture to fracture. Fractures parallel to the core axis should be ignored as sampling errors.

In certain cases the index can be recalculated over a normalized footage (for example a bench height) for interpretive use.

R.Q.D. may be used to classify the rock mass following Deere's scheme:

<u>RQD</u>	<u>Rock Classification</u>
0 - 25%	Very poor
25 - 50%	Poor
50 - 75%	Fair
75 - 90%	Good
90 - 100%	Excellent

Fracture Frequency or Fracture Index

This is an invaluable index of a rock mass and may be recorded in a number of ways:

- 1) When mapping exposures, either a cut slope or in a tunnel, it should be measured as the ratio of the number of fractures per foot of true spacing. It can be measured either per joint/bedding set, or for a rock mass.

- 2) For engineering logging it is almost invariably recorded as the number of natural fractures per unit length of core recovered. Depending on the logging requirement, the fracture frequency may be measured for each run or over a normalized footage, and representative sections of core only may be measured in certain circumstances.

It has been found from experience that fracture frequency/index is of most use for surface investigations whereas R.Q.D. holds similar prevalence for underground analyses. It is usual to record only natural fractures in the above assessments and departure from that specification should be recorded.

PART 3 - MAPPING SURFACE AND UNDERGROUND FEATURES

The principles for mapping surface and underground exposures are generally similar, although the underground openings may provide better three dimensional information.

The basic methods should be suitable for all rock types, but the mapping procedures are subdivided into three basic stages:

- 1) Major Feature Mapping.
- 2) Detailed Mapping.
- 3) Specific Mapping of Critical Features.

All attempts to strictly delineate the boundaries of these stages are doomed to failure and these recommendations should only be used as general guidelines. The objective is to initiate procedures which define, and then successively refine, information on those features which will be critical to stability.

MAJOR FEATURE MAPPING

The first step is to prepare a plan of the area with grid and magnetic north, if plans at a suitable scale are not available. A scale of **1:500** is the most useful general purpose scale but **1:1000** or **1:250** may be required for certain projects. It is most convenient to record information directly on to a working plan and transfer it to the master plan in the office.

In order to record the location of each feature it is necessary to use a system of reference points with known coordinates. These may be already available from surveys. If not, a special survey will be required, if pacing from known locations is found inadequate.

The location of each feature is measured from a tape stretched between reference points. In an underground opening two tapes may be used, one on either side of the opening. Intersections of major features with the tape(s) can thus be measured and recorded.

The major features should include the following:

- 1) Faults.
- 2) Rock type contacts, including weathering and alteration.
- 3) Fold axes.
- 4) Typical prominent bedding planes or joint sets.

In all cases the orientation should be measured using a compass or conventional surveying. The nature of infilling and the orientation of any slickensides or displacement of marker beds associated with faults should also be recorded.

The features are relatively large scale in relation to the slope and should be recorded on plans and sections on the same scale as the highway layout plans and sections. The use of transparent overlays is recommended for this purpose to avoid









<u>FEATURE</u>	<u>SYMBOL</u>	<u>CODING</u>
Rock Contact		
Syncline		
Anticline		
Fault		F
Bedding		B
Joint		J
Vein		V
Lineation		

Figure 8: Symbols for geological features.

confusion by detail. The symbols **recommended** for recording the major features are shown in Figure 8.

In order that the construction personnel can readily make use of this data, significant geological contacts and major zones of weakness should be marked in the field with **colour** coded stakes or spray painting.

This general scale of mapping will delineate the structural domains. In the case of metamorphic or volcanic rocks, major faults and contacts will be the main boundaries. Sedimentary rock types may show, in addition, distinct structural domains due to folding.

DETAILED MAPPING

Once the major features have been delineated it is possible to decide which areas should be mapped in detail. The locations of features can be determined from a tape using the same reference points discussed above.

Experience has shown that it is not necessary to map every feature. Indeed, it is often a mistake since it becomes difficult to distinguish major features from minor ones.

This stage of mapping should define the location and the orientation of fold axes. Where tight folding has occurred the amplitude and wavelength of folds should be measured. Since jointing will be associated, in most cases, with the folding, all joints should be related to representative bedding orientations.

The location, orientation, persistence, infilling and surface roughness should be recorded on a simple code form of the type shown on Figure 9. This code form fits into a field note book and enables the data to be easily punched onto cards which can then be read into computer data as input to programs for spherical projection analysis.

The presentation of detailed mapping data can be done in two ways:

- 1) The more important discontinuities, persistent categories 1 and 2, can be plotted on the same structural plans as the major features (see "Major Feature Mapping") using the symbols presented in Figure 8.
- 2) Oriented data can be plotted on an equal area projection with different symbols being used for different features.

In general, both methods should be used since they complement one another. The plan shows the spatial relationship while the projections define the angular relationships.

Wherever possible, color photographs should be taken of the exposure mapped, regardless of mapping method, as a useful adjunct to the structural data.

Three different methods of detailed mapping are suggested, and detailed below. The particular technique should be pertinent to the specific project.

Joint Set Mapping

In each structural domain typical discontinuity sets should be mapped for the following parameters (see Part 2).

- 1) Discontinuity Type
- 2) Orientation
- 3) Infilling
- 4) Surface Properties
- 5) Spacing
- 6) Persistence

In the case of typical joint and bedding sets at least 50 sample measurements should be taken per set. In some rock types and locations definitive sets may be difficult to delineate, under these circumstances only those features **which** will affect the stability of the slope should be mapped. This would include those features which are **more** Persistent, and those of adverse orientation.

Window Mapping

The "window" mapping technique involves the detailed mapping of representative **segments** or "windows" of a fixed size, spaced at fixed intervals in the exposures. The intervening areas are reviewed for similarity of structure with the adjacent "windows", and any variations or major structural features are mapped in detail. This form of mapping can be combined with standard geological (rock type/grade) mapping with little additional time requirements.

In each "window" the mean orientation for each discontinuity set is recorded, either as several individual joint measurements, or as the mean of several measurements. The characteristics of the discontinuities of the sets visible within the **window** are also noted.

The sizes of the window and the intervening section of unmapped rock face should be chosen to suit the project. The following examples are taken **from** recent projects where window mapping was used:

- 1) Slopes 30 ft. windows every 150 ft.
- 2) Tunnels 10 ft. windows every 50 ft. on both walls

Line Mapping

An alternative for isolating sample areas to be mapped is to use the line sampling method. This involves recording every structural feature which intersects a scan line which may be painted on a rock face or be represented by a tape stretched along a face or tunnel wall.

One advantage of this technique is that line sampling corrections may be applied to the data should detailed statistical analysis be required. However, it can be a tedious routine for mapping large areas.

SPECIFIC MAPPING OF CRITICAL FEATURES

In some instances it will be necessary to further refine the information if preliminary analysis has shown a particular

set(s) of features to be critical to stability. Each joint set should be treated independently. In addition to all the factors outlined in the previous sections, the apparent spacing between the joints of the same set should be measured with a minimum, mean and maximum value. The true spacing can be computed from the apparent spacing along a particular direction if the orientation of the mapping line is known (see Figure 6 in Part 2).

In order to estimate the shear strength of critical **discontinuities**, it may be necessary to make detailed shape and roughness measurements on the surfaces, and strength tests of infilling materials may be required.

PRIORITY IN GEOTECHNICAL MAPPING

The preceding sections are a guide and each geologist or engineer should realize that some flexibility is required. In many cases it may be possible to merge various stages.

The following factors should be regarded as the order of priority:

- 1) The orientation and location of major faults and weak zones and the infillings.
- 2) The orientation and location of contacts of major rock types.
- 3) The orientation of persistent discontinuities.
- 4) The spacing of persistent discontinuities.
- 5) The infilling of discontinuities.
- 6) The surface properties of features.

PART 4 - GEOTECHNICAL MAPPING FROM DIAMOND DRILL HOLES

Diamond core drilling is one of the most expensive forms of geological data collection, and generally forms the major expenditure in an exploration program. In consequence, it is essential that the maximum amount of data is obtained from the drill core, in addition to putting the resulting hole to maximum use, e.g. by measuring water levels, and permeability; installing piezometers, etc.

Drill core can be a valuable source of geotechnical and engineering information pertaining to rock conditions at depth. The amount and type of geotechnical detail recorded will vary depending on the project and the individual hole. As a result, data recording can vary from a **summary** log indicating the basic generalities of the rock characteristics, to a detailed log of the orientation and nature of every discontinuity.

It is valuable to photograph each core box (35 mm color slides are preferred). These photographs provide a permanent record of core condition from which considerable information of **geotechnical** value can be obtained later.

All logs should be filed with a cover sheet, see Figure 10, giving relevant drill hole data such as collar coordinates, **borehole** orientation, **borehole** survey data, length, core size, etc., plus any relevant information from the driller's logs.

Accurate discontinuity orientation is only possible when the logged orientations are corrected for hole deviation at close intervals along the hole. This is best performed by a computer program which interpolates absolute hole orientation between survey points, and corrects individual readings accordingly. Hole surveys should be taken every 100 to 200 ft.

Drilling Information

Problems encountered in the drilling of the hole frequently tell more about the ground conditions than can be obtained from logging of the recovered core. Thus, a geotechnical logging method should contain the following information, in addition to a record of geological features.

A **summary** of the drilling events, based on verbal conversation with the drillers, should be noted. This **summary** enables a reconstruction of events that allows the engineer to see exactly what occurred in the drilling of the hole and also may aid in the interpretation of core condition. Items such as the use of bentonitic mud; the rods becoming stuck or hard to turn; requirement for replacement of core catcher or bit, including specific type; deviations in usual drilling techniques; etc., all add to this documentation and serve to produce a log that can be used in the interpretation of the ground conditions.

This information should be recorded on a driller's sheet. If and when zones of water loss are encountered, the specific depth should be noted and shown on the log; a general statement should be made if none are encountered. Driller's data sheets, with water levels, can be used on each core hole to provide additional information.

BASIC DRILL HOLE DATA															
PAGE <u>1</u> Of <u>23</u>															
PROJECT: <i>PALABORA COPPER PIT</i>	BOREHOLE no.: <i>LK-150</i>														
LOCATION: <i>+ 24105,84 X / -14284,06 Y</i>															
CLIENT:															
DRILLING CONTRACTOR : <i>PMC Drill</i>															
DRILLING METHOD: <i>Diamond Coring</i>	MACHINE: <i>Longyear 38</i>														
CORE BARREL B BIT DESIGN: <i>BQ</i>	ORIENTATION OF MOLE: <i>89° 52' 50"</i>														
DATUM: <i>MSL</i>	ELEVATION of COLLAR: <i>+ 387,51m</i>														
OVERBURDEN THICKNESS: <i>12.0m</i>	DATE HOLE STARTED: <i>3/7/75</i>														
DEPTH DRILLED INTO ROCK: <i>1460.90m</i>	DATE HOLE COMPLETED: <i>12/8/77</i>														
TOTAL DEPTH OF HOLE: <i>1472.90m</i>	REFERENCE NO.:														
LOGGED BY: <i>T.A.H.</i>	CASING RECORD:														
NOTES : <i>Circulating medium :- water</i> <i>Inclination surveys (GYRO):-</i> <table style="margin-left: 40px;"> <tr> <td><i>Collar</i></td> <td><i>- 64' 39' 14"</i></td> </tr> <tr> <td><i>250m</i></td> <td><i>- 60' 14' 20"</i></td> </tr> <tr> <td><i>500m</i></td> <td><i>- 55' 05' 23'</i></td> </tr> <tr> <td><i>750m</i></td> <td><i>- 53' 10' 08"</i></td> </tr> <tr> <td><i>1000m</i></td> <td><i>- 52' 09' 31.</i></td> </tr> <tr> <td><i>1230m</i></td> <td><i>- 50' 35' 41"</i></td> </tr> <tr> <td><i>1470m</i></td> <td><i>- 48' 01' 52"</i></td> </tr> </table>		<i>Collar</i>	<i>- 64' 39' 14"</i>	<i>250m</i>	<i>- 60' 14' 20"</i>	<i>500m</i>	<i>- 55' 05' 23'</i>	<i>750m</i>	<i>- 53' 10' 08"</i>	<i>1000m</i>	<i>- 52' 09' 31.</i>	<i>1230m</i>	<i>- 50' 35' 41"</i>	<i>1470m</i>	<i>- 48' 01' 52"</i>
<i>Collar</i>	<i>- 64' 39' 14"</i>														
<i>250m</i>	<i>- 60' 14' 20"</i>														
<i>500m</i>	<i>- 55' 05' 23'</i>														
<i>750m</i>	<i>- 53' 10' 08"</i>														
<i>1000m</i>	<i>- 52' 09' 31.</i>														
<i>1230m</i>	<i>- 50' 35' 41"</i>														
<i>1470m</i>	<i>- 48' 01' 52"</i>														

Figure 10: Drill hole cover sheet.

Rubblized zones within the hole that cave should be given special emphasis and noted on the log. If the caving ground is brought to the surface in the barrel, a description of it should also be noted (sand size, gravel size, etc.).

Areas that require grouting in order to continue coring should be noted and the log should indicate the specific zones grouted, how much grout was used, and the hardness and description of the grout core.

GEOTECHNICAL LOGGING

The objective of a geotechnical log is to record information from the drill hole that reflects the condition of the ground penetrated. This information comes both from the drilling process and from the recovered core.

The data recorded should be relevant to the scope of the project; the logging detail and format for a tunnel should reflect the problems of underground excavation and support; data obtained from holes drilled for slope investigations should reflect the larger scale of a slope.

The information should also be directly useful in the interpretation of either the mechanical or hydrological properties of the rock mass. Geologic information (that which enables interpretation of the spatial variability of the several parameters) should be recorded and handled in the manner preferred by the responsible geologist(s). There is an overlap in that alteration, for instance, will affect the strength of the rock materials. Probably the most important aspect of the entire geological/geotechnical investigation is the definition of the fault population as faults frequently control water migration and strength properties. Typically geotechnical problem areas or failure situations in rock materials will directly relate to the occurrence of faults.

The following sections describe oriented core and geological engineering logging methods and show typical logging sheets. The parameters that are recorded are all described in detail in Part 2 of this manual.

ORIENTED CORE LOGGING

Where the core can be successfully oriented, valuable information can be obtained on the spacial relationships of the natural discontinuities in the rock. Because of the complexity of reducing the resulting orientation for the orientation of the drill hole, it is recommended that the oriented data is recorded in a format suitable for direct key-punching. This will permit data reduction and subsequent analysis usually by stereographic projection.

A Structural Mapping Coding Form (Figure 11) permits recording of details regarding the orientation and nature of the discontinuities. The data are recorded as follows:

- 1) Job Number
This is unique to the project.

- 2) Data Unit
Up to 7 characters to detail, for example, borehole number **DD77803**.
- 3) Location
Recorded to the nearest 0.1 ft. in columns 1 to 4. All other columns are filled with details of parameters described in Part 2 of this manual.

GEOLOGICAL ENGINEERING LOGGING

This logging technique is often performed **immediately** the core is recovered and, consequently, usually requires full-time rig supervision. It can be carried out with oriented core logging.

Most of the logging form (Figure 12) is self-explanatory, the details of parameters recorded being included as Part 2 of this manual. Other information is detailed below.

- 1) Type of Drilling
usually "Rotary Core" followed by the qualifying drilling medium "**Mudflush**" or "Waterflush".
- 2) Reference Elevation
Definition of the datum from which down-hole depths are measured, e.g. drill floor.
- 3) Drilling Progress
A line to indicate the end of run footage, with the down-hole depth recorded above the line. Data and shift (AM or PM) should also be recorded below the footage line at shift changes.
- 4) Rate of Advance
~~Time~~ per unit length of hole drilled. Filled in as a histogram, and shaded to highlight runs of slow drilling.
- 5) R.Q.D. and Core Recovery
Plotted graphically for better definition of possible weak zones. These are calculated for the core run interval shown.
- 6) Depth
The short lines usually represent 1/2 ft. increments; each 5 ft. line should be labelled. Down-hole depths at major rock type contacts should be included as accurately as possible and a line drawn across the rest of the log.
- 7) Reduced Level
After the **hole** has been surveyed this column can be completed with details of elevations, rather than down-hole depths, for major contacts.
- 8) Water Level
A line is drawn to indicate shift change hole depth and a record made of the fluid level-in the hole, measured from the reference elevation.

- 9) Test Results
Details of sample location, sample type, Atterberg test results, penetration tests, etc. are included in this column.
- 10) Bed/Fol
Representative inclinations of bedding or foliation with respect to the core axis are recorded.
- 11) Instrumentation and Legend
Both columns are for graphic representation of data. The former **is** used to represent in-hole installations, for example **piezometers**, with details of grout, fill, cave, etc. The latter is a geological legend, and should comply with a standard, either local to the project or following A.G.I. **recommendations**.
- 12) Description
The escription follows the procedure outlined in Part 2, Section'1 with major **rock unit** descriptions running across the **whole** column, and minor details, with **foot-**ages, being indented 1cm from the left.
- 13) Remarks
This space is used for indications of casing depths, hole surveys, zones of caving, etc.

Type of Drilling		Coordinates		DRILLHOLE No.								
ROTARY CORE MUD FLUSH		77,441.8		77-852								
		15,793.8		Sheet 11 of 15								
Rig		Dip		Location								
LONGYEAR 44 WIRELINE		30°		SLIDE AREA								
Bit		Azimuth		Reference elevation								
MS DIAMOND				DBLL FLOOR								
Drilling Progress	Rate of Advance Min./m	R O D	Core Recovery %	Depth m	Reduced Level	Water Level	Test Results	Bed/Fol	Fracture Index	Stratigraphic Unit	Legend	Description
	10 20 30 40 50	0 50 100	0 50 100	180								CONGLOMERATE cont'd.
	10	70	100	181					0			180.59-181.37 v. weak, poorly cemented congl. w. a silty matrix
	10	70	100	182					0			181.37-181.71 weak, med. to c. tuff. sandstone.
22/1 PM	10	72	100	183					0			182.18-183.00 mod. str., well cemented congl. w. a siliceous matrix, sl. calcareous. 183.13-183.18 Sample #37, n.c. 183.00-183.20 med. to c. tuff. sandstone. 183.20-184.60 sl. weath., mass., dk. green, mod. str. sandy siltstone. 183.38-183.52 fine to med. congl. siliceous matrix.
	10	100	100	184					0			184.60-185.83 well graded, str. congl. well cemented; siliceous matrix.
	10	100	100	185					0			185.83-187.57 mod. str., generally well cemented congl. w. a sandy siltstone to green sandstone matrix, also some siliceous matrix.
	10	97	100	186					0			187.57-189.28 str. c. congl. w. a siliceous matrix, some breaks along large clast boundaries.
	10	76	100	187					0			188.84-189.03 calcareous matrix. 189.28-190.80 mod. weak to mod. str. congl. w. a sandstone matrix, some weakly cemented zones.
	10	73	92	188								
				189								
				190								
Contractor JOKO				Logged by JG/NR				Remarks				
Date started 18 JAN 78				Checked by MM								
Date finished 23 JAN 78				Date 22 JAN 78								
Golder Associates										Scale: 1:50		metric

Figure 12: Geological engineering logging format.

PART 5 - GEOTECHNICAL SAMPLING

Most field programs undertaken for the collection of geological data also provide an ideal opportunity to assemble geotechnical data required for slope design projects or other engineering problems. Various mechanical indices can be derived and samples can be taken for laboratory testing at a later date. This part of the manual briefly describes techniques that can be used to collect samples for laboratory testing.

GEOTECHNICAL SAMPLING

Some, but by no means all, of the samples used for strength testing are obtained from **borehole** core. The special drilling techniques required to recover these samples are discussed in Part 8 but no mention is made of the preservation of the core for testing.

The information recorded on the geotechnical log becomes very useful when the classification can be "calibrated" with laboratory-determined strength parameters. Thus, enough core samples suitable for testing should be preserved, representative of each rock type, alteration state and rock quality class. If these are carefully described (photographed if possible), preserved and stored, there is no **immediate** requirement to do the testing.

In addition to the categories above, samples should also be taken of core sections separated by gouge zones.

The sample length should be at least **2-1/2** times the core diameter.

When clean joints in hard rock specimens have been collected for shear testing, it is probably satisfactory to transport these to the laboratory or testing station in a normal core box. If it is considered that excessive movement may damage the surfaces, the two pieces of core can be taped or wired together.

For the weaker materials, and the sections of harder core with gouge zones, it is useful to retain the sample's natural moisture content. For this reason careful preservation of the sample must be ensured. At each stage of the wrapping procedure the sample should be **labelled** with:

Sample number, including drill hole identification;
Depth interval, and Down-hole direction.

In addition an index card, preferably in duplicate or triplicate, should be filled in with all of the above information plus a geological description.

The selected samples should be wrapped in two layers of Saran wrap (or similar), and two layers of aluminum foil. They may be waxed should particular conditions indicate that the sample will further dry out. The lengths of wrapped core can then be placed in a core box, with suitably placed spacers, for transportation.

The samples in the core box can be protected from desiccation and damage in transit by pouring a suitable quantity of mixed,

two-part expanded polyurethane foam to completely enclose each individual sample in the box. This method preserves both the sample's condition and moisture content for later testing in the laboratory.

Index cards should be tied to each sample in the foamed core box, and copies kept on site and sent to the laboratory. In this way the sample does not have to be exposed in order to identify its various characteristics.

Samples for shear testing are also collected by methods other than core drilling. The most obvious of such methods is to use a geologist's **hammer** to chip the required sample out of the rock mass. This will sometimes work but a great deal of time and energy can be expended in attempts to collect an "undisturbed" sample.

In soft materials such as coal measure rocks, the National Coal Board in England has successfully used a chain saw fitted with a tungsten-carbide tipped chain to remove samples for shear testing.

PART 6 • PHOTOGRAPHIC TECHNIQUES

Color photographs are an invaluable aid to the interpretation of geological and geotechnical data. A clear scale should always be included in the picture since one project may require photography of the geology in varying detail, e.g. pit faces and core, or underground drifts and stopes.

It is preferable to use a diapositive transparency film for 35 mm color slides. The use of electronic flash or photoflood units permits the photography to be independent of external light conditions.

The color slides should be indexed and filed in suitable trays or boxes. When required, they can be projected on a screen or alternatively examined with a hand lens on a light table. For scale measurements the photos can be projected onto the rear of a ground-glass sheet, e.g. through a light table, and the size adjusted to natural scale, see Figure 6.1.

EXPOSURE PHOTOGRAPHY

Slopes

Geological interpretation from slope photography may be carried out in varying detail depending on the complexities of the project.

Aerial photography is often used at the beginning of a project in an attempt to delineate large-scale structures, such as folds, major faults and major rock contacts.

Photography can be used by the engineer to show rock contacts and some joint set orientations. In addition, areas of potential stability problems can often be isolated from a detailed study of such photographs.

Photographs should be taken as a routine compliment to face mapping. It is often useful to carry a wide-angle lens for use when berm widths restrict the amount of space available. The section of face to be photographed should be marked with spray paint to delineate, for example, windows or fracture sets mapped, and should also show some reference information to assist in filing the photograph. A suitable scale may also be worked directly into the rock. Close-ups of critical details may also be warranted using geological hammers, pocket knives or coins for scale depending on the detail in the photograph.

Tunnels

A different set of conditions are encountered when photographing exposures underground. Often the tunnel walls are covered in dust or mud and, prior to mapping or photography, an attempt must be made to clean off the rock. For drifts and ddits less than about 15 ft. wide, a short focal length lens should be used, e.g. 28 mm. In this case it should be borne in mind that most standard flash units will not illuminate as wide an angle as the lens will cover and suitable adaptations, like photofloods, may be needed. The wall should be marked to show the area mapped, its location and sometimes each discontinuity plane mapped.

The most successful technique for underground photography is to mount the camera on a tripod and then use the flash a number of times to evenly illuminate the face from different positions. Experience will give indications as to the correct exposure settings.

CORE PHOTOGRAPHY

Color photographs of drill core provide a permanent record of the core condition upon recovery, and hence can be an invaluable aid to the interpretation of ground conditions. The photographs show detail which cannot be easily recorded on drill logs and they can be filed for ready reference by both geologists and engineers.

Even with a good camera, where possible core should not be split until the film has been developed and satisfactory photographs obtained.

All core photos should include ample, clear identification of hole number, footage, and the core direction (way up). In addition, it is essential that core be photographed dry.

A **28 mm**, wide-angle lens has proved to be most convenient when photographing core. A suitable frame can be constructed of dimensions to suit the size of the core boxes and the width to height ratio of the **35 mm** transparency. A title block should be included to indicate project number and name, drill hole number and footage interval. A meter scale should also be shown.

Subdued daylight provides the best lighting for core photography and direct sunlight should not be used. Flash or **photo-floods** may be needed in adverse natural lighting conditions in which case different film requirements must be observed with regard to flash or floodlamp type. Regardless of the lighting system used, consistency is of the utmost importance for interpretation of the core slides, as similar colors will be recorded differently in varying lighting conditions.

PHOTOGRAMMETRY

Although not yet in wide use, photogrammetric methods offer considerable advantages in the interpretation of photographs of exposed surfaces.

Various different methods can be used to produce a stereoscopic model from which coordinates may be measured to an accuracy of about 1 in 5,000. The field set-up requires that the rock face has targets painted on it for photogrammetric measurement.

For simpler stereoscopic viewing of slope or underground exposures there is a stereo attachment for a **Pentax** camera which splits the **field** of view and produces a negative with a double **image**.

PART 7 - CORE ORIENTATION AND HOLE SURVEYING

A variety of **borehole** techniques and drilling equipment may be used to gain further data useful in the engineering assessment of a particular site. They include methods of recovering the maximum amount of intact core, methods of absolute orientation of that core, and down-hole logging techniques as described below:

- 1) Triple tube core barrel
- 2) Craelius core orientation
- 3) Christensen-Hugel orientation
- 4) Sperry Sun Single Shot camera
- 5) **Borehole** periscope and camera
- 6) Down-hole geophysics

Manufacturers should be referred to for greater details.

STRUCTURAL DRILLING

The requirements for structural drilling are somewhat more stringent than those for normal exploratory drilling. The aim is not only to recover a sample of the rock material but to recover a sample of the rock mass complete with **discontinuities**. This means that each piece of core must be recovered in its correct order.

It is essential for detailed logging to lay out the core in a V-shaped guide rail. The core can be fitted together and depths marked at regular intervals. The time taken to do this will be amply repaid by speed of mapping.

Positive incentives for skill and motivation of the drillers are required and for this reason footage bonuses must be avoided.

The absolute cost of this type of drilling will be somewhat higher than that of exploration drilling. However, the cost must be viewed in the light of the additional information obtained.

TRIPLE TUBE CORE BARREL

On all engineering/geotechnical drilling programs, maximum intact recovery of core is essential. It is often the soft or broken zones which will play a major role in stability problems, and it is these zones that are most difficult to recover. The **Longyear** Q-3 series triple tube **wireline** core barrel has been found, after extensive field proving, to be the most effective and reliable coring method.

Regular **Q** series **wireline** barrels can easily be converted to triple tube core barrels and all necessary parts can be ordered in either 5 or 10 ft. sizes. Instead of a simple double tube set-up, in which the core is usually hammered from the core tube, a third tube is added, split lengthwise and nested in the inner tube. Its inside surface is plated with hard, low-friction chrome for smooth core entry. Coring with the triple tube barrel proceeds in the usual manner and the core laden inner tube assembly is retrieved through the drill string. The core lifter and spring case is removed and the split tube is **hydrau-**

lically pumped from the inner tube. One-half of the split tube is carefully **lifted** off and the core can be inspected in a virtually undisturbed **condition** prior to transfer to the core box.

The combination of a step-type lifter case and face discharge diamond coring bit helps **eliminate** core erosion particularly when **drilling** in soft **conditions**. A special brass piston with an O-ring seal is used to extrude the split tube, incorporating a pump-out group designed to utilize the rig's grout pump.

The split tubes are manufactured in paired sets and matched **numbers** should always be used together. The walls of the tubes are fairly thin and, as they can easily be damaged through negligence, spare sets of splits should always be available and securely stored. Damaged splits are useful for carrying core which can then be transferred from split tube to core box with little or no disturbance.

CORE ORIENTATION

The dip and dip **direction** of discontinuities are most important in slope **stability** evaluations. Consequently, however successful a **drilling** program has been in terms of core recovery, the most valuable information of all will have been lost if no effort has been made to orient the core.

Relative Orientation

One approach to **this** problem is to use inclined boreholes to check or to deduce the **orientation** of structural features. For example, if surface mapping suggests a strong concentration of planes dipping at 30° in a dip direction of 130° , a hole drilled in the direction of the normal to these planes, i.e. **dipping** at 60° in a dip direction of 310° , will intersect these planes at right angles and the accuracy of the surface mapping prediction can be checked. This approach is useful for **checking** the dip and **dip** direction of critical planes.

Alternatively, if two or more non-parallel boreholes have been drilled in a rock mass in which there are recognizable marker horizons, the orientation and inclination of these horizons can be deduced **using** graphical techniques.

Absolute Orientation

A second approach is to attempt to orient the core itself and, while the techniques available abound with practical difficulties **which** are the despair of many drillers, these methods do provide some of the best results currently obtainable. In fact, the greatest possible service **which** could be rendered to the rock engineer by the manufacturers of drilling equipment would be the production of simple core orientation systems.

Craelius Core Orientator

One of the best core orientation devices is the Craelius Core Orientator manufactured by Atlas Copco. It consists of a metal holder, of the same diameter as the core, which **contains** six movable pins. It is clamped in the front of the core barrel and lowered into the hole. Its orientation is fixed by the

orientation of the rigid core-barrel or by a simple marker within the device. When the six pins come into contact with the end of the hole, where the core will usually have broken off or parted on an inclined surface, these pins take up the profile of the core stub. The pins are locked in place and the device released to move up the core-barrel as drilling proceeds. When the core is removed, the core orientation tool is matched to the upper end of the core and the first piece of core is oriented with respect to the known orientation of the device at the time of the fixing of the pins. Provided that good core recovery has been achieved, it should then be possible to reconstruct the core **which** is then oriented with respect to the first piece.

A technique currently being tested as a means of eliminating shortened drilling runs and drilling difficulties is to lower the craelius on the **wireline** overshot, take the impression of the core stub on the pins, and then remove the craelius **prior to drilling** the run. In this way a **quick** check can be made to ensure the device has operated correctly and the drilled run can then be of the standard **5** or **10** ft. This is most useful for taking further orientations since the drill rods may be broken at the same place each run without pulling the diamond bit back from the end of the hole too far.

For a detailed **review** of both the overall planning of an oriented coring program and step-by-step procedures for inspecting, maintaining, adjusting and using the craelius core orientator the reader is referred to the Craelius Manual.

Christensen-Hugel Orientation

An alternative method is used with the Christensen-Hugel core barrel. Three tungsten **carbide** points scribe the core continuously while coring. The reference marks are then oriented absolutely by a magnetic, or gyroscopic survey instrument mounted in the core barrel. This technique is most successful **when** the ground being drilled is hard and non-magnetic.

The Christensen-Hugel manual should be referred to for details of this orientation method.

HOLE SURVEYING

An integral part of any oriented core logging program is hole surveying. It is essential that the plunge and trend of the hole are known at enough intervals to interpolate the exact deviation of any depth. Golder Associates has developed a computer program which will handle this deviation interpolation. The most **commonly** used survey tools are the single- or **multi-shot** camera magnetic surveying instruments, (Eastman and Sperry Sun are most **commonly** used) the **Tro-Pari** Surveying instrument, and the acid test.

Sperry Sun Single Shot

As an example of the photographic methods available a description of the Sperry Sun single shot is given. This system can conveniently be used for hole surveying when the Craelius core orientator is being used for core orientation.

The single shot is a magnetic survey instrument which is used to obtain records, on film, of the inclination and direction of inclination (or plunge and trend) at various depths in a **borehole**. The presence of steel will obviously affect the compass, and non-magnetic rods are used to hold the instrument below all casing and drill rods. The inclination unit is a form of inverted plum bob which is combined with the magnetic compass into a single unit available for a number of angles of plunge. The **borehole** orientation indicated by the compass-angle unit is recorded on a film disc when a preset timer illuminates 2 small lamps in the body of the instrument. Special loading and developing tanks permit handling of the photographic discs without the necessity of a darkroom.

It has been found from extensive field experimentation that hole surveys should be taken every 100 to 300 ft. and more frequently ~~when~~ the deviation exceeds 1° in 100 ft. The delay caused in taking the survey, usually about 30 minutes per shot, is easily compensated by the additional information available from a well surveyed hole.

The single shot camera must be retrieved and reloaded after every shot. This feature is the only major difference compared to the multi-shot camera which is preloaded with four film discs, preset at different time intervals to allow hole **surveys** at several depths without removal of the instrument.

Tro-Pari Surveying Instrument

The Tro-Pari **Borehole** Surveying Instrument comprises a unit mounted in gimbals and is provided with a clockwork mechanism to clamp a compass to indicate trend and simultaneously to clamp the unit in its plumb position to indicate plunge.

By means of a timing ring suitably calibrated in five-minute divisions, the unit may set to lock after a lapse of time sufficient to allow the placing of the instrument at the desired point in the drill hole where readings are to be taken. The maximum time lapse obtainable with the instrument designed for use in E or A size holes is 1 hour 30 minutes which is considered to be ample time to lower to the greatest depths that may be drilled with this size of equipment. A larger adaptor has been developed for larger diameter holes such as B and N sizes and a correspondingly greater time lapse provided for.

Acid Test

This method is the most basic of all surveying techniques and will give a measure of hole inclination only. It is taken as a standard practice in most drilling companies and all drillers are familiar with the test.

Surveying drill holes for inclination is based on the **solubility** of glass in hydrofluoric acid. A glass vial or bottle is partially filled with a 4 percent solution of dilute **hydrofluoric acid** and lowered to the desired position in the hole in a special case, called a clinometer. The clinometer must have joints that are water-tight under heavy pressure, otherwise the glass tube will be crushed.

By leaving the clinometer in position for the proper length of time a line is etched along the surface contact of the acid and inside wall of the tube. The angle of this etched line with the long axis of the tube, read with a protractor, gives the inclination of the drill hole at the depth tested. The angle, as read, must be corrected for error due to capillary attraction within the tube.

Several tests may be made at the same time by inserting clinometers at the desired intervals in the string of drill rods. Tests are ordinarily made at intervals of 30 m to 100 m, depending on depth of hole.

As soon as the clinometer is removed from the hole, the bottle is emptied and washed. A tag showing job number, hole number, depth of test and date should be inserted in the bottle for later reference.

OTHER BOREHOLE METHODS

The following types are available but due to a number of factors, are at best only reliable when used as an adjunct to core logging for geological data collection purposes.

Borehole Periscope

This is an optical device which transmits an annular image of the borehole wall through a series of lenses and prisms to the surface. It is located in a series of connected rigid pipes. This instrument is limited to a depth of 30 m but has the advantage that no electronics are involved and orientation is directly measured from a reference line on the rigid pipes.

Borehole Cameras

Both the television and colour multiple shot types are available. Our experience is that these instruments are generally unreliable and difficult to maintain. The capital cost is currently in excess of \$50,000 and a further disadvantage lies in the difficulty of obtaining absolute orientation (by either magnetic or gyroscopic methods). However, it must be admitted that, in the hands of specialist operators, these instruments can provide very valuable information. It seems more than likely that, with developments in the field of electronics, better and more reliable instruments of this type will become available in the years to come.

Impression Packer

The impression packer is an inflatable rubber tube, the outside of which is coated with a soft, wax-like film. The tube is lowered down the hole on the wireline and inflated against the side of the hole so that fracture lines in the rock are impressed on the wax film. The tube is deflated and pulled from the hole and the orientation of the instrument is determined from a compass set in its base. The dip and strike of fractures can be determined from the inclination of line in the film. This is a simple and relatively inexpensive means of orienting fractures in drill holes.

Geophysical Methods

These methods were largely developed for the oil industry but have varied applications within other fields of mining. They are found to be most useful **when** "calibrated" by comparing the geophysical signature with the drill core and logs from some holes. Geophysical surveying is usually handled by the client directly and sub-contracted to a logging outfit.

The methods currently used Include:

- Gamma** Ray neutron logging
- Density logging
- Resistivity and Self-Potential logging
- Seismic logging

The civil engineering profession has a great deal to learn from the oil industry in this area of **borehole** interpretation, and other well logging devices such as the Televiwer are bound to find greater applications in site investigation in the future.

Appendix 7

APPENDIX 7

Computer program for slope stability analysis

a) General two-dimensional analysis (BASIC)

PREFACE

SARMA NON-VERTICAL SLICE STABILITY ANALYSIS

Copyright - Evert Hoek, 1985. This program is one of a series of geotechnical programs developed as working tools and for educational purposes. Use of the program is not restricted but the user is responsible for the application of the results obtained from this program.

GENERAL TWO-DIMENSIONAL SLOPE STABILITY ANALYSIS

By Evert Hoek
 Colder Associates, Vancouver, Canada

INTRODUCTION

The following analysis, originally published by Sarma (1979) and modified by this author, is a general method of limit equilibrium analysis which can be used to determine the stability of slopes of a variety of shapes. Slopes with complex profiles with circular, non-circular or planar sliding surfaces or any combination of these can be analysed using this method. In addition, active-passive wedge failures such as those which occur in spoil piles on sloping foundations or in clay core dam embankments can also be analysed. The analysis allows different shear strengths to be specified for each slice side and base. The freedom to change the inclination of the slice sides also allows the incorporation of specific structural features such as faults or bedding planes. External forces can be included for each slice and submergence of any part of the slope is automatically incorporated into the analysis.

The geometry of the sliding mass is defined by the coordinates $XT_i, YT_i, XB_i, YB_i, XT_{i+1}, YT_{i+1}$ and XB_{i+1}, YB_{i+1} of the corners of a number of three- or four-sided elements as shown in figure 1. The phreatic surface is defined by the coordinates XW_i, YW_i and XW_{i+1}, YW_{i+1} of its intersection with the slice sides. A closed form solution is used to calculate the critical horizontal acceleration K_c required to induce a state of limiting equilibrium in the sliding mass. The static factor of safety F is then found by reducing the shear strength values $\tan \phi$ and c to $\tan \phi/F$ and c/F until the critical acceleration K_c is reduced to zero.

In order to determine whether the analysis is acceptable, a check is carried out to determine whether all the effective normal stresses acting across the bases and sides of the slices are positive. If negative stresses are found, the slice geometry or the groundwater conditions must be changed until the stresses are all positive. An additional check for moment equilibrium is described but it has not been incorporated into the program listed at the end of the paper because it involves a significant increase in computational effort and because it is seldom required for normal slope stability problems.

GEOMETRICAL CALCULATIONS

The geometry of the i th slice is defined in figure 1. Note that the value of the x coordinate should always increase from the toe of the slope. Assuming that ZW_i, δ_i and d_i are available from the previous slice:

$$d_{i+1} = \{ (XT_{i+1} - XB_{i+1})^2 + (YT_{i+1} - YB_{i+1})^2 \}^{1/2} \quad (1)$$

$$\delta_{i+1} = \text{Arcsin} \{ (XT_{i+1} - XB_{i+1}) / d_{i+1} \} \quad (2)$$

$$b_i = XB_{i+1} - XB_i \quad (3)$$

$$\alpha_i = \text{Arctan} \{ (YB_{i+1} - YB_i) / b_i \} \quad (4)$$

$$W_i = \frac{1}{2}\gamma_r \left\{ (YB_i - YT_{i+1})(XT_i - XB_{i+1}) + (YT_i - YB_{i+1})(XT_{i+1} - XB_i) \right\} \quad (5)$$

$$ZW_{i+1} = (YW_{i+1} - YB_{i+1}) \quad (6)$$

where γ_r is the unit weight of the material forming the slice and W_i is the weight of the slice.

CALCULATION OF WATER FORCES

In order to cover all possible groundwater conditions, including submergence of any part of the slope, the four cases defined in figure 2 have to be considered. In all cases, the uplift U_i acting on the base of the slice is given by:

$$U_i = \frac{1}{2}\gamma_w \left\{ (YW_i - YB_i + YW_{i+1} - YB_{i+1}) \cdot b_i / \cos \alpha_i \right\} \quad (7)$$

where γ_w is the unit weight of water.

Case 1 - no submergence of slice

$$YT_i > YW_i \text{ and } YT_{i+1} > YW_{i+1}$$

$$P_{w_i} = \frac{1}{2}\gamma_w \left\{ (YW_i - YB_i)^2 / \cos \delta_{i+1} \right\} \quad (8)$$

$$P_{w_{i+1}} = \frac{1}{2}\gamma_w \left\{ (YW_{i+1} - YB_{i+1})^2 / \cos \delta_{i+1} \right\} \quad (9)$$

Case 2 - submergence of side i only

$$YT_i < YW_i \text{ and } YT_{i+1} > YW_{i+1}$$

$$P_{w_i} = \frac{1}{2}\gamma_w \left\{ (2YW_i - YT_i - YB_i)(YT_i - YB_i) / \cos \delta_i \right\} \quad (10)$$

$$P_{w_{i+1}} = \frac{1}{2}\gamma_w \left\{ (YW_{i+1} - YB_{i+1})^2 / \cos \delta_{i+1} \right\} \quad (11)$$

$$WW_i = \frac{1}{2}\gamma_w \left\{ (YW_i - YT_i)^2 (XT_{i+1} - XT_i) / (YT_{i+1} - YT_i) \right\} \quad (12)$$

$$WH_i = \frac{1}{2}\gamma_w (YW_i - YT_i)^2 \quad (13)$$

where WW_i and WH_i are the vertical and horizontal forces applied to the surface of the slice as a result of the submergence of part of the slice. Note that the horizontal force WH_i acts in a positive direction when $YT_{i+1} > YT_i$ and in a negative direction when $YT_{i+1} < YT_i$.

Case 3 - submergence of side i+1 only

$$YT_i > YW_i \text{ and } YT_{i+1} < YW_{i+1}$$

$$P_{w_i} = \frac{1}{2}\gamma_w \left\{ (YW_i - YB_i)^2 / \cos \delta_i \right\} \quad (14)$$

$$P_{w_{i+1}} = \frac{1}{2}\gamma_w \left\{ (2YW_{i+1} - YT_{i+1} - YB_{i+1})(YT_{i+1} - YB_{i+1}) / \cos \delta_{i+1} \right\} \quad (15)$$

$$WW_i = \frac{1}{2}\gamma_w \left\{ (YW_{i+1} - YT_{i+1})^2 (XT_{i+1} - XT_i) / (YT_{i+1} - YT_i) \right\} \quad (16)$$

$$WH_i = \frac{1}{2}\gamma_w (YW_{i+1} - YT_{i+1})^2 \quad (17)$$

Case 4 - complete submergence of slice i

$$XT_i < XW_i \text{ and } XT_{i+1} < XW_{i+1}$$

$$PW_i = \frac{1}{2} \gamma_w \left| (2YW_i - YT_i - YB_i)(YT_i - YB_i) / \cos \delta_i \right| \quad (18)$$

$$PW_{i+1} = \frac{1}{2} \gamma_w \left| (2YW_{i+1} - YT_{i+1} - YB_{i+1})(YT_{i+1} - YB_{i+1}) / \cos \delta_{i+1} \right| \quad (19)$$

$$WW_i = \frac{1}{2} \gamma_w \left| (YW_i - YT_i + YW_{i+1} - YT_{i+1})(XT_{i+1} - XT_i) \right| \quad (20)$$

$$WH_i = \frac{1}{2} \gamma_w \left| (YW_i - YT_i + YW_{i+1} - YT_{i+1})(YT_{i+1} - YT_i) \right| \quad (21)$$

WATER FORCES ON THE FIRST AND LAST SLICE SIDES

Although the water force PW_i acting on the first slice side and the force PW_{n+1} acting on the $n+1$ th slice side (which could be a tension crack) are calculated by means of the equations listed above, these forces are not normally used in the calculation of critical acceleration. These forces can be important when the slope toe is submerged or when a tension crack is filled with water and the simplest way to incorporate these forces into the analysis is to treat them as external forces. Hence, the vertical and horizontal components of these forces are given by:

$$TV_i = PW_i \cdot \sin \delta_i \quad (22)$$

$$TH_i = PW_i \cdot \cos \delta_i \quad (23)$$

$$TV_n = PW_{n+1} \cdot \sin \delta_{n+1} \quad (24)$$

$$TH_n = PW_{n+1} \cdot \cos \delta_{n+1} \quad (25)$$

where n is the total number of slices included in the analysis.

CALCULATION OF CRITICAL ACCELERATION K_c

The critical acceleration K_c required to bring the slope to a condition of limiting equilibrium is given by

$$K_c = AE/PE \quad (26)$$

where

$$AE = a_m + a_{n-1} \cdot e_n + a_{n-2} \cdot e_n \cdot e_{n-1} + \dots + a_1 \cdot e_n \cdot e_{n-1} \dots e_3 \cdot e_2 \quad (27)$$

$$PE = p_n + p_{n-1} \cdot e_n + p_{n-2} \cdot e_n \cdot e_{n-1} + \dots + p_1 \cdot e_n \cdot e_{n-1} \dots e_3 \cdot e_2 \quad (28)$$

$$a_i = Q_i \{ (W_i + TV_i) \cdot \sin(\phi_{s_i} - \alpha_i) - TH_i \cdot \cos(\phi_{s_i} - \alpha_i) + R_i \cdot \cos \phi_{s_i} + S_{i+1} \cdot \sin(\phi_{s_i} - \alpha_i - \delta_{i+1}) - S_i \cdot \sin(\phi_{s_i} - \alpha_i - \delta_i) \} \quad (29)$$

$$p_i = Q_i \cdot W_i \cdot \cos(\phi_{s_i} - \alpha_i) \quad (30)$$

$$e_i = Q_i (\cos(\phi_{s_i} - \alpha_i + \phi_{s_i} - \delta_i) / \cos \phi_{s_i}) \quad (31)$$

$$Q_i = \cos \phi_{s_{i+1}} / \cos(\phi_{s_i} - \alpha_i + \phi_{s_{i+1}} - \delta_{i+1}) \quad (32)$$

$$S_i = c_{s_i} \cdot d_i - P W_i \cdot \tan \phi_{s_i} \quad (33)$$

$$S_{i+1} = c_{s_{i+1}} \cdot d_{i+1} - P W_{i+1} \cdot \tan \phi_{s_{i+1}} \quad (34)$$

$$R_i = a_i \cdot b_i / \cos \alpha_i - U_i \cdot \tan \phi_{s_i} \quad (35)$$

CALCULATION OF FACTOR OF SAFETY

For slopes when the critical acceleration K_c is not equal to zero, the static factor of safety is calculated by reducing the shear strength simultaneously on all sliding surfaces until the acceleration K_c , calculated by means of equation 26, reduces to zero. This is achieved by substitution, in equations 29 to 35, of the following shear strength values

$$c_{s_i}/F, \tan \phi_{s_i}/F, a_i/F, \tan \phi_{s_i}/F, c_{s_{i+1}}/F \text{ and } \tan \phi_{s_{i+1}}/F$$

CHECK ON ACCEPTABILITY OF SOLUTION

Having determined the value of K for a given factor of safety, the forces acting on the sides and base of each slice are found by progressive solution of the following equations, starting from the known condition that $E_1 = 0$.

$$E_{i+1} = a_i - p_i \cdot K + E_i \cdot e_i \quad (36)$$

$$X_i = (E_i - P W_i) \tan \phi_{s_i} + c_{s_i} \cdot d_i \quad (37)$$

$$N_i = \begin{aligned} & \frac{1}{\cos \alpha_i} \cdot [T V_i + X_{i+1} \cdot \cos \delta_{i+1} + X_i \cdot \cos \delta_i \\ & - E_{i+1} \cdot \sin \delta_{i+1} + E_i \cdot \sin \delta_i + U_i \cdot \tan \phi_{s_i} \cdot \sin \alpha_i \\ & - c_{s_i} \cdot b_i \cdot \tan \alpha_i] \cos \phi_{s_i} / \cos(\phi_{s_i} - \alpha_i) \end{aligned} \quad (38)$$

$$T S_i = (N_i - U_i) \tan \phi_{s_i} + c_{s_i} \cdot b_i / \cos \alpha_i \quad (39)$$

The effective normal stresses acting across the base and the sides of a slice are calculated as follows :

$$\sigma_{s_i}' = (N_i - U_i) \cdot \cos \alpha_i / b_i \quad (40)$$

$$\sigma_{s_i}'' = (E_i - P W_i) / d_i \quad (41)$$

$$\sigma_{s_{i+1}}' = (E_{i+1} - P W_{i+1}) / d_{i+1} \quad (42)$$

In order for the solution to be acceptable, all effective normal stresses must be positive.

A final check on to determine whether the equilibrium conditions are satisfied for each slice is recommended by Sarma. Referring to figure 1 and taking moments about the lower left hand corner of the slice :

$$\begin{aligned}
& N_i Z_i - X_{i+1} \cdot b_i \cdot \cos(\alpha_i + \delta_{i+1}) / \cos \alpha_i - E_i Z_i + \\
& E_{i+1} (Z_{i+1} + b_i \cdot \sin(\alpha_i + \delta_{i+1}) / \cos \alpha_i) - \\
& W_i (XG_i - X_{a_i}) + KcW_i (YG_i - Y_{a_i}) - TV_i (X_i - XG_i) + \\
& TH_i (Y_i - YG_i) = 0
\end{aligned} \tag{43}$$

where XG_i, YG_i are the coordinates of the centre of gravity of the slice and X_i, Y_i are the coordinates of the point of action of the force T_i .

Starting from the first slice at the toe of the slope, where $Z_i = 0$, assuming a value of Z_i , the moment arm Z_{i+1} can be calculated or vice versa. The values of Z_i and Z_{i+1} should lie within the slice boundary, preferably in the middle third.

COMPUTER SOLUTION FOR SARMA ANALYSIS

A listing of a computer program for the analysis presented above is given in appendix 1 at the end of this paper. This program has been written in the simplest form of BASIC and great care has been taken to ensure that there are no machine-dependent commands in the program. Hence, it should be possible to key this program into any computer which runs Microsoft or equivalent BASIC and to modify it for any other form of BASIC. The program has also been carefully prepared so that it can be compiled into machine language using a BASIC compiler. The compiled program will run about six times faster than the program listed in appendix 1.

A graphics option is built into the program which allows the user to view the geometry of the slope being analysed. This option assumes that BASICA or an equivalent form of BASIC which supports graphics is available and that the computer has IBM compatible graphics capability. If these facilities are not available the graphics option can be disabled as described in appendix 1.

A critical component of the program is the factor of safety iteration in which the shear strength values are progressively reduced (or increased) until the static factor of safety (for $K = 0$) is found. Experience has shown that this iteration can be a very troublesome process and that severe numerical instability can occur if inappropriate values of F are used. The iteration technique used in the listed program is described below.

Figure 3 gives a plot of factor of safety F versus acceleration K for a range of friction angles for a typical slope analysis. This plot reveals that the curve of F vs K closely resembles a rectangular hyperbola and this suggests that a plot of $1/F$ vs K should be a straight line. As shown in figure 4, this is an acceptable assumption within the range of interest, ie from $K = K_c$ to $K = 0$ although, for significantly larger or significantly smaller values of K , the curve is no longer linear. This observation has been found to be true for a wide range of analyses.

Sarma and Bhawe (1974) plotted the values of the critical acceleration K_c against the static factor of safety F for a large number of stability analyses and found an approximately linear relationship defined by

$$F = 1 + 3.33 K_c \tag{44}$$

While this relationship does not provide sufficient accuracy for the very wide range of problems encountered when applying this analysis to rock

mechanics problems, it does give a useful point close to the $K = 0$ axis on the plot of $1/F$ vs K as shown in figure 4. A linear interpolation or extrapolation, using this point and the value of K_c (at $F = 1$), gives an accurate estimate of the static factor of safety. This technique has proved to be very fast and efficient and has been incorporated into the program. For critical cases, in which it is considered essential to plot the complete F vs K curve, an optional subroutine has been provided in the program to enable the user to produce such a plot.

PROBLEMS WITH NEGATIVE STRESSES

The effective normal stresses across the sides and base of each slice are calculated by means of equations 40 to 42 and, in order for the solution to be acceptable, these stresses must all be positive. The reasons for the occurrence of negative stresses and some suggested remedies are discussed below.

Negative stresses occur near the top of a slope when the lower portion of the slope is less stable and hence tends to slide away from the upper portion of the slope. This is the condition which leads to the formation of tension cracks in actual slopes and the negative stresses in the numerical solution can generally be eliminated by placing a tension crack at an appropriate position in the slope.

Negative stresses at the toe of a slope are sometimes caused by an excessively strong toe. This can occur when the upward curvature of a deep-seated failure becomes too severe in the toe region. Flattening the curvature or reducing the shear strength along the base will generally solve this problem.

Excessive water pressures within the slope can give rise to negative stresses, particularly near the top of the slope where the normal stresses are low. Reducing the level of the phreatic surface in the region in which negative stresses occur will usually eliminate these negative stresses.

Inappropriate selection of the slice geometry, particularly the inclination of the slice sides, can give rise to negative stress problems. This is an important consideration in rock mechanics when preexisting failure surfaces such as joints and faults are included in the analysis. If a potential failure path with a lower shear strength than that of the pre-existing surface exists in the sliding mass, negative stresses can occur along the pre-existing surface which has been chosen as a slice side. Sarma (1979) has shown that the best critical slice side inclinations are approximately normal to the basal failure surface. In the case of a circular failure in homogeneous soil, these slice sides are approximately radial to the centre of curvature of the failure surface.

A rough or irregular failure surface can also give rise to negative stress problems if it causes part of the sliding mass to be significantly more stable than an adjacent part. During the early stages of development of this program, the author compared answers against solutions for the same problem obtained from Bishop circular failure analyses. It was found that, in order to obtain absolute agreement between the solutions, the coordinates of the failure surface had to be calculated to ensure that the slice base inclinations were identical in the two analyses. Consequently, for critical problems, reading the slice base coordinates from a drawing may not be adequate and it may be necessary to calculate these coordinates to ensure that undulations are not built into the analysis.

DRAINAGE OF SLOPES

Three options for analysing the influence of drainage upon the stability of slopes have been included in the program listed in appendix 1.

The first option involves inserting a value for zero for the unit weight of water during initial entry of the data. This will activate an automatic routine in the program which will set all water forces to zero and give the solution for a fully drained slope.

The second option provides the user with the facility for changing the unit weight of water during operation of the program. This results in a pore-pressure ratio (r_u) type of analysis such as that commonly used in soil mechanics (see Bishop and Morgenstern (1960)). This analysis is useful for sensitivity studies on the influence of drainage on slope stability since it provides the user with a very fast means of changing the water pressures throughout the slope.

The final method of analyzing the influence of drainage is to change the phreatic surface coordinates on each slice boundary. This method is rather tedious but it probably represents the actual field conditions more realistically than the r_u analysis described above.

The water pressure distributions assumed in this analysis are illustrated in figures 1 and 2 and these distributions are considered to be representative of those most commonly occurring in the field. There are, however, situations in which these water pressure distributions are inappropriate. The best example of such a situation is a dam foundation in which the water pressure distribution is modified by the presence of grout and drainage curtains. The simplest way to account for such changes in the analysis presented here is to calculate the change in total uplift force on the base of each slice influenced by drainage and grouting and then to apply this change as a stabilizing external force acting normal to the slice base.

INCORPORATION OF NON-LINEAR FAILURE CRITERIA

Hoek (1982) has discussed the question of non-linear failure criteria for heavily jointed rock masses and has given an example of the analysis of a large open pit mine slope in such materials. Since the Sarma analysis calculates the effective normal stresses on each slice side and base, these values can be used to determine the instantaneous cohesion and friction angle acting on these surfaces. An iterative technique is used to change these shear strength values until the difference between factors of safety calculated in successive iterations is acceptably small. Three or four iterations are usually sufficient to give an acceptable answer.

The iterative process described above is relatively easy to build into the analysis presented in appendix 1 but, in the interests of space, this has not been done in this paper. In addition, non-linear analyses are generally only carried out for fairly complex problems and only after a large number of sensitivity studies using linear failure criteria have been performed. In such cases, the user is generally seeking a fundamental understanding of the mechanics of the slope behaviour and it is advantageous to carry out the non-linear analysis manually in order to enhance this understanding.

RECOMMENDED STEPS IN CARRYING OUT AN ANALYSIS

When applying this analysis to an actual slope problem a great deal of time can be wasted if too detailed an analysis is attempted at the beginning of the study.

The first step in any analysis involves a determination of the most critical failure surface. Except where this surface has been clearly pre-defined by existing geological weakness planes or observed failure surface, some form of search for the critical failure surface must be carried out. A good starting point for such a search is a set of charts such as those devised by Hoek and Bray (1981) and reproduced in figures 5 and 6. These give a first estimate of the location of the centre of rotation of a critical circle and the position of a tension crack in a homogeneous slope.

Based upon some estimate or educated guess of the critical failure surface location, the sliding mass is divided into slices, using the fewest possible number of slices to approximate the geometry. Usually three or four slices will suffice at this stage since only a very crude analysis is required to check the critical failure geometry.

A number of trial analyses with different failure surface locations should then be carried out. It will be found that a set of critical conditions will quickly be found and a more refined model can then be constructed. Unless the slope geometry is extremely complex, five to ten slices will generally be found to give an acceptable level of accuracy for this refined analysis.

Sarma (1979) suggests that the optimum inclination of the slice sides should be determined by varying the inclination of each slice side while keeping the others fixed. The optimum inclination for each slice side is that which gives the minimum factor of safety for the complete slope. In relatively simple slopes in which the range of shear strengths is fairly limited, the factor of safety is relatively insensitive to slice side inclination and, in such cases, it is generally acceptable to set the slice side inclination normal to the failure surface.

EXAMPLE 1 - SPOIL PILE ON A WEAK FOUNDATION

A common problem which occurs in the strip mining of coal involves failure of spoil (waste material) piles placed on weak inclined foundations. One such problem has been studied in considerable detail by Coulthard (1979) and the results which he obtained are reproduced below by means of the Sarma non-vertical slice method.

The failure geometry, reconstructed from field measurements by the Australian CSIRO, is illustrated in figure 7. This shows that the failure involves downward movement of an "active" wedge and outward movement along the weak inclined base of the "passive" wedge. The shear strengths on the inclined base and on the two internal shear failure surfaces are based upon laboratory strength test results.

In order to demonstrate the negative stress problem discussed above, the first analysis carried out is for a waste pile with a high groundwater table - a situation which would be most unlikely to occur in an actual spoil pile. The results of the analysis carried out for these conditions are listed in table 1 and a plot of the graph of factor of safety versus acceleration is given by the dashed line in figure 8. Note that negative stresses occur on both internal shear surfaces in this analysis and the calculated factor of safety of 0.26 is unacceptable. It is also important

to note that the plot of F vs K has an asymptote of $F = 0.428$ and that factors of safety of less than this value are meaningless.

This example demonstrates that, under certain circumstances, the iteration technique used in the program (and all other iteration techniques tried during the development of the program) will choose the incorrect solution. As shown in figure 8, the factor of safety for $K = 0$ is 0.48 whereas the second root of 0.26 has been chosen by the iteration technique. Fortunately, this problem is very rare and, as far as the author has been able to ascertain, is always associated with negative stresses which generate the message that the solution is unacceptable. Nevertheless, for critical problems, it is recommended that the curve of factor of safety versus acceleration be plotted out to ensure that the correct solution has been chosen.

The second solution is for a drained spoil pile. A factor of safety of 1.20 is obtained for this case and all the effective normal stresses are positive. The plot of factor of safety versus acceleration, given as the solid line in figure 8, shows that the value of 1.20 is well above the asymptote of 0.428 which, interestingly, is the same as for the previous analysis.

A third analysis, using the same geometry as illustrated in figure 7 but with the slope drained and the cohesion on side 2 reduced to zero, produces a factor of safety of 1.00. This limiting equilibrium condition is identical to that obtained by Coulthard (1979) using a two-wedge analysis similar to that proposed by Seed and Sultan (1967) for sloping core embankment dams.

EXAMPLE 2 - OPEN PIT COAL MINE SLOPE

Figure 9 illustrates the geometry of a slope problem in a large open pit coal mine. A thin coal seam is overlain by soft tuff and existing failures in the slope show that sliding occurs along the coal seam with the toe breaking out through the soft tuff. In the case illustrated, a reservoir close to the crest of the slope recharges the slope with water and results in the high groundwater surface illustrated. Laboratory tests and back analysis of previous failures give a friction angle of 18 degrees and a cohesion of zero along the coal seam and a friction angle of 30 degrees and cohesion of 2 tonnes/sq.m for failure through the soft tuff. The unit weight of the tuff is 2.1 tonnes/cu.m and the unit weight of water is 1.0 tonne/cu.m.

A printout produced by the program listed in appendix 1 is reproduced in table 2 and this shows that the factor of safety for the slope illustrated in figure 9 is 1.17. A sensitivity study of drainage shows that 50% drainage (reducing the unit weight of water to 0.5 tonnes/cu.m) increases the factor of safety to 1.41 while complete drainage of the slope gives a factor of safety of 1.65. In the actual case upon which this example is based, the reservoir above the slope was drained but in adjacent slopes long horizontal drain holes were used to reduce the water pressures in the slopes.

EXAMPLE 3 - PARTIALLY SUBMERGED ROCKFILL SLOPE

Figure 10 illustrates the geometry of a rockfill slope placed underwater onto a sandy river bottom. The rockfill is partially submerged and the

failure surface (determined by a critical failure search using a conventional vertical slice analysis) involves both the rockfill and the sand base. A printout of the slope geometry, material properties and calculated factor of safety is given in table 3.

It is interesting to note that the critical acceleration for this slope is 0.2106. This means that, for a pseudo-static analysis of earthquake loading, a horizontal acceleration of 0.21g would be required to induce failure in the slope. Factors of safety corresponding to different pseudo-static horizontal acceleration levels can be found by using the optional subroutine, included in the program, to produce a plot similar to that illustrated in figure 8. In the actual case upon which this example was based, a more complete dynamic earthquake analysis was performed but in many cases a pseudo-static check on stability under earthquake loading is acceptable.

ACKNOWLEDGEMENTS

The author wishes to acknowledge the interest and support of many of his colleagues in Colder Associates in the development of the program listed in appendix 1. Special thanks are due to Mr Ken Inouye and Mr Trevor Fitzell for their practical assistance in writing and debugging parts of the program.

REFERENCES

1. Bishop, A.W. and N.R. Morgenstern 1960. Stability coefficients for earth slopes. *Geotechnique* 10(4), 129-50.
2. Coulthard, M.A. 1979. *Back-analysis of observed spoil failures*. Tech. Rep. No. 83, Div. Appl. Mach., Aust. Corm. Sci. Ind. Res. Org., Melbourne.
3. Hoek, E. 1983. Strength of jointed rock masses. *Geotechnique* 33(3), 187-223.
4. Sarma, S.K. 1979. Stability analysis of embankments and slopes. *J. Geotech. Engrg Div., Am. Soc. Civ. Engrs* 105, No. GT12. 1511-24.
5. Sarma, S.K. and H.V. Bhave 1974. Critical acceleration versus static factor of safety in stability analysis of earth dams and embankments. *Geotechnique* 24(4), 661-5.
6. Seed, H.B. and H.A. Sultan 1967. Stability analyses for a sloping core embankment. *J. Soil Mech. Foundas Div., Am. Soc. Civ. Engrs* 93, No. SMA, 45-67.

Figure 1: Definition of geometry and forces acting on ith slice.

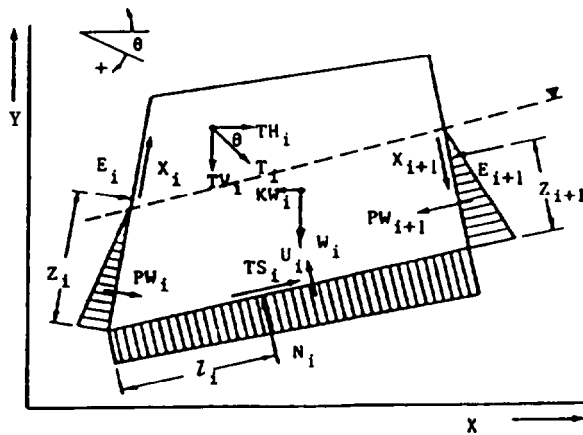
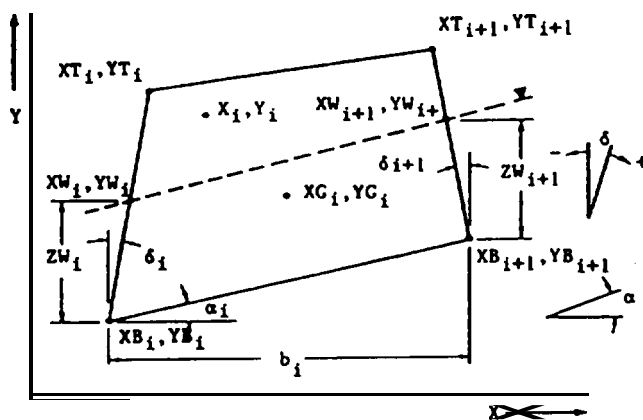


Figure 2: Definition of water forces.

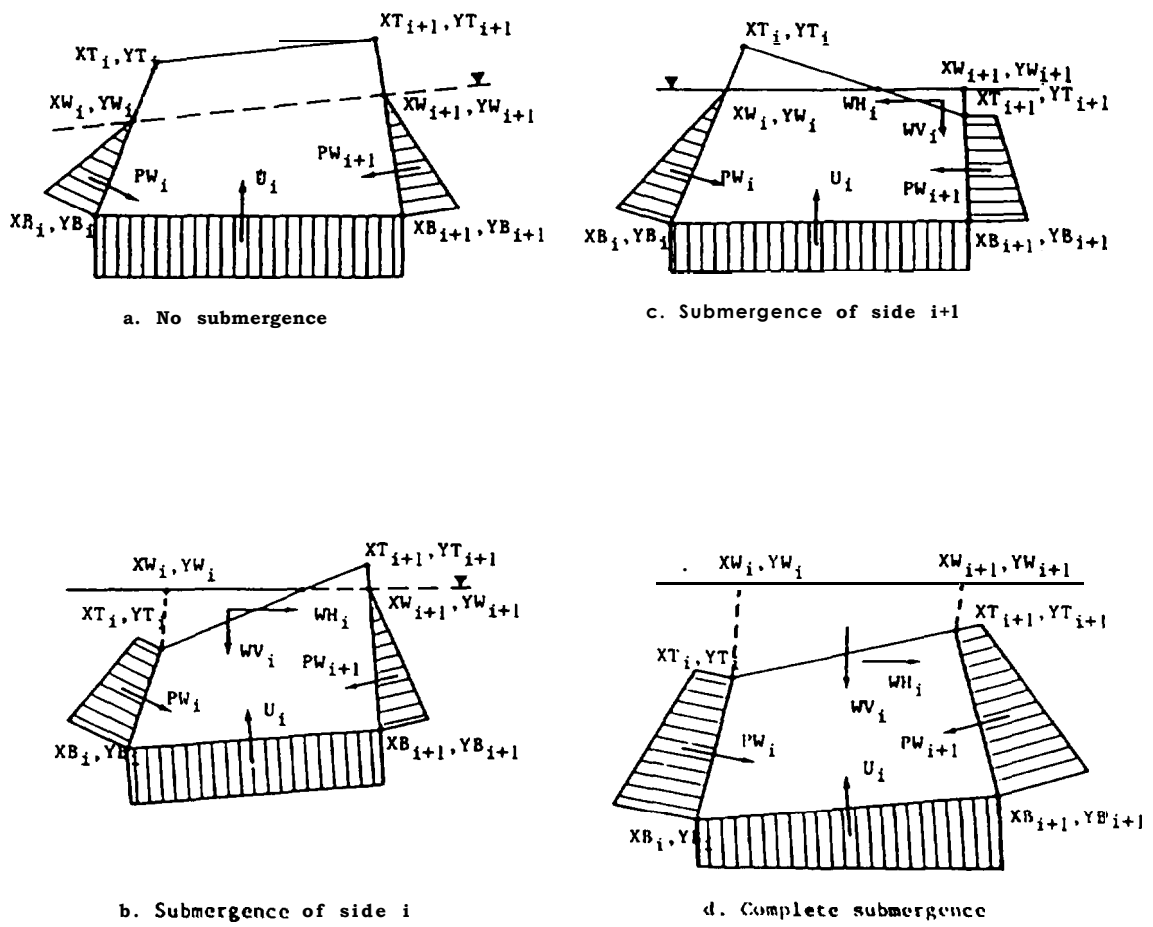


Figure 3: Factor of safety versus acceleration for a typical slope.

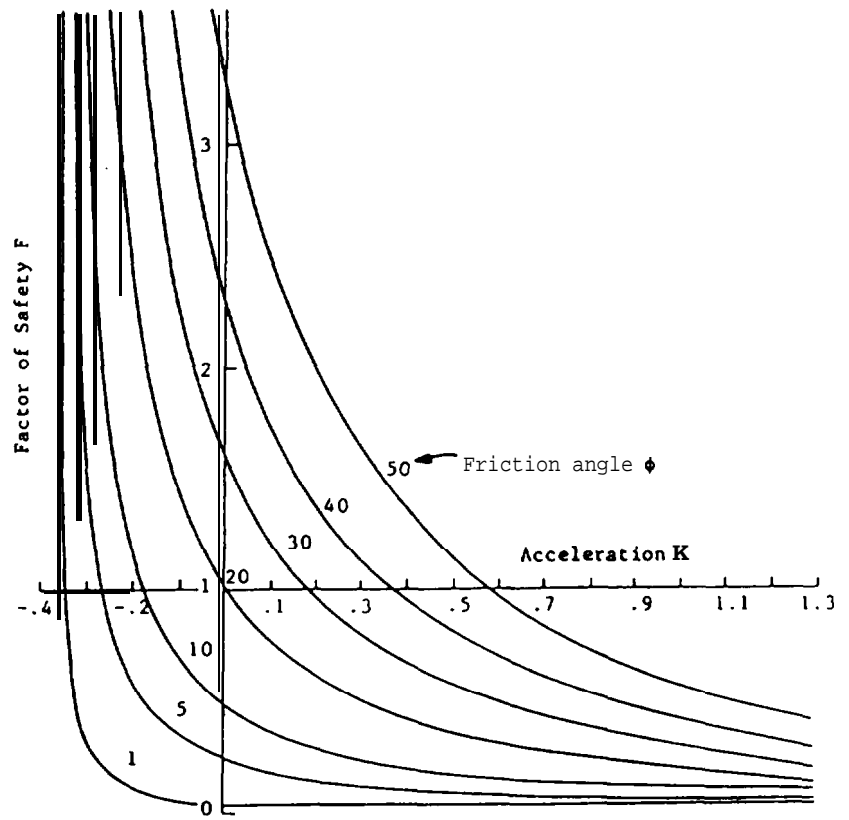


Figure 4: Plot of reciprocal of factor of safety versus acceleration.

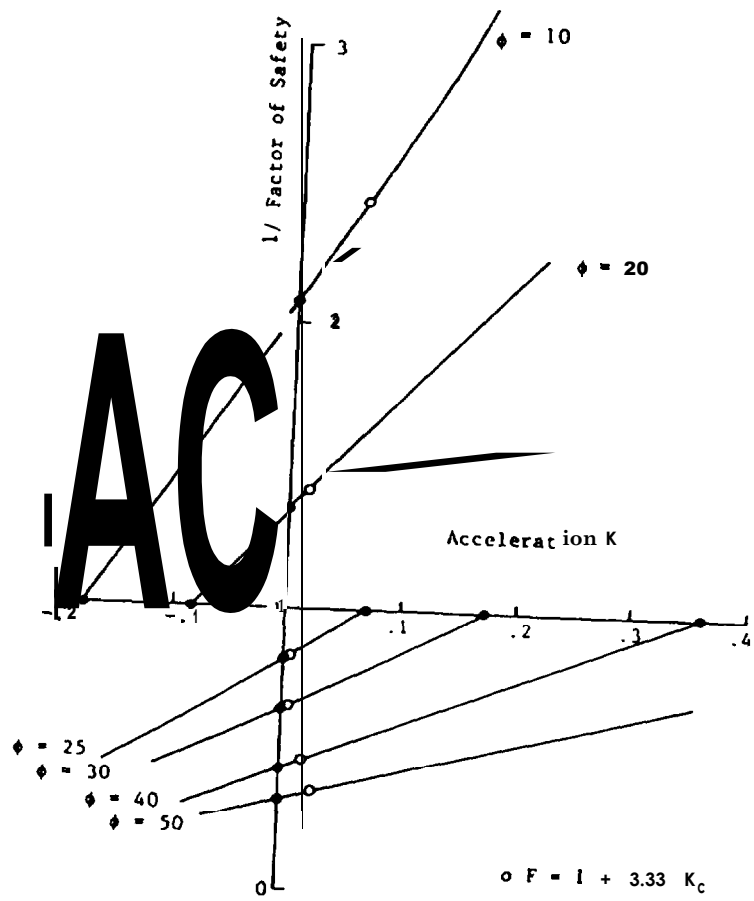


Figure 5: Approximate locations of the centre of curvature of a circular failure surface and a tension crack in a drained homogeneous slope.

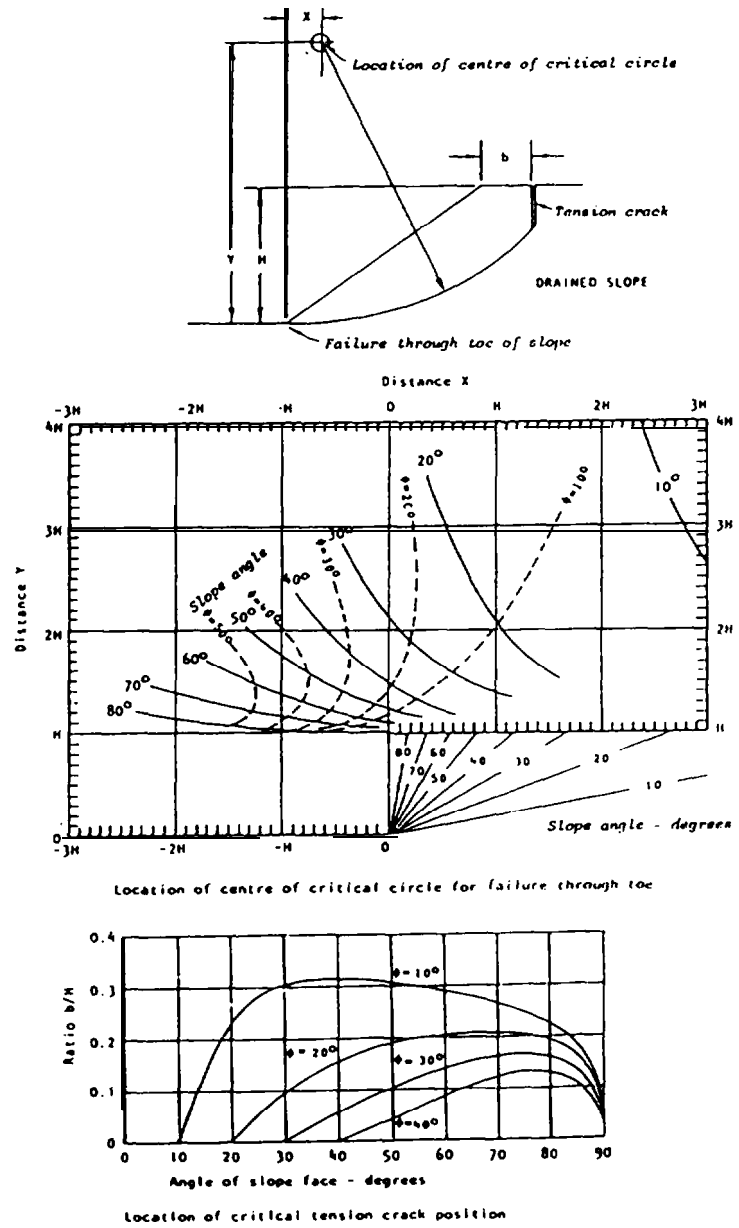


Figure 6: Approximate locations of the centre of curvature of a circular failure surface and a tension crack in a homogeneous slope with groundwater present.

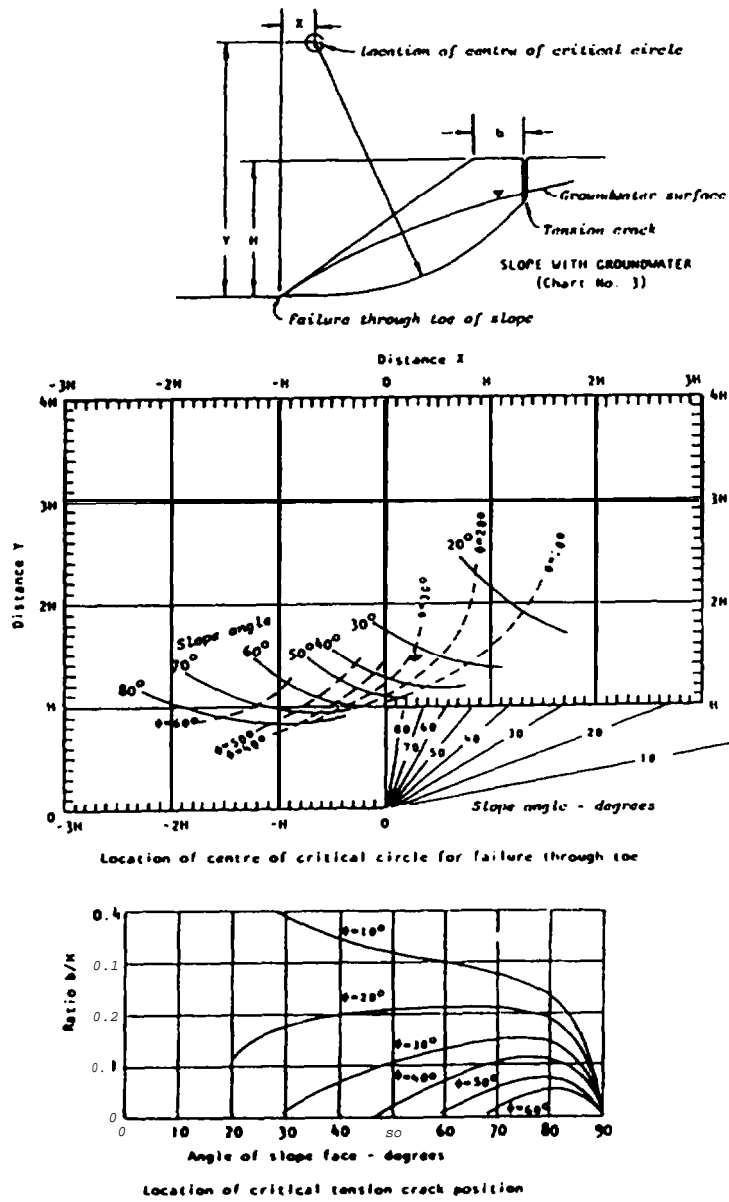


Figure 7: Geometry of a spoil pile on a weak foundation analysed by Coulthard (1979).

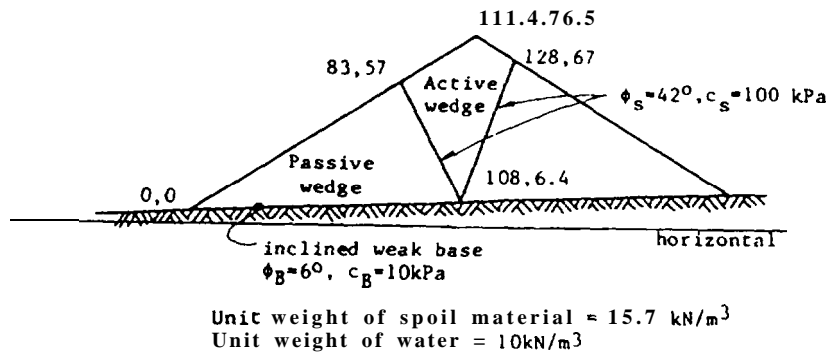


Figure 8: Plot of factor of safety versus acceleration K for a spoil pile on an inclined weak foundation.

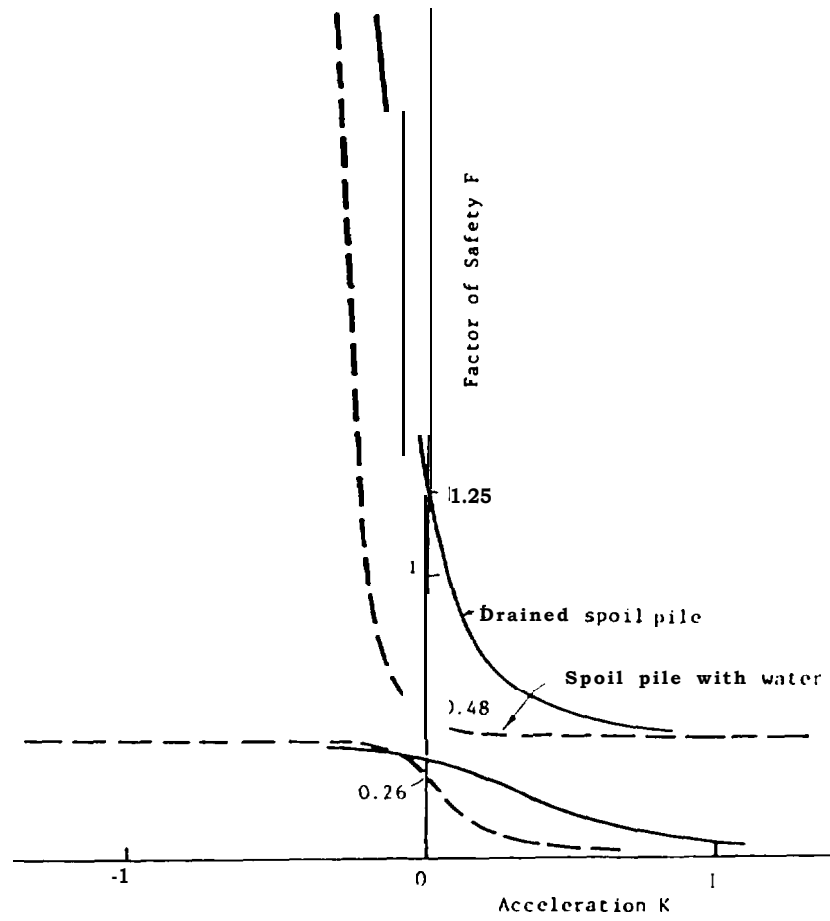


Figure 9: **Geometry for an Open pit coal mine slope.**

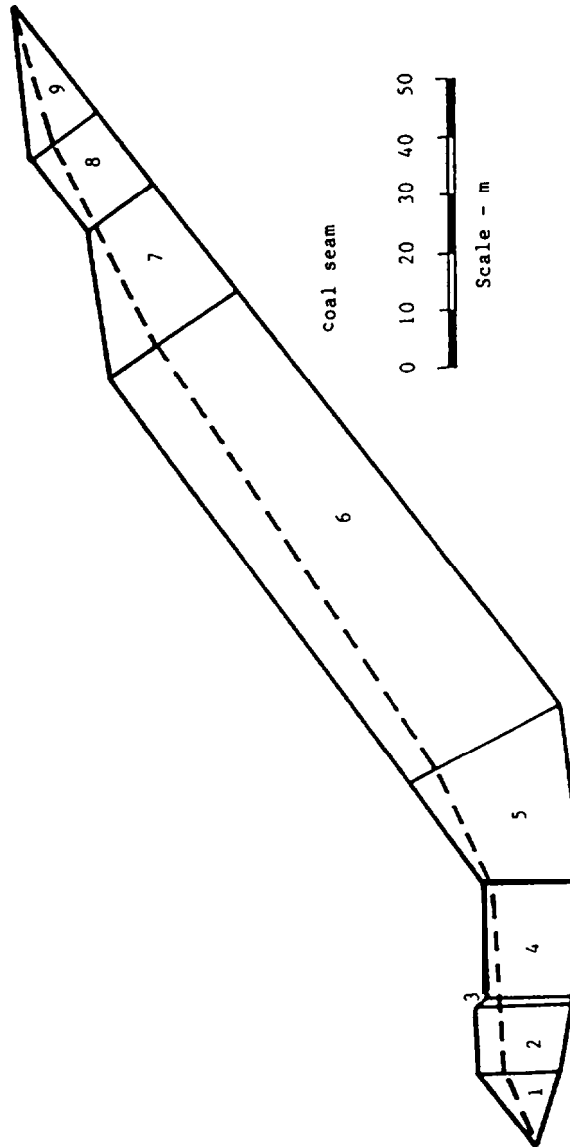


Table 1: Printout for analysis of stability of spoil pile on a weak foundation (figure 7).

SARMA NON-VERTICAL SLICE ANALYSIS

Analysis no. 1 - Spoil pile on a weak foundation

Unit weight of water = 10

Side number	1	2	3
Coordinate xt	0.00	83.00	111.40
Coordinate yt	0.00	57.00	76.50
Coordinate xw	0.00	83.00	128.00
Coordinate yw	0.00	57.00	67.00
Coordinate xb	0.00	108.00	128.00
Coordinate yb	0.00	6.40	67.00
Friction angle	0.00	42.00	0.00
Cohesion	0.00	100.00	0.00

Slice number	1	2
Rock unit weight	15.70	15.70
Friction angle	6.00	42.00
Cohesion	10.00	100.00
Force T	0.00	0.00
Angle theta	0.00	0.00

Effective normal stresses		
Base	147.15	-14.13
Side	0.00	-130.64

Acceleration          **Factor of Safety = 0.26**
Negative effective normal stresses - **solution unacceptable**

Table 2: Printout for analysis of stability of open pit coal mine slope (figure 9).

SARMA NON-VERTICAL SLICE ANALYSIS

Analysis no. 2 - Open pit coal mine slope with tuff overlying coal seam.

Unit weight of water = 1

Side number	1	2	3	4	5	6
Coordinate xt	4.00	17.00	29.00	30.00	50.00	68.00
Coordinate yt	17.00	26.00	26.00	24.00	25.00	37.00
Coordinate xw	4.00	17.00	29.00	30.00	50.00	70.00
Coordinate yw	17.00	23.00	22.00	22.00	24.00	33.00
Coordinate xb	4.00	17.00	29.00	30.00	50.00	80.00
Coordinate yb	17.00	12.00	10.00	10.00	8.00	11.00
Friction angle	0.00	30.00	30.00	30.00	30.00	18.00
Cohesion	0.00	2.00	2.00	2.00	2.00	0.00

Slice number	1	2	3	4	5	6
Rock unit weight	2.10	2.10	2.10	2.10	2.10	2.10
Friction angle	30.00	30.00	30.00	30.00	30.00	30.00
Cohesion	2.00	2.00	2.00	2.00	2.00	2.00
Force T	0.00	0.00	0.00	0.00	0.00	0.00
Angle theta	0.00	0.00	0.00	0.00	0.00	0.00

Effective normal stresses						
Base	29.91	37.07	22.52	29.22	44.54	27.92
Side	0.00	23.69	41.25	48.08	60.63	63.72

Side number	7	8	9	10
Coordinate xt	140.00	165.00	178.00	204.00
Coordinate yt	88.00	90.00	99.00	103.00
Coordinate xw	146.00	166.00	180.00	204.00
Coordinate yw	80.00	89.00	96.00	103.00
Coordinate xb	155.00	173.00	186.00	204.00
Coordinate yb	65.00	80.00	89.00	103.00
Friction angle	18.00	18.00	18.00	0.00
Cohesion	0.00	0.00	0.00	0.00

Slice number	7	8	9
Rock unit weight	2.10	2.10	2.10
Friction angle	30.00	30.00	30.00
Cohesion	2.00	2.00	2.00
Force T	0.00	0.00	0.00
Angle theta	0.00	0.00	0.00

Effective normal stresses			
Base	18.89	11.90	6.64
Side	14.41	11.11	3.25

Acceleration Kc = 0.1008

Factor of Safety = 1.17

APPENDIX 1-BASIC COMPUTER PROGRAM FOR SARMANON-VERTICAL SLICE ANALYSIS.

The BASIC program listed on the following pages has been written for use on microcomputers which run Microsoft or equivalent BASIC. In order to utilize the graphics option (lines 6410-6970) it is necessary to use BASICA or an equivalent BASIC which supports graphics commands and to run the program on a computer fitted with an IBM or compatible graphics card. If no graphics facilities are available, the graphics subroutine may be disabled by deleting line 1800 and the function key display can be removed by deleting lines 4750 and 4760.

The program can be compiled using a BASIC compiler and this produces a machine language program which runs about six times faster than the BASIC program. The compiled program may not drive printers fitted with serial interfaces (RS232C) and the printer manual should be consulted for instructions on initializing the printer. If it proves impossible to drive the printer from the compiled program, it will be found that the BASIC program will drive almost any printer.

The function keys for the main program execute the following operations:

F1 - Print : prints the tabulated data and calculates critical acceleration and factor of safety as shown in tables 1 to 3.

F2 - Calculate : recalculates the critical acceleration and the factor of safety using the displayed data.

F3 - fos vs k : activates a subroutine to calculate values of the acceleration K for different factors of safety. A new display is used for this subroutine.

F4 - drain : enables the user to edit the line which displays the unit weight of water. This is used to change the unit weight of water in sensitivity studies using a portpressure ratio (r_u) approach.

F5 - file : displays the data files already stored on the disk and requests a new file name. Stores the displayed data on a disk file.

F6 - restart : returns to the first page display which asks various questions before the data array is displayed.

F7 - quit : exits the program and returns to BASIC. The program may be reactivated by typing RUN and pressing enter.

F8 - view : activates the graphics display if a suitable graphics card is fitted.

TABLE 4 - DEFINITION OF ARRAY A(J,K) FOR SARMA ANALYSIS

Side number	1	k	k+1
coordinate xt	A(1,1)	A(1,k)	A(1,k+1)
coordinate yt	A(2,1)	A(2,k)	A(2,k+1)
coordinate xw	A(3,1)	A(3,k)	A(3,k+1)
coordinate yw	A(4,1)	A(4,k)	A(4,k+1)
coordinate xb	A(5,1)	A(5,k)	A(5,k+1)
coordinate yb	A(6,1)	A(6,k)	A(6,k+1)
friction angle ϕ_B	A(7,1)	A(7,k)	A(7,k+1)
cohesion c_B	A(8,1)	A(8,k)	A(8,k+1)
Slice number	1	k	
rock unit weight γ_r	A(10,1)	A(10,k)	
friction angle ϕ_s	A(11,1)	A(11,k)	
cohesion c_s	A(12,1)	A(12,k)	
force T	A(15,1)	A(15,k)	
angle theta θ	A(16,1)	A(16,k)	
side length d	A(17,1)	A(17,k)	A(17,k+1)
side angle δ	A(18,1)	A(18,k)	A(18,k+1)
base length b	A(19,1)	A(19,k)	
base angle α	A(20,1)	A(20,k)	
slice weight W	A(21,1)	A(21,k)	
uplift force U	A(22,1)	A(22,k)	
water force PW	A(23,1)	A(23,k)	A(23,k+1)
base cohesion a/F	A(24,1)	A(24,k)	
base friction $TM \phi_s/F$	A(25,1)	A(25,k)	
side cohesion c_s/F	A(26,1)	A(26,k)	A(26,k+1)
side friction $Tan \phi_s/F$	A(27,1)	A(27,k)	A(27,k+1)
calculated R	A(28,1)	A(28,k)	
calculated S	A(29,1)	A(29,k)	A(29,k+1)
calculated Q	A(30,1)	A(30,k)	
calculated e	A(31,1)	A(31,k)	
calculated p	A(32,1)	A(32,k)	
calculated a	A(33,1)	A(33,k)	
calculated E	A(34,1)	A(34,k)	A(34,k+1)
calculated x	A(35,1)	A(35,k)	
calculated N	A(36,1)	A(36,k)	
calculated TS	A(37,1)	A(37,k)	
calculated σ_B	A(38,1)	A(38,k)	
calculated σ_s	A(39,1)	A(39,k)	A(39,k+1)

```

10 * SARMA - NON-VERTICAL SLICE METHOD OF SLOPE STABILITY ANALYSIS
20 * Version 1.0 - Written by Dr.E.Hoek, Colder Associates, January 1986
30 * Reference : Sarma, S.K. (1979), Stability analysis of embankments
40 * and slopes, J. Geotech. Engg. Div., ASCE., Vol. 105,
50 * No. CT12. pages 1511-1524.
60 *
70 * Dimensioning of variables
80 *
90 STATUS="i":RAD=3.141593/180:F=1:M=1
100 DIM A(39,50),WH(50),WH(50),ACC(10),ACL(100)
110 DIM PB(50),PS(50),PHALP(50),ZW(50),FL(100)
120 DIM THETA(50),TV(50),TH(50),ZWT(50)
130 *
140 * Defioitiw of function keys
150 *
160 KEY OFF: FOR I = 1 TO 8:KEY I,"":NEXT I
170 KEY 1,"a":KEY 2,"b":KEY 3,"c":KEY 4,"d"
180 KEY 5,"e":KEY 6,"f":KEY 7,"g":KEY 8,"h"
190 *
200 * Display of first page
210 *
220 SCREEN 0,0:WIDTH 80:CLS:LOCATE8,17:COLOR 0.7:
230 PRINT " SARMA NUN-VERTICAL SLICK STABILITY ANALYSIS "
240 COLOR7,0:LOCATE 11.12
250 PRINT "Copyright - Bvert Hoek, 1985. This program is one of"
260 LOCATE 12.12
270 PRINT "a series of geotechnical programs developed as working"
280 LOCATE 13.12
290 PRINT "tools and for educational purposes. Use of the program"
300 LOCATE 14.12
310 PRINT "is not restricted but the user is responsible for the"
320 LOCATE 15.12
330 PRINT "application of the results obtained from this program."
340 LOCATE 18,25:PRINT "Press any key to continue"
350 IF LEN(INKEY$) = 0 THEN 350
360 *
370 * Display of second page
380 *
390 CLS:LOCATE 25.12
400 PRINT "to terminate input enter ";
410 LOCATE 25,37:COLOR 0,7:PRINT " q ";:COLOR 7.0
420 LOCATE 25,41:PRINT "in response to any question";
430 LOCATE 10,12
440 INPUT "Do you wish to read data from a disk file (y/n) ? : ",DISK$
450 IF LEFT$(DISK$,1)="q" OR LEFT$(DISK$,1)="Q" THEN 6980
460 IF LEN(DISK$)=0 THEN 430
470 IF LEFT$(DISK$,1)="Y" OR LEFT$(DISK$,1)="y" THEN 660
480 LOCATE 11,12
490 INPUT "Number of slices to be included in analysis : ",NUM$
500 IF LEFT$(NUM$,1)="q" OR LEFT$(NUM$,1)="Q" THEN 6980
510 IF LEN(NUM$)=0 THEN 480 ELSE NUM=VAL(NUM$)
520 FLAG2=0:LOCATE 12.12
530 INPUT "Unit weight of water = ",WATER$
540 IF LEFT$(WATER$,1)="q" OR LEFT$(WATER$,1)="Q" THEN 6980

```

```

550 IF LEN(WATER$)=0 THEN 520 ELSE WATER =VAL(WATER$)
560 IF WATER = 0 THEN FLAG2=1
570 FLAG3=0: LOCATE 13.12
580 INPUT "Are shear strengths uniform throughout slope (y/n) ? ",STRENGTH$
590 IF LEFT$(STRENGTH$,1)="q" OR LEFT$(STRENGTH$,1)="Q" THEN 6980
600 IF LEN(STRENGTH$)=0 THEN 570
610 IF LEFT$(STRENGTH$,1)="Y" OR LEFT$(STRENGTH$,1)="y" THEN FLAG3=1
620 N=NUM+1:GOTO 1950
630 '
640 ' Data entry from a disk file
650 '
660 CLS: LOCATE 8,1:PRINT STRING$(80,45)
670 PRINT:PRINT "Sarma data files on disk ";
680 PRINT:FILES "A:SARMA*.DAT":PRINT:PRINT STRING$(80,45):PRINT
690 INPUT "Enter filename (without extension): ",FILE$
700 CLS:OPEN "A:"+FILE$+".DAT" FOR INPUT AS #1
710 LINK INPUT#1, TITLE$: INPUT#1,N: INPUT#1,WATER
720 RAD=3.141593/180:F=1:M=1:NUM=N-1
730 INPUT#1,FLAG2: INPUT#1,FLAG3:INPUT#1,FLAG4
740 FOR K = 1 TO N:FOR J=1 TO 39:INPUT#1,A(J,K):NEXT J:NEXT K
750 INPUT#1,ACC: INPUT#1,ACC(2): INPUT#1,FOS
760 CLOSE #1:F=1:FLAG6=1:STATUS="e":GOTO 1950
770 '
780 ' Display of data array
790 '
800 CLS: LOCATE 1,1:PRINT "Analysis no. ";TITLE$
810 LOCATE 3,1:COLOR 15,0:PRINT "Side number":COLOR 7,0
820 LOCATE 4,1:PRINT "coordinate xt"
830 LOCATE 5,1:PRINT "coordinate yt"
&O LOCATE 6,1:PRINT "coordinate xw"
850 LOCATE 7,1:PRINT "coordinate yw"
860 LOCATE 8,1:PRINT "coordinate xb"
870 LOCATE 9,1:PRINT "coordinate yb"
880 LOCATE 10,1:PRINT "friction angle"
890 LOCATE 11,1:PRINT "cohesion"
900 LOCATE 12,1:PRINT "unit weight of water = "
910 LOCATE 12,23:PRINT WATER
920 LOCATE 13,1:COLOR 15.0
930 PRINT "Slice number":COLOR 7.0
940 LOCATE 14,1:PRINT "rock unit weight"
950 LOCATE 15,1:PRINT "friction angle"
960 LOCATE 16,1:PRINT "cohesion"
970 LOCATE 17,1:PRINT "force T ":LOCATE 18.1
980 PRINT "angle theta"
990 GOSUB 1040
1000 IF STATUS="i" THEN GOSUB 1140:RETURN ELSE RETURN
1010 '
1020 ' Subroutine for slice number display
1030 '
1040 COLOR 15,0: LOCATE 3,22:PRINT M: LOCATE 13,27:PRINT M
1050 LOCATE 3,32:PRINT M+1:COLOR 7,0:IF N=M+1 THEN RETURN
1060 COLOR 15,0: LOCATE 13,37:PRINT M+1: LOCATE 3.42
1070 PRINT M+2:COLOR 7,0:IF N=M+2 THEN RETURN
1080 COLOR 15,0: LOCATE 13,47:PRINT M+2: LOCATE 3.52

```

```

1090 PRINT M+3:COLOR 7,0:IF N=M+3 THEN RETURN
1100 COLOR 15,0:LOCATE 13,57:PRINT M+3:LOCATE 3.62
1110 PRINT M+4:COLOR 7,0:IF N=M+4 THEN RETURN
1120 COLOR 15,0:LOCATE 13,67:PRINT M+4:LOCATE 3.72
1130 PRINT M+5:COLOR 7,0:RETURN
1140 LOCATE 20.13
1150 PRINT "Note: coordinates must increase from slope toe to crest"
1160 LOCATE 22.13
1170 PRINT "To edit title or data array, use direction keys to move"
1180 LOCATE 23.13
1190 PRINT "highlighted window. Factor of safety calculation will"
1200 LOCATE 24.13
1210 PRINT "commence autcaatically when all data has been entered.:";
1220 RETURN
1230
1240 ' Entry and display of title
1250 '
1260 IF FLAG6=1 OR STATUS="e" THEN 1300
1270 LOCATE 1,1:COLOR 0,7:PRINT "Analysis no.":COLOR 2.0
1280 LOCATE 1,14:LINE INPUT "",TITLE$
1290 IF LEN(TITLE$)=0 THEN TITLE$=PREVT$
1300 LOCATE 1,1:PRINT "Analysis no. "
1310 IF STATUS="r" THEN LOCATE 1,14:PRINTSTRING$(66," ")
1320 LOCATE 1,14:PRINT TITLE$
1330 PREVT$=TITLE$:RETURN
1340 '
1350 ' Subroutine for entry of data into array a(j,k)
1360
1370 IF STATUS="i" THEN FLAG6=0
1380 IF FLAG20=1 THEN FLAG6=1:FLAG20=0 ' 1st column
1390 IF FLAG21=1 THEN K=M:J=PREVJ-1:FLAG21=0 ' locate cursor
1400 IF FLAG23=1 THEN K=M+4:J=PREVJ-1:FLAG23=0 ' locate cursor
1410 IF FLAG2=0 THEN 1440 ' water present
1420 IF J=3 AND FLAG2=1 THEN J=5 ' drained
1430 IF FLAG2=1 THEN A(3,K)=A(5,K):A(4,K)=A(6,K) ' yw=yb
1440 IF J=7 AND K=1 THEN J=10:GOTO 1500 ' first slice
1450 IF FLAG3=0 THEN 1500 ' variable strength
1460 IF J=7 THEN A(7,K)=A(11,1):FLAG6=1 ' uniform strength
1470 IF J=8 THEN A(8,K)=A(12,1):FLAG6=1
1480 IF J=9 AND FLAG12=0 THEN J=10 ' skip space
1490 IF J=10 THEN A(10,K)=A(10,1):FLAG6=1
1500 IF J=9 AND FLAG12=0 THEN J=10 ' skip space
1510 IF K=1 OR FLAG3=0 THEN 1540 ' variable strength
1520 IF J=11 THEN A(11,K)=A(11,1):FLAG6=1 ' uniform strength
1530 IF J=12 THEN A(12,K)=A(12,1):FLAG6=1
1540 IF J=13 THEN J=15 ' skip space
1550 IF J=16 AND A(15,K)=0 THEN J=0:K=K+1:RETURN ' no forces
1560 IF J=17 THEN J=0:K=K+1:RETURN ' next column
1570 IF J<=8 THEN X=18+(10*(K-M)):Y=J+3 ' cursor location
1580 IF J>=10 AND J<=12 THEN X=23+(10*(K-M)):Y=J+4
1590 IF J>=15 AND J<=16 THEN X=23+(10*(K-M)):Y=J+2
1600 IF FLAG6=1 THEN GOSUB 1880 ELSE GOSUB 1650 ' cursor operation
1610 RETURN
1620 '

```

```

1630 ' Subroutine for cursor movement and display of array a(j,k)
1640 '
1650 FLAG10=0:FLAG11=0:FLAG12=0:FLAG13=0
1660 FLAG14=0:GOSUB 1900
1670 Q$=INKEY$:IF Q$="" THEN 1670 'scan keyboard
1680 IF LEN(Q$)=2 THEN Q$=RIGHT$(Q$,1)
1690 IF Q$="K" THEN GOSUB 1870:FLAG10=1:RETURN 'left
1700 IF Q$="M" THEN GOSUB 1870:FLAG11=1:RETURN 'right
1710 IF Q$="H" THEN GOSUB 1870:FLAG12=1:RETURN 'up
1720 IF Q$="P" THEN GOSUB 1870:FLAG13=1:RETURN 'down
1730 IF Q$="A" THEN GOSUB 1870:FLAG14=1:RETURN 'print
1740 IF Q$="B" THEN GOSUB 1870:FLAG15=1:RETURN 'calculate
1750 IF Q$="C" THEN GOSUB 1870:FLAG16=1:RETURN 'f.o.s vs K
1760 IF Q$="D" THEN GOSUB 1870:FLAG25=1:RETURN 'drain
1770 IF Q$="E" THEN GOSUB 1670:FLAG17=1:RETURN 'file
1780 IF Q$="F" THEN GOSUB 1870:FLAG26=1:RETURN 'restart
1790 IF Q$="G" OR Q$="Q" THEN FLAG18=1:RETURN 'quit
1800 IF Q$="H" THEN FLAG27=1:RETURN 'view
1810 IF Q$="0" THEN 1890 'enter zero
1820 IF Q$="-" THEN 1890 'enter minus
1830 IF Q$="." THEN 1890 'enter period
1840 IF VAL(Q$)<1 OR VAL(Q$)>9 THEN 1670 'enter nuder
1850 LOCATE Y,X:PRINT VAL(Q$)
1860 LOCATE Y,X+2:INPUT "",IN$:A(J,K)=VAL(Q$+IN$)
1870 LOCATE Y,X:PRINT " "
1880 LOCATE Y,X:PRINT USING "####.##";A(J,K):RETURN 'display entry
1890 LOCATE Y,X:PRINT " ";PRINT Q$:GOTO 1860
1900 LOCATE Y,X:COLOR 0,7
1910 PRINT " ":COLOR 7,0:RETURN
1920 '
1930 ' Data entry wd display of array a(j,k)
1940 '
1950 F=1:M=1:GOSUB 800:GOSUB 1260 'screen display
1960 FOR K=1 TO 6:FOR J=1 TO 17
1970 IF FLAG1=1 THEN 2140
1980 IF FLAG23=1 THEN FLAG6=0:GOTO 2000
1990 IF FLAG22=1 THEN FLAG6=1:GOTO 2140
2000 IF FLAG10=1 THEN GOSUB 2500 'left
2010 IF FLAG11=1 THEN GOSUB 2610 'right
2020 IF FLAG12=1 THEN GOSUB 2720 'up
2030 IF FLAG13=1 THEN GOSUB 2840 'down
2040 IF FLAG14=1 THEN GOSUB 5710 'print
2050 IF FLAG15=1 THEN F=1:GOTO 3050 'calculate
2060 IF FLAG16=1 THEN 5130 'f.o.s vs K
2070 IF FLAG17=1 THEN 6310 'file
2080 IF FLAG18=1 THEN 6980 'quit
2090 IF FLAG19=1 THEN 2190 'next page
2100 IF FLAG25=1 THEN FLAG25=0:GOSUB 2950 'drain
2110 IF FLAG26=1 THEN 2120 ELSE 2130
2120 FLAG26=0:STATUS="i":TITLE$="":GOTO 390 'restart
2130 IF FLAG27=1 THEN 6440 'view
2140 IF K<N THEN 2160 'check end
2150 IF J=7 THEN 3040 'end input
2160 IF K=6 AND J=9 THEN 2180 'first page

```



```

2170 GOSUB 1370:NEXT J:NEXT K
2180 FLAG1=0:IF STATUS="e" THEN 4240
2190 M=M+5:GOSUB 800
2200 FOR K=M TO M+5:FOR J=1 TO 17
2210 IF STATUS="e" THEN 2230
2220 IF K=M AND J<=8 THEN FLAG20=1:GOTO 2460
2230 IF FLAG19=1 THEN FLAG6=1:GOTO 2430
2240 IF FLAG21=1 THEN FLAG6=0:GOTO 2460
2250 IF FLAG22=1 THEN FLAG6=1:GOTO 2430
2260 IF FLAG23=1 THEN FLAG6=0:GOTO 2460
2270 IF FLAG10=1 THEN GOSUB 2500
2280 IF FLAG11=1 THEN GOSUB 2610
2290 IF FLAG12=1 THEN GOSUB 2720
2300 IF FLAG13=1 THEN GOSUB 2840
2310 IF FLAG14=1 THEN GOSUB 5710
2320 IF FLAG15=1 THEN F=1:GOTO 3050
2330 IF FLAG16=1 THEN 5130
2340 IF FLAG17=1 THEN 6310
2350 IF FLAG18=1 THEN 6980
2360 IF FLAG25=1 THEN FLAG25=0:GOSUB 2950
2370 IF FLAG26=1 THEN 2360 ELSE 2390
2380 FLAG26=0:STATUS="i":TITLE$="":GOTO 390
2390 IF FLAG27=1 THEN 6440
2400 IF FLAG19=1 THEN K=M:J=1:GOTO 2190
2410 IF FLAG22=1 AND M=6 THEN M=1:GOTO 1950
2420 IF FLAG22=1 AND M>=11 THEN K=M:J=1:M=M-10:GOTO 2190
2430 IF K<N THEN 2450
2440 IF J=7 THEN 3040
2450 IF K=M+5 AND J=9 THEN 3040
2460 GOSUB 1370:NEXT J:NEXT K
2470 '
2480 ' Subroutine to move cursor left
2490 '
2500 IF K=2 AND J=8 THEN K=K:GOTO 2560
2510 IF K=2 AND J=9 THEN K=K:GOTO 2560
2520 IF K=1 THEN K=1:GOTO 2560
2530 IF M>=6 AND K=M THEN 2570
2540 IF K>M THEN K=K-1
2550 IF J=17 AND A(16,K)=0 THEN K=K+1:GOTO 2560
2560 J=J-1:FLAG10=0:RETURN
2570 FLAG22=1:PREVJ=J:FLAG10=0:RETURN
2580 '
2590 ' Subroutine to move cursor right
2600 '
2610 IF K=M+5 AND J<=9 THEN 2680
2620 IF K=M+4 AND J>9 THEN 2680
2630 IF K<N THEN K=K+1
2640 IF J=17 AND A(16,K)=0 THEN K=K-1:GOTO 2670
2650 IF J<=7 AND K=N THEN K=N
2660 IF J>7 AND K=N THEN K=NUM
2670 J=J-1:FLAG11=0:RETURN
2680 FLAG19=1:PREVJ=J:FLAG11=0:RETURN
2690 '
2700 ' Subroutine to move cursor up

```

'cursor operation
'display 1st page
'renumber columns
'second page

'left
'right
'up
'd a m
'print
'calculate
'f.o.s vs K
'file
'quit
'drain

'restart
'view

'check end
'end input

'limit left
'limit left

'previous page
'left
'blank cell
'keep line

'next page
'next page
'right
'blank cell
'limit right
'limit right
'keep line

```

2710 '
2720 IF J=2 AND K=1 THEN 2730 ELSE 2740
2730 STATUS="r":GOSUB 1270:STATUS="e":J=1:K=1:GOTO 2800 'edit title
2740 IF J=2 THEN J=1:GOTO 2800 'limit up
2750 IF J=6 AND FLAG2=1 THEN J=2:GOTO 2800 'drained
2760 IF K=1 AND J=11 THEN J=6:GOTO 2800 '1st column
2770 IF J=11 THEN J=8:GOTO 2800 'skip space
2780 IF J=16 THEN J=12:GOTO 2800 'skip space
2790 IF J>=3 AND J<=17 THEN J=J-2:FLAG12=0:GOTO 2800 'up
2800 FLAG12=0:RETURN
2810 '
2820 ' Subroutine to move cursor down
2830 '
2840 IF K=N AND J=7 THEN J=6:GOTO 2910 'last column
2850 IF J=1 AND K=1 THEN J=2:K=2:GOTO 2830 'exit title
2860 IF FLAG2=1 AND J=3 THEN J=5:GOTO 2910 'skip space
2870 IF J=9 THEN J=10:GOTO 2910 'skip space
2880 IF J=13 THEN J=15:GOTO 2910 'skip space
2890 IF J=16 AND A(J,K)=0 THEN J=15:GOTO 2910 'dam limit
2900 IF J=17 THEN J=16:GOTO 2910 'down limit
2910 FLAG13=0:RETURN
2920 '
2930 ' Subroutine to drain by changing unit weight of water
2940 '
2950 LOCATE 12,1:PRINT STRING$(30," "):COLOR 0.7
2960 LOCATE 12,1:PRINT "unit weight of water"
2970 COLOR 7,0:LOCATE 12,23:INPUT "=" ,WATER
2980 LOCATE 12,1:PRINT STRING$(30," "):LOCATE 12,1
2990 PRINT "unit weight of water = ";WATER
3000 J=J-1:RETURN
3010
3020 ' Calculation of slice parameters
3030 '
3040 IF STATUS="e" THEN 4240
3050 GOSUB 3320:FOR K=1 TO N:GOSUB 3430:NEXT K 'd & delta
3060 FOR K=1 TO NUM:GOSUB 3490:NEXT K 'b, alpha, W & U
3070 WAT=.5*WATER:GOSUB 3580 'water forces
3080 FOR K=1 TO N:A(24,K)=A(12,K)/F:A(26,K)=A(8,K)/F 'cb/F, cs/F
3090 PB(K)=A(11,K)*RAD:PS(K)=A(7,K)*RAD 'deg to radians
3100 A(25,K)=TAN(PB(K))/F 'tanphi/F
3110 A(27,K)=TAN(PS(K))/F 'tanphi/F
3120 PB(K)=ATN(A(25,K)):PS(K)=ATN(A(27,K)) 'effective phi
3130 PHALP(K)=PB(K)-A(20,K):THETA(K)=A(16,K)*RAD 'phi-alpha
3140 TV(K)=A(15,K)*SIN(THETA(K))+WW(K) 'TV
3150 IF A(16,K)=90 THEN TH(K)=0:GOTO 3180 'vertical
3160 IF A(16,K)=270 THEN TH(K)=0:GOTO 3180 'force
3170 TH(K)=A(15,K)*COS(THETA(K)) 'TH
3180 TH(K)=TH(K)+WH(K):NEXT K
3190 TV(N-1)=TV(N-1)-A(23,N)*SIN(A(18,N)) 'water in
3200 TH(N-1)=TH(N-1)-A(23,N)*COS(A(18,N)) 'tension crack
3210 TV(1)=TV(1)+A(23,1)*SIN(A(18,1)) 'submerged toe
3220 TH(1)=TH(1)+A(23,1)*COS(A(18,1)) 'submerged toe
3230 '
3240 ' Calculation of Kc

```

```

3250 '
3260 FOR K=2 TO N:GOSUB 3880:NEXT K ' S
3270 FOR K=1 TO NUM:GOSUB 3890: NEXT K ' R,Q,e,P,a,Kc
3280 GOTO 4050
3290 '
3300 ' Subroutine for display of "calculating"
3310 '
3320 IF FLAG15=0 THEN LOCATE 20,7:PRINT STRING$(70," ")
3330 LOCATE 22,7:PRINT STRING$(70," ")
3340 LOCATE 23,7:PRINT STRING$(70," ")
3350 LOCATE 24,7:PRINT STRING$(70," ");
3360 LOCATE 22,28:COLOR 0,7
3370 PRINT " C A L C U L A T I N G ":COLOR 7,0
3380 FOR J=17 TO 39:FOR K= 1 TO N
3390 A(J,K)=0:NEXT K:NEXT J:RETURN
3400 '
3410 ' Subroutines for calculation of slice geometry
3420 '
3430 IF A(4,K)<A(6,K) THEN A(4,K)=A(6,K):A(3,K)=A(5,K) ' check water
3440 DSQ=(A(1,K)-A(5,K))^2+(A(2,K)-A(6,K))^2
3450 IF DSQ=0 THEN A(17,K)=0 ELSE A(17,K)=SQR(DSQ) ' d
3460 IF A(2,K)-A(6,K)=0 THEN A(18,K)=0:RETURN
3470 A(18,K)=ATN((A(1,K)-A(5,K))/(A(2,K)-A(6,K))) ' delta
3480 RETURN
3490 A(19,K)=A(5,K+1)-A(5,K) ' b
3500 IF A(19,K)=0 THEN A(20,K)=0:GOTO 3520
3510 A(20,K)=ATN((A(6,K+1)-A(6,K))/A(19,K)) ' alpha
3520 A(21,K)=(A(6,K)-A(2,K+1))*(A(1,K)-A(5,K+1))
3530 A(21,K)=A(21,K)+(A(2,K)-A(6,K+1))*(A(1,K+1)-A(5,K))
3540 A(21,K)=.5*A(10,K)*A(21,K):RETURN ' w
3550 '
3560 ' Subroutine for calculation of water forces
3570 '
3580 FOR K=1 TO NUM:ZW(K)=A(4,K)-A(6,K)
3590 ZW(K+1)=A(4,K+1)-A(6,K+1)
3600 A(22,K)=WAT*(ZW(K)+ZW(K+1))*A(19,K)
3610 A(22,K)=ABS(A(22,K)/COS(A(20,K))):NEXT K ' U
3620 FOR K=1 TO N:ZWT(K)=A(4,K)-A(2,K)
3630 IF ZWT(K)>0 THEN 3650
3640 A(23,K)=WAT*ABS(ZW(K)^2/COS(A(18,K))):GOTO 3670 ' PW
3650 A(23,K)=WAT*(ZWT(K)+ZW(K)) ' submerged
3660 A(23,K)=A(23,K)*ABS((A(2,K)-A(6,K))/COS(A(18,K))) ' PW
3670 NEXT K
3680 FOR K=1 TO NUM
3690 IF ZWT(K)>=0 AND ZWT(K+1)>=0 THEN 3700 ELSE 3740
3700 WW(K)=WAT*(ZWT(K)+ZWT(K+1)) ' WW full,
3710 WH(K)=WW(K)*ABS((A(1,K+1)-A(1,K))) ' submerged
3720 WH(K)=WAT*(A(2,K+1)-A(2,K))*(ZWT(K)+ZWT(K+1)) ' WH
3730 IF A(2,K+1)<A(2,K) THEN WH(K)=-WH(K):GOTO 3840
3740 IF ZWT(K)>=0 AND ZWT(K+1)<=0 THEN 3750 ELSE 3790
3750 WW(K)=WAT*ZWT(K)^2*(A(1,K+1)-A(1,K)) ' WW side i
3760 IF A(2,K+1)-A(2,K)=0 THEN WW(K)=0:GOTO 3780
3770 WW(K)=ABS(WW(K)/(A(2,K+1)-A(2,K))) ' submerged
3780 WH(K)=WAT*ZWT(K)^2:GOTO 3840 ' hw

```

```

3790 IF ZWT(K)<=0 AND ZWT(K+1)>=0 THEN 3800 ELSE 3840
3800 WW(K)=WAT*ZWT(K+1)^2*(A(1,K+1)-A(1,K)) ' WW side i+1
3810 IF A(2,K+1)-A(2,K)=0 THEN WW(K)=0:GOTO 3830
3820 WW(K)=ABS(WW(K))/(A(2,K+1)-A(2,K)) ' submerged
3830 WH(K)=-WAT*(ZWT(K+1))^2
3840 NEXT K:RETURN
3850 '
3860 ' Subroutines for calculation of S,R,Q,e,p and s
3870 '
3880 A(29,K)=A(26,K)*A(17,K)-A(23,K)*A(27,K):RETURN ' S
3890 A(28,K)=A(24,K)*A(19,K)
3900 A(28,K)=A(28,K)/COS(A(20,K))-A(22,K)*A(25,K) ' R
3910 A(30,K)=COS(PB(K)-A(20,K)+PS(K+1)-A(18,K+1))
3920 A(30,K)=COS(PS(K+1))/A(30,K) ' O
3930 A(31,K)=A(30,K)*COS(PB(K)-A(20,K)+PS(K)-A(18,K))
3940 A(31,K)=A(31,K)/COS(PS(K)) ' e
3950 A(32,K)=A(30,K)*A(21,K)*COS(PB(K)-A(20,K)) ' p
3960 A(33,K)=(A(21,K)+TV(K))*SIN(PHALP(K))
3970 A(33,K)=A(33,K)+TH(K)*COS(PHALP(K))
3980 A(33,K)=A(33,K)+A(28,K)*COS(PB(K))
3990 A(33,K)=A(33,K)+A(29,K+1)*SIN(PHALP(K)-A(18,K+1))
4000 A(33,K)=A(33,K)-A(29,K)*SIN(PHALP(K)-A(18,K))
4010 A(33,K)=A(33,K)*A(30,K):RETURN ' a
4020 '
4030 ' Calculation of Kc and FOS
4040 '
4050 GOSUB 4540
4060 IF FLAG7=1 OR FLAG8=1 THEN 4090
4070 IF F<>1 THEN 4160
4080 IF (Z2+A(32,NUM))=0 THEN ACC(1)=0:GOTO 4230
4090 ACC(1)=(Z3+A(33,NUM))/(Z2+A(32,NUM)) ' Kc
4100 IF FLAG8=1 THEN 4190
4110 ACC=ACC(1):IF FLAG7 = 1 THEN 5290
4120 F=1+3.33*ACC(1) ' FOS estimate
4130 IF F<=0 THEN F=.1
4140 IF F>5 THEN F=5
4150 GOTO 3080 ' recalculate K
4160 ACC(2)=(Z3+A(33,NUM))/(Z2+A(32,NUM)) ' new K
4170 Y=1/F:FS=1-ACC(1)*(1-Y)/(ACC(1)-ACC(2)):FOS=1/FS ' FOS
4180 F=FOS:FLAG8=1:GOTO 3080
4190 FLAG8=0:FLAG4=0:FOR K=1 TO NUM:GOSUB 4810:NEXT K ' normal stresses
4200 FOR K=1 TO NUM:GOSUB 4840:NRXT K
4210 IF FLAG15=1 AND M>=6 THEN 4220 ELSE 4230
4220 F=1:M=1:STATUS="e":FLAG6=1:FLAG15=0:GOTO 1950
4230 LOCATE 22,28:PRINT
4240 WSUB 5020:LOCATE 22,7:COLOR 15,0
4250 LOCATE 22,7:COLOR 15,0
4260 PRINT "Acceleration Kc = ";
4270 LOCATE 22,27:PRINT USING "##.###";ACC;
4280 LOCATE 22,47:PRINT "Factor of safety = ";
4290 LOCATE 22,66:PRINT USING "##.##";FOS;:COLOR 7,0
4300 IF FLAG4=0 AND ABS(ACC(2))>.1 THEN 4310 ELSE 4340
4310 LOCATE 23,7:COLOR 15
4320 PRINT "Large extrapolation - plot of fos vs K suggested";

```

```

4330 LOCATE 23,59:PRINT "to check fos";:COLOR 7,0
4340 IF FLAG4=0 THEN 4410 ELSE LOCATE 23,7:COLOR 15.0
4350 PRINT "Negative effective normal stresses - "
4360 LOCATE 23,50:PRINT "solution unacceptable"
4370 COLOR 7.0
4380 '
4390 ' Control of screen displays
4400 '
4410 STATUS="e":FLAG15=0:GOSUB 4610
4420 IF STATUS="e" THEN 4440
4430 FLAG6=1:STATUS="e":GOTO 1950
4440 IF FLAG19=1 THEN 4450 ELSE 4460 ' next page
4450 FLAG21=1:FLAG3=0:FLAG19=0:GOTO 2200
4460 IF FLAG22=1 AND K=7 THEN 4470 ELSE 4480 ' previous page
4470 FLAG23=1:FLAG3=0:FLAG22=0:GOTO 1960
4480 IF FLAG22=1 AND K>=11 THEN 4490 ELSE 4500 ' previous page
4490 FLAG23=1:FLAG3=0:FLAG22=0:GOTO 2200
4500 FLAG6=0:FLAG3=0:J=1:K=1:M=1:GOTO 1960
4510 '
4520 ' Subroutine for calculation of K
4530 '
4540 Z1=1:Z2=0:Z3=0
4550 FOR K=NUM TO 2 STEP-1
4560 Z1=Z1*A(31,K):Z2=Z2+A(32,K-1)*Z1
4570 Z3=Z3+A(33,K-1)*Z1:NEXT K:RETURN
4580 '
4590 ' Display of function key
4600 '
4610 LOCATE 25 1:PRINT "1";
4620 WCATE 25,3:COLOR 0,7:PRINT "print";
4630 COWR 7,0:LOCATE 25,10:PRINT "2";
4640 LOCATE 25,12:COLOR 0,7:PRINT "calculate";
4650 COLOR 7,0:LOCATE 25,23:PRINT "3";
4660 WCATK 25,25:COLOR 0,7:PRINT "fos vs K";
4670 COWR 7,0:LOCATE 25,35:PRINT "4";
4680 LOCATE 25,37:COLOR 0,7:PRINT "drain";
4690 COLOR 7,0:LOCATE 25,44:PRINT "5";
4700 WCATE 25,46:COLOR 0,7:PRINT "file";
4710 COLOR 7,0:LOCATE 25,52:PRINT "6";
4720 LOCATE 25,54:COLOR 0,7:PRINT "restart";
4730 COLOR 7,0:LOCATE 25,63:PRINT "7";
4740 LOCATE 25,65:COLOR 0,7:PRINT "quit";
4750 COLOR 7,0:LOCATE 25,70:PRINT "8";
4760 LOCATE 25,72:COLOR 0,7:PRINT "view";
4770 COLOR 7,0:RETURN
4780 '
4790 ' Subroutine for calculation of effective normal stresses
4800 '
4810 A(34,K+1)=A(33,K)+A(34,K)*A(31,K)-ACC(1)*A(32,K) ' Ei+J
4820 A(35,K)=(A(34,K)-A(23,K))*A(27,K)+A(26,K)*A(17,K) ' Xi
4830 RETURN
4840 A(36,K)=A(21,K)+TV(K)+A(35,K+1)*COS(A(18,K+1))
4850 A(36,K)=A(36,K)-A(35,K)*COS(A(18,K))
4860 A(36,K)=A(36,K)-A(34,K+1)*SIN(A(18,K+1))

```



```

5410 LOCATE 25,59:PRINT "F3";:LOCATE 25,62:COLOR 0.7
5420 PRINT "restart";:COLOR 7.0
5430 LOCATE 25,71:PRINT "F4";:LOCATE 25,74:COLOR 0,7
5440 PRINT "quit";:COLOR 7,0:FLAG16=0
5450 Q$=INKEY$:IF Q$=" " THEN 5450
5460 IF Q$ = "a" THEN GOSUB 5550:GOTO 5450
5470 IF Q$ = "b" THEN 5500
5480 IF Q$ = "c" THEN 390
5490 IF Q$ = "d" THEN 6980 ELSE 5450
5500 F= 1: FLAG30= 1: GOTO 5280
5510 FLAG30=0: FLAG7=0:STATUS$="e": FLAG6=1: F=1:M=1:GOTO 1950
5520 '
5530 ' Subroutine for printing fos vs K
5540 '
5550 LPRINT:LPRINT:LPRINT:LPRINT
5560 LPRINT TAB(13) "Analysis no. ";:LPRINT TITLES
5570 LPRINT TAB(13) "Plot of factor of safety";
5580 LPRINT TAB(38) "versus acceleration K"
5590 LPRINT:LPRINT TAB(19) "f.o.s";
5600 LPRINT TAB(32) "acc. K";
5610 LPRINT TAB(44) "1/fos":LPRINT
5620 FOR L= 1 TO FIN-1
5630 LPRINT TAB(18) USING "##.###";FL(L);
5640 LPRINT TAB(31) USING "##.###";ACL(L);
5650 LPRINT TAB(43) USING "##.###";1/FL(L):NEXT L
5660 LPRINT:LPRINT:LPRINT:LPRINT
5670 RETURN
5680 '
5690 ' Subroutine for printing array ad results
5700
5710 PREVJ=J:PREVK=K:PREVM=M:FLAG14=0
5720 LPRINT:LPRINT:LPRINT:LPRINT:LPRINT:LPRINT
5730 LPRINT TAB(23) "SARMA NON-VERTICAL SLICE ANALYSIS":LPRINT
5740 LPRINT "Analysis no. ";:LPRINT TAB(14) TITLES
5750 LPRINT:LPRINT "Unit weight of water =";
5760 LPRINT TAB(23) WATER: X1=I: X2=N
5770 IF X2>6 THEN X2=X1+5
5780 T1=20:LPRINT:LPRINT "Side number";
5790 FOR X=X1 TO X2:LPRINT TAB(T1);:LPRINT USING "##";X;
5800 T1=T1+10:NEXT X:X3=X2
5810 IF X2=N THEN LPRINT
5820 T1=16:LPRINT "Coordinate xt";:J=1:GOSUB 6220
5830 T1=16:LPRINT "Coordinate yt";:J=2:GOSUB 6220
5840 T1=16:LPRINT "Coordinate xw";:J=3:GOSUB 6220
5850 T1=16:LPRINT "Coordinate yw";:J=4:GOSUB 6220
5860 T1=16:LPRINT "Coordinate xb";:J=5:GOSUB 6220
5870 T1=16:LPRINT "Coordinate yb";:J=6:GOSUB 6220
5880 T1=16:LPRINT "Friction angle";:J=7:GOSUB 6220
5890 T1=16:LPRINT "Cohesion";:J=8:GOSUB 6220
5900 T1=25:LPRINT:LPRINT "Slice number";
5910 IF X2=N THEN X3=X2-1 ELSE X3=X2
5920 FOR X=X1 TO X3:LPRINT TAB(T1);:LPRINT USING "##";X;
5930 T1=T1+10:NEXT X
5940 IF X2=N THEN LPRINT

```

```

5950 T1=21:LPRINT "Rockunit weight";:J=10:GOSUB 6220
5960 T1=21:LPRINT "Frictionangle";:J=11:GOSUB 6220
5970 T1=21:LPRINT "Cohesion";:J=12:GOSUB 6220
5980 T1=21:LPRINT "ForceT";:J=15:GOSUB 6220
5990 T1=21:LPRINT "Angletheta";:J=16:GOSUB 6220:LPRINT
6000 LPRINT "Effective normal stresses "
6010 T1=21:LPRINT "Base";:J=38:GOSUB 6220
6020 T1=16:LPRINT "Side";:J=39:GOSUB 6220:LPRINT:LPRINT
6030 IF X2=N THEN 6100
6040 IF X2<N THEN X1=X1+6:X2=N
6050 IF X2<X1+5 THEN 6060 ELSE X2=X1+5
6060 IF X1=13 OR X1=27 THEN 6080
6070 LPRINT:LPRINT:GOTO 5780
6080 LPRINT:LPRINT:LPRINT:LPRINT:LPRINT
6090 LPRINT:LPRINT:LPRINT:LPRINT:GOTO 5780
6100 LPRINT TAB(7) "Acceleration Kc = ";
6110 LPRINT TAB(27);:LPRINT USING "##.###";ACC;
6120 LPRINT TAB(47) "Factor of Safety = ";
6130 LPRINT TAB(66);:LPRINT USING "##.##";FOS
6140 IF FLAG4=0 THEN 6170
6150 LPRINT TAB(7) "Negativ effective normal stresses";
6160 LPRINT TAB(45) "- solution unacceptable":GOTO 6200
6170 IF FLAG4=0 AND ABS(ACC(2))<.1 THEN 6200
6180 LPRINT TAB(7) "Large extrapolation - plot of fos";
6190 LPRINT TAB(44) "vs K suggested to check fos"
6200 J=PREVJ-1:K=PREVK:M=PREVM
6210 LPRINT:LPRINT:LPRINT:RETURN
6220 FORK=X1 TO X3:LPRINT TAB(T1);:GOSUB 6240
6230 T1=T1+10:NEXT K:LPRINT:RETURN
6240 IF A(J,K)=0 THEN 6260
6250 IF ABS(A(J,K))>99999! OR ABS(A(J,K))<8.999999E-03 THEN 6270
6260 LPRINT USING "####.##";A(J,K);:RETURN
6270 LPRINT USING "##.##^####";A(J,K);:RETURN
6280 '
6290 ' Storage of data on disk file
6300 '
6310 CLS:LOCATE 8,1:PRINT STRING$(80,45)
6320 PRINT:PRINT "Sarva data files on disk ";
6330 PRINT:FILES "A:SARVA*.DAT":PRINT:PRINT STRING$(80,45):PRINT
6340 INPUT "Enter filename (without extension): ",FILE$
6350 OPEN "A:"+FILE$+".DAT" FOR OUTPUT AS #2
6360 PRINT#2,TITLE$:PRINT#2,N:WRITE#2,WATER
6370 WRITE#2,FLAG2:WRITE#2,FLAG3:WRITE#2,FLAG4
6380 FOR K=1 TO N:FOR J=1 TO 39:WRITE#2,A(J,K):NEXT J:NEXT K
6390 WRITE#2,ACC:WRITE#2,ACC(2):WRITE#2,FOS:CLOSE#2
6400 FLAG6=1:STATUS="e":F=1:M=1:FLAG17=0:GOTO 1950
6410 '
6420 ' Graphical display of geometry
6430 '
6440 SCREEN 1,1:COLOR 8,1:XA=0:XB=0:YA=0:YB=0
6450 JMIN=1:JMAX=5:DJ=2:KMIN=1:KMAX=N
6460 DK=N-1:GOSUB 6830:XMIN=MIN ' min x
6470 JMIN=1:JMAX=5:DJ=2:KMIN=1:KMAX=N
6480 DK=N-1:GOSUB 6910:XMAX=MAX ' max x

```



```

6490 JMIN=2:JMAX=6:DJ=2:KMIN=1:KMAX=N
6500 DK=1:GOSUB 6830:YMIN=MIN
6510 JMIN=2:JMAX=6:DJ=2:KMIN=1:KMAX=N
6520 DK=1:GOSUB 6910:YMAX=MAX
6530 XSC=270/(XMAX-XMIN):YSC=160/(YMAX-YMIN)
6540 IF XSC<YSC TREN 6560
6550 SC=YSC:GOTO 6570
6560 SC=XSC
6570 LNY=199
6580 XADJ=(319/SC-(XMAX-XMIN))/2
6590 YADJ=(199/SC-(YMAX-YMIN))/2
6600 XMIN=XMIN-XADJ:YMIN=YMIN-YADJ
6610 FOR K=1 TO N-1
6620 XA=(A(1,K)-XMIN)*SC:YA=LNY-(A(2,K)-YMIN)*SC
6630 XB=(A(1,K+1)-XMIN)*SC:YB=LNY-(A(2,K+1)-YMIN)*SC
6640 LINE (XA,YA)-(XB,YB),3
6650 XA=(A(5,K)-XMIN)*SC:YA=LNY-(A(6,K)-YMIN)*SC
6660 XB=(A(5,K+1)-XMIN)*SC:YB=LNY-(A(6,K+1)-YMIN)*SC
6670 LINE (XA,YA)-(XB,YB),3
6680 XA=(A(1,K)-XMIN)*SC:YA=LNY-(A(2,K)-YMIN)*SC
6690 XB=(A(5,K)-XMIN)*SC:YB=LNY-(A(6,K)-YMIN)*SC
6700 LINE (XA,YA)-(XB,YB),3
6710 XA=(A(3,K)-XMIN)*SC:YA=LNY-(A(4,K)-YMIN)*SC
6720 XB=(A(3,K+1)-XMIN)*SC:YB=LNY-(A(4,K+1)-YMIN)*SC
6730 LINE (XA,YA)-(XB,YB),1
6740 NEXT K
6750 XA=(A(1,N)-XMIN)*SC:YA=LNY-(A(2,N)-YMIN)*SC
6760 XB=(A(5,N)-XMIN)*SC:YB=LNY-(A(6,N)-YMIN)*SC
6770 LINE (XA,YA)-(XB,YB),3
6780 LOCATE25,9:PRINT "press any key to return";
6790 IF LEN(INKEY$)=0 THEN 6790
6800 FLAG27=0:SCREEN 0,0,0:WIDTH 80
6810 STATUS="e":FLAG6=1:F=1:M=1:GOTO 1950
6820 '
6830 ' Subroutine to find MIN in range
6840 '
6850 MIN=A(JMIN,KMIN)
6860 FOR J=JMIN TO JMAX STEP DJ
6870 FOR K=KMIN TO KMAX STEP DK
6880 IF MIN>A(J,K) THEN MIN=A(J,K)
6890 NBXT K:NEXT J:RETURN
6900 '
6910 ' Subroutine to find MAX in range
6920 '
6930 MAX=A(JMIN,KMIN)
6940 FOR J=JMIN TO JMAX STEP DJ
6950 FOR K=KMIN TO KMAX STEP DK
6960 IF MAX<A(J,K) THEN MAX=A(J,K)
6970 NEXT K:NEXT J:RETURN
6980 CLS:END

```

' min y
' max y
' scale factor

' center plot

' top surface

' failure surface

' slice sides

' water surface

' nth slice side

' reset screen
' return

Appendix 8

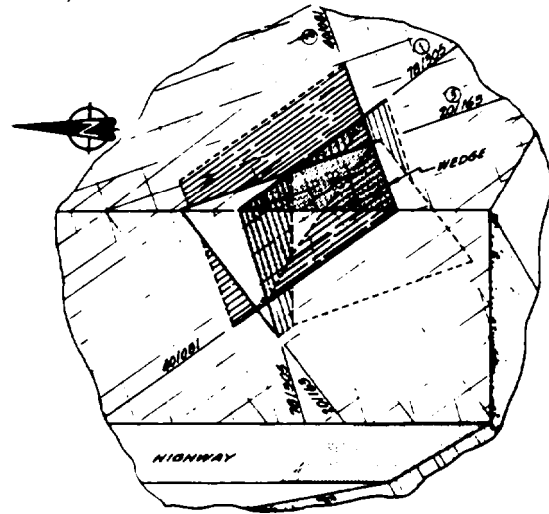
LIST OF PRACTICUMS

		<u>PAGE</u>
Practicum I :	Stereo plots of structural geology data	2
Practicum II:	Stability evaluation related to structural geology	9
Practicum III:	Analysis of direct shear strength test results	14
Practicum IV:	Analysis of point load test results	16
Practicum V:	Influence of geology and weather conditions on groundwater levels	16
Practicum VI:	Calculation of permeability from falling head test results	19
Practicum VII :	Plane failure - analysis and stabilization	20
Practicum VIII:	Wedge failure analysis	25
Practicum IX:	Circular failure analysis	26
Practicum X:	Toppling failure analysis	29
Practicum XI :	Blast design	31
Practicum XI I:	Design of controlled blasting pattern	52
Practicum XIII:	Control of damage from blast vibrations	33
Practicum XIV:	Plotting and interpretation of movement monitoring results	54

PRACTICUM I
Stereo plots of structural geology data

Given: A structural geology mapping program for a proposed highway produced the following results for the orientation of the fractures (format-diD/dio direction).

40/080
45/090
20/160
80/310
83/312
82/305
23/175
43/078
37/083
20/150
21/151
39/074
70/300
75/305
15/180
80/010
31/081



Required:

- (a) Plot the orientation of each fracture as a pole on a stereo-net using the equal area net and tracing paper provided.
- (b) Estimate and plot the position of the mean pole of each set of fractures.
- (c) Determine the maximum concentration of each set of poles using the Denness type B cell counting net.
- (d) Determine the angle between the mean poles with the steepest and shallowest dips.
- (e) Draw great circles of the three mean poles on a separate piece of tracing paper.
- (f) Determine the dip and trend of the line of intersection between the joint sets with the steepest and intermediate dip angles.

PRACTICUM I - SOLUTION
Stereo plots of structural geology data

Methods of plotting stereo plots are described in Chapter 3 of the manual.

(a) The poles of the 17 planes are plotted on Figure I-1 which shows that there are three sets of fractures.

(b) The mean pole of each of the three fracture sets is as follows:

Set 1 - 78/305
set 2 - 40/081
set 3 - 20/163

There is one pole (80/010) that does not belong to any of the three fracture sets.

(c) The maximum concentration of each set of poles is found using Figure 3.6 in the manual.

set 1 - 4 poles out of 17 poles = 24%
set 2 - 5 poles out of 17 poles = 29%
Set 3 - 4 poles out of 17 poles = 24%

A computer plot of this data is shown in Figures I-2a, b, c.

(d) The angles between the mean poles of joint sets 1 and 3 is determined by rotating the stereo-net until both mean poles lie on the same great circle. The number of divisions on this great circle is 94 degrees as shown by the dotted line on Figure I-1.

(e) The great circles of the three mean poles are plotted on Figure I-3.

(f) The dip and trend of the line of intersection of joint sets 1 and 2 is also shown on Figure I-3. The values are as follows:

Dip, θ_i = 27'
Dip direction, α_i = 029°

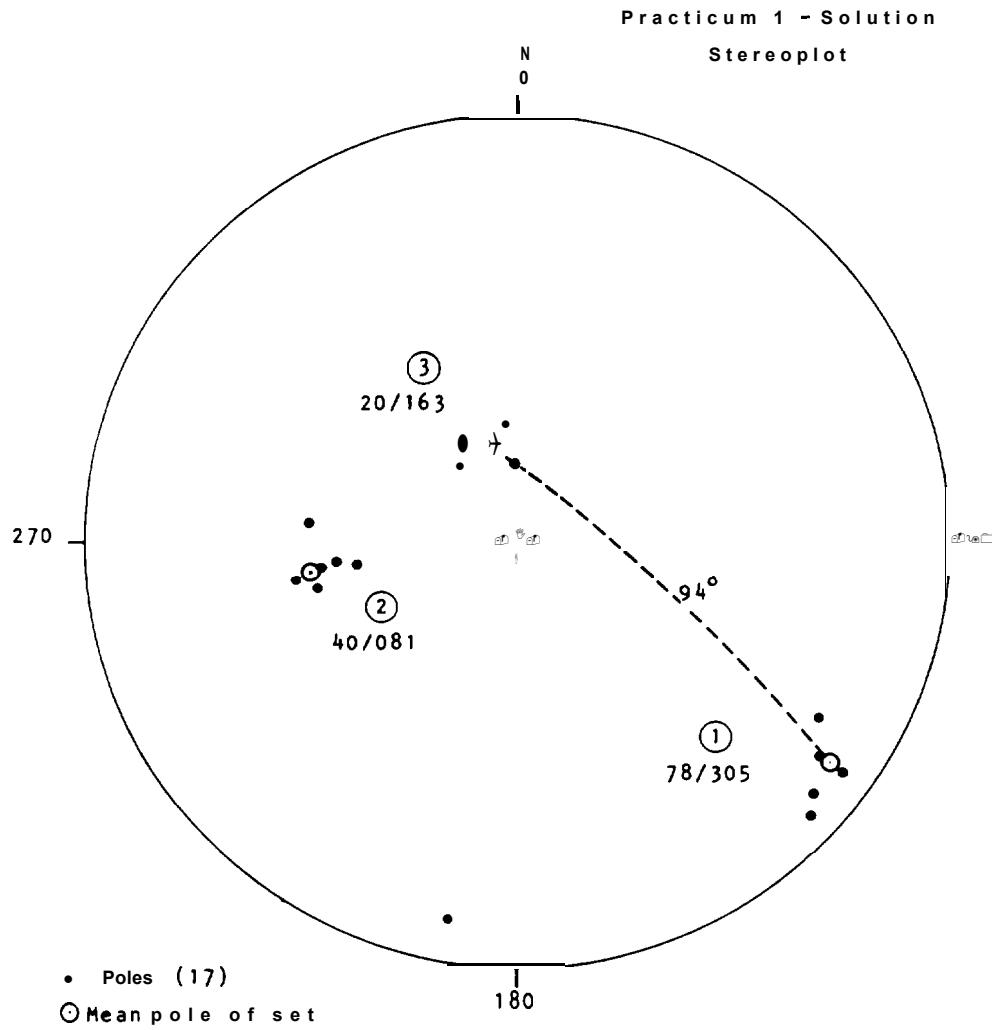


Figure 1.1: Plot of poles of structural mapping data.

0 80215860 -- FEDERAL HIGHWAY -- GEOLOGY DATA,
 TRAVERSE -- ALL DATA

HISTOGRAMS OF THE POLE ANGLES

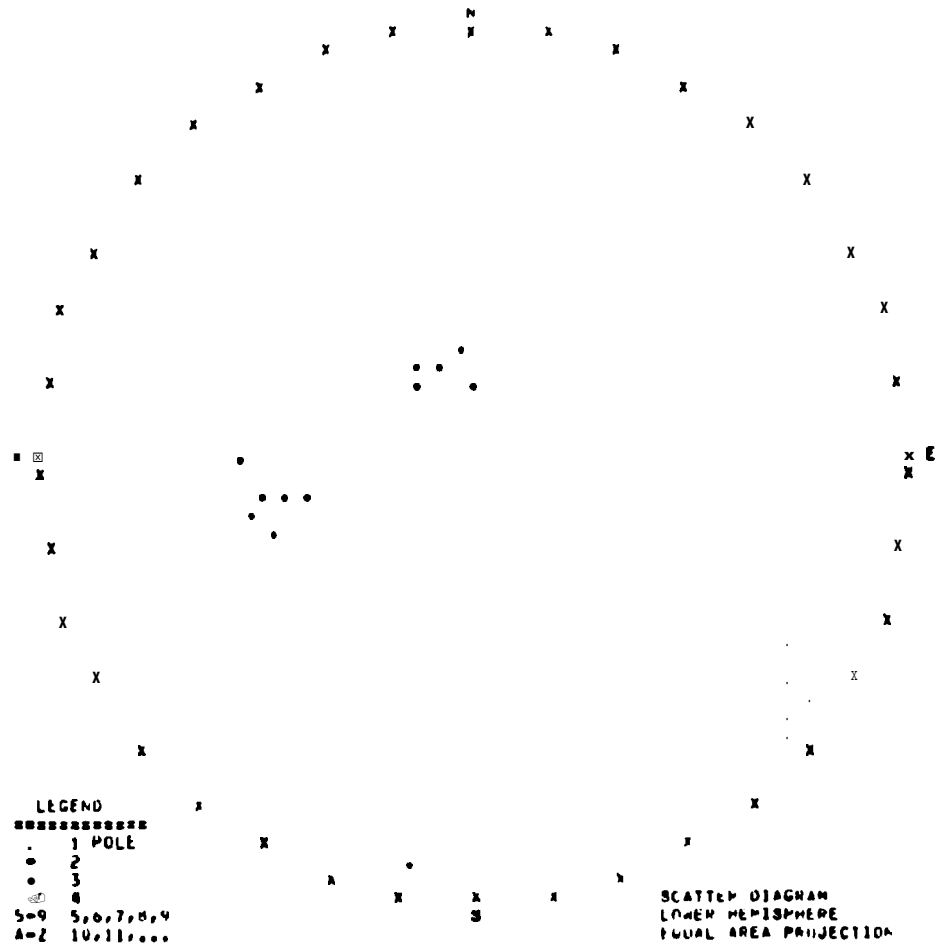
RANGE (DEGREES)	NUMBER OF POLES	DIP PERCENT OF TOTAL	CUMULATIVE NO. OF POLES	CUMULATIVE PERCENT
0 - 10	0	0.00	0	0.00
11 - 20	3	17.65	3	17.65
21 - 30	2	11.76	5	29.41
31 - 40	4	23.53	9	52.94
41 - 50	2	11.76	11	64.71
51 - 60	0	0.00	11	64.71
61 - 70	1	5.88	12	70.59
71 - 80	3	17.65	15	76.47
81 - 90	2	11.76	17	100.00

RANGE (DEGREES)	NUMBER OF POLES	DIP - DIRECTION PERCENT OF TOTAL	CUMULATIVE NO. OF POLES	CUMULATIVE PERCENT
0 - 10	1	5.88	1	5.88
11 - 20	1	0.00	1	5.88
21 - 30	1	0.00	1	5.88
41 - 40	0	0.00	1	5.88
51 - 60	0	0.00	1	5.88
61 - 70	0	0.00	1	5.88
71 - 80	0	0.00	1	5.88
81 - 90	3	17.65	4	23.53
91 - 100	0	0.00	7	41.18
101 - 110	0	0.00	7	41.18
111 - 120	0	0.00	7	41.18
121 - 130	0	0.00	7	41.18
131 - 140	0	0.00	7	41.18
151 - 160	1	5.88	8	47.06
161 - 170	2	11.76	10	58.82
171 - 180	0	0.00	10	58.82
181 - 190	2	11.76	12	70.59
191 - 200	0	0.00	12	70.59
201 - 210	0	0.00	12	70.59
211 - 220	0	0.00	12	70.59
221 - 230	0	0.00	12	70.59
231 - 240	0	0.00	12	70.59
241 - 250	0	0.00	12	70.59
251 - 260	0	0.00	12	70.59
261 - 270	0	0.00	12	70.59
271 - 280	0	0.00	12	70.59
281 - 290	0	0.00	12	70.59
291 - 300	1	5.88	13	76.47
301 - 310	3	17.65	16	94.12
311 - 320	1	5.88	17	100.00
321 - 330	0	0.00	17	100.00
331 - 340	0	0.00	17	100.00
341 - 350	0	0.00	17	100.00
351 - 360	0	0.00	17	100.00

Practicum I - Solution
 Stereoplots
 Figure I.2a

STEREO 8021586D -- FEDERAL HIGHWAY -- GEOLOGY DATA.
 TRAVERSE -- ALL DATA

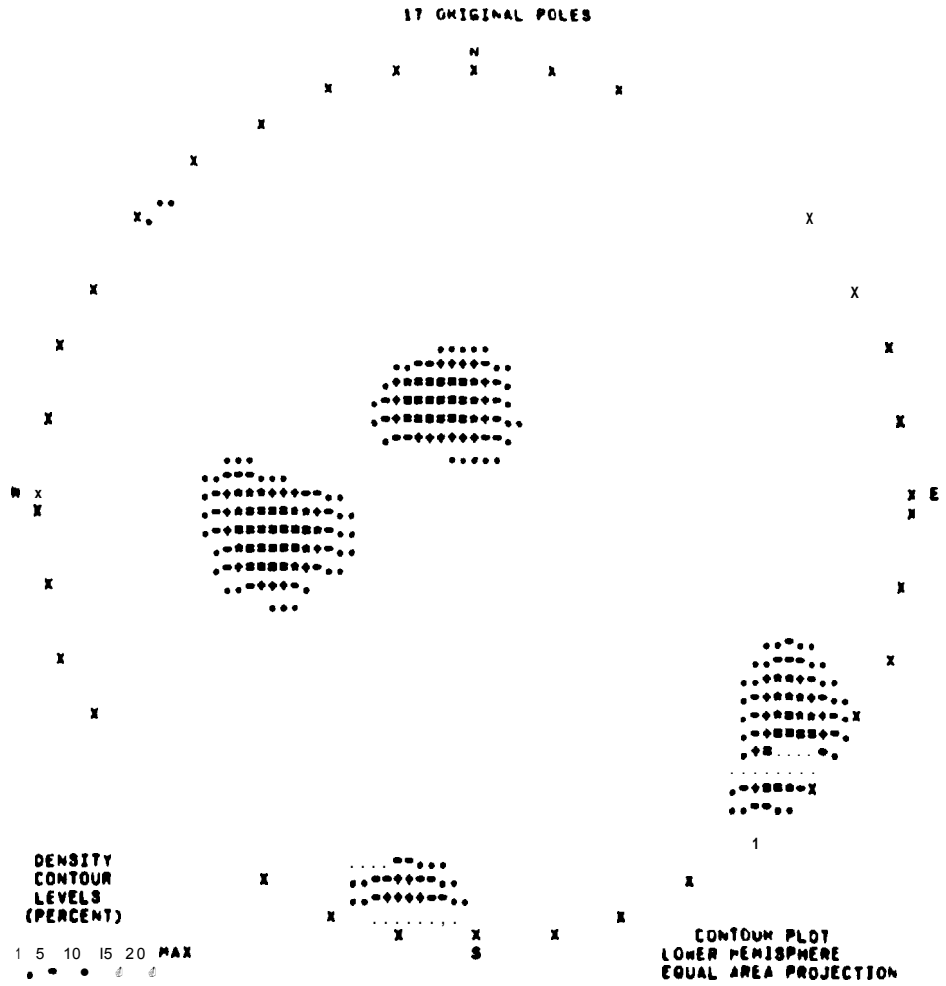
17 ORIGINAL POLES



Practicum I - Solution
 Stereoplots

Figure I.2b

STEREO 80215860 -- FEDERAL HIGHWAY -- GEOLOGY DATA.
TRAVERSE -- ALL DATA



Practicum I - Solution
Stereoplots

Figure I.2c

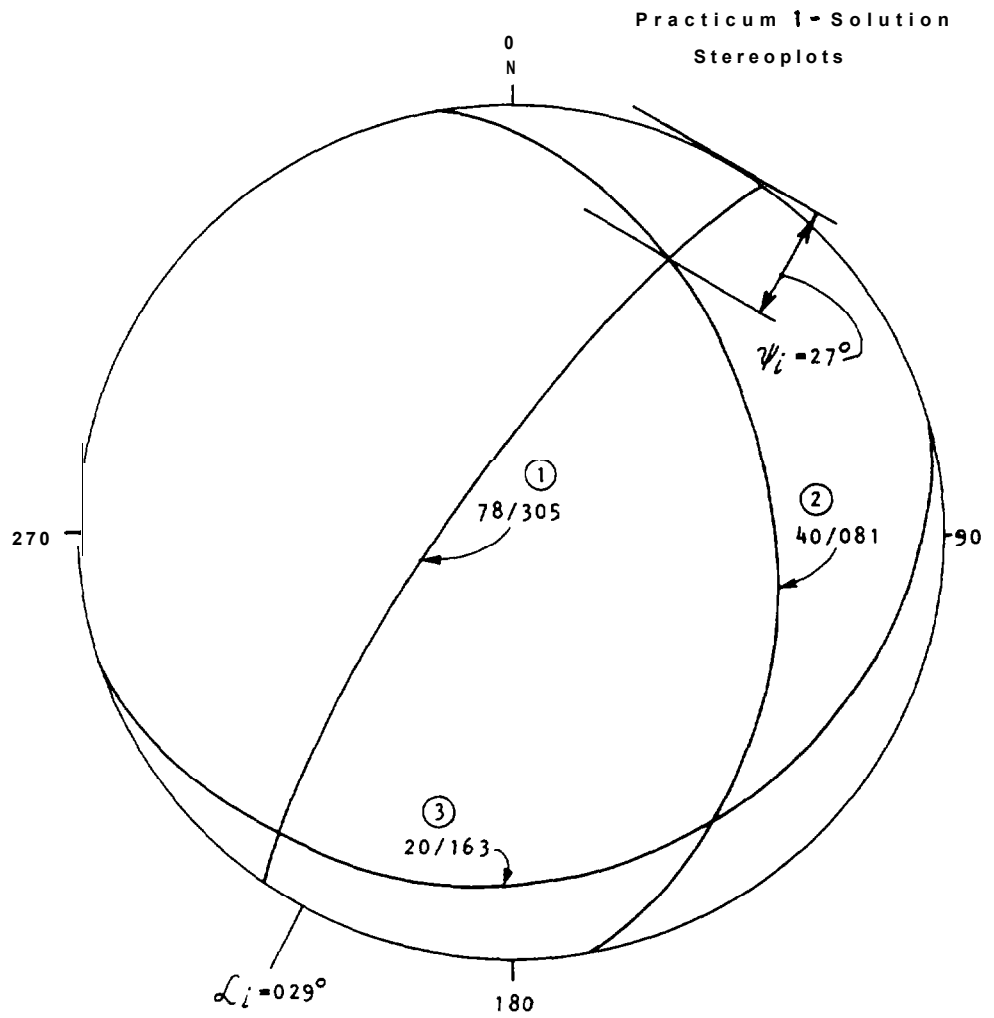


Figure 1.3: Great circles of mean poles. .





TABLE 2 (Continued)
 ROCK MASS CLASSES DETERMINED FROM TUNNELLING
 QUALITY INDEX (Q)

	Description
Less than 0.01	Exceptionally Poor
0.01 to 0.1	Extremely Poor
0.1 to 1	Very Poor
1 to 4	Poor
4 to 10	Fair
10 to 40	Good
40 to 100	Very Good
100 to 400	Extremely Good
More than 400	Exceptionally Good

TABLE 2 (Continued)
NGI CLASSIFICATION SYSTEM

c)	Squeezing rock, plastic flow of incompetent rock under the influence of high rock pressure.	SRF
N.	Mild squeezing rock pressure	5-10
O.	Heavy squeezing rock pressure	10-20
d)	Swelling rock, chemical swelling activity depending on presence of water	
P.	Mild swelling rock pressure	5-10
R.	Heavy swelling rock pressure	10-20

ADDITIONAL NOTES ON THE USE OF THESE TABLES

When making **estimates** of the rock mass **quality (Q)** the following guidelines should be followed, **in** addition to the notes listed in the tables:

- When **borehole** core is unavailable, **RQD** can be estimated from the number of joints per unit volume. In which the number of joints per metre for each **joint** set are added. A simple relation can be used to convert this number to **RQD** for the case of clay free rock masses:

$$RQD = 115 - 3.3J_v \text{ (approx.)}$$
 where J_v = total number of joints per m^3
 $(RQD = 100 \text{ for } J_v < 4.5)$
- The parameter J_n representing the number of joint sets will often be affected by **foliation**, schistosity, slaty cleavage or bedding etc. If strongly developed, these parallel "joints" should obviously be counted as a complete **joint** set. However, if there are few "joints" **visible**, or only occasional breaks in the core due to these features, then it will be more appropriate to count them as "random joints" when evaluating J_n .
- The parameters J_r and J_a (representing shear strength) should be relevant to the weakest significant **joint** set or clay filled **discontinuity** in the given zone. However, if the joint set or discontinuity **with** the minimum value of (J_r/J_a) is favourably oriented for **stability**, then a second, less favourably oriented joint set or **discontinuity** may sometimes be more **significant**, and its higher value of J_r/J_a should be used when evaluating **Q**. The value of J_r/J_a should in fact relate to the surface most likely to allow failure to initiate.
- When a rock mass contains clay, the factor SRF appropriate to **loosening** loads should be evaluated. In such cases, the strength of the intact rock is of little interest. However, when jointing is **minimal** and clay is completely absent the strength of the intact rock may become the weakest link, and the stability will then depend on the rock-stress/rock-strength. A strongly **anisotropic** stress field **is** unfavourable for stability and is roughly accounted for as in note 2 in the table for stress **reduction** factor evaluation.
- The compressive and tensile strengths (σ_c and σ_t) of the intact rock should be evaluated in the saturated condition if this **is appropriate** to **present** or future in situ **conditions**. A very conservative estimate of strength should be made for those rocks that deteriorate when exposed to moist or saturated **conditions**.

TABLE 2 (Continued)

NGI CLASSIFICATION SYSTEM

	J_w	approx. water pressure (Kgf/cm ²)		
5. JOINT WATER REDUCTION FACTOR				
A. Dry excavations or minor inflow, i.e. < 5 lit/min. locally.	1.0	< 1.0		
B. Medium inflow or pressure, occasional outwash of joint fillings	0.66	1.0 - 2.5	1. Factors C to F are crude estimates. Increase J_w if drainage measures are installed.	
C. Large inflow or high pressure in competent rock with unfilled joints	0.5	2.5 - 10.0		
O. Large inflow or high pressure, considerable outwash of fillings	0.33	2.5 - 10.0		
E. Exceptionally high inflow or pressure at blasting. decaying with time.	0.2 - 0.1	> 10	2. Special problems caused by ice formation are not considered.	
F. Exceptionally high inflow or pressure continuing without decay	0.1 - 0.05	> 10		
6. STRESS REDUCTION FACTOR				
a) Weakness zones are intersecting excavation, which may cause loosening of rock mass when tunnel is excavated.				
			SRF	
A. Multiple occurrences of weakness zones containing clay or chemically disintegrated rock, very loose surrounding rock (any depth)		10.0	1. Reduce these values of SRF by 25 - 50% if the relevant shear zones only influence, but do not intersect the excavation.	
B'. Single weakness zones containing clay, or chemically disintegrated rock (excavation depth < 50 m)		5.0		
C. Single weakness zones containing clay, or chemically disintegrated rock (excavation depth > 50 m)		2.5		
D. Multiple shear zones in competent rock (clay free), loose surrounding rock (any depth)		7.5		
E. Single shear zones in competent rock (clay free), (depth of excavation < 50 m)		5.0	2. For strongly anisotropic virgin stress field (if measured): when $5 \leq \sigma_1/\sigma_3 \leq 10$, reduce σ_c to $0.8\sigma_c$ and σ_t to $0.8\sigma_t$. When $\sigma_1/\sigma_3 > 10$, reduce σ_c and σ_t to $0.6\sigma_c$ and $0.6\sigma_t$, where σ_c = unconfined compressive strength, and σ_t = tensile strength (point load) and σ_1 and σ_3 are the major and minor principal stresses.	
F. Single shear zones in competent rock (clay free), (depth of excavation > 50 m)		2.5		
G. Loose open joints, heavily jointed or 'sugar cube' (any depth)		5.0		
b. Competent rock, rock stress problems			SRF	
H. Low stress, near surface	>200	>13	2.5	
J. Medium stress	200-10	13-0.66	1.0	
K. High stress, very tight structure (usually favourable to stability, may be unfavourable for wall stability)	10-5	0.66-0.33	0.5-2	3. Few case records available where depth of crown below surface is less than span width. Suggest SRF increase from 2.5 to 5 for such cases (see H).
L. Mild rock burst (massive rock)	5-2.5	0.33-0.16	5-10	
M. Heavy rock burst (massive rock)	< 2.5	< 0.16	10-20	

TABLE 2 (Continued)
NGI CLASSIFICATION SYSTEM

4. JOINT ALTERATION NUMBER	Ja	ϕ_r (approx.)	
a. Rock wall contact.			
A. Tightly healed, hard, non-softening, impermeable filling	0.75	-	
B. Unaltered joint walls, surface staining only	1.0	(25° - 35°)	
C. Slightly altered joint walls non-softening mineral coatings, sandy particles, clay-free disintegrated rock, etc.	2.0	(25° - 30°)	1. Values of ϕ_r , the residual friction angle, are intended as an approximate guide to the mineralogical properties of the alteration products, if present.
D. Silty- , or sandy-clay coatings, small clay-fraction (non-softening)	3.0	(20° - 25°)	
E. Softening or low friction clay mineral coatings, I.e. Kaolinite, mica . Also chlorite, talc, gypsum and graphite, etc., and small quantities of swelling clays. (Discontinuous coatings, 1-2 mm or less in thickness.)	4.0	(8' - 16°)	
b) Rock wall contact before 10 cms shear.			
F. Sandy particles, clay-free disintegrated rock, etc.	4.0	(25° - 30°)	
G. Strongly over-consolidated, non-softening clay mineral fillings (continuous. < 5 mm thick).	6.0	(16° - 24°)	
H. Medium or low over-consolidation softening, clay mineral fillings (continuous. < 5 mm thick).	8.0	(12° - 16°)	
J. Swelling clay fillings, i.e. montmorillonite (continuous, < 5 mm thick). Values of Ja depend on percent of swelling clay-size particles , and access to water.	8.0 - 12.0	(6' - 12°)	
c) No rock wall contact when sheared.			
K. Zones or bands of disintegrated	6.0		
L. or crushed rock and clay (see 6,	8.0		
M. H and J for clay conditions).	8.0 - 12.0	(6° - 24°)	
N. Zones or bands of silty- or sandy-clay, small clay fraction, (non-softening).	5.0		
O. Thick, continuous zones or	10.0 - 13.0		
P. bands of clay (see G, H, and	13.0 - 20.0	(6° - 24°)	
R. J for clay conditions).			

TABLE 2

NGI CLASSIFICATION SYSTEM

Description	Value	Notes
1. ROCK QUALITY DESIGNATION	RQD	
A. Very Poor	0 - 25	1. Where RQD is reported or measured as ≤ 10 (including 0), a nominal value of 10 is used to evaluate Q . 2. RQD intervals of 5, i.e. 100, 95, 90, etc., are sufficiently accurate.
B. Poor	25 - 50	
C. Fair	50 - 75	
D. Good	75 - 90	
E. Excellent	90 - 100	
2. JOINT SET NUMBER	J_n	
A. Massive, no or few joints	0.5 - 1.0	
B. One joint set	2	
C. One joint set plus random	3	
D. Two joint sets	4	
E. Two joint sets plus random	6	
F. Three joint sets	9	1. For intersections use $13.0 \times J_n$
G. Three joint sets plus random	12	2. For portals use $(2.0 \times J_n)$
H. Four or more joint sets, random, heavily jointed 'sugar cube', etc.	15	
J. Crushed rock, earthlike	20	
3. JOINT ROUGHNESS NUMBER	J_r	
a) Rock wall contact and b) Rock wall contact before 10 cms shear.		
A. Discontinuous joints	4	
B. Rough or irregular, undulating	3	
C. Smooth, undulating	2	
D. Slickensided, undulating	1.5	1. Add 1.0 if the mean spacing of the relevant joint set is greater than 3 m.
E. Rough or irregular, planar	1.5	
F. Smooth, planar	1.0	
G. Slickensided, planar	0.5	2. $J_r = 0.5$ can be used for planar, slickensided joints having lineations provided the lineations are orientated for minimum strength.
c) No rock wall contact when sheared.		
H. Zone containing clay minerals thick enough to prevent rock wall contact.	1.0	
J. Sandy, gravelly or crushed zone thick enough to prevent rock wall contact	1.0	

TABLE I - CSIR GEOMECHANICS CLASSIFICATION OF JOINTED ROCK MASSES
A. CLASSIFICATION PARAMETERS AND THEIR RATINGS

PARAMETER		RANGES OF VALUES							
1	Strength of intact rock material	Point load strength index	> 8 MPa	4-8 MPa	2-4 MPa	1-2 MPa	For this low range - uniaxial compressive test is preferred		
		Uniaxial compressive strength	> 200 MPa	100 - 200 MPa	50 - 100 MPa	25 - 50 MPa	10-25 MPa	3-10 MPa	1-3 MPa
	Rating	15	12	7	4	2	1	0	
2	Drill core quality RQD	90% - 100%	75% - 90%	50% - 75%	25% - 50%	< 25%			
	Rating	20	17	13	8	3			
3	Spacing of joints	> 3m	1-3m	0.3-1m	50 - 300 mm	< 50 mm			
	Rating	30	25	20	10	5			
4	Condition of joints	Very rough surfaces Not continuous No separation Hard joint wall rock	Slightly rough surfaces Separation < 1mm Hard joint wall rock	Slightly rough surfaces Separation < 1mm Soft joint wall rock	Slickensided surfaces Gauge < 5 mm thick or Joints open 1-5mm Continuous joints	Soft gauge > 5mm thick or Joints open > 5mm Continuous joints			
	Rating	25	20	12	6	0			
5	Ground water	Inflow per 10m tunnel length	None		< 25 litres/min	25 - 125 litres/min	> 125 litres/min		
		Ratio $\frac{\text{joint water pressure}}{\text{major principal stress}}$	OR		OR	OR	OR		
	General conditions	OR		OR	OR	OR			
	Rating	OR		OR	OR	OR			
		0	0.0 - 0.2	0.2 - 0.5	> 0.5				
		OR	OR	OR	OR	OR			
		Completely dry	Moist only (interstitial water)		Water under moderate pressure	Severe water problems			
		OR	OR	OR	OR	OR			
		10	7	4	0				

B. RATING ADJUSTMENT FOR JOINT ORIENTATIONS

Strike and dip orientations of joints		Very favourable	Favourable	Fair	Unfavourable	Very unfavourable
Ratings	Tunnels	0	-2	-5	-10	-12
	Foundations	0	-2	-7	-15	-25
	Slopes	0	-5	-25	-50	-60

C. ROCK MASS CLASSES DETERMINED FROM TOTAL RATINGS

Rating	100-81	80-61	60-41	40-21	< 20
Class No	I	II	III	IV	V
Description	Very good rock	Good rock	Fair rock	Poor rock	Very poor rock

the orientations of many types of excavation can be, and normally are, adjusted to avoid the maximum effect of unfavorably oriented major joints. However, this choice is not available in the case of tunnels, and more than half the case records were in this category. The parameters J_n , J_r and J_a appear to play a more important general role than orientation, because the number of joint sets determines the degree of freedom for block movement (if any), and the frictional and dilational characteristics can vary more than the down-dip gravitational component of unfavorably oriented joints. If joint **orientation** had been **included**, the classification would have been less general, and its essential simplicity **lost**".

The general relationship of qualitative rock classes to the value of Q are presented on Table 2.

several times this size and the smallest fragments less than half the size. (Clay particles are of course excluded.)

The second quotient (J_r/J_a) represents the roughness and frictional characteristics of the joint walls or filling materials. This quotient is weighted in favor of rough, unaltered joints in direct contact. It is to be expected that such surfaces will be close to peak strength, and that they will therefore be especially favorable to tunnel stability. When rock joints have thin clay mineral coatings and fillings, the strength is reduced significantly. Nevertheless, rock wall contact after small shear displacements have occurred may be a very important factor for preserving the excavation from ultimate failure. Where no rock wall contact exists, the conditions are extremely unfavorable to tunnel stability. The "friction angles" given in Table 2 are slightly below the residual strength values for most clays, and are possibly downgraded by the fact that these clay bands or fillings may tend to consolidate during shear, at least if normally consolidated or if softening and swelling has occurred. The swelling pressure of montmorillonite may also be a factor here.

The third quotient (J_w/SRF) consists of two stress parameters. SRF is a measure of:

- (1) loosening load in the case of an excavation through shear zones and clay bearing rock,
- (2) rock stress in competent rock, and
- (3) squeezing loads in plastic incompetent rocks.

It can be regarded as a total stress parameter. The parameter J_w is a measure of water pressure, which has an adverse effect on the shear strength of joints due to a reduction in effective normal stress. Water may, in addition, cause softening and possible outwash in the case of clay-filled joints. It has proved impossible to combine these two parameters in terms of interblock effective normal stress, because paradoxically a high value of effective normal stress may sometimes signify less stable conditions than a low value, despite the higher shear strength. The quotient (J_w/SRF) is a complicated empirical factor describing the "active stresses".

It appears that the rock tunneling quality Q can now be considered as a function of only three parameters which are crude measures of:

- (1) block size (RQD/J_n)
- (2) interblock shear strength (J_r/J_a)
- (3) active stress (J_w/SRF)

Undoubtedly, there are several other parameters which could be added to improve the accuracy of the classification system. One of these would be joint orientation. Although many case records include the necessary information on structural orientation in relation to excavation axis, it was not found to be the important general parameter that might be expected. Part of the reason for this may be that

Appendix 9 Rock mass classification systems

Introduction

Rock mass classification systems have been developed in order to relate the performance of excavations made in different rock masses. These empirical systems quantify those factors which affect the performance of rock which are then combined to produce a rating number. The relationship between this rating number and the strength of the rock mass is given in Table IV on page 5.26.

The two most widely used classification systems are those developed by the Council for Scientific and Industrial Research (CSIR) in South Africa and the Norwegian Geotechnical Institute (NGI). These systems are described on the following pages:

CSIR Classification

The CSIR Geomechanics Classification for jointed rock masses, by Bieniawski, considers the strength of the intact rock, RQD, joint condition, and groundwater conditions. It recognizes that each parameter does not necessarily contribute equally to the behavior of the rock mass. Bieniawski therefore applied a series of importance ratings to his parameters. A number of points or a rating is allocated to each range of values for each parameter and an overall rating for the rock mass is arrived at by adding the ratings for each of the parameters. Table 1 presents the CSIR system including the rating adjustment for joint orientation (Part B) and qualitative descriptions for each rock class (Part C).

In applying data to the CSIR system, the following parameter classifications are used:

Intact rock strength
Joint spacing
Effect of joint orientations

NGI Classification

Barton, Lien and Lunde of the Norwegian Geotechnical Institute (NGI) proposed an index (Q) for the determination of the tunnelling quality of a rock mass from an evaluation of a large number of case histories. The numerical value of this index Q is defined by:

$$Q = \frac{RQD}{J_n} \times \frac{J_r}{J_a} \times \frac{J_w}{SRF}$$

and the definition of these parameters is presented in Table 2.

In explaining how they arrived at the equation used to determine the index Q, Barton, Lien and Lunde offer the following comments:

"The first quotient (RQD/J_n), representing the structure of the rock mass, is a crude measure of the block or part it is size, with the two extreme values (100/0.5 and 10/20) differing by a factor of 400. If the quotient is interpreted in units of centimeters, the extreme "particle sizes" of 200 to 0.5 cm are seen to be crude but fairly realistic approximations. Probably the largest blocks should be



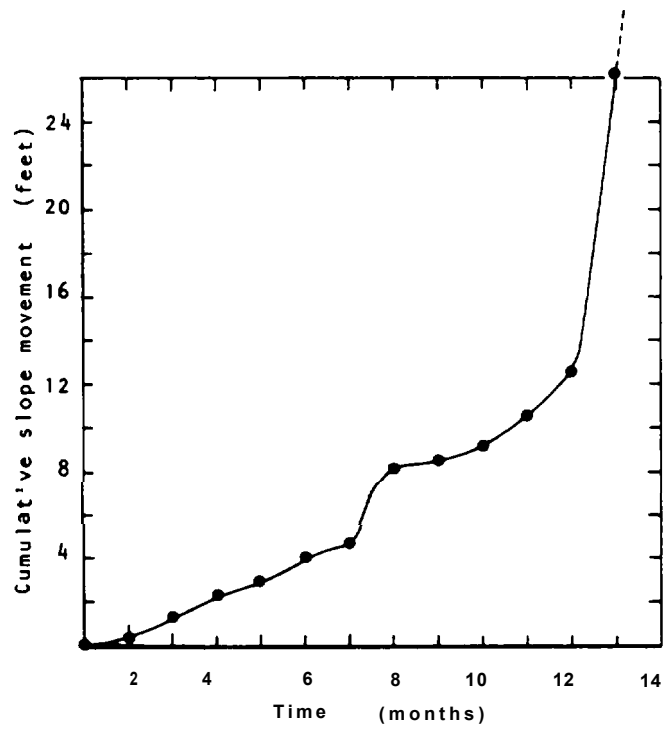


Figure XIV.1: Slope movement monitoring.

PRACTICUM XIV
Plotting and interpreting movement monitoring results

In order to obtain a warning of failure of a potentially unstable slope, a surface movement monitoring system has been set up using EDM equipment. The distances between the base station and the fastest moving prism measured at monthly intervals with this equipment on the slope are as follows:

<u>Month</u>	<u>Distance</u>
	822.83
2	822.51
3	821.52
4	820.54
5	819.92
6	818.82
7	818.24
8	814.63
9	814.30
10	813.65
11	812.34
12	810.37
13	796.59

Required:

Plot the slope movement against time to determine the months in which acceleration occurs and the onset of slope failure.

PRACTICUM XIV - SOLUTION
Plotting and interpreting movement monitoring results

The data for the cumulative slope movement against time is as follows:

<u>Month</u>	<u>Distance</u>
1	0
2	0.32
3	1.31
4	2.29
5	2.91
6	4.01
7	4.59
8	8.20
9	8.53
10	9.18
11	10.49
12	12.46
13	26.24

A plot of this data is shown on Figure XIV-1. This plot shows that acceleration occurs in months 8 and 12 and that the onset of failure occurs in month 13.

PRACTICUM XIII
Blast damage control

Given: A rock slope for a highway is to be excavated by blasting. An unlined railroad tunnel runs parallel to and 150 ft. from the center of the rock to be blasted and it is imperative that there be no damage to the tunnel. At one end of the tunnel there is some sensitive electrical switching equipment that must also be protected from blast vibration damage.

Required:

- (a) Determine the maximum allowable charge weight per delay to assure that the blast vibrations are below the damage threshold values for the tunnel and the electrical equipment.
- (b) If the blast hole diameter is 51 mm (2 inches), would it be necessary to protect the electrical equipment from flyrock damage?

PRACTICUM XIII - SOLUTION
Blast damage control

Methods of controlling blast damage are described in the third part of Chapter 11.

- (a) Allowable charge weights per delay are determined from damage threshold vibration levels for different structures listed on page 11.37 and from equation (124) on page 11.34. The equation for the allowable charge weight per delay is:

$$V = k(R/\sqrt{W})^n$$

If $k = 200$ and $n = -1.5$ and the threshold for rock falls in unlined tunnels is 12 in/sec., then at $R = 150$ ft., the allowable instantaneous charge is:

$$W = 530 \text{ lb/delay}$$

If the threshold for damage to the electrical equipment is 0.5 in/sec., the allowable instantaneous charge is:

$$W = 7\text{-}1/2 \text{ lb/delay}$$

Note: Figure 11.16 can also be used to determine allowable charge weights.

- (b) From Figure 11.18 boulders as big as 3 ft. (1 m) in diameter could be thrown 150 ft. (45 m) when using a 2 inch (51 mm) diameter drill hole. Therefore, the electrical equipment should be protected from flyrock with blast mats.

PRACTICUM XI I
Control led blasting design

Given: A 20 ft. high slope has been excavated for a highway by blasting and in one section, where the rock is weak, it is required that the face be trimmed back by 8 ft. It is necessary that control led blasting be used for this trimming operation to ensure there is no overbreak and that the new face is stable.

Required:

- (a) What is the most appropriate type of controlled blasting for this operation?
- (b) If the diameter of the blast holes is 2-1/2 inches, what hole spacing and explosive charge (lb/ft. of hole) should be used for the final line of holes?
- (c) If the only explosive available has a diameter of 1 inch and a specific gravity of 1.1, determine how the explosive can be distributed in the hole to achieve the required charge.
- (d) Is it necessary that a second row of blast holes be drilled between the present face and the final line? If this is necessary, how far should this row be from the final line and what detonation sequence should be used?

PRACTICUM XI I - SOLUTION
Controlled blasting design

Methods of controlled blasting are described in the second part of Chapter 11.

- (a) Cushion blasting should be used to remove the 8 ft. thick slice of rock. In highway construction, it is rarely necessary to use line drilling because it is expensive and is only used where very high quality slopes are required. Preshearing would be used where the burden is about equal to the cut height. Refer to Figures 11.8, 11.10, and 11.12 for typical hole layouts.
- (b) For a hole diameter of 2-1/2 inches in weak rock, a spacing of 3 ft. and an explosive load of 0.1 lb/ft. should be used (see Table VII).
- (c) The weight per foot of the diameter explosive is calculated as follows;

$$\begin{aligned} \text{Weight/ft.} &= \text{density} \times \text{area} \\ &= 1.1 \times 62.4 \times \pi (\text{diameter})^2/4 \\ &= 0.37 \text{ lb/ft.} \end{aligned}$$

Because the required charge is 0.1 lb/ft., spacers must be used between sticks of explosive to distribute the charge uniformly up the hole. A suitable charge would be 4 inch long sticks separated by 8 inch long spaces.

- (d) Table VI I shows that the burden between the final line and the next row of holes should be 4 ft. Therefore, a row of holes should be drilled midway between the face and the final line. This row would be detonated before the final line and the final line would be detonated on a single delay.

PRACTICUM XI
Blast design

Given: A 20 ft. high rock bench is to be excavated by blasting. The blast holes will be 2-1/2 inches in diameter and the explosive to be used has a specific gravity of 1.3 and is available in diameter of 1-1/2 inches and 2 inches. The broken rock will be mucked by a front-end loader with a maximum vertical reach of 16 ft.

Required:

- (a) Determine a suitable blast hole pattern, i.e. the burden spacing and length of the holes.
- (b) Determine the depth of subgrade drilling required.
- (c) Determine a suitable specific charge (lb/yd³), from Figure 11.5 in the manual, and the required explosive load per hole.
- (d) Determine the length of explosive column so that the length of unloaded hole is approximately equal to the burden.

PRACTICUM XI - SOLUTION
Blast design

Methods of blast design are described in Chapter 11.

- (a) This bench can be blasted in a single lift because most percussion drills can drill to a depth of 20 ft. with good directional control and penetration rate and it would not be dangerous for the loader to dig a 20 ft. high muck pile.

From Figure 11.5 a burden of about 7 ft. will produce maximum boulder sizes of about 3 ft. which can be readily handled by a loader. If the spacing/burden ratio is 1.25, the spacing is:

$$\begin{aligned}\text{Spacing} &= 7 \times 1.25 \\ &= 9 \text{ ft.}\end{aligned}$$

- (b) The subgrade depth is usually about one-third of the burden, so the holes should be drilled about 2.5 ft. below the required first grade. Therefore, the required hole depth is 22.5 ft.
- (c) From Figure 11.5, a powder factor of 0.6 lb/yd³ will produce the required fragmentation at a burden of 7 ft. The explosive load per hole is calculated as follows:

$$\begin{aligned}\text{Volume of rock per hole} &= 20 \times 7 \times 9/27 \\ &= 46.7 \text{ cu.yd.}\end{aligned}$$

$$\begin{aligned}\text{Explosive per hole} &= 46.7 \times 0.6 \\ &= 28 \text{ lb.}\end{aligned}$$

- (d) The weight of explosive per foot of drill hole is calculated as follows:

$$\begin{aligned}\text{Weight/ft.} &= \text{density} \times \text{area} \\ &= 1.3 \times 62.4 \times \frac{\pi}{4} (\text{explosive diameter})^2 \\ &= 1.77 \text{ lb/ft.} - 2 \text{ inch diameter explosive} \\ &= 1.0 \text{ lb/ft.} - 1\text{-}1/2 \text{ inch diameter explosive}\end{aligned}$$

The length of explosive column is calculated as follows:

$$\begin{aligned}\text{Column length} &= \text{explosive weight/weight per ft.} \\ &= 16 \text{ ft.} - 2 \text{ inch diameter explosive} \\ &= 28 \text{ ft.} - 1\text{-}1/2 \text{ inch diameter explosive}\end{aligned}$$

Because the required length of unloaded hole is 7 ft., i.e. equal to the burden, the 2 inch diameter explosive would be used. The unloaded length for 2 inch explosive is $22.5 - 16 = 6.5$ ft.

PRACTICUM X - SOLUTION
Toppling failure analysis

10. Methods of analysis of toppling failure are described in Chapter

(a) The factor against sliding is determined by the methods described in Chapter 7; the equation for a dry slope is:

$$F = \frac{C.A + W \cos \alpha \cdot \tan \phi}{W \sin \alpha}$$

$$= 2.0$$

where: A = base area of block
 = 6 ft.
 W = weight of block/ft.
 = 150 x 6 x 20
 = 18,000 lb/ft.

(b) From the dimensions given on Figure X-1, the following values are obtained to test stability conditions.

$$Y/\Delta x = 3.3$$

$$\cot 15 = 3.7$$

The block is just stable because $3.3 < 3.7$.

(c) If a further 0.4 ft. of erosion of the fault occurs, toppling is likely to occur because $Y/\Delta x = 20/5.6 = 3.6$.

(d) Stabilization measures which could be used on this slope include:

Filling the tension crack with clay to prevent infiltration of water and build-up of water pressure both in the tension crack and on the fault at the base.

Application of shotcrete to the fault to prevent further erosion.

Blasting to flatten the slope angle and reduce the dimension Y.

PRACTICUM X
Toppling failure analysis

Given: A 20 ft. high natural slope with an overhanging face at an angle of 75 degrees exists above a highway. There is a fault, with a dip angle of 15 degrees towards the highway, at the toe of this slope which is weathering and undercutting the face. A tension crack has developed behind the crest of the slope indicating that the face is marginally stable (Figure X-1). The friction angle (ϕ) of the fault is 20 degrees and the cohesion (C) is 500 psf. The slope is dry.

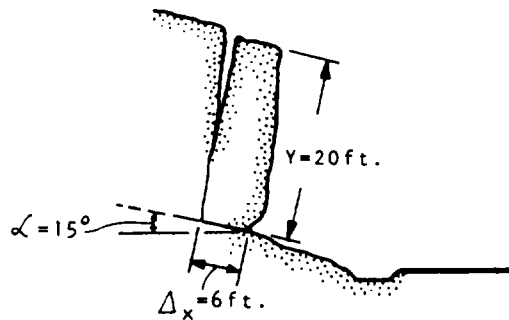


Figure X.1: Toppling failure.

Required:

- (a) Calculate the factor of safety of the block against sliding if the density of the rock is 150 lb/cu.ft.
- (b) Is the block stable against toppling as defined by the relation:

$$Y/\Delta x < \cot\alpha - \text{stable}$$
- (c) How much more erosion of the fault must occur before failure occurs?
- (d) What stabilization measures would be appropriate for this slope?

This shows that the slope height must be reduced by 22 ft. by unloading the crest to increase the factor of safety from 1.0 to 1.3. Note that this would only be correct if the groundwater level dropped by an equivalent amount.

- (d) The critical failure circle and critical tension crack for a slope with groundwater present are located using the graphs in Figure 9.5b.

For a slope angle of 60 degrees and a friction angle of 30 degrees, the coordinates of the center of the circle are:

$$x = 0.35.H$$

$$= -24.5 \text{ ft.}, \text{ i.e. } 24.5 \text{ ft. horizontally beyond the toe}$$

$$Y = H$$

$$= 70 \text{ ft. i.e. } 70 \text{ ft. above the toe}$$

The location of the tension crack behind the crest is:

$$b/H = 0.13$$

$$b = 9.1 \text{ ft.}$$

This critical circle is shown in Figure IX-2.

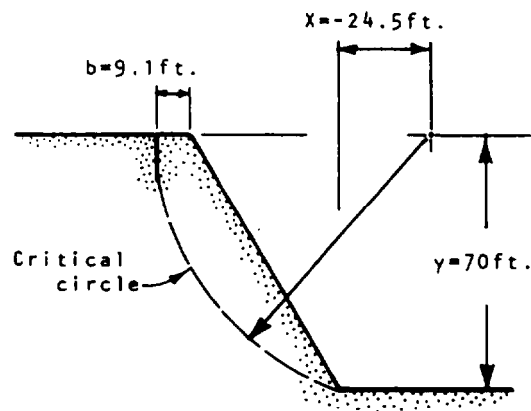


Figure IX-2 Position of Critical Circle and Critical Tension Crack

PRACTICUM IX - SOLUTION
Circular failure analysis

9. Method of analysis of circular failures is described in Chapter

- (a) The groundwater level shown in Figure IX-1 corresponds to groundwater condition 3 on page 9.9 in the manual, so chart number 3 on page 9.11 is used in the analysis.

$$\text{When } \phi = 30' \text{ and } F = 1, \tan \phi/F = 0.58$$

The intersection of this value for $\tan \phi/F$ and the curve for slope angle of 60 degrees gives:

$$C/\gamma HF = 0.086$$

$$\begin{aligned} \text{Limiting cohesion, } C &= 0.086 \times 160 \times 70 \times 1.0 \\ &= \underline{963 \text{ psf}} \end{aligned}$$

- (b) If the slope were completely drained, failure chart 1 would be used for the analysis.

$$\begin{aligned} C/\gamma H \tan \phi &= 963/160.70 \cdot \tan 30 \\ &= 0.15 \end{aligned}$$

The intersection of this inclined line with the curved line for a slope angle of 60 degrees gives:

$$\tan \phi/F = 0.52$$

$$F = \frac{\tan 30}{0.52}$$

$$= 1.11$$

This factor of safety is less than that usually accepted for a temporary slope, i.e. $F = 1.2$, so draining the slope would not be an effective means of stabilization.

- (c) When $F = 1.3$ and $\phi = 30^\circ$, then $\tan \phi/F = 0.44$

On chart number 3 the intersection of this horizontal line with the curved line for a slope angle of 60 degrees gives:

$$c/\gamma HF = .096$$

$$H = \frac{963}{160 \times 1.3 \times 0.096}$$

$$= 48 \text{ ft.}$$

PRACTICUM IX
Circular failure analysis

Given: A 70 ft. high rock cut with a face angle of 60 degrees has been excavated in highly weathered granitic rock. A tension crack has opened behind the crest and it is likely that the slope is on the point of failure, i.e. the factor of safety is approximately 1.0. The friction angle of the material is estimated to be 30 degrees, its density is 160 lb/cu.ft., and the position of the water table is shown on the sketch of the slope (Figure IX-1). The rock contains no continuous joints and the most likely type of failure mode is a circular failure.

Required:

- (a) Do a back-analysis of the failure to determine the limiting value of the cohesion when the factor of safety is 1.0.
- (b) Using the strength parameters calculated in question (a), determine the factor of safety for a completely drained slope. Would drainage of the slope be a feasible method of stabilization.
- (c) Using the groundwater level shown in Figure IX-1 and the strength parameters calculated in question (a), calculate the reduction in slope height, i.e. amount of unloading of the slope crest required to increase the factor of safety to 1.3.
- (d) For the slope geometry and groundwater level shown in Figure IX-1, find the coordinates of the center of the critical circle and the position of the critical tension crack.

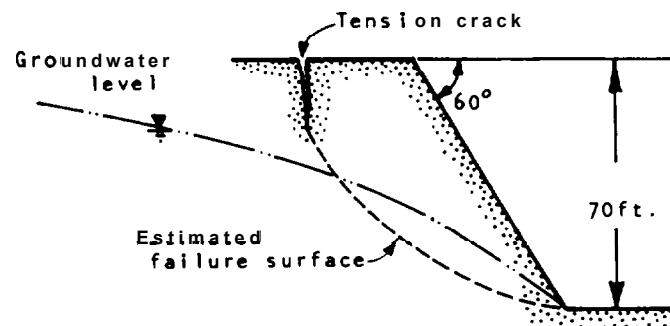


Figure IX.1 : Slope geometry for circular failure.

PRACTICUM VI I I
Wedge failure analysis

Given: A rock cut has been excavated with a face angle of 55 degrees in rock containing two major joint sets which form a wedge and are oriented as follows:

$$\begin{aligned}\text{Set A} &= \text{dip } (\psi_A) = 50^\circ, \text{ dip direction } (\alpha_A) = 140^\circ \\ \text{Set B} &= \text{dip } (\psi_B) = 60^\circ, \text{ dip direction } (\alpha_B) = 250^\circ\end{aligned}$$

The friction angle of set A is 30 degrees and of set B is 45 degrees, and there is no cohesion on either set. Assume that the slope is drained.

Required:

- (a) Determine the factor of safety of the wedge using the friction-only design charts (pages 8-13 to 8-20). Is this a potentially unstable wedge?
- (b) Calculate the dip (ψ_i) and dip direction (α_i) of the line of intersection of the wedge and determine if the slope face undercuts the wedge.

$$\tan \psi_i = \tan \psi_A \cdot \cos(\alpha_A - \alpha_i) = \tan \psi_B \cdot \cos(\alpha_B - \alpha_i) \quad (i)$$

$$\tan \alpha_i = \frac{\tan \psi_A \cdot \cos \alpha_A - \tan \psi_B \cdot \cos \alpha_B}{\tan \psi_B \cdot \sin \alpha_B - \tan \psi_A \cdot \sin \alpha_A} \quad (ii)$$

This equation gives two solutions 180 degrees apart; the correct value lies between α_A and α_B .

PRACTICUM VI I I - SOLUTION
Wedge failure analysis

1. Analysis of wedge failures is discussed in Chapter 8 and Appendix 1.

- (a) The factor of safety for friction only and a drained slope is:

$$F = A \tan \phi_A + B \tan \phi_B \quad (iii)$$

Constants A and B are obtained from the charts on page 8.14 for a dip difference of 10 degrees, and a dip direction difference of 110 degrees.

$$A = 1.0, B = 0.57$$

$$\begin{aligned}F &= 1 \tan 35 + 0.57 \tan 50 \\ &= 1.38.\end{aligned}$$

This is a potentially unstable wedge because water pressure could reduce the factor of safety to below 1.0.

- (b) Solution of equation (ii) gives $\alpha_i = 7.6^\circ$ or 187.6° . Because α_i must be between α_A and α_B , the correct value is 187.6° . Substitution of this value in equation (i) gives $\psi_i = 38.8^\circ$. If the face is cut at 55 degrees, the slope will undercut the wedge and sliding could occur. The stereoplot on Figure 8.3 illustrates the relationship between the slope angle, the dip of the line of intersection and the friction angle, i.e. $\psi_f - \phi > \psi_i$ - stable.

Slope reinforcement with rock bolts

- (a) The factor of safety of planar slope failure reinforced with rock bolts is calculated using equation (65) on page 7.17. In this case where the slope is drained and the cohesion is zero,

$$c = u = v = 0$$

$$\text{Therefore: } F = \frac{(W \cos \psi_p + T \cos \theta) \tan \phi}{W \sin \psi_p - T \sin \theta}$$

Where W is the weight of the sliding block. Using (46) on page 7.5 with

$$\begin{aligned} H &= 40', \psi_p = 35^\circ, \theta = 60^\circ, z/H = 0.38 \\ W &= 132,000 (0.86 \cot 35 - \cot 60) \\ &= 85913 \text{ lb/ft.} \end{aligned}$$

The factor of safety of the reinforced slope with $T = 25,000 \text{ lb/ft}$ and $\phi = 0$ is:

$$\begin{aligned} F &= \frac{(85913 \cos 35 + 25,000 \cos 0) \tan 37}{85913 \sin 35 - 25,000 \sin 0} \\ &= \frac{71,870}{49,277} \\ &= 1.46 \end{aligned}$$

- (b) If the bolts are installed at a flatter angle so that $\theta = 40$, then the factor of safety is:

$$\begin{aligned} F &= \frac{(85913 \cos 35 + 25,000 \cos 40) \tan 37}{85913 \sin 35 - 25,000 \sin 40} \\ &= \frac{67,463}{33,207} \\ &= 2.03 \end{aligned}$$

This shows the significant improvement that can be achieved by installing bolts at an angle flatter than the normal to the failure surface. The optimum angle is when:

$$\begin{aligned} \theta &= 90 - \phi \text{ see page 2.10} \\ &= 90 - 37 \\ &= 53^\circ \text{ and factor of safety} = 2.21 \end{aligned}$$

- (c) The rock bolt pattern should be laid out so that the distribution of bolts on the slope is as even as possible. If four bolts are installed in each vertical row and each row is 8 ft. apart, then the bolts are on an approximate 8 ft. square pattern and the bolt load per foot of slope is 25,000 lb.

Slope stabilization by unloading

The factor of safety is calculated using the design charts on Figure 7.3. The following values are obtained for the four constants:

$$\begin{aligned} P &= 1.74 && \text{when } \psi_p = 35, z/H = 0, \theta = 60 \\ Q &= 0.46 \\ R &= 0 \\ s &= 0 \\ F &= \frac{(0.42) + (0.46 \cot 35) \tan 37}{0.46} \\ &= \frac{0.92}{0.46} \\ &= \underline{2.0} \end{aligned}$$

Note that in case (c) the factor of safety for a 40 ft. high drained slope with cohesion = 500 psf was 1.56.

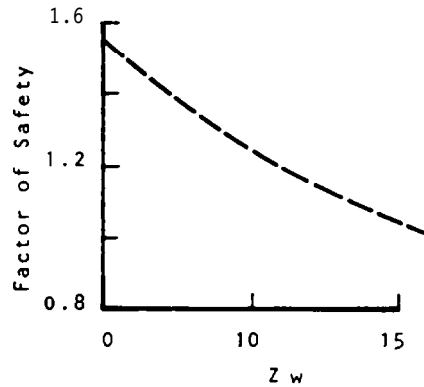
= 1.05 - this indicates that the slope is close to failure.

- (c) If the slope was drained so there was no water in the tension crack, i.e. $Z_w = 0$, then factors R and S become zero while factors P and Q remain unchanged. The new factor of safety is:

$$F = \frac{(0.17) + (0.35 \cot 35) \tan 37}{0.35}$$

= 1.56 - this is usually an adequate factor of safety

- (d) The plot of factor of safety against depth of water in the tension crack (Z_w) is nearly linear which shows that a significant decrease in the water level is required to improve the factor of safety. It also shows that the slope must remain drained if it is to be stable with an adequate factor of safety.



- (e) If the slope is drained and the cohesion on the failure plane is reduced from 500 psf to zero by blast vibrations, then the new factor of safety is:

$$F = \frac{0 + (0.35 \cot 35) \tan 37}{0.35} = 1.08$$

Note: Factors P, Q, R, S are the same as in case (c).

The loss of cohesion reduces the factor of safety from 1.56 to 1.08 which illustrates the sensitivity of the slope to the cohesion on the failure plane.

- (f) Figure 7.6a shows that the critical tension crack depth is 14.7 ft. (i.e. $z/H = 0.37$) which is close to the present position of the tension crack.

PRACTICUM VII - SOLUTION
Plane failure - analysis and stabilization

Analysis of plane failure is described in Chapter 7.

- (a) Factor of safety calculations: the factor of safety is calculated using equation (48) on page 7.5. The constants P, Q, R and S in this equation are obtained from the design charts in Figure 7.3. For this practicum the following values were obtained for the constants.

$$P = 1.1 \text{ when } \psi_p = 35^\circ, Z/H = 0.38$$

$$Q = 0.35$$

$$R = \frac{\gamma_w}{\gamma} \cdot \frac{Z_w}{Z} \cdot \frac{Z}{H}$$

$$= \frac{62.4}{165} \cdot \frac{10}{15} \cdot \frac{15}{40}$$

$$= 0.09$$

$$S = 0.16 \text{ when } \psi_p = 35^\circ, W/H = 0.25$$

$$F = \frac{(2 \times 500/165 \times 40) 1.1 + (0.35 \cot 35 - 0.09 (1.1 + 0.16)) \tan 37}{0.35 + 0.09 \times 0.16 \times \cot 35}$$

$$= \frac{(0.17) + (0.39) \tan 37}{.}$$

= 1.24 - This is usually a marginal factor of safety.

- (b) If the tension crack is completely filled with water, i.e. $Z_w = 15$, the parameters R and S will change, but parameters P and Q will be unchanged. The new values of R and S are as follows:

$$R = \frac{62.4}{165} \cdot \frac{15}{15} \cdot \frac{15}{40}$$

$$= 0.14.$$

$$S = 0.22 \text{ when } \psi_p = 35^\circ: Z_w/H = 0.38$$

The new factor of safety is:

$$F = \frac{(0.17) + (0.35 \cot 35 - 0.14 (1.1 + 0.22)) \tan 37}{. + 0.14 \times 0.22 \times \cot 35}$$

$$= \frac{(0.17) + (0.32) \tan 37}{0.39}$$

- (b) Calculate the new factor of safety if the bolts are installed at a different angle so that the angle θ is increased from 0 to 40° .
- (c) If the working load for each bolt is 50,000 lb., suggest a bolt layout, i.e. the number of bolts per vertical row and the horizontal and vertical spacing between bolts to achieve a bolt load of 25,000 lb/ft. of slope length.

Slope Stabilization by Unloading

Calculate the factor of safety for a drained slope with cohesion = 500 psf if the slope height is reduced from 40 ft. to 25 ft. by excavating the crest of the slope to the level of the base of the tension crack.

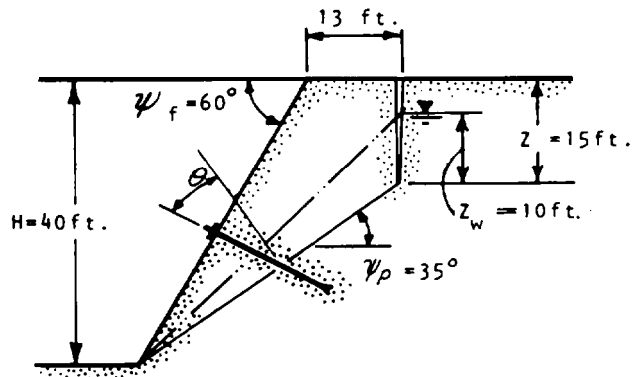


Figure VIII.1: Plane failure geometry.

PRACTICUM VI I
Plane failure - analysis and stabilization

Given: A 40 ft. high rock slope has been excavated at a face angle of 60 degrees. The rock in which this cut has been made contains continuous fractures that dip at an angle of 35 degrees into the excavation. The 15 ft. deep tension crack is 13 ft. behind the crest and is filled with water at a height of 10 ft. above the failure surface (Figure VII.1). The strength parameters of the failure surface are as follows:

$$\begin{aligned} \text{cohesion } c &= 500 \text{ psf} \\ \text{friction angle } \phi &= 37^\circ \end{aligned}$$

The unit weight of the rock is 165 lb/cu.ft. and the unit weight of water is 62.4 lb/ft.³.

Required:

Assuming that a plane slope failure is the most likely type of failure, determine the following:

- (a) Calculate the factor of safety of the slope for the conditions given in the sketch. Use design charts on Figure 7.3 in the manual.
- (b) Determine the new factor of safety if the tension crack was completely filled with water due to run-off collecting on the crest of the slope.
- (c) Determine the new factor of safety if the slope was completely drained.
- (d) Plot the relationship between the factor of safety and the depth of water in the tension crack.
- (e) Determine the new factor of safety if the cohesion was to be reduced to zero due to excessive vibrations from nearby blasting operations, assuming that the slope was still completely drained.
- (f) Determine whether the 15 ft. deep tension crack is the critical depth. Use the charts on Figure 7.6a in the manual.

Slope Reinforcements Using Rock Bolts

- (a) It is proposed that the drained slope with zero cohesion be reinforced by installing tensional rock bolts anchored into sound rock beneath the failure plane. If then rock bolts are installed at right angles to the failure plane, i.e. $\delta = 0$, and the total load on the anchors per lineal foot of slope is 25,000 lb., calculate the factor of safety.

PRACTICUM VI
Calculation of permeability from falling head test results

Given: A Falling Head Permeability Test is carried out in a rock of uniform permeability. The borehole diameter is 3 inches and the inside diameter of the drill rods is 2.36 inches. The drill rods are lifted from the bottom of the hole and a packer is installed (to create a seal to prevent water seepage up the annulus between the outside of the rods and the borehole) such that the test zone is 40 inches long.

The water level in the rods at rest is 164 ft. below the hole collar and water is added raising the water level to 115 ft. below the hole collar. After 30 seconds (t_1) and 150 seconds (t_2) the water levels in the rods have fallen by 16 ft. and 32 ft. respectively.

Required:

Calculate the coefficient of permeability of the rock assuming that the borehole is vertical and that the tests carried out below the water level.

PRACTICUM VI - SOLUTION
Calculation of permeability from falling head test results

Methods of interpreting falling head tests results are described in Chapter 6.

Coefficient of permeability can be calculated using:

$$k = \frac{A}{F(t_2 - t_1)} \cdot \log_e \frac{H_1}{H_2} \quad (\text{equation 35 in manual})$$

The first step in this analysis is to calculate the shape factor, F from the equation given in 3rd case (page 6.13 in manual).

$$\begin{aligned} F &= \frac{2\pi L}{\log_e(2L/D)} \\ &= \frac{2 \cdot \pi \cdot 40}{\log_e(2 \cdot 40/3)} \\ &= 76.5 \end{aligned}$$

The second step is to calculate cross-sectional area A of the water column in the rods.

$$\begin{aligned} \text{from } A &= \pi d^2/4 \\ A &= 4.4 \text{ inches}^2 \end{aligned}$$

The third step is to calculate the water levels H_1 and H_2 at different times t_1 and t_2 .

$$\begin{aligned} H_1 \text{ (after 30 seconds)} &= 164 - (115 + 16) \\ &= 33 \text{ ft.} = 396 \text{ inches} \\ H_2 \text{ (after 150 seconds)} &= 164 - (115 + 32) \\ &= 17 \text{ ft.} = 204 \text{ inches} \end{aligned}$$

Substituting in equation 35.

$$\begin{aligned} k &= \frac{4.4}{76.5(150-30)} \log_e 396/204 \\ &= 3.2 \times 10^{-4} \text{ in/sec.} \\ &= 8 \times 10^{-4} \text{ cm/sec.} \end{aligned}$$

PRACTICUM V - SOLUTION

Influence of geology and weather conditions on groundwater levels

Methods of evaluating groundwater conditions in slopes is described in Chapter 6.

Figures V.2 a, b, c show the positions of the phreatic line under the various conditions.

In general, the rock near the surface of the slope has been disturbed by blasting and has undergone stress relief so it will have a higher permeability than the undisturbed rock. When the permeability is high, the rock drains readily and the phreatic line has a relatively flat gradient.

If the face freezes and the water cannot drain from the slope then phreatic line will rise behind the face. The same situation arises when heavy infiltration exceeds the rate at which the rock will drain.

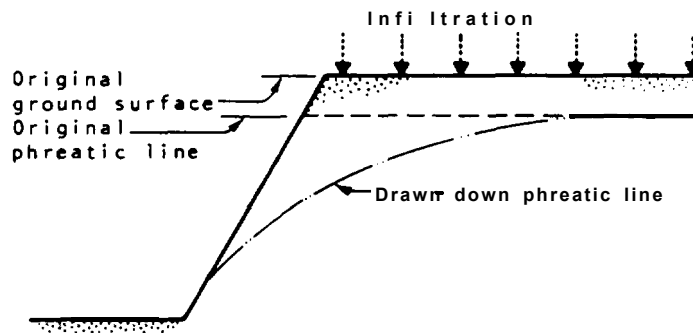


Figure V.2a Position of the phreatic line before and after excavation.

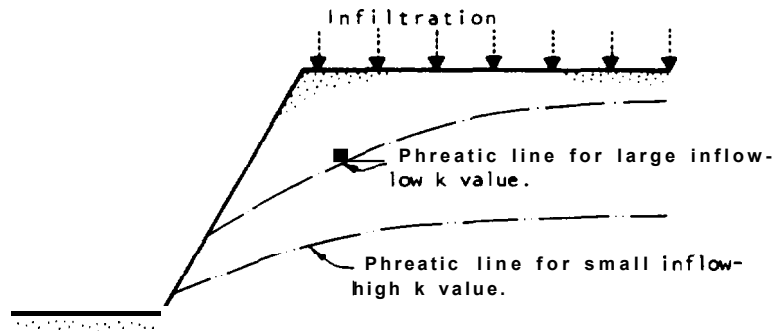


Figure V.2b Relative positions of the phreatic line for variations of inflow and permeability.

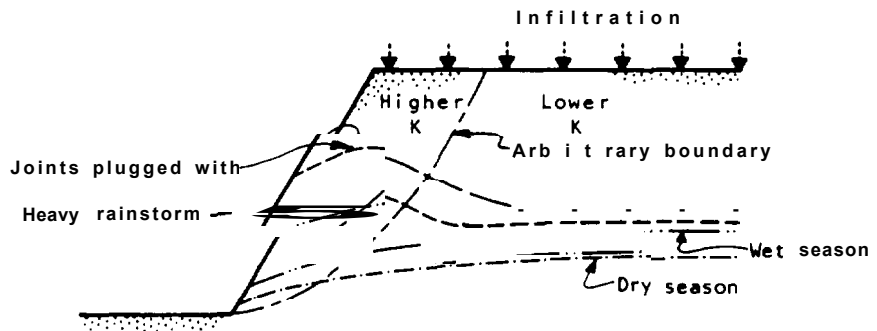


Figure V.2c Hypothetical positions of the phreatic line in a jointed rock slope.

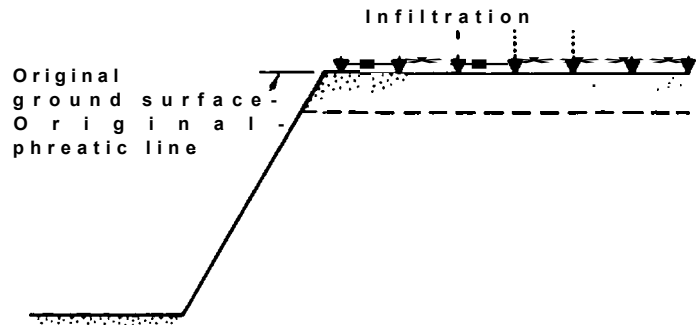


Figure V.1a Position of the phreatic line before and after excavation.

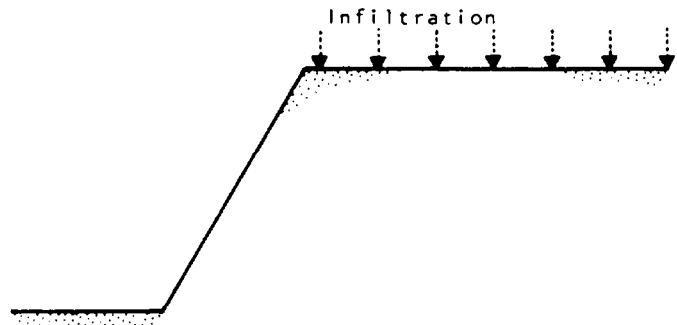


Figure V.1b Relative positions of the phreatic line For variations of inflow and permeability.

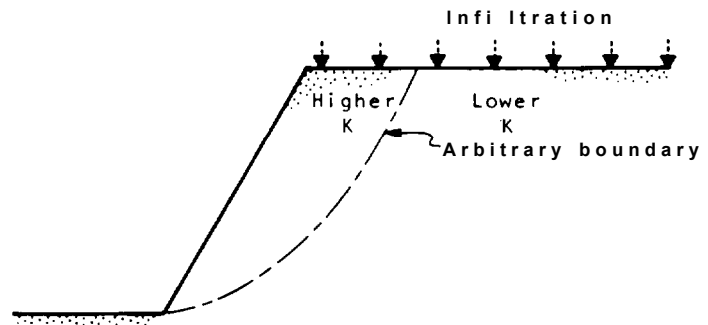


Figure V.1c Hypothetical positions of the phreatic line in a jointed rock slope.

PRACTICUM IV
Analysis of point load test results

Given: A series of point load tests on pieces of core 2.4 inches in diameter gave an average point load strength index of 10.2 when the core was loaded diametrically.

Required:

Determine the average uniaxial compressive strength of the samples.

PRACTICUM IV - SOLUTION
Analysis of point load test results

Methods of analysis of point load test results are given in Chapter 5.

The relationship between point load strength index (I_s) and uniaxial compressive strength (σ_c) for 2.4 inch diameter core is:

$$\text{where } \sigma_c = 24.5 I_s$$

is in MPa

$$\begin{aligned} \sigma_c &= 24.5 \times 10.2 \\ &= 250 \text{ MPa} \\ &= \underline{56,245 \text{ psi}} \end{aligned}$$

PRACTICUM V
Influence of geology and weather conditions on groundwater levels

- (a) On the cross-section shown in Figure V1a draw the approximate position of the phreatic line after excavation of the slope.
- (b) On the cross-section shown in Figure V1b draw the approximate positions of the phreatic line for two conditions:
- (1) large inflow, low permeability
 - (2) small inflow, high permeability
- (c) On the cross-section shown in Figure V1c draw the approximate positions of the phreatic line for the following conditions:
- (1) joints on slope face plugged with ice
 - (2) immediately following a heavy rainstorm
 - (3) wet season
 - (4) dry season

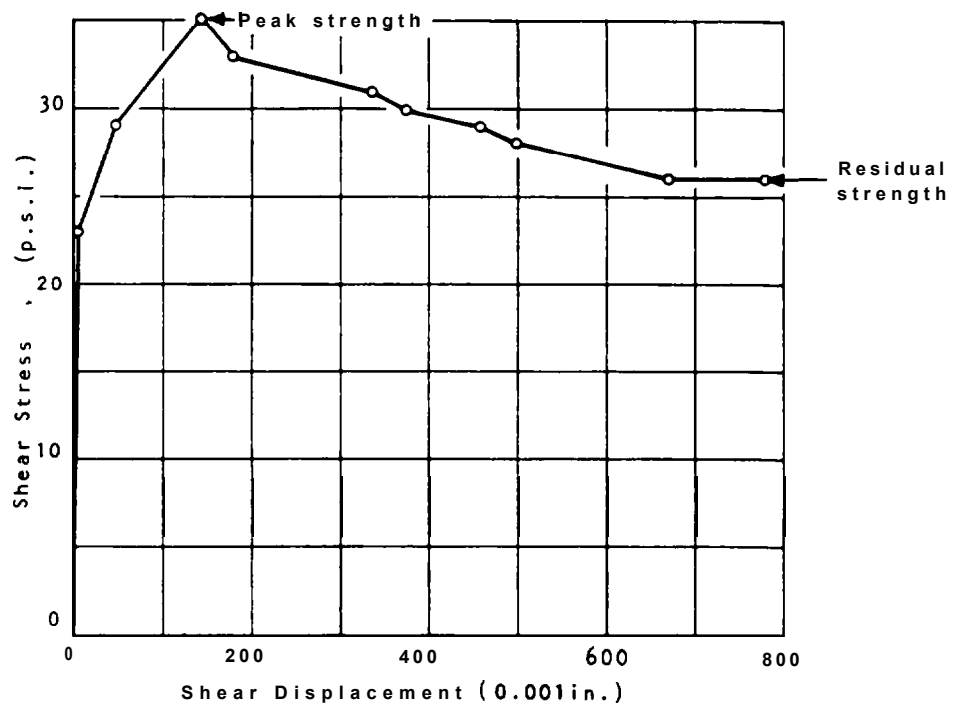


Figure III, 1: Plot of shear strength against shear displacement

PRACTICUM III
Analysis of direct shear strength test results

Given: The following table of results was obtained from a direct shear box test on a planar discontinuity in a sample of weathered granite. The average normal load on the sample was 30 psi .

<u>Shear Stress (psi)</u>	<u>Shear Displacement (0.001 inches)</u>
23	2
29	47
35	142
33	177
31	335
30	370
29	457
28	496
26	673
26	780

Required:

- (a) Plot a graph of shear stress against shear displacement with shear stress on the vertical axis.
- (b) From the graph determine the peak shear strength and peak friction angle of the surface.
- (c) From the graph determine the residual shear strength and residual friction angle of the surface.

PRACTICUM III - SOLUTION
Analysis of direct strength shear test results

Methods of evaluating shear strength test results are described in Chapter 5.

- (a) The graph of shear stress against shear displacement is shown on Figure III-1.
- (b) The peak strength is 35 psi from which the peak friction angle is:

$$\begin{aligned}
 \phi_p &= \tan^{-1} \frac{(\text{Shear stress})}{(\text{normal stress})} \\
 &= \tan^{-1} \frac{(35)}{(30)} \\
 &= 49^\circ
 \end{aligned}$$

- (c) The residual strength is 26 psi and the residual friction angle is:

$$\begin{aligned}
 \phi_r &= \tan^{-1} \frac{(26)}{(30)} \\
 &= 41^\circ
 \end{aligned}$$

Practicum II - Solution
Stability evaluation

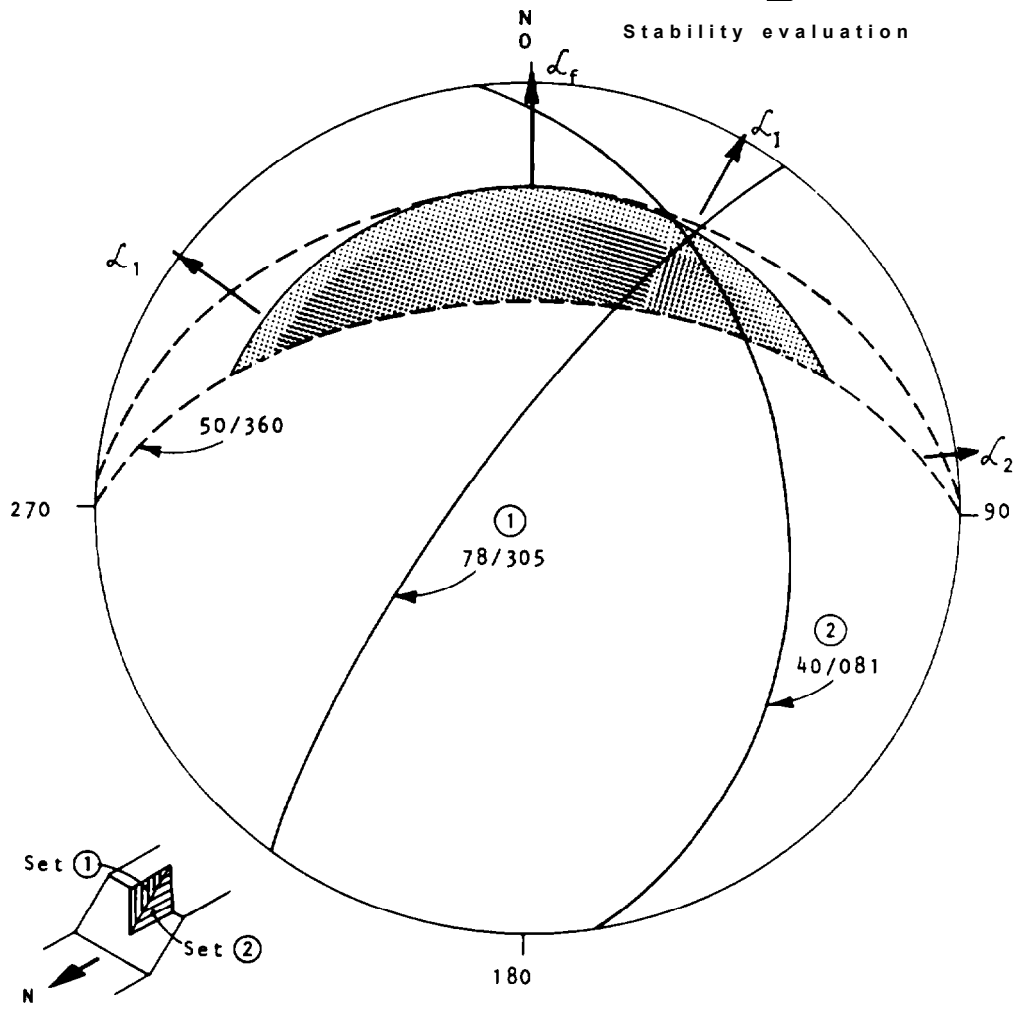


Figure 11.4: Stability conditions on north dipping slope-wedge failure on joint set 1 and joint set 2.

Practicum II - Solution
Stability evaluation

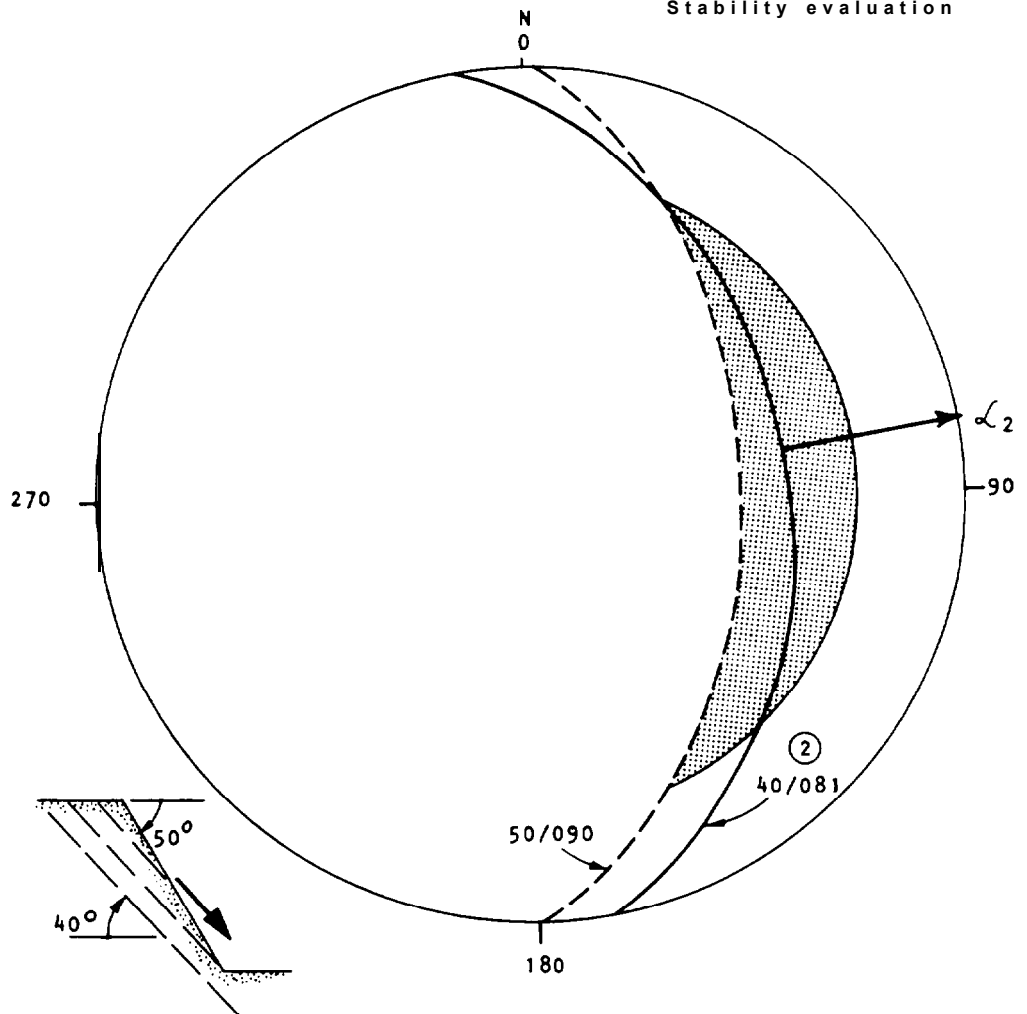


Figure II.3: Stability conditions on east dipping slope-sliding failure on joint set 2.

Practicum II - Solution
Stability evaluation

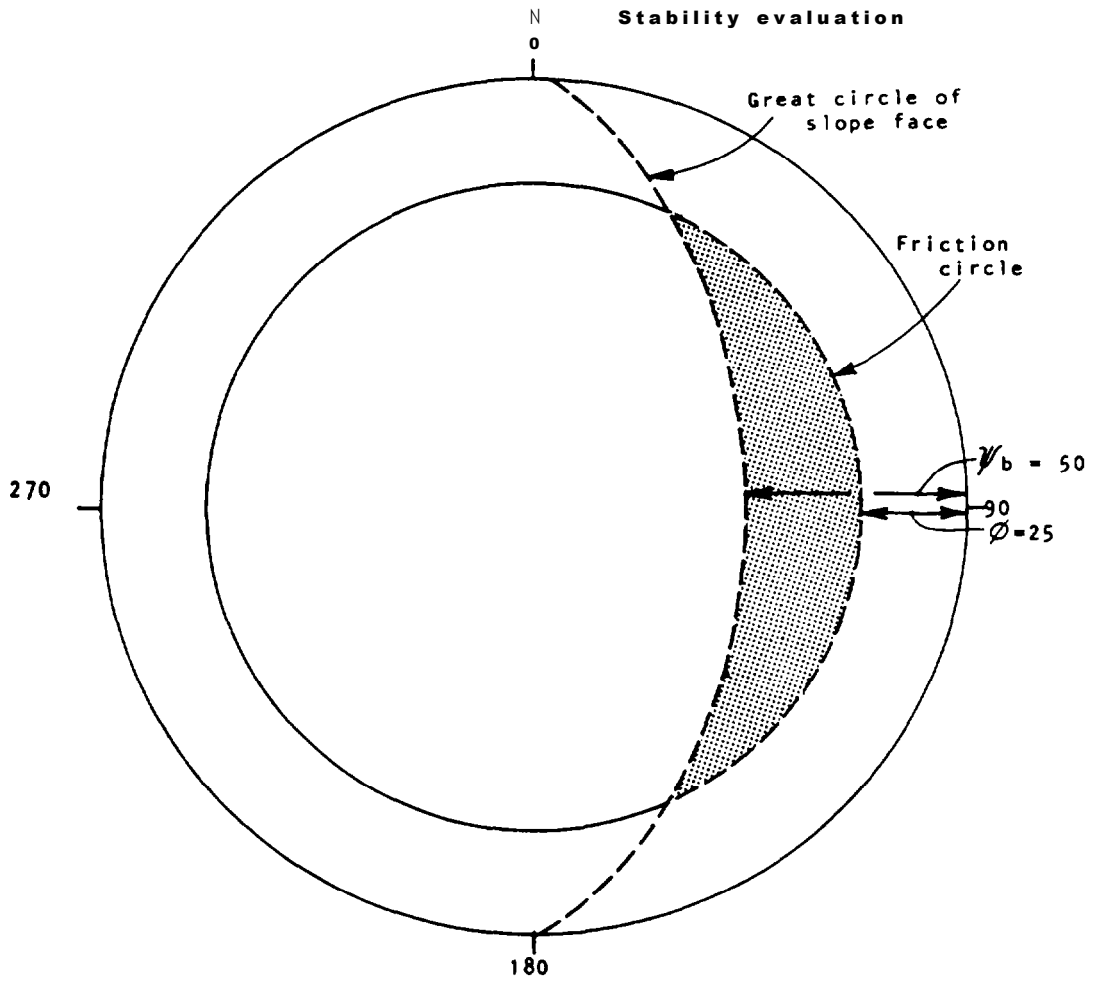


Figure II. 2: Great circle of slope and friction circle.

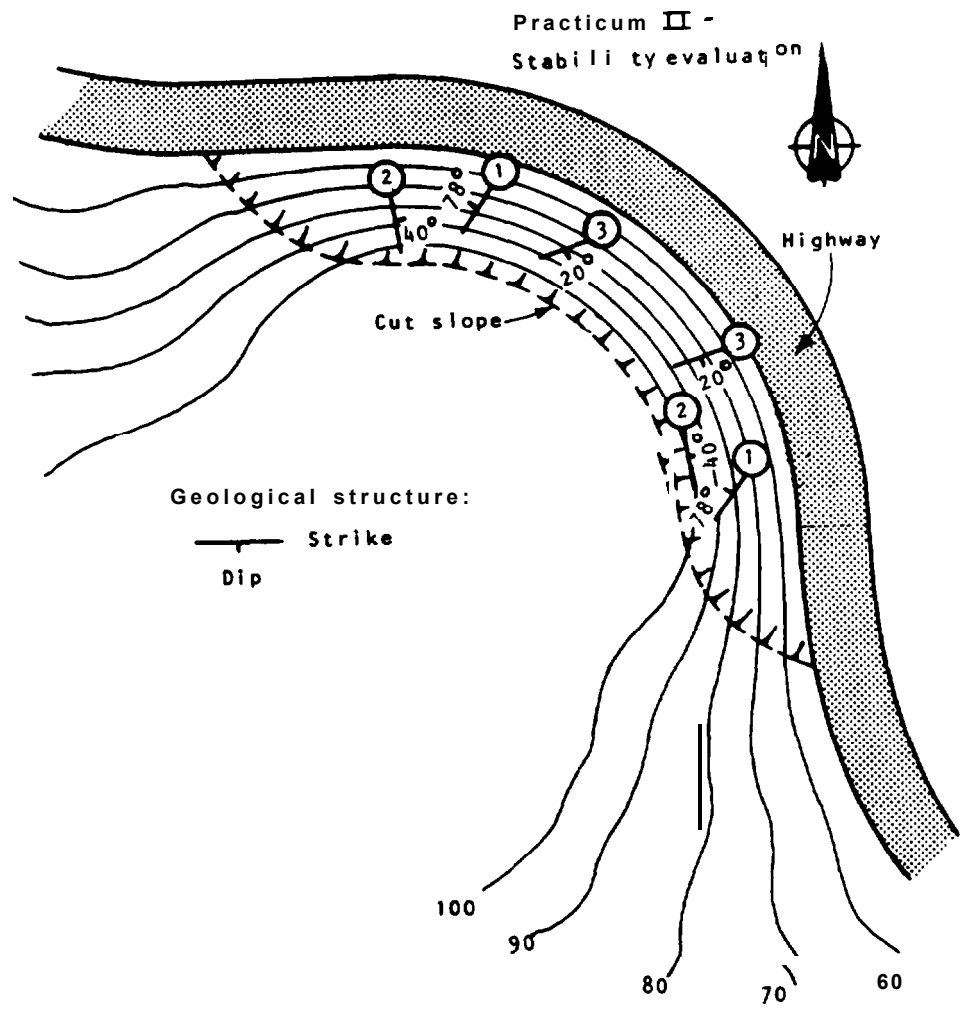


Figure 11.1: Cut slope and geological structures above highway.

PRACTICUM I

Slope stability evaluation related to structural geology

Given: In order to make a 90 degree curve in the highway a 50 ft. high rock cut has been excavated that follows the curve of the highway. The slope is 50 ft. high and the face is cut at an angle of 50 degrees.

The joints in the rock at the site form three sets with the following orientations:

Set 1 78/305
Set 2 40/081
Set 3 20/163

Figure I-1 shows the alignment of the highway and the orientation of the three sets in the slope.

The friction angle of the joint surfaces is 25 degrees.

Required:

- (a) On a piece of tracing paper draw a great circle representing the 50 degree slope face and a 25 degree friction circle.
- (b) Determine the most likely mode of failure, i.e. planar, wedge or toppling, on the following slopes:
 - (1) East dipping slope.
 - (2) North dipping slope.
- (c) State the joint set or sets on which sliding would occur on each slope.
- (d) Determine the steepest possible slope angle for these two slopes assuming that only the orientation of the fractures and the friction angle of the surfaces have to be considered.

PRACTICUM II - SOLUTION

Slope stability evaluation related to structural geology

Methods of evaluating slope stability are described in Chapter 3.

- (a) Figure II-2 shows the great circle of the slope at a face angle of 50 degrees. Note that there is no reference direction on this great circle because it will be rotated to follow the curvature of the slope.

A 25 degree friction circle is plotted on the same diagram as the great circle.

- (b) The stability evaluation is carried out by placing first the tracing of the great circles (Figure I-3) and then the tracing of the slope face and friction circle (Figure II-2) on the equal area net. The tracing of the slope great circle is rotated to the corresponding orientation of the slope face to give the following results:

East dipping slope: Sliding failure possible on joint set (Figure II-3). Sliding could be prevented by cutting the slope at 40 degrees coincident with the joint surfaces. If the friction angle had been greater than 40 degrees then sliding would not occur on these planes.

North dipping slope: Wedge failure possible on joint sets 1 and 2 (Figure II-4). Sliding could be prevented by cutting the slope at an angle of 27 degrees so that the wedges are not undercut by the slope.